

Acetylation Mechanism and HDAC Enzymes in Neurodegenerative Diseases

THESIS

Submitted to the Delhi Technological University For the
award of the degree of

DOCTOR OF PHILOSOPHY

Submitted by

Rohan Gupta
(2K18/PHDBT/501)

Guide

Prof. Pravir Kumar, PhD
Professor, Head, and Dean (International Affairs)
Department of Biotechnology
Delhi Technological University, DELHI



Department of Biotechnology
Delhi Technological University
(Formerly Delhi College of Engineering)
Shahbad Daulatpur, Main Bawana Road, Delhi-110042, INDIA

September 2022

Copyright ©Delhi Technological University-2022
All rights reserved.

Acetylation Mechanism and HDAC Enzymes in Neurodegenerative Diseases

THESIS

Submitted to the Delhi Technological University For the
award of the degree of

DOCTOR OF PHILOSOPHY

Submitted by

Rohan Gupta
(2K18/PHDBT/501)

Guide

Prof. Pravir Kumar, PhD
Professor, Head, and Dean (International Affairs)
Department of Biotechnology
Delhi Technological University, DELHI



Department of Biotechnology
Delhi Technological University
(Formerly Delhi College of Engineering)
Shahbad Daultapur, Main Bawana Road, Delhi-110042, INDIA

September 2022

Dedicated
to
My
Parents

DECLARATION

I hereby declare that the thesis entitled “**Acetylation and Mechanism and HDAC Enzymes in Neurodegenerative Diseases**” submitted by me, for the award of the degree of *Doctor of Philosophy* to **Delhi Technological University (Formerly DCE)** is a record of *bona fide* work carried out by me under the guidance of Prof. Pravir Kumar.

I further declare that the work reported in this thesis has not been submitted and will not be submitted, either in part or in full, for the award of any other degree or diploma in this Institute or any other Institute or University.

Name: Rohan Gupta
Reg No: 2K18/PHDBT/501
Department of Biotechnology
Delhi Technological University (DTU)
Shahbad Daulatpur, Bawana Road, Delhi-110042
Place: New Delhi
Date: 20.09.2022

CERTIFICATE

This is to certify that the thesis entitled “**Acetylation Mechanism and HDAC Enzymes in Neurodegenerative Diseases**” submitted by **Mr. Rohan Gupta** to **Delhi Technological University (Formerly DCE)**, for the award of the degree of “Doctor of Philosophy” in Biotechnology is a record of *bona fide* work carried out by him. Rohan Gupta has worked under my guidance and supervision and has fulfilled the requirements for the submission of this thesis, which to our knowledge has reached requisite standards.

The results contained in this thesis are original and have not been submitted to any other university or institute for the award of any degree or diploma.

Prof. Pravir Kumar, PhD
Professor and Head of Department
Dean (International Affairs)
Department of Biotechnology
Delhi Technological University
Shahbad Daulatpur, Bawana Road, Delhi-110042
Place: New Delhi
Date: 20.09.2022

ABSTRACT

Neurodegenerative diseases, including Alzheimer's disease and Parkinson's disease are characterized by the loss of neuronal cells due to the accumulation of toxic proteins, namely β -amyloid, tau, α -synuclein, and others. Studies have demonstrated that several contributing factors, such as aging, mitochondrial dysfunction, DNA damage, misfolded protein aggregation, impaired ubiquitin-proteasome system and autophagy-lysosomal pathway, and environmental toxins involved in the progression and pathogenesis of Alzheimer's and Parkinson's disease. However, post-translational modifications play a crucial role in the alteration of misfolded protein aggregates and impaired protein degradation pathways. Post-translational modifications are covalently attached modifications that alter the functions of proteins without changing the structure of protein. Additionally, lysine residues are known for the post-translational modifications, namely acetylation, ubiquitination, and SUMOylation. In acetylation, histone deacetylases and its interactors cause transcriptional deregulation, and cause mitochondrial dysfunction, apoptosis, inflammatory response, and cell-cycle impairment, that cause brain homeostasis and neuronal cell death. Another regulatory post-translational modification involved in the pathogenesis of neurodegenerative diseases are ubiquitination and SUMOylation for the degradation of the misfolded proteins. Additionally, mounting evidence demonstrated that heavy metals, such as copper, chromium, cobalt, and nickel, increases the β -amyloid and tau aggregation in the pathogenesis of Alzheimer's and Parkinson's disease by activating different signaling events. For instance, copper induces the formation of reactive oxygen species to cause mitochondrial dysfunction and DNA damage, whereas, chromium elevates neuroinflammatory response and neuronal apoptosis. Similarly, cobalt increases tau hyperphosphorylation and promotes tau aggregation, whereas, nickel elevates β -amyloid aggregation. Moreover, integration of omics data and deciphering the mechanism of a biological regulatory network could be a promising approach to reveal the molecular mechanism involved in the progression of

complex diseases, including Alzheimer's and Parkinson's. Despite having an overlapping mechanism in the etiology of Alzheimer's and Parkinson's disease, the exact mechanism and signaling molecules behind them are still unknown. Further, the acetylation mechanism and histone deacetylase enzymes provide a positive direction towards studying shared phenomenon between Alzheimer's disease and Parkinson's disease pathogenesis. Herein, we employed an integrative approach to analyze the transcriptomics data that established a potential relationship between Alzheimer's and Parkinson's disease. Firstly, we aim to investigate the potential conventional biomarkers and regulatory TFs involved in the pathogenesis of AD and PD simultaneously with the help of microarray datasets and the network-biology approach. The identified proteomics and transcriptomics signatures were further analyzed to investigate the potential lysine residue for acetylation and deacetylation activity, along with the determination of the type of histone deacetylase enzyme being involved in the disease progression. Lately, the study focuses on investigating conserved amino acid residues involved in the lysine-acetylation/deacetylation process along with the structural selectivity of molecular signatures, which could be crucial for protein acetylation or deacetylation activity. Further, we aim to investigate the potential acetylation/ubiquitination/SUMOylation crosstalk sites in the histone deacetylase interactors, which causes NDDs. Further, we aim to identify the influence of post-translational modifications on structural features of proteins and the impact of lysine mutation on disease susceptibility. Additionally, we aim to examine the impact of the mutation on acetylated lysine for the ubiquitination and SUMOylation. Moreover, we aim to identify the crucial proteins involved in metal toxicity-induced Alzheimer's disease through network biology, followed by identifying regulatory transcription factors associated with crucial proteins. Further, we aim to determine the critical lysine residue and the role of CREBBP-induced acetylation on transcription factors. Lately, we have focused on identifying micro RNAs associated with CREBBP and transcription factors simultaneously. Lastly, we aim to identify

the potential long non-coding RNA, serving as a sponge to micro RNAs. Lastly, we investigate the potential histone deacetylase 10 inhibitor using machine learning approach.

Our results highlighted the importance of CREBK292 and HINFPK330 as a potential biomarker in Alzheimer's and Parkinson's pathology. Further, we reported the importance of PARP1 as a crucial regulatory molecule in Alzheimer's disease and Parkinson's disease. Lately, we demonstrated that the OIP5-AS1/miR-129-5p/CREBBP axis is a potential therapeutic target in metal toxicity-induced Alzheimer's disease pathogenesis. Lastly, we reported the role of anti-psychotic drugs, namely Zimeldine and Dibenzapine as potential histone deacetylase 10 inhibitors in Alzheimer's disease therapeutics.

ACKNOWLEDGEMENT

First and foremost, I am thankful to almighty GOD for keeping me fit, healthy and energetic during entire course of my Ph.D. work.

*I would like to express my gratitude to **Prof. Jai Prakash Saini**, Vice chancellor, Delhi Technological University, Delhi for providing this opportunity to carry out this work in this prestigious institute. Further, I express my gratitude to **Prof. Yogesh Singh**, former Vice chancellor Delhi Technological University, Delhi for providing me opportunity and infrastructure to carry out this work.*

*With pleasure, I acknowledge my deep sense of gratitude and indebtedness to my guide and mentor **Prof. Pravir Kumar**, Professor, DRC Chairman and Head, Department of Biotechnology, Delhi Technological University, Delhi, for their enlightening guidance, intelligent approach, constructive critique, whole hearted and ever available help, which has been the primary impetus behind the research. Without the wise advice and able guidance, it would have been impossible to complete the thesis in this manner. Here, I would also like to thanks **Prof. Jai Gopal Sharma**, Former Head of the Department, department of Biotechnology, for providing me the infrastructure and smooth functioning of official work.*

*The constant guidance and encouragement received from **Dr. Rashmi Ambasta**, CSIR Scientist, Delhi Technological University, Delhi, has been of great help in carrying out the present work and is acknowledged with reverential thanks.*

*I wish to record my thanks and gratitude to my External DRC experts, **Prof. Suhel Parvez** (Department of Toxicology and In-Charge, Jamia Hamdard) and **Prof. S K Khare** (IIT Delhi) for their valuable guidance, critical and constructive discussion during this work.*

*I would like to thank my fellow lab mates especially **Dia Advani**, **Smita Kumari**, **Rahul Tripathi**, and **Sudhanshu Sharma** for helping and encouraging me throughout my research. Moreover, I wish to thanks my juniors, namely **Mehar Sahu** and **Neetu Rani** for their support during my research work. This would be incomplete without saying thanks to my senior **Dr. Dhiraj Kumar**, who have corrected me several times during my initial days of career.*

I would also like to thanks the Senior Management and technical staff of DTU, who help me to carry out my research work.

*Thanks are due to the wonderful friends in my life who were always on the stand by to bring me to positivity, hope and smiles when things didn't seem favoring and it seemed a far-fetched journey. Special mention is deserved for all my friends, especially **Sunil Kumar**, **Ashish Ganguli**, **Megha Khandelwal**, and **Archit** who have always been my guiding light when I didn't*

*believe in myself. I would also like to thanks my dear and lovely niece, **Kashvi** for releasing my stress during my research work. Lastly, I would to express my gratitude to my sister **Dr. Nikita Gupta**, who always stood beside mi in my ups and downs.*

*Finally, I want to dedicate this thesis to my parents, **Mr. Anil Kumar Gupta** and **Mrs. Babita Gupta**, whose loving support has been my strongest inspiration. Their sacrifice allowed me to pursuit my dream and has made Ph.D. study seems completely painless.*

TABLE OF CONTENTS

<i>Declaration</i>		V
<i>Certificate</i>		VI
<i>Abstract</i>		VII
<i>Acknowledgement</i>		X
<i>List of Figures</i>		XIV
<i>List of Tables</i>		XIX
Chapter 1	Introduction	1
1.1.	Overview	2
1.2.	Motivation of Research	2
1.3.	Aim and Objectives	3
1.3.1.	Aim	3
1.3.2.	Objectives	3
1.4.	Summary of Thesis	3
Chapter 2	Review of Literature	6
2.	Introduction	7
2.1.	Neurodegenerative Diseases	9
2.1.1.	Alzheimer's Disease	9
2.1.2.	Parkinson's Disease	12
2.2.	Post-Translational Modifications in Neurodegeneration	14
2.2.1.	Role in Misfolded Protein Aggregates	17
2.3.	Acetylation in Alzheimer's and Parkinson's Disease Pathology	20
2.4.	Classification of Histone Deacetylases Enzymes Superfamily	22
2.5.	Histone Deacetylases Enzymes Mediated Neurotoxicity	29
2.5.1.	Alzheimer's Disease	31
2.5.2.	Parkinson's Disease	34
2.6.	Acetylation and Histone Deacetylase Enzymes Interfere Biological and Cellular Process in Alzheimer's and Parkinson's Disease	35
2.6.1.	Synaptic Plasticity and Transmission	36
2.6.2.	Neurogenesis and Neural Migration	39
2.6.3.	Oxidative Stress and Autophagy	42
2.6.4.	Inflammatory and Immune Response	45
2.7.	Histone Deacetylases Inhibitors in Alzheimer's and Parkinson's Therapeutics	47
2.7.1.	Role of Chemically Synthesized Compounds	48
2.7.2.	Implementation of Natural Compounds and Micro-RNAs	50
2.7.3.	Emergence Of Multi-Target Drug Ligand as a Potential Therapeutic Agents in Alzheimer's and Parkinson's Pathology	53
Chapter 3	Materials and Methodology	58
3.	Introduction	59
3.1.	Data Collection	59

3.2.	Data Processing and Filtration	60
3.3.	Protein-Protein Interaction Analysis	60
3.4.	Network Clustering and HUB Signature Identification	61
3.5.	Functional Enrichment Analysis of HUB Signatures	61
3.6.	Objective 1: To Identify Novel Common Biomarkers in AD and PD Based on Multi-Omics Approach	62
3.6.1.	Identification of HUB Signatures-Transcription Factors Regulatory Network and Cellular Localization Prediction	62
3.6.2.	Prediction of Acetylation Signatures and Deacetylation Sites	62
3.6.3.	Prediction of Conserved Lysine Residues	63
3.7.	Objective 2: To Dissect Histone Deacetylase Mechanism and Key Lysine Residues in Association with Novel Biomarkers	63
3.7.1.	Integrate Post-Translational Modifications sites	63
3.7.2.	Structural Analysis of HUB Signatures	64
3.7.2.1.	Secondary Structure Analysis	64
3.7.2.2.	Disorder Prediction	64
3.7.2.3.	<i>In-Situ</i> Crosstalk Analysis	64
3.7.2.4.	Hotspot Analysis	64
3.7.3.	Impact of Lysine Mutation	66
3.7.3.1.	Lysine Mutation and Disease Susceptibility	66
3.7.3.2.	Impact of Lysine Mutation on Protein Stability	66
3.7.4.	Impact of Lysine Mutation on Acetylation, Ubiquitination, and SUMOylation	66
3.8.	Objective 3: To Identify Potential Micro-RNAs and Biomarkers Regulatory Network in The Pathogenesis of Neurodegenerative Diseases	67
3.8.1.	Identification of HUB Proteins-Transcription Factors Association	68
3.8.2.	Prediction of Putative Acetylation Sites	68
3.8.3.	Identification of Micro-RNAs Interact with Transcription Factors and Acetylating Enzyme	68
3.8.4.	Expression of Micro-RNAs in Brain and Prediction of Putative Long Non-Coding RNA	68
3.9.	Objective 4: To Explore Novel Histone Deacetylase Inhibitor Using Machine Learning Approach	69
3.9.1.	Data Collection and Target Refinement	69
3.9.2.	Molecular Descriptors Calculation	70
3.9.3.	Machine Learning Model Preparation	70
3.9.4.	ADMET Analysis and Blood Brain Barrier Prediction	70
3.9.5.	Molecular Docking and Molecular Dynamic Simulation	71
3.10.	Statistical Analysis	71
Chapter 4	CREB1^{K292} and HINFP^{K330} As Putative Common Therapeutic Targets in Alzheimer's and Parkinson's Disease	72

4	Introduction	73
4.1.	Results and Discussion	74
4.1.1.	Transcriptomics Signatures Involved in Alzheimer's and Parkinson's Pathology	74
4.1.2.	Protein-Protein Interaction network in Alzheimer's and Parkinson's Disease	75
4.1.3.	Protein-Protein Interaction Network Clustering and Proteomic Signatures in Alzheimer's and Parkinson's Pathogenesis	78
4.1.4.	Functional Enrichment Analysis of HUB Proteins in Alzheimer's and Parkinson's Pathology	82
4.1.5.	Transcription Factors Associated with HUB Proteins	84
4.1.6.	Cellular Location and Acetylation Signatures of Hub Proteins and Transcription Factors in Alzheimer's and Parkinson's Disease	86
4.1.7.	Potential Lysine Residues for Protein Acetylation	89
4.1.8.	Conserved Amino Acid Residues at Protein Acetylation Sites	92
4.2.	Conclusion and Summary	96
4.3.	Highlights of the Study	98
Chapter 5	Computational Analysis Indicates That PARP1 Acts as a Histone Deacetylases Interactor Sharing Common Lysine Residues for Acetylation, Ubiquitination, and SUMOylation in Alzheimer's and Parkinson's Disease	99
5.	Introduction	100
5.1.	Results and Discussion	101
5.1.1.	Integration of Proteomics Data and Post-Translational Modifications Sites	101
5.1.2.	Molecular Functions and Biological Pathways of Top Interacting HDAC Partners	103
5.1.3.	Structural Characterization of PARP1, NPM1, and CDK1	105
5.1.4.	Impact of Lysine Mutation on PARP1	110
5.1.5.	Potential Lysine Residues Involved in Acetylation, Ubiquitination, and SUMOylation	111
5.2.	Conclusion and Summary	115
5.3.	Highlights of the Study	118
Chapter 6	Integrative Analysis of OIP5-AS1/MIR-129-5P/CREBBP Axis as a Potential Therapeutic Target in The Pathogenesis of Metal Toxicity-Induced Alzheimer's Disease	119
6.	Introduction	120
6.1.	Results and Discussion	121
6.1.1.	Genes Involved in Metal Toxicity-Induced Alzheimer's Disease	121
6.1.2.	Gene Set Enrichment Analysis of Common Genes	121
6.1.3.	Protein-Protein Interaction Analysis and HUB Proteins in Network	126

6.1.4.	Regulatory Post-Transcriptional Signatures in the Regulation of HUB Proteins Activity	130
6.1.5.	Literature Validation of Regulatory Molecules and Protein Sub-Cellular Localization	131
6.1.6.	Potential Acetylated Lysine Residues of Regulatory Molecules	132
6.1.7.	Micro-RNAs Regulating the Activity of Identified Signatures	133
6.1.8.	6OIPS-AS1 Regulates the Expression and Activity of hsa-mir-129-5P and hsa-mir-335-5P In the Pathogenesis of Metal Toxicity-Induce AD	135
6.2.	Conclusion and Summary	137
6.3.	Highlights of the Study	144
Chapter 7	Identification of Novel Histone Deacetylase 10 Inhibitor for Alzheimer's Disease Therapeutics	145
7.	Introduction	146
7.1.	Results and Discussion	146
7.1.1.	Data Collection and Preprocessing	146
7.1.2.	Machine Learning Model Preparation and Evaluation	147
7.1.3.	ADMET Analysis and Blood Brain Barrier of Selected Compounds	148
7.1.4.	Molecular Docking Studies of Selected Compounds	150
7.2.	Conclusion and Summary	151
Chapter 8	Summary, Discussion, and Future Perspectives	153
Annexure		
Annexure 1	Box plots of Alzheimer's disease (GSE1297 and GSE28146) and Parkinson's disease (GSE7621 and GSE19587) before and after normalization of microarray datasets	160
Annexure 2	(A) histograms of microarray datasets of Alzheimer's disease (GSE1297 and GSE28146) and Parkinson's disease (GSE7621 and GSE19587). (B) volcano plots of publicly available microarray datasets for GSE1297, GSE28146, GSE7621, and GSE19587	161
Annexure 3	Prediction of putative lysine residues and HDAC enzymes in the CREB1	162
Annexure 4	Prediction of putative lysine residues and HDAC enzymes in the HINFP	163
Annexure 5	List of anti-depressive drugs used as a test set	164
Annexure 6	List of compounds used as training set for HDAC10 inhibitors	170
References		181
List of Publications		253
Curriculum Vitae		257

LIST OF FIGURES

Figure Number	Title of the Figure	Page Number
Chapter 2		
Figure 2.1	Epigenetic modifications in neurodegenerative diseases	8
Figure 2.2	APP processing cascade in Alzheimer's disease	10
Figure 2.3	α -synuclein in the pathophysiology of Parkinson's disease	14
Figure 2.4	Implementation of different post-translational modifications in neurodegenerative diseases (NDDs)	19
Figure 2.5	Domain architectures and position of post-translational modifications in the neurotoxic proteins involved in the pathogenesis and progression of Alzheimer's disease and Parkinson's disease	22
Figure 2.6	Classification of histone deacetylase enzymes and their domain structure	25
Figure 2.7	Interplay between the histone deacetylase (HDAC) biological activity and etiology of neurodegenerative disorders	33
Figure 2.8	Role of histone deacetylase enzymes in synaptic plasticity and transmission	38
Figure 2.9	Involvement of histone deacetylase enzymes in neurogenesis and neural migration	41
Figure 2.10	Histone deacetylase modulates autophagic cell death and oxidative stress	44
Figure 2.11	Histone deacetylase enzymes regulates neuroinflammation in neurodegeneration	47
Figure 2.12	Histone deacetylase inhibitors as a potential multi-target directed ligand	55
Chapter 3		
Figure 3.1	Workflow of the current study. The study is divided according to the different objectives as mentioned in the figure	65
Chapter 4		
Figure 4.1	It represents the protein-protein interaction network of the top 15 ranked or HUB genes involved in Alzheimer's disease, Parkinson's disease, Alzheimer's disease-Parkinson's disease union merged network, and Alzheimer's disease-Parkinson's disease intersection merged network	76
Figure 4.2	Represents the bar graph of the top 10 biological processes, molecular functions, and biological pathways of HUB proteins along with their p-value and involved HUB proteins	83
Figure 4.3	Part A of the figure represents the PPI network of HUB genes with associated regulatory transcription factors. Part B of the figure demonstrated the biological significance of top interacting transcription factors in the progression of Alzheimer's disease and Parkinson's disease along with their degree of node and interacting partners	85
Figure 4.4	Part A of the figure denotes the acetylation signatures of non-histone protein substrates. Part B of the figure represents the relative expression of substrate with respect to change in	88

	histone acetylation status at particular lysine residue	
Figure 4.5	Multiple sequence analysis of potential acetylation/deacetylation-lysine residues by taking 21 window sizes. 21 window size was taken by lysine at the center and placed ten amino acids on both sides	94
Figure 4.6	Literature validation of the involvement of HDAC interaction with CREB1 and HINFP	98
Chapter 5		
Figure 5.1	Interactive Venn analysis of AD, PD, and HDAC interactors collected during the data extraction from different databases. Bar graph analysis of protein extracted from databases for AD, PD, and HDAC interactors was given in the figure. PPI network of cluster 1 including 33 proteins extracted from the core PPI network after clustering analysis. Graphical representation of acetylation, ubiquitination, SUMOylation sites in protein present in the cluster 1	102
Figure 5.2	(A) Graphical representation of acetylation, ubiquitination, SUMOylation sites in protein present in the cluster 1 (B) Molecular functions of top 33 proteins involved in HDAC interactors, Alzheimer's and Parkinson's disease	105
Figure 5.3	(A) Stack-bar representation of 'K' modified sites (B) Secondary-structure representation in PARP1, CDK1, and NPM1	106
Figure 5.4	Classification of PTM sites of PARP1, NPM1, and CDK1 into ordered and disordered region	107
Figure 5.5	Crosstalk analysis between acetylation, ubiquitination, and SUMOylation in PARP1, CDK1, and NPM1 (B) Identification of Hotspot regions in PARP1 and CDK1	109
Figure 5.6	Impact of lysine mutation in hotspot sites on disease susceptibility	110
Figure 5.7	Impact of lysine mutation on protein stability and investigation of acetylated lysine residue mutations on ubiquitination and SUMOylation	112
Figure 5.8	Mechanism of PARP1 acetylation in neurodegenerative diseases	116
Chapter 6		
Figure 6.1	Gene set enrichment analysis of common genes between chromium, cobalt, copper, and nickel-associated Alzheimer's disease	125
Figure 6.2	It represents the protein-protein interaction network of 199 common genes between chromium, cobalt, copper, and nickel associate metal toxicity induced Alzheimer's disease	127
Figure 6.3	(A) it represents the clustering protein-protein interaction network and aims to identify the highly-dense or connected region in the global biological interaction network. (B) It represents the top 10 ranked HUB genes in the network. Here, darker is the color of the node; more is the rank of the HUB gene	129
Figure 6.4	Protein-protein interaction network of transcription factors-HUB genes through Cytoscape Software: network analysis	130

	from network analyst identified the potential transcription factors associated with HUB genes	
Figure 6.5	Micro-RNAs interacting with putative acetylated transcription factors and acetylating enzyme CREBBP were identified	134
Figure 6.6	Involvement of predicted micro-RNAs, such as hsa-miR-338-5p, hsa-miR-335-5p, hsa-miR-429, hsa-miR-200c-3p, and hsa-miR-129-5p in the brain disease	135
Figure 6.7	Pathway analysis of hsa-miR-335-5p and hsa-miR-129-5p with the help of TissueAtlas database	137
Figure 6.8	Mechanism of long non-coding RNA and micro-RNAs in metal toxicity-induced Alzheimer's disease	139

LIST OF TABLES

Table Number	Title of the Table	Page Number
Chapter 2		
Table 2.1	Classification of HDAC superfamily along with their substrates (histone and non-histone), catalytic active ligand binding sites, and molecular function	27
Table 2.2	Administration effects of histone deacetylase inhibitors in cellular and animal models and their implications in neurodegenerative disorders	49
Table 2.3	Neuroprotective role of biomolecules and micro-RNAs mediated inhibition of histone deacetylase enzymes	52
Chapter 4		
Table 4.1	Datasets obtained from the gene expression omnibus database for Alzheimer's and Parkinson's disease	74
Table 4.2	(A) Parameters and characteristics feature of complex Alzheimer's disease, Parkinson's disease, Alzheimer's-Parkinson's disease intersection network, and Alzheimer's-Parkinson's disease union networks; (B) characteristic features of top 5 ranked clusters from Alzheimer's disease, Parkinson's disease, Alzheimer's-Parkinson's disease merged network; (C) parameters of HUB genes protein-protein interaction network	77
Table 4.3	List of HUB genes identified in different protein-protein interaction networks and list of common proteins that were found in the cluster of all three protein-protein interaction networks such as Alzheimer's disease, Parkinson's disease, and Alzheimer's-Parkinson's disease union network	79
Table 4.4	Role of HUB genes in the pathogenesis of Alzheimer's disease and Parkinson's disease identified with the help of MalaCards	81
Table 4.5	List of common crucial lysine residues in CREB1 and HINFP	92
Table 4.6	Secondary structure of the protein acetylation sites predicted by PSIPRED: protein structure prediction server	96
Chapter 5		
Table 5.1	Functional enrichment analysis (biological pathways and molecular functions) involved in top interacting histone deacetylase interactors	103
Table 5.2	List of histone deacetylase interactors having more than 50 lysine modified sites (acetylation, ubiquitination, and SUMOylation)	105
Table 5.3	List of post-translational modification and non-post-translational modification sites of PARP1, NPM1 and CDK1 (histone deacetylase interactors) in coiled, helix, and strand region	108
Table 5.4	Impact of PARP1's "K" mutation to either Q or L on disease susceptibility predicted with the help of Pmut, PolyPhen2, Panther, and SNAP2	111
Table 5.5	Physical significance of lysine (K) residue in PARP1 acetylation, ubiquitination, and SUMOylation through an online analysis tool known as MutPred2	113
Chapter 6		

Table 6.1	Gene set enrichment analysis (GO analysis and Pathway analysis) of 199 common genes related to metal toxicity and Alzheimer's disease	121
Table 6.2	Characteristics and parameters of core, cluster, HUB genes, transcription factors, and micro-RNAs protein-protein interaction network	127
Table 6.3	Top interacting transcriptional regulatory factors involved in metal toxicity induced Alzheimer's disease	131
Table 6.4	Prediction of CREBBP-induced acetylation sites of identified transcription factors through Deep PLA and GPS-PAIL	132

Chapter 7

Table 7.1	List of 16 anti-depressive drugs as a potential HDAC10 inhibitors predicted from machine learning classification	147
Table 7.2	List of compounds selected from blood-brain barrier prediction	148
Table 7.3	ADMET analysis of 14 potential anti-depressive drugs as histone deacetylase 10 inhibitor	149
Table 7.4	Structural similarity comparison of selected ant-depressive drugs with histone deacetylase 10 known inhibitor i.e., pracinostat	150
Table 7.5	Molecular docking analysis of 7 predicted ant-depressive compounds and their comparison with known HDAC10 inhibitor	150

CHAPTER I

Introduction

CHAPTER I: INTRODUCTION

1.1.OVERVIEW

Alterations in transcriptional machinery play critical function in the development and progression of central nervous system (CNS) disorders, including neurodegenerative diseases (NDDs). NDDs are characterized by loss of motor neurons leading to neuronal death that causes Alzheimer's Disease (AD), Parkinson's Disease (PD), Huntington's Disease (HD) and Amyotrophic Lateral Sclerosis (ALS) [1,2]. Although different experimental models have been developed to understand the molecular phenomenon of biomarkers and pathophysiology of disease progression, research has yet to provide a therapeutic approach [3]. Epigenetic modifications such as DNA methylation, histone post-translational modifications (PTMs) and RNA interference result in altered transcriptional activity and gene expression patterns [4]. Mounting evidence suggests a plausible connection for targeting histone PTMs with their specific inhibitor for treating neurologic deficits, including synaptogenesis, neurogenesis, neural plasticity and cognition [5–7]. Histone acetylation and deacetylation are covalent but reversible modifications that alter transcriptional activity via modulation of histone and non-histone substrate acetylation status [8,9]. Recently, the reversal of histone acetylation through inhibition of histone deacetylase (HDAC) activity at specific lysine-residue through HDAC inhibitors, naturally-occurring biomolecules, micro-RNAs (miRNAs), and multi-target drug ligands has emerged as a potential therapeutic agent to treat NDDs.

1.2.MOTIVATION OF RESEARCH

- Lysine acetylation and deacetylation of substrates are involved in transcriptional regulation.
- Inhibition of HDAC enzymes or activation of histone acetyltransferase (HAT) enzymes provides promising therapeutic avenues against NDDs.

- However, traditional HDAC inhibitors have limitations, such as specificity and selectivity. Similarly, current therapeutic biomarkers failed to show effective treatment or diagnosis.
- Thus, there is a growing need to identify novel biomarkers with site-specific acetylation that will eliminate the issues with current HDAC inhibitors.
- In addition, multi-target drug ligand targeting HDACs will provide a cost-effective and less toxic therapeutic approach in NDDs therapeutics.

1.3.AIM AND OBJECTIVES

1.3.1. AIM:

- Molecular signaling effects of HDAC inhibitors and key lysine residues in neurodegenerative diseases.

1.3.2. OBJECTIVES:

- To identify novel common biomarkers in AD and PD based on a multi-omics approach.
- To dissect the HDAC mechanism and critical lysine residues associated with novel biomarkers.
- To identify potential miRNA – biomarkers regulatory networks in the pathogenesis of neurodegenerative diseases.
- To explore novel HDAC inhibitors using a machine learning approach.

1.4.SUMMARY OF THE THESIS

The thesis is structured into eight different chapters. Chapter 1 briefly discuss the overview of the topic, motivation or rationale of the current study, aims and objectives of the research work, and overview of the current study. Chapter 2 introduces the etiology of the acetylation mechanism and HDAC enzymes and associated signaling pathways and molecules known for the onset and progression of NDDs, especially AD and PD. Additionally, chapter 2 reviews the interplay of HDAC in neurologic function and highlights the complex nature of HDAC in neurogenesis, neural plasticity, and synaptic function. Chapter 2 also reflects the role of HDAC

in regulating biologic and cellular phenomena, such as inflammatory response, oxidative stress, and autophagic degradation. Lately, chapter 2 describes the role of HDAC as a potential therapeutic target and potential implementation of HDAC inhibitors, such as natural compounds, multi-target ligands, miRNAs, and chemically synthesized compounds in the progression and pathogenesis of NDDs, namely AD and PD. Chapter 3 is dedicated to the methodology adopted, experimental procedures performed and tools and techniques used to realize the above objectives. In chapter 4, we aim to investigate the potential conventional biomarkers and regulatory transcription factors (TFs) involved in the pathogenesis of AD and PD, simultaneously with the help of microarray datasets and the network-biology approach. The identified proteomics and transcriptomics signatures were further analyzed to investigate the potential lysine residue for acetylation and deacetylation activity, along with the determination of the type of HDAC enzyme involved in the disease progression. Lastly, the study investigates conserved amino acid residues involved in the lysine-acetylation/deacetylation process along with the structural selectivity of molecular signatures, which could be crucial for protein acetylation or deacetylation activity. Chapter 5 of the thesis deals with identifying potential lysine residues of non-histone substrates involved in the crosstalk between acetylation, ubiquitination, SUMOylation, and HDAC interactors that regulate the pathogenesis of AD and PD. Herein, we integrated AD and PD-related genes with HDAC interactors and identified the HUB genes through protein-protein interaction (PPI) network and clustering analysis. Further, we examined the molecular functions and biological pathways in which shared genes (AD, PD, and HDAC) were involved. Lastly, PTM data were integrated through dbPTM and PLMD databases on 32 proteins, which are the regulatory sequences. Afterward, the proteins with high frequency for acetylation, ubiquitination, and SUMOylation were extracted among the 32 selected proteins. Finally, structural features and crosstalk sites were identified, along with the impact of lysine mutation on disease

susceptibility and protein stability. Lastly, our study investigates the potential implementation of the loss of crucial lysine residues on ubiquitination and SUMOylation function. Thus, till date, this is the first study that deals with the crosstalk of acetylation with ubiquitination and SUMOylation simultaneously among HDAC interactors. Chapter 6 of the thesis is dedicated to identifying potential miRNAs and long non-coding RNAs that will regulate the acetylation status of neurotoxic proteins involved in the pathology of metal toxicity-induced AD. Here, we aim to identify the mechanism of CREBBP acetyltransferase in the pathogenesis of metal toxicity-induced AD. Further, we aim to determine the potential miRNA regulates the acetylation level of non-histone substrates through the regulation of CREBBP. Lastly, we investigate the implication of long non-coding RNAs that serves as a sponge to a particular micro-RNA.

In chapter 7 of the thesis, we recognize the potential inhibitor of class IIb HDAC inhibitor that may be involved in the reversal of AD pathology. Herein, we employed machine learning algorithms and IC_{50} value-based compound screening to identify potential HDAC inhibitors. Lately, we have applied ADMET analysis and blood-brain barrier (BBB) prediction to assess the pharmacokinetic and pharmacodynamic properties of the selected compounds. Lastly, molecular docking analysis of the shortlisted compounds was performed to select the best possible HDAC inhibitor. Finally, the results obtained through various experimental and virtual screening procedures have been discussed in Chapter 6. Further, chapter 6 also deals with the conclusion and future perspectives of the current study.

CHAPTER II

Review of Literature

CHAPTER II: REVIEW OF LITERATURE

2. INTRODUCTION

Transcriptional dysregulation plays an essential character in the progression and development of numerous brain disorders such as AD, PD, ALS, and HD [10–12]. Although various animals and diseased cellular models have been designed to study the selective biomarkers, molecular mechanism and pathophysiology of neurological diseases but clinical implications have failed to provide a promising approach to correct cognitive impairment [13].

HAT is an essential enzyme in the acetylation process. In contrast, HDAC carries out the deacetylation of histone proteins on their protruding N-terminal lysine residue of histone and non-histone substrates, which is involved in the regulation of diverse cellular and molecular functions [14]. They alter the transcriptional regulation, gene expression patterns, metabolic processes, and energy homeostasis in a specific cell [15,16]. HAT carries the acetyl group to the lysine residue from acetyl coenzyme A, decreasing the overall positive charge on histone and thus, inhibiting DNA-histone interaction and promoting euchromatin [17]. This phenomenon is associated with enhanced gene transcription, whereas, histone deacetylation promotes compact chromatin organization that leads to the downregulation of transcription process [18]. HDAC inhibitors are considered a promising therapeutic in reversing memory dysfunction and cognitive defects that eliminate these diverse molecular and cellular functions of HDAC enzymes in the brain [19,20]. Evidence suggests that HDAC has been characterized as a therapeutic marker for various human disorders such as cancer, depression, diabetes, and CNS diseases [21–25] **[Figure 2.1]**.

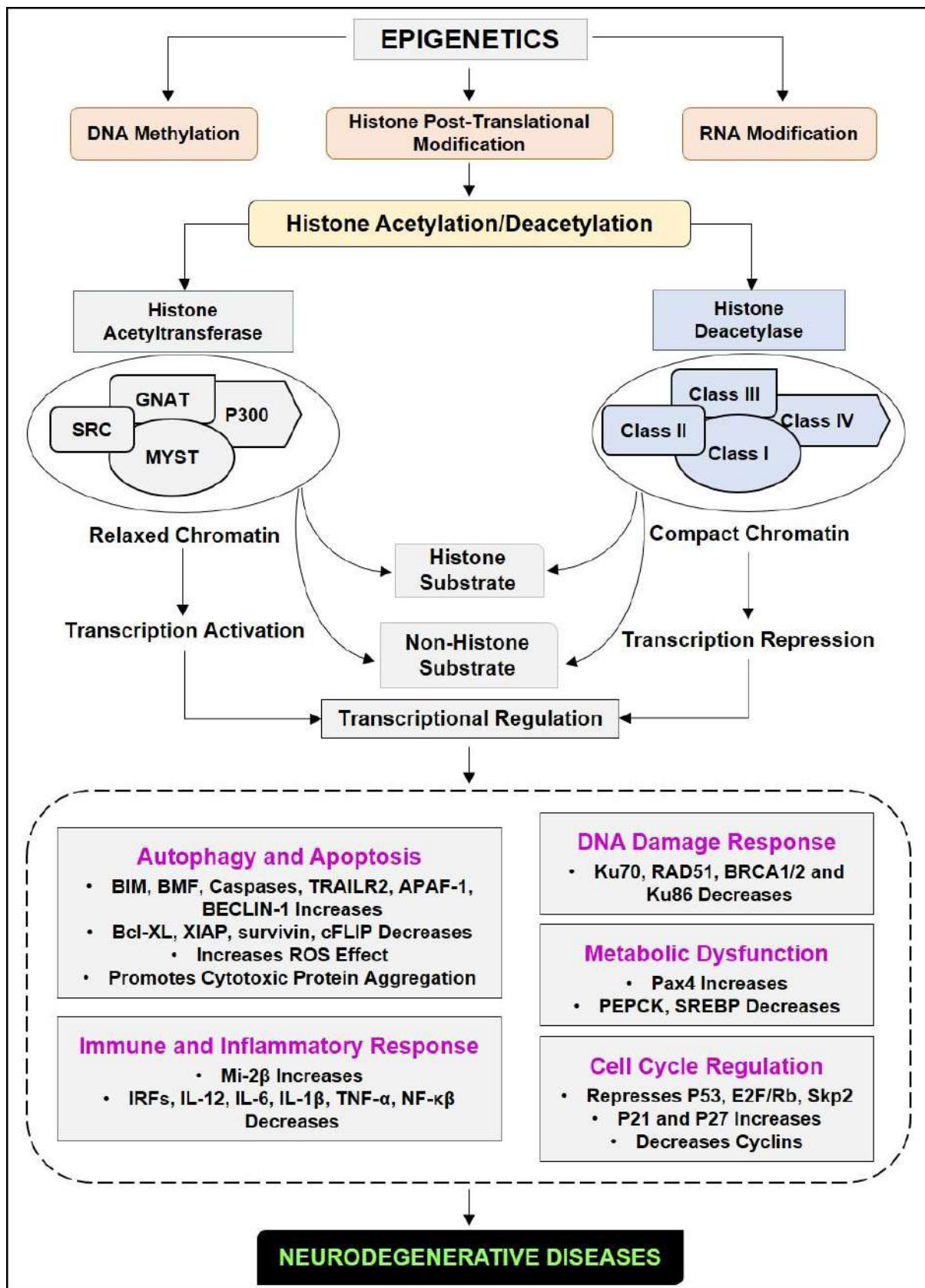


Figure 2.1: Epigenetic modifications in neurodegenerative diseases: Functional effect of epigenetics-based chromatin remodeling/histone post-translational modification in neurodegeneration via histone acetylation/deacetylation carried out by two classes of enzymes are histone acetyltransferase and histone deacetylases which modulate transcriptional status of histone and non-histone substrates.

For the past two decades, researchers have focused on the impact of these covalent histone modifications on brain diseases. Apart from these modifications, some TFs also bring remodeling of chromatin in neurodegeneration. Two major gene silencing complexes, REST and polycomb proteins, were viewed as the chromatin remodelers in the brain through histone acetylation and methylation effects on synaptic vesicles protein, channels, and adhesion proteins [26,27]. These chromatin-associated modifications were highly regulated in neurological disorders, which alter transcriptional regulation along with gene expression [28]. Epigenetic modifications are known to participate in the pathogenesis of NDDs. For this reason, researchers have hypothesized that small molecule inhibitors have the capability to regulate these altered covalent epigenetic modifications [29]. The process of acetylation and deacetylation respectively targets both histone and non-histone substrates that carried out transcriptional regulation [30]. Histone deacetylation through HDAC enzymes compacts chromatin structure and favors transcription repression. Further, HDACs negatively regulate biological processes, including apoptosis and autophagy, DNA damage response, immune and inflammatory response, metabolic dysfunction, and cell cycle regulation [31].

2.1. NEURODEGENERATIVE DISEASES

2.1.1. ALZHEIMER'S DISEASE

AD is one of the most prominent types of dementia worldwide, which can be characterized by the deposition and accumulation of neurotoxic protein, namely neurofibrillary tangles and senile plaques in the medial temporal lobe and neocortical structures [32]. Studies have demonstrated that the accumulation of misfolded β -amyloid ($A\beta$) and tau hyperphosphorylation are the significant reasons for the deposition of neurofibrillary tangles and plaques [33,34]. Currently, there are around 52 million AD patients worldwide, and studies have predicted that this number would be doubled in every 5 years and will increase to reach 150 million by 2050. Until now, no effective treatment is available for AD, which will impact

the global economy [35,36]. A β is generated through proteolytic processing of A β precursor protein through the combined action of α -secretase, β -secretase, and γ -secretase [37]. Amyloid precursor protein (APP) is cleaved via two pathways, namely the amyloidogenic pathway and the non-amyloidogenic pathway. In the amyloidogenic pathway, APP is firstly cleaved by β -secretase to generate C-terminal fragments β (C99) and N-terminal soluble APP β , which is further cleaved by γ -secretase to generate extracellular A β and APP intracellular domain. On the other hand, in the non-amyloidogenic pathway, APP is cleaved with the action of α -secretase to produce α -C terminal fragment (C83), and the N-terminal fragment soluble APP α , which is on proteolytic action of γ -secretase generate extracellular P3 peptide and the APP intracellular domain [37–39] [Figure 2.2].

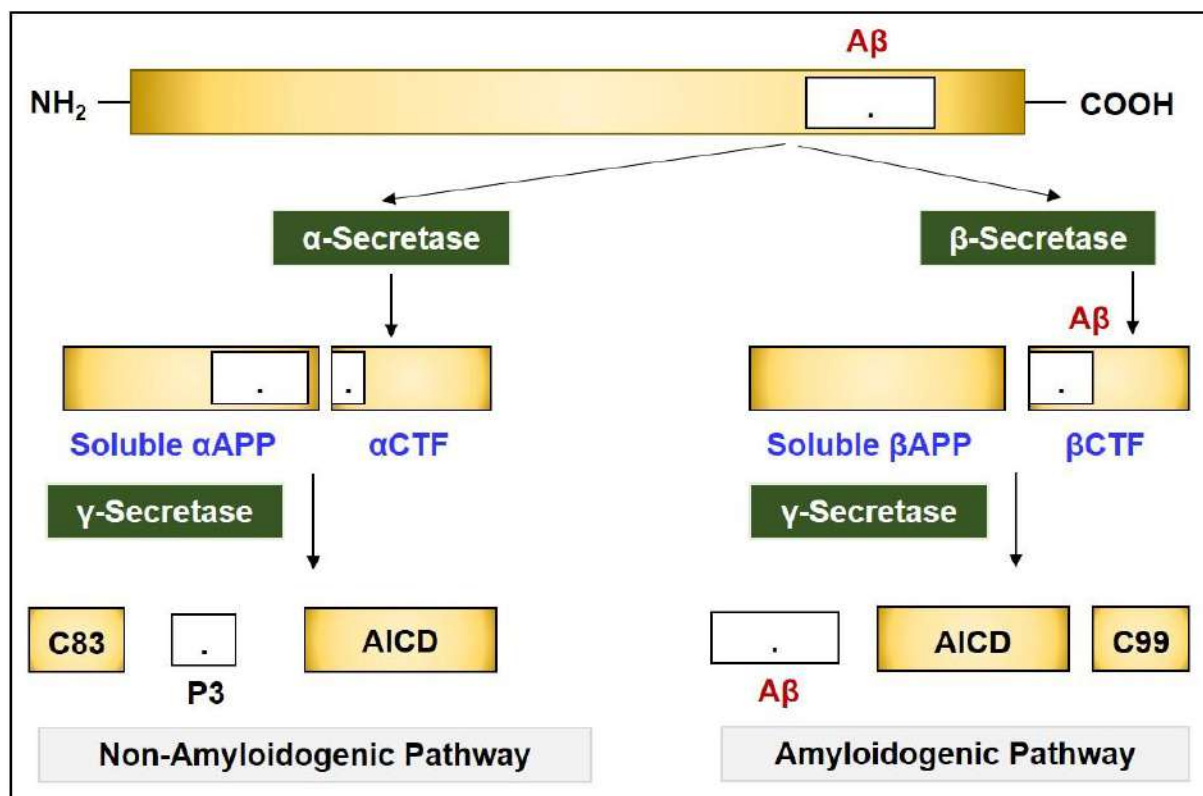


Figure 2.2: APP processing cascade in Alzheimer’s disease: The amyloid precursor protein (APP) can be processed by two pathways: the non-amyloidogenic α -secretase pathway and the amyloidogenic β -secretase pathway. In the non-amyloidogenic pathway, α -secretase cleaves in the middle of the β -amyloid (A β) region to release the soluble APP-fragment sAPP- α . The APP C-terminal fragment 83 (APP-CTF83, α CTF) is then cleaved by γ -secretase to release the APP intracellular domain (AICD) and P3 fragment. In the amyloidogenic pathway, β -secretase cleaves APP to produce the soluble fragment sAPP- β . APP-CTF99 (β CTF) is then cleaved by γ -secretase to produce A β 40, A β 42, and AICD.

Recent studies have identified various contributing factors that elevate the progression of AD, namely DNA damage response, aging, genetic factors, protein misfolding, protein degradation pathways, membrane damage, and mitochondrial dysfunction [40]. For example, mutations in the *APP*, *Presenilin-1*, and *Presenilin-2* genes increase A β production and accumulation, whereas, defects in DNA damage repair result from a mutation in breast cancer type 1 (BRAC1) and other DNA repair genes facilitate the A β accumulation in the cerebral cortex [41]. Likewise, impaired energy metabolism implicates mitochondrial dysfunction in AD through reduced glucose utilization in the hippocampus and cortex [42]. Additionally, Adler et al., 2018 demonstrated the linkage between aging and AD through hippocampal subfield morphometry and found similar histology of neurons in AD pathogenesis and aging [43]. Likewise, Liyanage et al., 2019 highlighted the importance of misfolded proteins as a potential therapeutic target in the pathogenesis and progress of AD. It concluded that misfolded proteins increase neurotoxicity in the hippocampus and cerebral cortex, leading to neuronal cell death [44]. Protein degradation pathways, namely ubiquitin-proteasome system (UPS) and autophagy-lysosomal pathway (ALP), play a critical role in the pathogenesis of AD. For instance, ubiquitin-B mutant protein, a mutant ubiquitin, has been shown to inhibit ubiquitin-dependent proteolysis in neuronal cells, whereas, Presenilin-1 deficiency or mutation causes the mammalian target of rapamycin complex 1 activation that inhibits transcription factor EB-mediated autophagy and lysosomal biogenesis [45,46]. In addition, various PTMs, such as acetylation, phosphorylation, SUMOylation, and others, are involved in regulating UPS and ALP to maintain the protein homeostasis network to achieve protein balance [47].

Despite having a worldwide problem, only two classes of drugs, namely cholinesterase inhibitors and N-methyl d-aspartate antagonists, have been approved to treat AD. Acetylcholinesterase inhibitors, which are classified as reversible, irreversible, and pseudo-reversible, act by blocking cholinesterase enzymes from breaking down acetylcholinesterase,

which results in increasing acetylcholinesterase levels in the synaptic cleft [48,49]. On the other hand, overactivation of N-methyl d-aspartate receptors leads to increasing levels of influx calcium ions, which promotes cell death and synaptic dysfunction. N-methyl d-aspartate receptor antagonist prevents overactivation of N-methyl d-aspartate receptor glutamate receptor and hence, calcium ions influx, and restores its normal activity [50].

2.1.2. PARKINSON'S DISEASE

PD is the second most progressive NDD characterized by the loss of neuronal cells in the substantia nigra *pars compacta* [51]. There are two forms of PD: familial and sporadic [52].

The familial form is caused by genetic aberrations, among others, in the gene for α -synuclein [53,54]. The cause for sporadic PD is unknown, but some progress has been made in searching for potential causes, implicating both genetic and environmental factors [55]. According to

Braak's hypothesis, sporadic PD is caused by a pathogen that enters the body through the nasal cavity and subsequently is swallowed and reaches the gut, initiating Lewy pathology in the nose and the digestive tract [56]. Early PD symptoms include bradykinesia, tremor, rigidity, and postural disability caused by the accumulation of toxic α -synuclein in the basal ganglia.

The incidence and prevalence of PD increase with increasing age, which is known to present in almost 1% of the people over the age of 60. Further, the genetic forms of PD include only 5-10% of all cases [57]. Genetic factors, such as genetic mutations in α -synuclein, ubiquitin C-terminal hydrolase like 1, parkin, Leucine-rich repeat kinase 2 (LRRK2), PINK 1 and DJ-1 genes were responsible for the onset of PD [58,59]. Duplication or triplication of the SNCA gene in affected members leads to PD symptoms developing at a later age in the fourth or fifth decades, raising the possibility that overexpression of SNCA may be a factor in sporadic disease [60,61].

Additionally, mutations in the LRRK2 gene are the most common feature of familial PD, whereas, a single mutation in DJ-1 with an autosomal recessive inheritance pattern is known to cause PD [62,63].

Apart from genetic factors, environmental factors play an essential role in the pathophysiology of PD [64]. For instance, exposure to pesticides, heavy metals, and air pollution increase the concentration of

reactive oxygen species (ROS) inside the brain, which leads to oxidative stress, and, ultimately, dopaminergic neuronal cell death [65]. Not limited to this, PD is also caused by the incidence of head injury, where mild to moderate head injury was associated with a higher risk of the onset of PD [66]. The characteristics features of PD are neuronal cell death and aggregation of toxic protein, termed “Lewy Bodies” [67]. Pathogenic mutations directly influence abnormal protein aggregates that damage the ability of cellular machinery to detect and degrade misfolded aggregates [68]. The accumulated misfolded protein aggregates enhance the generation of ROS inside the brain that directly induces oxidative stress, which leads to mitochondrial dysfunction and impaired dopamine metabolism [69] [Figure 2.3]. Further, studies have demonstrated that endotoxicity derived from increasing dopamine levels, dopamine oxidation, and dopamine reactive catabolites are recognized as one of the major causes of oxidative stress in PD. Further, several PTMs of neurotoxic proteins have been involved in the pathogenesis of PD through increasing misfolded protein aggregation [70,71]. For instance, phosphorylation of α -synuclein, PARKIN, and Drp-1 causes the formation of inclusion bodies to increase E3 ligase activity and mitochondrial localization, respectively. Likewise, SUMOylation of α -synuclein, PARKIN, and Drp-1 causes enhanced aggregation propensity, self-ubiquitination, and mitochondrial localization, respectively [72].

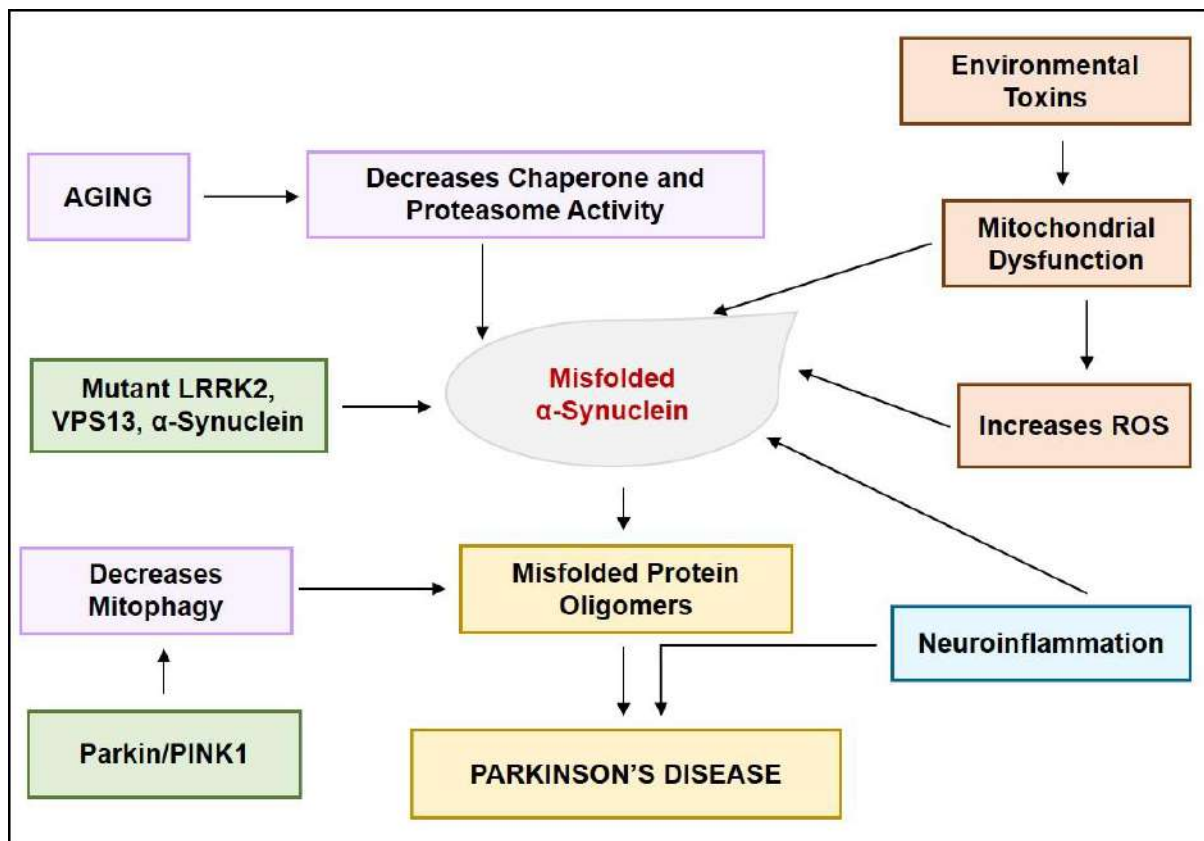


Figure 2.3: α -synuclein in the pathophysiology of Parkinson's disease: The crucial neurotoxic protein in the pathogenesis of Parkinson's disease is α -synuclein. Environmental toxins increase the concentration of reactive oxygen species that causes mitochondrial dysfunction and ultimately leads to the generation of misfolded protein aggregates. Neuroinflammation and ubiquitin E3 ligase PARKIN deficiency also lead to neuronal cell death through misfolded protein aggregation.

2.2. POST-TRANSLATIONAL MODIFICATIONS IN NEURODEGENERATION

PTMs and protein-quality control systems, for instance, a molecular chaperone, UPS, and ALP are crucial factors responsible for the accumulation of misfolded proteins [73]. Aberrant PTMs in the cellular milieu modulates dysregulated conformation, enzymatic activity, protein turnover rate, and toxic aggregates generation, which causes different proteinopathies [74]. PTMs are considered as covalent or enzymatic modifications of protein occurring after protein synthesis. PTMs generally occur in the amino acid side chain or at the protein's C-terminal or N-terminal, depending upon the type of modification. PTMs are classified into different groups such as the addition of functional groups/chemical groups (acetylation, methylation, formylation, phosphorylation, amidation, and others), the addition of polypeptide chain (ubiquitination, SUMOylation, neddylation), the addition of complex molecules

(palmitoylation, oxidation, glycation, pegylation, carbamylation, and others), and amino acids modifications (racemization, citrullination, isoaspartate, proteolytic cleavage) [75]. Different studies demonstrated the implementation of different aberrant PTMs in the pathogenesis of proteinopathies disorders such as cancer, heart disease, NDDs, diabetes, and metabolic syndromes [76]. Common NDDs such as AD, PD, HD and Spinocerebellar ataxias are best described as progressive and slow neuronal death due to misfolded and pathogenic protein aggregates, whereas, another common NDD, ALS, also characterizes protein aggregation but is a rather very fast progressing disease with a median survival time ranging from 20 to 48 months. The neuronal cell death causes brain cellular machinery malfunction, which results in memory impairment, synaptic dysfunction, learning disability, and cognitive defects [77]. These NDDs can be further classified into amyloidosis, tauopathies, synucleinopathies, and transactivation response DNA binding protein-43 proteinopathies (TDP-43), depending upon the pathogenic protein accumulated.

Many studies have been conducted to explain the exact mechanism of protein aggregation and its pathogenicity in NDDs, which concluded that dysregulated PTMs are crucial for neuronal proteinopathies [78–80]. For example, in AD and PD, a decrease in H3 and H4 acetylation causes transcriptional deactivation, which leads to a decrease in neurotrophic factor expression. A decrease in H3 and H4 acetylation also causes an increase in A β plaques, neurofibrils tangles, and deposition of Lewy bodies [81]. Apart from acetylation, another modification is methylation. Studies show that hypermethylation through the addition of methyl groups causes transcription deactivation, leading to the accumulation of toxic proteins and, ultimately, neuronal cell death [82]. Similarly, hyperphosphorylation of tau protein, α -synuclein, and mutant htt causes their misfolding and subsequent aggregation [83]. Ubiquitination, SUMOylation, and neddylation are crucial for misfolded protein degradation through a polypeptide chain made up of small chemical groups. Aberrant ubiquitination, SUMOylation,

and neddylation hamper the lysosomal degradation pathway and ubiquitin-proteasome degradation pathway, which causes the accumulation of toxic proteins [84–86].

Further, studies demonstrated the role of the addition of complex molecules to the protein's side chain in the progression and pathogenesis of NDDs. For instance, glycation causes the formation of β -sheets in A β , α -synuclein, superoxide dismutase 1 (SOD1), TDP-43 and prion protein structure, which causes the generation of fibrillar structures and misfolded proteins [87]. Similarly, palmitoylation and carbamylation disrupt synaptic plasticity and neural differentiation, which causes the accumulation of toxic proteins that lead to memory impairment and cognitive defects [88,89]. Moreover, aberrant S-nitrosylation alters mitochondrial function, synaptogenesis, misfolded protein fragmentation, apoptosis, and autophagy, which leads to the accumulation of excessive nitric oxide and ultimately causes neuronal cell death [90]. Similarly, myristoylation is the addition of myristate to the N-terminal of newly synthesized glycine residue followed by caspase cleavage. However, myristoylation has been considered as both neuroprotective as well as neurotoxic. Studies demonstrated that myr-ctPAK2 prevents neuronal apoptosis, whereas, myr- huntingtin provides an additional link between caspases and positive autophagy [91]. Likewise, succinylation has been involved in AD progression with site-specific succinylation of A β peptides and tau tangles, which promotes amyloidosis and tauopathy, respectively [92]. Further, mounting evidence demonstrated that irregular PTMs hamper endoplasmic reticulum functioning, which leads to the progression of NDDs. These data suggest that PTM enzymes have beneficial therapeutic activity in neuronal dysfunction. Thus, various drugs have been tested for NDDs but with low success, highlighting the gaps in comprehending their pathogenic mechanism. To date, no full-proof medicine is available that can block the progression of NDDs by inhibiting or modulating the activity of PTM enzymes [93,94].

2.2.1. ROLE IN MISFOLDED PROTEIN AGGREGATION

During the translation process, a newly synthesized protein falls off as a chain of amino acids in the cytoplasm, forming linear polypeptides that interact with each other to form an adequately folded native protein structure. This native 3D conformation of a protein symbolizes a biologically active protein [95]. However, a protein's failure to fold into its native conformation results in the inception of inactive misfolded proteins that eventually give rise to abnormal protein clusters [96]. In their non-native state, misfolded proteins expose their inner hydrophobic core to the outer hydrophilic environment, which accumulates and leads to the formation of toxic aggregates [97]. It has been established that intracellular and extracellular pathogenic protein aggregates are the main culprit in many NDDs that disrupt neuronal homeostasis [98]. These pathogenic proteins can also self-replicate and can be transmitted from one cell to another, thus promoting their neuropathogenicity [94]. In healthy conditions, cells have a highly orchestrated machinery to maintain the protein quality control system, consisting of chaperones, a UPS, and an ALP. Chaperones are protein superfamilies defined as the first line of defense against protein aggregation, which helps a misfolded protein reach its native conformation, thus preventing aggregation [99]. Various chaperones, such as heat shock protein (HSP90), HSP70, HSP60, HSP40, and small HSPs, play a crucial role in maintaining protein homeostasis. However, when the chaperone system is overburdened and/or mutated, they cannot perform their normal functions, contributing to its dysfunction and protein aggregation. Beyond a threshold, when chaperones cannot maintain protein homeostasis, cells are overburdened with non-functional proteins, where the UPS comes into action for the breakdown of those abnormal proteins. The ubiquitin E3 ligase has played a decisive role in the UPS, where the non-functional protein is tagged with another ubiquitin. The process of tagging a protein with multiple ubiquitin moieties serves as a signal for its breakdown by the proteasome [100]. In NDDs, ubiquitinated proteins have been observed in many protein

aggregates, suggesting a dysfunction in the UPS machinery. An E3 ligase, HRD1, can reduce the A β aggregation by ubiquitination of APP protein, whereas, the knockdown of CHIP, an E3 ligase, showed PolyQ aggregation in ALS [101]. Also, the autophagy-lysosome system is used to degrade bulk protein aggregates, which cannot be degraded by the UPS system. In the autophagy system, abnormal protein aggregates are degraded by enzymes present in the lysosome's acidic milieu. Macroautophagy and chaperone-mediated autophagy are the two main types of autophagic processes involved in protein degradation. In macroautophagy, aberrant proteins are engulfed by autophagosomes; this double-membraned autophagosome then fuses with the lysosomes to form autolysosomes, where abnormal proteins are deposited and then degraded by the enzymes present in it [102,103]. Chaperone-mediated autophagy targets specific abnormal proteins with the KFERQ motif, which are recognized by the HSC70 chaperone, and forms a complex that interacts with lysosome membrane receptors. Abnormal proteins are then deposited in lysosomes' lumen for degradation [104].

However, many PTMs can also cause protein aggregation in NDDs, depending upon the amino acid residues modified by them. For example, phosphorylation of A β at S8 residue promotes A β aggregation and its toxicity in AD [105]. Similarly, SUMOylation refers to a covalent attachment of small Ubiquitin-like modifiers (SUMO) to the amino acid residues, where SUMOylation at K75 residue of SOD1 has been reported to stimulate the aggregation of fALS-linked SOD1 mutants in ALS [106]. Some important PTMs such as acetylation, nitrosylation, glycation, nitration, palmitoylation, and carbamylation promote toxic aggregation in the NDDs. Acetylation is the covalent coupling of an acetyl group on amino acid residues, and acetylation at K145 and K192 within the RRM domain of TDP-43 protein leads to pathogenic aggregation of TDP-43 proteins in ALS [107]. Glycation involves the attachment of the sugar molecules to the polypeptide chain of proteins. MGO-induced glycation has been reported to promote huntingtin aggregation and toxicity in HD models [108].

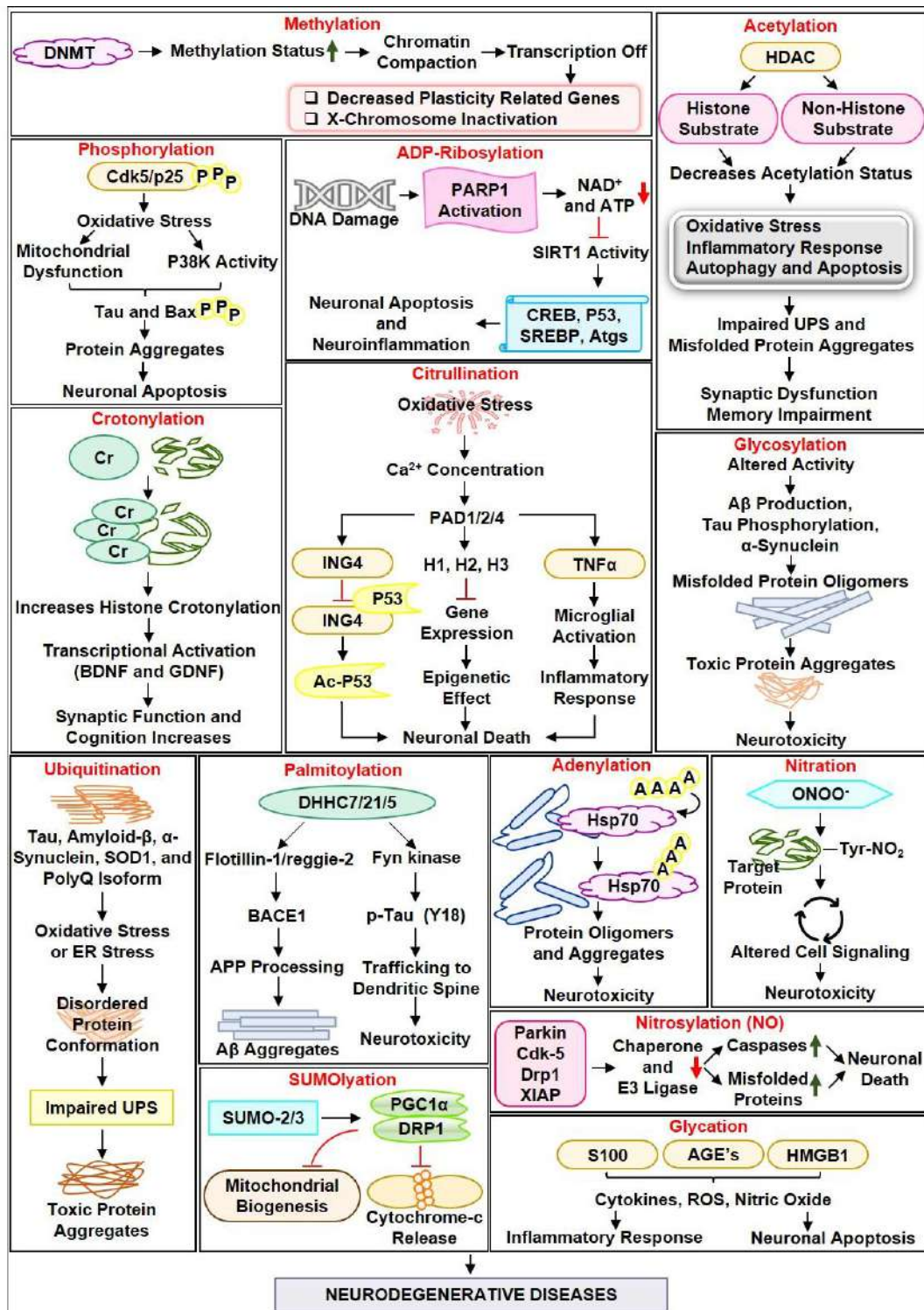


Figure 2.4: Implementation of different post-translational modifications in neurodegenerative diseases (NDDs): post-translational modifications of histone and non-histone substrates were involved in the pathogenesis and progression of deadly NDDs, such as Alzheimer's Disease (AD), Parkinson's Disease (PD), Amyotrophic Lateral Sclerosis (ALS), and Huntington's Disease (HD). More than 50 PTMs have been discovered so far in which phosphorylation, Acetylation, ubiquitination, SUMOylation, and palmitoylation were prominent were regulating different cell-signaling cascades involved in the pathogenesis of NDDs. Other PTMs such as Glycosylation, nitration, amidation, adenylation, citrullination, crotonylation, and methylation are also involved in the progression of NDDs. PTMs alter substrate protein activity, which causes an increase in stress conditions such as oxidative stress and ER stress. An increase in oxidative stress increases mitochondrial dysfunction, inflammatory response, neuronal apoptosis, autophagic cell death, and DNA damage response. This molecular phenomenon causes synaptic dysfunction, impaired neural plasticity, and memory impairment leading to neurodegeneration.

Furthermore, nitration involves the addition of the nitro group to the polypeptide chain, and research has shown that nitration at Y39 of α -synuclein facilitates its oligomer formation [109]. Palmitoylation is the covalent linkage of palmitate to cysteine residues, and palmitoylation of APP at C186 and C187 promotes A β aggregation in AD [110]. Additionally, nitrosylation covalently attaches nitric oxide moiety to cysteine residues, S-Nitrosylation of deubiquitinase enzyme UCHL1 at C90, C152, and C220 induces α -synuclein aggregation in PD [111]. Carbamylation refers to the covalent adduction of carbamoyl moiety to amino acid residues, and one study showed that carbamylation stimulates tau aggregation and induces amyloidogenesis [89]. Glutathionylation is a covalent linkage of glutathione moiety to cysteine groups, S-Glutathionylation of SOD1 at C111 increases the propensity of SOD1 towards aggregation [112].

Moreover, Truncation is a PTM that refers to the N-terminal or C-terminal termination of a protein chain, and it has been observed that truncation of α -synuclein's C-terminal stimulates aggregation of α -syn in PD [70]. Glycosylation is the covalent adduction of the carbohydrate moiety to proteins. In AD, it has been observed that tau glycosylation amplifies aberrant tau hyperphosphorylation [113]. Additionally, ADP-ribosylation is the coupling of ADP-ribose to proteins, and in ALS, it has been observed that ADP-ribosylation induces TDP-43 aggregation [114]. Further, trans-glutamination results in isopeptide bond formation between the γ -carboxamide group of glutamines in one protein and the ϵ -amino group of lysine in another protein. [Figure 2.4].

2.3. ACETYLATION IN ALZHEIMER'S AND PARKINSON'S DISEASE PATHOLOGY

Acetylation, a lysine-induced PTM, is the process of transfer of acetyl group from acetyl coenzyme A to the specific site of a polypeptide chain. Basically, acetylation changes the overall charge of the histone protein from positive to neutral and thus enhances the

transcriptional activity. Acetylation occurs on both histone and non-histone substrates, which is carried out with the help of enzymes called as lysine acetyltransferases (KAT and GNAT). Mounting evidence suggests that dysfunction in lysine acetylation is associated with the pathogenesis and progression of various NDDs, namely AD and PD. For example, in APP/PS1 mice model, decreased histone H4 acetylation levels that cause impaired memory formation, whereas, a decrease in histone H3 acetylation at lysine 9 causes an increased tau pathology [115,116]. Marzi et al., 2018 demonstrated that in entorhinal cortex samples from AD, an altered histone H3 acetylation at lysine 27 causes an increase in the progression of A β and tau-related pathology [117]. In another study, the authors of AD patients observed the hypoacetylation of AD hippocampus through GTPase-mediated mechanisms [118]. Apart from histone substrates, deregulated acetylation status of non-histone substrates is also involved in the progression of AD. For instance, acetylation of Beclin-1 through p300 inhibits autophagosome formation and maturation that leads to the impaired autophagic flux, whereas, acetylation of tau causes tau-interactome changes that result in tau degradation and leads to the recovery of synaptic pathology [119,120]. Further, Min et al., 2010 demonstrated that acetylation of tau inhibits its degradation that contributes to tauopathy [121]. Subsequently, another study concluded that acetylation of tau at lysine 274 and lysine 281 inhibits the expression of long-term potentiation at hippocampal synapses that contribute to AD pathology [122] **[Figure 2.5]**.

The altered acetylation status of both histone and non-histone substrates is involved in the pathogenesis and progression of PD **[Figure 2.5]**. For example, site-specific acetylation of H2A, H2B, H3, and H4 was found in dopaminergic neurons of PD patients when compared with matched controls [123]. Further, the administration of sirtuin 2 causes enhanced dopaminergic neuronal cell death through microglial activation [124]. Additionally, Yakhine-Diop et al., 2019 demonstrated that inhibition of HATs activity promotes neuroprotection

through enhanced mitophagy [125]. Not limited to this, acetylation of neurotoxic proteins, namely α -synuclein, promotes its oligomerization and aggregation, leading to the progression of PD [126]. For instance, N-terminal acetylation of α -synuclein induces transient helical propensity and decreased aggregation rates in the intrinsic disorder monomer [127].

Moreover, increased acetylation of peroxiredoxin ½ and NDUFV1 through HDAC6 inhibition promotes neuroprotection and rescues dopaminergic neuronal cell death [128,129]. Another study found that acetylation and phosphorylation of PGC-1 α promote nuclear translocation and protect from oxidative stress [130]. Thus, from the above-mentioned evidences, it will be concluded that site-specific acetylation of neurotoxic proteins is associated with the pathogenesis and progression of NDDs, especially AD and PD.

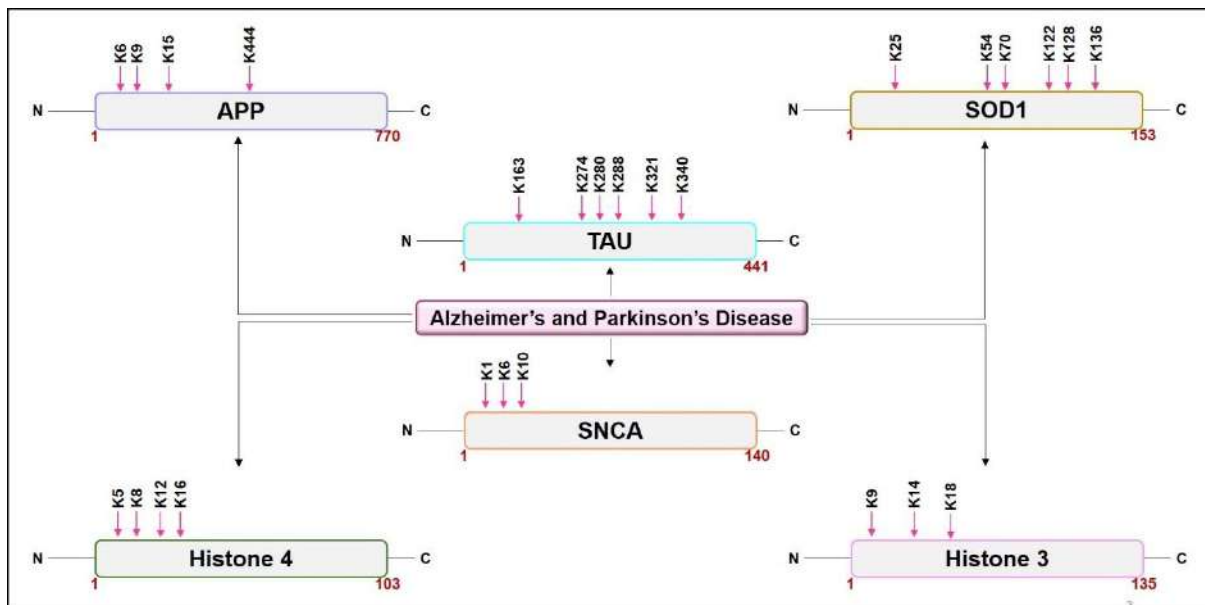


Figure 2.5: Domain architectures and position of post-translational modifications in the neurotoxic proteins involved in the pathogenesis and progression of Alzheimer's and Parkinson's disease.

2.4. CLASSIFICATION OF HISTONE DEACETYLASES ENZYMES SUPERFAMILY

There are 18 mammalian HDAC discovered, which were divided into two families (HDAC family and sirtuins regulator family), and four classes based on their sequence and structure similarities to yeast deacetylases [Figure 2.6]. Class I (HDAC1, HDAC2, HDAC3, and

HDAC8), Class IIa (HDAC4, HDAC5, HDAC7, and HDAC9), Class IIb (HDAC6 and HDAC10), Class III (Sir1, Sir2, Sir3, Sir4, Sir5, Sir6, and Sir7), and Class IV (HDAC11). Class I have sequence similarity to yeast transcription regulator reduced potassium dependency 3 (Rpd3) protein, while Class II has sequence similarity to yeast HDAC-A 1 (Hda1) protein. Rpd3 has 35%-49% homology to Hos1, Hos2, and Hos3 found in yeast, while Hda1 has 21%-28% homology to these proteins. Thus, it can be concluded that mammalian deacetylases (Class I and Class II) are somehow related to yeast hos protein. Mammalian class I, class II (IIa and IIb), and class IV belongs to the arginase/deacetylase superfamily of catalytic enzymes containing amido hydrolases, whereas, class III containing sirtuins belongs to nicotinamide adenine dinucleotide and flavin adenine dinucleotide (NAD/FAD) binding domain superfamily of enzymes containing carboxy-terminal domain, pyruvate oxidase, and decarboxylase middle domain. Class I HDAC is considered a transcription repressor because they bind to DNA as a corepressor recruited by TFs. They can be found in both cytoplasm and nucleus and are ubiquitously expressed to perform tissue-specific functions. For example, HDAC1, HDAC2, and HDAC3 regulate the deacetylation activity of MAP kinase phosphatase, and this histone modification increases intrinsic mitogen-activated protein kinase (MAPK) and alteration in innate immune signaling [131]. At the same time, class II HDAC can be translocated between the nucleus and cytoplasm associated with transcription dysregulation, as in the case of class I HDAC. The mechanism and distribution of HDAC11 (Class IV HDAC) are not well established. However, studies suggested the role of HDAC11 in regulating the expression of DNA replication factor CDT1 and interleukin 10 (IL10). Further, Finnin et al., 1999 [132] proposed that the catalytic mechanism followed by arginase dependent family required a transition metal ion which is zinc (Zn^{2+}) and shares a common structural motif sequence. Moreover, catalysis of histone and non-histone substrates by HDAC commences with intermediate chelation of water and the carbonyl group of acetylated lysine residue to the

central Zn²⁺ atom, which results in histidine (HIS¹³²) protonation followed by protonation of water due to rate-determining step that is nucleophile attack and deprotonation of HIS¹³¹. This result in the generation of hydroxide ion, which facilitates the stabilization of acyloxanion generated due to carbonyl attack of acetyl groups and thus interacts with the hydroxyl group at tyrosine (TYR²⁹⁷). The resulting complex leads to the formation of acetate ion and the production of terminal ammonium on the lysine side chain. Importantly, at the last step of this process HIS¹³¹ and not HIS¹³² is protonated, and the catalytic complex consists of a Zn²⁺ atom bound by two histidine and aspartic acid dyads (HIS¹³¹-ASP¹⁶⁶, HIS¹³²-ASP¹⁷³), one tyrosine (TYR²⁹⁷), and the proton donor molecule which is coordinated with two aspartic acids (ASP²⁵⁸ and ASP¹⁶⁸), and a histidine (HIS¹⁷⁰). The model of HDAC catalysis seems to be more analogous to classical metalloenzymes such as thermolysin and carboxypeptidase [133,134]. Later studies on catalytic activities showed that class IIa HDAC does not form a complex with histone terminal and has less catalytic activity than class IIb and class I due to the replacement of conserved tyrosine residue accountable for a catalytic mechanism with histidine in class II HDAC [135–137]. Experiments performed by Fischle and colleagues confirmed the proposed mechanism. They demonstrated that Class IIb HDAC (HDAC4 and HDAC5) do not possess catalytic activity in isolation but are found in complex with HDAC3 in association with transcriptional repressor complex containing silencing mediator for retinoid and thyroid receptors and nuclear receptor corepressor (N-CoR). Furthermore, it was discovered that class II HDACs are bound to heterochromatin protein 1 and C-terminal binding protein, which facilitates transcriptional repression and downregulated expression [138,139] [**Table 2.1**].

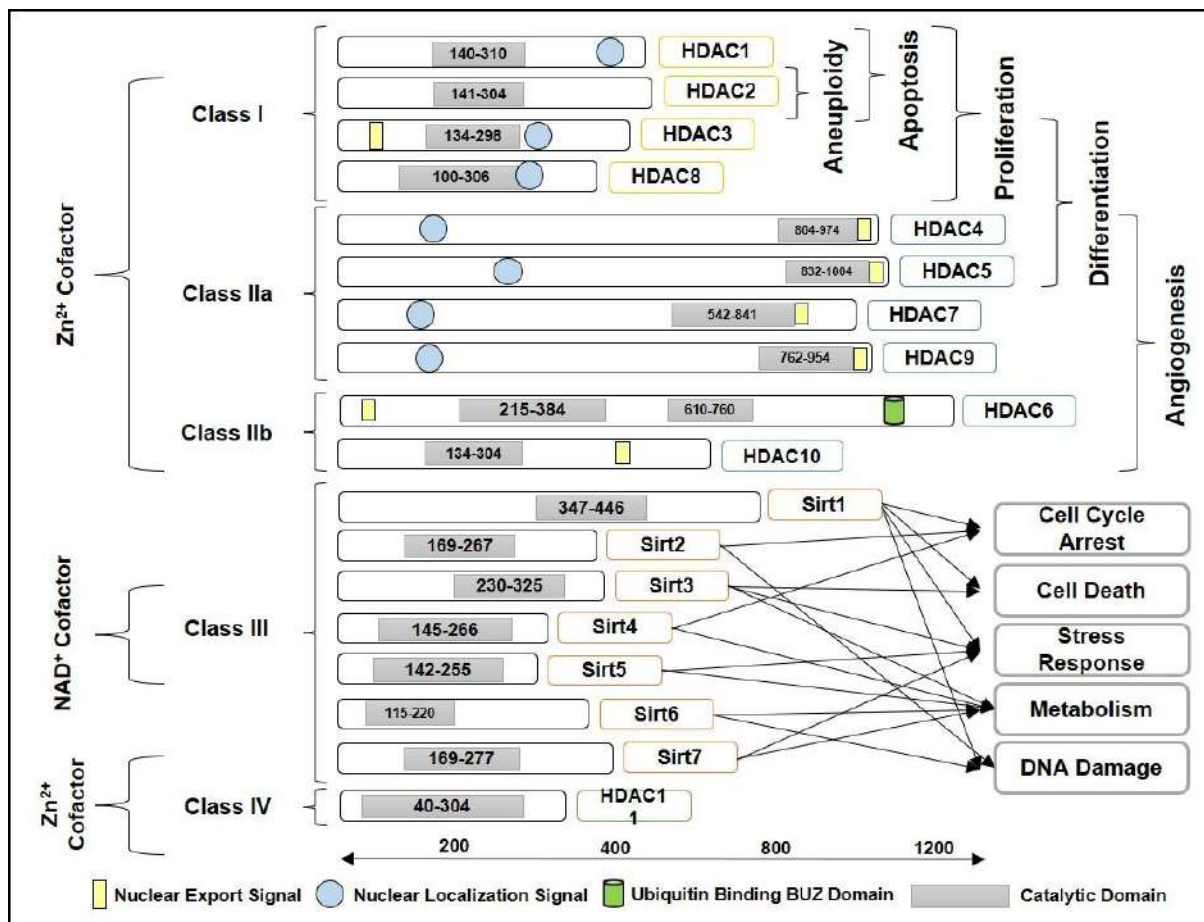


Figure 2.6: Classification of histone deacetylase enzymes and their domain structure: Metal-dependent and arginase-dependent histone deacetylase (HDAC) enzymes superfamily was divided into four subgroups that are Class I (HDAC1, HDAC2, HDAC3, and HDAC8), Class IIa (HDAC4, HDAC5, HDAC7, and HDAC9), Class IIb (HDAC6 and HDAC10), Class III consisting of sirtuins (Sirt 1–7), and Class IV (HDAC11) according to their homology similarity along with the biological process regulated by them. The figure also represents the nuclear localization signal, nuclear export signal, ubiquitin-binding site, and catalytic sites.

Class III HDAC or sirtuins family have vigorous deacetylase activity and are known to regulate mitochondrial activity in numerous biological and cellular signaling pathways [140–144]. Compared with the classical HDAC, sirtuins require NAD⁺ as a cofactor for their catalytic activity. It consists of a large Rossmann fold and small zinc-binding, which form a cleft amidst where conserved catalytic residues of sirtuins reside, which then interact with the substrate after forming a tunnel between them [145]. Deacetylation catalysis performed by sirtuins is the thermodynamically stable reaction followed by the generation of 2'-AADPR, which in turn catalyzes the formation of an ester through amide resulting in the breakdown of NAD⁺ [146]. As a predominant regulator of the transcriptional machinery, HDAC's catalytic activity should be highly regulated at each and every step. There are several governing phenomena

among which PPI and HDACs PTMs are studied thoroughly, whereas alternative RNA splicing, availability of co-factors, subcellular localization, and proteolytic processing of HDACs are equally important but less studied. The formation of the complex with another protein substrate to induce their catalytic activity is a common mechanism to control HDAC activity. For example, HDAC1 and HDAC2 are found in multiprotein complexes such as paired amphipathic helix protein Sin3a, N-CoR, and REST corepressor 1 (CoREST). Sin3 and N-CoR share the same structural components and consist of HDAC1, HDAC2, retinoblastoma binding protein 7 (RbAp46), and retinoblastoma binding protein 4 (RbAp48). A study established that the association of HDAC1 and HDAC2 with the CoREST complex is necessary for catalytic activity, and the activity of HDAC1 increases in association with the Sin3 corepressor multiprotein complex.

Moreover, HDAC proteins undergo several PTMs striking their activity. Phosphorylation is essential in regulating HDAC1/2 activity, which is a reversible reaction monitored by protein phosphatase 1 (PP1) [147]. Mitotic disruption without affecting G1/S repression results in hyperphosphorylation of HDAC2. Similarly, the activity of HDAC3 also increases phosphorylation due to CK2 and DNA-dependent protein kinase catalytic subunit. Further, the hyperphosphorylation of HDAC3 with glycogen synthase kinase 3 beta (GSK3 β) protects against HDAC3-induced neurodegeneration [148]. Protein phosphatase 1b and protein phosphatase 2A perform phosphorylation of Class II HDAC and regulate their catalytic activities. Phosphorylation of HDAC6 at S22 and T30 by Aurora A kinase leads to tubulin deacetylation activation [149,150]. HDAC5 consists of 17 conserved phospho-acceptor residues, which explain the importance of phosphorylation-mediated regulation of structure and function. In HDAC5, phosphorylation by PKD and CaMKII at Ser259 and Ser498 induces nuclear export that prevents binding of 14-3-3 proteins, while phosphorylation of protein kinase A (PKA) at Ser279 induces nuclear retention [151–154]. HDAC4 and HDAC5 regulate the

activity of myocyte enhancer factor (MEF) 2 dependent transcription upon ubiquitination and SUMOylation, which has a significant role in regulating HDAC's expression [155,156].

Table 2.1: Classification of HDAC superfamily along with their substrates (histone and non-histone), catalytic active ligand binding sites, and molecular function [157–161]

Class	Name	Amino Acids	Family and Co-Factor	Subcellular Localization	Tissue Distribution	Yeast Homologous	Substrates Specificity	Catalytic Sites	Molecular Function
I	HDAC1	482	Arginase/ Histone Deacetylase Family and Zinc Dependent	Nucleus	Ubiquitous Expression with higher levels in heart and pancreas and lower level in brain and lungs	Rpd3	p53, RUNX3, AR, SMAD7, STAT3, E2F1, MyoD	HIS ¹⁴⁰ , HIS ¹⁴¹ , GLY ¹⁴⁹ , PHE ¹⁵⁰ , ASP ¹⁷⁶ , HIS ¹⁷⁸ , ASP ²⁶⁴ , LEU ²⁷¹	Chromatin modeler, transcriptional inhibition, cell proliferation regulator, tumorigenesis
	HDAC2	488		Nucleus and Cytoplasm			STAT3, BTCL6, Glucocorticoid Receptor, YY1	HIS ¹⁴¹ , HIS ¹⁴² , GLY ¹⁵⁰ , PHE ¹⁵¹ , ASP ¹⁷⁷ , HIS ¹⁷⁹ , ASP ²⁶⁵ , LEU ²⁷² , GLY ³⁰² , TYR ³⁰⁴	Chromatin remodeling, transcriptional repression, modulation of plasticity, memory, and senescence
	HDAC3	428		Nucleus, Cytosol, and Cytoplasm			STAT3, GATA1, RelA, MEF2D, YY1, SHP	HIS ¹³⁴ , HIS ¹³⁵ , GLY ¹⁴³ , PHE ¹⁴⁴ , ASP ¹⁷⁰ , HIS ¹⁷² , ASP ²⁵⁹ , LEU ²⁶⁶ , GLY ²⁹⁶ , TYR ²⁹⁸	Transcriptional control, cell cycle progression, cell cycle-dependent DNA damage and repair, apoptosis
	HDAC8	377		Nucleus and Cytoplasm			Expressed in most tissues with higher levels in brain, heart, kidney, and pancreas	ND	TYR ¹⁰⁰ , ASP ¹⁰¹ , TRP ¹⁴¹ , HIS ¹⁴² , HIS ¹⁴³ , GLY ¹⁵¹ , PHE ¹⁵² , ASP ¹⁷⁸ , HIS ¹⁸⁰ , PHE ²⁰⁸ , ASP ²⁶⁷ , MET ²⁷⁴ , GLY ³⁰⁴ , TYR ³⁰⁶
IIa	HDAC4	1084		Nucleus and Cytoplasm	Ubiquitous expressed with higher expression in Brain, heart, and skeletal muscles	Hda1	GCMa, GATA1, HP-1, importin 1 (CRM1), nucleoporin 155 (Nup155)	HIS ⁸⁰² , HIS ⁸⁰³ , GLY ⁸¹¹ , PHE ⁸¹² , ASP ⁸⁴⁰ , HIS ⁸⁴² , ASP ⁹³⁴ , GLY ⁹⁷⁴	Cellular differentiation and development, involvement in block of muscle differentiation, neuron survival
	HDAC5	1122		Nucleus and Cytoplasm	Brain, heart, and skeletal muscles		RUNX3, SMAD7, HP-1, GCMa	HIS ⁸³² , HIS ⁸³³ , GLY ⁸⁴¹ , PHE ⁸⁴² , ASP ⁸⁷⁰ , HIS ⁸⁷² , ASP ⁹⁶⁴ , GLY ¹⁰⁰⁴	Cellular differentiation and development, involvement in block of muscle differentiation, regulation of nuclear genes that promote cardiac hypertrophy

	HDAC7	952		Nucleus and Cytoplasm	Platelet, lung, heart, skeletal muscles, and pancreas		FLAG1, FLAG2	PHE ⁵⁴² , ASP ⁶²⁶ , HIS ⁶⁶⁹ , HIS ⁶⁷⁰ , GLY ⁶⁷⁸ , PHE ⁶⁷⁹ , ASP ⁷⁰⁷ , HIS ⁷⁰⁹ , PHE ⁷³⁸ , ASP ⁸⁰¹ , PRO ⁸⁰⁹ , LEU ⁸¹⁰	Cellular differentiation and development, involvement in block of muscle differentiation
	HDAC9	1011		Nucleus	Brain and skeletal muscles		ND	HIS ⁷⁸² , HIS ⁷⁸³ , GLY ⁷⁹¹ , PHE ⁷⁹² , ASP ⁸²⁰ , HIS ⁸²² , ASP ⁹¹⁴ , GLY ⁹⁵⁴	Cellular differentiation and development, regulation of nuclear genes that promote cardiac hypertrophy
I Ib	HDAC6	1215		Nucleus and Cytoplasm	Brain, heart, liver, kidney, and pancreas		HSP70, HSP90, α-tubulin, SHP, SMAD7	HIS ²¹⁵ , HIS ²¹⁶ , GLY ²²⁴ , TYR ²²⁵ , ASP ²⁵³ , HIS ²⁵⁵ , ASP ³⁴⁶ , GLY ³⁸⁴	Microtubule stability and function, ubiquitin proteasome system, autophagy
	HDAC 10	669		Nucleus and Cytoplasm	Spleen, liver, and kidney		HSP90	HIS ¹³⁴ , HIS ¹³⁵ , GLY ¹⁴³ , PHE ¹⁴⁴ , ASP ¹⁷² , HIS ¹⁷⁴ , ASP ²⁶⁵ , GLY ³⁰³	Transcriptional repression, HSP-mediated regulation of VEGFR
III	SIRT1	747	Sirtuin Regulator Containing Carboxyl Terminal Domain Family and NAD Dependent	Nucleus, Cytoplasm	Brain, heart, and kidney	Sir2, Hst1, Hst2, Hst3, and Hst4	H3K9, H3K14, H3K56, H4K16, H1K26, p53, FOXO1, FOXO3, FOXO4, PARP-1, APE1, DNA-PK, RARβ, PGC1α, PPARγ, NF-κB, IGF1, Ku70	ILE ³⁴⁷ , HIS ³⁶³ , VAL ⁴¹² , PHE ⁴¹⁴ , GLY ⁴¹⁵ , GLU ⁴¹⁶ , ASN ⁴¹⁷ , LEU ⁴¹⁸ , LYS ⁴⁴⁴ , VAL ⁴⁴⁵ , ARG ⁴⁴⁶	Modulation of the mitochondrial functions, anti-inflammatory mediator
	SIRT2	389		Cytoplasm	Brain, and skeletal muscles		H4K16, H3K56, α-tubulin	ILE ¹⁴⁰ , HIS ¹⁵⁸ , VAL ²⁰² , PHE ²⁰⁴ , GLY ²⁰⁵ , GLU ²⁰⁶ , ASN ²⁰⁷ , LEU ²⁰⁸ , GLU ²³⁴ , VAL ²³⁵ , GLN ²³⁶	Regulation of the microtubule acetylation and stability
	SIRT3	399		Nucleus, Mitochondria	Ubiquitarian		H4K16, Acetyl-coA synthetase, glutamate dehydrogenase, Ku70, isocitrate dehydrogenase	ILE ²³⁰ , HIS ²⁴⁸ , VAL ²⁹² , PHE ²⁹⁴ , GLY ²⁹⁵ , GLU ²⁹⁶ , PRO ²⁹⁷ , LEU ²⁹⁸ , GLU ³²³ , VAL ³²⁴ , GLU ³²⁵	Deacetylation of several key metabolic enzymes, acetyl coenzyme a synthetase, glutamate dehydrogenase
	SIRT4	314		Mitochondria			Glutamate dehydrogenase	VAL ¹⁴⁵ , HIS ¹⁶¹ , VAL ²³² , PHE ²³⁴ , GLY ²³⁵ , ASP ²³⁶ , THR ²³⁷ , VAL ²³⁸ , GLN ²⁶⁴ , VAL ²⁶⁵ , TYR ²⁶⁶	Regulation of insulin secretion

	SIRT5	310		Mitochondria			Cytochrome c, Carbamoyl phosphate synthetase 1, Urate oxidase	ILE ¹⁴² , HIS ¹⁵⁸ , VAL ²²¹ , PHE ²²³ , GLY ²²⁴ , GLU ²²⁵ , ASN ²²⁶ , LEU ²²⁷ , VAL ²⁵³ , VAL ²⁵⁴ , TYR ²⁵⁵ ,	Deacetylation of cytochrome c, apoptosis initiation, promotion of neuronal death
	SIRT6	355		Nucleus			H3K9, H3K56, PARP-1, DNA-PK	VAL ¹¹⁵ , HIS ¹³³ , LEU ¹⁸⁶ , TRP ¹⁸⁸ , GLU ¹⁸⁹ , ASP ¹⁹⁰ , SER ¹⁹¹ , LEU ¹⁹² , GLN ²¹⁸ , ILE ²¹⁹ , ARG ²²⁰	Modulation of gene expression, apoptosis, cellular senescence
	SIRT 7	400		Nucleolus			H3K18, RNA Pol I complex, RNA Pol II complex	CYS ¹⁶⁹ , HIS ¹⁸⁷ , VAL ²³⁷ , PHE ²³⁹ , GLY ²⁴⁰ , GLU ²⁴¹ , ARG ²⁴² , GLY ²⁴³ , LYS ²⁷² , VAL ²⁷³ , TYR ²⁷⁷	Activation Of RNA polymerase I transcription
IV	HDAC 11	347	Arginase/ Histone Deacetylase Family and Zinc Dependent	Nucleus	Brain, testis, kidney, and heart	Rpd3	ND	LYS ⁴¹ , GLY ¹⁴⁰ , PHE ¹⁴¹ , HIS ¹⁴² , HIS ¹⁴³ , GLY ¹⁵¹ , PHE ¹⁵² , CYS ¹⁵³ , ASP ¹⁸¹ , HIS ¹⁸³ , ASN ²⁵⁷ , ASP ²⁶¹ , SER ³⁰¹ , GLY ³⁰² , TYR ³⁰⁴	Carcinogenesis, expression modulation of the gene encoding interleukin 10 (IL10)

2.5. HISTONE DEACETYLASE ENZYMES MEDIATED NEUROTOXICITY

HDACs are known to regulate the gene expression pattern, which is involved in the pathogenesis and progression of various life-threatening diseases, namely diabetes, cancer, NDDs, stroke, and others. Mounting evidence sheds light on the possible implication of HDAC enzymes in NDDs causing neurotoxicity. For instance, HDAC1 decreases the potential of binding of motor proteins and α -tubulin with cargo proteins, whereas, overexpression of the HDAC1/2 complex inhibits the apoptotic process by decreasing p53 acetylation and PUMA expression. Hence, inhibition of HDAC1 and HDAC2 in Schwann cells and conditional knockout mouse model targeting retinal ganglion cells promised neuroprotective effects [162,163]. In the PD model (*in vivo and in vitro*), inhibition of HDAC 1 and HDAC2 complex with K560 in 1-methyl-4-phenyl-1,2,3,6-tetrahydropyridine (MPTP) induced neurotoxicity promotes neuroprotection and increases XIAP expression [164]. Further, the R6/2 mice model

and Ube3a-maternal deficient mice model demonstrated the neurotoxic effect of HDAC1 and HDAC3 complex. Increased expression of HDAC1/2 has a detrimental effect on ubiquitin-protein ligase E3A, also promoting decreased acetylation of histone H3 and H4 causing intellectual and development deficits [165,166]. In one study, it was seen that c-Abl tyrosine kinase activity increases HDAC2 gene expression in the neuronal model and knocked out the Npc1 mouse model mediated through the c-Abl/HDAC2 signaling pathway [167]. Moreover, cognitive impairment caused by the decreased synapse number and synaptic plasticity due to overexpression of HDAC2 results in acetylation of H4 histone on specific lysine residues, such as Lys¹² and Lys⁵ [168]. Likewise, HDAC3 promotes the inhibition of the neuroprotective cell cycle inhibitory protein cyclin-dependent kinase inhibitor 1A (CDKN1A) when in complex with HDAC1, whereas, in a non-neuronal experimental model, HDAC3 is known to be CDKN1A inhibitor [169–172]. Further, HDAC3 is also linked to the onset of AD and PD, two common forms of neurodegeneration where it promotes A β and LRRK2-induced cell death [173–175]. In another experimental condition, it was shown that HDAC3 increases tau phosphorylation, increases A β expression in the brain and periphery regions, and causes memory and cognitive impairment in the 3xTg-AD mice model [176]. Nuclear exportation of HDAC4 is linked with detrimental effects on neuronal cell life, and brain-derived neurotrophic factor (BDNF) treatment suppresses the nuclear transport while administration of the Calcium/calmodulin-dependent protein kinase inhibitors upsurges in nuclear accumulation [177]. In another experiment performed on dopaminergic neurons overexpressing A53T mutant α -synuclein treated with MPTP *in vitro* and *in vivo*, intracellular nuclear transport of HDAC4 was shown to be involved in the pathogenesis of PD where it causes dopaminergic cell death, resulting in suppression of cAMP response element-binding protein (CREB), MEF2A, and enhanced neuronal apoptosis [178]. Moreover, inhibition of HDAC6 with a selective inhibitor causes neurite extension, reverse oxidative stress-induced neuronal cell

death, reverse impaired axonal transport through recruitment of kinesin and dynein motor complexes, enhance microtubule stability, mitochondrial transport [179–182] improves memory and cognitive conditions in disease phenotypes such as AD, Tauopathy, HD, Charcot-Marie-Tooth disease both in cell culture and animal experimental models [78,183–186] whereas its overexpression reduces tau degradation and increases its accumulation in the brain which promotes toxicity [78]. Altogether, these studies proved the plausible implications of selective or pan HDAC inhibitors as therapeutic agents in NDDs.

2.5.1. ALZHEIMER'S DISEASE

AD is the most prevalent NDD in the elderly. It is characterized by neurotoxic A β oligomer aggregates and tau hyperphosphorylation leading to neuronal dysfunction and, ultimately, neuronal cell death. Recently, histone deacetylation and HDAC have been implicated in neuronal dysfunction, cognitive defects, memory and learning impairment and decreased synaptic plasticity *in vivo* and *in vitro* AD experimental models [158,187,188]. For example, Mahady et al., 2018 [189] found that HDAC and sirtuin expression in post-mortem frontal cortex tissue correlated to the degree of cognitive impairment. HDAC1 and 3 were increased in mild and moderate AD versus non-impaired subjects. HDAC2 was relatively constant, whereas HDAC4 significantly increased in mild and moderately impaired cases. Interestingly, HDAC4 was found to decrease in severe AD. HDAC6 increased continuously throughout disease progression from non- to severe cognitive impairment. Increased APP expression in cultured cortical neurons decreased H3 and H4 acetylation.

In contrast, increased histone acetylation via HDAC inhibitor improved memory and cognitive function in aged neurons. Thus, it may be concluded that H3 and H4 hyperacetylation and HDAC inhibitors mitigated AD by enhancing memory function and improving cognition [24,190–192]. Prolonged administration of sodium butyrate (NaB) increased H3 and H4 acetylation, and p53 acetylation improved cognition and memory and re-established synaptic

plasticity. In aged murine studies, transcriptional p53 deregulation has been linked to tau hyperphosphorylation and A β aggregation, i.e., pathologic changes consistent with AD [193–196]. Further, the dose-dependent administration of 4-phenylbutyric acid in Tg2576 AD mice enhanced spatial memory and cognitive function in the hippocampus through normalizing tau hyperphosphorylation without alteration in A β concentration [197]. 4-phenylbutyric acid also increased H3 acetylation status. H4 acetylation increased glutamate receptor 1, postsynaptic density protein 95 and microtubule-associated protein 2 expressions resulting in transcriptional repression. In the fear mice model, HDAC inhibitors altered H3/H4 acetylation in synaptogenesis genes to improve spatial and contextual learning [115,168,198–200]. In 3xTg AD murine studies, W2, a mercaptoacetamide-based class II HDAC inhibitor, decreased tau hyperphosphorylation and A β concentration by increasing β - and γ -secretase expression, thus improving memory and learning [201].

Moreover, neuron-specific HDAC2 over-expression reduced spine density, synapse number/plasticity and cognitive function and thus negatively regulated memory and learning ability mediated through transcriptional repression [168]. In the AD murine model, HDAC6 expression led to A β deposition and mitochondrial trafficking impairment, causing cognitive and memory impairment [202]. HDAC2 is deregulated in the nucleus basalis of Meynert, and its reduction decreases the expression of genes involved in the memory-associated immune signaling cascade. Also, over-expressed HDAC2 and HDAC5 reduced BDNF production, decreased H3 and H4 acetylation and increased A β aggregation [203,204]. Increased HDAC3 and 1 activity in primary culture neurons and SHSY-5Y neuronal cells cause histone hypoacetylation, increased A β oligomers mediated hippocampal impairment, and long-term memory and synaptotoxicity lead to cognitive defects and memory impairment [205,206]. Further, HDAC inhibitor MGCD0103 in primary neurons of AD mice ameliorated histone hypoacetylation, impaired α -tubulin acetylation, tau protein phosphorylation, and A β toxicity,

thus preventing neuronal loss [207]. Because HDAC appears strongly associated with histone hypoacetylation and transcriptional regulation of genes associated with AD, developing a specific HDAC inhibitor is of therapeutic importance [Figure 2.7].

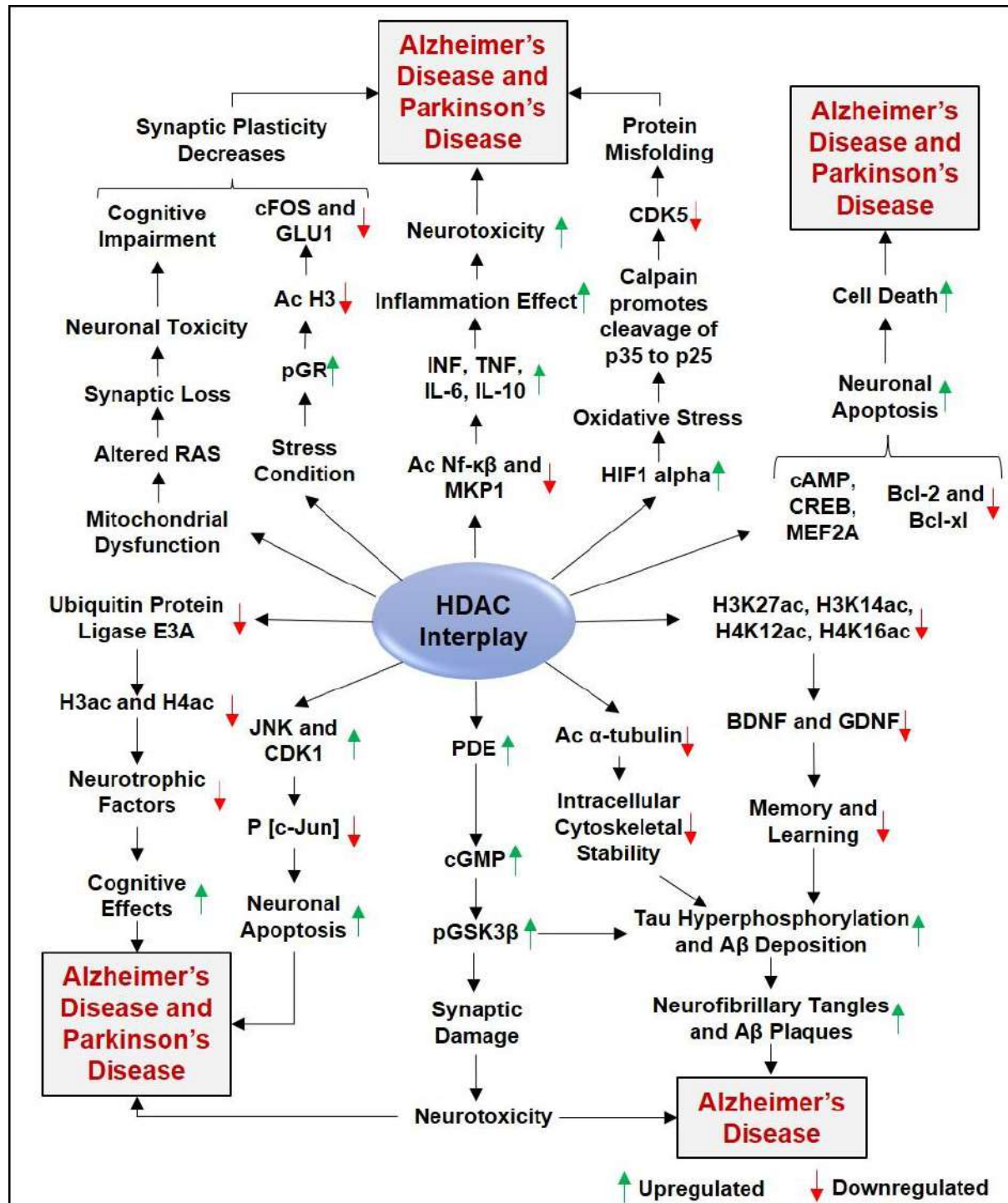


Figure 2.7: Interplay between the histone deacetylase (HDAC) biological activity and etiology of neurodegenerative disorders. Histone deacetylase manipulates various signaling cascades such as proteasomal degradation, inflammation, apoptosis, and autophagic cell death. Moreover, histone deacetylase decreases the acetylation level of neuroprotective proteins, such as brain-derived neurotrophic factor (BDNF), GDNF, α -Tubulin, and other neurotrophic factors leading to memory

impairment. Altogether, HDAC cause neurotoxicity and eventually leads to neuronal cell death by mitochondrial dysfunction, inflammation effect, increasing oxidative stress, and decreases the activity of pro-survival factors such as Bcl-2 and Bcl-xl. HDAC was also known to regulate intracellular cytoskeletal stability causing tau hyperphosphorylation and toxic amyloid protein. HDAC decreases the expression of ubiquitin-protein ligase E3 causes proteasomal degradation, and cognitive defects lead to Alzheimer's and Parkinson's disease.

2.5.2. PARKINSON'S DISEASE

PD is the most common neurodegenerative brain disorder [273,274]. It is characterized by motor dysfunction, sleep behavior disorders, mood disturbance, cognitive decline and dementia caused by Lewy body aggregation and dopaminergic neuronal loss in the substantia nigra *pars compacta*. Data implicates α -synuclein mediated transcriptional deregulation and altered histone acetylation in PD in animal and cell culture models [208,209]. Pan-HDAC inhibitors have been used as a therapeutic agent to alter HDAC activity in PD models [29]. For example, valproate prevented dopaminergic neuronal degeneration in the substantia nigra *pars compacta* and inhibited α -synuclein accumulation in the MPTP and rotenone-induced PD models [210]. Valproic acid (VPA) increased H3 and H4 acetylation, increased neurotrophic glial cell line-derived neurotrophic factor and BDNF expression, and ameliorated cognitive defects *in vitro* and *in vivo* PD models [211,212]. Furthermore, valproate activated neuroprotection molecular targets such as GSK3 β , Akt/Erk pathway, Na⁺ and K⁺ channels, the oxidative phosphorylation pathway, and the suppression of neuroinflammation and oxidative stress associated markers [213]. Administration of 4-phenylbutyric acid in the transgenic fly PD model and 6-hydroxydopamine induced rat model prevented dopaminergic neuronal loss mediated by increased histone acetylation, BDNF and glial cell line-derived neurotrophic factor expression, reduced caspase-3 and attenuation of inflammatory response and oxidative stress [214–216] [Figure 2.7].

In a transgenic PD animal model, 4-phenylbutyric acid prevented loss of dopaminergic neurons and 3,4-dihydroxy phenylacetic acid, reduced motor defects and cognitive impairment, up-regulated DJ-1 expression and inhibited α -synuclein accumulation and cytotoxicity [217–219]. Trichostatin A increased histone H3 and H4 acetylation, inhibited inflammatory response,

prevented microglial cells apoptosis and up-regulated BDNF and glial cell line-derived neurotrophic factor expression in dopaminergic neurons, and MPTP and rotenone treated neuron-glia co-cultures [220–222]. In SHSY-5Y neuroblastoma cell culture and PD mice model, HDAC1/2 inhibitor K560 attenuated dopaminergic neuronal cell death mediated through decreased ROS production, anti-inflammatory effect, and increased anti-apoptotic XIAP expression, decreased p53 phosphorylation and inhibited MAPK activation [164]. HDAC6 promotes deacetylation of cortactin, HSP90, and α -synuclein, prevents misfolded protein accumulation, promotes autophagy in the aggresomes, and protects from α -synuclein cytotoxicity mediated dopaminergic neuronal cell death [223–228]. In the *Drosophila* model of PD, inhibition of HDAC6 with tubastatin prevented protein aggregation. It protected against neuronal degeneration via ROS-induced oxidative stress reduction, increased peroxiredoxin1/2 acetylation, and improved microtubule axonal transport [128,229]. VPA in SHSY-5Y culture and LRRK2-R1441G PD mice model attenuates dopaminergic cell death through increased acetylation, reduced microglial activation and inflammatory response, reduced pro-apoptotic genes expression, and decreased Bax/Bcl-2 ratio resulted into increased motor neuron functions [230,231]. Harrison et al., 2013 [232] demonstrated that nicotinamide in the lactacystin PD rat model prevented neuronal apoptosis and increased neurotrophic factor expression. Although pharmacologic inhibition of HDAC appears promising and effective, additional studies are required to understand their exact mechanism of action in developing an isoform-specific HDAC inhibitor for PD.

2.6. ACETYLATION AND HISTONE DEACETYLASE ENZYMES INTERFERE WITH BIOLOGICAL AND CELLULAR PROCESSES IN ALZHEIMER'S AND PARKINSON'S DISEASE

CNS development and function depend on gene expression regulation in response to external stimulus and internal stress signaling. PTMs and chromatin remodeling mechanisms are

essential in regulating neural gene expression mediated neurogenesis, neural migration, synaptic plasticity and transmission, glial cell differentiation, and neural behavior [233]. Moreover, these modifications do not only regulate neural gene expression but are also involved in higher-order brain functions such as memory and cognition. HDAC provides an essential function in neural cell lineage, i.e., HDAC inhibition promotes increased neural differentiation [234]. Interestingly, HDAC appears to be involved in both neurotoxic and neuroprotective effects in neuronal function regulation in aging and age-related disorders.

Additionally, Transcriptional regulation through HAT and HDAC has been extensively studied as the therapeutic targets for NDD. Before the development and prosecution of HDAC inhibitors, the exact mechanism of different HDACs in the pathogenesis of neurological defects must be understood. HDAC causes chromatin condensation leading to transcriptional repression of regulatory genes involved with normal CNS function. These include neural differentiation and plasticity, synaptogenesis, synaptic function, cognition and neurological behavior. HDAC regulate these processes through modulation of signaling pathways or molecules. HDACs are also involved in biological processes and molecular phenomena that include oxidative stress, inflammatory response, autophagic cell death, mitochondrial dysfunction, cell-cycle progression, and ubiquitin-proteasome degradation. In the next section, we discuss the potential of HDAC in neurological defects mediated through different signaling cascades leading to abnormal cell death.

2.6.1. SYNAPTIC PLASTICITY AND TRANSMISSION

Synapses degeneration caused by plasticity impairment and transmission deficit promotes neuronal cell death involved in NDD. Synapse plasticity and memory potential in the brain region is highly controlled with transcriptional process and positive gene regulation provided by histone acetylation [235]. In the hippocampal CA1 region, HAT Kat2a was upregulated and is involved in synaptic plasticity and memory consolidation mediated through nuclear factor

kappa-light-chain-enhancer of activated B cells (NF- κ B) pathway, the dysregulation of which occurs in NDD and dementia [236]. Similarly, increased Tip60 expression required for upregulation of synaptic proteins and early environmental benefits cause restoration of cognitive functions and memory impairment mediated through H4K45 and H4K12 hyperacetylation in human APP overexpressing flies' model [237]. L. Peng et al., 2019 [238] demonstrated that lipopolysaccharides-induced neonatal inflammation reduces H4K12ac and c-FOS expression, enhancing spatial cognitive impairment and inducing memory deficits. However, specific Trichostatin A-induced inhibition improved lipopolysaccharides-induced neurologic deficits that were mediated via increased acetylation and c-FOS in murine hippocampus. Also, decreased ANP32A expression in the human tau transgenic mice model caused H3K9 and 14, H4K5 and 12 acetylations that promoted increased expression of synaptophysin, glutamate receptor 1 and synapsin-1 associated with synaptic function and memory consolidation. Selective inhibition of HDAC1 and 2 co-repressor complexes, including CoREST with Rodin-A, promoted increased spine density, improved long-term potentiation, and synaptic protein expression to improve synaptopathies [239]. Further, selective inhibition of class I HDAC with MS-275 caused increased miniature inhibitory post-synaptic currents plasticity and synaptic transmission in the hippocampus, improved synaptic and memory function [240]. A recent study highlighted the potential of HDAC and phosphodiesterase type 5 dual inhibitor CM-414 in synaptopathies. Administration of CM-414 in Tg2576 mice decreased A β and tau, increased inactive GSK3 β and decreased dendritic spine density associated with cognitive defects mediated through increased synaptic transmission [241,242]. TF Sp3 is upregulated in AD patients that interact with HDAC2, facilitates its recruitment to synaptic proteins, and isoform-specific inhibition of HDAC2-Sp3 complex causes restoration of synaptic functions and ameliorates memory impairment in the CK-p25 mouse model [24,243,244]. The HDAC2 inhibitor, NaB, promoted H3K9 and H3K14

acetylation, increased synaptosome-associated protein 25 (SNAP25) expression and up-regulated neurotransmitter release in a hypoxia-mediated neurodegeneration rodent model. Also, HDAC2 inhibition with vorinostat restored memory deficits and synaptic function via increased synaptic numbers, a finding not observed in a knockout HDAC2 mouse model [168]. BDNF, also known to regulate synaptic plasticity and transmission and memory consolidation, was down-regulated in NDDs [245–247]. In 3xTg-AD mice, HDAC inhibitors, such as sulforaphane, NaB, and Trichostatin A, increase BDNF activity that, causes an enhanced H3 and H4 acetylation and subsequent increase in microtubule-associated protein 2, synaptophysin and post-synaptic density protein 95 (PSD-95) expression [248,249].

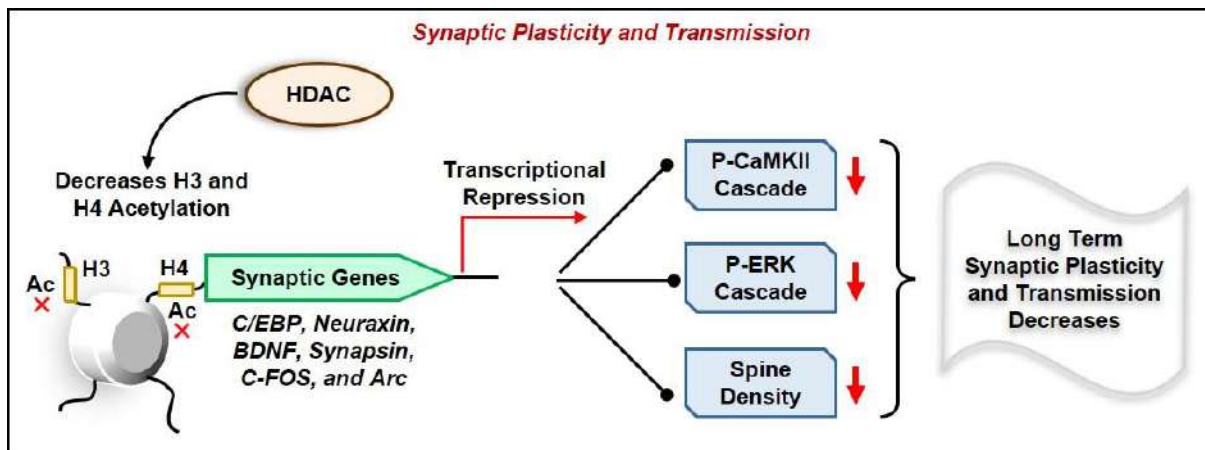


Figure 2.8: Role of histone deacetylase enzymes in synaptic plasticity and transmission: histone deacetylase decreases overall histone acetylation and thus inhibits transcriptional activation of genes involved in synaptogenesis and synaptic plasticity. Consequently, transcriptional repression of genes decreases spine density and synapse number, inhibits the p-ERK pathway, and deregulates the p-CaMKII signaling cascade, decreasing synaptic plasticity and transmission.

However, administration of the HDAC2 selective inhibitor, NaB, in the rat hippocampus ameliorated ethanol-induced memory impairment and N-methyl-D-aspartate receptor-dependent long-term synaptic depression mediated through positive regulation of glutamate receptor subunit epsilon-2 [250,251]. Chronic treatment of HDAC2 with CI-994 increased H3 acetylation and GABAergic and glutamatergic plasticities in dopaminergic neurons to improve cognitive and synaptic function [252]. Inhibition of HDAC3 provoked H3 and H4 acetylation in the hippocampal and infra limbic cortex region along with positive regulation of gene

expression [253]. VPA and vorinostat ameliorated fear conditioning, increased histone acetylation and improved synaptic and memory function [254,255]. Post-natal ethanol exposure increased HDAC1-3 expression, up-regulated caspase-3 activity, decreased H3 and H4 acetylation and repressed synaptic plasticity genes. Trichostatin A administration reversed H3 and H4 deacetylation, prevented caspase-3 over-expression and positively regulated BDNF, Egr1 and Arc to improve synaptogenesis and cognition [256]. In class IIa HDAC, inhibition of HDAC5 mediated by antidepressants such as imipramine and reboxetine increased H3 and H4 acetylation, increased BDNF expression, and enhanced vesicular glutamate transporter 1 activity to protect against cognitive and synaptic defects [257,258]. Environmental enrichment mediated HDAC3 inhibition and miR-132 upregulation prevents A β oligomers from inducing synaptotoxicity, causing synaptic plasticity impairment and long-term potentiation [205]. Unfortunately, the role of HDAC4, 7, 9 and 10 in regulating synaptic transmission and function remains largely unclear. Additional research is clearly warranted to more fully understand the HDAC mechanism of action in synaptic defect-induced neurodegeneration [Figure 2.8].

2.6.2. NEUROGENESIS AND NEURAL MIGRATION

HDAC1 and 2 are highly expressed in neuroepithelial cells (NEC) and neural progenitor cells (NPC) during cortical development, wherein HDAC1 is primarily expressed in glial cells while HDAC2 is expressed in mature neuronal cells in the neocortex. Genetic ablation of *hdac1* or 2 did not alter brain phenotypic expression or contribute to other brain abnormalities [259]. Simultaneous deletion of both proteins in NPC and astrocytes through glial fibrillary acidic protein promoter (GFAP)-Cre results in cell death-induced pathology, including that of the hippocampus, cortex and cerebellum. These results implicate HDAC1 and 2 in brain development, wherein redundancy in one protein might be compensated by the other [260]. Hagelkruys et al., 2014 [261] demonstrated that genetic ablation of *hdac1/2* did not alter brain development using *Nestin*-Cre, in which mice that lacked both proteins showed CNS-related

abnormalities along with reduced proliferation and premature differentiation of NPC. In another study, *hdac1* was implicated in maintaining neural cell proliferation in NSC in zebrafish [107]. This finding was mediated through prevention from premature cell cycle exit and differentiation in which *hdac1* deletion promoted reduced proliferation and reduced brain size. Tang et al., 2019 [262] demonstrated that genetic knockout *hdac1* and 2 resulted in decreased NPC via apoptotic cell death followed by reduced neocortex size. The study concluded that HDAC1 and 2 were critical for maintaining the density of NPC, neural migration and differentiation, and for correctly positioning NPC in the developing cortex. The external granule layer (EGL) in the developing cerebellar cortex demonstrated increased HDAC1 expression. The study also demonstrated that in Purkinje cells, GABAergic interneurons and migrating granule neurons, HDAC1 expression was low, and HDAC2 was high [263]. Thus, it may be concluded that HDAC1 and 2 were critical regulators of adult neurogenesis, wherein HDAC1 was essential for NPC proliferation, whereas HDAC2 regulated differentiation and maturation [Figure 2.9]. HDAC3 is the only HDAC in which deletion causes an adverse effect on neural proliferation and differentiation. Calcium/Calmodulin Dependent Protein Kinase II Alpha (*CaMK2a*)-*Cre* and *Thy-1*-*Cre* mediated knockout *hdac3* mice demonstrated neurologic deficits in the forebrain [264]. HDAC3 is required for cell cycle progression mediated through cyclin-dependent kinase 1 (CDK1), and genetic knockdown of HDAC3 resulted in reduced NPC proliferation and neuronal differentiation in the hippocampus [265]. However, in the cortex, siRNA-mediated *hdac3* knockdown resulted in increased neural differentiation via increased *BDNF*, tubulin beta 3 class III (*Tubb3*) and neurogenin-2 (*Neurog2*) expression [266]. TF TLX has an essential role in NSC proliferation via the recruitment of specific HDAC to target loci such as p21 and phosphatase and tensin homolog (*Pten*) and promotes neuronal growth [267]. Ankyrin repeats domain-containing protein 11 (ANKRD11) that interacts with HDAC3 and positively regulates gene expression associated

with neurogenesis, while genetic deletion of *hdac3* causes decreased precursor proliferation. Unfortunately, little is known about the involvement of HDAC8 in neural differentiation and migration. However, in retinoic acid-treated P19 embryonic carcinoma cells, HDAC8 regulated neuronal differentiation via cell cycle progression in which genetic deletion led to the formation of embryonic bodies [268]. HDAC8 deacetylates complex cohesion proteins involved in cohesion function, affecting transcription and mitosis mediated through the loss of topologically associated domain functions [269,270].

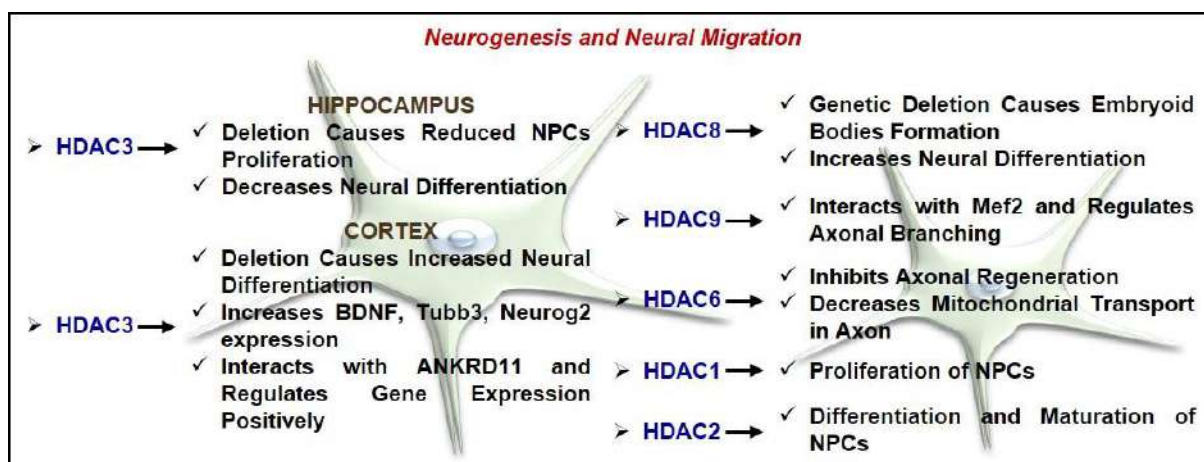


Figure 2.9: Involvement of histone deacetylase enzymes in neurogenesis and neural migration: HDAC enzymes modulate transcriptional activity of histone and non-histone substrates that are involved in neuronal functions such as neurogenesis, neural migration, synaptic plasticity, synaptogenesis, and synaptic transmission. Genetic deletion of HDAC3 in hippocampal neurons inhibits neural differentiation, whereas, in the cortex neurons, HDAC3 deletion increases neural differentiation. HDAC9 and HDAC6 overexpression negatively regulate the transcriptional activity of genes involved in neurogenesis and thus inhibits axonal regeneration and mitochondrial transport in axons. Further, HDAC1 regulates the proliferation of neural progenitor cells (NPCs), while HDAC2 regulates the differentiation and maturation of NPCs. Genetic deletion of HDAC8 causes embryoid body formation and consequently increases neural differentiation.

In class IIa, genetic deletion of *hdac4* promotes abnormal cerebellum development, including Purkinje neurons. Similarly, CaMK-Cre or Thy1-Cre mediated *hdac4* deletion did not impart abnormalities, thereby implicating early embryonic mechanisms in knockout *hdac4* mediated cerebellum defects [271–273]. Further, HDAC5 and 9 deletions did not alter neurogenesis and neural cell migration long with neuronal deficits. However, HDAC9 interaction with MEF2 regulated axonal branching in an activity-dependent manner [274,275]. In contrast, HDAC6 promoted axonal elongation through its localization in the distal end of axons and regulated

microtubule stabilization to enhance neuronal function and neurogenesis. Further, HDAC6 inhibited axonal regeneration mediated through deacetylating calcium-binding outer mitochondrial protein, resulting in decreased mitochondrial transport in axons [276,277]. Despite mounting evidence, the full potential of HDAC in adult neurogenesis and neural migration remains to be elucidated.

2.6.3. OXIDATIVE STRESS AND AUTOPHAGY

Oxidative stress is essential in the etiology of neurodevelopmental disorders and NDD. Oxidative stress increases HDAC expression causing transcriptional repression and subsequent cell death. HDAC inhibitors, such as Trichostatin A, VPA, NaB, SAHA, and 4-phenylbutyric acid, have neuroprotective effects against oxidative stress, neuroinflammatory response, mitochondrial dysfunction, calcium signaling defects, and excitotoxicity. In SHSY-5Y dopaminergic neurons, 6-hydroxydopamine-induced oxidative stress results in increased HDAC activity. At the same time, the administration of VPA and NaB reversed HDAC over-expression, increased H3 acetylation, reduced Bax/Bcl2 ratio, increased BDNF expression, and decreased pro-apoptotic factors activity [215,231]. Additionally, HDAC inhibitor butyrate in C57BI/6 female mice improved metabolism via reduced oxidative stress and apoptosis markers along with altered antioxidant activity [278]. Moreover, the administration of NaB in Sprague Dawley rat ganglion and PC12-NeuroD6 cells ameliorated oxidative stress-induced cell death and induced neurodevelopment and neurogenesis mediated through increased H3 and H4 acetylation, increased CREB activity and enhanced oxidative phosphorylation biogenesis thereby reducing mitochondrial dysfunction [279,280]. Additionally, NaB increased protein kinase C δ expression in cultured neurons, brain slices and animal models through Sp1, 3 and 4 regulated increase in H4 acetylation and increased CBP/CREB binding, resulting in augmentation of dopaminergic neuronal cell death [281]. Administration of hydroxamate-based HDAC inhibitors, such as BRD3811 and PCI-34051, ameliorated oxidative stress-

induced neurotoxic effects through histone hyperacetylation and inhibited HDAC [282,283]. In mouse neural stem cells, NaB and VPA inhibited HDAC1 activity, reduced nitric oxide production and induced NSC proliferation via decreased tumor necrosis factor-alpha (TNF- α) and COX2 [284]. Dose-dependent pharmacologic inhibition of HDAC2 with Trichostatin A in ethanol-treated SK-N-MC ameliorated oxidative stress-induced cell death through decreased ROS production and increased memory function [285,286]. In AD, neuronal and murine model over-expressing tau increased oxidative stress-induced cell death mediated by HDAC6 and 2 overexpression [213,214]. Increased insoluble tau led to neurofibrillary tangle formation, impaired proteasomal degradation and decreased microtubule stability. Vorinostat ameliorated traumatic brain injury and exhibited anti-depressant activity associated with reduced oxidative stress and neuroinflammatory response in mice neuronal tissue via H3 and H4 acetylation, HDAC and nuclear factor erythroid 2-related factor 2 (Nrf2)/ARE pathways [287,288]. Moreover, HDAC inhibitors, namely ING-6 and -66, promoted selective HDAC6 and hypoxia-inducible factor (HIF1) prolyl hydroxylase inhibition along with Nrf2 activation leading to neuroprotection by reducing oxidative stress response [289]. Administration of VPA in the MPTP-treated PD mouse model attenuated neuronal cell death induced by increased oxidative stress and ameliorated histone hypoacetylation [290]. Wang et al., 2017 [291] demonstrated that a ketogenic diet ameliorated oxidative stress-induced neuronal cell death in Sprague-Dawley rats post spinal cord injury. They concluded that the ketogenic diet inhibited HDAC activity and increased H3 and H4 acetylation. Moreover, this diet increased the expression of antioxidant-related genes such as SOD1 and Forkhead Box O3a (FOXO3a). Thus, hypoacetylation of histone and non-histone substrates due to increased HDAC activity caused oxidative stress [Figure 2.10].

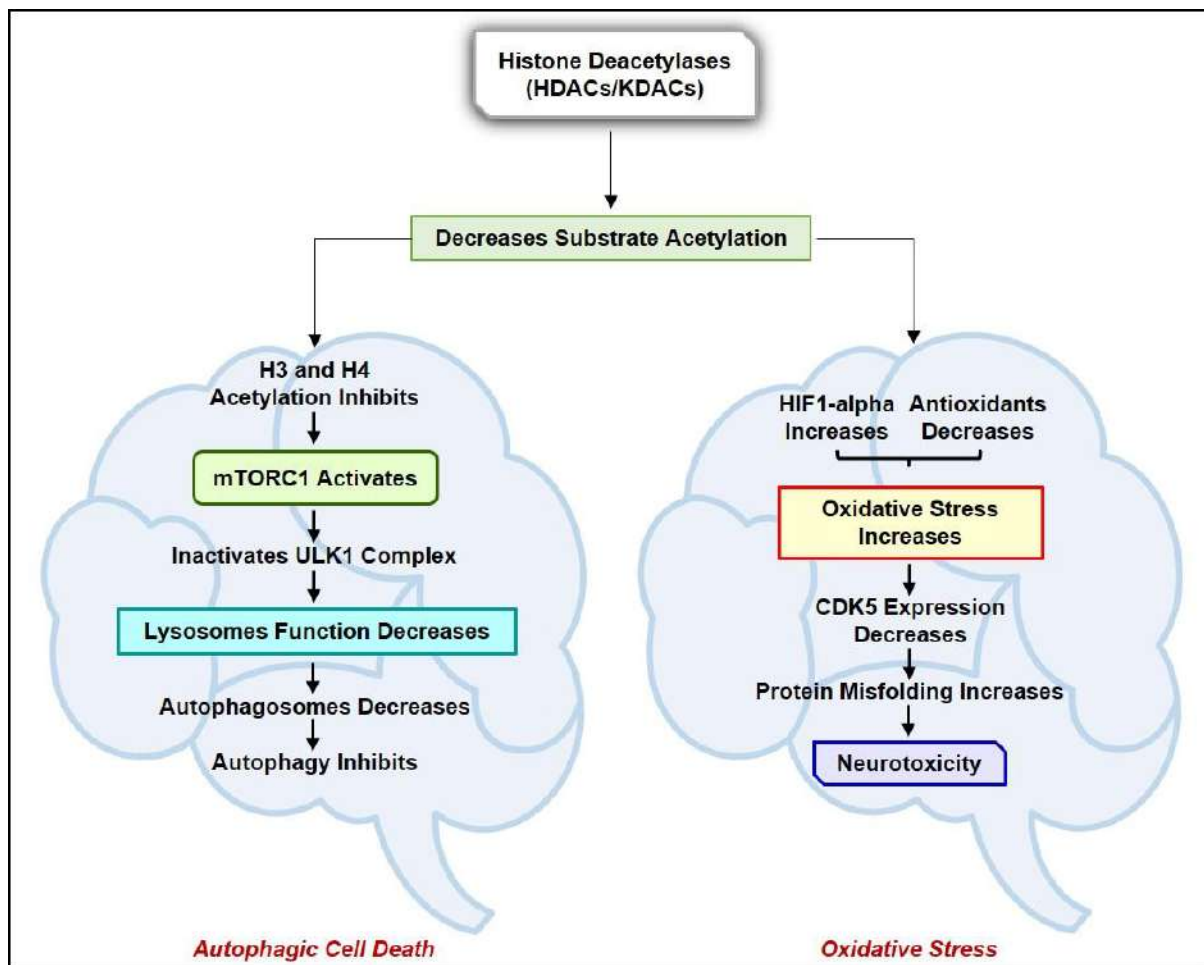


Figure 2.10: Histone deacetylase modulates autophagic cell death and oxidative stress: A decrease in histone acetylation results in autophagy impairment through mammalian target of rapamycin complex 1 activation and consequently decreases in lysosomes function and autophagosomes formation. Additionally, activation of glycogen synthase kinase 3 beta through decreased H3 and H4 acetylation results in synaptic damage, and an increase in misfolded protein aggregates causes a decrease in synaptic plasticity and an increase in neurotoxicity, respectively. Moreover, enhanced histone deacetylases activity increases hypoxia-inducible factor 1-alpha activity and decreases antioxidants expression, which in turn increases oxidative stress-mediated decrease in cyclin-dependent kinase 5 expressions, resulting in protein misfolding aggregation and consequently increases neurotoxicity.

Autophagy interference induces stress responses such as oxidative stress, endoplasmic reticulum stress, proteasome and aggresomes, and UPS via transcriptional regulating enzymes known as HDACs. In HeLa cells, HDAC6 functions to autophagy degradation of misfolded huntingtin aggregates, while in the mice model of HD, VCP mutations cause disease phenotypes mediated through impaired aggresomes followed by autophagic degradation of misfolded proteins rescued by HDAC6 overexpression [292]. Similarly, the HDAC1 and 3 selective inhibitors 4b in N171-82Q transgenic mice ameliorated behavioral defects through I kappa B kinase (IKK) activation, increased mHtt degradation in the proteasome and the

lysosomes, and increased autophagic degradation [293]. However, in the AD mice model, HDAC6 played a different role as it increased tau hyperphosphorylation and impaired autophagy leading to misfolded protein accumulation [294]. Zhang et al., 2014 [185] demonstrated that selective HDAC6 inhibition with tubastatin A and ACY-1215 alleviates neurological defects, reduces tau hyperphosphorylation, and promotes autophagic clearance of A β aggregates in the AD transgenic mice model. Microtubule-associated protein tau inhibited the IST1 factor associated with ESCRT-III expression, followed by reduced autophagosome-lysosome fusion required for autophagic degradation of misfolded protein aggregates leading to enhanced LC3-II and sequestosome I activity [295]. Recently, Wu et al., 2020 [296] demonstrated the different regulatory functions of yeast Rpd3 and its mammalian homolog HDAC1 in autophagy. Cholesterol derivatives increased dephosphorylation and nucleus-cytoplasm shifting of the BmRpd3/HsHDAC1 complex via mammalian target of rapamycin (mTOR) complex inhibition and autophagic induction. Unfortunately, there is limited evidence on the functional effect of HDAC, apart from HDAC6, on autophagy in neurologic defects. Additional research is clearly required to characterize HDAC in autophagic degradation of misfolded protein aggregates to more fully understand their potential role in cognition and memory [Figure 2.10].

2.6.4. INFLAMMATORY AND IMMUNE RESPONSE

Pathogenesis and progression of various neurologic defects have been associated with microglial activation and subsequent release of toxic cytokines. HDAC regulates inflammatory response and microglial activation through modulation of histone acetylation, which consequently activates pro-inflammatory genes and suppresses anti-inflammatory genes. Durham et al., 2017 [297] observed that specific KO of HDAC1 or 2 and selective inhibition of HDAC activity with MS-275, apicidine, or MI-192 in BV-2 murine microglia activated with lipopolysaccharides decreased pro-inflammatory cytokines TNF- α and interleukin 6 (IL-6)

expression. Pharmacologic inhibition of HDAC1 with SAHA in a mouse model of cerebral occlusion attenuated ischemia-induced H3 deacetylation, decreased COX2 expression, nitric oxide synthase and IL1 β mRNA expression, and increased Bcl-2 and HSP70 expression [298,299]. Trichostatin A administration increased the expression of inflammatory markers such as TNF- α , IL-6, and nitric oxide synthase during lipopolysaccharides induction in glial cultures and hippocampal tissues [300]. The time and dose-dependent administration of VPA in primary neurons or enriched glial cultures exhibited chromatin condensation and DNA fragmentation [193]. Subsequent apoptotic cell death was mediated through disruption of the mitochondrial membrane potential and increased acetylation. VPA promoted neuroprotection against glutamate excitotoxicity in rat cortical neurons through HSP70 induction and increased specificity protein 1 (Sp1) acetylation and subsequent association with acetyltransferase p300 [301]. Likewise, Chen et al., 2018 [302], demonstrated that VPA administration following spinal cord injury caused a phenotypic microglia shift from M1 to M2, followed by microglial deactivation. VPA induced STAT1/NF- κ B acetylation and inhibited HDAC3 activity and the inflammatory response [Figure 2.11].

Similarly, SB administration in C57Bl/6NTac mice and a rodent model of hypoxia-ischemia stimulated neurogenesis, inhibited microglial activation, up-regulated the anti-inflammatory marker IL10 and decreased pro-inflammatory cytokine expression [303,304]. MS-275 and SAHA increased mGlu2 expression in dorsal root ganglion and spinal cord via increased p65/RelA acetylation, thus inhibiting neuroinflammatory response in a mouse model of persistent inflammatory pain [305]. Further, specific administration of DMA-PB in the traumatic brain injury rodent model enhanced H3 acetylation associated with the reduced neuroinflammatory response [306]. Park et al., 2016 [307] observed that NaB administration decreased lipid peroxides and serum GFAP, inhibited over-expression of pro-inflammatory cytokines in the cortex and striatum, and thus exhibited an anti-neuroinflammatory effect.

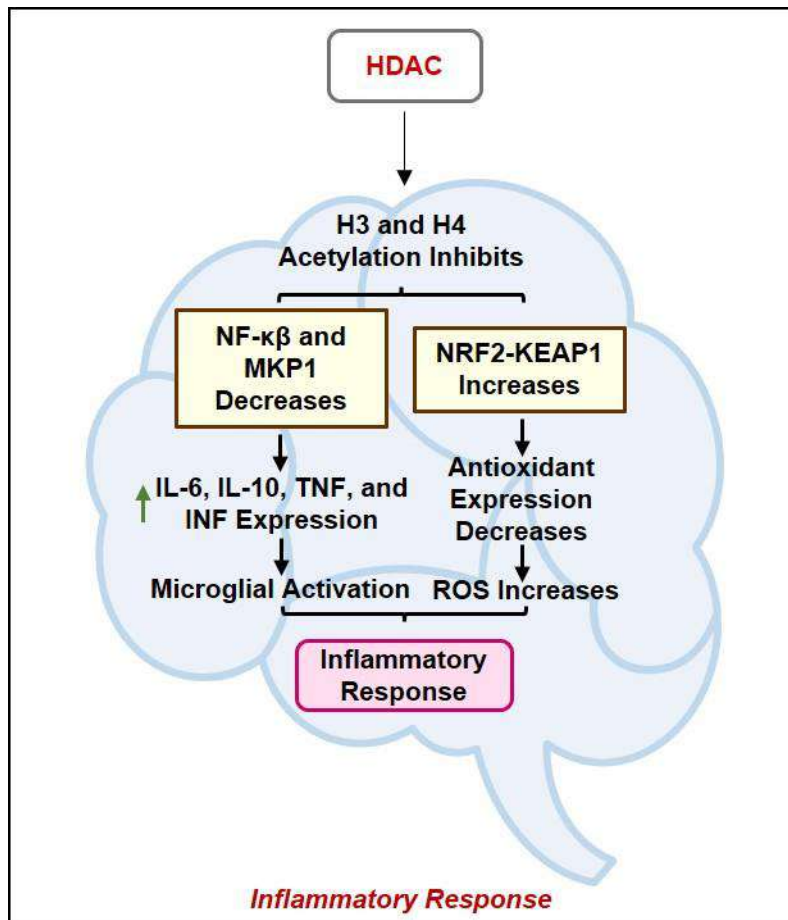


Figure 2.11: Histone deacetylase enzymes regulate neuroinflammation in neurodegeneration: HDAC decreases histone acetylation resulting in increased pro-inflammatory cytokines expression and decreased production of antioxidants. This will increase reactive oxygen species production and microglial activation that exhibit neuroinflammation.

2.7. HISTONE DEACETYLASES INHIBITORS IN ALZHEIMER'S AND PARKINSON'S THERAPEUTICS

Evolving research on the role of histone erasers (HDAC) and writers (HAT) in the human nervous system has improved our understanding of their potential involvement in neurodevelopmental deficits and NDDs. It is widely recognized that these enzymes modulate synaptic plasticity, cognition, neural plasticity, neural differentiation and neurogenesis. These processes are mediated through various biological and molecular pathways impacting neuronal function and potentially cell death. Further, it is well-established that these enzymes function through the deacetylation of histone and non-histone substrates along with interaction with each other. Thus, inhibiting specific HDAC enzymes and activating HAT enzymes is crucial

to promote neuroprotection. The following section discusses the potential mechanisms of HDAC inhibitors in the pathogenesis of NDDs.

2.7.1. ROLE OF CHEMICALLY-SYNTHEZIZED COMPOUNDS

HDAC inhibitors have been divided into four groups based on structural and functional groups [255]. These include hydroxamate, tetra-peptide, aliphatic acid and benzamide inhibitors. Hydroxamate inhibitors have a short half-life and exhibit prolonged effects [376]. These include Trichostatin A, pyridoxamine, scriptaid and SAHA. Trichostatin A inhibits HDAC6 activity, decreases calpain acetylation, and reduces calcium ions-induced neuronal cell death [308]. SAHA decreases histone acetylation and increases SMN2 expression in neuronal ectodermal tissues [309]. Further, non-selective hydroxamate inhibitors promote neuroprotection against ROS-mediated oxidative stress-induced neuronal cell death [282]. Moreover, VPA, Trichostatin A and NaB up-regulate BDNF and glial cell line-derived neurotrophic factor expression via increased histone acetylation and are neuroprotective in NDD [211]. PBA ameliorates disease progression via significantly increased DJ-1 expression (300%) in N27 dopamine cell lines, thus decreasing oxidative stress and α -synuclein toxicity [218]. PBA is neuroprotective in MPTP and rotenone-induced toxicity in mice models and ALS, HD and SMA models [310–312]. For neuroprotection, 4-phenylbutyric acid alters tau pathology by increasing inactive GSK3 β [313]. SB and 4-phenylbutyric acid enhance tissue damage in the hypoxia mice model, whereas VPA reduces lesion volume and neurologic defects post-CNS injury [197] [**Table 2.2**].

Apicidin regulates HDAC2-3 activity and is neuroprotective against MPTP-induced neurotoxicity [159]. In cortical neurons, apicidine increased protein acetylation and HSP70 expression [314], whereas, oral administration of MS-275 inhibited microglial activation, amyloid deposition and aggregation in the hippocampus and cortex and minimized the production of pro-inflammatory cytokines and nitric oxide. MS-275 can cross the BBB and has

a critical role in the development of any therapeutics for NDD [315].

Table 2.2: Administration effects of histone deacetylase inhibitors in cellular and animal models and their implications in neurodegenerative disorders

Inhibitor	Disease	Model	Interactions	Results	Dose	References
MS-275/Entinostat	AD	APP/PS1-21 Mice Model	TNF, IL-1 β , and iNOS	Increases Acetylation, promotes neuroprotection	20 ng/ml	[316]
Vorinostat/SAHA	PD	Mesencephalic neuron–glia cultures and reconstituted cultures	GDNF and BDNF	prolongation cell survival and protection against neurotoxin-mediated cell death of dopaminergic neurons	1.25 μ M	[212]
	PD	SH-SY5Y neuroblastoma cells	GAPDH, α -synuclein, CBP, P/CAF	Prevention against alpha synuclein mediated neurotoxicity	10 μ M	[317]
	AD	Neuro-2a luciferase reporter cell line	GRN	Increases GRN expression level and promote neuroprotection	0.51 μ M	[318]
	AD	APP ^{swe} /PS1 ^d E9 Mice Model	–	Rescue contextual memory formation and increases histone acetylation	100 mg/kg	[199]
Trichostatin A	PD	mesencephalic neuron-glia cultures	BDNF and GDNF	Neuroprotection	50 nM and 100 nM	[211]
	PD	SH-SY5Y Cell Line	NRSF, UCH-L1, mGluR1 and BDNF	Protect against MPTP mediated neurotoxicity	1 mg/kg	[319]
	AD	APP ^{swe} /PS1 δ E9 transgenic (Tg) mice	Gelsolin and A β	Increases gelsolin mediated clearance of A β , promotes neuroprotection	5 mg/kg	[320]
	AD	Swiss Albino Mice	BDNF	Provides neuroprotection and rescue memory deficits	0.5 and 1 mg/kg	[286]
Sodium butyrate [NaB]	PD	6-hydroxydopamine Rat Model	BDNF	Increases global H acetylation and upregulation of BDNF expression, reduces motor deficits	150 and 300 mg/kg	[215]
	PD	Rotenone Induced Drosophila Model	Sin3A complex	Rescue locomotor deficits, induces neuroprotection, and decreases rotenone-mediated dopamine deficiency	10 mM	[216]
	PD	Cell Culture and Transgenic Drosophila	Sin3A complex	Rescues toxicity associated with syn ^{WT} and syn ^{NLS} constructs in SH-SY5Y cells	100 and 200 mM	[317]
	PD	Dopaminergic Cell Model	P53, H3	Reverse the acetylation level of histone proteins, Reverses DNA damage due to transcriptional dysregulation		[321]
	AD	APPPS1-21	Myst4, Fmn2, Marcks11, Gsk3 β , GluR1, Snap25, Prkca, and Shank3	Increases histone acetylation levels, restores memory functions	1.2 g/kg	[322]
	AD	Sprague–Dawley (SD) Rats	Nrf2	Increases hippocampus associated memory and learning ability, promotes global hypo acetylation	840 mg/kg/day	[323]
Phenyl butyrate/ Sodium Phenylbutyrate	PD	Cell Culture and Animal Model	PARK7 and DJ1	Upregulate expression of DJ1 and provides neuroprotection		[218]
	PD	MPTP Mouse Model	P21, Nf-kB	Regulate neuroinflammation and	100 mg/kg body wt/d	[324]

				oxidative stress		
	AD	Tg2576 Mouse Model	GSK3 β , GluR1, PSD-95	Rescue brain histone acetylation and decreases tau phosphorylation	200 mg/kg	[197]
	AD	Tg2576 Mouse Model	NR2B, SAP102	Promotes synaptic plasticity and structural modification, reverse memory deficits and abnormalities in spine density	200 mg/kg	[200]
	PD	Mesencephalic neuron-glia cultures Mice Model	GDNF and BDNF	Protection against DA neuronal death, increases neurotropic factors expression in astrocytes	0.6 mM	[212]
Valproate/ Valproic Acid [VPA]	PD	Rotenone Induced PD mouse Model	α -Synuclein	Increases H3 acetylation and reduces neurotoxicity	2% VPA	[325]
	PD	MPTP Mouse Model	H3 and α -Synuclein	Promotes histone hyperacetylation and promotes neuroprotection	400 mg/kg	[326]
	PD	SH-SY5Y Cell Culture	HSP70, Akt, ERK1/2, Bcl-2	Provide Neuroprotection against DA cell death	5 mM	[327]
	AD	APP(V717F) Mice Model	GSK3 β and A β	Reduces A β deposition and rescue GSK3 β mediated neurotoxicity	400 mg/kg	[328]
	AD	APP23/ APP751	APP, BACE1, and PS1	Inhibits APP processing, neurite plaque formation, and rescue memory deficits	30 mg/kg	[329]
	AD	CA1 pyramidal neuronal Rat Model	HDAC3	Reduces amyloid- β -oligomer-induced synaptic plasticity impairment	20 μ M	[173]
RGFP966	PD	SH-SY5Y Cells, C57BL/6 mice	HDAC1, HADC2, p53, XIAP	Protection against MPTP induced toxicity and DA neuronal cell death	45 mg/kg/day	[164]

2.7.2. IMPLEMENTATION OF NATURAL COMPOUNDS AND MICRO-RNAs

Along with the positive effects of the HDAC inhibitors discussed above, natural-occurring biomolecules and small non-coding miRNA also play a pivotal role in neuroprotection via altering the histone acetylation level [330]. Curcumin, a natural flavonoid, has been found to be a potential neuroprotective role. Along with SAHA, a specific HDAC inhibitor, curcumin was found to induce neuroprotection in the AD cell culture model. Curcumin and SAHA have a synergistic effect on neuronal apoptosis due to A β toxicity at the concentration level of 1 μ M and 5 μ M for SAHA and curcumin, respectively [331]. Also, curcumin was found to regulate neuropathic pain by altering the HAT activity and transcriptional regulation of BDNF and Cox-2 genes [332]. Experiments performed by Kwon et al., 2010 confirmed the possible

implications of resveratrol and melatonin in the neuroprotection from A β -induced neurotoxicity. Melatonin and resveratrol attenuate neuronal cell apoptosis via inducing Sirt1 class III HDACs. At the concentration level of 20 μ M and 500 μ M for resveratrol and melatonin, respectively, expression activity of Extracellular signal-regulated kinases (ERK) increases while the level of ROS decreases and restores intracellular Glutathione (GSH) levels [333]. The *in vitro* analysis concluded that resveratrol deacetylates histone H3K9 and (NF- κ B-p65) K310, which promotes transcriptional attenuation of NOX and NF- κ B-p65 and eventually decreases cell apoptosis and DNA damage [334]. Melatonin, another naturally occurring HDAC inhibitor, promotes the induction of the glial cell-derived neurotrophic factors potent factor for alleviating neuronal apoptosis. Melatonin induces hyperacetylation of histone H3 via inhibiting HDAC3, HDAC5, and HDAC7 and regulates gene expression with the help of activating neuroprotective signaling pathways such as ERK 1/2 and PI3K/Akt along with an increase in NeuroD, GDNF and BDNF gene expression level both *in vitro* and *in vivo* [335]. Melatonin, a pleiotropic molecule, regulates the acetylation level of histone H3 proteins via increasing the expression of CBP/p300 along with the ERK signaling pathway, due to which expression level of Neurogenin1 and NeuroD1 increases, which promotes neuronal differentiation [336]. Melatonin also increases cell proliferation and cell survival rate, which promotes neurogenesis in the hippocampal region and decreases memory deficits [337]. Nicotine and cocaine, two chief agents of drug abuse, increase the accumulation of the FosB gene through the hyperacetylation of H3 and H4 at the promoter region, which is necessary for the behavioral addict. Further, nicotine-induced hyperacetylation of histone increases cognitive performance and has a significant role in synaptic plasticity via altering transcriptional regulation of gene expression [338].

Small non-coding miRNA acts as a repressor of the gene expression phenomenon, which is modulated at the transcriptional level, regulated by epigenetic alterations and involved in the

modification of several biological functions such as cell differentiation, cell survival, axonal regeneration, DNA damage repair, shortening of telomere, inflammation, apoptosis, and autophagy. For example, HDAC3 regulated the expression pattern of miR29 and reduced the binding of HDAC3 and EZH2, which resulted in hyperacetylation of histones and reduced H3K27 trimethylation [339]. MiR-124 and miR-9 provide a significant role in regulating the expression level of HDAC5, which is the direct interacting partner of neural membrane glycoprotein GPM6A and plays a pivotal role in neural differentiation and elongation. HDAC5 regulated the expression pattern of transcriptional factor MEF2C. miRNAs such as miR-124 and miR-9 regulate neural elongation via inhibiting HDAC5 activity through regulation of the HDAC5-MEF2C-GPM6A pathway [340]. Mir-9, which is highly expressed in the neural region, also regulates long-term memory and improves neuronal cell survival post-ischemic stroke via inhibiting the expression activity of HDAC4, leading to an increase in H3 and H4 acetylation status. In the study conducted, the expression level of miR9 slightly increased after 20h of OGD treatment implicated the neural regeneration. Here, Sreekala et al., 2019 found that upregulation of miR-9 prevents neuronal apoptosis via targeting Bcl-2, while inhibition results in increased expression of BACE1 and CREB1 involved in resetting memory deficits [341] [Table 2.3].

Table 2.3: Neuroprotective role of biomolecules and micro-RNAs mediated inhibition of histone deacetylase enzymes

Compound	Disease	Model	Interactors	Biological Function	Dose	References
Curcumin	AD	(N2a/APP ^{swe}) and (N2a/APP ^w) AD Cell Model	BACE1, PS1, P300	Inhibit H3 acetylation, decreases BACE1 and PS1 expression	20µM	[342]
	AD	Rat pheochromocytoma PC12 cells AD model	Akt, CBP, p300, EP300	Decreases neuronal cell apoptosis, promotes neuroprotection	5µM	[331]
	AD	Chronic Constriction Injury (CCI) Rat Model	BDNF and Cox-2	Curcumin inhibits the acetylation of H3 through reduction in p300/CBP activity and its binding to BDNF and Cox-2	40 and 60 mg/kg	[332]
Resveratrol	AD	HT22 hippocampal cell line	GSK3β, AMPK, GSH	Promotes neuroprotection and decreases oxidative stress, induces SIRT1 activity	20µM	[333]
<i>Withania somnifera</i>	AD	SH-SY5Y cell culture model	NLRP3, HDAC2	Inhibits the neuroinflammatory	50 nM–1 µM	[343]

				response through inhibiting the activity of NLRP3 and HDAC2		
Protopine	AD	3xTg-AD and P301S tau transgenic models of AD	HDAC6, HSC70, UPS	Promotes ubiquitination and degradation of pathological tau aggregates	289.47 ng/g	[344]
Oleuropein Aglycone	AD	Patient samples	AMPK/mTOR	Induce autophagy and reverses cognitive impairment	12.5 mg/kg	[345]
Melatonin	AD	HT22 hippocampal cell line	GSK3 β , AMPK, GSH	Acts as SIRT1 modulators promotes deacetylation of histones	500 μ M	[333]
miR-124	—	P19 cells and primary neurons	HDAC5, MEF2C	Inhibitor of HDAC5, increases neurite elongation	0.4 μ g	[340]
	AD	Mice Model	Sirt1	Improved synaptic plasticity and enhanced expression of BDNF	—	[346]
miR-134	AD	Hippocampal CA1 neurons	CREB, YY1, and Sirt1	Promotes neuroprotection with increase in the expression level of neurotropic factors such as CREB and BDNF	—	[347]
miR-149-5p	AD	293/APP ^{sw} cells	BACE1, KAT8	miR-149-5p regulated KAT8 and H4K16ac expression in an AD cell model, which may be associated with the pathological process of AD	—	[348]
miR-149	AD	SH-SY5Y cells	BACE1 and HDAC4	Overexpression of miR-149 may suppress A β accumulation and promote neuronal viability by targeting BACE1 in AD model cells	—	[349]
miR-138-5p	PD	SH-SY5Y Cell Culture Model	Sirt1, Beclin1, P62	Suppress MnCl ₂ induced autophagy, provide neuroprotection	—	[350]
miR-212-5p	PD	MPTP-induced mouse model	SIRT2, p62, LC3 B	Promotes neuroprotection through enhanced autophagy	—	[351]

2.7.3. EMERGENCE OF MULTI-TARGET DRUG LIGAND AS A POTENTIAL THERAPEUTIC AGENTS IN ALZHEIMER'S AND PARKINSON'S PATHOLOGY

To overcome problems of toxicity and isoform-selectivity, multi-targeted ligands open up new doors for the development of therapeutic agents in neurodegeneration. However, it is a well-established fact that chemical molecules able to modulate the activity of two or more targets have a synergistic or additive effect at low dose concentration along with the increase in pharmacokinetic properties [352]. This strategy shows possible implications in the case of NDDs because of their multifactorial state of origin with a special focus on AD and PD. Thus, the effect of a particular drug may be nullified due to the emergence of different pathological

pathways, which can be overcome by using multi-target drug ligands, in which one formulation consists of different drugs targeting different biological processes. The development and prosecution of multi-target drug ligands are emerging approach because of high patient compliance, ease of administration, development, and cost-effectiveness [353,354] **[Figure 2.12]**.

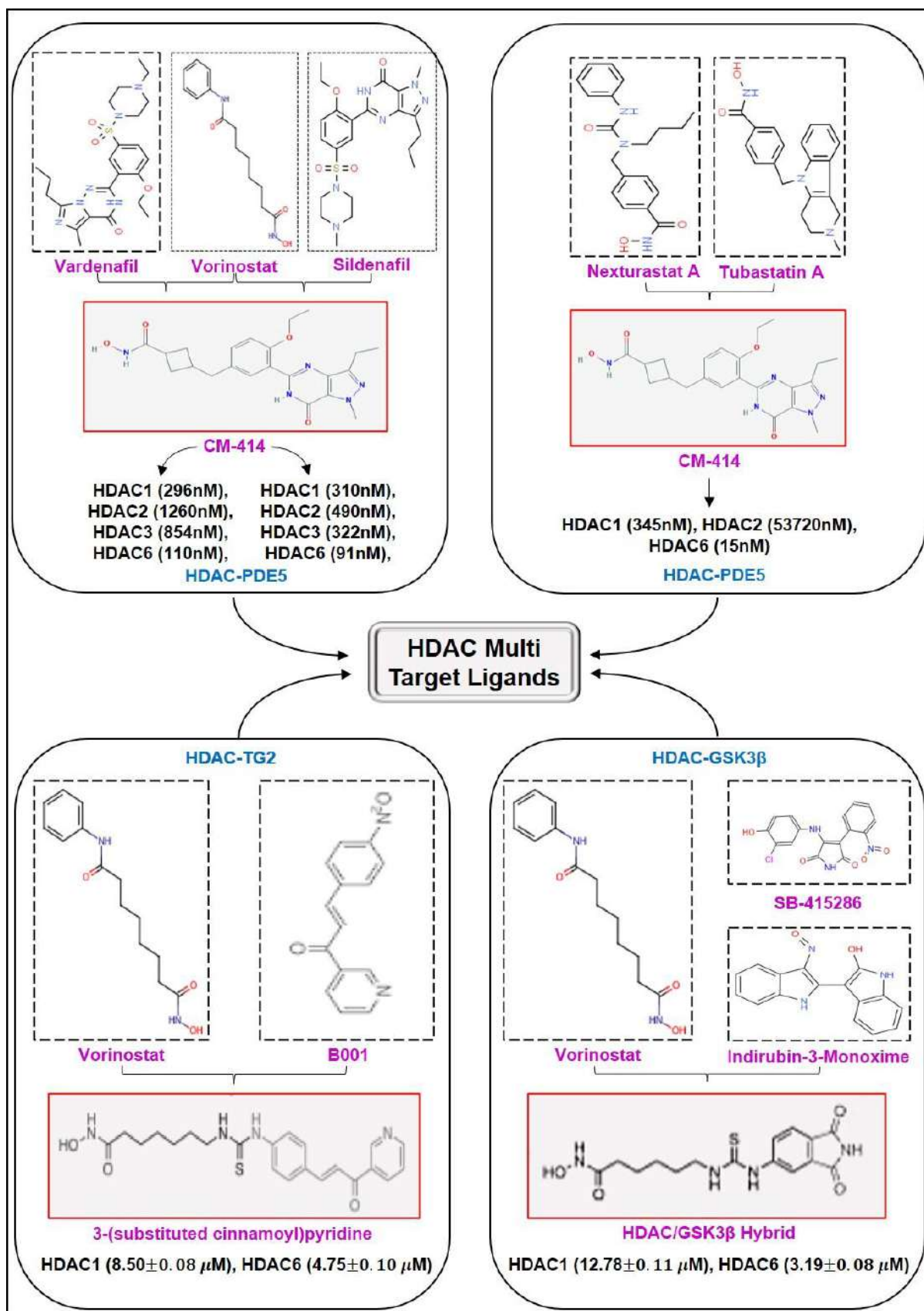


Figure 2.12: Histone deacetylase inhibitors as a potential multi-target directed ligand: Isoform selectivity of HDAC inhibitors remains the key issue to be addressed, which causes neuronal toxicity and side effects. Multi-target ligand approach becomes an emerging technique to develop dual inhibitor affecting HDAC and key proteins involved in Alzheimer's disease pathology. Till now the combination of HDAC inhibitors with

phosphodiesterase type 5 (PDE5), transglutaminase 2 (TG2), and glycogen synthase kinase 3 beta (GSK3 β) Inhibitors have been discovered as a therapeutic approach for Alzheimer's disease. Vorinostat remains the preferable HDAC inhibitor for developing a multi-target ligand. CM-414 is a multi-target ligand developed from the combination of Vorinostat and Vardenafil, Vorinostat and Sildenafil, and Tubastatin A and Nexturastat A having greater IC₅₀ value as compared to compounds when used alone. Further, 3-(substituted cinnamoyl) pyridine was developed from the combination of Vorinostat, an HDAC inhibitor and B001, a TG2 inhibitor having an IC₅₀ value of $8.50 \pm 0.08 \mu\text{M}$ and $4.75 \pm 0.10 \mu\text{M}$ for HDAC1 and HDAC6, respectively. Similarly, GSK3 β and HDAC hybrid based on multi-target ligand was developed from a combination of Vorinostat and SB-415286, and Vorinostat and Indirubin-3-Monoxime reflect an IC₅₀ value of $12.78 \pm 0.11 \mu\text{M}$ and $3.19 \pm 0.08 \mu\text{M}$ for HDAC1 and HDAC6, respectively.

Drugs such as MK-4305, A₂A/MAOB, memoquin, and ChE-MAOB inhibitors have been administered in the treatment of AD and PD, which promotes inhibition of A β aggregates [355–358]. In order to develop a multi-targeted ligand based on HDAC, a pharmacophore model of different hydrophobic cap moieties should be identified, which can be used as a therapeutic agent in HDAC-mediated neurotoxicity. Herein, we explain some recently developed HDAC-based multi-directed ligands. Collateral modulation of HDAC and phosphodiesterase type 5 has been developed in the treatment of NDD using the combination of Vorinostat and Tadalafil, a known phosphodiesterase type 5 inhibitor [359,360]. Inhibition of HDAC and phosphodiesterase type 5 modulates the global histone acetylation level associated with long-term memory. Three models with different cap moieties, such as Sildenafil, Vardenafil, and Tadalafil associated with HDAC inhibitor, have been developed in which CM-414 emerged as a promising agent in the treatment of AD. The compound exhibits strong inhibitory activity against phosphodiesterase type 5 and HDAC6 but lower inhibitory activity against class I HDAC *in vitro*. The hepatic cell line THLE-2 culture model confirmed that it modulated the acetylation level of H3 histone and tubulin, while in the animal model, it showed a decrease in APP and tau expression levels [359]. Similarly, combinations of Vardenafil and Vorinostat and Tubastatin A and Nexturastat A targeting activity of HDAC6 and phosphodiesterase type 5 have been developed aimed at the induction of H3 and tubulin acetylation [360,361]. The combined administration of Tubastatin A and Ebselen showed a neuroprotective effect in PC-12 cells against ROS-mediated toxicity, which is higher than the administration of both compounds alone at concentrations of $5 \mu\text{M}$ and $10 \mu\text{M}$, respectively [362]. Transglutaminase

2 (TG2), which is highly resistant to proteolytic conversion, forms A β aggregates. Simultaneous inhibition of TG2 and HDAC protects neuronal cell death. The combination of vorinostat and 3-(substituted cinnamoyl) pyridine as an interacting partner induced acetylation of histone H3 and tubulin. In SHSY-5Y cell culture, the assay confirmed its inhibitory activity at 50 μ M and protected neurons against glutamate [5 mM] induced toxicity [363]. Additionally, inhibiting HDAC and GSK3 β with a dual inhibitor is a promising therapeutic strategy for minimizing the etiology of AD. The combination of hydroxamic acid and phthalimide moiety is known to modulate H3 acetylation, inhibit tau hyperphosphorylation at a concentration level up to 100 μ M in SH5Y cells and promote the neuroprotective effects in neurons with toxic 6-hydroxydopamine [364]. Moreover, the compound can provide neurogenesis and decreased neuroinflammation. NF- κ B is a transcription factor causing inflammation in various NDDs regulated by HDAC activity. Developing HDAC and NF- κ B-based dual inhibitor is a promising strategy for providing neuroprotection. The combination of chalcones-based HDAC and NF- κ B dual inhibitor promotes the neuroprotective effect and inhibits both HDAC and TNF- α induced NF- κ B activity at concentration levels 60-190 μ M and 8-41 μ M, respectively [365].

CHAPTER III

Materials and Methodology

CHAPTER III: MATERIALS AND METHODOLOGY

3. INTRODUCTION

The following chapter describe the tools and techniques used in the study to achieve pre-defined objectives. Initially, we have discussed the common techniques that implemented in the study, namely data collection and pre-processing, PPI network analysis, network clustering, and HUB signatures identification. Lately, we have divided our methodology as per the objective's requirement. For objective 1, techniques such as identification of acetylation signatures, involvement of potential HDAC enzymes, and critical lysine residues involved in disease pathogenesis. Likewise, for objective 2, techniques, namely crosstalk between lysine-induced PTMs, impact of lysine mutation on disease pathogenesis, and impact of lysine mutation on ubiquitination and SUMOylation. Additionally, for objective 3, we have focused on the role of lysine acetylation on metal toxicity-induced AD, whereas, for objective 4, we have focused on machine learning algorithms to identify novel HDAC inhibitor [Figure 3.1].

3.1. DATA COLLECTION AND MINING

The microarray gene expression datasets for AD and PD were obtained from NCBI-GEO database (<https://www.ncbi.nlm.nih.gov/geo/>) [366]. Further, data from two databases, such as DisGeNET (<https://www.disgenet.org/>) [367] and the comparative toxicogenomics database (<http://ctdbase.org/>) [368] were collected for genes associated with the progression of AD and PD. Similarly, Information related to HDAC interactors were extracted from two databases, such as comparative toxicogenomics database and HIPPIE (<http://cbdm-01.zdv.uni-mainz.de/~mschaefer/hippie/>) [369]. In addition, the datasets related to trace elements, namely chromium, cobalt, copper, and nickel were obtained from the online freely accessible comparative toxicogenomics database version 2019 (<http://ctdbase.org/>) [368]. For evaluation of protein structure, high-resolution co-crystallized HDAC6 and HDAC10 protein structures were extracted from RCSB PDB database (<https://www.rcsb.org/>) [370]. Similarly, the

compounds datasets for training data were extracted from binding database (<https://www.bindingdb.org/bind/index.jsp>) [371] and test sets were collected from DrugBank database (<https://go.drugbank.com/>) [370].

3.2. DATA PREPROCESSING AND FILTERATION

The datasets were analyzed in R-environment for data normalization and data pre-processing. Further, Limma was used to identify differential expressed genes in both AD and PD compared to controls. The p-value <0.05 and $| \text{Log}_2 \text{FC} | > 1.1$ was regarded as cut-off criteria to screen for significant differential expressed genes. The BioMart data-mining tool (<https://m.ensembl.org/info/data/biomart/index.html>) was applied to convert probe symbols into gene symbols. The databases were searched for duplicates, and redundancy in data was removed manually. Lastly, Venn analysis was performed using the online tool called as Venny 2.1 (<https://bioinfo.gp.cnb.csic.es/tools/venny/>) to identify common signatures. Additionally, these structures additionally went through the dock prep section of UCSF Chimera 1.10 (<https://www.cgl.ucsf.edu/chimera/>) [372] on account of including charges and missing residues. Binding and catalytic mode information of HDAC6 and HDAC10 has been studied from different scientific sources. Protein Pdb structures undergo energy minimization through ModRefiner: High-Resolution Protein structure Refinement (<https://zhanglab.ccmb.med.umich.edu/ModRefiner/>) [373] from Zhang Lab available online freely.

3.3. PROTEIN-PROTEIN INTERACTION ANALYSIS

The interaction network of common signatures was obtained from STRING database version 11.0 (<https://string-db.org/>) [374]. The search criteria in the STRING database are limited to a confidence score of 0.5. The obtained networks were imported into Cytoscape software version 3.8.0 (<https://cytoscape.org/>) [375] for protein data integration, PPI network visualization, and PPI network analysis. Subsequently, node degree, number of edges, clustering coefficient,

network homogeneity, shortest path length, and network density of AD and PD PPI network were calculated.

3.4. NETWORK CLUSTERING AND HUB SIGNATURE IDENTIFICATION

The AD and PD networks were merged using network merge tool of cytoscape based on two methods, namely network union and network intersection. Afterwards, network clustering was performed through molecular complex detection (<http://apps.cytoscape.org/apps/mcode>) [376] plugin of Cytoscape software. The clusters so formed were analyzed and visualized on different parameters such as the number of proteins (nodes) and physical interactions between them (edges), network clustering coefficient, characteristics path length, network centralization and homogeneity, and network density. The clusters of all PPI networks were statistically analyzed and ranked separately based on node degree. Lastly, the HUB proteins were identified using CytoHubba (<http://apps.cytoscape.org/apps/cytohubba>) [377] through default parameters.

3.5. FUNCTIONAL ENRICHMENT ANALYSIS OF HUB SIGNATURES

HUB proteins overrepresentation was performed through bioinformatics resource EnrichR (<http://amp.pharm.mssm.edu/Enrichr/>) [378] and QuickGO (<https://www.ebi.ac.uk/QuickGO/>) [379] to identify the molecular function, biological process, cellular function. Further, pathway analysis of HUB proteins was carried out using freely accessible online databases and tools such as the REACTOME database (<https://reactome.org/>) [380] and FunRich version 3.1.3 (<http://funrich.org/>) [381]. For statistical assessment of GO analysis and pathway analysis a p-value, less than 0.05 was considered significant, and fold enrichment value was taken considered. Here, p-value reflects the chance of observing “n” number of genes in a gene list annotated to a specific term, whereas, fold enrichment of a term was designated as overrepresented compared to the background, where overrepresentation is denoted as positive fold enrichment.

3.6. OBJECTIVE 1: TO IDENTIFY NOVEL COMMON BIOMARKERS IN AD AND PD BASED ON MULTI-OMICS APPROACH

In this section, we have presented a detailed picture of tools used to crucial signatures that involved in the pathogenesis of AD and PD, simultaneously. Further, we discussed the techniques implemented to identify the acetylation signatures of HUB signatures, that is, common proteins and TFs. In addition, we have defined the tools and techniques to determine the critical acetylated residues and their respective HDAC enzymes in the pathogenesis of AD and PD.

3.6.1. IDENTIFICATION OF HUB SIGNATURES-TRANSCRIPTION FACTORS REGULATORY NETWORK AND CELLULAR LOCALIZATION PREDICTION

The subcellular localization of HUB genes was calculated to understand the mechanism of action of protein and its associated functions using CELLO version 2.5: subCELLular LOcalization predictor (<http://cello.life.nctu.edu.tw/>) [382]. To identify the TFs that control the HUB proteins at a transcriptional level, TFs-target interactions were obtained from JASPAR version 8 (<http://jaspar.genereg.net/>) [383] and an interaction network between TFs and HUB proteins was created using NetworkAnalyst tool version 3.0 (<https://www.networkanalyst.ca/home.xhtml>) [384].

3.6.2. PREDICTION OF ACETYLATION SIGNATURES AND DEACETYLATION SITES

Based on the previous experimental studies, it was evident that acetylation signatures were associated with the pathogenesis of AD and PD through altering gene expression patterns. Thus, we used the Epigenomics Roadmap CHIP-seq dataset, which is an inbuilt feature of EnrichR for their potential acetylation marks of HUB proteins. Moreover, acetylation sites in CREB1 and HINFP have been predicted through machine learning algorithm-based, freely accessible online tools such as MuSite Deep (<https://www.musite.net/>) [385] and PSKAcePred

(http://bioinfo.ncu.edu.cn/inquiries_PSKAcePred.aspx) [386]. Lastly, the type of deacetylating enzyme associated with CREB and HINFP was predicted with the help of a freely accessible online web server named Deep-PLA (<http://deeppla.cancerbio.info/index.html>) [387].

3.6.3. PREDICTION OF CONSERVED LYSINE RESIDUES

The conserved sequence was predicted using multiple sequence alignment of 21 window sizes of lysine site residues that are ten residues on both left and right end containing lysine acetylating site in the middle for both CREB1 and HINFP using ClustalW multiple sequence alignment tool (<https://www.genome.jp/tools-bin/clustalw>) [388]. Additionally, the structural selectivity of lysine acetylating sites has been predicted with the help of PSIPRED: protein structure prediction server (<http://bioinf.cs.ucl.ac.uk/psipred/>) [389]. Subsequently, the secondary structure of the protein has been correlating with their respective protein acetylating sites.

3.7. OBJECTIVE 2: TO DISSECT HISTONE DEACETYLASE MECHANISM AND KEY LYSINE RESIDUES IN ASSOCIATION WITH NOVEL BIOMARKERS

In the following section, we have described the tools and techniques to identify the potential crosstalk between acetylation, ubiquitination, and SUMOylation in AD and PD pathogenesis, simultaneously in relation with HDAC interactors.

3.7.1. INTEGRATE POST-TRANSLATIONAL MODIFICATION SITES

Two databases, such as dbPTM (<http://dbptm.mbc.nctu.edu.tw/>) [390] and PLMD (<http://plmd.biocuckoo.org/>) [391] were used to extract the information of PTM (Acetylation, Ubiquitination, and SUMOylation) on regulatory proteins. Once the data were extracted, they were combined manually, and redundancy in PTM sites was removed. The PTM sites are sorted out according to PTM and modification sites.

3.7.2. STRUCTURAL ANALYSIS OF HUB SIGNATURES

3.7.2.1. SECONDARY STRUCTURE ANALYSIS

PTM influence the secondary structure of the protein, which regulates its biological functions. We extract the protein secondary structure information from DISOPRED3 (<http://bioinf.cs.ucl.ac.uk/psipred/>) [392] on both PTM and non-PTM lysine residue. DISOPRED3 is an open-source tool created by the UCL Department of Computer Science: Bioinformatics Group. The output was classified into three categories, such as coiled, helix, and strand.

3.7.2.2. DISORDER PREDICTION

The sequence for regulatory proteins-containing PTMs were extracted from the PMLD database. Structural order and disorder for these proteins were predicted through DISOPRED3, which uses PSIPRED software for disorder prediction. The extracted data were separated into two categories, such as the ordered region and the disordered region, as analyzed from the output.

3.7.2.3. *IN-SITU* CROSSTALK ANALYSIS

In-situ crosstalk analysis was performed to check the competition of PTMs on the same site. Data collected from PLMD and dbPTM were used to identify different PTMs on the same amino acid residues. The residues which have more than one PTMs were selected for further analysis.

3.7.2.4. HOTSPOT ANALYSIS

For all the identified PTM crosstalk sites, a motif of +7 and -6 amino acid stretch was extracted from the PLMD database from the corresponding protein sequence. For each identified acetylation site, the frequency of probable PTM site was calculated in the vicinity for the defined motif. Every motif containing ≥ 2 lysine residues, excluding the central lysine residue, was called a PTM hotspot region. Further, if a motif contained ≥ 2 PTMs on the same site, it

will be considered a PTM crosstalk hotspot.

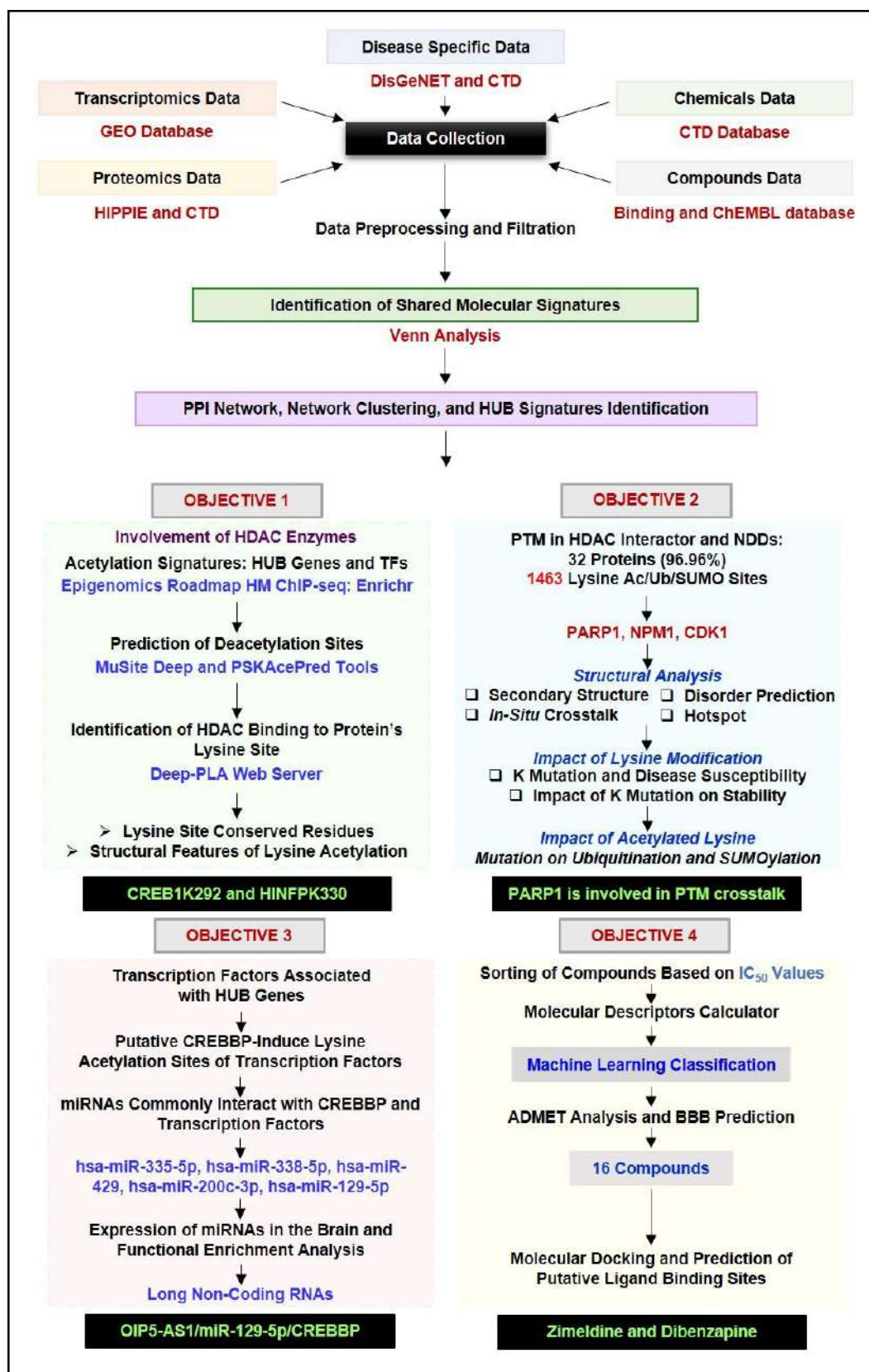


Figure 3.1: Workflow of the current study. The study is divided according to the different objectives as mentioned in the figure.

3.7.3. IMPACT OF LYSINE MODIFICATION

3.7.3.1. LYSINE MUTATION AND DISEASE SUSCEPTIBILITY

The functional impact of lysine mutations was studied with the help of online tools such as Pmut (<http://mmb.irbbarcelona.org/PMut/>) [393], PolyPhen2 (<http://genetics.bwh.harvard.edu/pph2/>) [394], PANTHER (<http://www.pantherdb.org/tools/csnpscoreForm.jsp>) [395], and SNAP2 (<https://roslab.org/services/snap/>) [396]. The obtained results were transformed into numerical values in order to visualize them on the stack bar graph. The particular mutation is said to be disease susceptible if its confidence score is greater than or equal to '3', which is called a threshold value.

3.7.3.2. IMPACT OF LYSINE MUTATION ON PROTEIN STABILITY

The protein structure was analyzed for force field energy upon lysine mutation. The lysine residue was mutated into glutamine (Q) and Leucine (L), and their total energy was calculated with the help of an online prediction tool that is DynaMut (<http://biosig.unimelb.edu.au/dynamut/>) [397]. The variation in the energy was estimated to observe the impact of lysine mutation on poly (ADP-ribose) polymerase 1 (PARP1) protein stability.

3.7.4. IMPACT OF LYSINE MUTATION ON ACETYLTATION, UBIQUITINATION, AND SUMOYLATION

To investigate the contribution of lysine in acetylation, ubiquitination and SUMOylation on the nearby sites, substitute lysine residue to glutamine (Q) and leucine (L). MutPred2 (<http://mutpred.mutdb.org/>) [398], an online tool was used to predict the physical significance of lysine mutation on acetylation, ubiquitination, and SUMOylation. The same tool was also used to predicted the affected motifs and pathogenic score upon lysine mutation either with glutamine and leucine. Further, BDM-PUB (<http://bdmpub.biocuckoo.org/>) [399] and

SUMOGO (<http://predictor.nchu.edu.tw/SUMOGO/>) [400] were employed to predict the potential ubiquitination and SUMOylation on nearby sites, respectively. The sites which are affected due to modification of lysine by either glutamine and leucine were tallied. The affected sites were classified into two groups that are gain in function on nearby sites and loss of function on nearby sites.

3.8. OBJECTIVE 3: TO IDENTIFY POTENTIAL MICRO-RNAs AND BIOMARKERS REGULATORY NETWORK IN THE PATHOGENESIS OF NEURODEGENERATIVE DISEASES

In the following section, we have discussed the tools and techniques that have been employed to identify the potential regulatory network of biomarkers-miRNAs in the pathogenesis of metal toxicity-induced AD. Herein, we identified the TFs-HUB markers interaction followed by putative lysine sites of TFs. Lately, through the different tools, we have identified putative miRNAs and long ncRNAs in the pathogenesis of metal toxicity-induced AD.

3.8.1. IDENTIFICATION OF HUB PROTEINS-TRANSCRIPTION FACTORS ASSOCIATION

It is a well-established fact that regulatory biomolecules, such as TF's, play a crucial role in gene regulation. TFs determine the transcriptional fate of target genes and, based on that, activates or deactivates the transcriptional activity of a particular gene. HUB genes were analyzed with JASPAR (<http://jaspar.genereg.net/>) [383], an open-source and online database of curated TFs. The information extracted from JASPAR was imported into NetworkAnalyst version 3.0 (<https://www.networkanalyst.ca/>) [384], an online freely available tool to form an interaction network between genes-TFs. Top interacting nodes were selected for further investigation and analysis.

3.8.2. PREDICTION OF PUTATIVE ACETYLATION SITES

Acetylation is a lysine-specific PTM, which promotes euchromatin structure and activates the transcription process. To find out the potential acetylated lysine residues of identified TFs, two online web-servers, such as Deep PLA (<http://deeppla.cancerbio.info/>) [387] and GPS-PAIL (<http://pail.biocuckoo.org/>) [401] were used. The study is restricted to identify the potential CREBBP induced acetylation sites. Deep PLA is a deep neural network-based online prediction tool, where four models are combined into one complete connection layer. Similarly, GPS-PAIL is a machine learning-based online prediction tool, which predicts acetylated sites of seven different acetyltransferases.

3.8.3. IDENTIFICATION OF MICRO-RNAs INTERACT WITH TRANSCRIPTION FACTORS AND ACETYLATED ENZYME

miRNA are post-transcriptional regulators, which regulate the expression of particular proteins. To predict the putative miRNAs bound with CREBBP and identified TFs simultaneously, we used an online integrated miRNA target database known as mirDIP (<https://ophid.utoronto.ca/mirDIP/>) [402]. Only those miRNAs with confidence scores high (top 5%) and very high (top 1%) were selected for further studies. Further, the Venny tool was used to identify the common miRNAs among identified TFs and acetylating enzyme. Moreover, the predicted miRNAs were subjected to TissueAtlas (<https://ccb-web.cs.uni-saarland.de/tissueatlas/>) [403], an online web server to identify the potential of predicted miRNAs for expressing in healthy brain tissues.

3.8.4. EXPRESSION OF MICRO-RNAs IN BRAIN AND PREDICTION OF PUTATIVE LONG NON-CODING RNA

It is crucial to validate that the predicted miRNAs are involved in the pathogenesis of AD and CNS diseases. MIENTURNET (<http://userver.bio.uniroma1.it/apps/mienturnet/>) [404], an online web tool devised for miRNA functional enrichment analysis and miRNA-target

prediction. Similarly, miRNAs involved in signaling transduction were predicted using the MIENTURNET web tool. Further, it is a well-established notion that gene expression is regulated by non-coding RNAs, such as long non-coding RNAs and circular RNAs. Thus, it is equally important to identify the long non-coding RNAs that will regulate the activity of selected miRNAs in the pathogenesis of AD. StarBase V2.0 (<http://starbase.sysu.edu.cn/>) [405] was used to identify the potential non-coding RNA that simultaneously binds with selected miRNAs.

3.9. OBJECTIVE 4: TO EXPLORE NOVEL HISTONE DEACETYLASE INHIBITOR USING MACHINE LEARNING APPROACH

HDAC inhibitors known to promote neuroprotection through inhibition of HDAC activity. Thus, identification of novel HDAC inhibitor is critical to reverse AD and PD pathology. Thus, we have defined a methodology consisting of machine learning algorithms and toxicological analysis of anti-psychotic drugs that targets HDAC10 to reverse AD and PD pathology.

3.9.1. DATA COLLECTION AND TARGET REFINEMENT

A total of 543 compounds annotated with IC₅₀ values for human HDAC3 were downloaded from the ChEMBL database (<https://www.ebi.ac.uk/chembl/>) [406]. and submitted for data pre-processing. First, the compounds without definite IC₅₀ values were discarded. Second, the salt components were removed from the compounds with the “SaltRemover” function of RDKit. The compounds were then neutralized and canonicalized by the “Uncharged” and “standardize smiles” methods of MolVS (version 0.1.1). Third, for any compound with multiple IC₅₀ values determined by different bioassays, de-duplication was applied by averaging the IC₅₀ values as its bioactivity. Thus, 476 compounds were extracted as training set. For test set, anti-depressive drugs were collected from ChEMBL Database. After removing duplications and other filters, a total of 239 compounds were selected as test set.

3.9.2. MOLECULAR DESCRIPTORS CALCULATION

Apart from the descriptors-based molecular features, two types of fingerprints were calculated with RDKit (version 2019.9.3) and used for modeling, i.e., MACCS keys (166 bits) and Morgan2 fingerprints (1024 bits). Unlike descriptors, no feature selection was applied to molecular fingerprints [407].

3.9.3. MACHINE LEARNING MODEL PREPERATION

Compounds having the highest inhibitory effect that is $IC_{50} < 40$ nM were classified as inhibitor/actives, while the compounds having weak inhibitory potential that is $IC_{50} > 40$ nM were classified as non-inhibitor/decoys. In order to compute the 2D and 3D chemical, physical, and geometrical properties freely available software and tools were used such as DataWarrior (<http://www.openmolecules.org/datawarrior/>) [408] from openmolecules and ACD ChemSketch (<https://www.acdlabs.com/resources/freeware/chemsketch/>) [409] used to draw the chemical structure and to calculate molecular properties. Machine learning models were applied to test set data in order to compute their binding effect with the help of freely available software Weka 3.8 (<https://www.cs.waikato.ac.nz/ml/weka/>) developed by The University of Waikato (New Zealand) [39]. Weka developed four classification model based on different algorithms which are as follow random forest model, deep learning model, logistic model, and k-star model.

3.9.4. ADMET ANALYSIS AND BLOOD BRAIN BARRIER PREDICTION

Pharmacokinetic and pharmacodynamics properties were used to study the pharmacological action of compounds administered to a particular cell. The compounds obtained from data sorting and filtering were subjected to analyze ADMET properties, bioactivity score, and BBB permeability using different online web servers, such as LightBBB (<http://bioanalysis.cau.ac.kr:7030/>) [410], CBLigand (<https://www.cbligand.org/BBB/>) [411], and admetSAR (<http://lmmd.ecust.edu.cn/admetSar2/>) [412]. Further structural comparison

between HDAC10 control drug, namely pracinostat and selected anti-depressive drugs were calculated with the help of ChemMine tools (<https://chemminetools.ucr.edu/>) [413].

3.9.5. MOLECULAR DOCKING AND MOLECULAR DYNAMIC SIMULATION

In order to check the binding efficiency of filtered compounds with HDAC10, molecular docking studies were performed with the help of freely available web service Webina 1.0.3 (<https://durrantlab.pitt.edu/webina/>) [414]. Total binding energy and binding pose of ligand to specific HDAC were examined carefully. Before docking studies, ligand set preparation is done with the help of the OpenBabel tool (http://openbabel.org/wiki/Main_Page) [415], which converts the ligand format from mol to mol2.

3.10. STATISTICAL ANALYSIS

All the data are expressed as mean + SEM. The statistical measurement was done using one way ANOVA followed by Tukey's multiple comparison test. The statistically significant values were considered for $p < 0.05$.

CHAPTER IV

CREB1^{K292} and HINFP^{K330} as Putative Common Therapeutic Targets in Alzheimer's and Parkinson's Disease

CHAPTER IV: CREB1^{K292} AND HINFP^{K330} AS PUTATIVE COMMON THERAPEUTIC TARGETS IN ALZHEIMER'S AND PARKINSON'S DISEASE

4. INTRODUCTION

Integration of omics data and deciphering the mechanism of a biological regulatory network could be a promising approach to reveal the molecular mechanism involved in the progression of complex diseases, including AD and PD. Despite having an overlapping mechanism in the etiology of AD and PD, the exact mechanism and signaling molecules behind them are still unknown. Further, the acetylation mechanism and HDAC enzymes provide a positive direction towards studying shared phenomenon between AD and PD pathogenesis. For instance, increased expression of HDACs causes a decrease in protein acetylation status, resulting in decreased cognitive and memory function. Herein, we employed an integrative approach to analyze the transcriptomics data that established a potential relationship between AD and PD. Data preprocessing and analysis of four publicly available microarray datasets revealed 10 HUB proteins, namely CDC42, CD44, FGFR1, MYO5A, NUMA1, TUBB4B ARHGEF9, USP5, INPP5D, and NUP93 that may be involved in the shared mechanism of AD and PD pathogenesis. Further, we identified the relationship between the HUB proteins and TFs that could be involved in the overlapping mechanism of AD and PD. CREB1 and HINFP were the crucial regulatory TFs that were involved in the AD and PD crosstalk. Further, lysine acetylation sites and HDAC enzyme prediction revealed the involvement of 15 and 27 potential lysine residues of CREB1 and HINFP, respectively. Our results highlighted the importance of HDAC1(K292) and HDAC6(K330) association with CREB1 and HINFP, respectively, in AD and PD crosstalk. In conclusion, our study potentially highlighted the crucial proteins, TFs, biological pathways, lysine residues, and HDAC enzymes shared between AD and PD at the molecular level. The findings can be used to study molecular studies to identify the possible relation in AD-PD crosstalk.

4.1. RESULTS AND DISCUSSION

4.1.1. TRANSCRIPTOMICS SIGNATURES INVOLVED IN ALZHEIMER'S AND PARKINSON'S PATHOLOGY

The obtained datasets were normalized through quantile normalization and log₂ transformation. Statistically, in microarray data, the intensity values are relative numbers, and thus log₂ transformation is necessary to make variations similar across the order of magnitude. Boxplots of data before normalization and after normalization were prepared to check the background corrections in the datasets [Annexure 1]. Further, independent histograms of normalized data with a color intensity such as green for control and red for the disease were prepared to check the variation in the required datasets [Annexure 2(A)]. Our results identified 4736 (GSE7621), 2961 (GSE19587), 1989 (GSE1297), and 3634 (GSE28146) DEGs [Table 4.1]. Independent volcano plots of different datasets were used to measure the extent of DEGs in AD and PD [Annexure 2(B)]. After identifying DEGs, the probe IDs were converted into respective gene symbols, and then Venn analysis of DEGs was performed. Venn analysis results demonstrated 579 DEGs in AD while 406 DEGs in PD.

Table 4.1: Datasets obtained from the gene expression omnibus database for Alzheimer's and Parkinson's disease

GEO Accession Number	Platform	Total Samples	Control Samples	Disease Samples	Total DEGs	Upregulated DEGs	Downregulated DEGs
Alzheimer's Disease							
GSE1297	Affymetrix Human Genome U133A Array	31	9	22	1989	949	1040
GSE28146	Affymetrix Human Genome U133 Plus 2.0 Array	30	8	22	3634	1718	1916
Parkinson's Disease							
GSE7621	Affymetrix Human Genome U133 Plus 2.0 Array	25	9	16	4736	2508	2228
GSE19587	Affymetrix Human Genome U133A 2.0 Array	22	10	12	2961	1457	1504

4.1.2. PROTEIN-PROTEIN INTERACTION NETWORK IN ALZHEIMER'S AND PARKINSON'S DISEASE

PPI interaction analysis confirmed the presence of 492 proteins with 2335 physical interactions and 311 proteins and 1014 physical interactions in the AD and PD network, respectively. The clustering coefficient of AD and PD networks was found to be 0.244 and 0.248, which implies the higher co-expression of DEGs in AD networking than PD networking. Further, the characteristic path length of AD and PD networks are 3.504 and 3.390, respectively. Herein, the network centralization was found to be 0.107 and 0.200, whereas, the network heterogeneity was found to be 1.028 and 1.057 for AD and PD PPIs network, respectively. The analysis found out that the network density of AD and PD networks is 0.019 and 0.021, respectively, which implements that particular node in the PD PPI network has more participants compared to the AD PPI network [**Figure 4.1**].

Further, network biology using PPI networking becomes the important tool to establish a relationship between two proteins and identify the interactive pattern of proteomics data [416]. In addition, PPI networking provides an in-depth understanding of the biological characteristics of proteins encoded through DEG's and helps in estimating their biological significance [417]. PPI network is characterized by the presence of nodes and edges along with other topological features, namely clustering coefficient, characteristics path length, network density, and network centralization [418]. The protein in the networks were represented as nodes marked in a circle, while their biological association with other proteins were represented as edges marked as lines [419]. The clustering of the network determines the extent up to which genes in the network co-expressed in biological conditions based on distance calculation. Thus, the higher the clustering coefficient, the lower the probability of proteins co-expressing in the biological network [420]. Characteristic path length denotes the best possible configuration of the biological network [421] [**Table 4.2**].

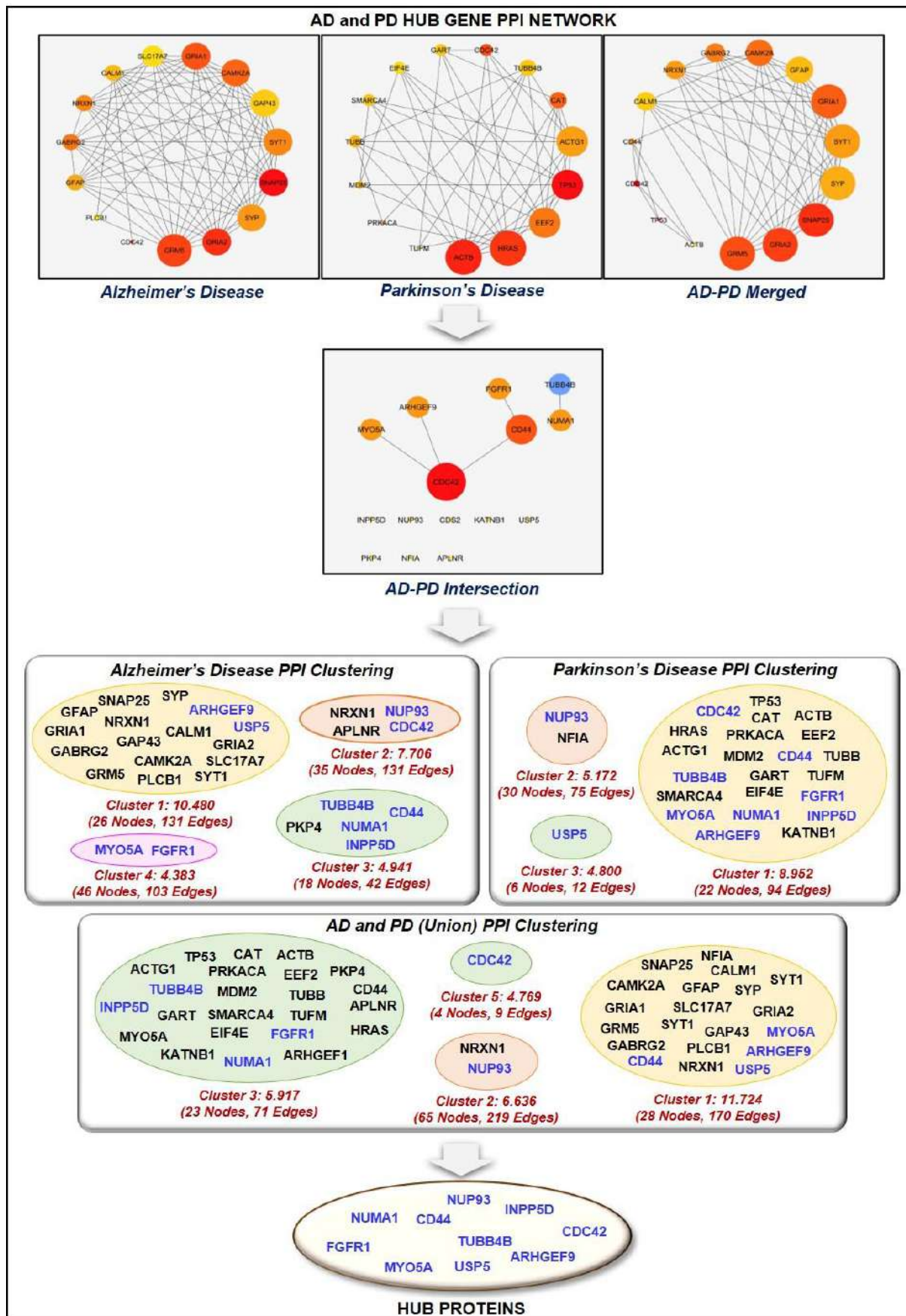


Figure 4.1: It represents the protein-protein interaction network of the top 15 ranked or HUB genes involved in Alzheimer's disease, Parkinson's disease, Alzheimer's disease-Parkinson's disease union merged

network, and Alzheimer's disease-Parkinson's disease intersection merged network. Further, the top 15 proteins of the individual network were mapped against the clusters of AD, PD, AD-PD intersection, and AD-PD union network to extract HUB proteins.

Network homogeneity refers to non-uniformity in character [422,423], while network centralization or centrality identifies the network's essential vertices or proteins [424,425]. Another essential feature of biological networks is network density, which measures the average number of connections of a particular protein or node divided by the total number of participant proteins in the network [426]. Statistically, the topological coefficient is a relative measure for the extent to which a particular protein in the given network shares neighbors with other proteins. The proteins that have one or no neighbors are assigned a topological coefficient of zero [427]. The topological analysis of the PPI network provides a way to identify HUB proteins, which pass signaling stimulus to other proteins or nodes in the network. Subsequently, HUB proteins were identified based on topological features of the PPT network, especially node degree (number of proteins interact with single protein), which may serve as potential biomarkers in AD and PD therapeutics.

Table 4.2: (A) Parameters and characteristics features of complex Alzheimer's disease, Parkinson's disease, Alzheimer's-Parkinson's disease intersection network, and Alzheimer's-Parkinson's disease union networks; (B) characteristic features of top 5 ranked clusters from Alzheimer's disease, Parkinson's disease, Alzheimer's-Parkinson's disease merged network; (C) parameters of HUB genes protein-protein interaction network

Network	Nodes	Edges	Clustering Coefficient	Network Density	Network Heterogeneity	Network Centralization	Characteristics Path Length
(A) CHARACTERISTICS FEATURES OF CORE PPI NETWORK							
AD	492	2335	0.244	0.019	1.028	0.107	3.504
PD	311	1014	0.248	0.021	1.057	0.2	3.39
AD-PD	784	3344	0.243	0.011	1.091	0.1	3.878
COMMON	19	5	0	0.029	1.556	0.154	1.727
(B) CHARACTERISTICS FEATURES OF AP, PD, and AD-PD CLUSTERS PPI NETWORK							
B.1 Alzheimer's Disease							
Cluster 1 (12.847)	188	1214	0.412	0.069	0.877	0.265	2.586
Cluster 2 (8.47)	148	631	0.334	0.058	0.782	0.155	2.67
Cluster 3 (7.553)	205	778	0.345	0.037	0.813	0.155	3.163
Cluster 4 (5.531)	80	224	0.406	0.071	1.023	0.447	2.553
Cluster 5 (4.897)	28	71	0.469	0.188	0.745	0.316	2.225
B.2 Parkinson's Disease							

Cluster 1 (7.974)	152	610	0.39	0.053	0.983	0.402	2.559
Cluster 2 (5.856)	96	284	0.294	0.062	0.709	0.141	2.849
Cluster 3 (4.239)	91	195	0.32	0.048	0.828	0.144	3.274
Cluster 4 (2.963)	26	40	0.246	0.123	0.704	0.17	2.975
Cluster 5 (2.629)	34	36	0.415	0.082	0.899	0.267	3.449
B.3 AD-PD Merged Union Network							
Cluster 1 (12.947)	188	1214	0.412	0.069	0.877	0.265	2.586
Cluster 2 (8.216)	147	608	0.335	0.057	0.787	0.158	2.697
Cluster 3 (7.703)	342	1321	0.347	0.023	0.874	0.175	3.499
Cluster 4 (5.557)	211	589	0.309	0.027	0.834	0.122	3.735
Cluster 5 (4.479)	145	327	0.344	0.031	1.078	0.306	3.518
(C) CHARACTERISTICS FEATURES OF AP, PD, and AD-PD HUB GENES PPI NETWORK							
AD	15	76	0.841	0.724	0.33	0.236	1.314
PD	15	47	0.594	0.448	0.38	0.308	1.59
AD-PD	15	58	0.845	0.552	0.345	0.187	1.667
COMMON	15	5	0	0.048	1.304	0.192	1.727

4.1.3. PROTEIN-PROTEIN INTERACTION NETWORK CLUSTERING AND PROTEOMIC SIGNATURES IN ALZHEIMER'S AND PARKINSON'S PATHOGENESIS

The merging of two PPI networks was done in two steps. In the first step, the PPIs network of AD and PD were combined by the union to ensure complete coverage of relevant proteins involved in the study, followed by extracting common proteins (nodes) of individual PPIs networks. AD-PD union PPI network consists of 784 proteins and 3344 physical/functional interactions, while the AD-PD intersection biological network consists of 19 proteins and 5 physical/functional interactions [Figure 4.1]. The top 15 highly connected proteins of individual AD, PD, AD-PD (union), and AD-PD (intersection) PPI networks were extracted. The HUB proteins were marked according to their presence in the respective PPI cluster. CDC42, CD44, FGFR1, MYO5A, NUMA1, TUBB4B, ARHGEF9, USP5, INPP5D, and NUP93 were found to be the most prominent proteins found in clusters of AD, PD, and AD-PD (union) PPIs networks [Table 4.3].

Table 4.3: List of HUB genes identified in different protein-protein interaction networks and list of common proteins that were found in the cluster of all three protein-protein interaction networks such as Alzheimer's disease, Parkinson's disease, and Alzheimer's-Parkinson's disease union network

	Rank	HUB Genes	Alzheimer's Disease	Parkinson's Disease	Merged Network (Intersection)	Frequency
Alzheimer's Disease	1	SNAP25	Cluster 1		Cluster 1	2
	2	CDC42	Cluster 2	Cluster 1	Cluster 5	3
	3	GRIA2	Cluster 1		Cluster 1	2
	4	GRM5	Cluster 1		Cluster 1	2
	5	GRIA1	Cluster 1		Cluster 1	2
	6	CAMK2A	Cluster 1		Cluster 1	2
	7	GABRG2	Cluster 1		Cluster 1	2
	8	SYT1	Cluster 1		Cluster 1	2
	9	NRXN1	Cluster 1		Cluster 2	2
	10	SYP	Cluster 1		Cluster 1	2
	11	GFAP	Cluster 1		Cluster 1	2
	12	CALM1	Cluster 1		Cluster 1	2
	13	GAP43	Cluster 1		Cluster 1	2
	14	SLC17A7	Cluster 1		Cluster 1	2
	15	PLCB1	Cluster 1		Cluster 1	2
Parkinson's Disease	1	TP53		Cluster 1	Cluster 3	2
	2	ACTB		Cluster 1	Cluster 3	2
	3	HRAS		Cluster 1	Cluster 3	2
	4	CDC42	Cluster 2	Cluster 1	Cluster 5	3
	5	CAT		Cluster 1	Cluster 3	2
	6	EEF2		Cluster 1	Cluster 3	2
	7	PRKACA		Cluster 1	Cluster 3	2
	8	ACTG1		Cluster 1	Cluster 3	2
	9	TUBB		Cluster 1	Cluster 3	2
	10	MDM2		Cluster 1	Cluster 3	2
	11	GART		Cluster 1	Cluster 3	2
	12	TUBB4B	Cluster 3	Cluster 1	Cluster 3	3
	13	SMARCA4		Cluster 1	Cluster 3	2
	14	TUFM		Cluster 1	Cluster 3	2
	15	EIF4E		Cluster 1	Cluster 3	2
Merged Network (Union)	1	CDC42	Cluster 2	Cluster 1	Cluster 5	3
	2	TP53		Cluster 1	Cluster 3	2
	3	SNAP25	Cluster 1		Cluster 1	2
	4	GRIA2	Cluster 1		Cluster 1	2
	5	GRM5	Cluster 1		Cluster 1	2
	6	GRIA1	Cluster 1		Cluster 1	2
	7	CAMK2A	Cluster 1		Cluster 1	2
	8	GABRG2	Cluster 1		Cluster 1	2
	9	CD44	Cluster 3	Cluster 1	Cluster 1	3
	10	NRXN1	Cluster 1		Cluster 1	2
	11	SYT1	Cluster 1		Cluster 1	2
	12	SYP	Cluster 1		Cluster 1	2
	13	GFAP	Cluster 1		Cluster 1	2
	14	CALM1	Cluster 4		Cluster 1	2

Merged Network (Intersection)	15	ACTB		Cluster 1	Cluster 3	2
	1	CDC42	Cluster 2	Cluster 1	Cluster 5	3
	2	CD44	Cluster 3	Cluster 1	Cluster 1	3
	3	FGFR1	Cluster 4	Cluster 1	Cluster 3	3
	4	MYO5A	Cluster 4	Cluster 1	Cluster 1	3
	5	NUMA1	Cluster 3	Cluster 1	Cluster 3	3
	6	TUBB4B	Cluster 3	Cluster 1	Cluster 3	3
	7	ARHGEF9	Cluster 1	Cluster 1	Cluster 1	3
	8	CDS2				0
	9	KATNB1		Cluster 1	Cluster 3	2
	10	USP5	Cluster 1	Cluster 3	Cluster 1	3
	11	PKP4	Cluster 3		Cluster 3	2
	12	NFIA	Cluster 1	Cluster 2	Cluster 1	3
	13	APLN	Cluster 2		Cluster 3	2
	14	INPP5D	Cluster 3	Cluster 1	Cluster 3	3
15	NUP93	Cluster 2	Cluster 2	Cluster 2	3	

Table 4.4 describes the role of HUB proteins in the pathogenesis of AD and PD. Here, our network analysis study demonstrates the involvement of CDC42, CD44, FGFR1, MYO5A, NUMA1, TUBB4B, ARHGEF9, USP5, INPP5D, and NUP93 in the onset and progression of AD and PD. Studies demonstrated that these proteins were associated with different biological processes. For instance, activation of FAK/Rac1/CDC42-GTPase signaling rescued impaired microglial migration response to A β 42 in triggering receptor expressed on myeloid cells 2 loss-of-function [428]. Similarly, inhibition of FGFR1 effectively blocked the GLP-promoted NPC proliferation in the mouse model of AD [429]. However, the exact role of FGFR1 and CDC42 in AD and PD crosstalk is still missing. In addition, Lim et al., 2018 concluded that CD44 activates tau pathology, whereas, Neal et al., 2018 concluded that GPNMB attenuates astrocyte inflammatory response through CD44 receptor [430,431]. Further, loss of MYO5A resulted in structural and functional alterations in the rat brain through alterations in dopamine metabolism, whereas TUBB4B may be a part of the signaling cascade involved in the etiology of PD and is related to inflammatory response [432]. ARHGEF9 that encodes collybistin involved in the postsynaptic clustering of glycine and inhibitor gamma-aminobutyric acid receptors [433]. Further, Griffin et al., 2020 concluded the upregulation of ARHGEF9 during astroglia response to A β oligomers [434].

Table 4.4: Role of HUB genes in the pathogenesis of Alzheimer's disease and Parkinson's disease identified with the help of MalaCards

HUB Genes	Description	Involvement in Alzheimer's Disease	Involvement in Parkinson's Disease
CDC42	Cell Division Cycle 42	Establishment of neuron polarity, regulation of cell morphology and mortality, and cell-cycle regulation	Inhibits the activating features of microglia
TUBB4B	Tubulin Beta 4B	Regulates inflammatory response	Serve as a target for PD associated toxins
CD44	CD44 Molecule (Indian Blood Group)	Interacts with mutant p53 activity	Causes α -Synuclein induced migration of BV-2 microglial cells
FGFR1	Fibroblast Growth Factor Receptor 1	Involved in axonal projection and inhibits the apoptosis	Elevate the DA levels and protects the specific midbrain neurons
MYO5A	Myosin VA (Heavy Chain, Myosin)	Induced cell motility	Mutant MYO5A exhibits alterations in dopamine metabolism
NUMA1	Nuclear Mitotic Apparatus Protein 1	Identify transported MSC in the brain	Help in mitotic spindle formation
ARHGEF9	CDC42 Guanine Nucleotide Exchange Factor (GEF) 9	Role in integrin signaling and axon guidance signaling	Encodes synaptic proteins and loss of function results in intellectual disability
USP5	Ubiquitin Specific Peptidase 5	Compromised tau levels	Deletion causes increased p53 activity
INPP5D	Inositol Polyphosphate-5-Phosphatase, 145kDa	Modulating Inflammatory Response	Involved in immune response
NUP93	Nucleoporin 93kDa	Promotes nuclear accumulation of mRNA	Inhibits mRNA transport

USP5, a stress granule protein, increases TNF- α expression through the ubiquitin-proteasome pathway and regulates inflammatory response through Smurf1 [435]. Recently, Tsai et al., 2021 demonstrated that INPP5D was positively associated with amyloid plaque density in the human brain [436]. Thus, these evidences concluded that the above-mentioned HUB proteins are associated with neurological disease in some manner through regulation of different biological phenomena, yet their relationship in AD and PD crosstalk is still missing. Further, HUB proteins, namely NUMA1 and NUP93, lack the potential involvement in the pathogenesis of either AD and PD.

4.1.4. FUNCTIONAL ENRICHMENT ANALYSIS OF HUB PROTEINS IN ALZHEIMER'S AND PARKINSON'S PATHOLOGY

To identify the complicated relationship between highly dense connected components of PPI networks (AD, PD, AD-PD union, and AD-PD intersection), pathway analysis and GO analysis was performed. Moreover, we extracted the top 10 biological pathways, cellular components, and molecular functions of highly interconnected proteins involved in neurodegeneration, as demonstrated in **Figure 4.2**. Moreover, after GO analysis, the extracted highly interconnected proteins were subjected to pathway analysis, which enables to identification of the molecular pathway followed by the interconnected proteins in the progression of AD and PD. **Figure 4.2** demonstrates the top 10 biological pathways in which these proteins were involved. Gap junction (TUBB4B), GnRH signaling pathway (CDC42), and Rap1 signaling pathway (CDC42 and FGFR1) were critical pathways in which HUB proteins were involved and maybe potential biological pathway targets for AD and PD crosstalk. For instance, Esteves et al., 2017 demonstrated that nicotine effectively prevented prefrontal long-term potentiation and memory deficits induced by streptozotocin in AD [437], whereas, Carvajal-Oliveros et al., 2021 demonstrated that nicotine suppresses PD like phenotype induced by synphilin-1 overexpression through increased dopamine levels [438]. Similarly, a study concluded that balance between dopamine and adenosine signals regulates the PKA/Rap1 pathway in spiny neurons, where D1R and A2AR agonist enhanced PKA-mediated Rap1 phosphorylation *in vivo* and *in vitro* [439]. Further, studies demonstrated that impaired GnRH production is directly linked to oxidative stress and mitochondrial dysfunction in neurons [440,441]. Another significantly enriched pathway is the gap junction that is involved in the pathogenesis of AD and PD [442,443]. For instance, Angeli et al., 2020 demonstrated the altered expression of glial gap junction proteins, namely Cx43, Cx30, and Cx47 in the 5XFAD model of AD [444], whereas, Maulik et al., 2020 concluded that A β regulates gap junction protein connexin 43 in

cultured primary astrocytes [445]. Consistent with this, the results demonstrated the importance of CDC42, TUBB4B, and FGFR1 in the pathogenesis of AD and PD. Further, these three HUB proteins were a potential target for identifying the relationship between AD and PD.

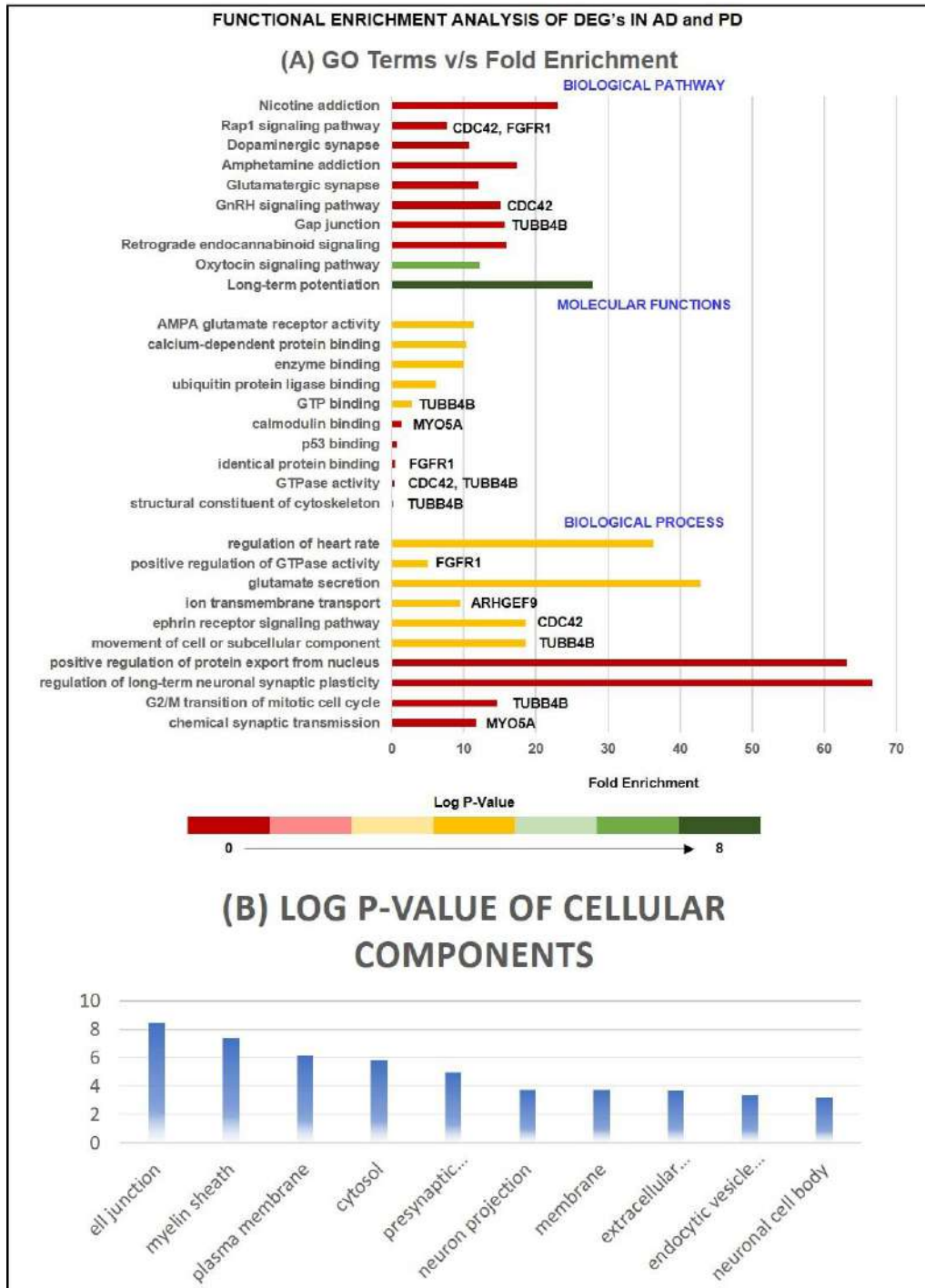


Figure 4.2: Represents the bar graph of the top 10 biological processes, molecular functions, and biological pathways of HUB proteins along with their p-value and involved HUB proteins. The axis of the bar represents the p-value. The figures also represent the critical cellular components in which HUB proteins lie with their corresponding p-value. Terms with a P-value ≤ 0.05 were considered as significant.

4.1.5. TRANSCRIPTION FACTORS ASSOCIATED WITH HUB PROTEINS

Further, we identified HUB proteins-TF interaction and detected central regulatory molecules using topological features. Thus, we extracted seven regulatory TFs, namely FOXC1 (8), GATA2 (5), CREB1 (4), FOXL1 (3), NFIC (3), HINFP (3), and SREBF1 (3). Subsequently, the cross-validation of TFs in the pathogenesis of AD and PD was identified with the help of MalaCards. TFs are transcriptional regulators that are involved in the pathogenesis of AD and PD [446–449]. In this study, we also studied the potential relationship between TFs and HUB proteins in order to identify mutual transcriptional regulators of identified HUB proteins. The identified TFs are FOXC1, GATA2, CREB1, FOXL1, NFIC, HINFP, and SREBF1 as a regulator of HUB proteins commonly expressed in AD and PD pathogenesis [Figure 4.3]. For instance, Xu et al., 2019 concluded that deletion of CREB1 diminishes the effect of DJ1 on TH regulation through deregulation of CaMKK β /CaMIV/CREB1 pathway [450]. Similarly, deletion of CREB1 promotes pro-inflammatory changes in the mouse hippocampus [451]. Moreover, He et al., 2021 concluded that deacetylation of EZH2 through SIRT6 causes an increased association between EZH2 and FOXC1 that exerts anti-inflammatory response, whereas, Emelyanove et al., 2018 concluded the positive correlation between dopamine and GATA2 expression in PD [452,453]. FOXL1 is implemented in the pathogenesis of NDDs, while, NFIC was identified as novel loci in the AD [454–456]. Studies demonstrated that HINFP is a co-activator in the sterol regulated transcription of PCSK9, a target gene of SREBP2 involved in the tau alterations, which contribute to disturbed cholesterol homeostasis in AD [457][458]. Lastly, genetic mutation analysis concluded that genetic polymorphism rs11868035 was associated with susceptibility to PD in the Chinese population [459,460]. Thus, the evidences mentioned above prove the potential link of identified TFs in the progression and pathogenesis of AD and PD and acts as a specific biomarker for their therapeutics. However, their potential role in AD and PD crosstalk is still missing.

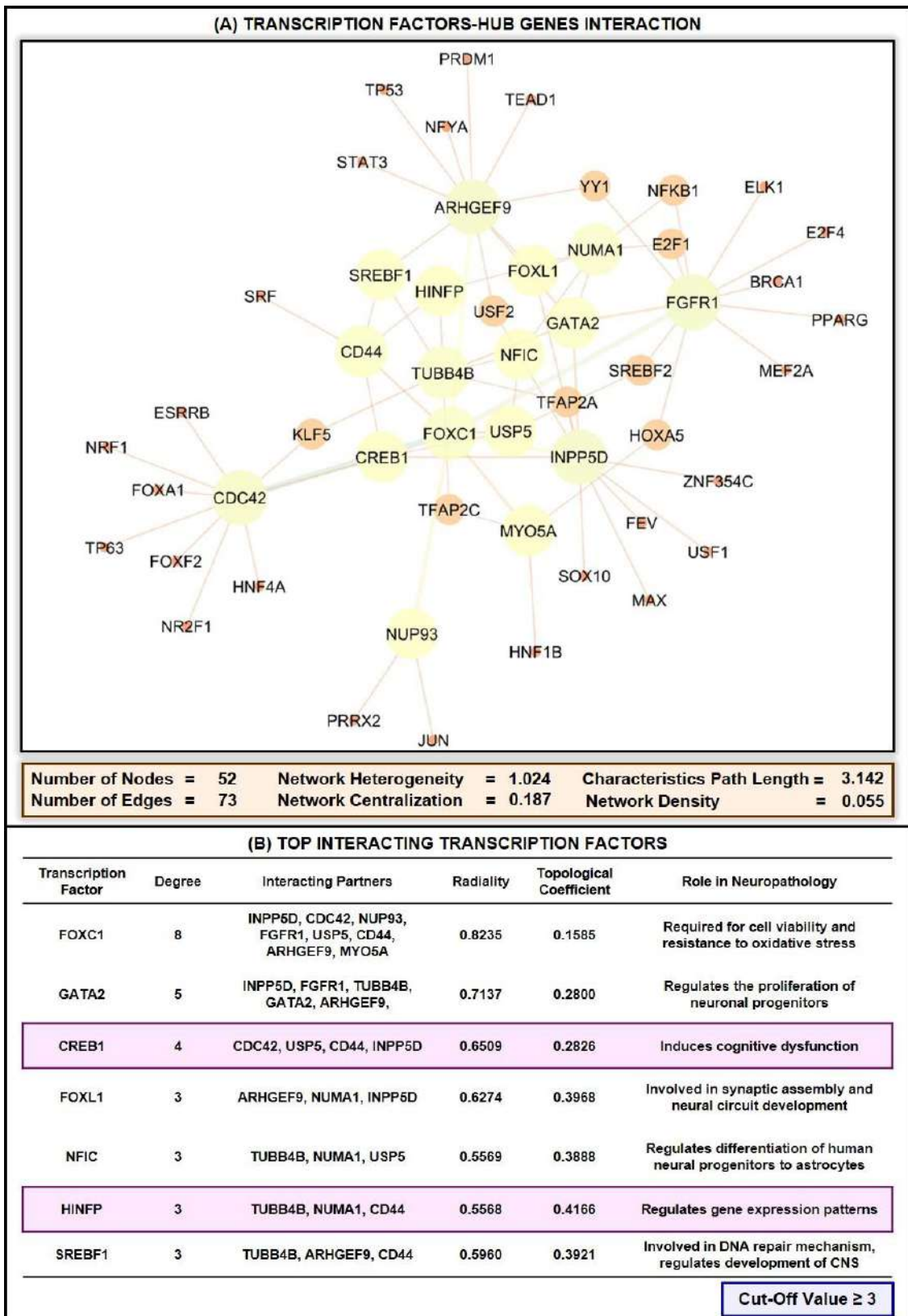


Figure 4.3: Part A of the figure represents the PPI network of HUB genes with associated regulatory transcription factors. FGFR1 with the highest degree of node interacts with 12 transcription factors such as BRCA1, FOXC1, GATA2, YY1, MEF2A, HOXA5, PPARG, E2F1, NFKB1, ELK1, SREBF2, and E2F4. Similarly, INPP5D and ARHGEF9 interact with ten transcription factors each such as FEV, ZNF354C, CREB1, FOXC1, GATA2, FOXL1, TFAP2A, MAX, USF1, USP2, SOX10, and FOXC1, GATA2, FOXL1, YY1,

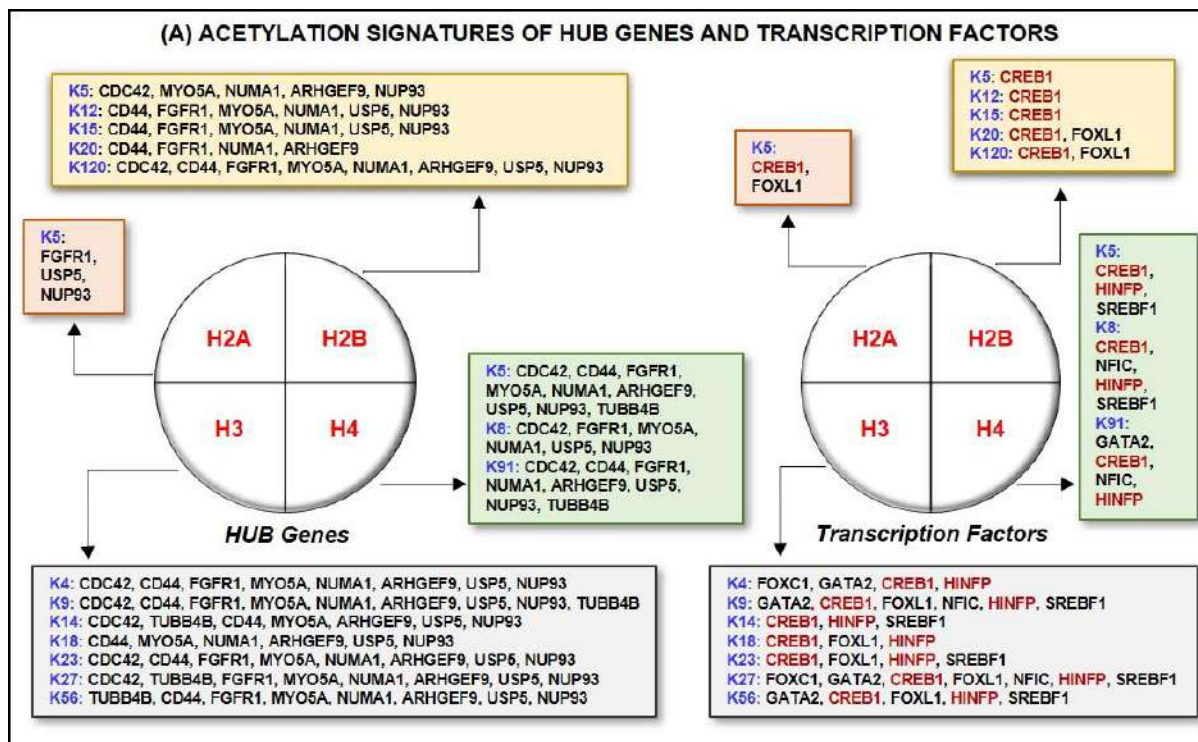
NFYA, STAT3, TP53, USF2, SREBF1, TEAD1, PRDM1 respectively. Moreover, the HUB gene CDC42 (10), TUBB4B (7), and NUMA1 (6) involved in the PPI network of HUB genes and transcription factors. CDC42 interacts with NR2F1, CREB1, FOXC1, HNF4A, KLF5, FOXF2, TP63, FOXA1, NRF1, and ESRRB, TUBB4B interacts with GATA2, NFIC, HINFP, TFAP2A, KLF5, SREBF1, and TFAP2C, and NUMA1 interacts with GATA2, FOXL1, NFIC, E2F1, HINFP, and NFKB1. Further analysis revealed that CD44 interacts with CREB1, FOXC1, SRF, HINFP, and SREBF1 while USP5 and MYO5A interact with CREB1, FOXC1, NFIC, SREBF2, and FOXC1, HOXA5, TFAP2C, HNF1B, respectively. Further analysis shows the interaction of NUP93 with three transcription factors, such as PRRX2, JUN, and FOXC1. Among the transcription factors, FOXC1 (8) has the highest degree of node followed by GATA2 (5), CREB1 (4), FOXL1 (3), NFIC (3), HINFP (3), and SREBF1 (3). FOXC1 forms biological association with INPP5D, CDC42, NUP93, FGFR1, USP5, CD44, ARHGEF9, MYO5A, while GATA2 interacts with INPP5D, FGFR1, TUBB4B, GATA2, ARHGEF9. Similarly, CREB1 interacts with CDC42, USP5, CD44, INPP5D, FOXL1 interacts with ARHGEF9, NUMA1, INPP5D, NFIC interacts with TUBB4B, NUMA1, USP5, HINFP interacting partners are TUBB4B, NUMA1, CD44, and SREBF1 interacts with TUBB4B, ARHGEF9, CD44. the total number of nodes and edges in HUB genes and transcription factors protein-protein interaction network are 52 and 73. the other parameters of the biological network are network heterogeneity (1.024), network centralization (0.187), network density (0.055), and characteristics path length (3.142). Part B of the figure demonstrated the biological significance of top interacting transcription factors in the progression of Alzheimer's disease and Parkinson's disease along with their degree of node and interacting partners. The figure also reflects the radiality and topological coefficient of the top-ranked transcription factors in the protein-protein interaction network.

4.1.6. CELLULAR LOCATION AND ACETYLATION SIGNATURES OF HUB PROTEINS AND TRANSCRIPTION FACTORS IN ALZHEIMER'S AND PARKINSON'S DISEASE

Herein, we analyzed the cellular location of HUB proteins with CELLO version 2.5: subCELLular LOcalization predictor. Among the extracted 10 HUB proteins, 40% were cytoplasmic proteins, 50% were nuclear protein, and 10% were extracellular proteins. CD44 (1.974), FGFR1 (2.078), INPP5D (3.954), MYO5A (3.300), and NUMA1 (1.858) were predicted as nuclear proteins, while CDC42 (2.037) was predicted as extracellular protein. Similarly, ARHGEF (2.770), NUP93 (2.534), TUBB4B (3.682), and USP5 (2.207) were predicted as cytoplasmic proteins. Studies demonstrated that acetylation activates STAT3 through the nuclear translocation of CD44, whereas, acetylation of histone proteins controls FGFR1 polymorphisms and isoform splicing [461,462]. In addition, lysine acetylation of SCF FBXL19 ubiquitin E3 ligase increases its activity and stabilization that targets CDC42 for its ubiquitination and degradation [463].

HUB genes and TFs were analyzed for their acetylation signature to understand the involvement of acetylation and deacetylation process associated with HUB genes and TFs in the pathogenesis of AD and PD. Herein, CDC42 (10), CD44 (11), FGFR1 (11), MYO5A (13),

NUMA1 (14), ARHGEF9 (11), USP5 (14), and NUP93 (15) were predicted as the most non-histone acetylating substrates among HUB proteins, while CREB1 (16) and HINFP (10) were predicted as non-histone acetylating substrates among TFs [Figure 4.4]. Lately, to study the epigenetic regulation of HUB proteins and TFs, we investigated histone modification sites found in the coding region of HUB proteins and TFs implicated with NDDs and identified a range of sites [464,465]. Thus, this raises the possibility that PTMs, namely acetylation, deacetylation, ubiquitination, SUMOylation, methylation, and others, are the primary means of alteration in these proteins that need further investigation.



(B) RELATIVE EXPRESSION OF GENES WITH RESPECT TO HISTONE ACETYLATION

Genes	CDC42	TUBB4B	CD44	FGFR1	NUMA1	NFIA	INPP5D	NUP93	USP5	ARHGEF9	MYO5A
H2AK5	0	0	0	0.091	0	0	0	0.178	0.178	0	0
H2BK5	0.393	0	0	0	0.393	0	0	0.393	0	0.393	0.393
H2BK12	0	0	0.314	0.239	0.314	0	0	0.135	0.314	0	0.314
H2BK15	0	0	0.2	0.153	0.2	0	0	0.152	0.2	0	0.2
H2BK20	0	0	0.0965	0.096	0	0	0	0	0	0.096	0
H2BK120	0.348	0	0.348	0.174	0.174	0	0	0.347	0.174	0.174	0.174
H3K4	0.337	0	0.202	0.282	0.282	0	0	0.282	0.282	0.282	0.282
H3K9	0.584	0.239	0.252	0.269	0	0.584	0.212	0.251	0.584	0	0.584
H3K14	0.177	0.177	0.403	0	0	0	0	0.403	0.177	0.177	0.403
H3K18	0.366	0	0.484	0	0.484	0.439	0	0.484	0.484	0.484	0.484
H3K23	0	0	0	0	0.171	0	0.171	0.171	0.171	0	0.194
H3K27	0.513	0.234	0	0.236	0.294	0.294	0.513	0.513	0.513	0.513	0.513
H3K56	0	0.387	0.29	0	0.387	0.289	0	0.387	0.289	0.3871	0.387
H4K5	0.485	0.485	0.262	0.485	0.485	0.485	0	0.485	0.485	0.485	0.485
H4K8	0.516	0	0	0.516	0.516	0	0	0.229	0.516	0	0.516
H4K91	0.295	0	0.236	0.295	0.236	0.295	0.236	0.295	0.236	0.295	0

Figure 4.4: Part A of the figure denotes the acetylation signatures of non-histone protein substrates, such as HUB genes and transcription factors. CREB1 and HINFP are the most prominent acetylated transcription factors, whereas, CDC42, CD44, TUBB4B are the most crucial non-histone protein acetylated substrates. Additionally, part B of the figure represents the relative expression of substrate with respect to change in histone acetylation status at particular lysine residue in a tabular format.

Further, histone acetylation signatures are primarily related to the markers of activity at regulatory elements, namely promoters and enhancers [466]. Moreover, understanding the specific role of histone acetylation at different genomic elements has the potential to improve disease therapeutics through increasing the target specificity [467]. In addition, histone signatures enable to understand the biological phenomenon, namely chromosome packaging, transcriptional activation, and DNA packaging.

4.1.7. POTENTIAL LYSINE RESIDUES FOR PROTEIN ACETYLATION

Correlation between acetylation and HDAC enzymes has been studied extensively in the past [291,468,469]. For instance, MS-275, a class I HDAC inhibitor, promotes rapid acetylation of the YB-1 RNA-binding protein at K81 [470], whereas, HDAC1 complex is able to regulate histone H3 acetylation at K18 [471]. Further, Topuz et al., 2019 demonstrated that administration of HDAC inhibitor, namely NaB increases H2B acetylation at K5 that leads to increased spatial learning and long-term memory in rat hippocampus [472]. Similarly, Choi et al., 2017 demonstrated that increased acetylation of peroxiredoxin 1 at K197 through HDAC6 inhibition leads to recovery of A β -induced impaired axonal transport [473]. In addition, the role of SIRT1 in regulating pathogenic tau acetylation at K174 and in suppressing the spread of tau pathology has been demonstrated in a mouse model of tauopathy [474]. Thus, based on the above-mentioned evidences we identified acetylation sites and HDAC enzymes of CREB1 and HINFP through two online tools, namely MuSite deep and PSKAcePred. For MuSite Deep, statistically, a high confidence score relates to the high probability of lysine acetylation at a particular lysine amino acid. A score above 0.5 is considered as a high confidence score and a high probability of lysine acetylation, whereas, score below 0.2 is considered as a low confidence score where the probability of lysine acetylation is negligible, and a score between 0.2 to 0.5 is considered as the site with moderate probability. Further, for PSKAcePred, a score above 0.7 is considered a high confidence score, and the probability of lysine acetylation is

very high, whereas, a score between 0.5 to 0.7 is considered a moderate confidence score, and the probability of lysine acetylation is relatively less as compared to acetylation at high confidence score lysine site. CREB1 peptide sequence (P16220.2) has 15 potential acetylating lysine residues. The respective acetylation-sites prediction scores, with the help of MuSite deep and PSKAcePred, as shown in **Annexure 3**. MuSite predicted K330 as an essential lysine acetylation site with a high confidence score of 0.557. similarly, PSKAcePred predicted K94, K292, K303, K304, and K309 as potential protein acetylation-lysine residues with a high confidence score of 0.872, 0.737, 0.856, 0.924, and 0.994, respectively. From the protein acetylation-site prediction of CREB1, it may be concluded that K304, K309, and K330 were essential acetylating lysine residues. The type of HDAC enzymes involved in the deacetylation of CREB1 was predicted and found out that HDAC1, HDAC2, and SIRT7 were important in CREB1 deacetylation where HDAC1 was involved in K292 (3.35) deacetylation, HDAC2 involved in K330 (10.67), and SIRT7 involved in K94 (13.26), K303 (12.54), and K304 (12.90) deacetylation. The results demonstrated that the binding propensity of SIRT7 and HDAC2 is very low as compared to the binding propensity of HDAC1. Thus, the results show that K292 is a critical lysine residue for CREB1 acetylation and deacetylation process with HDAC1 is its deacetylating enzyme involved in the pathogenesis of AD and PD. In addition, Hassen et al., 2019 [475] demonstrated the acetylation of CREB1 at K330 and K136, whereas, Paz et al., 2014 demonstrated that sirtuin 1 directly downregulates the CREB transcriptional activity by binding and deacetylating CREB at K136, thereby reducing CREB interaction with CBP [476]. Further, Lu et al., 2003 confirmed the acetylation of CREB1 at K91, K94, and K136 within the activation domain through CBP. However, they also concluded that that single mutation of the putative CBP acetylation sites has no significant effect on the transactivation potential of CREB [477]. Thus, these evidences suggest the possibility of CREB1 acetylation and its binding with HDAC enzymes in regulation of gene transcription.

Moreover, HINFP (AAH17234.1) consists of 27 potential lysine-acetylating residues such as K6, K10, K31, K94, K96, K164, K174, K181, K185, K197, K213, K236, K256, K285, K294, K301, K330, K335, K346, K352, K366, K367, K371, K382, K439, K446, and K504 as observed from **Annexure 4**. MuSite Deep predicted all 27 sites as potential lysine-acetylating residues with no residue of high confidence score. However, five sites were predicted as potential acetylation sites with a moderate score, such as K6: 0.318, K213: 0.311, K330: 0.420, K371: 0.354, and K382: 0.269. Thus, predicted acetylation sites were essential for triggering protein acetylation results in transcription initiation. Among the predicted acetylating-lysine residues, HDAC6 (K6 and K330), HDAC1 (K382), and SIRT1 (K371) were important deacetylating residues involved in protein deacetylation resulted in the progression of AD and PD. However, the binding score of HDAC6 (2.74 and 3.84) was predicted higher than HDAC1 (6.53) and SIRT1 (7.01). Similarly, PSKAcePred predicted 15 potential lysine-acetylating sites in which 8 sites were predicted as potential lysine acetylation sites with a high confidence score. K31: 0.730, K96: 0.766, K174: 0.779, K330: 0.726, K335: 0.930, K367: 0.904, K371: 0.911, and K446: 0.719. Further, the HDAC enzyme prediction tool predicted that SIRT1 (K31:6.51 and K371:7.01), SIRT2 (K446:0.95), SIRT7 (K174:13.26), HDAC1 (K367:4.23), and HDAC6 (K330:3.84 and K335:2.74) were crucial enzymes involved in the regulation of HINFP deacetylating activity. A comparative analysis of both the acetylation prediction tools and the type of deacetylating enzyme reflected that K330 and K371 were crucial protein acetylating-lysine residue with HDAC6 and SIRT1 as its interacting partners. However, the confidence score of SIRT1 is lower than HDAC6, while the confidence of K330 is higher than that of K371. Thus, it will be concluded that K330 interacts with HDAC6 to carry out HINFP deacetylation in AD and PD progression. Further, till now, no proteomic study has evident the implementation of acetylation sites and HDAC binding residue in the activation domain of HINFP. However, mounting evidence suggests that HAT1, an acetyltransferase binding to

HINFP promoters, have specific stimulatory effect on H4 gene transcription. In addition, the authors concluded that HAT1 promotes the accumulation of newly synthesized H4 dimers without affecting levels of histones embedded in nucleosome [478]. Another study concluded that HINFP forms a functional complex with NPAT that recruits HAT cofactor TRRAP to facilitate the histone 4 acetylation at PCSK9 promoter[458]. Thus, this *in-silico* analysis could be a milestone in providing an avenue for identifying crucial acetylation or deacetylation patterns of CREB1 and HINFP to minimize AD and PD progression [Table 4.5].

Table 4.5: List of common crucial lysine residues in CREB1 and HINFP

CREB1	
Lysine Residue	Interactor
K94	SIRT7
K292	HDAC1
K303	SIRT7
K304	SIRT7
HINFP	
K31	SIRT1
K174	SIRT7
K330	HDAC6
K335	HDAC6
K367	HDAC1
K371	SIRT1

4.1.8. CONSERVED AMINO ACID RESIDUES AT PROTEIN ACETYLATION SITES

The predicted protein acetylation sites were analyzed for the conserved lysine residues, which could be crucial for lysine selectivity and specificity for the acetylation process and binding of deacetylating enzymes. CREB1 has 15 potential lysine residues represented by 16220.2, while

HINFP has 27 potential lysine residues represented by AAH17234.1. The MSA analysis of predicted lysine residues for acetylation revealed the conservation of negative charged glutamic acid (E) and neutrally charged leucine (L), methionine (M), valine (V), and glutamine (Q) in close association with the positively charged lysine residue as shown in **Figure 4.5**. These conserved residues provided the suitable environment and favorable conditions for associated potential lysine residues for the acetylation process, thus imparting lysine selectivity and specificity for the acetylation and deacetylation. However, further investigations are required to excavate the potential of conserved residues in the acetylation and deacetylation process of CREB1 and HINFP. However, glutamic acid is most prominent compared to other conserved amino acids as it will decrease the overall positive charge of lysine and impart a negative charge to the lysine site that will promote acetylation and deacetylation reactions. For instance, Nguyen et al., 2016 concluded that glutamine triggers acetylation-dependent degradation of glutamine synthetase, whereas, Son et al., 2020 demonstrated that leucine regulates autophagy through acetylation of the mammalian target of rapamycin complex 1 [479,480]. Moreover, the role of methionine involvement on lysine acetylation is not studied so far in AD and PD, but yet at the same time demonstrated the potential relationship between methionine and lysine acetylation in other neurological defects. For instance, Chiki et al., 2021 concluded that the presence of oxidation of methionine at position 8 and acetylation at K6 resulted in dramatic inhibition of Httex1 fibrilization [481]. Thus, these studies correlate with our results and suggest that glutamic acid (E), leucine (L), methionine (M), valine (V), and glutamine (Q) could be critical amino acid residues in acetylation and HDAC binding.

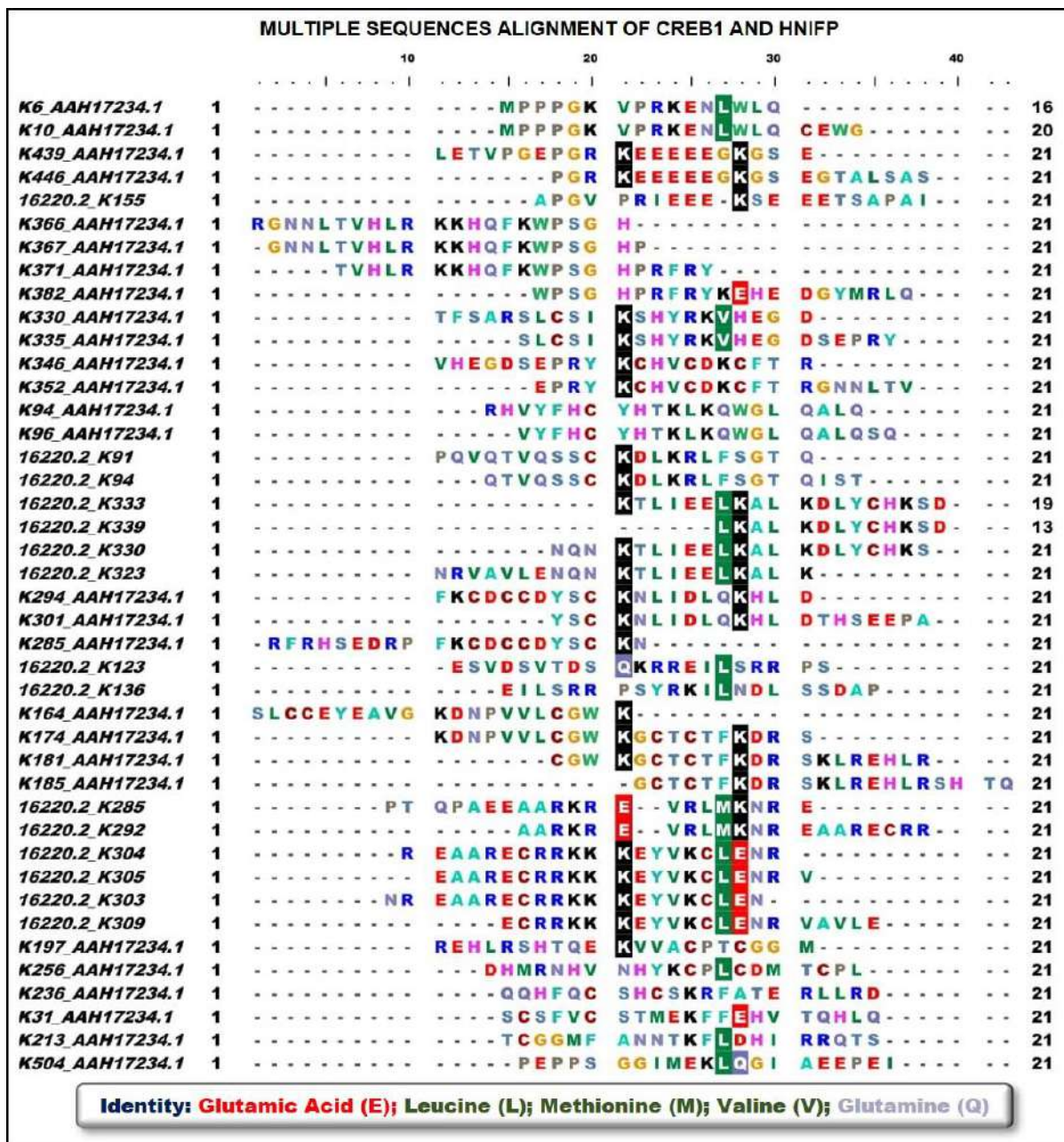


Figure 4.5: Multiple sequence analysis of potential acetylation/deacetylation-lysine residues by taking 21 window sizes. 21 window size was taken by lysine at the center and placed ten amino acids on both sides.

Further, structural information of CREB reveals that it consists of 11 exons and 3 isoforms that are produced through alternative splicing [482]. Primary structure studies of CREB identified the presence of four functional domains, namely Q1 basal transcriptional activity domain, kinase inducible domain, a glutamine-rich region, and basic region/leucine zipper domain [483]. Thus, this relates to the importance of glutamine in the structural activity of CREB1. Similarly, structural information of HINFP concludes the interaction of HINFP produced TF

with methyl-CpG-binding protein-2, a component of the HDAC complex and plays an important role in transcription repression. Sekimata et al., 2004 demonstrated that HINFP, through its DNA-binding activity, acts as a sequence-specific (conserved CGGAC core) transcriptional repressor [484], whereas, Medina et al., 2008 concluded that PSCR motif is required for activation of histone H4 gene transcription and promotes its binding with DNA [485]. Further, the study revealed the presence of acetylated H4 histone in the binding activity of HINFP to USF and GAL4-AH [486]. In addition, a study concluded that lysine residues control the conformational dynamics of proteins [487]. Thus, it is equally important to identify the structural features of CREB1 and HINFP that were involved in the acetylation mechanism. Thus, the potential and possible acetylation-lysine residues were analyzed for their structural selectivity for lysine recognition pattern and potential deacetylating enzyme attachment, as discussed in **Table 4.6**. The structural pattern of the putative deacetylating enzyme attachment binding to potential acetylation or deacetylation lysine residues revealed the presence of alpha-helix, strand, and coil region in the CREB1 and HINFP peptide. However, an in-depth analysis of the structural configuration of CREB1 and HINFP revealed that the helix region is predominant over the strand/coil region in the acetylation of CREB1. Study by Maltsev et al., 2012 concluded the involvement of helix structure in the acetylation process, where acetylation increases α -helicity of the first six residues of α -synuclein [488]. Similarly, the coil region is dominant over the helix/strand region in the potential lysine-acetylation of HINFP. The results correlates the study by Kulemziana et al., 2016, which concluded that lysine acetylation promotes interaction between Smc coiled coils interaction that is required for cohesion ring assembly [489]. Further, the results were analyzed precisely and revealed the involvement of structural selectivity in acetylation and deacetylation of CREB1 and HINFP. In addition, the results also provide an avenue of helix and coil region in the acetylation of predicted lysine residues of CREB1 and HINFP, respectively.

Table 4.6: Secondary structure of the protein acetylation sites predicted by PSIPRED: protein structure prediction server

CREB1			HNIFP					
Residue	Structure Prediction (PSIPRED)	Score (10)	Residue	Structure Prediction (PSIPRED)	Score (10)	Residue	Structure Prediction (PSIPRED)	Score (10)
91	Coil	4	6	Coil	9	301	Helix	9
94	Strand	3	10	Coil	8	330	Helix	3
123	Helix	8	31	Helix	6	335	Coil	5
136	Helix	9	94	Coil	8	346	Strand	4
155	Coil	5	96	Coil	1	352	Coil	9
285	Helix	9	164	Coil	8	366	Helix	3
292	Helix	9	174	Coil	9	367	Coil	1
303	Helix	9	181	Coil	4	371	Coil	9
304	Helix	9	185	Coil	1	382	Coil	4
305	Helix	9	197	Coil	9	439	Helix	6
309	Helix	9	213	Coil	6	446	Coil	9
323	Helix	9	236	Coil	8	504	Helix	9
330	Helix	9	256	Coil	8			
333	Helix	9	285	Coil	5			
339	Coil	0	294	Strand	1			

4.2. CONCLUSION AND SUMMARY

In conclusion, the present study focuses on the crosstalk between AD and PD at the molecular level. Through this study, we identified the relationship between DEG's, HUB proteins, TFs, acetylation, and HDAC enzymes in the shared pathogenesis of AD and PD. Our findings highlighted the crucial role of CDC42, TUBB4B, and FGFR1 in the AD and PD crosstalk through Gap junction (TUBB4B), GnRH signaling pathway (CDC42), and Rap1 signaling pathway (CDC42 and FGFR1). In addition, the present study identified the potential TFs that regulate the expression of HUB proteins at the transcriptional level through biological network analysis. Our analysis identified FOXC1, GATA2, CREB1, FOXL1, NFIC, HINFP, and SREBF1 as potential TFs that regulate the activity of HUB proteins shared between AD and PD. Our bioinformatic analysis also revealed the effect of subcellular localization of HUB proteins and TFs in the AD and PD crosstalk. Lately, the study identified the 15 potential lysine residues and 27 potential lysine residues in CREB1 and HINFP, respectively. The study

revealed that among 15 possible lysine residues of CREB1, only 4 lysine residues, namely K91, K94, K136, and K330 had been studied in the past, while K123, K155, K285, K292, K303, K304, K305, K309, K323, K333, and K339 have been reported first time for their role in acetylation process. Similarly, among HINFP, all 27 lysine residues have been reported for the first time. Further, *in-silico* analysis of CREB1 and HINFP revealed the importance of HDAC1 for its deacetylation activity at K292 of CREB1 and HDAC6 for its deacetylation activity at K330 of HINFP. This will provide a way to study the role of acetylation and HDAC enzymes in the transcriptional activity of CREB1 and HINFP in AD and PD crosstalk. Further, the computational analysis identified the importance of negative charged glutamic acid (E) and neutrally charged leucine (L), methionine (M), valine (V), and glutamine (Q) amino acid residues in the acetylation mechanism of CREB1 and HINFP in AD and PD crosstalk. The study also highlighted the importance of the helix region over the strand/coil region in the acetylation of CREB1. Similarly, the coil region is dominant over the helix/strand region in the potential lysine-acetylation of HINFP. Thus, this study highlighted the importance of two prominent biological pathways for the progression of AD and PD simultaneously, such as HDAC1-CREB1-TUBB4B/CDC42/CD44 and HDAC6-HINFP-TUBB4B/CDC42/CD44 [Figure 4.6]. Further studies are required to generate the potential treatments targeting the above-mentioned biological pathways to treat AD and PD's adverse effects. However, the current study is associated with some sort of limitation as the study uses only microarray data, which is not as comprehensive as transcriptomics data analysis. Thus, there is a growing need to simultaneously analyze the different types of AD and PD datasets, namely microarray data, epigenetic data, and RNA data, to extract the novel biomarkers involved in disease pathology.

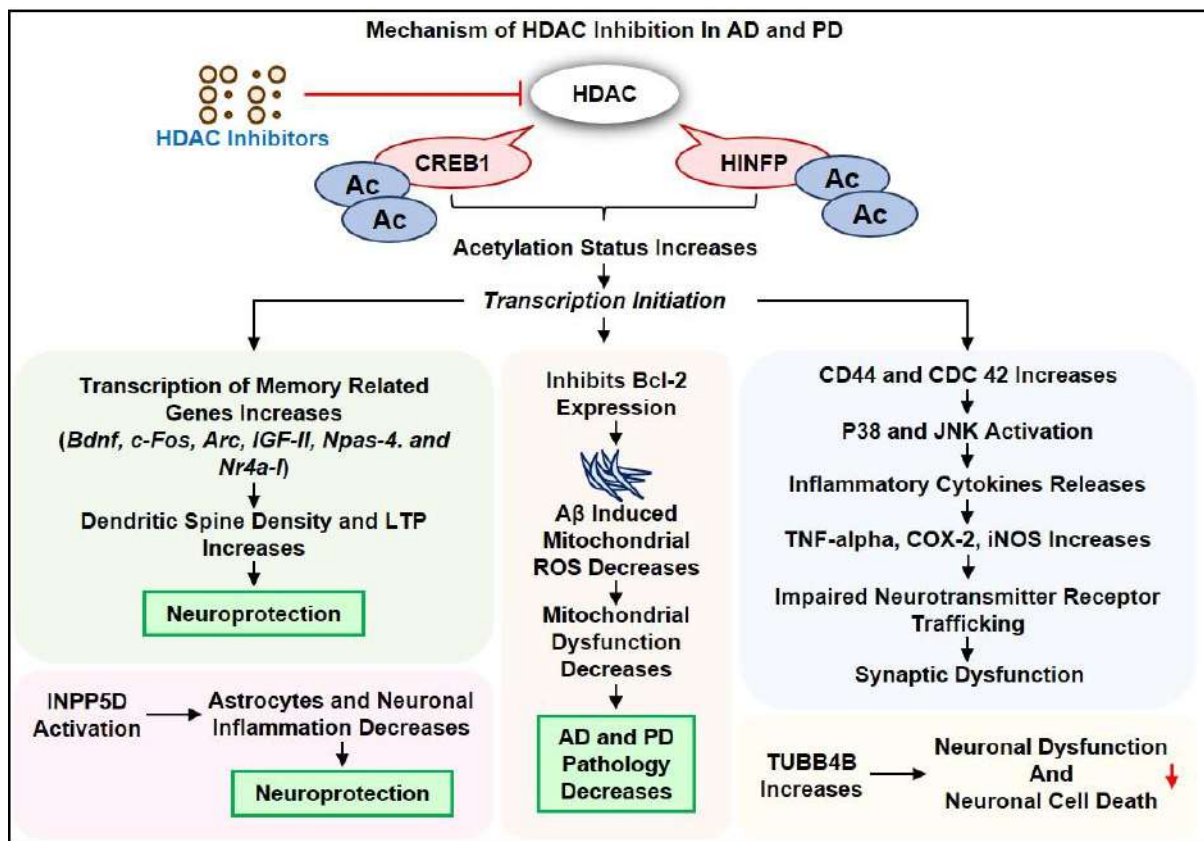


Figure 4.6: Literature validation of the involvement of HDAC interaction with CREB1 and HINFP. HDAC inhibitors cause a decrease in HDAC activity followed by the increased acetylation status of CREB1, and HINFP causes positive transcriptional regulation. Increased transcriptional activity causes an increase in transcription of memory associated genes, and Bcl-2 expression leads to an increase in cognitive function and memory function. The increased acetylation status of CREB1 and HINFP causes INPP5D and TUBB4B activation, which decreases neuronal cell death and leads to neuroprotection.

4.3. HIGHLIGHTS OF THE STUDY

- 4.3.1. TUBB4B, CDC42, and CD44 were identified as common molecules in AD and PD
- 4.3.2. CREB1 and HINFP are promising regulatory molecule involved in disease progression
- 4.3.3. K292 and K330 are crucial protein lysine-acetylation sites for CREB1 and HINFP respectively
- 4.3.4. Glutamic acid (E), leucine (L), methionine (M), valine (V), and glutamine (Q) are conserved amino acid residues that facilitates protein acetylation/deacetylation
- 4.3.5. Involvement of alpha-helix (CREB1) and coil (HINFP) in the structural selectivity for acetylation and deacetylation activity
- 4.3.6. Identified HDAC1-CREB1-TUBB4B/CDC42/CD44 and HDAC6-HINFP-TUBB4B/CDC42/CD44 as a promising target pathway

CHAPTER V

Computational Analysis Indicates That PARP1 Acts as a Histone Deacetylases Interactor Sharing Common Lysine Residues for Acetylation, Ubiquitination, and SUMOylation in Alzheimer's and Parkinson's Disease

CHAPTER V: COMPUTATIONAL ANALYSIS INDICATES THAT PARP1 ACTS AS A HISTONE DEACETYLASES INTERACTOR SHARING COMMON LYSINE RESIDUES FOR ACETYLATION, UBIQUITINATION, AND SUMOYLATION IN ALZHEIMER'S AND PARKINSON'S DISEASE

5. INTRODUCTION

Lysine residues are known for the PTMs acetylation, ubiquitination, and SUMOylation. In acetylation, HDAC and its interactors cause transcriptional deregulation, and cause mitochondrial dysfunction, apoptosis, inflammatory response, and cell-cycle impairment, that cause brain homeostasis and neuronal cell death. Another regulatory PTMs involved in the pathogenesis of NDDs are ubiquitination and SUMOylation, for the degradation of the misfolded proteins. Thus, we aim to investigate the potential acetylation/ubiquitination/SUMOylation crosstalk sites in the HDAC interactors, which causes NDDs. Further, we aim to identify the influence of PTMs on structural features of proteins and the impact of putative lysine mutation on disease susceptibility. Lastly, we aim to examine the impact of the putative mutation on acetylated lysine for the ubiquitination and SUMOylation. Herein, we integrate 1455 genes, 3094 genes, and 1940 genes related to HDAC interactors, AD, and PD, respectively. Further, PPI network and PTMs integrations from different databases identified 32 proteins that are associated with HDAC, AD, and PD with 1489 potential lysine modified sites. HDAC interactors poly (ADP-ribose) polymerase 1 (PARP1), nucleophosmin (NPM1), and CDK1 involved in the progression of NDDs and 64% and 75% of PTM sites in PARP1, NPM1, and CDK1 fall into coiled and ordered regions, respectively. Moreover, 15 putative lysine sites have been found in crosstalk and K148, K249, K528, K637, K700, and K796 of PARP1 are crosstalk hotspots. Loss of acetylated hotspot sites results in loss of ubiquitination and SUMOylation function on nearby sites, which is relatively higher when compared to gain of function.

5.1. RESULTS AND DISCUSSION

5.1.1. INTEGRATION OF PROTEOMICS DATA AND POST-TRANSLATIONAL MODIFICATIONS SITES

After collecting data for HDAC interactors from two databases, such as HIPPIE and CTD, Venn analysis was performed to investigate the common interactors among both databases. 1657 proteins were obtained from HIPPIE, and 1804 proteins were collected from the CTD database. The HDAC interactors were associated with class I, class II, and class IV HDACs. Venn analysis demonstrated that there are 1455 (72.6%) proteins that were common in both the databases. Similarly, for AD and PD associated protein, data were collected from CTD and DisGeNET. In CTD, 23268 and 23680 proteins were associated with AD and PD, respectively, whereas, in DisGeNET, 3397 and 2078 proteins were involved in the pathogenesis of AD and PD, respectively. Further, Venn analysis demonstrated the involvement of 3094 (13.1%) and 1940 (8.1%) proteins that were common in both the databases. Furthermore, HDAC interactor, AD, and PD data were combined manually to check the common proteins among them. 185 proteins (7.7%) were found to be involved in the pathogenesis of AD and PD, which are associated with HDAC interactors **[Figure 5.1]**.

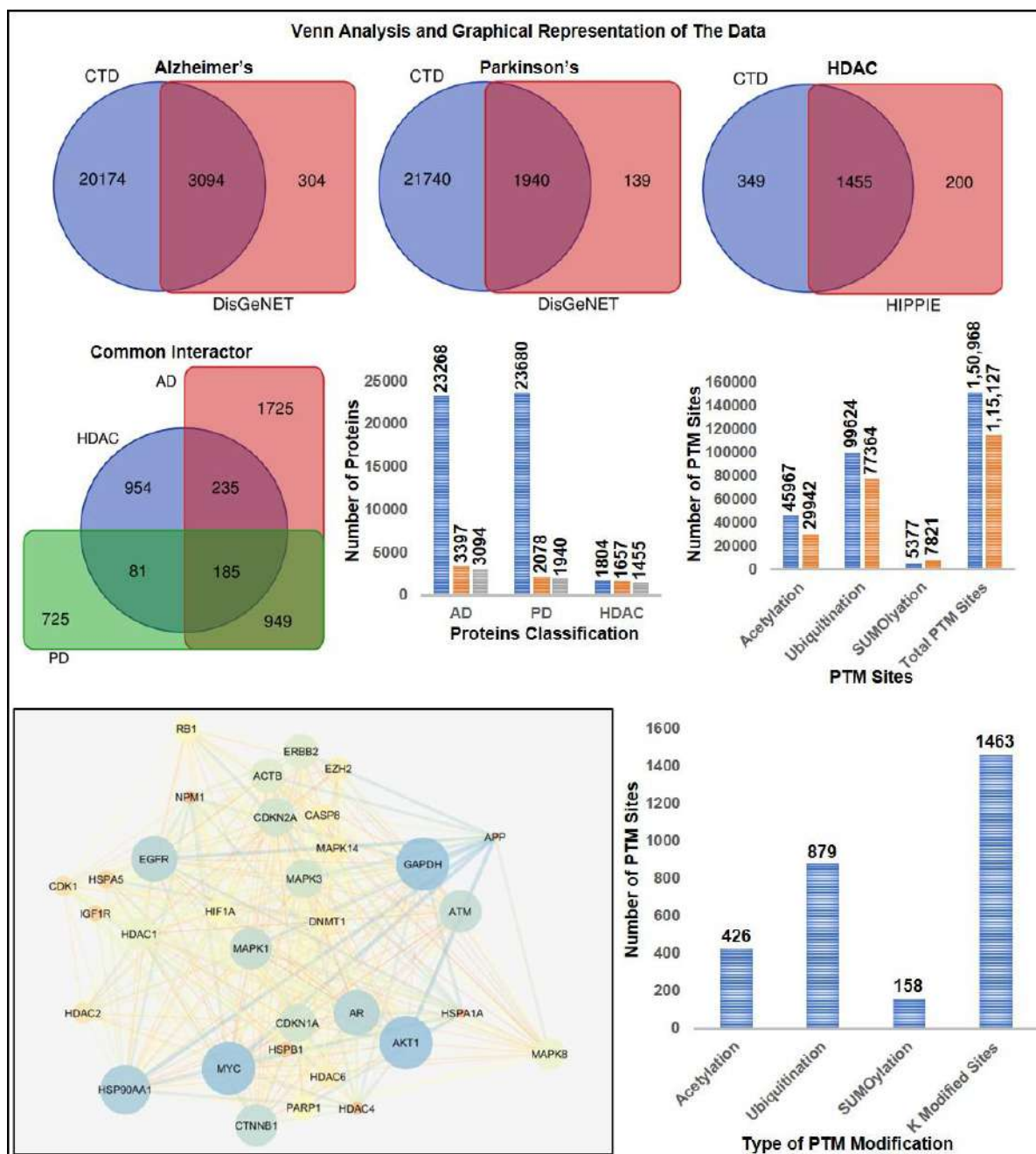


Figure 5.1: Interactive Venn analysis of AD, PD, and HDAC interactors collected during the data extraction from different databases. For AD and PD, databases such as CTD and DisGeNET were used, whereas HDAC interactors databases such as CTD and HIPPIE were used. The figure also shows the Venn analysis of common genes involved in AD, PD, and HDAC interactors. Later on, bar graph analysis of protein extracted from databases for AD, PD, and HDAC interactors was given in the figure. The blue colour in the graph represents the CTD database. The orange colour represents the DisGeNET database for AD and PD, whereas, the HIPPIE database for HDAC interactors. Similarly, grey colour represents the common among them. In the second bar graph, the blue colour denotes the dbPTM database, whereas the orange colour represents the PLMD database. PPI network of cluster 1 including 33 proteins extracted from the core PPI network after clustering analysis. Graphical representation of acetylation, ubiquitination, SUMOylation sites in protein present in the cluster 1.

Moreover, PPI network and clustering analysis demonstrated the involvement of 33 proteins as top-ranked proteins, which are associated with HDAC interactors and pathogenesis of NDDs. Further, 1,50,968 PTM sites and 1,15,127 PTM sites were collected from dbPTM database and PLMD database, respectively. A total of 45967 and 29942 acetylation sites, 99624 and 77364 ubiquitination sites, and 5377 and 7821 SUMOylation sites were extracted from the dbPTM and PLMD database. The extracted PTM sites were mapped to respective proteins. A total of 1463 potential acetylation (426), ubiquitination (879), and SUMOylation (158) sites were identified among 32 potential proteins for crosstalk analysis [Figure 5.1].

5.1.2. MOLECULAR FUNCTION AND BIOLOGICAL PATHWAYS OF TOP INTERACTING HDAC PARTNERS

A total of 33 proteins identified through clustering analysis involving HDAC interactors, AD, and PD were subjected to gene set enrichment analysis. Through this, molecular functions and biological processes involved in the pathogenesis of AD and PD through HDAC interaction were determined. The cut-off p-value for identifying molecular function and biological pathways was set at less than 0.05, as shown in Table 5.1.

Table 5.1: Functional enrichment analysis (biological pathways and molecular functions) involved in top interacting histone deacetylase interactors

Molecular Function	Number of Genes	Percentage of Genes	Fold Enrichment	P-Value	Mapped Genes
MOLECULAR FUNCTION					
Protein serine/threonine kinase activity	7	21.21	12.78	9.58384E-07	ATM; CDK1; MAPK8; AKT1; MAPK1; MAPK3; MAPK14;
Transcription regulator activity	6	18.18	3.96	0.0035	HDAC1; EZH2; HDAC2; HDAC4; RB1; HDAC6;
Transcription factor activity	2	6.06	1.31	0.45	MYC; HIF1A;
Transmembrane receptor protein tyrosine kinase activity	3	9.09	29.50	0.000142	IGF1R; ERBB2; EGFR;
Chaperone activity	5	15.15	21.83	3.04388E-06	HSPB1; HSPA5; NPM1; HSPA1A; HSP90AA1;
DNA-methyltransferase activity	1	3.03	138.29	0.0072	DNMT1;
BIOLOGICAL PATHWAY					
Glypican pathway	26	81.25	3.82	6.10568E-13	AR; HSPB1; ATM; CDK1 ; NPM1 ; CTNNB1; HSPA1A; MAPK8; MYC; IGF1R; HDAC1; HIF1A; APP; AKT1; HDAC2; CASP8; MAPK1; ERBB2; MAPK3; CDKN2A; RB1; HSP90AA1; EGFR; CDKN1A; GAPDH; MAPK14;
TRAIL signaling pathway	27	84.37	4.00	2.91586E-14	AR; HSPB1; ATM; CDK1 ; NPM1 ; CTNNB1; HSPA1A; MAPK8; MYC; IGF1R; HDAC1; PARP1 ; HIF1A;

					APP; AKT1; HDAC2; CASP8; MAPK1; ERBB2; MAPK3; CDKN2A; RB1; HSP90AA1; EGFR; CDKN1A; GAPDH; MAPK14;
Glypican 1 network	26	81.25	3.94	2.93211E-13	AR; HSPB1; ATM; CDK1 ; NPM1 ; CTNNB1; HSPA1A; MAPK8; MYC; IGF1R; HDAC1; HIF1A; APP; AKT1; HDAC2; CASP8; MAPK1; ERBB2; MAPK3; CDKN2A; RB1; HSP90AA1; EGFR; CDKN1A; GAPDH; MAPK14;
Integrin-linked kinase signaling	21	65.62	6.31	7.17368E-14	AR; HSPB1; ATM; CDK1 ; NPM1 ; CTNNB1; MAPK8; MYC; HDAC1; PARP1 ; HIF1A; AKT1; HDAC2; CASP8; MAPK1; MAPK3; CDKN2A; RB1; HSP90AA1; CDKN1A; MAPK14;
AP-1 transcription factor network	20	62.5	6.33	4.19493E-13	AR; HSPB1; ATM; CDK1 ; NPM1 ; CTNNB1; MAPK8; MYC; HDAC1; HIF1A; AKT1; HDAC2; CASP8; MAPK1; MAPK3; CDKN2A; RB1; HSP90AA1; CDKN1A; MAPK14;
Arf6 downstream pathway	25	78.12	3.82	3.54199E-12	AR; HSPB1; ATM; CDK1 ; NPM1 ; CTNNB1; HSPA1A; MAPK8; MYC; IGF1R; HDAC1; HIF1A; AKT1; HDAC2; CASP8; MAPK1; ERBB2; MAPK3; CDKN2A; RB1; HSP90AA1; EGFR; CDKN1A; GAPDH; MAPK14;

Among macular functions Protein serine/threonine kinase activity (21.21%), Transcription regulator activity (18.18%), Transcription factor activity (6.06%), Transmembrane receptor protein tyrosine kinase activity (9.09%), Chaperone activity (15.15%), DNA-methyltransferase activity (3.03%) was highly enriched having a p-value less than 0.05 [Figure 5.2 (A)]. Similarly, among different biological pathways, Glypican pathway (81.25%), TNF-related apoptosis-inducing ligand (TRAIL) signaling pathway (84.37%), Glypican 1 network (81.25%), Integrin-linked kinase signaling (65.62%), AP-1 transcription factor network (62.50%), and ADP-ribosylation factor 6 (Arf6) downstream pathway (78.12%) [Figure 5.2 (B)]. However, from table 5.1, it will be observed that only two pathways, such as the TRAIL signaling pathway and Integrin-linked kinase signaling, constitute nucleophosmin (NPM1), cyclin-dependent kinase 1 (CDK1), and PARP1 (highlight in blue script with a green fill). Thus, the above-said pathways were crucial in the AD and PD pathogenesis with HDAC interactors.

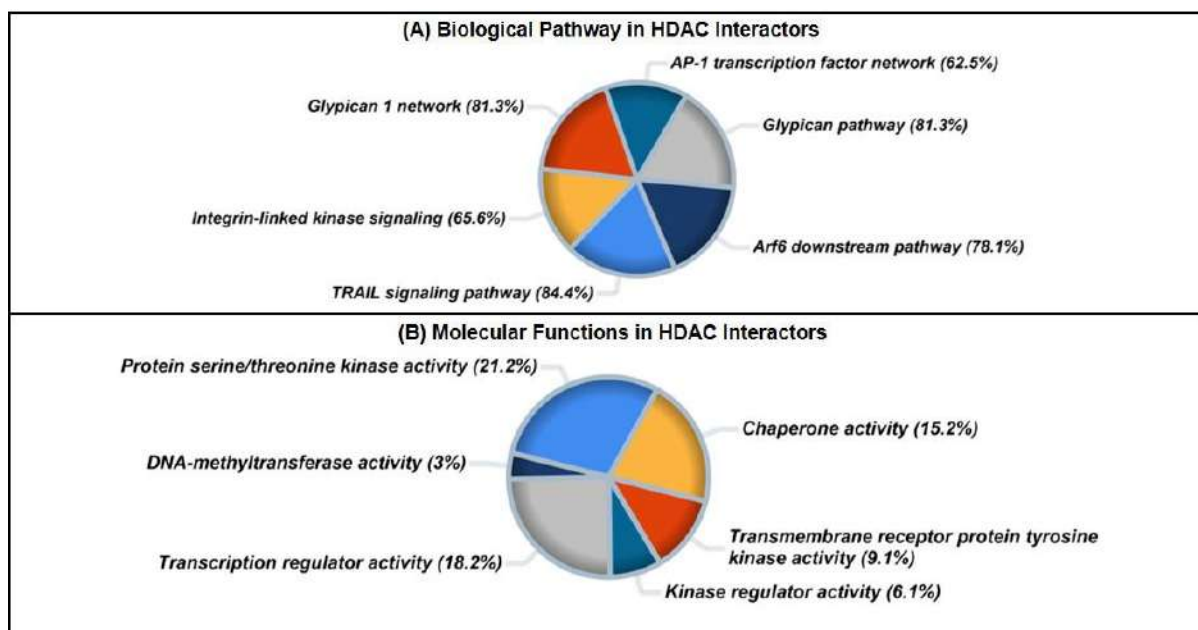


Figure 5.2: (A) Graphical representation of acetylation, ubiquitination, SUMOylation sites in protein present in the cluster 1 (B) Molecular functions of top 33 proteins involved in HDAC interactors, Alzheimer's and Parkinson's disease.

5.1.3. STRUCTURAL CHARACTERIZATION OF PARP1, NPM1, AND CDK1

For crosstalk analysis, a protein should be selected on the basis that the individual frequency of acetylation, ubiquitination, and SUMOylation is ≥ 10 [Table 5.2].

Table 5.2: List of histone deacetylase interactors having more than 50 lysine modified sites (acetylation, ubiquitination, and SUMOylation). The proteins marked in blue colour and filled with grey colour represents those proteins have individual acetylation, ubiquitination, and SUMOylation sites more than 10

	Acetylation	Ubiquitination	SUMOylation	K Modified Sites
HSP90AA1	50	101	4	155
DNMT1	44	94	8	146
PARP1	65	43	33	141
HSPA5	29	52	2	83
NPM1	27	27	26	80
HIF1A	9	61	5	75
ATM	5	69	1	75
HSPA1A	29	41	5	75
CDK1	15	42	15	72
GAPDH	27	26	6	59

Thus, PARP1, NPM1, and CDK1 were found to be the most prominent protein for crosstalk between acetylation, ubiquitination, and SUMOylation [Figure 5.3].

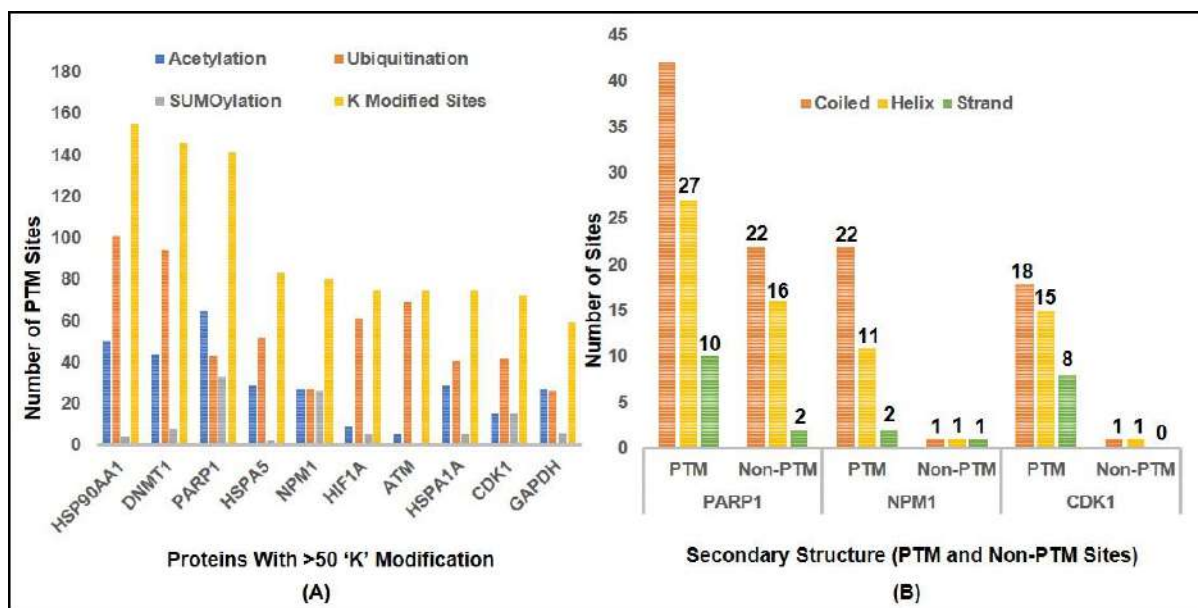


Figure 5.3: (A) Stack-bar representation of 'K' modified sites (B) Secondary-structure representation in PARP1, CDK1, and NPM1.

Secondary structure analysis of PARP1, NPM1, and CDK1 revealed the importance of coiled structure as compared to helix and strand in the PTM region. A coiled region regulates protein interactions and aggregation propensity, and thus mutations, which impair coiled regions, deregulate aggregation and protein activity, whereas, mutations, which increase coiled structure enhance aggregation propensity [490]. In PARP1, 42 PTM sites fall into the coiled region, whereas, 22 and 18 PTM sites formed a coiled structure in NPM1 and CDK1, respectively.

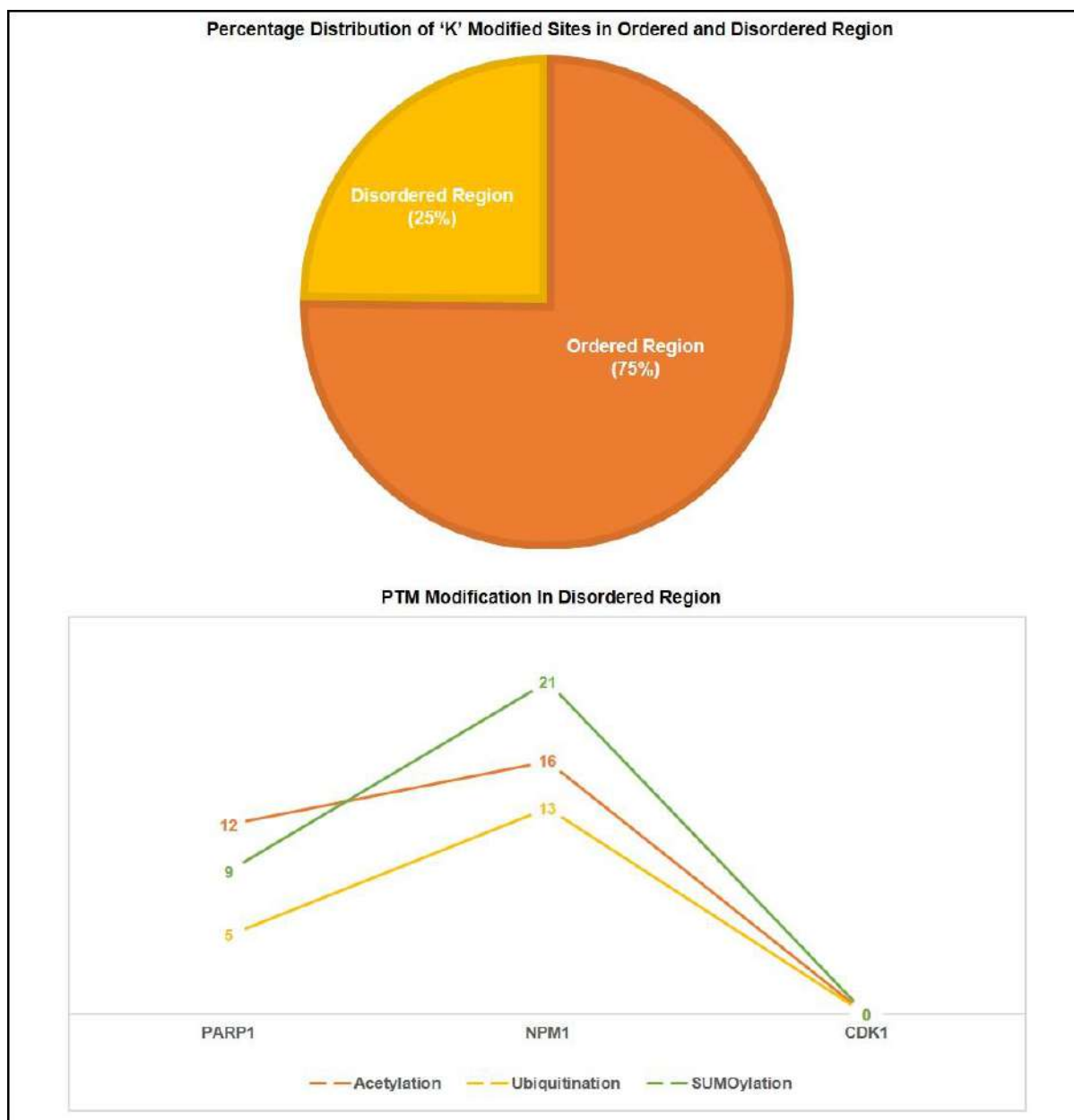


Figure 5.4: **Classification of PTM sites of PARP1, NPM1, and CDK1 into ordered and disordered region.**

Further, our analysis demonstrates that the frequency of helix structure is greater in PARP1 (27), NPM1 (11), and CDK1 (15) PTM sites as compared to non-PTM sites [Table 5.3]. However, in NPM1, the frequency of strands is almost equal in both PTM and non-PTM sites. Moreover, PTMs preferred disordered regions as compared to the ordered region, which affecting its functions and interactions. Further, the involvement of PTM in the disordered region influences disorder to order transition, thus altering protein's stability and its associated mechanisms.

Table 5.3: List of post-translational modification and non-post-translational modification sites of PARP1, NPM1 and CDK1 (histone deacetylase interactors) in coiled, helix, and strand region

	PARP1		NPM1		CDK1	
	PTM	Non-PTM	PTM	Non-PTM	PTM	Non-PTM
Coiled	42	22	22	1	18	1
Helix	27	16	11	1	15	1
Strand	10	2	2	1	8	0

This mechanism could be beneficial in diversifying the functional effect of protein by forming new structural sites or PPI by providing a binding region. Interestingly, our analysis of PTM sites revealed that 75% of sites fall in the ordered region, whereas, 25% of sites fall in the disordered region [Figure 5.4]. Our data suggest that there is no PTM site in the disordered region for CDK1. Similarly, PARP1 has 12 acetylation, 9 SUMOylation, and 5 ubiquitination sites fall in the disordered region, whereas, NPM1 has 16 acetylation, 21 SUMOylation, and 13 ubiquitination sites fall in the disordered region. Although previous studies reported that acetylation, ubiquitination, and SUMOylation preferred the ordered region, and thus PARP1 has more acetylation and ubiquitination sites in the ordered region, which is 53 and 38, respectively. However, in NPM1, the number of acetylation sites in the ordered region is less than that of the disordered region, whereas, the number of ubiquitination sites in the ordered region (18) is higher than that of ubiquitination sites in the disordered region (13). Similarly, the SUMOylation sites of PARP1 in the ordered region (24) is greater than that of the disordered region (9), whereas, the SUMOylation sites of NPM1 in the ordered region (5) is less than that of the disordered region (21). Thus, our study demonstrates the deviation in NPM1, whereas, PARP1 data goes well with previously reported literature for acetylation, ubiquitination, and SUMOylation. Moreover, to identify PTM hotspots and crosstalk hotspots and their susceptibility to neurodegeneration, we separated the proteins based on PTM sites and hotspot sites. *In-situ* crosstalk analysis in PARP1 revealed 15 potential acetylation/ubiquitination/SUMOylation sites, 19 acetylation/ubiquitination sites, 7

acetylation/SUMOylation sites, and 3 ubiquitination/SUMOylation sites. Similarly, in CDK1, there are 11 acetylation/ubiquitination/SUMOylation sites, 3 acetylation/ubiquitination sites, and 4 ubiquitination/SUMOylation sites [Figure 5.5 (A)].

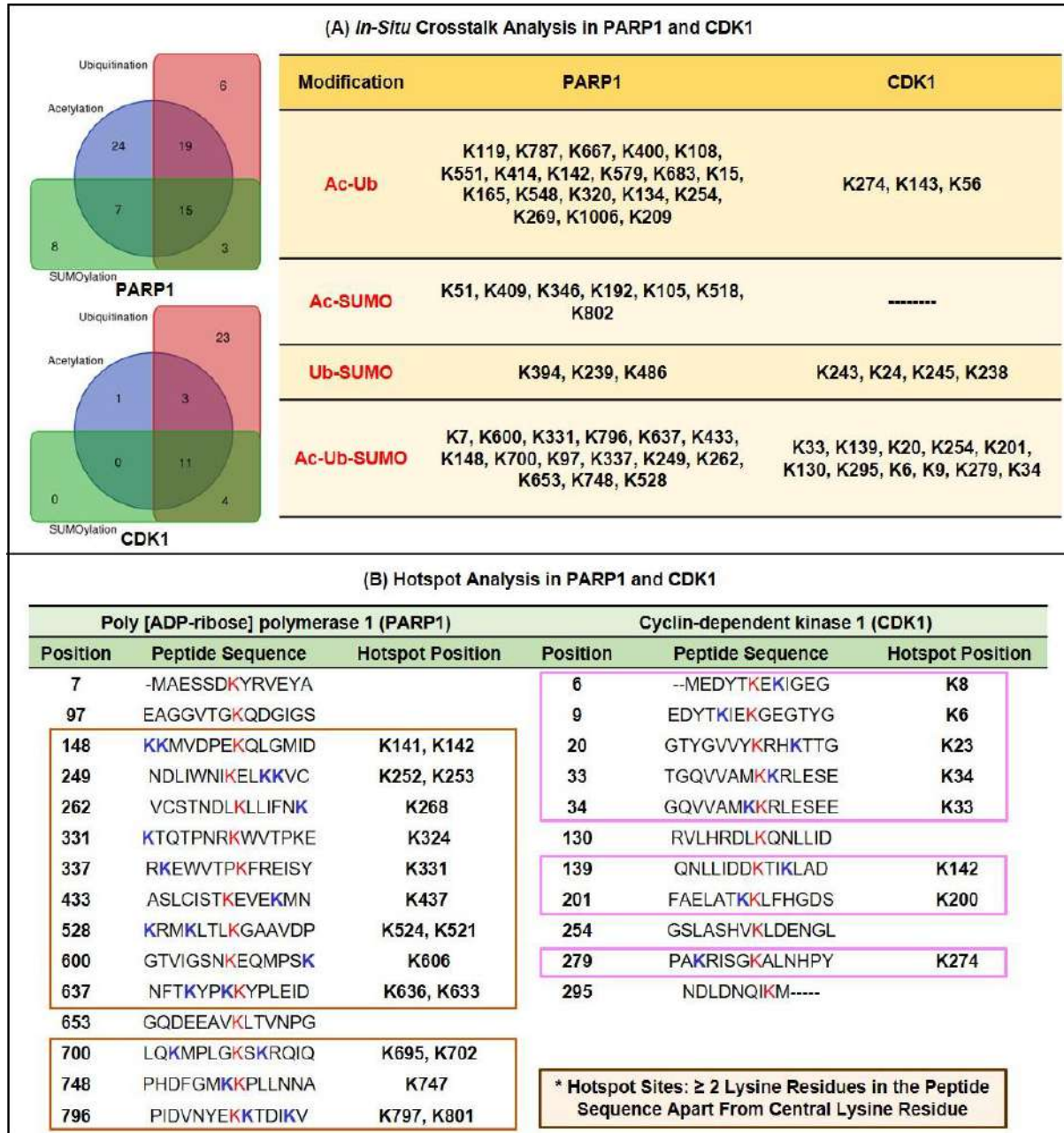


Figure 5.5: Crosstalk analysis between acetylation, ubiquitination, and SUMOylation in PARP1, CDK1, and NPM1 (B) Identification of Hotspot regions in PARP1 and CDK1.

The acetylation/ubiquitination/SUMOylation crosstalk sites of CDK1 and PARP1 were selected to identify crosstalk hotspots. Later on, we selected high density stretches containing the +7 and -6 motif starch, excluding the central PTM. Our analysis observed that K148, K249,

K528, K637, K700, and K796 have crosstalk hotspots in PARP1, whereas, no such hotspot has been observed in CDK1 [Figure 5.5 (B)].

5.1.4. IMPACT OF LYSINE MUTATION ON PARP1

The disease susceptibility of putative lysine mutation, either with glutamine and leucine, were investigated through mutational analysis tools such as PANTHER, Pmut, PolyPhen2, and SNAP2. Our results observed that all sites have an impact on disease susceptibility. However, K249, K331, K337, K528, K600, K637, K700, and K796 have a high confidence score on disease susceptibility. The highly intolerant mutation that is disease susceptible were shown in [Figure 5.6] and [Table 5.4].

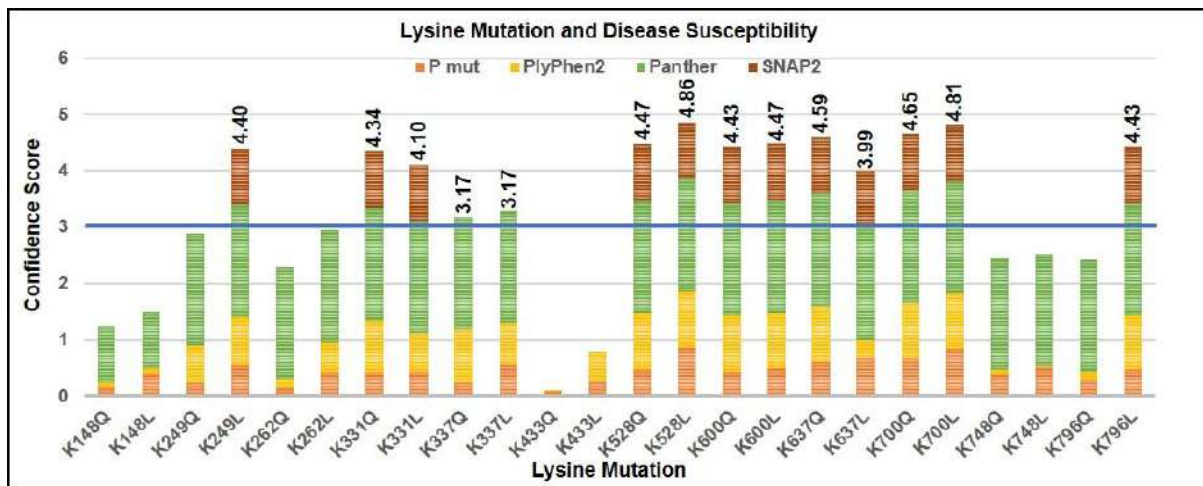


Figure 5.6: Impact of lysine mutation in hotspot sites on disease susceptibility. The selected lysine residues such as K148, K249, K262, K331, K337, K433, K528, K600, K637, K700, K748, and K796 were subjected to mutation with both glutamine or leucine. Afterwards, the mutations were checked for their impact on disease susceptibility. The results indicate that mutations such as K249L, K331Q, K331L, K337Q, K337L, K528Q, K528L, K600Q, K600L, K637Q, K637L, K700Q, K700L, and K796L have a pathogenic score above than 3 (taken as reference).

Mutational analysis study also revealed that mutation of K249, K331, and K796 residue with leucine decreases PARP1 stability, whereas, mutation of K331, K528, K600, K637, and K700 with glutamine decreases PARP1 stability. However, the decrease in PARP1 stability at K331 is higher when mutated with glutamine as compared to mutation with leucine [Figure 5.7 (A)]. Thus, the investigation suggests that mutation with glutamine on crosstalk sites impacts the stability of PARP1 to a great extent as compared to leucine.

Table 5.4: Impact of PARP1's "K" mutation to either Q or L on disease susceptibility predicted with the help of Pmut, PolyPhen2, Panther, and SNAP2

Residue	Pmut	PolyPhen2	Panther	SNAP2	Confidence
K148Q	0.16	0.075	1	0	1.235
K148L	0.39	0.097	1	0	1.487
K249Q	0.23	0.656	2	0	2.886
K249L	0.54	0.86	2	1	4.4
K262Q	0.15	0.138	2	0	2.288
K262L	0.42	0.529	2	0	2.949
K331Q	0.42	0.924	2	1	4.344
K331L	0.41	0.696	2	1	4.106
K337Q	0.24	0.935	2	0	3.175
K337L	0.56	0.731	2	0	3.291
K433Q	0.08	0.005	0	0	0.085
K433L	0.26	0.522	0	0	0.782
K528Q	0.47	1	2	1	4.47
K528L	0.86	1	2	1	4.86
K600Q	0.43	1	2	1	4.43
K600L	0.48	0.999	2	1	4.479
K637Q	0.61	0.988	2	1	4.598
K637L	0.68	0.318	2	1	3.998
K700Q	0.66	0.997	2	1	4.657
K700L	0.84	0.979	2	1	4.819
K748Q	0.38	0.084	2	0	2.464
K748L	0.51	0.01	2	0	2.52
K796Q	0.28	0.148	2	0	2.428
K796L	0.47	0.961	2	1	4.431

"Probably Begin" and "Neutral" Marked as 0
 "Possible Damage" Marked as 1
 "Probably Damaging" and "Effect" Marked as 2

5.1.5. POTENTIAL LYSINE RESIDUES INVOLVED IN ACETYLTATION, UBIQUITINATION, AND SUMOYLATION

Herein, we investigated the impact of an acetylated lysine residue on ubiquitination and SUMOylation, either at the same location or at the nearby sites. Our data revealed that putative mutation in 15 lysine-acetylated sites (K7, K97, K148, K249, K262, K331, K337, K433, K528, K600, K637, K653, K700, K748, K796) out of a total of 65 acetylated sites in PARP1 affect the process of ubiquitination to a great extent as compared to SUMOylation [Table 5.5]. Table 5.5 demonstrates the functional impact of putative lysine residue mutation on acetylation, ubiquitination, and SUMOylation. Further, the collective results depict the role of putative lysine mutation on other cellular functions. The results revealed that mutation in K7, K249, K337, K528, and K796 results in loss of acetylation on the same site, whereas, loss of lysine on K637 results in loss of acetylation at K633. Similarly, loss of putative lysine residue on K7

results in loss of ubiquitination at K7, whereas, loss of putative lysine residue on K600 results in loss of SUMOylation at K600. Further, our analysis demonstrates that putative mutation in lysine either with glutamine or leucine at K528 results in loss of acetylation at K528, loss of ubiquitination at K528, and loss of SUMOylation at K524 with ELME000051, ELME000231, ELME000336, and PS00005 as affected motifs.

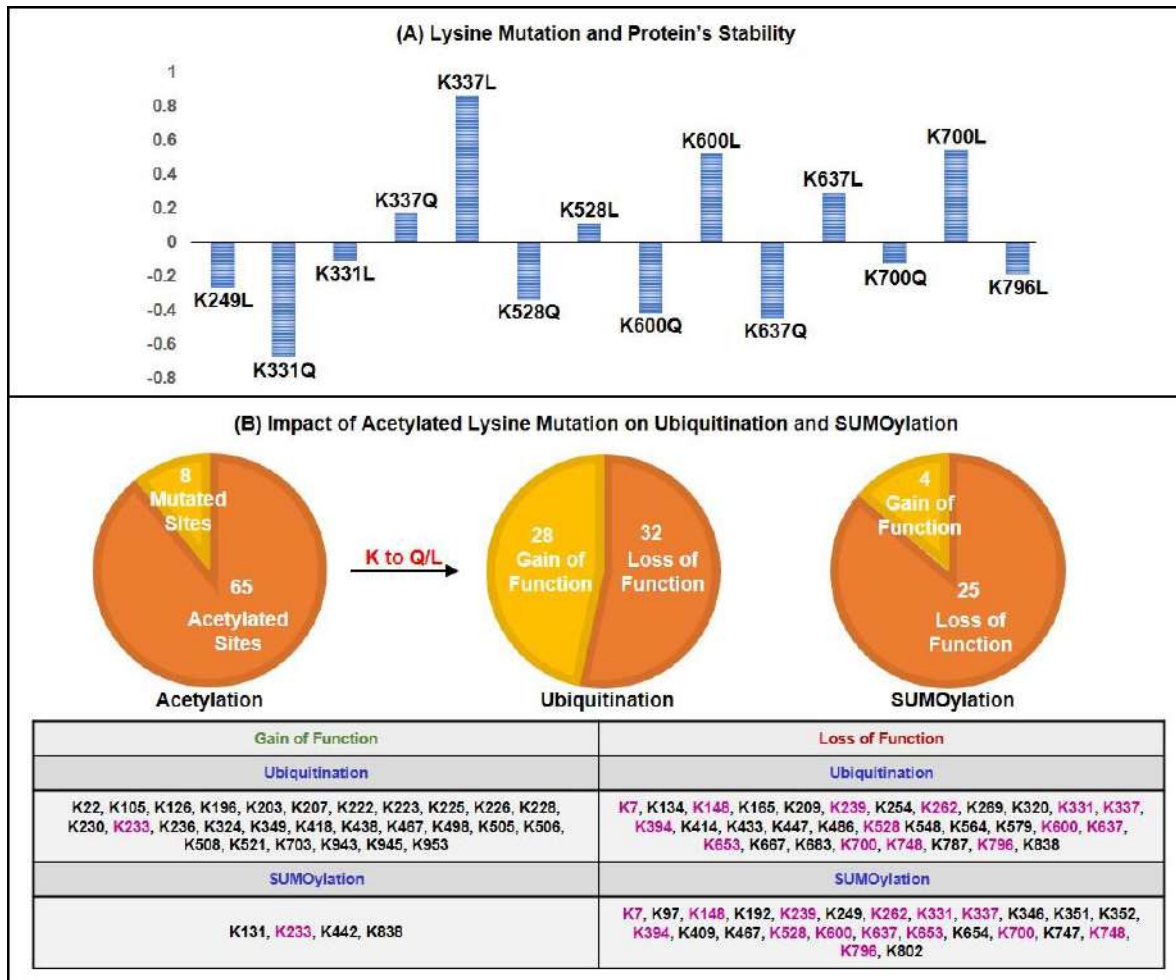


Figure 5.7: Impact of lysine mutation on protein stability. Afterward, the selected disease susceptible mutations were subjected to investigate their impact on protein structure stability. The results indicate that mutations such as K337Q, K337L, K528L, K600L, K637L, and K700L have positive energy value and increases protein stability. Similarly, K249L, K331Q, K331L, K528Q, K600Q, K637Q, K700Q, and K796L have negative energy value and thus, decreases the stability of the protein. (B) Investigation of acetylated lysine residue mutations on ubiquitination and SUMOylation. Here the results suggest that out of a total of 65 potential lysine sites, 15 sites were mutated and predicted the change in ubiquitination and SUMOylation states of the PARP1. The results suggested that total of 28 sites have a gain of ubiquitination, whereas, 32 sites have loss of ubiquitination when mutated with either glutamine or leucine. Similarly, 4 sites have gain of SUMOylation, whereas, 25 sites have loss of SUMOylation when mutated with both glutamine or leucine. Further, K233 have gain of both ubiquitination and SUMOylation, whereas, 14 sites have loss of both ubiquitination and SUMOylation as represented with pink colour in the figure.

The results collectively show the importance of K528 of PARP1, which regulates acetylation, ubiquitination, and SUMOylation collectively in NDDs such as AD and PD. Further, SUMOgo

and BDM-PUB predict 117 SUMOylation sites and 80 ubiquitination sites, respectively. The cut-off value for SUMOylation and ubiquitination prediction was set at 0.5 and 1.5, respectively, which filters 12 SUMOylation sites and 39 ubiquitination sites in PARP1. Through the *in-silico* approach, we substitute the lysine residue with glutamine and leucine, which promotes neutral side chain and hydrophobic side chain, respectively. The predicted residues were then compared with the integrated ubiquitination and SUMOylation residues. Here, we classified the affected ubiquitination and SUMOylation sites into two groups, which are the gain of function on nearby sites and loss of function on nearby sites. Our prediction demonstrated that loss of crucial lysine residue alters the ubiquitination function to a great extent as compared to SUMOylation. In ubiquitination, 28 sites were resulted in a gain of function, whereas, 32 sites resulted in the loss of function. Similarly, in SUMOylation, only 4 sites were predicted to gain in function, whereas, 25 sites resulted in the loss of function [Figure 5.7 (B)]. Further, our results suggest that loss of lysine residue at crucial sites either with glutamine and leucine resulted in both ubiquitination and SUMOylation gain in function at K233. Similarly, 14 sites (K7, K148, K239, K262, K331, K337, K394, K528, K600, K637, K653, K700, K748, K798) predicted to the loss in function for both ubiquitination and SUMOylation upon lysine substitution with either glutamine or leucine.

Table 5.5: Physical significance of lysine (K) residue in PARP1 acetylation, ubiquitination, and SUMOylation through an online analysis tool known as MutPred2 (<http://mutpred.mutdb.org/>)

Lysine Residue	Mutation	Affected Molecular Mechanism (P ≤ 0.05)	Affected Motifs	Pathogenic Score
K7	Lys(K)-Gln(Q)	_____	_____	0.273
	Lys(K)-Leu(L)	Loss of Intrinsic disorder Loss of Acetylation at K7 Loss of Phosphorylation at Y9 Loss of Methylation at K7 Loss of Ubiquitylation at K7	ELME000149 PS00005	0.517
K97	Lys(K)-Gln(Q)	_____	_____	0.196
	Lys(K)-Leu(L)	_____	_____	0.383
K148	Lys(K)-Gln(Q)	_____	ELME000155 PS00347	0.545
	Lys(K)-Leu(L)	Gain of Loop Altered Transmembrane protein		0.742
K249	Lys(K)-	_____	_____	0.479

	Gln(Q)			
	Lys(K)- Leu(L)	Altered Coiled Loss of Intrinsic disorder Gain of Loop Loss of Helix Altered Disordered interface Loss of Acetylation at K249	ELME000002	0.737
K262	Lys(K)- Gln(Q)	—	—	0.453
	Lys(K)- Leu(L)	Altered Coiled	—	0.771
K331	Lys(K)- Gln(Q)	—	—	0.272
	Lys(K)- Leu(L)	Altered Transmembrane protein	—	0.575
K337	Lys(K)- Gln(Q)	Loss of Acetylation at K337	ELME000064 ELME000117 ELME000133 ELME000136 ELME000159	0.694
	Lys(K)- Leu(L)	Loss of Acetylation at K337	—	0.825
K433	Lys(K)- Gln(Q)	—	—	0.113
	Lys(K)- Leu(L)	—	—	0.385
K528	Lys(K)- Gln(Q)	—	—	0.370
	Lys(K)- Leu(L)	Loss of Intrinsic disorder Loss of Acetylation at K528 Loss of Strand Loss of Helix Loss of SUMOylation at K524 Loss of Ubiquitylation at K528 Loss of Methylation at K528	ELME000051 ELME000231 ELME000336 PS00005	0.687
K600	Lys(K)- Gln(Q)	Loss of SUMOylation at K600 Gain of GPI-anchor amidation at N599	PS00005	0.718
	Lys(K)- Leu(L)	Loss of SUMOylation at K600		0.862
K637	Lys(K)- Gln(Q)	Gain of Strand Loss of Acetylation at K633 Altered Transmembrane protein	ELME000163 ELME000233	0.713
	Lys(K)- Leu(L)	Loss of Acetylation at K633 Altered Transmembrane protein	ELME000120 ELME000233	0.886
K653	Lys(K)- Gln(Q)	—	—	0.273
	Lys(K)- Leu(L)	—	—	0.489
K700	Lys(K)- Gln(Q)	—	—	0.499
	Lys(K)- Leu(L)	Altered Coiled	ELME000333	0.768
K748	Lys(K)- Gln(Q)	—	—	0.562
	Lys(K)- Leu(L)	Altered Coiled	—	0.775
K796	Lys(K)- Gln(Q)	Loss of Acetylation at K796 Altered Transmembrane protein Altered Coiled Gain of Proteolytic cleavage at D791	ELME000020 ELME000120 ELME000173 ELME000233	0.546
	Lys(K)- Leu(L)	Altered Ordered interface Loss of Acetylation at K796 Altered Transmembrane protein Altered Coiled Gain of Proteolytic cleavage at D791		0.776

5.2. CONCLUSION AND SUMMARY

NDDs such as AD and PD are best characterized as progressive loss of neuronal cells leading to memory deficits and cognitive dysfunction. Mounting evidence suggests the possible implementation of PTMs in the pathogenesis of NDDs. One important PTM is acetylation, which is the process of the addition of the acetyl group to the N-terminal lysine residue. Acetylation and deacetylation are reversible processes, which are carried out with the help of HATs and HDACs enzymes, respectively. HATs/HDACs promote euchromatin and heterochromatin structure, respectively, which involves in the transcriptional regulation. Apart from acetylation, ubiquitination and SUMOylation are two important PTMs, which help in the removal of misfolded toxic protein aggregates such as A β and α -synuclein. The common characteristics feature of acetylation, ubiquitination, and SUMOylation is the involvement of lysine (K) residue, and thus crosstalk between three PTMs becomes a fascinating topic for research. Studies indicate that acetylation of PARP1 leads to its hyperactivation, which will intensify oxidative stress and causes mitochondrial dysfunction and, subsequently, neuronal cell death through parthanatos. Mounting evidence indicates that PARP1 acetylation increases A β and α -synuclein aggregates, which increases neurotoxicity [491]. Studies demonstrated that activation of PARP1 decreases A β clearance and increases AIF expression. Love et al., 1999 first reported the activation of PARP1 in brain samples of AD patients. The authors conducted immunostaining analysis, which indicated the increased levels of PAR in AD patients in frontal and temporal lobes as compared to control patients [492]. Similarly, Abeti et al., 2011 in mixed cultures of hippocampal neurons and glial cells from Sprague-Dawley rat concluded that PARP1 activation leads to oxidative stress in the presence of A β causes metabolic failure and neuronal death [493]. Further, Li et al., 2010 in ischemic mice demonstrated that PARP1 causes nuclear translocation of AIF, which results in neuronal cell death, whereas, in another

study conducted on rats concluded that PARP1 increased expression causes suppression of AIF protein expression [494]. In MPTP mouse model of PD, FAF1 plays a key role in PARP-1 dependent necrosis in response to oxidative stress. Further, FAF1 depletion prevented PARP1-linked downstream events such as mitochondrial depolarization and nuclear translocation of AIF [495]. [Figure 5.8].

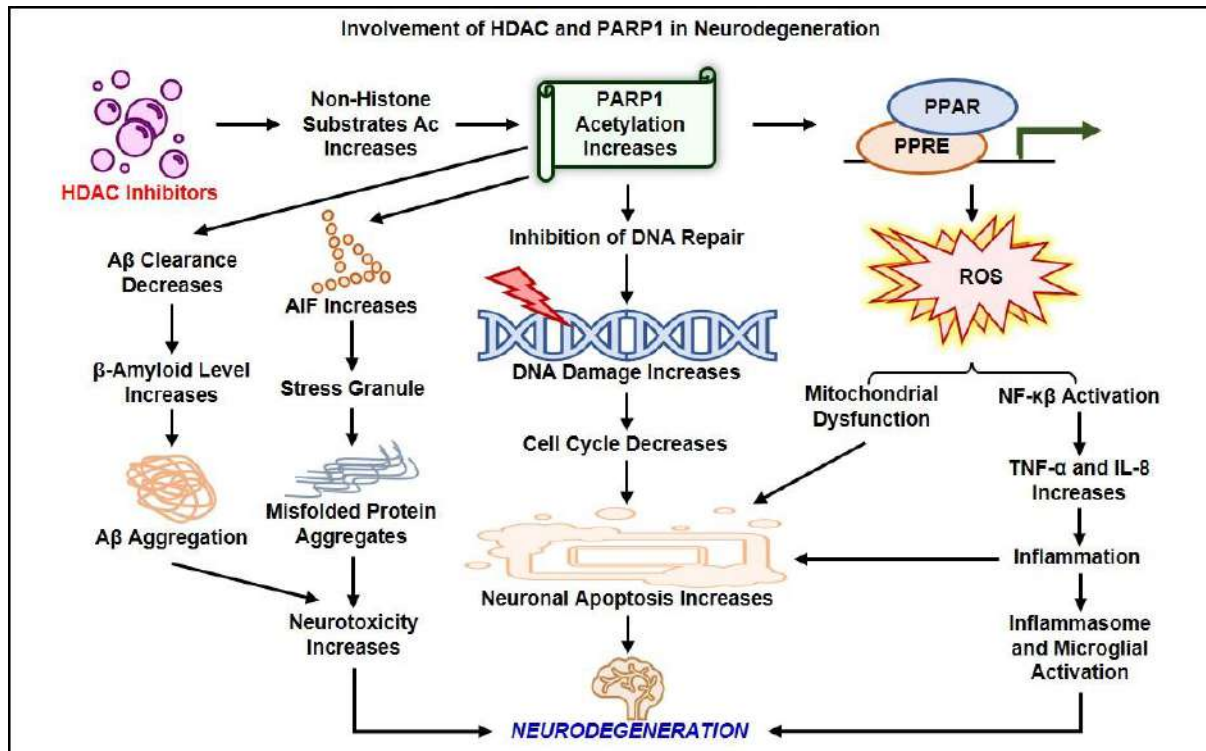


Figure 5.8: Mechanism of PARP1 acetylation in neurodegenerative diseases. Similarly, increased PARP1 acetylation causes inhibition of DNA repair and increased ROS activity, which decreases cell-cycle activity and increases mitochondrial dysfunction, respectively. Decreased cell-cycle regulation and increased mitochondrial dysfunction causes increased neuronal apoptosis, which results in memory impairment and cognitive defects. Increased ROS activity by increased PARP1 acetylation lead to NF-κB activation, which increases pro-inflammatory cytokines release and results in microglial activation.

In this study, we have examined the PTMs and their crosstalk in HDAC interactors, which are involved in the progression of NDDs such as AD and PD. The interactors of HDAC and proteins involved in AD and PD were collected from different databases such as HIPPIE, CTD, and DisGeNET. Venn analysis and PPI interaction of HDAC interactors, AD, and PD demonstrated the involvement of the Top 33 proteins. Gene set enrichment analysis of 33 proteins confirmed the involvement of six different molecular functions and biological pathways in the pathogenesis of AD and PD through HDAC interactors. Protein

serine/threonine kinase activity (21.21%), Transcription regulator activity (18.18%), Transcription factor activity (6.06%), Transmembrane receptor protein tyrosine kinase activity (9.09%), Chaperone activity (15.15%), DNA-methyltransferase activity (3.03%) were top-ranked molecular functions performed by HDAC interactors having a p-value less than 0.05. Similarly, Glypican pathway (81.25%), TRAIL signaling pathway (84.37%), Glypican 1 network (81.25%), Integrin-linked kinase signaling (65.62%), AP-1 transcription factor network (62.50%), and Arf6 downstream pathway (78.12%) were top-ranked biological pathways involved in the pathogenesis of AD and PD. Lately, 1,50,968 PTMs sites from dbPTM and 1,15,127 PTMs sites from PLMD were integrated to 32 proteins in which 1489 were acetylation, ubiquitination, and SUMOylation sites. Among 32 proteins, only three proteins, such as PARP1, NPM1, and CDK1, have individual acetylation, ubiquitination, and SUMOylation frequency greater than 10. Secondary structure prediction confirmed 42, 22, and 18 PTMs sites formed coiled structure in PARP1, NPM1, and CDK1 respectively, demonstrating that the probability of PTMs site is higher in the coiled region as compared to helix and strand region. However, in NPM1, the probability of forming a strand region is higher as compared to PARP1 and CDK1. Further investigation revealed that 75% of PTMs sites were associated with the ordered region, whereas, 25% of PTMs sites were associated with the disordered region. Thus, it will be concluded that PTM distribution is higher in the ordered region as compared to the disordered region. Further, crosstalk analysis of acetylation, ubiquitination, and SUMOylation sites in PARP1 revealed that 19 PTM sites were associated with acetylation and ubiquitination crosstalk. Similarly, acetylation-SUMOylation (7 sites), ubiquitination-SUMOylation (3 sites), and acetylation-ubiquitination-SUMOylation (15 sites) were identified. Hotspot analysis identified that K148, K249, K528, K637, K700, and K796 have potential crosstalk sites having ≥ 2 potential lysine residue in the vicinity of +7 and -6 motif sequence. In order to predict crucial crosstalk sites, the impact of putative lysine mutation

on disease susceptibility was predicted, which demonstrated that among hotspot sites, K249L, K528Q, K528L, K637Q, K637L, K700Q, K700L, K796L were involved in the progression of NDDs. Further, our study investigated the role of putative lysine mutation on ubiquitination and SUMOylation, which shows that putative mutation in lysine residue will result in loss of SUMOylation and ubiquitination function. However, the gain of function after putative lysine mutation will also be observed, but the frequency is low as compared to the loss of function. In conclusion, K249, K331, K337, K528, K600, K637, K700, and K796 of PARP1 play a vital role in ubiquitination, acetylation, and SUMOylation crosstalk, which can potentially be useful for newer leads into acetylation mechanism, HDAC interactions, disease progression, biomarkers, or as a therapeutic target. Further, from this study, we also concluded that site-specific inhibition of PARP1 acetylation (K249, K331, K337, K528, K600, K637, K700, and K796) and simultaneous activation of ubiquitination and SUMOylation at the same residues rescue neuronal cell death that involved in AD pathology.

5.3. HIGHLIGHTS OF THE STUDY

5.3.1. Lysine residues are important for acetylation, ubiquitination, and SUMOylation crosstalk

5.3.2. HDAC interactors such as PARP1, NPM1, and CDK1 acts as a central player in PTM crosstalk

5.3.3. K249, K331, K337, K528, K600, K637, K700, and K796 involved in PTM crosstalk

5.3.4. Loss of acetylation causes loss of ubiquitination and SUMOylation function

CHAPTER VI

Integrative Analysis of OIP5-AS1/MIR-129-5P/CREBBP Axis as a Potential Therapeutic Target in The Pathogenesis of Metal Toxicity-Induced Alzheimer's Disease

CHAPTER VI: INTEGRATIVE ANALYSIS OF OIP5-AS1/MIR-129-5P/CREBBP AXIS AS A POTENTIAL THERAPEUTIC TARGET IN THE PATHOGENESIS OF METAL TOXICITY-INDUCED ALZHEIMER'S DISEASE

6. INTRODUCTION

NDDs, namely AD, is characterized by the accumulation of toxic A β aggregates and insoluble tau tangles. Mounting evidence demonstrated that heavy metals, such as copper, chromium, cobalt, and nickel, increases the A β and tau aggregation in the pathogenesis of AD by activating different signaling events. For instance, copper induces the formation of ROS to cause mitochondrial dysfunction and DNA damage, whereas, chromium elevates neuroinflammatory response and neuronal apoptosis. Similarly, cobalt increases tau hyperphosphorylation and promotes tau aggregation, whereas, nickel elevates A β aggregation. Further, acetylation, a lysine-specific post-translational modification, has been linked to transcriptional activation, which regulates the transcription of genes associated with metal toxicity-induced AD. However, miRNAs can reduce the activity of acetyltransferase, which decreases the transcriptional activation and thus inhibits the pathogenesis of AD. In contrast, long non-coding RNAs modulate the expression of specific miRNA and serve as a sponge to particular miRNA. In this study, we aim to identify the crucial proteins involved in metal toxicity-induced AD through network biology, followed by identifying regulatory TFs associated with crucial proteins. Further, we aim to determine the critical lysine residue and the role of CREBBP-induce acetylation on TFs. Lately, we have focused on identifying miRNAs associated with CREBBP and TFs simultaneously. Lastly, we aim to identify the potential long non-coding RNA, serving as a sponge to miRNAs. Our results demonstrated that the OIP5-AS1/miR-129-5p/CREBBP axis is a potential therapeutic target in metal toxicity-induced AD pathogenesis.

6.1. RESULTS AND DISCUSSION

6.1.1. GENES INVOLVED IN METAL TOXICITY-INDUCED ALZHEIMER'S DISEASE

Data extraction from the CTD database identified that genes involved in chromium, cobalt, copper, and nickel toxicity are 2149, 4804, 5862, and 7649, respectively. The Venn analysis of the genes revealed that 376 genes were common among them. Similarly, a total of 3397 genes involved in AD pathogenesis were extracted from the DisGeNET database. Furthermore, Venn analysis of metal toxicity linked genes and AD-related genes identified 199 shared genes.

6.1.2. GENE SET ENRICHMENT ANALYSIS OF COMMON GENES

A total of 199 common genes identified in metal toxicity and AD were subjected to functional enrichment analysis such as GO analysis and pathway analysis. Gene set enrichment analysis of common genes enables identifying cellular functions, molecular functions, biological processes, and pathways. The cut-off p-value for identifying cellular, molecular, biological, and pathway functions was set at less than 0.05, as shown in **Table 6.1**.

Table 6.1: Gene set enrichment analysis (GO analysis and Pathway analysis) of 199 common genes related to metal toxicity and Alzheimer's disease

Name	Fold enrichment	P-value	Genes Mapped
Biological Process			
Apoptosis	4.206953589	0.000145225	TP53; CASP3; MAPK9; BCL2; BAX; CASP7; BBC3; CASP9; BCL2L11; CASP8;
Regulation of cell cycle	8.125736768	0.000372966	MAPK9; CDKN1A; CCNE2; CHEK2; KLF4;
Anti-apoptosis	11.58336557	0.000376289	SOD2; GPX1; FAS; IGF1;
Protein metabolism	1.747940437	0.004511294	PARP1; MMP1; MMP2; ADAMTS1; EIF4A1; HSPA5; MMP13; ANPEP; BMP1; CALR; CCT2; DNAJB1; DPP4; F3; HSPA9; HSPB1; HSPH1; HYOU1; PDIA6; RPL15; SERPINA1; SERPINC1; SERPING1; SQSTM1; THOP1;
Metabolism	1.593812016	0.008086365	CAT; NQO1; GSR; SOD1; HMOX1; PTGS2; GPT; NOS2; TXN; GSK3 β ; LYZ; G6PD; HMGCR; NAT10; ACHE; ALDH1L1; CD36; CYCS; FDPS; GCHFR; GPX4; IDH2; LDHA; NME1; PHYHD1; PRDX1; PSAT1; SIRT1; TXNRD1;
Signal transduction	1.339959419	0.009037422	MAPK8; MAPK1; AKT1; MAPK3; TNF; MAPK9; VEGFA; CCND1; FYN; IRS1; PLK1; CDK1; MAP2K4; EGFR; ICAM1; CHEK2; LDLR; NOTCH1; PLK2; SGK1; TGFB1; TGFB1; AGT; ARHGEF2; ATM; BMP4; CCL5; CD44; CD68; CXCR4; DENR; DKK1; DUSP6; EDN1; FAS; FGFR4; FZD4; GDF15; GPNMB; HSP90AB1; IGF1; IGF2; IL1RL1; MAPK14; NTS; PGF; PHB;

			PRKCD; RAB31; RGCC; RGS2; S100A6; ST13; STIP1; TAX1BP1; TGFB2; TLR4;
Cellular Component			
Extracellular	3.124166679	3.33129E-21	CAT; SOD1; IL6; TNF; CXCL8; CDKN1A; VEGFA; GPT; GPX1; STAT3; TF; IFNG; TIMP1; TXN; APOA1; EGFR; ICAM1; IL1B; LYZ; MMP1; MMP2; MT2A; TFRC; VIM; ADAMTS1; C3; EGR1; FABP3; G6PD; HMGCR; IL4; MMP13; TGFB1; TGFB1; ACHE; ADM; AGT; ALB; ANPEP; APOB; APOC3; BMP1; BMP4; CALR; CCL2; CCL5; CFB; CFI; CXCL1; DKK1; DPP4; EDN1; F3; FAS; FGFR4; FN1; GDF15; HMGB1; HSP90AB1; IGF1; IGF2; IL10; IL1RL1; IL2; NME1; NTS; PDIA6; PGF; PHB; RGS2; SERPINA1; SERPINC1; SERPING1; SHBG; THOP1; TXNRD1;
Extracellular space	5.943226358	3.12411E-16	SOD1; IL6; HMOX1; TNF; CXCL8; VEGFA; APOA1; EGFR; ICAM1; IL1B; LYZ; MMP2; IL4; MMP13; TGFB1; TGFB1; ADM; AGT; ALB; APOC3; CALR; CCL2; CXCL1; EDN1; F3; FN1; HMGB1; IGF1; IL10; IL2; SERPINA1; SERPINC1;
Cytosol	3.311818965	4.53947E-15	TP53; CASP3; GSR; SOD1; HMOX1; MAPK8; MAPK1; AKT1; MAPK3; CDKN1A; CCND1; FYN; GPX1; IRS1; RELA; BCL2; HDAC1; BAX; CASP7; PLK1; CASP9; CDK1; MAP2K4; NOS2; TXN; GSK3β; TCF4; VIM; BCL2L11; CASP8; CCNE2; EIF4A1; G6PD; NOTCH1; ARHGEF2; CALR; CCT2; CYCS; DNAJB1; FAS; GART; HSP90AB1; HSPH1; LDHA; MAPK14; PPIA; PRKCD; PSAT1; RPL15; S100A6; SQSTM1; TXNRD1;
Exosomes	2.533787837	3.15643E-14	NQO1; GSR; SOD1; GPT; TF; BAX; CASP9; CDK1; TXN; APOA1; EGFR; ICAM1; LYZ; SLC2A1; TFRC; VIM; C3; EIF4A1; FABP3; G6PD; HSPA5; NOTCH1; PCNA; TGFB1; TGFB1; AGT; ALB; ALDH1L1; ANPEP; APOB; CALR; CCT2; CD36; CD44; CFI; CXCR4; DNAJB1; DPP4; FAS; FDPS; FN1; GART; GPX4; HSP90AB1; HSPA9; HSPB1; HSPH1; HYOU1; LDHA; NME1; OPTN; PDIA6; PHB; PPIA; PRDX1; PRKCD; PSAT1; RBM3; RPL15; S100A6; SERPINA1; SERPING1; SLC2A3; SQSTM1; ST13; STIP1; TAX1BP1; TPM1; TXNRD1;
Nucleoplasm	4.679352988	9.37804E-12	TP53; CASP3; JUN; MAPK8; MAPK1; AKT1; MAPK3; MAPK9; CDKN1A; CCND1; RELA; MYC; CASP7; PLK1; CDK1; ATF2; CCNE2; MCM2; PCNA; ATM; DUSP6; HMGB1; MAPK14; PHB; PPARGC1A; SFPQ; SIRT1; SQSTM1;
Cytoplasm	1.61016101	1.28598E-11	CAT; TP53; NQO1; CASP3; GSR; HIF1A; SOD1; JUN; MAPK8; MAPK1; PTGS2; AKT1; MAPK3; MAPK9; PARP1; CDKN1A; VEGFA; CCND1; FYN; GPT; GPX1; IRS1; RELA; STAT3; TF; BCL2; HDAC1; BAX; CASP7; NFE2L2; PLK1; BBC3; CASP9; CDK1; MAP2K4; NOS2; TXN; AHR; APOA1; ATF2; EGFR; GSK3β; ICAM1; IL1B; MT2A; SLC2A1; VIM; BCL2L11; C3; CASP8; CHEK2; CREBBP; EIF4A1; ESR1; FABP3; G6PD; HSPA5; PCNA; PLK2; PPARA; SGK1; SLC11A2; SLC40A1; TGFB1; TGFB1; ADM; AGT; ALB; ALDH1L1; ARHGEF2; ATM; BMP1; C1QBP; CALR; CCL5; CCT2; CD36; CD44; CXCR4; CYCS; DHFR; DNAJB1; DUSP6; EDN1; FAS; FDPS; FZD4; GCHFR; GPX4; HMGB1; HSP90AB1; HSPA9; HSPB1; HSPH1; HYOU1; IGF1; KLF4; LDHA; MAPK14; NFIA; NME1; OPTN; PHB; PPIA; PRDX1; PRKCD; RAB31; RGCC; RGS2; S100A6; SERPINA1; SFPQ; SIRT1; SQSTM1; ST13; STIP1; TAX1BP1;

			TGFBR2; THOP1; TLR4; TPM1; TXNRD1;
Molecular Functions			
Protein serine/threonine kinase activity	4.303851101	5.27737E-06	MAPK8; MAPK1; AKT1; MAPK3; MAPK9; PLK1; CDK1; GSK3β; CHEK2; PLK2; SGK1; ATM; MAPK14; PRKCD;
Peroxidase activity	18.53093404	5.61002E-05	PTGS2; GPX1; GPX4; PRDX1;
Metallopeptidase activity	6.417319661	0.000113325	MMP1; MMP2; ADAMTS1; MMP13; ANPEP; BMP1; THOP1;
Cytokine activity	6.057503589	0.000162709	IL6; CXCL8; IFNG; IL1B; IL4; IL10; IL2;
Superoxide dismutase activity	61.74895155	0.000346553	SOD1; SOD2;
Chaperone activity	5.144142997	0.00044355	HSPA5; CALR; CCT2; HSP90AB1; HSPA9; HSPB1; HYOU1;
Biological Pathways			
AP-1 transcription factor network	4.375449634	1.06375E-30	TP53; CASP3; HIF1A; IL6; JUN; HMOX1; MAPK8; MAPK1; PTGS2; AKT1; MAPK3; TNF; CXCL8; MAPK9; CDKN1A; VEGFA; CCND1; FYN; RELA; STAT3; TF; BCL2; HDAC1; IFNG; MYC; BAX; CDK1; MAP2K4; NOS2; TIMP1; TXN; ATF2; FOS; GSK3β; ICAM1; MMP1; MMP2; MT2A; SLC2A1; TCF4; TFRC; BCL2L11; CASP8; CREBBP; DDIT3; EGR1; ESR1; IL4; SGK1; SP1; TGFB1; ACHE; ADM; AGT; ATM; BHLHE40; CCL2; CXCR4; DKK1; EDN1; GJA1; HSPB1; IL10; IL2; JUNB; KLF4; LDHA; MAPK14; NTS; PPARGC1A; PRDX1; PRKCD; TGFBR2;
Integrin-linked kinase signaling	4.21157898	4.56458E-30	TP53; CASP3; HIF1A; IL6; JUN; HMOX1; MAPK8; MAPK1; PTGS2; AKT1; MAPK3; TNF; CXCL8; MAPK9; PARP1; CDKN1A; VEGFA; CCND1; FYN; RELA; STAT3; TF; BCL2; HDAC1; IFNG; MYC; BAX; CDK1; MAP2K4; NOS2; TIMP1; TXN; ATF2; FOS; GSK3β; ICAM1; MMP1; MMP2; MT2A; SLC2A1; TCF4; TFRC; BCL2L11; CASP8; CREBBP; DDIT3; EGR1; ESR1; IL4; SGK1; SP1; TGFB1; ACHE; ADM; AGT; ATM; BHLHE40; CCL2; CXCR4; DKK1; EDN1; GJA1; HSPB1; IL10; IL2; JUNB; KLF4; LDHA; MAPK14; NTS; PPARGC1A; PRDX1; PRKCD; TGFBR2;
TRAIL signaling pathway	2.837162097	1.33272E-28	CAT; TP53; CASP3; HIF1A; IL6; JUN; HMOX1; MAPK8; MAPK1; PTGS2; AKT1; MAPK3; TNF; CXCL8; MAPK9; PARP1; CDKN1A; SOD2; VEGFA; CCND1; FYN; GPX1; IRS1; RELA; STAT3; TF; BCL2; HDAC1; IFNG; MYC; BAX; CASP7; PLK1; BBC3; CASP9; CDK1; MAP2K4; NOS2; TIMP1; TXN; ATF2; EGFR; FOS; GSK3β; ICAM1; MMP1; MMP2; MT2A; SLC2A1; TCF4; TFRC; VIM; BCL2L11; CASP8; CHEK2; CREBBP; DDIT3; EGR1; EIF4A1; ESR1; IL4; MMP13; PCNA; SGK1; SP1; TGFB1; ACHE; ADM; AGT; ATM; BHLHE40; BMP4; CCL2; CCL5; CXCR4; CYCS; DKK1; DUSP6; EDN1; FAS; FGFR4; FN1; GDF15; GJA1; HSPB1; IGF1; IGF2; IL10; IL2; JUNB; KLF4; LDHA; MAPK14; NME1; NTS; PPARGC1A; PRDX1; PRKCD; RGCC; SIRT1; TGFBR2;
VEGF and VEGFR signaling network	2.860893735	1.62998E-28	CAT; TP53; CASP3; HIF1A; IL6; JUN; HMOX1; MAPK8; MAPK1; PTGS2; AKT1; MAPK3; TNF; CXCL8; MAPK9; CDKN1A; SOD2; VEGFA; CCND1; FYN; GPX1; IRS1; RELA; STAT3; TF; BCL2; HDAC1; IFNG; MYC; BAX; PLK1; BBC3; CASP9; CDK1; MAP2K4; NOS2; TIMP1; TXN; ATF2; EGFR; FOS; GSK3β; ICAM1; MMP1;

			MMP2; MT2A; SLC2A1; TCF4; TFRC; BCL2L11; CASP8; CHEK2; CREBBP; DDIT3; EGR1; EIF4A1; ESR1; IL4; MMP13; PCNA; SGK1; SP1; TGFB1; ACHE; ADM; AGT; ATM; BHLHE40; BMP4; CCL2; CCL5; CXCR4; CYCS; DKK1; DUSP6; EDN1; FAS; FGFR4; FN1; GDF15; GJA1; HSP90AB1; HSPB1; IGF1; IGF2; IL10; IL2; JUNB; KLF4; LDHA; MAPK14; NME1; NTS; PGF; PPARGC1A; PRDX1; PRKCD; RGCC; SIRT1; TGFB2;
Signaling events mediated by VEGFR1 and VEGFR2	2.849811345	5.67443E-28	CAT; TP53; CASP3; HIF1A; IL6; JUN; HMOX1; MAPK8; MAPK1; PTGS2; AKT1; MAPK3; TNF; CXCL8; MAPK9; CDKN1A; SOD2; VEGFA; CCND1; FYN; GPX1; IRS1; RELA; STAT3; TF; BCL2; HDAC1; IFNG; MYC; BAX; PLK1; BBC3; CASP9; CDK1; MAP2K4; NOS2; TIMP1; TXN; ATF2; EGFR; FOS; GSK3β; ICAM1; MMP1; MMP2; MT2A; SLC2A1; TCF4; TFRC; BCL2L11; CASP8; CHEK2; CREBBP; DDIT3; EGR1; EIF4A1; ESR1; IL4; MMP13; PCNA; SGK1; SP1; TGFB1; ACHE; ADM; AGT; ATM; BHLHE40; BMP4; CCL2; CCL5; CXCR4; CYCS; DKK1; DUSP6; EDN1; FAS; FGFR4; FN1; GDF15; GJA1; HSP90AB1; HSPB1; IGF1; IGF2; IL10; IL2; JUNB; KLF4; LDHA; MAPK14; NME1; NTS; PPARGC1A; PRDX1; PRKCD; RGCC; SIRT1; TGFB2;
IFN-gamma pathway	2.849811345	5.67443E-28	CAT; TP53; CASP3; HIF1A; IL6; JUN; HMOX1; MAPK8; MAPK1; PTGS2; AKT1; MAPK3; TNF; CXCL8; MAPK9; CDKN1A; SOD2; VEGFA; CCND1; FYN; GPX1; IRS1; RELA; STAT3; TF; BCL2; HDAC1; IFNG; MYC; BAX; PLK1; BBC3; CASP9; CDK1; MAP2K4; NOS2; TIMP1; TXN; ATF2; EGFR; FOS; GSK3β; ICAM1; IL1B; MMP1; MMP2; MT2A; SLC2A1; TCF4; TFRC; BCL2L11; CASP8; CHEK2; CREBBP; DDIT3; EGR1; EIF4A1; ESR1; IL4; MMP13; PCNA; SGK1; SP1; TGFB1; ACHE; ADM; AGT; ATM; BHLHE40; BMP4; CCL2; CCL5; CXCR4; CYCS; DKK1; DUSP6; EDN1; FAS; FGFR4; FN1; GDF15; GJA1; HSPB1; IGF1; IGF2; IL10; IL2; JUNB; KLF4; LDHA; MAPK14; NME1; NTS; PPARGC1A; PRDX1; PRKCD; RGCC; SIRT1; TGFB2;

Among biological processes, apoptosis (5.1%), regulation of cell cycle (2.6%), anti-apoptosis (2%), protein metabolism (12.8%), and metabolism (14.8%) were top 5 ranked processes. Similarly, extracellular (39.2%), extracellular space (16.5%), cytosol (26.8%), exosomes (35.6%), and nucleoplasm (14.4%) were top-ranked cellular components, while protein serine/threonine kinase activity (7.1%), peroxidase activity (2%), metalloproteinase activity (3.6%), cytokine activity (3.6%), and superoxide dismutase activity (1%) were top-ranked molecular functions of common genes.

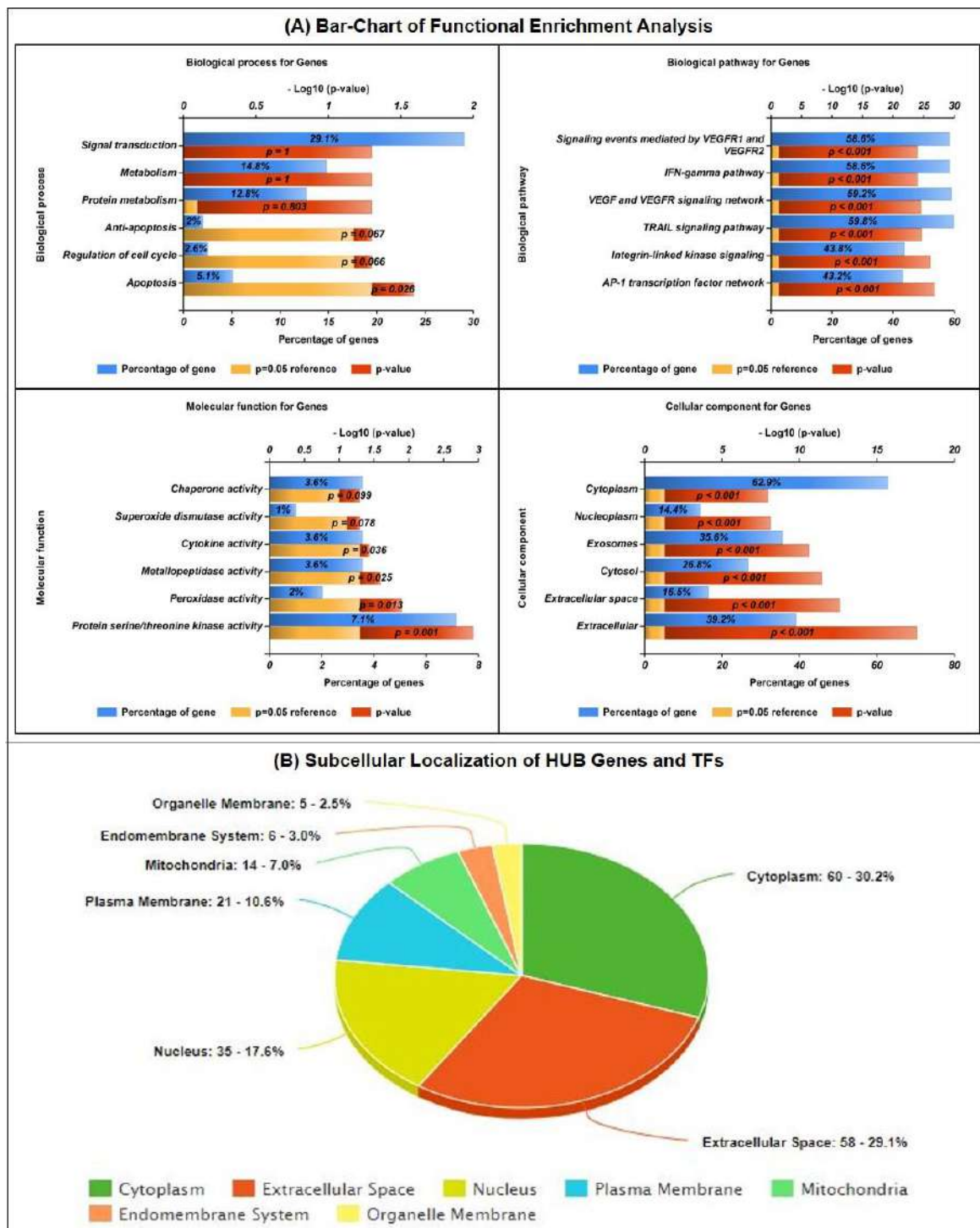


Figure 6.1: Gene set enrichment analysis of common genes between chromium, cobalt, copper, and nickel-associated Alzheimer's disease (FunRich and KEGG pathway database). (A) represents the bar-graph of biological process, cellular components, molecular function, and associated pathway. Among the biological process, signal transduction, metabolism, protein metabolism, anti-apoptosis, apoptosis, and cell cycle regulation with p-value 1, 1, 0.803, 0.067, 0.066, and 0.026 were top-ranked. Similarly, chaperon's activity, superoxide dismutase activity, cytokine activity, metalloproteinase activity, peroxidase activity, and protein serine/threonine kinase activity were top-ranked molecular functions. At the same time, cytoplasm, nucleoplasm, exosomes, cytosol, extracellular space, and extracellular were top-ranked cellular components. Moreover, signaling events mediated by VEGFR1 and VEGFR2 (58.6%), IFN-gamma pathway (58.6%), VEGF and VEGFR signaling network (59.2%), TRAIL signaling pathway (59.8%), integrin-linked kinase signaling (43.8%), and AP-1 transcription factor network (43.2%) were top-ranked biological pathway associated with shared genes. (B) Subcellular localization of the shared genes involved in metal toxicity-induced AD through BUSCA: Bologna Unified Subcellular Component Annotator.

Further, pathway analysis of common genes demonstrated the involvement of AP-1 transcription factor network (43.2%), Integrin-linked kinase signaling (43.8%), TRAIL Signaling pathway (59.8%), VEGF and VEGFR signaling cascade (59.2%), and VEGFR1 and VEGFR2 mediated signaling cascade (58.6%). Moreover, the fold enrichment value of the above-described cellular pathways is 4.375, 4.211, 2.837, 2.860, and 2.849, respectively. Thus, the results concluded that the common genes were mainly involved in apoptosis, and cell-cycle regulation causes neuronal cell death in metal toxicity induced AD.

Figure 6.1 (A) demonstrated the functional enrichment analysis of common genes such as cellular components, biological processes, molecular functions, and pathways. Further, subcellular localization prediction of shared genes involved in metal toxicity-induced AD indicates the crucial role of cytoplasm (60 genes: 30.2%). The analysis found that the percentage of genes present in the extracellular space (58 genes: 29.1%) is almost comparable to that of the cytoplasm. In addition, apart from the cytoplasm and extracellular space, the shared genes were found in the nucleus (35 genes: 17.6%), plasma membrane (21 genes: 10.6%), mitochondria (14 genes: 7.0%), endomembrane system (6 genes: 3.0%), and organelle membrane (5 genes: 2.5%) [**Figure 6.1 (B)**].

6.1.3. PROTEIN-PROTEIN INTERACTION ANALYSIS AND HUB PROTEINS IN NETWORK

To construct a global PPI network of common genes involved in metal toxicity and AD, the genes were entered as a list in the STRING database with a medium confidence score. The obtained output was imported into the Cytoscape software as input with the help of the Reactome FI plugin for data visualization. The results of the PPI network show 175 nodes and 1138 edges in the network [**Figure 6.2**]. Nodes represent the protein signature, while edges are the interaction between different signatures. The size of the particular node decreases as the degree of the node decreases. Similarly, the edge thickness depends on the experimental

validation of the interaction among two different nodes. The characteristics and parameters of the PPI network are given in **Table 6.2**.

Table 6.2: Characteristics and parameters of core, cluster, HUB genes, transcription factors, and micro-RNAs protein-protein interaction network

Network	Number of Nodes	Number of Edges	Clustering Coefficient	Network Density	Network Centralization	Network Heterogeneity	Characteristics Path Length	Average No of Neighbors
Core PPI	175	1138	0.422	0.075	0.36.	1.14	2.426	13.006
Cluster (11.524)	22	121	0.713	0.524	0.419	0.385	0.419	11
HUB Genes	10	40	0.916	0.889	0.139	0.148	1.111	8
Transcription Factors	47	73	0.071	0.068	0.202	0.896	3.192	3.106

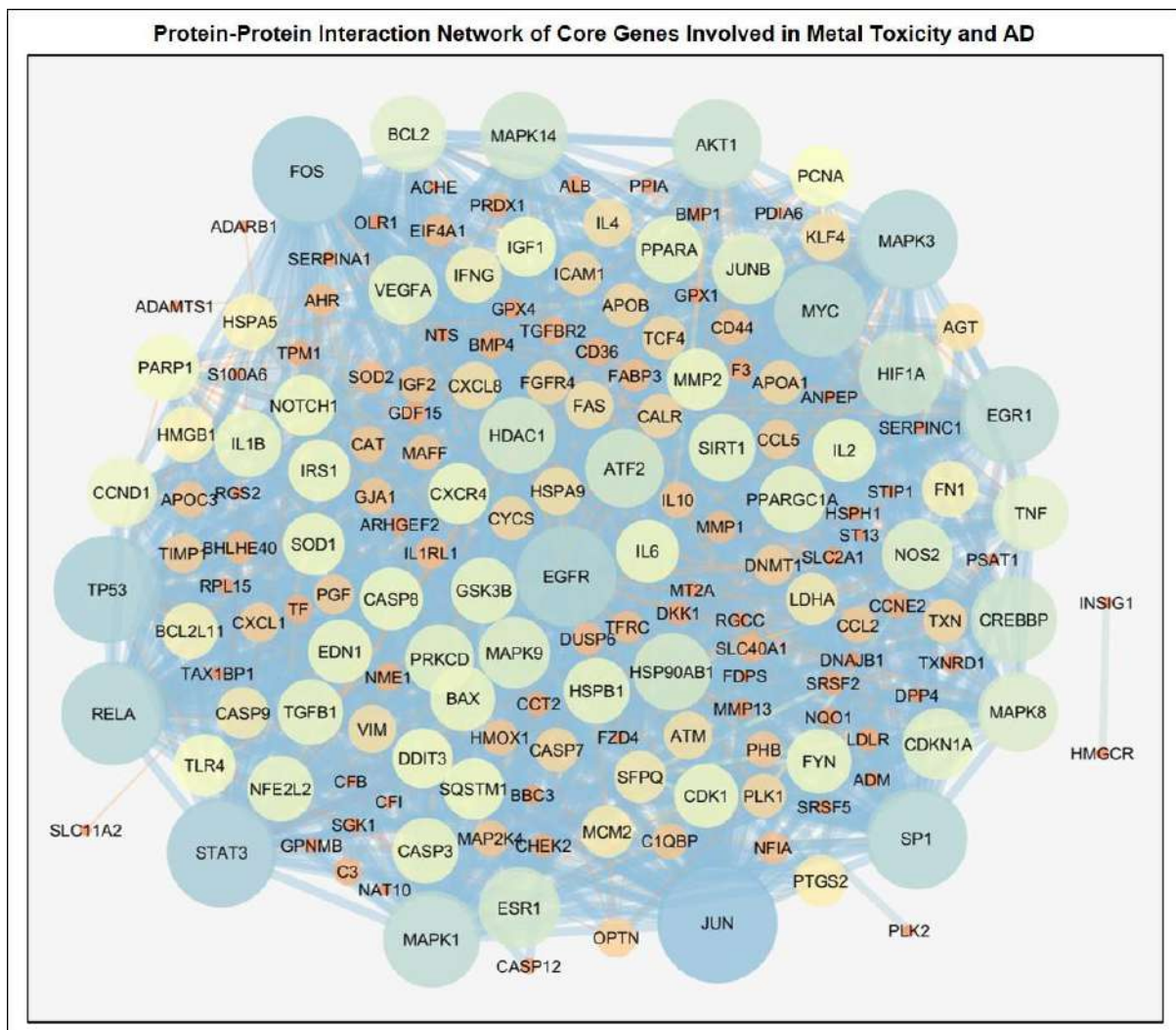


Figure 6.2: It represents the protein-protein interaction network of 199 common genes between chromium, cobalt, copper, and nickel associate metal toxicity induced Alzheimer's disease. The nodes in the network were ranked according to their degree. The size of the node decreases as the degree of node decreases. Similarly, the color of the node increases from a light color to dark color as the degree of the node decreases. Furthermore, the size of the edge between nodes depends on edge betweenness.

Further, the global PPI network clustering was carried out to extract the highly-dense connected region of the network with the help of M-Code [Figure 6.3 (A)]. Cluster 1 with an MCode score of 11.524, the number of nodes equal to 22, and the number of edges equal to 121 were selected for further investigations. Herein, we selected cluster 1 as it has a higher MCODE score and, thus, higher accuracy and biological significance than other predicted clusters. The density, centralization, and heterogeneity of the cluster network are 0.524, 0.419, and 0.385, respectively. Other parameters and characteristics of the cluster network are given in Table 6.2. Furthermore, the top 10 proteomic signatures or HUB genes were selected from the cluster network with the help of the CytoHubba. STAT3 (19), RELA (19), MAPK3 (18), C-FOS (17), EGFR (14), NOS2 (12), HIF1A (12), PTGS2 (7), MAPK8 (13), and AKT1 (12) were identified as HUB genes in the network [Figure 6.3 (B)]. The network density, network centralization, and network heterogeneity of the HUB genes network are 0.889, 0.139, and 0.148, respectively.

Protein-Protein Interaction Network of (B) Cluster Genes and (C) HUB Genes Involved in Metal Toxicity and AD

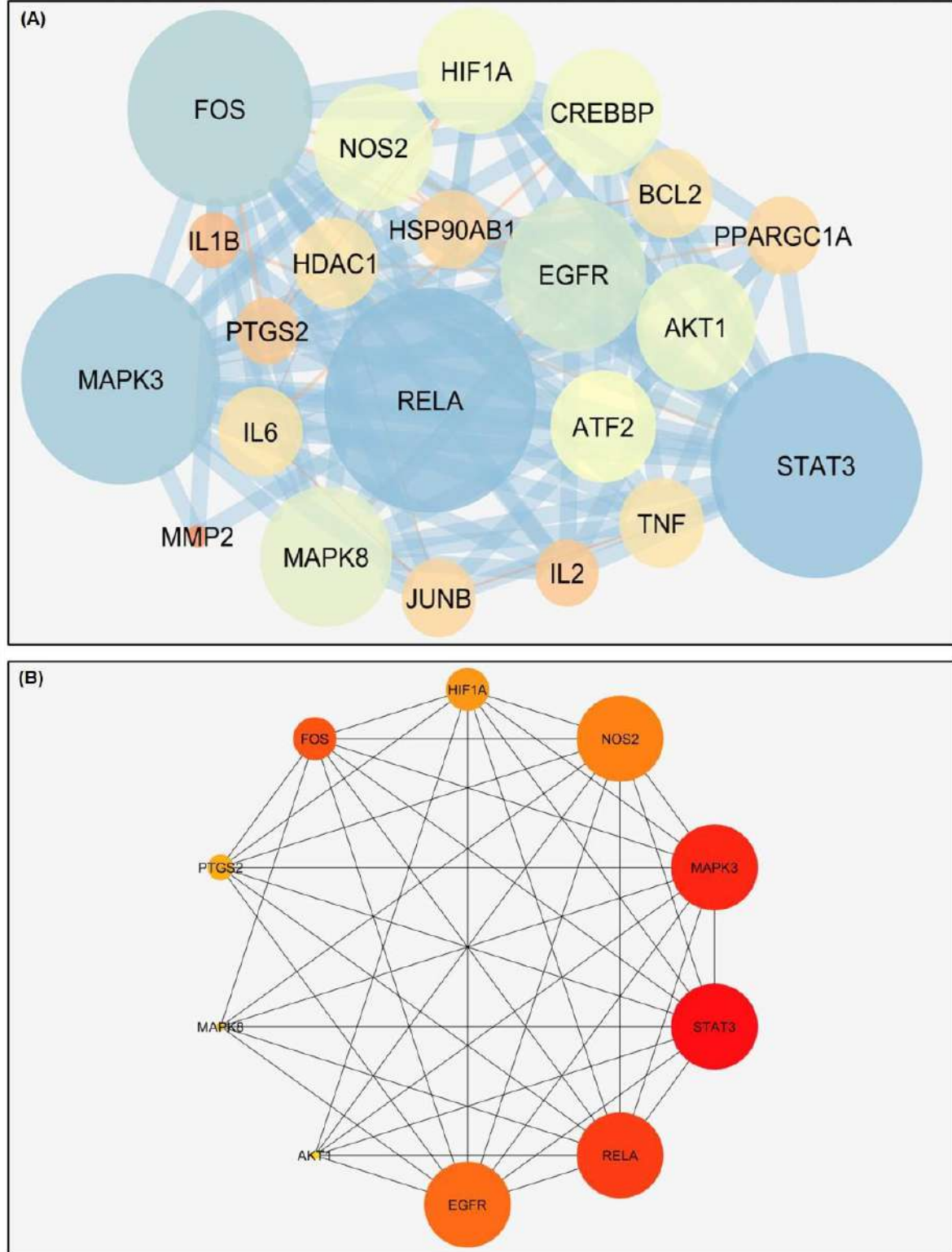


Figure 6.3: (A) it represents the clustering protein-protein interaction network and aims to identify the highly-dense or connected region in the global biological interaction network. (B) It represents the top 10 ranked HUB genes in the network. Here, darker is the color of the node; more is the rank of the HUB gene.

6.1.4. REGULATORY POST-TRANSCRIPTIONAL SIGNATURES IN THE REGULATION OF HUB PROTEINS ACTIVITY

The selected HUB genes were further analyzed to identify transcriptional signatures that are TFs involved in regulating metal toxicity induced AD. The HUB genes were analyzed with the JASPAR tool to identify regulatory TFs, and then with the help of network analyst interaction networks between HUB genes and TFs, were identified [Figure 6.4]. Analysis of the HUB genes-TFs network demonstrated 47 nodes and 73 edges in the network. Table 6.2 describes the parameters of the HUB genes-TFs interaction network. 47 TFs were identified, which regulate the transcriptional activity of HUB genes. To minimize the number of transcriptional signatures, the TFs with node degrees equal to or greater than 3 were selected for further investigations.

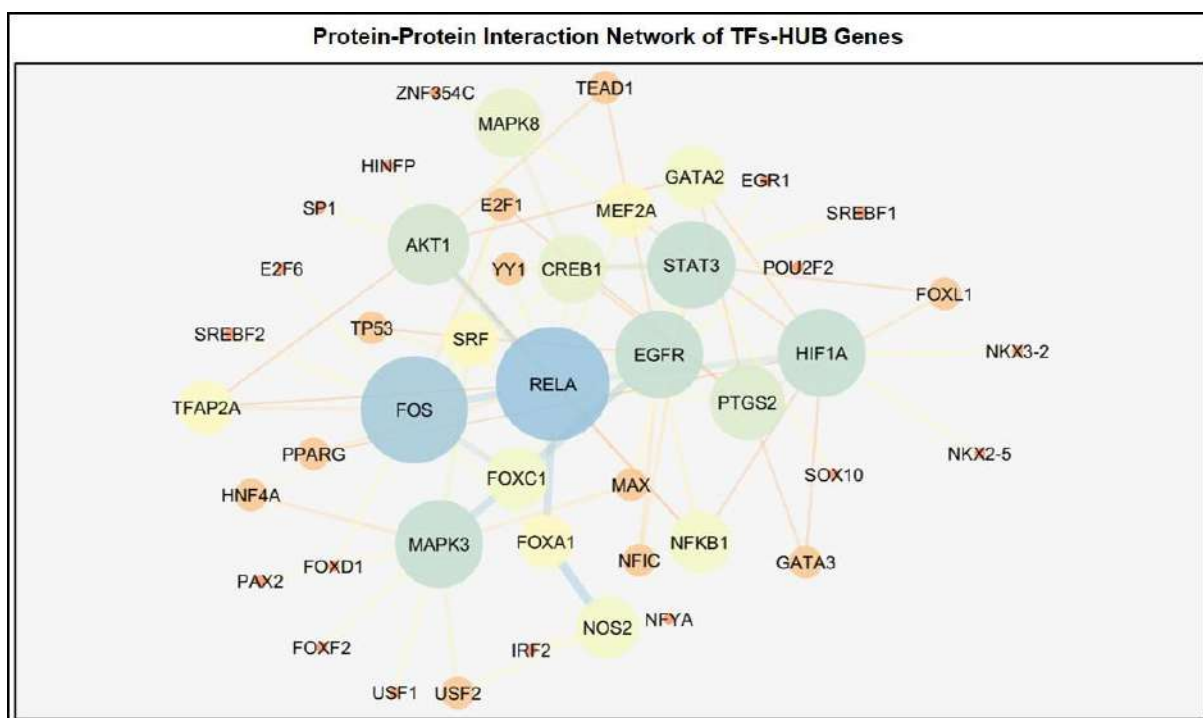


Figure 6.4: Protein-protein interaction network of transcription factors-HUB genes through Cytoscape Software: network analysis from network analyst identified the potential transcription factors associated with HUB genes. Among transcription factors, CREB1 (5), FOXC1 (4), GATA2 (4), NFκβ (4), SRF (3), TFAP2A (3), FOXA1 (3), and MEF2A (3) were the top interacting partners of HUB genes. Similarly, among HUB genes, FOS (11), RELA (9), MAPK3 (8), STAT3 (8), EGFR (8), HIF1A (8), AKT1 (6), PTGS2 (6), MAPK8 (5), and NOS2 (4) interacting partners.

The rationale behind selecting TFs with node degrees equal to or greater than 3 is to minimize

the number of TFs for further analysis. Another necessary explanation for selecting TFs with node degree equal to 3 or greater than 3 is to remove irrelevant TFs associated with molecular signatures of metal toxicity-induced AD. The node degree equal or greater than three signifies that a particular TFs is associated with either 3 molecular signatures or above 3 molecular signatures involved in metal toxicity-induced AD. Thus, these TFs have a higher weightage or higher probability of being involved in metal toxicity-induced AD. Thus, CREB1 (5), FOXC1 (4), GATA2 (4), NFKB1 (4), SRF (3), TFAP2A (3), FOXA1 (3), and MEF2A (3) were identified as top interacting TFs [Table 6.3].

Table 6.3: Top interacting transcriptional regulatory factors involved in metal toxicity induced Alzheimer's disease

TFs	Degree	Partners	Role in Disease Pathogenesis
CREB1	5	C-FOS, RELA, MAPK8, PTGS2, STAT3	Reduction in CREB1 activation promotes memory impairment
FOXC1	4	C-FOS, STAT3, EGFR, MAPK3	Mutation in FOXC1 cause neurodevelopmental disorder
GATA2	4	HIF1A, PTGS2, EGFR, AKT1	Reduction in GATA2 expression decreases neuroglobin expression
NFKB1	4	RELA, EGFR, AKT1, HIF1A	Regulate immunological response
SRF	3	MAPK3, MAPK8, C-FOS	Regulate LRP mediate amyloid- β clearance
TFAP2A	3	AKT1, RELA, C-FOS	Regulate the proliferation and apoptosis of neuronal cells
FOXA1	3	C-FOS, RELA, NOS2	Required for adult dopamine neuronal cells maintenance and functioning
MEF2A	3	RELA, MAPK8, HIF1A	Reduction in MEF2A expression causes decreased activity of anti-apoptotic genes

6.1.5. LITERATURE VALIDATION OF REGULATORY MOLECULES AND PROTEIN SUB-CELLULAR LOCALIZATION

Transcriptomics signatures and post-transcriptomics signatures were further investigated and validated to identify their potential role in regulating HUB genes or involvement in disease pathogenesis. The TFs were analyzed with MalaCards to extract the role of regulatory molecules in the progression of the disease [Table 6.3]. Furthermore, HUB genes were analyzed for their sub-cellular localization. Among the HUB genes, 50% were cytoplasmic (MAPK3, RELA, NOS2, MAPK8, AKT1), 30% were nuclear proteins (STAT3, C-FOS, HIF1A), 10% were endoplasmic reticulum complex protein (PTGS2), and 10% were Golgi

complex proteins (EGFR).

6.1.6. POTENTIAL ACETYLATED LYSINE RESIDUES OF REGULATORY MOLECULES

Acetylation of TFs at specific lysine residues causes transcriptional activation and thus promotes the cellular and biological processes. The identified TFs, such as CREB1, FOXC1, GATA2, NFKB1, SRF, TFAP2A, FOXA1, and MEF2A, were analyzed with Deep-PLA and GPS-PAIL to determine the crucial common CREBBP-induced acetylated lysine residues with high confidence score. For Deep-PLA, if the score is less than 5%, it must be said as acetylated lysine residue with high confidence, whereas, for GPS-PAIL, if the score is greater than 1.0, it is said to be acetylated lysine residue with high confidence. Our analysis identified a total of 4 acetylated lysine residues with high confidence, each one in four identified TFs. CREB1 (K122), GATA2 (K399), FOXA1 (K350), and NFKB (K967) were identified as critical lysine residues [Table 6.4].

Table 6.4: Prediction of CREBBP-induced acetylation sites of identified transcription factors through Deep PLA and GPS-PAIL

TF	Acetylation (CREBBP)		Common K Sites
	Deep PLA (Score < 5%)	GPS-PAIL (Score: > 1.0)	
CREB1	122	122, 271, 278, 289, 295, 316, 325	122
FOXC1	256	181, 552	--
GATA2	102, 281, 285, 399	324, 378, 389, 390, 399 , 403, 405, 406,	399
NFKB1	277, 431, 967	362, 425, 448, 896, 967	967
SRF	147, 154	506	--
TFAP2A	271	411, 427, 431, 434, 437	--
FOXA1	316, 350 , 389	6, 350	350
MEF2A	Nil	403, 498	--

FOXC1, SRF, TFAP2A, and MEF2A did not have any common acetylated lysine residue and thus were excluded for further analysis. Further, our prediction of CREBBP-induced acetylation sites for CREB coincides with the previously reported study. For instance, Lu et al., 2003 reported that the acetylation of CREB at K91, K94, K122, and K136 by CREBBP enhanced CREB-dependent transcription [477]. In addition, a previously published study

identified the GATA2 acetylation on K399 by p300, where the authors concluded that acetylation of GATA2 in 293T cells increases its DNA-binding activity [496].

6.1.7. MICRO-RNAs REGULATING THE ACTIVITY OF IDENTIFIED SIGNATURES

miRNAs are post-transcriptional regulators, which regulate the activity of a particular gene. Moving forward, we aim to identify the critical miRNAs that regulate the expression of CREBBP, CREB1, GATA2, NFKB1, and FOXA1. mirDIP, an online miRNA-target prediction tool, identified 379 miRNAs, 640 miRNAs, 145 miRNAs, 127 miRNAs, and 223 miRNAs in CREBBP, CREB1, GATA2, NFKB1, and FOXA1, respectively. Further, miRNAs having confidence score high or very high with a particular target, such as CREBBP (85 very high and 294 high), CREB1 (220 very high and 420 high), GATA2 (36 very high and 109 high), NFKB1 (32 very high and 95 high), and FOXA1 (71 very high and 152 high) were selected for further analysis. Moreover, Venn analyses were carried to identify the common miRNAs associated with CREBBP, CREB1, GATA2, NFKB1, and FOXA1 [Figure 6.5]. Our analysis identified five miRNAs, such as hsa-miR-338-5p, hsa-miR-335-5p, hsa-miR-429, hsa-miR-200c-3p, and hsa-miR-129-5p, were important miRNAs associated with all five selected targets. Furthermore, it is equally important to check whether the selected miRNA was expressed in brain tissues or not. For this, we analyzed the expression of putative miRNA in brain tissue samples from TissueAtlas, where we identified the expression of particular miRNA in the brain. hsa-miR-338-5p (23.09484), hsa-miR-335-5p (169.42783), hsa-miR-429 (4.26456), hsa-miR-200c-3p (2.72829), and hsa-miR-129-5p (251.58495) were expressed in 43, 46, 21, 28, and 47 brain tissue samples, respectively [Figure 6.5]. Further, we checked the role of putative miRNAs in the pathogenesis of AD. Our study identified that miRNAs, such as hsa-miR-335-5p (169.42783) and hsa-miR-129-5p (251.58495), were significantly enriched in the AD pathway with a p-value less than 0.05 [Figure 6.5]. Thus, hsa-miR-338-5p

(23.09484), hsa-miR-429 (4.26456), and hsa-miR-200c-3p (2.72829) were excluded from further analysis.

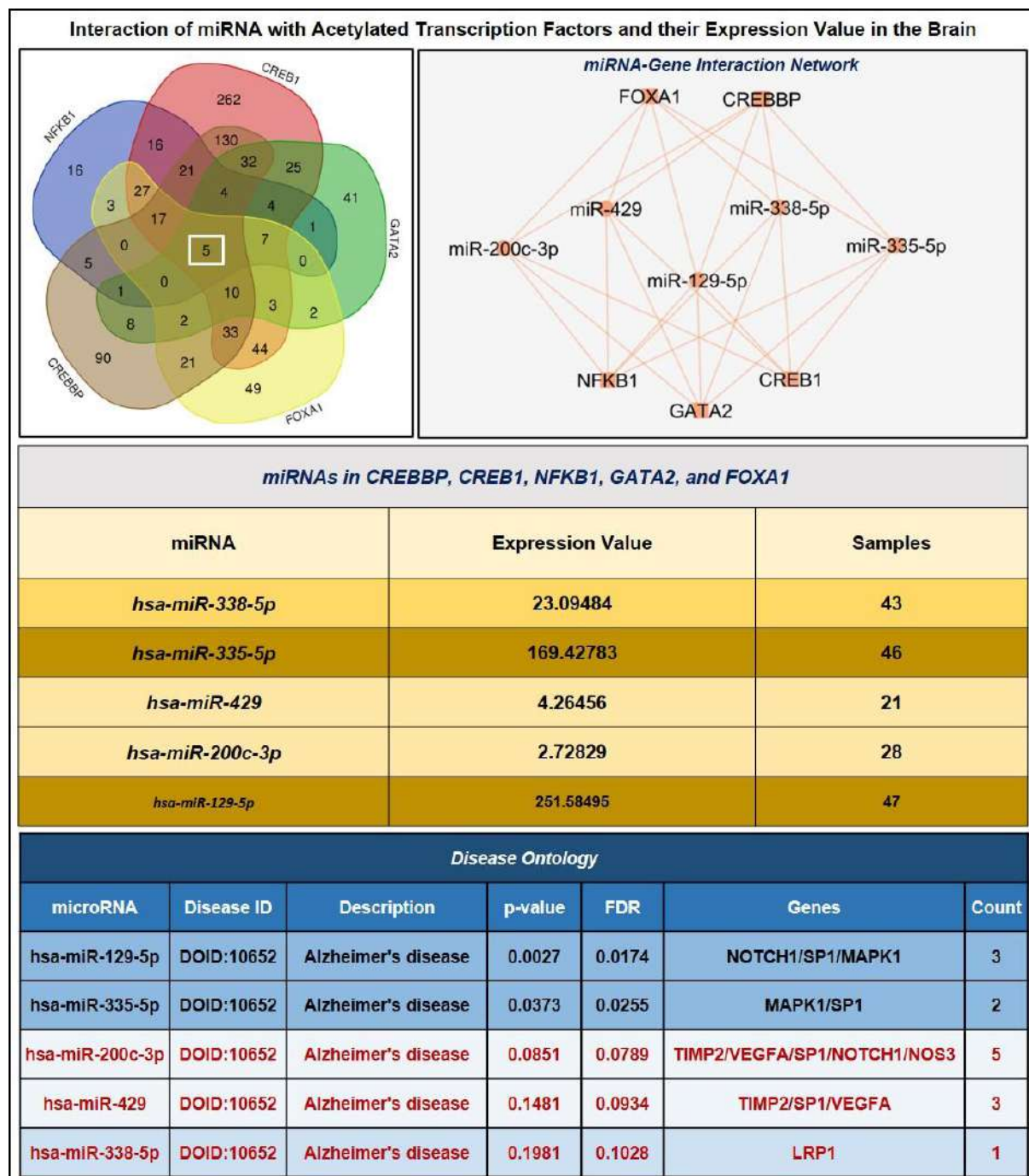


Figure 6.5: Micro-RNAs interacting with putative acetylated transcription factors and acetylating enzyme CREBBP were identified. Five micro-RNAs, such as hsa-miR-338-5p, hsa-miR-335-5p, hsa-miR-429, hsa-miR-200c-3p, and hsa-miR-129-5p, were common micro-RNAs interacting with acetylated transcription factors and CREBBP with the help of Venny 2.0 Software. Further, expression analysis of the predicted micro-RNAs in the brain tissue identified that micro-RNAs, namely hsa-miR-335-5p (169.427, 46 samples) and hsa-miR-129-5p (251.584, 47 samples), have the highest expression in the brain tissue among all five predicted micro-RNAs. Lately, network analysis of predicted micro-RNAs with identified transcription factors through Cytoscape software. Moreover, disease ontology analysis confirmed the involvement of hsa-miR-335-5p and hsa-miR-129-5p in the pathogenesis of Alzheimer's disease with the significantly enriched p-value of 0.0373 and 0.0174, respectively.

6.1.8. OIPS-AS1 REGULATES THE EXPRESSION AND ACTIVITY OF HSA-MIR-129-5P AND HSA-MIR-335-5P IN THE PATHOGENESIS OF METAL TOXICITY-INDUCE AD

Apart from AD, it is equally important to analyze the role of identified miRNAs in the pathogenesis and progression of brain diseases. hsa-miR-335-5p is involved in AD (0.03), developmental disorder of mental health (0.2), and tauopathy (0.03), whereas, hsa-miR-129-5p is involved in the pathogenesis of AD (0.002), dementia (0.107), Lewy body dementia (0.03), PD (0.13), and tauopathy (0.002). thus, the analysis concluded that both hsa-miR-335-5p and hsa-miR-129-5p are significantly involved in the pathogenesis of AD and tauopathy [Figure 6.6].

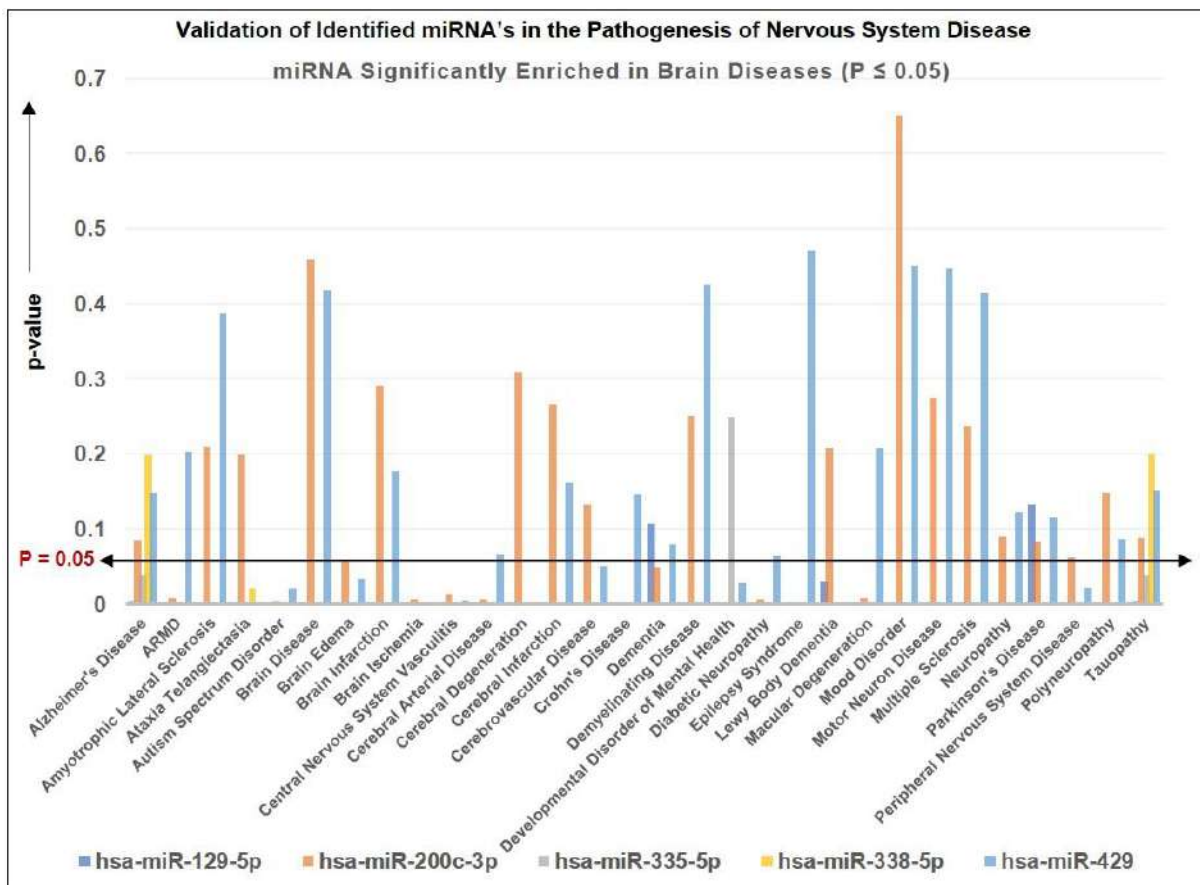


Figure 6.6: Involvement of predicted micro-RNAs, such as hsa-miR-338-5p, hsa-miR-335-5p, hsa-miR-429, hsa-miR-200c-3p, and hsa-miR-129-5p in the brain disease, such as Alzheimer's disease, Parkinson's disease, tauopathy, neuropathy, brain ischemia, brain edema, autism spectrum disorder, cerebral degeneration, and others through mirDIP database.

Further, our study also concluded that hsa-miR-338-5p is significantly enriched in the pathogenesis of Ataxia Telangiectasia (0.019), whereas, hsa-miR-429 is significantly enriched in autism spectrum disorder (0.020), brain edema (0.03), brain ischemia (0.001), CNS vasculitis (0.004), a developmental disorder of mental health (0.026), and peripheral nervous system disease (0.02). Similarly, hsa-miR-200c-3p is significantly enriched in ARMD (0.007), autism spectrum disorder (0.003), brain ischemia (0.005), CNS vasculitis (0.013), cerebral arterial disease (0.006), dementia (0.04), developmental disorder of mental health (0.0008), diabetic neuropathy (0.005), and macular degeneration (0.007). Further, we analyzed the signaling mechanism followed by hsa-miR-335-5p and hsa-miR-129-5p in the pathogenesis of AD. Our results demonstrated that hsa-miR-129-5p significantly enriches corticotropin-releasing hormone pathway (9.91805E-05), IL17 signaling pathway (0.000468125), EGF/EGFR signaling pathway (0.000533398), Interleukin-11 signaling pathway (0.000945926), and VEGFA-VEGFR2 (0.001582748) signaling pathway. Similarly, the TGF-beta signaling pathway (5.90563E-06), IL-2 signaling pathway (8.98756E-06), ErbB signaling pathway (9.29391E-05), B cell receptor signaling pathway (0.000115973), and IL-7 signaling pathway (0.000302961) are the top 5 signaling cascade in the hsa-miR-335-5p [Figure 6.7]. It is well-known that non-coding RNAs, namely long non-coding RNAs and circular RNAs, bind to the miRNA response element and alter the binding activity of miRNA to a target gene. Thus, keeping this in mind, we analyzed the putative long non-coding RNAs that alter the activity of five identified miRNAs. OIP5-AS1 is identified as long non-coding RNAs that alter the binding affinity of hsa-miR-335-5p and hsa-miR-129-5p to CREBBP in the pathogenesis of AD.

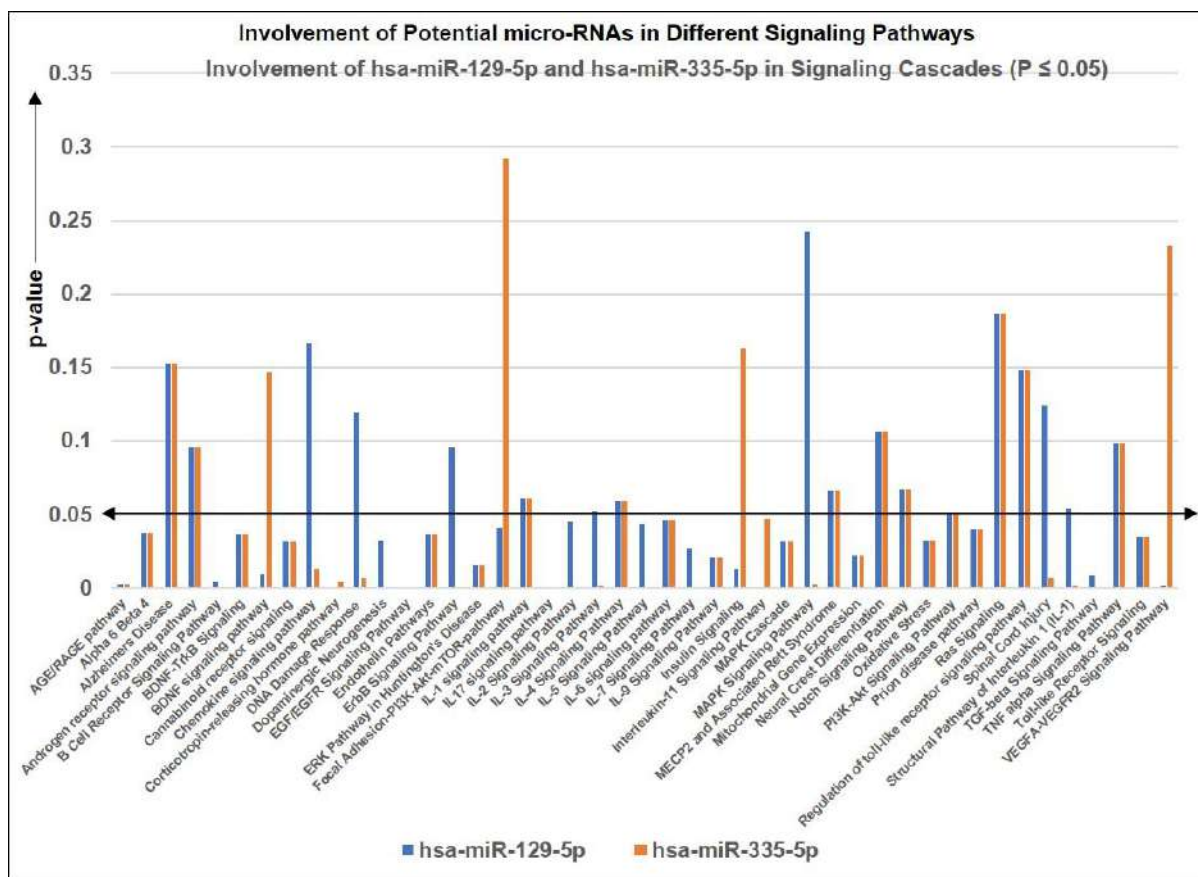


Figure 6.7: Pathway analysis of hsa-miR-335-5p and hsa-miR-129-5p with the help of TissueAtlas database: hsa-miR-129-5p is significantly enriched in corticotropin-releasing hormone pathway (9.91805E-05), IL17 signaling pathway (0.000468125), EGF/EGFR signaling pathway (0.000533398), Interleukin-11 signaling pathway (0.000945926), and VEGFA-VEGFR2 (0.001582748) signaling pathway, whereas, hsa-miR-335-5p is significantly enriched in TGF-beta signaling pathway (5.90563E-06), IL-2 signaling pathway (8.98756E-06), ErbB signaling pathway (9.29391E-05), B cell receptor signaling pathway (0.000115973), and IL-7 signaling pathway (0.000302961).

6.2. CONCLUSION AND SUMMARY

In the following study, we utilized a publicly accessible database, the CTD database and the DisGeNET database were used to identify common molecular signatures in metal toxicity and AD. The Venn analysis of genes involved in copper, chromium, cobalt, and nickel toxicity identified 376 shared genes. Furthermore, the Venn analysis of shared metal toxicity genes with the genes expressed in the AD revealed the presence of 199 common molecular genes that has been linked to heavy metal toxicity and AD. the gene set enrichment analysis of shared molecular targets identified the involvement of apoptosis, regulation of cell cycle, anti-apoptosis, protein metabolism, metabolism, signal transduction as the crucial biological process followed by shared molecular targets. Moreover, pathway analysis of common

molecular targets identified the potential involvement of AP-1 transcription factor network (43.2%), Integrin-linked kinase signaling (43.8%), TRAIL Signaling pathway (59.8%), VEGF and VEGFR signaling cascade (59.2%), and VEGFR1 and VEGFR2 mediated signaling cascade (58.6%). Further, the common molecular targets were analyzed to identify associated proteomic signatures, highly dense regions of the network, and highly connected nodes with the help of network biology. The PPI network has 175 nodes, and 1138 edges, where nodes were mapped according to their degree of nodes and edges were mapped according to FI score. Clustering of global PPI network identified highly dense regions with a clustering score of 11.524 with 22 nodes and 121 edges. Further investigation identified HUB genes in the cluster network, which are STAT3, MAPK3, RELA, C-FOS, EGFR, NOS2, HIF1A, PTGS2, MAPK8, and AKT1. PPI network analysis of HUB genes identified that the network has 10 nodes and 40 edges with network density and clustering coefficient of 0.889 and 0.916, respectively. Apart from identified 10 nodes or proteomic signatures or HUB genes, other nodes of cluster 1, such as IL2, IL6, Bcl-2, HDAC1, TNF, IL1 β , ATF2, and others were found to be associated with AD pathways through metal toxicity [Figure 6.8]. For instance, Cobalt chloride mimics hypoxia in R28 cells, which causes mitochondrial membrane potential disruption and activation of caspase 3 and ultimately leads to neuronal cell death. The same study also concluded that IL6 mediated its pro-survival effect against cobalt toxicity via STAT3 phosphorylation and activation of anti-apoptotic proteins [497]. Similarly, another study demonstrated that administration of cobalt nanoparticles causes an increase in inflammation-relation proteins, such as NLRP3 and IL1 β in C57BL/6J mice brain, suggesting the role of microglia-involved inflammation [498]. Further, Yubolphan et al., 2021 demonstrated that administration of nickel at 600.60 μ M and >1000 μ M in astrocytoma cells and primary human astrocytes, respectively, triggered apoptotic pathway through decreased activity of Bcl-2 and increased activity of caspase 3 [499].

Involvement of OIP5-AS1/miR-129-5p/CREBBP in the pathogenesis of metal toxicity-induced Alzheimer's disease

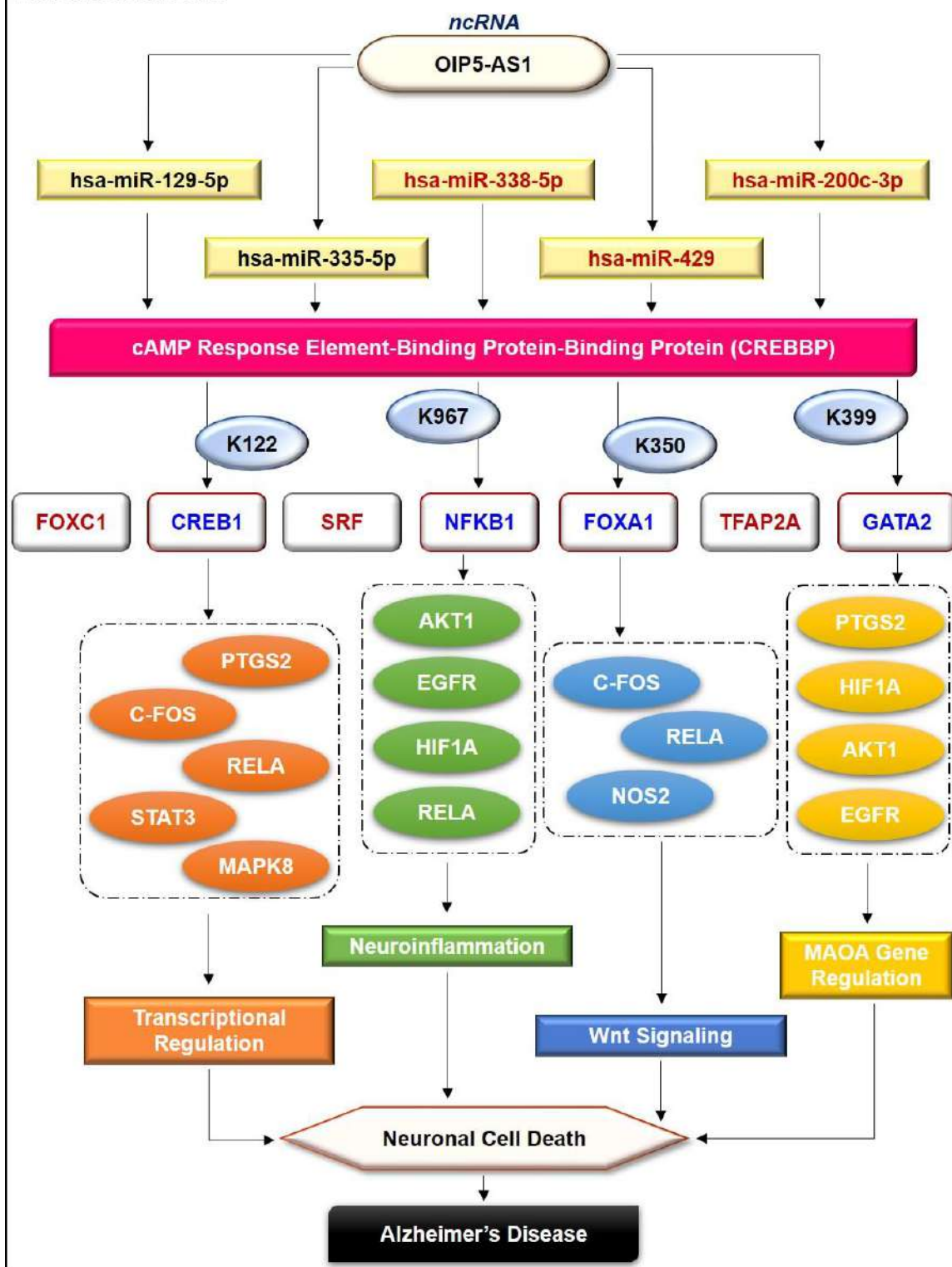


Figure 6.8: Mechanism of long non-coding RNA and micro-RNAs in metal toxicity-induced Alzheimer's disease: long non-coding RNA, namely Opa interacting protein 5 antisense RNA 1 (OIP5-AS1), alters the binding activity of hsa-miR-129-5p, hsa-miR-335-5p, hsa-miR-338-5p, hsa-miR-429, and hsa-miR-200c-3p to CREB Binding Protein (CREBBP), and thus alters the acetylation-inducing activity of CREBBP. CREBBP induces acetylation of CAMP responsive element binding protein 1 (CREB1) at lysine122, nuclear factor kappa-light-chain-enhancer of activated B cells (NFκβ) at lysine967, forkhead box A1 (FOXA1) at lysine350, and GATA binding protein 2 (GATA2) at lysine399. The acetylation of CREB1, NFκβ, FOXA1, and GATA2 increases their transcriptional activity, which further activates the activation of genes, such as PTGS2, C-

FOS, RELA, STAT3, MAPK8, AKT1, EGFR, HIF1A, and NOS2. The activation of such genes activates the different signaling cascades. For instance, acetylation of CREB1 activates transcriptional regulation, activation of NF κ B activates neuroinflammation cascade, acetylation of FOXA1 activates Wnt signaling pathway, and acetylation of GATA2 activates MAOA gene regulation pathway. Activation of these signaling pathways leads to neuronal cell death, which causes memory and synaptic impairment and ultimately leads to the pathogenesis of Alzheimer's disease.

Kitazawa et al., 2016 concluded that the copper-A β complex inhibits microglial phagocytosis and increases TNF- α and IL1 β clearance, leading to decreased activity of LRP1, which activates the inflammatory pathway [500,501]. Further, CREB1 (5), FOXC1 (4), GATA2 (4), NFKB1 (4), SRF (3), TFAP2A (3), FOXA1 (3), and MEF2A (3) were identified as top interacting TFs, which regulates the expression activity of HUB genes. Lately, literature validation confirmed the role of identified TFs in the pathogenesis and progression of AD [455,502–506]. For instance, activation of CREB1 and acquisition of transcription cofactors, such as CREBBP, is crucial for memory formation, whereas, deficiency of NFKB1 causes early onset of memory loss [507,508]. Similarly, silencing SRF reversed contractile protein content and rescued from a hypercontractile phenotype in AD, while TFAP2A is involved in the genetic variants associated with a high risk of dementia [509,510]. Lately, we identified the CREBBP-induced acetylation sites of the eight TFs. CREBBP, also called CBP or KAT3A is involved in acetylation by modulating different signaling pathways, such as calcium signaling, notch signaling, response to hypoxia, and NF- κ B signaling [511]. Recent studies demonstrated the potential link between metal toxicity and the acetylation process. For instance, Kang et al., 2004 concluded that copper at both toxic and non-toxic levels (100 or 200 μ M) causes histone hypoacetylation in Hep3B cultured cells through inhibiting specific HAT activity [512]. Further, it was concluded that administration of hexavalent chromium (10 μ M) downregulates histone H4 acetylation at K16 through activation of stressor protein Nupr1 [513]. Similarly, chromium (12.5 μ M) administration causes inhibition of biotinidase, which could be reversed by increased acetylation levels [514]. Recently, Zhou et al., 2021 demonstrated that administration of nickel causes a reduction in H3K9 acetylation levels, which leads to repression of H3K9-modulate neural genes expression [515]. Apart from nickel, copper, and

chromium, another metal that interferes with acetylation is cobalt. Evidence suggests the potential relationship between cobalt and acetylation status. For example, Guo et al., 2021 demonstrated that cobalt chloride administration at 400 μ M for 24 hours in the SHSY5Y cell culture model inhibits H3 and H4 acetylation [516]. The same study concluded that cobalt chloride selectively decreased the activity of HAT and did not alter the activity of HDAC. Thus, these evidences validate the role of metal toxicity and acetylation status. Further different studies also investigated the role of metal exposure on the expression of CREBBP. For example, administration of chromium hexavalent ion results in decreased expression of CREBBP protein, whereas, exposure to copper caused decreased expression of CREBBP mRNA [517,518]. However, in another study, it was concluded that administration of nickel monoxide results in increased expression of CREBBP mRNA [519]. Further, some evidences suggest the role of metal exposure on the activity of CREBBP and its targets. For instance, chromium inhibits the transcriptional activity of NF- κ B by decreasing the interaction between p65 and CBP [520]. Similarly, Cobalt causes increased activity of SRC protein, which activates HIF1A/STAT3/VEGFA and leads to binding of APEX1 to CREBBP promoter [521]. Thus, these evidences demonstrated the potential link between metal exposure and CREBBP and acetylation. However, no study was reported that concluded the exact role of metal exposure in CREBBP and its target acetylation. Thus, we aim to identify the potential targets of CREBBP involved in metal toxicity and AD pathogenesis. Our study identified that CREBBP-Induces CREB1, GATA2, NFKB1, and FOXA1 acetylation at K122, K399, K967, and K350. Thus, K122 of CREB1, K399 of GATA2, K967 of NFKB1, and K350 of FOXA1 were considered crucial lysine residues for the acetylation process in the pathogenesis of AD. In addition, post-transcriptional signatures, namely miRNA and long non-coding RNAs, regulate the expression of proteins, where long non-coding RNAs serve as a sponge for miRNA. Our results identified five potential miRNAs that were associated with CREBBP and identified TFs simultaneously,

such as hsa-miR-338-5p, hsa-miR-335-5p, hsa-miR-429, hsa-miR-200c-3p, and hsa-miR-129-5p. However, hsa-miR-335-5p and hsa-miR-129-5p, having expression values of 169.427 and 251.584, respectively, in the brain tissue, were selected for further studies. In addition, literature validation suggests the potential applicability of hsa-miR-335-5p and hsa-miR-129-5p in the pathogenesis and progression of AD. For instance, Wang et al., 2020 demonstrated that overexpression of miR-335-5p significantly decreased the expression of c-Jun N-terminal kinase 3 (JNK3) and A β and thus, inhibited the neuronal apoptosis in SH-SY5Y/APP_{swe} cells [522]. Similarly, overexpression of miR-129-5p rescued nerve injury and inflammatory response through decreased expression of SRY-box transcription factor 6 (SOX6) in the A β ₂₅₋₃₅-induced AD rat model [523]. In addition, Li et al., 2020 concluded that knockdown of miR-129-5p decreased the neuroprotective effects of exercise on cognition and neuroinflammation in the AD mice model [524]. Thus, it could be concluded that overexpression of both hsa-miR-335-5p and hsa-miR-129-5p promotes neuroprotection. Furthermore, disease ontology confirmed the involvement of hsa-miR-335-5p and hsa-miR-129-5p in the pathogenesis of AD, having a p-value of 0.0373 and 0.0027, respectively. Further, mounting evidence suggests the potential link between metal toxicity and miRNA expression. For instance, administration of cadmium at 0.6 mg/kg increased the expression levels of miR-21-5p, miR-34a-5p, miR-224-5p, miR-451-5p, and miR-1949, whereas, administration of cadmium in human prostrate epithelial cells at 10 μ M increases the expression of miR-96, miR-134, and miR-9 [525,526]. Similarly, administration of cobalt increases the pri-miRNA processing activity of DGCR8, which enhanced the expression of miR-9 [527]. Further, Jeon et al., 2014 concluded that administration of cobalt chloride-induced neuronal differentiation of human mesenchymal stem cells through upregulation of miR-124a, which inhibits the expression of SCP1 and SOX9 [528]. Chiou et al., 2015 demonstrated that administration of nickel contributes to EGFR mutation and miR-21 overexpression, whereas, Wu et al., 2017 concluded that upregulation of

miR-4417 contributes to nickel-induced fibrogenesis [529,530]. Another study identified that administration of arsenic in Patu8988 cells at 3 $\mu\text{mol/L}$ causes increased expression of miR-330-5p, whereas, administration of lead in blood samples of battery factory workers causes and upregulation of miR-520c-3p, miR-148a, miR-141, and miR-211 [531,532]. Jia et al., 2020 reported that chromium in exposed electroplating workers causes upregulation of miR-941 and miR-590-3p, whereas, Chandra et al., 2015 concluded that administration of chromium at 10 and 20 $\mu\text{g/ml}$ for 24 hours upregulated the expression of miR-34-5p [533,534]. Further, studies demonstrated that exposure to cobalt chloride regulates the expression of miR-129-5p and its target genes [535,536]. Moreover, pathway analysis demonstrated the possible pathways through which hsa-miR-335-5p and hsa-miR-129-5p are involved in the pathogenesis of AD [522,524]. hsa-miR-129-5p is involved in corticotropin-releasing hormone pathway, IL17 signaling pathway, EGF/EGFR signaling pathway, Interleukin signaling pathway, and VEGFA-VEGFR2 signaling pathway [537–541], whereas, hsa-miR-335-5p is involved in TGF-beta signaling pathway, IL-2 signaling pathway, ErbB signaling pathway, B cell receptor signaling pathway, and IL-7 signaling pathway [542–545]. Lastly, we identified the potential long non-coding RNA that is OPI5-AS1 that regulates the activity of hsa-miR-335-5p and hsa-miR-129-5p. Literature analysis validated our results as downregulation of OPI5-AS1 causes upregulation of has-miR-129-5p [546]. Thus, we concluded that downregulation of OPI5-AS1 causes upregulation of miR-129-5p, which modulate CREBBP-induced hyperacetylation of CREB1, GATA2, NFKB1, and FOXA1 acetylation at K122, K399, K967, and K350. Regulation of hyperacetylation of CREB1, GATA2, NFKB1, and FOXA1 modulate their transcriptional activation, neuroinflammation, Wnt Signaling, and MAOA gene regulation, respectively, which inhibits neuronal cell death. In addition, decreased neuronal cell death rescued memory impairment and cognitive defects, which inhibits the pathogenesis of AD. Thus, the OIP5-AS1/miR-129-5p/CREBBP axis could be a possible therapeutic target in metal

toxicity-induced AD. Further, these results provide a gateway for the future *in vivo* and *in vitro* studies targeting OIP5-AS1/miR-129-5p/CREBBP axis in a metal toxicity-induced AD.

6.3. HIGHLIGHTS OF THE STUDY

6.3.1. OIP5-AS1/miR-129-5p/CREBBP axis is involved in metal toxicity-induced AD

6.3.2. FOXC1, CREB1, SRF, NFKB1, FOXA1, TFAP2A, and GATA2 were identified as regulatory TFs

6.3.3. CREBBP-induces CREB1, GATA2, NFKB1, and FOXA1 acetylation at K122, K399, K967, and K350

6.3.4. miR-129-5p and miR-335-5p as potential post-transcriptional signatures involved in AD pathogenesis

6.3.5. miR-129-5p and miR-335-5p regulate the activity of CREBBP in metal toxicity-induced AD

6.3.6. OIP5-AS1 regulates the expression of miR-129-5p and miR-335-5p

CHAPTER VII

Identification of Novel Histone Deacetylase 10 Inhibitor for Alzheimer's Disease Therapeutics

CHAPTER VII: IDENTIFICATION OF NOVEL CLASS IIB HISTONE DEACETYLASE INHIBITOR FOR ALZHEIMER'S DISEASE THERAPEUTICS

7. INTRODUCTION

HDAC enzymes acts as potential chromatin modifier agents that targets the progression and pathogenesis of AD. Various studies have confirmed the overexpression of HDAC activity in the pathology of AD that causes transcriptional downregulation. Thus, inhibition of HDAC activity could be a promising therapeutic approach in reversing AD pathology. However, HDAC inhibitors are associated with some sort of limitations, such as isoform selectivity and specificity. Hence, we aim to set up a methodology describing the rational development of isoform-selective HDAC class Iib inhibitor targeting HDAC10. A convenient multistage virtual screening followed by machine learning and IC₅₀ screenings were used to classify the 239 anti-depressive compounds into inhibitors and non-inhibitors classes retrieved from the ChEMBL database. ADMET analysis identified the pharmacokinetics and pharmacodynamics properties of selected compounds. Molecular docking, along with mutational analysis of seven compounds, characterized the inhibiting potency. Herein, for the first time, we reported Zimeldine and Dibenzapine as the potential HDAC10 inhibitor, which interact central Zn²⁺ atom.

7.1. RESULTS AND DISCUSSION

7.1.1. DATA COLLECTION AND PREPROCESSING

Total of 543 compounds that binds with HDAC10 in *in vitro* and *in vivo* assay were extracted. After removing blanks and duplicates, a list of 503 compounds were selected for further steps. Lately, the compounds were filtered based on their IC₅₀ values. Sorting of compounds based on IC₅₀ value yield 122 inhibitors and 354 non-inhibitors. Similarly, for test set, 444 anti-depressive drugs were collected. After data processing and removing duplicates, a total of 283 compounds were selected. Further, only those compounds were selected for machine learning

classification those have passed phase IV of clinical trials.

A .pdb structure of HDAC10 (5TD7) were extracted form PDB database. The protein was processed and remove non-protein molecules and add hydrogen atoms. Further, energy minimization of HDAC10 was performed for efficient molecular docking.

7.1.2. MACHINE LEARNING MODEL PREPARATION AND EVALUATION

As mentioned above, three kinds of molecular features, i.e., MACCS keys (166 bits), Morgan2 fingerprints (1024 bits) and Mordred descriptors (27 descriptors after feature selection) and five ML algorithms (i.e., KNN, SVM, RF, XGBoost and DNN) were used for model building. All the models were tested and measured by AC, SE, SP, MCC and AUC. All the models showed pretty good and close performance on the test set. The MCC values of the models ranged from 0.514 to 0.739, while the AUC values were between 0.863 and 0.946. All the models could predict actives better than inactives as the mean value of SE was 0.921 while the average SP value was 0.705. For different feature sets, the classifiers built based on the Morgan2 fingerprints performed better than those based on the other two feature sets, as the average AUC was 0.934 for the Morgan2 fingerprints, 0.914 for the MACCS keys, and 0.893 for Mordred descriptors. The above data indicate that, among the three features, the Morgan2 fingerprints were the most suitable for building ML models to classify HDAC3 inhibitors. Further, the classification identified 16 anti-depressive drugs as potential HDAC10 inhibitor [Table 7.1].

Table 7.1: List of 16 anti-depressive drugs as a potential HDAC10 inhibitors predicted from machine learning classification

Class	SMILES	ChEMBL ID	NAME
Inhibitor	<chem>Cc1cc2c(s1)Nc1ccccc1N=C2N1CCN(C)CC1</chem>	CHEMBL715	OLANZAPINE
Inhibitor	<chem>COc1ccc2c(c1)N(C[C@H](C)CN(C)C)c1ccccc1S2</chem>	CHEMBL1764	LEVOMEPROMAZINE
Inhibitor	<chem>CN1CCN2c3ncccc3Cc3ccccc3C2C1</chem>	CHEMBL654	MIRTAZAPINE
Inhibitor	<chem>CN(C)c1ccc(O)c2c1C[C@H]1C[C@H]3[C@H](N(C)C)C(O)=C(C(N)=O)C(=O)[C@@]3(O)C(O)=C1C2=O</chem>	CHEMBL1434	MINOCYCLINE
Inhibitor	<chem>CN(C)CCN1C(=O)c2ccccc2N(C)c2ccccc21</chem>	CHEMBL1442422	DIBENZEPIN
Inhibitor	<chem>CN(C)CCCN1c2ccccc2Sc2ccnc21</chem>	CHEMBL2111030	PROTHIPENDYL
Inhibitor	<chem>CN(C)CC/C=C1/c2ccccc2CSc2ccccc21</chem>	CHEMBL1492500	DOTHIEPIN

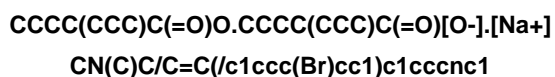
Inhibitor	<chem>C1c1ccc2c(c1)C(N1CCNCC1)=Nc1cccc1O2</chem>	CHEMBL1113	AMOXAPINE
Inhibitor	<chem>CN1CCC[C@H]1c1cccnc1</chem>	CHEMBL3	NICOTINE
Inhibitor	<chem>Cc1ccc(-c2nc3ccc(C)cn3c2CC(=O)N(C)C)cc1</chem>	CHEMBL911	ZOLPIDEM
Inhibitor	<chem>CO[C@]12C[C@@H](COC(=O)c3cncc(Br)c3)CN(C)[C@@H]1Cc1cn(C)c3cccc2c13</chem>	CHEMBL1372950	NICERGOLINE
Inhibitor	<chem>C#CCN(C)[C@H](C)Cc1cccc1</chem>	CHEMBL972	SELEGILINE
Inhibitor	<chem>CN1CCN(C(=O)OC2c3nccnc3C(=O)N2c2ccc(Cl)cn2)CC1</chem>	CHEMBL135400	ZOPICLONE
Inhibitor	<chem>OCCOCCN1CCN(C2=Nc3cccc3Sc3cccc32)CC1</chem>	CHEMBL716	QUETIAPINE
Inhibitor	<chem>CCCC(CCC)C(=O)O.CCCC(CCC)C(=O)[O-].[Na+]</chem>	CHEMBL2105613	DIVALPROEX SODIUM
Inhibitor	<chem>CN(C)C/C=C/c1ccc(Br)cc1)c1cccnc1</chem>	CHEMBL37744	ZIMELDINE

7.1.3. ADMET ANALYSIS AND BLOOD BRAIN BARRIER OF SELECTED COMPOUNDS

BBB permeability of 16 novels predicted hits were calculated with the help of CBLigand and LightBBB, which is necessary for any compound to be said as drug molecule. BBB prediction of 16 novel compounds identified that two compounds, namely MINOCYCLINE (CHEMBL1434) and NICERGOLINE (CHEMBL1372950) [Table 7.2]. Thus, 14 potential anti-depressive drugs were carried out for ADMET analysis with the help of online tool, namely admetSAR.

Table 7.2: List of compounds selected from blood-brain barrier prediction

SMILES	LightBBB	CBLigand
<chem>Cc1cc2c(s1)Nc1cccc1N=C2N1CCN(C)CC1</chem>	Permeable	Positive
<chem>COc1ccc2c(c1)N(C[C@H](C)CN(C)C)c1cccc1S2</chem>	Permeable	Positive
<chem>CN1CCN2c3ncccc3Cc3cccc3C2C1</chem>	Permeable	Positive
<chem>CN(C)c1ccc(O)c2c1C[C@H]1[C@H]3[C@H](N(C)C)C(O)=C(C(N)=O)C(=O)[C@@]3(O)C(O)=C1C2=O</chem>	Non-Permeable	Negative
<chem>CN(C)CCN1C(=O)c2cccc2N(C)c2cccc21</chem>	Permeable	Positive
<chem>CN(C)CCN1c2cccc2Sc2cccnc21</chem>	Permeable	Positive
<chem>CN(C)CC/C=C1c2cccc2CSc2cccc21</chem>	Permeable	Positive
<chem>C1c1ccc2c(c1)C(N1CCNCC1)=Nc1cccc1O2</chem>	Permeable	Positive
<chem>CN1CCC[C@H]1c1cccnc1</chem>	Permeable	Positive
<chem>Cc1ccc(-c2nc3ccc(C)cn3c2CC(=O)N(C)C)cc1</chem>	Permeable	Positive
<chem>CO[C@]12C[C@@H](COC(=O)c3cncc(Br)c3)CN(C)[C@@H]1Cc1cn(C)c3cccc2c13</chem>	Permeable	Negative
<chem>C#CCN(C)[C@H](C)Cc1cccc1</chem>	Permeable	Positive
<chem>CN1CCN(C(=O)OC2c3nccnc3C(=O)N2c2ccc(Cl)cn2)CC1</chem>	Permeable	Positive
<chem>OCCOCCN1CCN(C2=Nc3cccc3Sc3cccc32)CC1</chem>	Permeable	Positive



Permeable Positive
 Permeable Positive

ADMET analysis of novel compounds was carried out to check the pharmacokinetics and pharmacodynamics properties of lead compounds. In our study, we predict 10 ADMET properties of selected compounds out of them 3 of absorption properties, 1 of distribution properties, 2 of metabolism properties, 1 of excretion properties, and 3 of toxicity properties. For a compound to be an effective drug it must fulfill these parameters. Hepatotoxicity predicts the action of compound on normal liver function. Furthermore, if the given compound is found to be AMES positive, then it will be considered as mutagenic. Our study found out that only 7 compounds (OLANZAPINE, MIRTAZAPINE, DIBENZEPIN, PROTHIPENDYL, AMOXAPINE, QUETIAPINE, ZIMELDINE) were show promising results, whereas, other seven compounds were removed after ADMET analysis [Table 7.3].

Table 7.3: ADMET analysis of 14 potential anti-depressive drugs as histone deacetylase 10 inhibitor

Anti-Depressive Drugs	Adsorption			Distribution	Metabolism		Excretion	Toxicity		
	Water Solubility	Intestinal Absorption	Skin Permeability	VDss	CYP2D6 Substrate	CYP3A4 Substrate	Total Clearance	AMES Toxicity	Hepatotoxicity	Skin Sensitisation
OLANZAPINE	-3.656	91.841	-2.737	1.816	Yes	Yes	0.659	No	Yes	No
LEVOMEPROMAZINE	-4.483	93.306	-2.505	1.691	No	Yes	0.463	Yes	Yes	No
MIRTAZAPINE	-2.68	96.586	-2.568	1.226	No	Yes	0.745	No	Yes	No
DIBENZEPIN	-3.579	97.686	-2.541	1.158	No	Yes	0.71	No	No	No
PROTHIPENDYL	-3.681	95.109	-2.398	1.159	No	Yes	0.598	No	Yes	No
DOTHIEPIN	-2.841	82.458	-2.638	-1.125	No	Yes	0.786	No	Yes	No
AMOXAPINE	-4.221	92.727	-2.822	1.303	No	Yes	0.471	No	Yes	No
NICOTINE	-0.748	95.867	-2.143	0.577	No	No	0.858	No	Yes	Yes
ZOLPIDEM	-2.838	92.713	-2.773	-0.099	No	No	0.752	Yes	Yes	No
SELEGILINE	-2.29	94.876	-1.88	1.1	Yes	No	1.045	No	Yes	Yes
ZOPICLONE	-3.03	80.53	-2.769	-0.332	No	Yes	0.249	No	Yes	No
QUETIAPINE	-3.446	93.076	-2.665	1.23	Yes	Yes	0.636	No	Yes	No
DIVALPROEX SODIUM	-2.569	75.058	-2.735	-1.725	No	Yes	1.966	No	No	No
ZIMELDINE	-3.126	87.536	-2.561	0.685	Yes	Yes	1.249	No	Yes	No

Afterwards, Structural comparison of novel potential hits with HDAC10 known inhibitor, namely pracinostat were performed with the help of online tool, such as ChemMine.

ChemMine calculates the atom pair and maximum common substructure (MCS) similarities with the Tanimoto coefficient as the similarity measure. The MCS tool identifies the largest substructure two compounds have in common. The MCS method provides the most accurate and sensitive similarity measure, especially for compounds with large size differences [Table 7.4]. The results indicated that anti-depressive drugs, namely DIBENZEPIN, PROTHIPENDYL, and ZIMELDINE have maximum similarity with HDAC10 known inhibitor, namely pracinostat with MCS size of 13, 10, and 10, respectively [Table 7.4].

Table 7.4: Structural similarity comparison of selected ant-depressive drugs with histone deacetylase 10 known inhibitor i.e., pracinostat

SMILES	MCS Tanimoto	MCS Size	MCS Min	MCS Max
<chem>Cc1cc2c(s1)Nc1cccc1N=C2N1CCN(C)CC1</chem>	0.3495	8	0.3636	0.3077
<chem>CN1CCN2c3ncccc3Cc3cccc3C2C1</chem>	0.1795	7	0.3500	0.2692
<chem>CN(C)CCN1C(=O)c2cccc2N(C)c2cccc21</chem>	0.3714	13	0.5909	0.5000
<chem>CN(C)CCCN1c2cccc2Sc2ccnc21</chem>	0.2778	10	0.5000	0.3846
<chem>C1c1ccc2c(c1)C(N1CCNCC1)=Nc1cccc1O2</chem>	0.2000	8	0.3636	0.3077
<chem>OCCOCCN1CCN(C2=Nc3cccc3Sc3cccc32)CC1</chem>	0.1778	8	0.3077	0.2963
<chem>CN(C)C/C=C/c1ccc(Br)cc1)c1ccnc1</chem>	0.2857	10	0.5263	0.3846

7.1.4. MOLECULAR DOCKING STUDIES OF PREDICTED COMPOUNDS

Comparison between the full fitness of 7 anti-depressive compounds to 1 known inhibitor (Pracinostat) explained that the three compounds, such as Zimeldine, Prothipendyl, and Dibenapine have a higher binding affinity to HDAC10 due to which they have strong potential to be used as isoform-selective HDAC inhibitors. From the study of binding pocket and binding site analysis, it is cleared that Zimeldine and Dibenapine can be used to inhibit HDAC10, whereas, Prothipendyl is unable to bind with central Zn²⁺ atom and cannot be used as HDAC10 inhibitor.

Table 7.5: Molecular docking analysis of 7 predicted ant-depressive compounds and their comparison with known HDAC10 inhibitor

Compound	Docking Score	Residues
Pracinostat	-2890.03 Kcal/mol	PRO ¹³⁴ , HSD ¹³⁶ , HSD ¹³⁷ , PHE ¹⁴⁶ , HSE ¹⁷⁶ , TRP ²⁰⁵ , ASP ²⁶⁷ , GLU ²⁷⁴ , GLU ³⁰⁴ , GLY ³⁰⁵
Zimeldine	-2962.57 Kcal/mol	PRO ¹³⁴ , HSD ¹³⁶ , GLY ¹⁴⁵ , PHE ¹⁴⁶ , CYS ¹⁴⁷ , HSE ¹⁷⁶ , GLY ³⁰⁵

Mirtazapine	-2830.36 Kcal/mol	ASP ⁹³ , HSD ¹³⁴ , HSD ¹³⁵ , GLY ¹⁴³ , CYS ¹⁴⁵ , ASP ¹⁷⁰ , HSE ¹⁷² , TYR ¹⁹⁸ , PHE ¹⁹⁹ , PHE ²⁰⁰ , ASP ²⁵⁹ , LEU ²⁶⁶ , GLY ²⁹⁶ , TYR ²⁹⁸
Prothipendyl	-2892.25 Kcal/mol	PRO ¹³⁴ , HSD ¹³⁶ , HSD ¹³⁷ , GLY ¹⁴⁵ , TRP ²⁰⁵ , ASP ²⁶⁷ , GLU ²⁷⁴
Olanzapine	-2836.52 Kcal/mol	GLY ⁶⁰⁹ , PHE ⁶¹⁰ , CYS ⁶¹¹ , VAL ⁶¹⁶ , VAL ⁶¹⁹ , ALA ⁶²⁰ , GLY ⁶⁴³ , GLU ⁶⁵¹ , ASP ⁶⁵² , ALA ⁷⁴³ , ASP ⁷⁴⁷
Dibenzapine	-2915.14 Kcal/mol	GLY ¹⁴⁵ , PHE ¹⁴⁶ , CYS ¹⁴⁷ , ASP ²⁶⁷ , GLU ²⁷⁴ , GLU ³⁰⁴ , GLY ³⁰⁵
Amoxapine	-2809.27 Kcal/mol	TYR ¹⁰⁰ , ASP ¹⁰¹ , GLY ¹⁴⁰ , TRP ¹⁴¹ , HSD ¹⁴² , HSD ¹⁴³ , GLY ¹⁵¹ , PHE ¹⁵² , CYS ¹⁵³ , ASP ¹⁷⁸ , HSE ¹⁸⁰ , PHE ²⁰⁸ , GLN ²⁶³ , ASP ²⁶⁷ , GLY ³⁰³ , TYR ³⁰⁶
Quetiapine	-2810.47 Kcal/mol	ASP ⁹³ , HSD ¹³⁴ , HSD ¹³⁵ , GLY ¹⁴³ , CYS ¹⁴⁵ , ASP ¹⁷⁰ , HSE ¹⁷² , TYR ¹⁹⁸ , PHE ¹⁹⁹ , PHE ²⁰⁰ , ASP ²⁵⁹ , LEU ²⁶⁶ , GLY ²⁹⁶ , TYR ²⁹⁸

7.2. CONCLUSION AND SUMMARY

Ligand-based drug designing follows machine learning, and the molecular docking analysis approach based on the binding or full fitness energy of ligand to the receptor is considered as an effective tool in the drug detection procedure. Here we screen the data of anti-depressive from the ChEMBL compound library for HDAC10 by creating machine learning models, for example, logistic model, k-star model, random forest model, and deep learning model in order to classify them into inhibitors and non-inhibitors based on 2D/3D molecular and chemical properties. Total of around 1400 molecular descriptors belongs to the physical, chemical, and biological properties that were taken in order to classify the compounds. The average accuracy (94.53), precision (0.950), TP rate (0.950), FP rate (0.071), and area under the ROC curve of our generated models was quite high as compared to the previously created model for selecting a novel HDAC10 inhibitor. Consequently, 16 novel hits were identified through their BBB permeability and ADME properties. Also, the data for testing the inhibitor potential includes more than 6000 novel compounds. ADMET analysis of 16 novel hits explained the potential of compounds to be taken as a drug. Altogether, these compounds were subjected to molecular docking technique in order to check the binding efficiency of novel hits in the active position of HDAC10. Through molecular docking studies, the novel compounds with binding energy or full fitness for HDAC10 were selected for comprehensive analysis. The predicted compounds had the characteristics feature that is a central Zn²⁺ atom in its binding region. Out

of these Zimeldine, Prothipendyl, and Dibenapine possess the greater binding energy for the HDAC10.

In this study, we developed and identified a broad range inhibitor, which will be capable of inhibiting HDAC10 isoform as a therapeutic approach for Alzheimer's disease. Here, we deployed a machine learning classification algorithm in order to classify sets of compounds into inhibitors and non-inhibitors and after multiple level screening identified novel inhibitors known as Zimeldine and Dibenzapine. This study is a novel approach to incorporate machine learning classification and virtual screening of compounds based on IC₅₀ value and different types of molecular descriptors for the drug-discovery process. As a therapeutic approach, this study enables scientists to study the compound *in vitro* or *in vivo* studies. Although we have validated our results from multiple *in silico* approaches such as multiple-target validation and literature validation, there is a gap that will be filled by cell culture and animal model studies. From *in silico* studies, we identified the common residues through which inhibitor can potentially bind with the target, but the molecular mechanism behind the inhibition of target expression should be validated only from *in vitro* studies. Moreover, the work will further highlight the importance of epigenetic alterations in the pathology of NDDs such as AD.

CHAPTER VIII

Summary, Discussion, and Future Perspectives

CHAPTER VIII: SUMMARY, DISCUSSION, AND FUTURE PERSPECTIVES

NDDs, including AD and PD are characterized by the presence of misfolded protein aggregates, such as A β , tau, α -synuclein, and others that causes neuronal cell death. Further, excessive neuronal cell death due to protein aggregates causes synaptic dysfunction, memory impairment, and cognitive defects [547]. AD is the most prevalent form of dementia best characterized by the presence of amyloid plaques and neurofibrillary tangles produced by unsystematic proteolytic processing of amyloid peptide-protein and hyperphosphorylation of tau protein [548]. For example, Kollmer et al., 2019 demonstrated that A β fibrils from meningeal Alzheimer's brain tissue are polymorphic but consist of similarly structured protofibrils [549]. Similarly, Bu et al., 2017 concluded that blood-derived A β protein induces AD pathologies that result in functional impairment of neurons [550]. In contrast, PD, which is the second most common NDDs, is characterized by progressive loss of dopaminergic neurons in the substantia nigra *pars compacta*. The pathological feature of PD is the accumulation of toxic α -synuclein [551] protein and the formation of Lewy bodies, which causes neuronal cell death and ultimately leads to synaptic dysfunction and memory loss [552,553]. Mounting evidence suggests the common overlapping molecular phenomenon in the pathology of AD and PD. However, the exact molecular pathways and signaling molecules being involved are poorly understood. Moreover, the active treatment of AD and PD is still unknown due to a lack of understanding of the molecular mechanism of disease progression. Accumulating evidence suggests that protein acetylation and deacetylation play a significant role in the pathogenesis of AD and PD [121,554,555]. For instance, Choi et al., 2019 demonstrated that acetylation of tau facilitated the recruitment of Hsp40, Hsp70, and Hsp110, which causes tau association with E3 ligases and results in its degradation through proteasomal

pathway[120]. Similarly, Wang et al., 2020 concluded that AMPK reduces tau acetylation and rescues memory impairment by activating sirtuin 1 in APP/PS1 mice[556]. Further, Fan et al., 2020 concluded that PGC-1 α translocation due to its acetylation promotes neuroprotection from oxidative damage in PD experimental model [130]. Further, acetylation and deacetylation of transcription factors (TFs) play a vital role in regulating cellular and molecular processes, which activates different neuronal signal transduction pathways such as PI3K/Akt, MAPK pathways, cAMP/PKA pathways, and Ca²⁺/CaMK cascade. For instance, Fusco et al., 2016 concluded that acetylation of CREB1 at K122 increases the Hes-1 expression under low glucose concentration, facilitating neurogenesis by removing sirtuin 1 on the Hes-1 promoter region [557]. Similarly, Paz et al., 2014 demonstrated that acetylation of CREB at K136 facilitated its interaction with CBP bromodomain that augmented recruitment of this coactivator to the promoter [476]. Thus, these evidences concluded the importance of acetylation of TFs in gene regulation.

The present study focuses on the crosstalk between AD and PD at the molecular level. Through this study, we identified the relationship between DEG's, HUB proteins, TFs, acetylation, and HDAC enzymes in the shared pathogenesis of AD and PD. Our findings highlighted the crucial role of CDC42, TUBB4B, and FGFR1 in the AD and PD crosstalk through Gap junction (TUBB4B), GnRH signaling pathway (CDC42), and Rap1 signaling pathway (CDC42 and FGFR1). In addition, the present study identified the potential TFs that regulate the expression of HUB proteins at the transcriptional level through biological network analysis. Our analysis identified FOXC1, GATA2, CREB1, FOXL1, NFIC, HINFP, and SREBF1 as potential TFs that regulate the activity of HUB proteins shared between AD and PD. Our bioinformatic analysis also revealed the effect of subcellular localization of HUB proteins and TFs in the AD and PD crosstalk. Lately, the study identified the 15 potential lysine residues and 27 potential lysine residues in CREB1 and HINFP, respectively. The study revealed that among 15 possible

lysine residues of CREB1, only 4 lysine residues, namely K91, K94, K136, and K330 had been studies in the past, while K123, K155, K285, K292, K303, K304, K305, K309, K323, K333, and K339 have been reported first time for their role in acetylation process. Similarly, among HINFP, all 27 lysine residues have been reported for the first time. Further, *in-silico* analysis of CREB1 and HINFP revealed the importance of HDAC1 for its deacetylation activity at K292 of CREB1 and HDAC6 for its deacetylation activity at K330 of HINFP. This will provide a way to study the role of acetylation and HDAC enzymes in the transcriptional activity of CREB1 and HINFP in AD and PD crosstalk. Further, the computational analysis identified the importance of negative charged glutamic acid (E) and neutrally charged leucine (L), methionine (M), valine (V), and glutamine (Q) amino acid residues in the acetylation mechanism of CREB1 and HINFP in AD and PD crosstalk. The study also highlighted the importance of the helix region over the strand/coil region in the acetylation of CREB1. Similarly, the coil region is dominant over the helix/strand region in the potential lysine-acetylation of HINFP. Thus, this study highlighted the importance of two prominent biological pathways for the progression of AD and PD simultaneously, such as HDAC1-CREB1-TUBB4B/CDC42/CD44 and HDAC6-HINFP-TUBB4B/CDC42/CD44 (Figure 6). Further studies are required to generate the potential treatments targeting the above-mentioned biological pathways to treat AD and PD's adverse effects.

Moreover, the study highlighted the role of PTMs and their crosstalk in HDAC interactors, which are involved in the progression of NDDs such as AD and PD. The interactors of HDAC and proteins involved in AD and PD were collected from different databases such as HIPPIE, CTD, and DisGeNET. Venn analysis and PPI interaction of HDAC interactors, AD, and PD demonstrated the involvement of the Top 33 proteins. Gene set enrichment analysis of 33 proteins confirmed the involvement of six different molecular functions and biological pathways in the pathogenesis of AD and PD through HDAC interactors. Protein

serine/threonine kinase activity (21.21%), Transcription regulator activity (18.18%), Transcription factor activity (6.06%), Transmembrane receptor protein tyrosine kinase activity (9.09%), Chaperone activity (15.15%), DNA-methyltransferase activity (3.03%) were top-ranked molecular functions performed by HDAC interactors having a p-value less than 0.05. Similarly, Glypican pathway (81.25%), TRAIL signaling pathway (84.37%), Glypican 1 network (81.25%), Integrin-linked kinase signaling (65.62%), AP-1 transcription factor network (62.50%), and Arf6 downstream pathway (78.12%) were top-ranked biological pathways involved in the pathogenesis of AD and PD. Lately, 1,50,968 PTMs sites from dbPTM and 1,15,127 PTMs sites from PLMD were integrated to 32 proteins in which 1489 were acetylation, ubiquitination, and SUMOylation sites. Among 32 proteins, only three proteins, such as PARP1, NPM1, and CDK1, have individual acetylation, ubiquitination, and SUMOylation frequency greater than 10. Secondary structure prediction confirmed 42, 22, and 18 PTMs sites formed coiled structure in PARP1, NPM1, and CDK1 respectively, demonstrating that the probability of PTMs site is higher in the coiled region as compared to helix and strand region. However, in NPM1, the probability of forming a strand region is higher as compared to PARP1 and CDK1. Further investigation revealed that 75% of PTMs sites were associated with the ordered region, whereas, 25% of PTMs sites were associated with the disordered region. Thus, it will be concluded that PTM distribution is higher in the ordered region as compared to the disordered region. Further, crosstalk analysis of acetylation, ubiquitination, and SUMOylation sites in PARP1 revealed that 19 PTM sites were associated with acetylation and ubiquitination crosstalk. Similarly, acetylation-SUMOylation (7 sites), ubiquitination-SUMOylation (3 sites), and acetylation-ubiquitination-SUMOylation (15 sites) were identified. Hotspot analysis identified that K148, K249, K528, K637, K700, and K796 have potential crosstalk sites having ≥ 2 potential lysine residue in the vicinity of +7 and -6 motif sequence. In order to predict crucial crosstalk sites, the impact of lysine mutation on

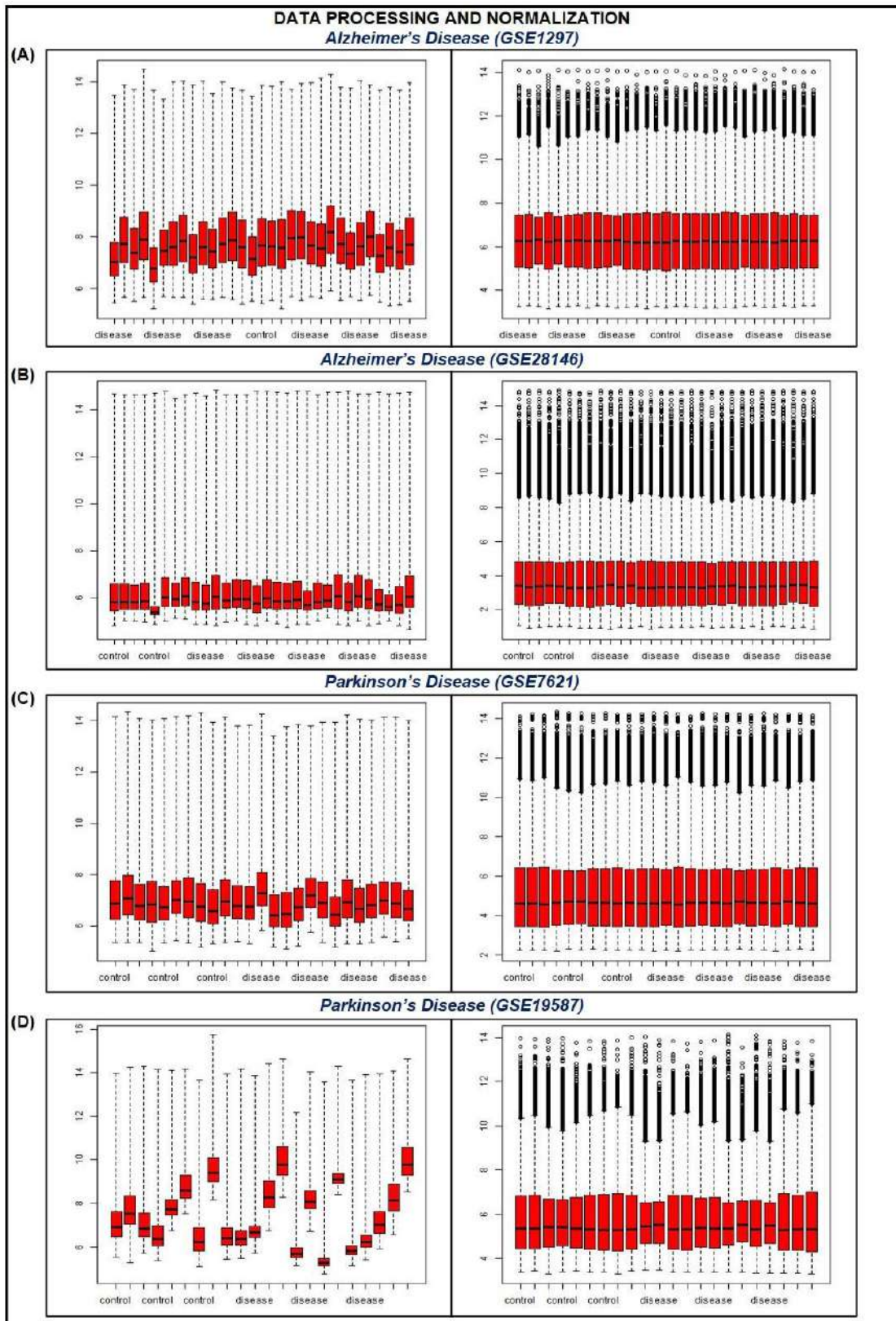
disease susceptibility was predicted, which demonstrated that among hotspot sites, K249L, K528Q, K528L, K637Q, K637L, K700Q, K700L, K796L were involved in the progression of NDDs. Further, our study investigated the role of lysine mutation on ubiquitination and SUMOylation, which shows that mutation in lysine residue will result in loss of SUMOylation and ubiquitination function. However, the gain of function after lysine mutation will also be observed, but the frequency is low as compared to the loss of function. In conclusion, K249, K331, K337, K528, K600, K637, K700, and K796 of PARP1 play a vital role in ubiquitination, acetylation, and SUMOylation crosstalk, which can potentially be useful for newer leads into acetylation mechanism, HDAC interactions, disease progression, biomarkers, or as a therapeutic target. Further, from this study, we also concluded that site-specific inhibition of PARP1 acetylation (K249, K331, K337, K528, K600, K637, K700, and K796) and simultaneous activation of ubiquitination and SUMOylation at the same residues rescue neuronal cell death that involved in AD pathology.

The study also discussed the potential of miRNAs and long non-coding RNA in relation with acetylation in the pathogenesis of metal toxicity-induced AD. we concluded that downregulation of OIP5-AS1 causes upregulation of miR-129-5p, which modulate CREBBP-induced hyperacetylation of CREB1, GATA2, NFKB1, and FOXA1 acetylation at K122, K399, K967, and K350. Regulation of hyperacetylation of CREB1, GATA2, NFKB1, and FOXA1 modulate their transcriptional activation, neuroinflammation, Wnt Signaling, and MAOA gene regulation, respectively, which inhibits neuronal cell death. In addition, decreased neuronal cell death rescued memory impairment and cognitive defects, which inhibits the pathogenesis of AD. Thus, the OIP5-AS1/miR-129-5p/CREBBP axis could be a possible therapeutic target in metal toxicity-induced AD. Further, these results provide a gateway for the future *in vivo and in vitro* studies targeting OIP5-AS1/miR-129-5p/CREBBP axis in a metal toxicity-induced AD. Lastly, we concluded the potential of Zimeldine and Dibenzapine as

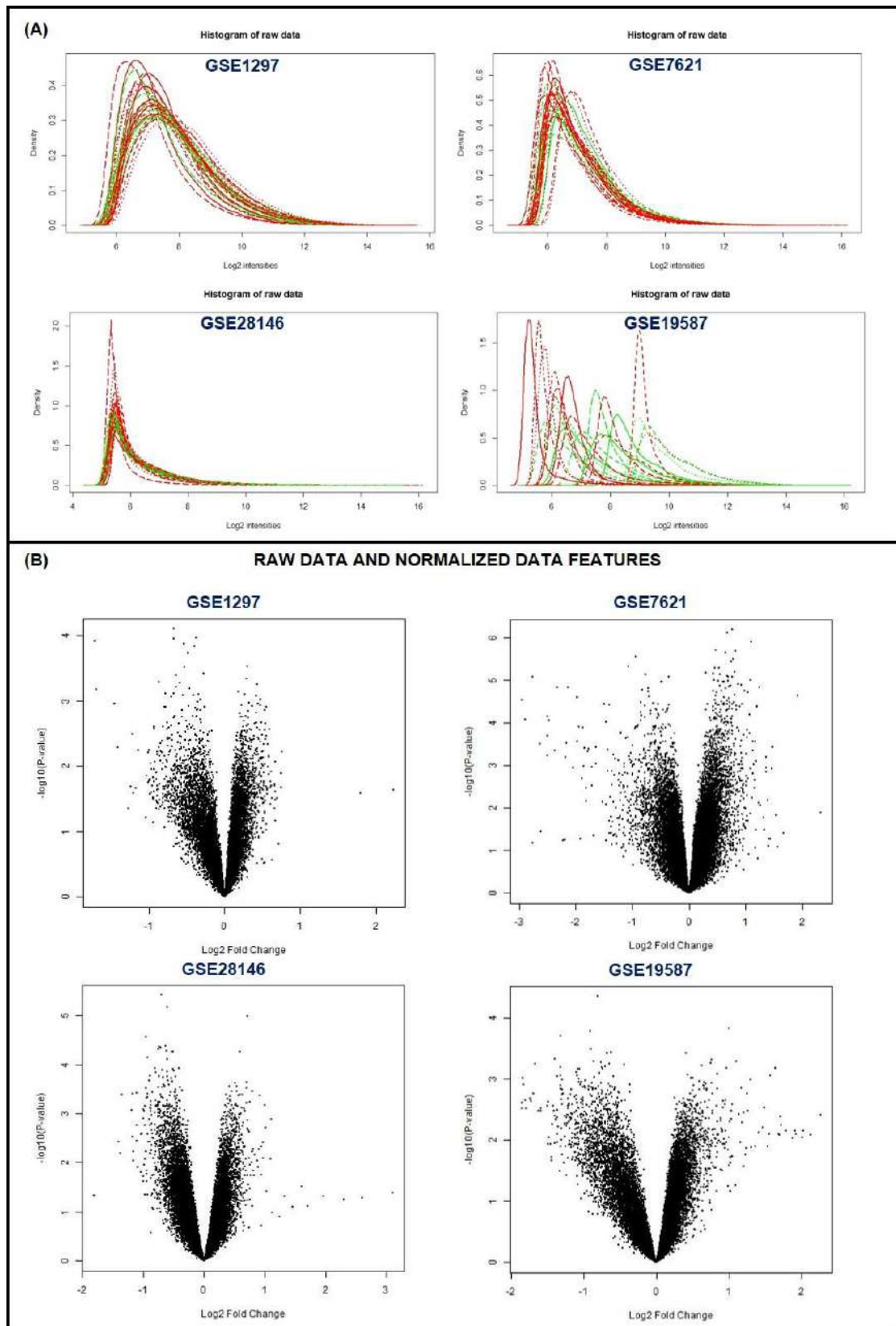
potential therapeutic compound against HDAC10 in AD therapeutics.

However, the current study is associated with some sort of limitation as the study uses only microarray data, which is not as comprehensive as transcriptomics data analysis. Thus, there is a growing need to simultaneously analyze the different types of AD and PD datasets, namely microarray data, epigenetic data, and RNA data, to extract the novel biomarkers involved in disease pathology. Further, there should be a greater number of control as well as disease samples to conclude a general discussion. In addition, samples from different tissue could be more beneficial in understanding the molecular mechanism and role of HDAC in AD and PD simultaneously. Further, the study is solely depending on the analysis parameters, such as log Fc value, node degree, network merging parameters, or acetylation signatures. Slightly changes in the analysis parameters or addition of other datasets might cause some deviation in the molecular signatures.

ANNEXURE



Annexure 1: Box plots of Alzheimer's disease (GSE1297 and GSE28146) and Parkinson's disease (GSE7621 and GSE19587) before and after normalization of microarray datasets



Annexure 2: (A) histograms of microarray datasets of Alzheimer’s disease (GSE1297 and GSE28146) and Parkinson’s disease (GSE7621 and GSE19587). (B) volcano plots of publicly available microarray datasets for GSE1297, GSE28146, GSE7621, and GSE19587

Annexure 3: Prediction of putative lysine residues and HDAC enzymes in the CREB1

MuSite Deep / Deep-PLA				
Residue	Score	Confidence	Type	FPR (%)
91	0.25	Low	SIRT7	14.7
94	0.166	Low	SIRT7	13.26
123	0.12	Low	HDAC6	2.74
136	0.309	Moderate	SIRT1	0.03
155	0.162	Low	SIRT1	3.35
285	0.129	Low	SIRT7	9.68
292	0.139	Low	HDAC1	4.96
303	0.114	Low	SIRT7	12.54
304	0.133	Low	SIRT7	12.9
305	0.185	Low	SIRT7	13.98
309	0.29	Moderate	----	----
323	0.318	Moderate	----	----
330	0.557	High	HDAC2	10.67
333	0.288	Moderate	SIRT6	6.92
339	0.199	Low	SIRT6	2.31
PSKAcePred / Deep-PLA				
Residue	Score	Confidence	Type	FPR (%)
91	0.692	Moderate	SIRT7	14.7
94	0.872	High	SIRT7	13.26
136	0.659	Moderate	SIRT1	0.03
292	0.737	High	HDAC1	3.35
303	0.856	High	SIRT7	12.54
304	0.924	High	SIRT7	12.9
305	0.653	Moderate	SIRT7	13.98
309	0.994	High	----	----

Annexure 4: Prediction of putative lysine residues and HDAC enzymes in the HINFP

MuSite Deep / Deep-PLA				
Residue	Score	Confidence	Type	FPR (%)
6	0.318	Moderate	HDAC6	2.74
10	0.164	Low	HDAC6	3.84
31	0.163	Low	SIRT1	6.51
94	0.176	Low	----	----
96	0.159	Low	----	----
164	0.206	Low	SIRT3	14.56
174	0.191	Low	SIRT7	13.26
181	0.182	Low	----	----
185	0.177	Low	SIRT3	14.94
197	0.168	Low	----	----
213	0.311	Moderate	----	----
236	0.189	Low	----	----
256	0.191	Low	----	----
285	0.174	Low	----	----
294	0.186	Low	----	----
301	0.21	Low	----	----
330	0.42	Moderate	HDAC6	3.84
335	0.198	Low	HDAC6	2.74
346	0.178	Low	HDAC6	6.3
352	0.228	Low	HDAC3	8.6
366	0.175	Low	HDAC1	5.8
367	0.157	Low	HDAC1	4.23
371	0.354	Moderate	SIRT1	7.01
382	0.269	Moderate	HDAC1	6.53
439	0.153	Low	SIRT2	4.77
446	0.11	Low	SIRT2	0.95
504	0.154	Low	SIRT1	6
PSKAcePred / Deep-PLA				
Residue	Score	Confidence	Type	FPR (%)
31	0.73	High	SIRT1	6.51
96	0.766	High	----	----
174	0.779	High	SIRT7	13.26
185	0.591	Moderate	SIRT3	14.94
197	0.65	Moderate	----	----
213	0.616	Moderate	----	----
236	0.522	Moderate	----	----
330	0.726	High	HDAC6	3.84
335	0.93	High	HDAC6	2.74
352	0.5	Moderate	HDAC3	8.6
366	0.629	Moderate	HDAC1	5.8
367	0.904	High	HDAC1	4.23
371	0.911	High	SIRT1	7.01
446	0.719	High	SIRT2	0.95
504	0.506	Moderate	SIRT1	6

Annexure 5: List of anti-depressive drugs used as a test compound

ChEMBL ID	Name	Molecular Formula
CHEMBL1696	DESIPRAMINE HYDROCHLORIDE	C18H23ClN2
CHEMBL517	DISOPYRAMIDE	C21H29N3O
CHEMBL1201293	ACAMPROSATE	C5H11NO4S
CHEMBL1201066	VENLAFAXINE HYDROCHLORIDE	C17H28ClNO2
CHEMBL595	PIOGLITAZONE	C19H20N2O3S
CHEMBL1199080	BRETYLIUM	C11H17BrN+
CHEMBL1200420	MIDAZOLAM HYDROCHLORIDE	C18H14Cl2FN3
CHEMBL1201082	FLUOXETINE HYDROCHLORIDE	C17H19ClF3NO
CHEMBL741	LAMOTRIGINE	C9H7Cl2N5
CHEMBL315795	CLOMETHIAZOLE	C6H8ClNS
CHEMBL1200322	ESCITALOPRAM OXALATE	C22H23FN2O5
CHEMBL715	OLANZAPINE	C17H20N4S
CHEMBL16	PHENYTOIN	C15H12N2O2
CHEMBL896	HYDROXYZINE	C21H27ClN2O2
CHEMBL636	RIVASTIGMINE	C14H22N2O2
CHEMBL2110816	BUTRIPTYLINE	C21H27N
CHEMBL418995	AMINEPTINE	C22H27NO2
CHEMBL511142	BUPRENORPHINE	C29H41NO4
CHEMBL1764	LEVOMEPRMAZINE	C19H24N2OS
CHEMBL654	MIRTAZAPINE	C17H19N3
CHEMBL1200399	BUSPIRONE HYDROCHLORIDE	C21H32ClN5O2
CHEMBL1201242	INDECAINIDE	C20H24N2O
CHEMBL631	PROPAFENONE	C21H27NO3
CHEMBL558	MEXILETINE	C11H17NO
CHEMBL490	PAROXETINE	C19H20FNO3
CHEMBL130	CHLORAMPHENICOL	C11H12Cl2N2O5
CHEMBL533	IBUTILIDE	C20H36N2O3S
CHEMBL1294	QUINIDINE	C20H24N2O2
CHEMBL1464	WARFARIN	C19H16O4
CHEMBL894	BUPROPION	C13H18ClNO
CHEMBL1200710	CLOMIPRAMINE HYDROCHLORIDE	C19H24Cl2N2
CHEMBL1234579	NITROUS OXIDE	N2O
CHEMBL350221	OXITRIPTAN	C11H12N2O3
CHEMBL54	HALOPERIDOL	C21H23ClFNO2
CHEMBL502	DONEPEZIL	C24H29NO3
CHEMBL667	ACETYLCHOLINE	C7H16NO2+
CHEMBL86304	MOCLOBEMIDE	C13H17ClN2O2
CHEMBL6437	MIANSERIN	C18H20N2
CHEMBL54976	TRYPTOPHAN	C11H12N2O2
CHEMBL1628234	DOXEPIN HYDROCHLORIDE	C19H22ClNO
CHEMBL1508	ESCITALOPRAM	C20H21FN2O
CHEMBL1628227	DOXEPIN	C19H21NO
CHEMBL1201314	VALGANCICLOVIR	C14H22N6O5
CHEMBL1434	MINOCYCLINE	C23H27N3O7

CHEMBL1621	PALIPERIDONE	C23H27FN4O3
CHEMBL1256818	DEXTROMETHORPHAN HYDROBROMIDE	C18H28BrNO2
CHEMBL297302	BENPERIDOL	C22H24FN3O2
CHEMBL14370	REBOXETINE	C19H23NO3
CHEMBL1200332	PROTRIPTYLINE HYDROCHLORIDE	C19H22ClN
CHEMBL2105581	VERALIPRIDE	C17H25N3O5S
CHEMBL439849	VILAZODONE	C26H27N5O2
CHEMBL70418	CLOBAZAM	C16H13ClN2O2
CHEMBL1722	METHYLPHENIDATE HYDROCHLORIDE	C14H20ClNO2
CHEMBL796	METHYLPHENIDATE	C14H19NO2
CHEMBL2364609	ESKETAMINE HYDROCHLORIDE	C13H17Cl2NO
CHEMBL22097	LORMETAZEPAM	C16H12Cl2N2O2
CHEMBL1112	ARIPIRAZOLE	C23H27Cl2N3O2
CHEMBL415	CLOMIPRAMINE	C19H23ClN2
CHEMBL643	PROMETHAZINE	C17H20N2S
CHEMBL1643	RIBAVIRIN	C8H12N4O5
CHEMBL1698	BUPROPION HYDROCHLORIDE	C13H19Cl2NO
CHEMBL58323	ERLOSAMIDE	C13H18N2O3
CHEMBL1237082	MECAMYLAMINE HYDROCHLORIDE	C11H22ClN
CHEMBL807	MEMANTINE	C12H21N
CHEMBL1237021	LURASIDONE	C28H36N4O2S
CHEMBL1491	AMLODIPINE	C20H25ClN2O5
CHEMBL652	FLECAINIDE	C17H20F6N2O3
CHEMBL2105732	LEVOMILNACIPRAN HYDROCHLORIDE	C15H23ClN2O
CHEMBL2105760	BREXPIRAZOLE	C25H27N3O2S
CHEMBL12	DIAZEPAM	C16H13ClN2O
CHEMBL640	PROCAINAMIDE	C13H21N3O
CHEMBL1059	PREGABALIN	C8H17NO2
CHEMBL455917	CHLORAL HYDRATE	C2H3Cl3O2
CHEMBL452	CLONAZEPAM	C15H10ClN3O3
CHEMBL1442422	DIBENZEPIN	C18H21N3O
CHEMBL1201222	LISDEXAMFETAMINE	C15H25N3O
CHEMBL1715	PIOGLITAZONE HYDROCHLORIDE	C19H21ClN2O3S
CHEMBL259209	MILNACIPRAN	C15H22N2O
CHEMBL395091	ESKETAMINE	C13H16ClNO
CHEMBL2111030	PROTHIPENDYL	C16H19N3S
CHEMBL545	ALCOHOL	C2H6O
CHEMBL243712	AMISULPRIDE	C17H27N3O4S
CHEMBL1492500	DOTHIEPIN	C19H21NS
CHEMBL1521	ZALEPLON	C17H15N5O
CHEMBL49	BUSPIRONE	C21H31N5O2
CHEMBL1113	AMOXAPINE	C17H16ClN3O
CHEMBL1286	LEVETIRACETAM	C8H14N2O2
CHEMBL1091	HYDROCORTISONE ACETATE	C23H32O6
CHEMBL108	CARBAMAZEPINE	C15H12N2O
CHEMBL2028019	CARIPRAZINE	C21H32Cl2N4O

CHEMBL207538	BREXANOLONE	C21H34O2
CHEMBL1762	TOCAINIDE	C11H16N2O
CHEMBL12713	SERTINDOLE	C24H26ClFN4O
CHEMBL477	ADENOSINE	C10H13N5O4
CHEMBL190	THEOPHYLLINE	C7H8N4O2
CHEMBL10878	AGOMELATINE	C15H17NO2
CHEMBL573	NIACIN	C6H5NO2
CHEMBL315838	ENCAINIDE	C22H28N2O2
CHEMBL968	FLURAZEPAM	C21H23ClFN3O
CHEMBL277062	BROMAZEPAM	C14H10BrN3O
CHEMBL657	DIPHENHYDRAMINE	C17H21NO
CHEMBL139	DICLOFENAC	C14H11Cl2NO2
CHEMBL669	CYCLOBENZAPRINE	C20H21N
CHEMBL596	FENTANYL	C22H28N2O
CHEMBL580	LORAZEPAM	C15H10Cl2N2O2
CHEMBL3	NICOTINE	C10H14N2
CHEMBL142438	NITROGEN	N2
CHEMBL27	PROPRANOLOL	C16H21NO2
CHEMBL1373	MODAFINIL	C15H15NO2S
CHEMBL135	ESTRADIOL	C18H24O2
CHEMBL1200781	CITALOPRAM HYDROBROMIDE	C20H22BrFN2O
CHEMBL1200492	NEFAZODONE HYDROCHLORIDE	C25H33Cl2N5O2
CHEMBL1089	PHENELZINE	C8H12N2
CHEMBL1218	RAMELTEON	C16H21NO2
CHEMBL1214124	PERAMPANEL	C23H15N3O
CHEMBL940	GABAPENTIN	C9H17NO2
CHEMBL36	PYRIMETHAMINE	C12H13ClN4
CHEMBL1237135	MAPROTILINE HYDROCHLORIDE	C20H24ClN
CHEMBL21731	MAPROTILINE	C20H23N
CHEMBL655	MIDAZOLAM	C18H13ClFN3
CHEMBL1200964	AMITRIPTYLINE HYDROCHLORIDE	C20H24ClN
CHEMBL628	PENTOXIFYLLINE	C13H18N4O3
CHEMBL568	OXAZEPAM	C15H11ClN2O2
CHEMBL1509	DROSPIRENONE	C24H30O3
CHEMBL1064	SIMVASTATIN	C25H38O5
CHEMBL549	CITALOPRAM	C20H21FN2O
CHEMBL668	PROTRIPTYLINE	C19H21N
CHEMBL644	TRIMIPRAMINE	C20H26N2
CHEMBL1431	METFORMIN	C4H11N5
CHEMBL52440	DEXTROMETHORPHAN	C18H25NO
CHEMBL85	RISPERIDONE	C23H27FN4O2
CHEMBL1200328	DULOXETINE HYDROCHLORIDE	C18H20ClNOS
CHEMBL90593	PRASTERONE	C19H28O2
CHEMBL526	PROPOFOL	C12H18O
CHEMBL103	PROGESTERONE	C21H30O2
CHEMBL646	TRIAZOLAM	C17H12Cl2N4

CHEMBL1201168	ISOCARBOXAZID	C12H13N3O2
CHEMBL1714	KETAMINE HYDROCHLORIDE	C13H17Cl2NO
CHEMBL911	ZOLPIDEM	C19H21N3O
CHEMBL45	MELATONIN	C13H16N2O2
CHEMBL273575	NOMIFENSINE	C16H18N2
CHEMBL95889	BETAINE	C5H12NO2+
CHEMBL537669	YOHIMBINE HYDROCHLORIDE	C21H27ClN2O3
CHEMBL1175	DULOXETINE	C18H19NOS
CHEMBL1372950	NICERGOLINE	C24H26BrN3O3
CHEMBL696	ETHOSUXIMIDE	C7H11NO2
CHEMBL220492	TOPIRAMATE	C12H21NO8S
CHEMBL267936	MECAMYLAMINE	C11H21N
CHEMBL1503	OMEPRAZOLE	C17H19N3O3S
CHEMBL637	VENLAFAXINE	C17H27NO2
CHEMBL2103822	TASIMELTEON	C15H19NO2
CHEMBL679	EPINEPHRINE	C9H13NO3
CHEMBL181	DIAZOXIDE	C8H7ClN2O2S
CHEMBL26	SULPIRIDE	C15H23N3O4S
CHEMBL13209	NITRAZEPAM	C15H11N3O3
CHEMBL24441	BETAHISTINE	C8H12N2
CHEMBL72	DESIPRAMINE	C18H22N2
CHEMBL28218	BROMPERIDOL	C21H23BrFNO2
CHEMBL1237044	TRAMADOL	C16H25NO2
CHEMBL25	ASPIRIN	C9H8O4
CHEMBL814	FLUVOXAMINE	C15H21F3N2O2
CHEMBL742	KETAMINE	C13H16ClNO
CHEMBL1771	CLOPIDOGREL	C16H16ClNO2S
CHEMBL972	SELEGILINE	C13H17N
CHEMBL1075	MORICIZINE	C22H25N3O4S
CHEMBL1201192	ARMODAFINIL	C15H15NO2S
CHEMBL777	CLAVULANIC ACID	C8H9NO5
CHEMBL41	FLUOXETINE	C17H18F3NO
CHEMBL451	CHLORDIAZEPOXIDE	C16H14ClN3O
CHEMBL41355	EZOZABINE	C16H18FN3O2
CHEMBL1101	BIPERIDEN	C21H29NO
CHEMBL967	TEMAZEPAM	C16H13ClN2O2
CHEMBL196	ASCORBIC ACID	C6H8O6
CHEMBL708	ZIPRASIDONE	C21H21ClN4OS
CHEMBL714	ALBUTEROL	C13H21NO3
CHEMBL40	PHENOBARBITAL	C12H12N2O3
CHEMBL1201010	FLUDROCORTISONE ACETATE	C23H31FO6
CHEMBL1068	OXCARBAZEPINE	C15H12N2O2
CHEMBL600	ACETYLCYSTEINE	C5H9NO3S
CHEMBL629	AMITRIPTYLINE	C20H23N
CHEMBL500	PINDOLOL	C14H20N2O2
CHEMBL771	CYCLOSERINE	C3H6N2O2

CHEMBL621	TRAZODONE	C19H22CIN5O
CHEMBL109	VALPROIC ACID	C8H16O2
CHEMBL126224	IPRINDOLE	C19H28N2
CHEMBL36715	PIRACETAM	C6H10N2O2
CHEMBL569713	SCOPOLAMINE	C17H21NO4
CHEMBL2107387	VORTIOXETINE HYDROBROMIDE	C18H23BrN2S
CHEMBL1437	NOREPINEPHRINE	C8H11NO3
CHEMBL135400	ZOPICLONE	C17H17CIN6O3
CHEMBL445	NORTRIPTYLINE	C19H21N
CHEMBL716	QUETIAPINE	C21H25N3O2S
CHEMBL278819	MINAPRINE	C17H22N4O
CHEMBL1201735	BUPROPION HYDROBROMIDE	C13H19BrCINO
CHEMBL2105613	DIVALPROEX SODIUM	C16H31NaO4
CHEMBL142703	VILDAGLIPTIN	C17H25N3O2
CHEMBL567	PERPHENAZINE	C21H26CIN3OS
CHEMBL42	CLOZAPINE	C18H19CIN4
CHEMBL1256841	NIALAMIDE	C16H18N4O2
CHEMBL37744	ZIMELDINE	C16H17BrN2
CHEMBL1118	DESVENLAFAXINE	C16H25NO2
CHEMBL92401	IPRONIAZID	C9H13N3O
CHEMBL1201728	DESVENLAFAXINE SUCCINATE	C20H31NO6
CHEMBL623	NEFAZODONE	C25H32CIN5O2
CHEMBL473	DOFETILIDE	C19H27N3O5S2
CHEMBL1678	DONEPEZIL HYDROCHLORIDE	C24H30CINO3
CHEMBL1201178	LISDEXAMFETAMINE DIMESYLATE	C17H33N3O7S2
CHEMBL59	DOPAMINE	C8H11NO2
CHEMBL1234886	OXYGEN	O2
CHEMBL2104993	VORTIOXETINE	C18H22N2S
CHEMBL2103774	TIBOLONE	C21H28O2
CHEMBL1496	ROSUVASTATIN	C22H28FN3O6S
CHEMBL661	ALPRAZOLAM	C17H13CIN4
CHEMBL691	ETHINYL ESTRADIOL	C20H24O2
CHEMBL118	CELECOXIB	C17H14F3N3O2S
CHEMBL2111101	PIMAVANSERIN	C25H34FN3O2
CHEMBL1140	NIACINAMIDE	C6H6N2O
CHEMBL1005	REMIFENTANIL	C20H28N2O5
CHEMBL656	OXYCODONE	C18H21NO4
CHEMBL99946	LEVOMILNACIPRAN	C15H22N2O
CHEMBL934	METYRAPONE	C14H14N2O
CHEMBL306700	VILOXAZINE	C13H19NO3
CHEMBL1200798	TRAZODONE HYDROCHLORIDE	C19H23Cl2N5O
CHEMBL521	IBUPROFEN	C13H18O2
CHEMBL3306803	LUMATEPERONE	C24H28FN3O
CHEMBL11	IMIPRAMINE	C19H24N2
CHEMBL1201156	NORTRIPTYLINE HYDROCHLORIDE	C19H22CIN
CHEMBL19019	NALTREXONE	C20H23NO4

CHEMBL1718	NALOXONE HYDROCHLORIDE	C19H22ClNO4
CHEMBL1615374	VILAZODONE HYDROCHLORIDE	C26H28ClN5O2
CHEMBL744	RILUZOLE	C8H5F3N2OS
CHEMBL3188993	QUETIAPINE FUMARATE	C46H54N6O8S2
CHEMBL1708	PAROXETINE HYDROCHLORIDE	C19H21ClFNO3
CHEMBL1201027	GLYCOPYRROLATE	C19H28BrNO3
CHEMBL659	GALANTAMINE	C17H21NO3
CHEMBL1692	IMIPRAMINE HYDROCHLORIDE	C19H25ClN2
CHEMBL70	MORPHINE	C17H19NO3
CHEMBL301265	PRAMIPEXOLE	C10H17N3S
CHEMBL3989861	DESVENLAFAXINE FUMARATE	C20H31NO7

Annexure 6: List of compounds used as training set for HDAC10 inhibitors

Molecule ChEMBL ID	Standard Value	Class
CHEMBL4066920	3.981	Inhibitor
CHEMBL4578278	3.981	Inhibitor
CHEMBL2018302	30000	Non-Inhibitor
CHEMBL4577299	7700	Non-Inhibitor
CHEMBL4283105	6400	Non-Inhibitor
CHEMBL4293438	30000	Non-Inhibitor
CHEMBL3347696	30000	Non-Inhibitor
CHEMBL4516095	14700	Non-Inhibitor
CHEMBL1091474	32.8	Inhibitor
CHEMBL4532304	660	Non-Inhibitor
CHEMBL2103863	3.981	Inhibitor
CHEMBL4468860	5011.87	Non-Inhibitor
CHEMBL98	97	Non-Inhibitor
CHEMBL4437432	4997	Non-Inhibitor
CHEMBL98	199.53	Non-Inhibitor
CHEMBL2105763	10	Inhibitor
CHEMBL4470067	19.95	Inhibitor
CHEMBL4545091	5300	Non-Inhibitor
CHEMBL1630208	3.7	Inhibitor
CHEMBL99	22.8	Inhibitor
CHEMBL98	430	Non-Inhibitor
CHEMBL99	31	Inhibitor
CHEMBL98	58	Non-Inhibitor
CHEMBL99	20.1	Inhibitor
CHEMBL251011	179	Non-Inhibitor
CHEMBL1631912	958	Non-Inhibitor
CHEMBL1631916	320	Non-Inhibitor
CHEMBL1631918	200	Non-Inhibitor
CHEMBL4554522	2690	Non-Inhibitor
CHEMBL1914702	776	Non-Inhibitor
CHEMBL466031	30000	Non-Inhibitor
CHEMBL466033	30000	Non-Inhibitor
CHEMBL3670680	8547	Non-Inhibitor
CHEMBL1631913	70.7	Non-Inhibitor
CHEMBL1631915	152	Non-Inhibitor
CHEMBL488747	19.2	Inhibitor
CHEMBL483892	34.3	Inhibitor
CHEMBL483693	18.5	Inhibitor
CHEMBL99	5	Inhibitor
CHEMBL4445342	2073	Non-Inhibitor
CHEMBL29362	280	Non-Inhibitor
CHEMBL1767031	100000	Non-Inhibitor

CHEMBL3793310	10200	Non-Inhibitor
CHEMBL2105763	1.96	Inhibitor
CHEMBL4294514	1510	Non-Inhibitor
CHEMBL1767032	100000	Non-Inhibitor
CHEMBL1767044	21800	Non-Inhibitor
CHEMBL1767045	98500	Non-Inhibitor
CHEMBL598797	125.89	Non-Inhibitor
CHEMBL4475240	1000	Non-Inhibitor
CHEMBL1088734	14.5	Inhibitor
CHEMBL3911566	11900	Non-Inhibitor
CHEMBL1094707	9.8	Inhibitor
CHEMBL3670668	316	Non-Inhibitor
CHEMBL466032	30000	Non-Inhibitor
CHEMBL2431862	3700	Non-Inhibitor
CHEMBL3098687	227	Non-Inhibitor
CHEMBL4093691	8230	Non-Inhibitor
CHEMBL356066	8.41	Inhibitor
CHEMBL609583	4.3	Inhibitor
CHEMBL564876	870	Non-Inhibitor
CHEMBL2152613	30000	Non-Inhibitor
CHEMBL99	32	Inhibitor
CHEMBL4534503	158.49	Non-Inhibitor
CHEMBL4466930	199.53	Non-Inhibitor
CHEMBL98	208	Non-Inhibitor
CHEMBL4438279	398.11	Non-Inhibitor
CHEMBL4537561	21000	Non-Inhibitor
CHEMBL4557665	10000	Non-Inhibitor
CHEMBL4469098	14000	Non-Inhibitor
CHEMBL4577107	1462.81	Non-Inhibitor
CHEMBL4207182	9100	Non-Inhibitor
CHEMBL466459	13300	Non-Inhibitor
CHEMBL4445862	164	Non-Inhibitor
CHEMBL2417782	6	Inhibitor
CHEMBL483254	10.24	Inhibitor
CHEMBL27759	3150	Non-Inhibitor
CHEMBL1767043	15400	Non-Inhibitor
CHEMBL4541796	50.12	Non-Inhibitor
CHEMBL471043	5430	Non-Inhibitor
CHEMBL470843	6100	Non-Inhibitor
CHEMBL1767033	100000	Non-Inhibitor
CHEMBL1767036	73300	Non-Inhibitor
CHEMBL1767039	23100	Non-Inhibitor
CHEMBL1631914	62.5	Non-Inhibitor
CHEMBL1631917	190	Non-Inhibitor
CHEMBL427510	29700	Non-Inhibitor
CHEMBL180911	1540	Non-Inhibitor

CHEMBL389687	46.1	Non-Inhibitor
CHEMBL1088736	5.8	Inhibitor
CHEMBL440018	3430	Non-Inhibitor
CHEMBL483254	4	Inhibitor
CHEMBL1914708	140	Non-Inhibitor
CHEMBL561604	250	Non-Inhibitor
CHEMBL446512	840	Non-Inhibitor
CHEMBL468595	17.5	Inhibitor
CHEMBL511715	471	Non-Inhibitor
CHEMBL1091475	10.7	Inhibitor
CHEMBL487106	17.6	Inhibitor
CHEMBL487742	55.7	Non-Inhibitor
CHEMBL27759	50100	Non-Inhibitor
CHEMBL98	456	Non-Inhibitor
CHEMBL467793	44.9	Non-Inhibitor
CHEMBL1767047	100000	Non-Inhibitor
CHEMBL227118	173	Non-Inhibitor
CHEMBL1094710	16.6	Inhibitor
CHEMBL4290191	7.55	Inhibitor
CHEMBL469275	891	Non-Inhibitor
CHEMBL2177587	3400	Non-Inhibitor
CHEMBL598797	26.1	Inhibitor
CHEMBL1767030	100000	Non-Inhibitor
CHEMBL1767037	100000	Non-Inhibitor
CHEMBL1767046	37800	Non-Inhibitor
CHEMBL513160	155	Non-Inhibitor
CHEMBL468842	73	Non-Inhibitor
CHEMBL511749	90.7	Non-Inhibitor
CHEMBL1243289	23900	Non-Inhibitor
CHEMBL3774414	1176	Non-Inhibitor
CHEMBL3917405	80	Non-Inhibitor
CHEMBL483893	13	Inhibitor
CHEMBL519491	36.1	Inhibitor
CHEMBL483494	112	Non-Inhibitor
CHEMBL4129930	10000	Non-Inhibitor
CHEMBL1796689	0.5	Inhibitor
CHEMBL3329621	0.2	Inhibitor
CHEMBL109654	1220	Non-Inhibitor
CHEMBL3356523	11	Inhibitor
CHEMBL4556817	1470	Non-Inhibitor
CHEMBL3622727	138	Non-Inhibitor
CHEMBL3622728	395	Non-Inhibitor
CHEMBL2414098	3	Inhibitor
CHEMBL467998	852	Non-Inhibitor
CHEMBL3262727	4130	Non-Inhibitor
CHEMBL3098604	30	Inhibitor

CHEMBL98	77	Non-Inhibitor
CHEMBL4452620	899	Non-Inhibitor
CHEMBL3827814	2.8	Inhibitor
CHEMBL483254	4.45	Inhibitor
CHEMBL99	34.5	Inhibitor
CHEMBL29814	50	Non-Inhibitor
CHEMBL99	38.1	Inhibitor
CHEMBL98	72	Non-Inhibitor
CHEMBL1087053	30000	Non-Inhibitor
CHEMBL4206537	100000	Non-Inhibitor
CHEMBL98	68.4	Non-Inhibitor
CHEMBL356769	3710	Non-Inhibitor
CHEMBL98	200	Non-Inhibitor
CHEMBL96051	300	Non-Inhibitor
CHEMBL1631910	1530	Non-Inhibitor
CHEMBL468841	401	Non-Inhibitor
CHEMBL483495	86.5	Non-Inhibitor
CHEMBL2425955	17500	Non-Inhibitor
CHEMBL3335283	94	Non-Inhibitor
CHEMBL3335300	29	Inhibitor
CHEMBL3621988	235	Non-Inhibitor
CHEMBL4210907	47900	Non-Inhibitor
CHEMBL4210107	7050	Non-Inhibitor
CHEMBL4213856	5890	Non-Inhibitor
CHEMBL3622533	2.8	Inhibitor
CHEMBL4205609	7740	Non-Inhibitor
CHEMBL4069287	5000	Non-Inhibitor
CHEMBL4210305	15500	Non-Inhibitor
CHEMBL520056	24.5	Inhibitor
CHEMBL483477	1350	Non-Inhibitor
CHEMBL3098695	113	Non-Inhibitor
CHEMBL1631911	683	Non-Inhibitor
CHEMBL511432	250	Non-Inhibitor
CHEMBL4532398	0.58	Inhibitor
CHEMBL2177582	5000	Non-Inhibitor
CHEMBL3356923	4	Inhibitor
CHEMBL3356927	14	Inhibitor
CHEMBL1094709	6.8	Inhibitor
CHEMBL471041	7360	Non-Inhibitor
CHEMBL2431902	50000	Non-Inhibitor
CHEMBL2431901	50000	Non-Inhibitor
CHEMBL99	8	Inhibitor
CHEMBL98	210	Non-Inhibitor
CHEMBL487533	188	Non-Inhibitor
CHEMBL469134	254	Non-Inhibitor
CHEMBL4551095	30000	Non-Inhibitor

CHEMBL4215954	100000	Non-Inhibitor
CHEMBL519668	27.7	Inhibitor
CHEMBL99	9	Inhibitor
CHEMBL1243261	9050	Non-Inhibitor
CHEMBL487741	64.7	Non-Inhibitor
CHEMBL3426803	40	Inhibitor
CHEMBL4202838	100000	Non-Inhibitor
CHEMBL3670675	723	Non-Inhibitor
CHEMBL519746	70.1	Non-Inhibitor
CHEMBL4095596	31	Inhibitor
CHEMBL356769	30000	Non-Inhibitor
CHEMBL4104247	10000	Non-Inhibitor
CHEMBL1767029	100000	Non-Inhibitor
CHEMBL1767038	100000	Non-Inhibitor
CHEMBL3827894	2.83	Inhibitor
CHEMBL3792392	78310	Non-Inhibitor
CHEMBL3981567	10000	Non-Inhibitor
CHEMBL4764787	5780	Non-Inhibitor
CHEMBL4086093	10000	Non-Inhibitor
CHEMBL2177588	1600	Non-Inhibitor
CHEMBL472631	7840	Non-Inhibitor
CHEMBL389688	28.3	Inhibitor
CHEMBL227119	178	Non-Inhibitor
CHEMBL2425953	10000	Non-Inhibitor
CHEMBL487107	15.8	Inhibitor
CHEMBL3098606	163	Non-Inhibitor
CHEMBL3098694	88	Non-Inhibitor
CHEMBL227120	176	Non-Inhibitor
CHEMBL98	1258.93	Non-Inhibitor
CHEMBL4468860	39810.72	Non-Inhibitor
CHEMBL1851943	1584.89	Non-Inhibitor
CHEMBL3958794	63.1	Non-Inhibitor
CHEMBL1851943	3162.28	Non-Inhibitor
CHEMBL2103863	7.943	Inhibitor
CHEMBL3971436	630.96	Non-Inhibitor
CHEMBL4214502	100000	Non-Inhibitor
CHEMBL3086767	5000	Non-Inhibitor
CHEMBL4218789	5240	Non-Inhibitor
CHEMBL4552057	1.43	Inhibitor
CHEMBL1767034	100000	Non-Inhibitor
CHEMBL1767035	100000	Non-Inhibitor
CHEMBL1767040	100000	Non-Inhibitor
CHEMBL1767041	100000	Non-Inhibitor
CHEMBL99	11.3	Inhibitor
CHEMBL487943	74.8	Non-Inhibitor
CHEMBL3828518	6.85	Inhibitor

CHEMBL4550526	5.7	Inhibitor
CHEMBL2364628	125.89	Non-Inhibitor
CHEMBL2170177	39810.72	Non-Inhibitor
CHEMBL3907295	25.12	Inhibitor
CHEMBL3670669	35	Inhibitor
CHEMBL3675758	126	Non-Inhibitor
CHEMBL99	34.81	Inhibitor
CHEMBL4777961	10000	Non-Inhibitor
CHEMBL2018302	25000	Non-Inhibitor
CHEMBL2018302	12.59	Inhibitor
CHEMBL3907295	19.95	Inhibitor
CHEMBL2431907	50000	Non-Inhibitor
CHEMBL4593729	2910	Non-Inhibitor
CHEMBL3086768	5000	Non-Inhibitor
CHEMBL4459443	10000	Non-Inhibitor
CHEMBL4534503	251.19	Non-Inhibitor
CHEMBL3621988	100	Non-Inhibitor
CHEMBL4438279	316.23	Non-Inhibitor
CHEMBL2105763	39.81	Inhibitor
CHEMBL4539040	16900	Non-Inhibitor
CHEMBL4517151	102	Non-Inhibitor
CHEMBL3827281	17.55	Inhibitor
CHEMBL98	170	Non-Inhibitor
CHEMBL2105763	0.5	Inhibitor
CHEMBL4536605	26000	Non-Inhibitor
CHEMBL2170177	20000	Non-Inhibitor
CHEMBL3940985	66200	Non-Inhibitor
CHEMBL1173445	2210	Non-Inhibitor
CHEMBL3827517	0.86	Inhibitor
CHEMBL180064	8780	Non-Inhibitor
CHEMBL3394285	6320	Non-Inhibitor
CHEMBL4561073	950	Non-Inhibitor
CHEMBL1213492	331	Non-Inhibitor
CHEMBL2364628	194	Non-Inhibitor
CHEMBL227118	270	Non-Inhibitor
CHEMBL3335288	774	Non-Inhibitor
CHEMBL326433	252	Non-Inhibitor
CHEMBL3356921	116	Non-Inhibitor
CHEMBL2179618	100	Non-Inhibitor
CHEMBL511749	794.33	Non-Inhibitor
CHEMBL4445881	199.53	Non-Inhibitor
CHEMBL4798571	246.53	Non-Inhibitor
CHEMBL487253	72	Non-Inhibitor
CHEMBL4066043	3000	Non-Inhibitor
CHEMBL4080014	20400	Non-Inhibitor
CHEMBL4087897	290	Non-Inhibitor

CHEMBL98	982	Non-Inhibitor
CHEMBL4078721	3.6	Inhibitor
CHEMBL4087616	10500	Non-Inhibitor
CHEMBL469274	28.2	Inhibitor
CHEMBL98	278	Non-Inhibitor
CHEMBL99	20	Inhibitor
CHEMBL471042	1580	Non-Inhibitor
CHEMBL4066920	5.012	Inhibitor
CHEMBL467792	690	Non-Inhibitor
CHEMBL561483	240	Non-Inhibitor
CHEMBL564382	4700	Non-Inhibitor
CHEMBL564916	73000	Non-Inhibitor
CHEMBL4218266	59800	Non-Inhibitor
CHEMBL4206021	18900	Non-Inhibitor
CHEMBL4217319	8240	Non-Inhibitor
CHEMBL4218915	100000	Non-Inhibitor
CHEMBL4099942	21	Inhibitor
CHEMBL4104117	9791	Non-Inhibitor
CHEMBL178456	10700	Non-Inhibitor
CHEMBL387924	11.1	Inhibitor
CHEMBL227170	42.1	Non-Inhibitor
CHEMBL427135	30000	Non-Inhibitor
CHEMBL3622533	3	Inhibitor
CHEMBL4078458	20000	Non-Inhibitor
CHEMBL3356931	189	Non-Inhibitor
CHEMBL3356939	6000	Non-Inhibitor
CHEMBL4790998	78.24	Non-Inhibitor
CHEMBL98	57.25	Non-Inhibitor
CHEMBL27759	11100	Non-Inhibitor
CHEMBL4280303	9.12	Inhibitor
CHEMBL3235463	100000	Non-Inhibitor
CHEMBL538364	100000	Non-Inhibitor
CHEMBL3235787	100000	Non-Inhibitor
CHEMBL3098690	93	Non-Inhibitor
CHEMBL3098605	649	Non-Inhibitor
CHEMBL3098691	125	Non-Inhibitor
CHEMBL4097399	30000	Non-Inhibitor
CHEMBL1767042	100000	Non-Inhibitor
CHEMBL3356929	9	Inhibitor
CHEMBL3356936	3930	Non-Inhibitor
CHEMBL556332	11000	Non-Inhibitor
CHEMBL4451623	1502	Non-Inhibitor
CHEMBL3356918	15	Inhibitor
CHEMBL3356926	7	Inhibitor
CHEMBL3356928	14	Inhibitor
CHEMBL3356933	310	Non-Inhibitor

CHEMBL98	80	Non-Inhibitor
CHEMBL3104851	8400	Non-Inhibitor
CHEMBL4464421	2.1	Inhibitor
CHEMBL2425956	29800	Non-Inhibitor
CHEMBL511749	316.23	Non-Inhibitor
CHEMBL3971436	316.23	Non-Inhibitor
CHEMBL2018451	158.49	Non-Inhibitor
CHEMBL4790678	5750	Non-Inhibitor
CHEMBL3356917	4	Inhibitor
CHEMBL3356919	11	Inhibitor
CHEMBL213934	5210	Non-Inhibitor
CHEMBL3098693	147	Non-Inhibitor
CHEMBL3098692	244	Non-Inhibitor
CHEMBL2431912	50000	Non-Inhibitor
CHEMBL3098602	10.6	Inhibitor
CHEMBL4079541	700	Non-Inhibitor
CHEMBL4066043	79.43	Non-Inhibitor
CHEMBL2018451	199.53	Non-Inhibitor
CHEMBL2170177	10000	Non-Inhibitor
CHEMBL3098604	30.3	Inhibitor
CHEMBL3098689	51	Non-Inhibitor
CHEMBL4548759	3000	Non-Inhibitor
CHEMBL3104855	8100	Non-Inhibitor
CHEMBL3356526	6	Inhibitor
CHEMBL4532181	5.012	Inhibitor
CHEMBL4541796	25.12	Inhibitor
CHEMBL4066043	316.23	Non-Inhibitor
CHEMBL598797	398.11	Non-Inhibitor
CHEMBL3958794	158.49	Non-Inhibitor
CHEMBL4571886	33730	Non-Inhibitor
CHEMBL4448385	10000	Non-Inhibitor
CHEMBL325676	270	Non-Inhibitor
CHEMBL3356524	32	Inhibitor
CHEMBL3356930	1170	Non-Inhibitor
CHEMBL3356932	6290	Non-Inhibitor
CHEMBL3356935	658	Non-Inhibitor
CHEMBL343448	11	Inhibitor
CHEMBL3098695	125	Non-Inhibitor
CHEMBL3356922	5	Inhibitor
CHEMBL1089495	374	Non-Inhibitor
CHEMBL3098697	6830	Non-Inhibitor
CHEMBL3353927	7	Inhibitor
CHEMBL3356924	2	Inhibitor
CHEMBL146250	3.9	Inhibitor
CHEMBL3353053	41000	Non-Inhibitor
CHEMBL4749146	10000	Non-Inhibitor

CHEMBL4514330	2670	Non-Inhibitor
CHEMBL2170166	1995.26	Non-Inhibitor
CHEMBL164868	40	Inhibitor
CHEMBL3098603	503	Non-Inhibitor
CHEMBL3098696	4890	Non-Inhibitor
CHEMBL4475116	320	Non-Inhibitor
CHEMBL4749655	2.5	Inhibitor
CHEMBL2425954	5140	Non-Inhibitor
CHEMBL3098602	11	Inhibitor
CHEMBL3356916	1	Inhibitor
CHEMBL3356937	81	Non-Inhibitor
CHEMBL3356938	2930	Non-Inhibitor
CHEMBL98	64	Non-Inhibitor
CHEMBL3098688	210	Non-Inhibitor
CHEMBL4636189	200000	Non-Inhibitor
CHEMBL178456	10650	Non-Inhibitor
CHEMBL4209463	100000	Non-Inhibitor
CHEMBL4784006	1000	Non-Inhibitor
CHEMBL3670674	294	Non-Inhibitor
CHEMBL2408778	51	Non-Inhibitor
CHEMBL98	432	Non-Inhibitor
CHEMBL98	686	Non-Inhibitor
CHEMBL3356915	11	Inhibitor
CHEMBL3356925	5	Inhibitor
CHEMBL4443548	9996	Non-Inhibitor
CHEMBL2012815	150	Non-Inhibitor
CHEMBL2179618	7570	Non-Inhibitor
CHEMBL4303643	15000	Non-Inhibitor
CHEMBL2170177	13000	Non-Inhibitor
CHEMBL98	460	Non-Inhibitor
CHEMBL3335298	136	Non-Inhibitor
CHEMBL3335299	25	Inhibitor
CHEMBL3233755	886	Non-Inhibitor
CHEMBL3356920	40	Inhibitor
CHEMBL99	61	Non-Inhibitor
CHEMBL3622730	1930	Non-Inhibitor
CHEMBL3338418	100000	Non-Inhibitor
CHEMBL99	1.61	Inhibitor
CHEMBL27759	1000	Non-Inhibitor
CHEMBL99	71	Non-Inhibitor
CHEMBL98	27	Inhibitor
CHEMBL1851943	82	Non-Inhibitor
CHEMBL2018302	3710	Non-Inhibitor
CHEMBL4445881	125.89	Non-Inhibitor
CHEMBL4531802	1000	Non-Inhibitor
CHEMBL4470067	15.85	Inhibitor

CHEMBL4445312	13000	Non-Inhibitor
CHEMBL343448	0.9	Inhibitor
CHEMBL3329622	0.5	Inhibitor
CHEMBL3593247	0.5	Inhibitor
CHEMBL1370863	200000	Non-Inhibitor
CHEMBL4642821	10000	Non-Inhibitor
CHEMBL4283683	10000	Non-Inhibitor
CHEMBL4460552	1.98	Inhibitor
CHEMBL4563988	1600	Non-Inhibitor
CHEMBL4280893	39500	Non-Inhibitor
CHEMBL4763995	10000	Non-Inhibitor
CHEMBL3338404	71100	Non-Inhibitor
CHEMBL2431906	50000	Non-Inhibitor
CHEMBL4060201	19	Inhibitor
CHEMBL4450128	9400	Non-Inhibitor
CHEMBL4781177	13.24	Inhibitor
CHEMBL3356527	9	Inhibitor
CHEMBL3356934	2990	Non-Inhibitor
CHEMBL3758457	42	Non-Inhibitor
CHEMBL3353925	11	Inhibitor
CHEMBL3098691	113	Non-Inhibitor
CHEMBL4126661	10000	Non-Inhibitor
CHEMBL2103863	52	Non-Inhibitor
CHEMBL4069287	13000	Non-Inhibitor
CHEMBL4095667	1256	Non-Inhibitor
CHEMBL4103801	33000	Non-Inhibitor
CHEMBL4165684	1870	Non-Inhibitor
CHEMBL4759256	420	Non-Inhibitor
CHEMBL2364628	1584.89	Non-Inhibitor
CHEMBL2179618	501.19	Non-Inhibitor
CHEMBL4475240	2511.89	Non-Inhibitor
CHEMBL2170166	3981.07	Non-Inhibitor
CHEMBL4562244	1995.26	Non-Inhibitor
CHEMBL4444176	268	Non-Inhibitor
CHEMBL98	70	Non-Inhibitor
CHEMBL3318732	85000	Non-Inhibitor
CHEMBL561209	91000	Non-Inhibitor
CHEMBL594544	42.6	Non-Inhibitor
CHEMBL4281014	2910	Non-Inhibitor
CHEMBL3426804	1800	Non-Inhibitor
CHEMBL3622731	751	Non-Inhibitor
CHEMBL3622729	37.4	Inhibitor
CHEMBL2417781	70	Non-Inhibitor
CHEMBL2364628	10000	Non-Inhibitor
CHEMBL99	37.9	Inhibitor
CHEMBL4785064	1.7	Inhibitor

CHEMBL4744689	2.3	Inhibitor
CHEMBL3310505	1	Inhibitor
CHEMBL3235118	3220	Non-Inhibitor
CHEMBL98	91.8	Non-Inhibitor
CHEMBL4082995	51.6	Non-Inhibitor
CHEMBL3605506	100000	Non-Inhibitor
CHEMBL4514808	923	Non-Inhibitor
CHEMBL3622533	4.1	Inhibitor
CHEMBL4087968	78	Non-Inhibitor
CHEMBL4531802	630.96	Non-Inhibitor
CHEMBL4562244	501.19	Non-Inhibitor
CHEMBL4466930	79.43	Non-Inhibitor
CHEMBL4531108	5900	Non-Inhibitor
CHEMBL4471619	30000	Non-Inhibitor
CHEMBL4579366	30000	Non-Inhibitor
CHEMBL4744479	8000	Non-Inhibitor
CHEMBL4450285	114	Non-Inhibitor
CHEMBL3235790	63900	Non-Inhibitor
CHEMBL483254	2.1	Inhibitor
CHEMBL98	150	Non-Inhibitor

REFERENCES

- [1] Peng C, Trojanowski JQ, Lee VMY. Protein transmission in neurodegenerative disease. *Nat Rev Neurol* 2020 164 2020;16:199–212. <https://doi.org/10.1038/s41582-020-0333-7>.
- [2] Hou Y, Dan X, Babbar M, Wei Y, Hasselbalch SG, Croteau DL, et al. Ageing as a risk factor for neurodegenerative disease. *Nat Rev Neurol* 2019 1510 2019;15:565–81. <https://doi.org/10.1038/s41582-019-0244-7>.
- [3] Abel T, Zukin RS. Epigenetic targets of HDAC inhibition in neurodegenerative and psychiatric disorders. *Curr Opin Pharmacol* 2008. <https://doi.org/10.1016/j.coph.2007.12.002>.
- [4] Miller JL, Grant PA. The Role of DNA Methylation and Histone Modifications in Transcriptional Regulation in Humans. *Subcell Biochem* 2013;61:289. https://doi.org/10.1007/978-94-007-4525-4_13.
- [5] Smrt RD, Zhao X. Epigenetic regulation of neuronal dendrite and dendritic spine development. *Front Biol (Beijing)* 2010;5:304. <https://doi.org/10.1007/S11515-010-0650-0>.
- [6] Sultan FA, Day JJ. Epigenetic mechanisms in memory and synaptic function. *Epigenomics* 2011;3:157. <https://doi.org/10.2217/EPI.11.6>.
- [7] Geng H, Chen H, Wang H, Wang L. The Histone Modifications of Neuronal Plasticity. *Neural Plast* 2021;2021. <https://doi.org/10.1155/2021/6690523>.
- [8] Qiu X, Xiao X, Li N, Li Y. Histone deacetylases inhibitors (HDACis) as novel therapeutic application in various clinical diseases. *Prog Neuro-Psychopharmacology Biol Psychiatry* 2017. <https://doi.org/10.1016/j.pnpbp.2016.09.002>.
- [9] Gupta R, Ambasta RK, Kumar P. Pharmacological intervention of histone deacetylase enzymes in the neurodegenerative disorders. *Life Sci* 2020;243:117278.

- <https://doi.org/10.1016/J.LFS.2020.117278>.
- [10] Abeliovich A, Gitler AD. Defects in trafficking bridge Parkinson's disease pathology and genetics. *Nature* 2016. <https://doi.org/10.1038/nature20414>.
- [11] Amemori T, Jendelova P, Ruzicka J, Urdzikova LM, Sykova E. Alzheimer's disease: Mechanism and approach to cell therapy. *Int J Mol Sci* 2015. <https://doi.org/10.3390/ijms161125961>.
- [12] Taylor JP, Brown RH, Cleveland DW. Decoding ALS: From genes to mechanism. *Nature* 2016. <https://doi.org/10.1038/nature20413>.
- [13] Poduri A, Evrony GD, Cai X, Walsh CA. Somatic mutation, genomic variation, and neurological disease. *Science (80-)* 2013. <https://doi.org/10.1126/science.1237758>.
- [14] Kawa IA, Masood A, Amin S, Mustafa MF, Rashid F. Clinical Perspective of Posttranslational Modifications. *Mol Nutr Vitam* 2019:37–68. <https://doi.org/10.1016/B978-0-12-811913-6.00002-3>.
- [15] Haberland M, Montgomery RL, Olson EN. The many roles of histone deacetylases in development and physiology: Implications for disease and therapy. *Nat Rev Genet* 2009. <https://doi.org/10.1038/nrg2485>.
- [16] Penney J, Tsai L-H. Histone deacetylases in memory and cognition. *Sci Signal* 2014. <https://doi.org/10.1126/scisignal.aaa0069>.
- [17] Bannister AJ, Kouzarides T. Regulation of chromatin by histone modifications. *Cell Res* 2011 213 2011;21:381–95. <https://doi.org/10.1038/cr.2011.22>.
- [18] Watts BR, Wittmann S, Wery M, Gautier C, Kus K, Birot A, et al. Histone deacetylation promotes transcriptional silencing at facultative heterochromatin. *Nucleic Acids Res* 2018;46:5426. <https://doi.org/10.1093/NAR/GKY232>.
- [19] Ganai SA, Ramadoss M, Mahadevan V. Histone Deacetylase (HDAC) Inhibitors - Emerging Roles in Neuronal Memory, Learning, Synaptic Plasticity and Neural

- Regeneration. Curr Neuropharmacol 2016;14:55.
<https://doi.org/10.2174/1570159X13666151021111609>.
- [20] Shukla S, Tekwani BL. Histone Deacetylases Inhibitors in Neurodegenerative Diseases, Neuroprotection and Neuronal Differentiation. *Front Pharmacol* 2020;11:537.
<https://doi.org/10.3389/FPHAR.2020.00537/BIBTEX>.
- [21] Damaskos C, Garmpis N, Valsami S, Kontos M, Spartalis E, Kalampokas T, et al. Histone Deacetylase Inhibitors: An Attractive Therapeutic Strategy Against Breast Cancer. *Anticancer Res* 2017. <https://doi.org/10.21873/anticancerres.11286>.
- [22] Fuchikami M, Yamamoto S, Morinobu S, Okada S, Yamawaki Y, Yamawaki S. The potential use of histone deacetylase inhibitors in the treatment of depression. *Prog Neuro-Psychopharmacology Biol Psychiatry* 2016.
<https://doi.org/10.1016/j.pnpbp.2015.03.010>.
- [23] Christensen DP, Dahllöf M, Lundh M, Rasmussen DN, Nielsen MD, Billestrup N, et al. Histone deacetylase (HDAC) inhibition as a novel treatment for diabetes mellitus. *Mol Med Cambridge Mass* 2011.
<https://doi.org/10.2119/molmed.2011.0002110.2119/molmed.2011.00021>. Epub 2011 Jan 25.
- [24] Gräff J, Rei D, Guan JS, Wang WY, Seo J, Hennig KM, et al. An epigenetic blockade of cognitive functions in the neurodegenerating brain. *Nature* 2012.
<https://doi.org/10.1038/nature10849>.
- [25] Blackwell L, Norris J, Suto CM, Janzen WP. The use of diversity profiling to characterize chemical modulators of the histone deacetylases. *Life Sci* 2008.
<https://doi.org/10.1016/j.lfs.2008.03.004>.
- [26] Hwang JY, Aromolaran KA, Zukin RS. The emerging field of epigenetics in neurodegeneration and neuroprotection. *Nat Rev Neurosci* 2017.

- <https://doi.org/10.1038/nrn.2017.46>.
- [27] Shimojo M, Hersh LB. Regulation of the cholinergic gene locus by the repressor element-1 silencing transcription factor/neuron restrictive silencer factor (REST/NRSF). *Life Sci* 2004;74:2213–25. <https://doi.org/https://doi.org/10.1016/j.lfs.2003.08.045>.
- [28] Narayanan M, Huynh JL, Wang K, Yang X, Yoo S, McElwee J, et al. Common dysregulation network in the human prefrontal cortex underlies two neurodegenerative diseases. *Mol Syst Biol* 2014. <https://doi.org/10.15252/msb.20145304>.
- [29] Harrison IF, Dexter DT. Epigenetic targeting of histone deacetylase: Therapeutic potential in Parkinson's disease? *Pharmacol Ther* 2013;140:34–52. <https://doi.org/10.1016/j.pharmthera.2013.05.010>.
- [30] Lee CY, Grant PA. Role of Histone Acetylation and Acetyltransferases in Gene Regulation. *Toxicopigenetics Core Princ Appl* 2019:3–30. <https://doi.org/10.1016/B978-0-12-812433-8.00001-0>.
- [31] Parbin S, Kar S, Shilpi A, Sengupta D, Deb M, Rath SK, et al. Histone Deacetylases: A Saga of Perturbed Acetylation Homeostasis in Cancer. *J Histochem Cytochem* 2014;62:11. <https://doi.org/10.1369/0022155413506582>.
- [32] Breijyeh Z, Karaman R, Muñoz-Torrero D, Dembinski R. Comprehensive Review on Alzheimer's Disease: Causes and Treatment. *Mol* 2020, Vol 25, Page 5789 2020;25:5789. <https://doi.org/10.3390/MOLECULES25245789>.
- [33] Iqbal K, Liu F, Gong C-X, Grundke-Iqbal I. Tau in Alzheimer Disease and Related Tauopathies. *Curr Alzheimer Res* 2010;7:656. <https://doi.org/10.2174/156720510793611592>.
- [34] Murphy MP, Levine H. Alzheimer's Disease and the β -Amyloid Peptide. *J Alzheimers Dis* 2010;19:311. <https://doi.org/10.3233/JAD-2010-1221>.
- [35] Yiannopoulou KG, Papageorgiou SG. Current and future treatments for Alzheimer's

- disease. *Ther Adv Neurol Disord* 2013;6:19–33.
<https://doi.org/10.1177/1756285612461679>.
- [36] Livingston G, Huntley J, Sommerlad A, Ames D, Ballard C, Banerjee S, et al. Dementia prevention, intervention, and care: 2020 report of the Lancet Commission. *Lancet* 2020;396:413–46. [https://doi.org/10.1016/S0140-6736\(20\)30367-6/ATTACHMENT/CEE43A30-904B-4A45-A4E5-AFE48804398D/MMC1.PDF](https://doi.org/10.1016/S0140-6736(20)30367-6/ATTACHMENT/CEE43A30-904B-4A45-A4E5-AFE48804398D/MMC1.PDF).
- [37] Steiner H, Capell A, Leimer U, Haass C. Genes and mechanisms involved in β -amyloid generation and Alzheimer's disease. *Eur Arch Psychiatry Clin Neurosci* 1999 2496 1999;249:266–70. <https://doi.org/10.1007/S004060050098>.
- [38] Chen GF, Xu TH, Yan Y, Zhou YR, Jiang Y, Melcher K, et al. Amyloid beta: structure, biology and structure-based therapeutic development. *Acta Pharmacol Sin* 2017 389 2017;38:1205–35. <https://doi.org/10.1038/aps.2017.28>.
- [39] Sun X, Chen WD, Wang YD. β -Amyloid: The key peptide in the pathogenesis of Alzheimer's disease. *Front Pharmacol* 2015;6:221. <https://doi.org/10.3389/FPHAR.2015.00221/BIBTEX>.
- [40] Armstrong RA. Risk factors for Alzheimer's disease. *Folia Neuropathol* 2019;57:87–105. <https://doi.org/10.5114/FN.2019.85929>.
- [41] Lin X, Kapoor A, Gu Y, Chow MJ, Peng J, Zhao K, et al. Contributions of DNA Damage to Alzheimer's Disease. *Int J Mol Sci* 2020;21. <https://doi.org/10.3390/IJMS21051666>.
- [42] Wang W, Zhao F, Ma X, Perry G, Zhu X. Mitochondria dysfunction in the pathogenesis of Alzheimer's disease: recent advances. *Mol Neurodegener* 2020 151 2020;15:1–22. <https://doi.org/10.1186/S13024-020-00376-6>.
- [43] Adler DH, Wisse LEM, Ittyerah R, Pluta JB, Ding SL, Xie L, et al. Characterizing the human hippocampus in aging and Alzheimer's disease using a computational atlas derived from ex vivo MRI and histology. *Proc Natl Acad Sci* 2018;115:4252–7.

- <https://doi.org/10.1073/PNAS.1801093115>.
- [44] Liyanage SI, Weaver DF. Misfolded proteins as a therapeutic target in Alzheimer's disease. *Adv Protein Chem Struct Biol* 2019;118:371–411. <https://doi.org/10.1016/BS.APCSB.2019.08.003>.
- [45] Zhang W, Xu C, Sun J, Shen HM, Wang J, Yang C. Impairment of the autophagy–lysosomal pathway in Alzheimer's diseases: Pathogenic mechanisms and therapeutic potential. *Acta Pharm Sin B* 2022;12:1019–40. <https://doi.org/10.1016/J.APSB.2022.01.008>.
- [46] Oddo S. The ubiquitin-proteasome system in Alzheimer's disease. *J Cell Mol Med* 2008;12:363. <https://doi.org/10.1111/J.1582-4934.2008.00276.X>.
- [47] Bustamante HA, González AE, Cerda-Troncoso C, Shaughnessy R, Otth C, Soza A, et al. Interplay between the autophagy-lysosomal pathway and the ubiquitin-proteasome system: A target for therapeutic development in alzheimer's disease. *Front Cell Neurosci* 2018;12:126. <https://doi.org/10.3389/FNCEL.2018.00126/BIBTEX>.
- [48] Sharma K. Cholinesterase inhibitors as Alzheimer's therapeutics (Review). *Mol Med Rep* 2019;20:1479–87. <https://doi.org/10.3892/MMR.2019.10374/HTML>.
- [49] Eldufani J, Blaise G. The role of acetylcholinesterase inhibitors such as neostigmine and rivastigmine on chronic pain and cognitive function in aging: A review of recent clinical applications. *Alzheimer's Dement Transl Res Clin Interv* 2019;5:175–83. <https://doi.org/10.1016/J.TRCI.2019.03.004>.
- [50] Wang R, Reddy PH. Role of Glutamate and NMDA Receptors in Alzheimer's Disease. *J Alzheimer's Dis* 2017;57:1041–8. <https://doi.org/10.3233/JAD-160763>.
- [51] Mhyre TR, Boyd JT, Hamill RW, Maguire-Zeiss KA. Parkinson's Disease. *Subcell Biochem* 2012;65:389. https://doi.org/10.1007/978-94-007-5416-4_16.
- [52] Tang Y, Xiao X, Xie H, Wan CM, Meng L, Liu ZH, et al. Altered functional brain

- connectomes between sporadic and Familial Parkinson's patients. *Front Neuroanat* 2017;11:99. <https://doi.org/10.3389/FNANA.2017.00099/BIBTEX>.
- [53] Chartier-Harlin MC, Kachergus J, Roumier C, Mouroux V, Douay X, Lincoln S, et al. α -synuclein locus duplication as a cause of familial Parkinson's disease. *Lancet* 2004;364:1167–9. [https://doi.org/10.1016/S0140-6736\(04\)17103-1](https://doi.org/10.1016/S0140-6736(04)17103-1).
- [54] Farrer M, Kachergus J, Forno L, Lincoln S, Wang DS, Hulihan M, et al. Comparison of kindreds with parkinsonism and α -synuclein genomic multiplications. *Ann Neurol* 2004;55:174–9. <https://doi.org/10.1002/ANA.10846>.
- [55] Modi P, Mohamad A, Phom L, ZevelouKoza, Das A, Chaurasia R, et al. Understanding Pathophysiology of Sporadic Parkinson's Disease in Drosophila Model: Potential Opportunities and Notable Limitations. *Challenges Park Dis* 2016. <https://doi.org/10.5772/63767>.
- [56] Rietdijk CD, Perez-Pardo P, Garssen J, van Wezel RJA, Kraneveld AD. Exploring Braak's Hypothesis of Parkinson's Disease. *Front Neurol* 2017;8. <https://doi.org/10.3389/FNEUR.2017.00037>.
- [57] DeMaagd G, Philip A. Parkinson's Disease and Its Management: Part 1: Disease Entity, Risk Factors, Pathophysiology, Clinical Presentation, and Diagnosis. *Pharm Ther* 2015;40:504.
- [58] Klein C, Westenberger A. Genetics of Parkinson's Disease. *Cold Spring Harb Perspect Med* 2012;2:a008888. <https://doi.org/10.1101/CSHPERSPECT.A008888>.
- [59] Sardi SP, Cedarbaum JM, Brundin P. Targeted Therapies for Parkinson's Disease: From Genetics to the Clinic. *Mov Disord* 2018;33:684–96. <https://doi.org/10.1002/MDS.27414>.
- [60] Ross OA, Braithwaite AT, Skipper LM, Kachergus J, Hulihan MM, Middleton FA, et al. Genomic investigation of α -Synuclein multiplication and parkinsonism. *Ann Neurol*

- 2008;63:743–50. <https://doi.org/10.1002/ANA.21380>.
- [61] Stefanis L. α -Synuclein in Parkinson's Disease. *Cold Spring Harb Perspect Med* 2012;2. <https://doi.org/10.1101/CSHPERSPECT.A009399>.
- [62] Li JQ, Tan L, Yu JT. The role of the LRRK2 gene in Parkinsonism. *Mol Neurodegener* 2014;9:47. <https://doi.org/10.1186/1750-1326-9-47>.
- [63] Tang B, Xiong H, Sun P, Zhang Y, Wang D, Hu Z, et al. Association of PINK1 and DJ-1 confers digenic inheritance of early-onset Parkinson's disease. *Hum Mol Genet* 2006;15:1816–25. <https://doi.org/10.1093/HMG/DDL104>.
- [64] Chen H, Ritz B. The Search for Environmental Causes of Parkinson's Disease: Moving Forward. *J Parkinsons Dis* 2018;8:S9. <https://doi.org/10.3233/JPD-181493>.
- [65] Ball N, Teo WP, Chandra S, Chapman J. Parkinson's Disease and the Environment. *Front Neurol* 2019;10:218. <https://doi.org/10.3389/FNEUR.2019.00218>.
- [66] Kenborg L, Rugbjerg K, Lee PC, Ravnskjaer L, Christensen J, Ritz B, et al. Head injury and risk for Parkinson disease: results from a Danish case-control study. *Neurology* 2015;84:1098–103. <https://doi.org/10.1212/WNL.0000000000001362>.
- [67] Gómez-Benito M, Granado N, García-Sanz P, Michel A, Dumoulin M, Moratalla R. Modeling Parkinson's Disease With the Alpha-Synuclein Protein. *Front Pharmacol* 2020;11:1. <https://doi.org/10.3389/FPHAR.2020.00356>.
- [68] Lim J, Yue Z. Neuronal aggregates: formation, clearance and spreading. *Dev Cell* 2015;32:491. <https://doi.org/10.1016/J.DEVCEL.2015.02.002>.
- [69] Guo CY, Sun L, Chen XP, Zhang DS. Oxidative stress, mitochondrial damage and neurodegenerative diseases. *Neural Regen Res* 2013;8:2003. <https://doi.org/10.3969/J.ISSN.1673-5374.2013.21.009>.
- [70] Oueslati A, Fournier M, Lashuel HA. Role of post-translational modifications in modulating the structure, function and toxicity of α -synuclein. Implications for

- Parkinson's disease pathogenesis and therapies. vol. 183. Elsevier B.V.; 2010.
[https://doi.org/10.1016/S0079-6123\(10\)83007-9](https://doi.org/10.1016/S0079-6123(10)83007-9).
- [71] He S, Wang F, Yung KKL, Zhang S, Qu S. Effects of α -Synuclein-Associated Post-Translational Modifications in Parkinson's Disease. *ACS Chem Neurosci* 2021;12:1061–71.
https://doi.org/10.1021/ACSCHEMNEURO.1C00028/ASSET/IMAGES/LARGE/CN1C00028_0002.JPEG.
- [72] Junqueira SC, Centeno EGZ, Wilkinson KA, Cimarosti H. Post-translational modifications of Parkinson's disease-related proteins: Phosphorylation, SUMOylation and Ubiquitination. *Biochim Biophys Acta - Mol Basis Dis* 2019;1865:2001–7.
<https://doi.org/10.1016/J.BBADIS.2018.10.025>.
- [73] Ren RJ, Dammer EB, Wang G, Seyfried NT, Levey AI. Proteomics of protein post-translational modifications implicated in neurodegeneration. *Transl Neurodegener* 2014.
<https://doi.org/10.1186/2047-9158-3-23>.
- [74] Stram AR, Payne RM. Post-translational modifications in mitochondria: protein signaling in the powerhouse. *Cell Mol Life Sci* 2016. <https://doi.org/10.1007/s00018-016-2280-4>.
- [75] Xu H, Wang Y, Lin S, Deng W, Peng D, Cui Q, et al. PTMD: A Database of Human Disease-associated Post-translational Modifications. *Genomics, Proteomics Bioinforma* 2018. <https://doi.org/10.1016/j.gpb.2018.06.004>.
- [76] Varland S, Osberg C, Arnesen T. N-terminal modifications of cellular proteins: The enzymes involved, their substrate specificities and biological effects. *Proteomics* 2015.
<https://doi.org/10.1002/pmic.201400619>.
- [77] Biroccio A, Del Boccio P, Panella M, Bernardini S, Di Ilio C, Gambi D, et al. Differential post-translational modifications of transthyretin in Alzheimer's disease: A

- study of the cerebral spinal fluid. *Proteomics* 2006. <https://doi.org/10.1002/pmic.200500285>.
- [78] Cook C, Stankowski JN, Carlomagno Y, Stetler C, Petrucelli L. Acetylation: A new key to unlock tau's role in neurodegeneration. *Alzheimer's Res Ther* 2014. <https://doi.org/10.1186/alzrt259>.
- [79] Olzscha H. Posttranslational modifications and proteinopathies: How guardians of the proteome are defeated. *Biol Chem* 2019;400:895–915. <https://doi.org/10.1515/hsz-2018-0458>.
- [80] Schaffert LN, Carter WG. Do post-translational modifications influence protein aggregation in neurodegenerative diseases: A systematic review. *Brain Sci* 2020;10. <https://doi.org/10.3390/brainsci10040232>.
- [81] Cobos SN, Bennett SA, Torrente MP. The impact of histone post-translational modifications in neurodegenerative diseases. *Biochim Biophys Acta - Mol Basis Dis* 2019;1865:1982–91. <https://doi.org/10.1016/J.BBADIS.2018.10.019>.
- [82] Lu H, Liu X, Deng Y, Qing H. DNA methylation, a hand behind neurodegenerative diseases. *Front Aging Neurosci* 2013. <https://doi.org/10.3389/fnagi.2013.00085>.
- [83] Geschwind DH. Tau phosphorylation, tangles, and neurodegeneration: The chicken or the egg? *Neuron* 2003. [https://doi.org/10.1016/S0896-6273\(03\)00681-0](https://doi.org/10.1016/S0896-6273(03)00681-0).
- [84] Kumar D, Ambasta RK, Kumar P. Ubiquitin biology in neurodegenerative disorders: From impairment to therapeutic strategies. *Ageing Res Rev* 2020. <https://doi.org/10.1016/j.arr.2020.101078>.
- [85] Princz A, Tavernarakis N. SUMOylation in Neurodegenerative Diseases. *Gerontology* 2020. <https://doi.org/10.1159/000502142>.
- [86] Chen Y, Neve RL, Liu H. Neddylation dysfunction in Alzheimer's disease. *J Cell Mol Med* 2012;16:2583–91. <https://doi.org/10.1111/J.1582-4934.2012.01604.X>.

- [87] Salahuddin P, Rabbani G, Khan RH. The role of advanced glycation end products in various types of neurodegenerative disease: a therapeutic approach. *Cell Mol Biol Lett* 2014. <https://doi.org/10.2478/s11658-014-0205-5>.
- [88] Cho E, Park M. Palmitoylation in Alzheimer's disease and other neurodegenerative diseases. *Pharmacol Res* 2016. <https://doi.org/10.1016/j.phrs.2016.06.008>.
- [89] Guru KrishnaKumar V, Baweja L, Ralhan K, Gupta S. Carbamylation promotes amyloidogenesis and induces structural changes in Tau-core hexapeptide fibrils. *Biochim Biophys Acta - Gen Subj* 2018. <https://doi.org/10.1016/j.bbagen.2018.07.030>.
- [90] Nakamura T, Tu S, Akhtar MW, Sunico CR, Okamoto S ichi, Lipton SA. Aberrant Protein S-nitrosylation in neurodegenerative diseases. *Neuron* 2013. <https://doi.org/10.1016/j.neuron.2013.05.005>.
- [91] Martin DDO, Hayden MR. Post-translational myristoylation at the cross roads of cell death, autophagy and neurodegeneration. *Biochem Soc Trans* 2015. <https://doi.org/10.1042/BST20140281>.
- [92] Alleyn M, Breitzig M, Lockey R, Kolliputi N. The dawn of succinylation: A posttranslational modification. *Am J Physiol - Cell Physiol* 2018. <https://doi.org/10.1152/ajpcell.00148.2017>.
- [93] Soto C. Unfolding the role of protein misfolding in neurodegenerative diseases. *Nat Rev Neurosci* 2003. <https://doi.org/10.1038/nrn1007>.
- [94] Agbas A. Trends of Protein Aggregation in Neurodegenerative Diseases. *Neurochem. Basis Brain Funct. Dysfunct.*, 2019, p. 1–26. <https://doi.org/10.5772/intechopen.81224>.
- [95] Merlini G, Bellotti V, Palladini G, Obici L, Casarini S, Perfetti V. Protein Aggregation 1) 2001;39:1065–75.
- [96] Shamsi TN, Athar T, Parveen R, Fatima S. A review on protein misfolding, aggregation and strategies to prevent related ailments. *Int J Biol Macromol* 2017;105:993–1000.

- <https://doi.org/10.1016/j.ijbiomac.2017.07.116>.
- [97] Malik R, Wiedau M. Therapeutic Approaches Targeting Protein Aggregation in Amyotrophic Lateral Sclerosis. *Front Mol Neurosci* 2020;13:1–6. <https://doi.org/10.3389/fnmol.2020.00098>.
- [98] Ross CA, Poirier MA. What is the role of protein aggregation in neurodegeneration? *Nat Rev Mol Cell Biol* 2005;6:891–8. <https://doi.org/10.1038/nrm1742>.
- [99] Ciechanover A, Kwon YT. Protein quality control by molecular chaperones in neurodegeneration. *Front Neurosci* 2017;11:1–18. <https://doi.org/10.3389/fnins.2017.00185>.
- [100] McNaught KSP, Olanow CW, Halliwell B, Isacson O, Jenner P. Failure of the ubiquitin proteasome system in Parkinson's disease. *Nat Rev Neurosci* 2001;2:589–94. <https://doi.org/10.1038/35086067>.
- [101] Zheng Q, Huang T, Zhang L, Zhou Y, Luo H, Xu H, et al. Dysregulation of ubiquitin-proteasome system in neurodegenerative diseases. *Front Aging Neurosci* 2016;8:1–10. <https://doi.org/10.3389/fnagi.2016.00303>.
- [102] Pan T, Kondo S, Le W, Jankovic J. The role of autophagy-lysosome pathway in neurodegeneration associated with Parkinson's disease. *Brain* 2008;131:1969–78. <https://doi.org/10.1093/BRAIN/AWM318>.
- [103] Eskelinen EL, Saftig P. Autophagy: A lysosomal degradation pathway with a central role in health and disease. *Biochim Biophys Acta - Mol Cell Res* 2009. <https://doi.org/10.1016/j.bbamcr.2008.07.014>.
- [104] Martini-Stoica H, Xu Y, Ballabio A, Zheng H. The Autophagy-Lysosomal Pathway in Neurodegeneration: A TFEB Perspective. *Trends Neurosci* 2016;39:221–34. <https://doi.org/10.1016/j.tins.2016.02.002>.
- [105] Rezaei-Ghaleh N, Amininasab M, Kumar S, Walter J, Zweckstetter M. Phosphorylation

- modifies the molecular stability of β -amyloid deposits. *Nat Commun* 2016;7:1–9. <https://doi.org/10.1038/ncomms11359>.
- [106] Banks CJ, Andersen JL. Mechanisms of SOD1 regulation by post-translational modifications. *Redox Biol* 2019;26:101270. <https://doi.org/10.1016/j.redox.2019.101270>.
- [107] Cohen TJ, Hwang AW, Restrepo CR, Yuan CX, Trojanowski JQ, Lee VMY. An acetylation switch controls TDP-43 function and aggregation propensity. *Nat Commun* 2015;6:1–13. <https://doi.org/10.1038/ncomms6845>.
- [108] Vicente Miranda H, Gomes MA, Branco-Santos J, Breda C, Lázaro DF, Lopes LV, et al. Glycation potentiates neurodegeneration in models of Huntington's disease. *Sci Rep* 2016;6:1–12. <https://doi.org/10.1038/srep36798>.
- [109] Zhang J, Li X, Li J Da. The Roles of Post-translational Modifications on α -Synuclein in the Pathogenesis of Parkinson's Diseases. *Front Neurosci* 2019;13. <https://doi.org/10.3389/fnins.2019.00381>.
- [110] Bhattacharyya R, Barren C, Kovacs DM. Palmitoylation of amyloid precursor protein regulates amyloidogenic processing in lipid rafts. *J Neurosci* 2013;33:11169–83. <https://doi.org/10.1523/JNEUROSCI.4704-12.2013>.
- [111] Kumar R, Jangir DK, Verma G, Shekhar S, Hanpude P, Kumar S, et al. S-nitrosylation of UCHL1 induces its structural instability and promotes α -synuclein aggregation. *Sci Rep* 2017;7:1–16. <https://doi.org/10.1038/srep44558>.
- [112] Wilcox KC, Zhou L, Jordon JK, Huang Y, Yu Y, Redler RL, et al. Modifications of superoxide dismutase (SOD1) in human erythrocytes: A possible role in amyotrophic lateral sclerosis. *J Biol Chem* 2009;284:13940–7. <https://doi.org/10.1074/jbc.M809687200>.
- [113] Liu F, Zaidi T, Iqbal K, Grundke-Iqbal I, Merkle RK, Gong CX. Role of glycosylation

- in hyperphosphorylation of tau in Alzheimer's disease. *FEBS Lett* 2002;512:101–6. [https://doi.org/10.1016/S0014-5793\(02\)02228-7](https://doi.org/10.1016/S0014-5793(02)02228-7).
- [114] McGurk L, Rifai OM, Bonini NM. Poly(ADP-Ribosylation) in Age-Related Neurological Disease. *Trends Genet* 2019. <https://doi.org/10.1016/j.tig.2019.05.004>.
- [115] Francis YI, Fa M, Ashraf H, Zhang H, Staniszewski A, Latchman DS, et al. Dysregulation of Histone Acetylation in the APP/PS1 Mouse Model of Alzheimer's Disease. *J Alzheimers Dis* 2009;18:131–9. <https://doi.org/10.3233/JAD-2009-1134>.
- [116] Klein HU, McCabe C, GJoneska E, Sullivan SE, Kaskow BJ, Tang A, et al. Epigenome-wide study uncovers large-scale changes in histone acetylation driven by tau pathology in aging and Alzheimer's human brains. *Nat Neurosci* 2018 221 2018;22:37–46. <https://doi.org/10.1038/s41593-018-0291-1>.
- [117] Marzi SJ, Leung SK, Ribarska T, Hannon E, Smith AR, Pishva E, et al. A histone acetylome-wide association study of Alzheimer's disease identifies disease-associated H3K27ac differences in the entorhinal cortex. *Nat Neurosci* 2018 2111 2018;21:1618–27. <https://doi.org/10.1038/s41593-018-0253-7>.
- [118] Santana DA, Bedrat A, Puga RD, Turecki G, Mechawar N, Faria TC, et al. The role of H3K9 acetylation and gene expression in different brain regions of Alzheimer's disease patients. <https://doi.org/10.2217/EPI-2022-0096> <https://doi.org/10.2217/EPI-2022-0096> 2022;14:651–70. <https://doi.org/10.2217/EPI-2022-0096>.
- [119] Esteves AR, Filipe F, Magalhães JD, Silva DF, Cardoso SM. The Role of Beclin-1 Acetylation on Autophagic Flux in Alzheimer's Disease. *Mol Neurobiol* 2019;56:5654–70. <https://doi.org/10.1007/S12035-019-1483-8/FIGURES/5>.
- [120] Choi H, Kim HJ, Yang J, Chae S, Lee W, Chung S, et al. Acetylation changes tau interactome to degrade tau in Alzheimer's disease animal and organoid models. *Aging Cell* 2020;19:e13081. <https://doi.org/10.1111/ACEL.13081>.

- [121] Min SW, Cho SH, Zhou Y, Schroeder S, Haroutunian V, Seeley WW, et al. Acetylation of Tau Inhibits Its Degradation and Contributes to Tauopathy. *Neuron* 2010;67:953–66. <https://doi.org/10.1016/J.NEURON.2010.08.044>.
- [122] Tracy TE, Gan L. Acetylated tau in Alzheimer’s disease: An instigator of synaptic dysfunction underlying memory loss. *BioEssays* 2017;39:1600224. <https://doi.org/10.1002/BIES.201600224>.
- [123] Park G, Tan J, Garcia G, Kang Y, Salvesen G, Zhang Z. Regulation of Histone Acetylation by Autophagy in Parkinson Disease *. *J Biol Chem* 2016;291:3531–40. <https://doi.org/10.1074/JBC.M115.675488>.
- [124] Harrison IF, Smith AD, Dexter DT. Pathological histone acetylation in Parkinson’s disease: Neuroprotection and inhibition of microglial activation through SIRT 2 inhibition. *Neurosci Lett* 2018;666:48–57. <https://doi.org/10.1016/J.NEULET.2017.12.037>.
- [125] Yakhine-Diop SMS, Niso-Santano M, Rodríguez-Arribas M, Gómez-Sánchez R, Martínez-Chacón G, Uribe-Carretero E, et al. Impaired Mitophagy and Protein Acetylation Levels in Fibroblasts from Parkinson’s Disease Patients. *Mol Neurobiol* 2019;56:2466–81. <https://doi.org/10.1007/S12035-018-1206-6/FIGURES/10>.
- [126] Trexler AJ, Rhoades E. N-terminal acetylation is critical for forming α -helical oligomer of α -synuclein. *Protein Sci* 2012;21:601–5. <https://doi.org/10.1002/PRO.2056>.
- [127] Kang L, Moriarty GM, Woods LA, Ashcroft AE, Radford SE, Baum J. N-terminal acetylation of α -synuclein induces increased transient helical propensity and decreased aggregation rates in the intrinsically disordered monomer. *Protein Sci* 2012;21:911–7. <https://doi.org/10.1002/PRO.2088>.
- [128] Jian W, Wei X, Chen L, Wang Z, Sun Y, Zhu S, et al. Inhibition of HDAC6 increases acetylation of peroxiredoxin1/2 and ameliorates 6-OHDA induced dopaminergic injury.

- Neurosci Lett 2017;658:114–20. <https://doi.org/10.1016/j.neulet.2017.08.029>.
- [129] Li B, Yang Y, Wang Y, Zhang J, Ding J, Liu X, et al. Acetylation of NDUFV1 induced by a newly synthesized HDAC6 inhibitor HGC rescues dopaminergic neuron loss in Parkinson models. *IScience* 2021;24:102302. <https://doi.org/10.1016/J.ISCI.2021.102302>.
- [130] Fan F, Li S, Wen Z, Ye Q, Chen X, Ye Q. Regulation of PGC-1 α mediated by acetylation and phosphorylation in MPP⁺ induced cell model of Parkinson's disease. *Aging (Albany NY)* 2020;12:9461. <https://doi.org/10.18632/AGING.103219>.
- [131] Jeong Y, Du R, Zhu X, Yin S, Wang J, Cui H, et al. Histone deacetylase isoforms regulate innate immune responses by deacetylating mitogen-activated protein kinase phosphatase-1. *J Leukoc Biol* 2013. <https://doi.org/10.1189/jlb.1013565>.
- [132] Finnin MS, Donigian JR, Cohen A, Richon VM, Rifkind RA, Marks PA, et al. Structures of a histone deacetylase homologue bound to the TSA and SAHA inhibitors. *Nature* 1999. <https://doi.org/10.1038/43710>.
- [133] Bertrand P. Inside HDAC with HDAC inhibitors. *Eur J Med Chem* 2010. <https://doi.org/10.1016/j.ejmech.2010.02.030>.
- [134] Vanommeslaeghe K, De Proft F, Loverix S, Tourwé D, Geerlings P. Theoretical study revealing the functioning of a novel combination of catalytic motifs in histone deacetylase. *Bioorganic Med Chem* 2005. <https://doi.org/10.1016/j.bmc.2005.04.001>.
- [135] Parra M. Class IIa HDACs - New insights into their functions in physiology and pathology. *FEBS J* 2015. <https://doi.org/10.1111/febs.13061>.
- [136] Jones P, Altamura S, De Francesco R, Gallinari P, Lahm A, Neddermann P, et al. Probing the elusive catalytic activity of vertebrate class IIa histone deacetylases. *Bioorganic Med Chem Lett* 2008. <https://doi.org/10.1016/j.bmcl.2008.02.025>.
- [137] Lahm A, Paolini C, Pallaoro M, Nardi MC, Jones P, Neddermann P, et al. Unraveling

- the hidden catalytic activity of vertebrate class IIa histone deacetylases. *Proc Natl Acad Sci U S A* 2007. <https://doi.org/10.1073/pnas.0706487104>.
- [138] Wang A, Kruhlak M, Wu J, Bertos N, Vezmar M, Posner B, et al. Regulation of histone deacetylase 4 by binding of 14-3-3 proteins. *Mol Cell Biol* 2000.
- [139] Zhou X, Richon VM, Rifkind RA, Marks PA. Identification of a transcriptional repressor related to the noncatalytic domain of histone deacetylases 4 and 5. *Proc Natl Acad Sci U S A* 2000.
- [140] Bao X, Wang Y, Li X, Li XM, Liu Z, Yang T, et al. Identification of “erasers” for lysine crotonylated histone marks using a chemical proteomics approach. *Elife* 2014. <https://doi.org/10.7554/eLife.02999>.
- [141] Simmons BJ, Cohen TJ, Bedlack R, Yao T. Histone Deacetylases: the Biology and Clinical Implication. *Handb Exp Pharmacol* 206 2011. <https://doi.org/10.1007/978-3-642-21631-2>.
- [142] Dokmanovic M, Clarke C, Marks PA. Histone Deacetylase Inhibitors: Overview and Perspectives. *Mol Cancer Res* 2007. <https://doi.org/10.1158/1541-7786.MCR-07-0324>.
- [143] Gray SG, Ekström TJ. The human histone deacetylase family. *Exp Cell Res* 2001. <https://doi.org/10.1006/excr.2000.5080>.
- [144] Rehan L, Laszki-Szczańchor K, Sobieszczańska M, Polak-Jonkisz D. SIRT1 and NAD as regulators of ageing. *Life Sci* 2014. <https://doi.org/10.1016/j.lfs.2014.03.015>.
- [145] Imai SI, Armstrong CM, Kaeberlein M, Guarente L. Transcriptional silencing and longevity protein Sir2 is an NAD-dependent histone deacetylase. *Nature* 2000. <https://doi.org/10.1038/35001622>.
- [146] Sauve AA, Wolberger C, Schramm VL, Boeke JD. The Biochemistry of Sirtuins. *Annu Rev Biochem* 2006. <https://doi.org/10.1146/annurev.biochem.74.082803.133500>.
- [147] Galasinski SC, Resing KA, Goodrich JA, Ahn NG. Phosphatase inhibition leads to

- histone deacetylases 1 and 2 phosphorylation and disruption of corepressor interactions. *J Biol Chem* 2002. <https://doi.org/10.1074/jbc.M201174200>.
- [148] Bardai FH, D’Mello SR. Selective toxicity by HDAC3 in neurons: regulation by Akt and GSK3beta. *J Neurosci* 2011;31:1746–51. <https://doi.org/10.1523/JNEUROSCI.5704-10.2011>.
- [149] Elias JE, Li J, Beausoleil SA, Gygi SP, Villen J, Schwartz D, et al. Large-scale characterization of HeLa cell nuclear phosphoproteins. *Proc Natl Acad Sci* 2004. <https://doi.org/10.1073/pnas.0404720101>.
- [150] Pugacheva EN, Jablonski SA, Hartman TR, Henske EP, Golemis EA. HEF1-Dependent Aurora A Activation Induces Disassembly of the Primary Cilium. *Cell* 2007. <https://doi.org/10.1016/j.cell.2007.04.035>.
- [151] Greco TM, Yu F, Guise AJ, Cristea IM. Nuclear Import of Histone Deacetylase 5 by Requisite Nuclear Localization Signal Phosphorylation. *Mol Cell Proteomics* 2010. <https://doi.org/10.1074/mcp.m110.004317>.
- [152] Backs J, Backs T, Bezprozvannaya S, McKinsey TA, Olson EN. Histone deacetylase 5 acquires calcium/calmodulin-dependent kinase II responsiveness by oligomerization with histone deacetylase 4. *Mol Cell Biol* 2008;28:3437–45. <https://doi.org/10.1128/MCB.01611-07>.
- [153] Walkinshaw DR, Weist R, Xiao L, Yan K, Kim GW, Yang XJ. Dephosphorylation at a conserved sp motif governs camp sensitivity and nuclear localization of class iia histone deacetylases. *J Biol Chem* 2013. <https://doi.org/10.1074/jbc.M112.445668>.
- [154] Jhun BS, Zhao J, Jin ZG, Wong C, Ha CH, Wang W, et al. PKA phosphorylates histone deacetylase 5 and prevents its nuclear export, leading to the inhibition of gene transcription and cardiomyocyte hypertrophy. *Proc Natl Acad Sci* 2010. <https://doi.org/10.1073/pnas.1000462107>.

- [155] Gregoire S, Yang X-J. Association with Class IIa Histone Deacetylases Upregulates the Sumoylation of MEF2 Transcription Factors. *Mol Cell Biol* 2006. <https://doi.org/10.1128/mcb.26.8.3335.2006>.
- [156] Potthoff MJ, Wu H, Arnold MA, Shelton JM, Backs J, McAnally J, et al. Histone deacetylase degradation and MEF2 activation promote the formation of slow-twitch myofibers. *J Clin Invest* 2007. <https://doi.org/10.1172/JCI31960>.
- [157] Mai A, Rotili D, Valente S, Kazantsev A. Histone Deacetylase Inhibitors and Neurodegenerative Disorders: Holding the Promise. *Curr Pharm Des* 2009. <https://doi.org/10.2174/138161209789649349>.
- [158] Ziemka-Nalecz M, Jaworska J, Sypecka J, Zalewska T, Ziemka-Nalecz M, Zalewska T. Histone Deacetylase Inhibitors: A Therapeutic Key in Neurological Disorders? *J Neuropathol Exp Neurol* 2018;77:855–70. <https://doi.org/10.1093/jnen/nly073>.
- [159] Micelli C, Rastelli G. Histone deacetylases: Structural determinants of inhibitor selectivity. *Drug Discov Today* 2015. <https://doi.org/10.1016/j.drudis.2015.01.007>.
- [160] Xu K, Dai X-LL, Huang H-CC, Jiang Z-FF. Targeting HDACs: A Promising Therapy for Alzheimer's Disease. *Oxid Med Cell Longev* 2011. <https://doi.org/10.1155/2011/143269>.
- [161] Li Z, Zhu WG. Targeting histone deacetylases for cancer therapy: From molecular mechanisms to clinical implications. *Int J Biol Sci* 2014. <https://doi.org/10.7150/ijbs.9067>.
- [162] Jacob C, Christen CN, Pereira JA, Somandin C, Baggiolini A, Lötscher P, et al. HDAC1 and HDAC2 control the transcriptional program of myelination and the survival of Schwann cells. *Nat Neurosci* 2011. <https://doi.org/10.1038/nn.2762>.
- [163] Lebrun-Julien F, Suter U. Combined HDAC1 and HDAC2 Depletion Promotes Retinal Ganglion Cell Survival After Injury Through Reduction of p53 Target Gene Expression.

- ASN Neuro 2015. <https://doi.org/10.1177/1759091415593066>.
- [164] Choong CJ, Sasaki T, Hayakawa H, Yasuda T, Baba K, Hirata Y, et al. A novel histone deacetylase 1 and 2 isoform-specific inhibitor alleviates experimental Parkinson's disease. *Neurobiol Aging* 2016. <https://doi.org/10.1016/j.neurobiolaging.2015.10.001>.
- [165] Bardai FH, Price V, Zaayman M, Wang L, D'Mello SR. Histone deacetylase-1 (HDAC1) is a molecular switch between neuronal survival and death. *J Biol Chem* 2012. <https://doi.org/10.1074/jbc.M112.394544>.
- [166] Jamal I, Kumar V, Vatsa N, Shekhar S, Singh BK, Sharma A, et al. Rescue of altered HDAC activity recovers behavioural abnormalities in a mouse model of Angelman syndrome. *Neurobiol Dis* 2017. <https://doi.org/10.1016/j.nbd.2017.05.010>.
- [167] Contreras PS, Gonzalez-Zuñiga M, González-Hódar L, Yáñez MJ, Dulcey A, Marugan J, et al. Neuronal gene repression in Niemann–Pick type C models is mediated by the c-Abl/HDAC2 signaling pathway. *Biochim Biophys Acta - Gene Regul Mech* 2016;1859:269–79. <https://doi.org/https://doi.org/10.1016/j.bbagr.2015.11.006>.
- [168] Guan JS, Haggarty SJ, Giacometti E, Dannenberg JH, Joseph N, Gao J, et al. HDAC2 negatively regulates memory formation and synaptic plasticity. *Nature* 2009. <https://doi.org/10.1038/nature07925>.
- [169] Knutson SK, Chyla BJ, Amann JM, Bhaskara S, Huppert SS, Hiebert SW. Liver-specific deletion of histone deacetylase 3 disrupts metabolic transcriptional networks. *EMBO J* 2008. <https://doi.org/10.1038/emboj.2008.51>.
- [170] Louis Sam Titus ASC, Yusuff T, Cassar M, Thomas E, Kretzschmar D, D'Mello SR. Reduced Expression of Foxp1 as a Contributing Factor in Huntington's Disease. *J Neurosci* 2017. <https://doi.org/10.1523/JNEUROSCI.3612-16.2017>.
- [171] Langley B, D'Annibale MA, Suh K, Ayoub I, Tolhurst A, Bastan B, et al. Pulse Inhibition of Histone Deacetylases Induces Complete Resistance to Oxidative Death in

- Cortical Neurons without Toxicity and Reveals a Role for Cytoplasmic p21^{and}waf1/cip1^{and} in Cell Cycle-Independent Neuroprotection. *J Neurosci* 2008;28:163 LP – 176. <https://doi.org/10.1523/JNEUROSCI.3200-07.2008>.
- [172] Harms C, Albrecht K, Harms U, Seidel K, Hauck L, Baldinger T, et al. Phosphatidylinositol 3-Akt-Kinase-Dependent Phosphorylation of p21^{and}Waf1/Cip1^{and} as a Novel Mechanism of Neuroprotection by Glucocorticoids. *J Neurosci* 2007;27:4562 LP – 4571. <https://doi.org/10.1523/JNEUROSCI.5110-06.2007>.
- [173] Krishna K, Behnisch T, Sajikumar S. Inhibition of Histone Deacetylase 3 Restores amyloid- β Oligomer-Induced Plasticity Deficit in Hippocampal CA1 Pyramidal Neurons. *J Alzheimer's Dis* 2016. <https://doi.org/10.3233/JAD-150838>.
- [174] Han KA, Shin WH, Jung S, Seol W, Seo H, Ko CM, et al. Leucine-rich repeat kinase 2 exacerbates neuronal cytotoxicity through phosphorylation of histone deacetylase 3 and histone deacetylation. *Hum Mol Genet* 2017. <https://doi.org/10.1093/hmg/ddw363>.
- [175] Mata IF, Wedemeyer WJ, Farrer MJ, Taylor JP, Gallo KA. LRRK2 in Parkinson's disease: protein domains and functional insights. *Trends Neurosci* 2006. <https://doi.org/10.1016/j.tins.2006.03.006>.
- [176] Janczura KJ, Volmar C-H, Sartor GC, Rao SJ, Ricciardi NR, Lambert G, et al. Inhibition of HDAC3 reverses Alzheimer's disease-related pathologies in vitro and in the 3xTg-AD mouse model. *Proc Natl Acad Sci* 2018. <https://doi.org/10.1073/pnas.1805436115>.
- [177] Bolger TA. Intracellular Trafficking of Histone Deacetylase 4 Regulates Neuronal Cell Death. *J Neurosci* 2005. <https://doi.org/10.1523/jneurosci.1826-05.2005>.
- [178] Wu Q, Yang X, Zhang L, Zhang Y, Feng L. Nuclear Accumulation of Histone Deacetylase 4 (HDAC4) Exerts Neurotoxicity in Models of Parkinson's Disease. *Mol Neurobiol* 2017. <https://doi.org/10.1007/s12035-016-0199-2>.

- [179] Dompierre JP, Godin JD, Charrin BC, Cordelieres FP, King SJ, Humbert S, et al. Histone Deacetylase 6 Inhibition Compensates for the Transport Deficit in Huntington's Disease by Increasing Tubulin Acetylation. *J Neurosci* 2007. <https://doi.org/10.1523/JNEUROSCI.0037-07.2007>.
- [180] Chen S, Owens GC, Makarenkova H, Edelman DB. HDAC6 Regulates mitochondrial transport in hippocampal neurons. *PLoS One* 2010. <https://doi.org/10.1371/journal.pone.0010848>.
- [181] Kim C, Choi H, Jung ES, Lee W, Oh S, Jeon NL, et al. HDAC6 inhibitor blocks amyloid beta-induced impairment of mitochondrial transport in hippocampal neurons. *PLoS One* 2012. <https://doi.org/10.1371/journal.pone.0042983>.
- [182] Jaffrey SR, Ratan RR, Rivieccio MA, D'Annibale MA, McLaughlin K, Langley B, et al. HDAC6 is a target for protection and regeneration following injury in the nervous system. *Proc Natl Acad Sci* 2009. <https://doi.org/10.1073/pnas.0907935106>.
- [183] Benoy V, Vanden Berghe P, Jarpe M, Van Damme P, Robberecht W, Van Den Bosch L. Development of Improved HDAC6 Inhibitors as Pharmacological Therapy for Axonal Charcot–Marie–Tooth Disease. *Neurotherapeutics* 2017. <https://doi.org/10.1007/s13311-016-0501-z>.
- [184] Guedes-Dias P, de Proença J, Soares TR, Leitão-Rocha A, Pinho BR, Duchen MR, et al. HDAC6 inhibition induces mitochondrial fusion, autophagic flux and reduces diffuse mutant huntingtin in striatal neurons. *Biochim Biophys Acta - Mol Basis Dis* 2015. <https://doi.org/10.1016/j.bbadis.2015.08.012>.
- [185] Zhang L, Liu C, Wu J, Tao JJ, Sui XL, Yao ZG, et al. Tubastatin A/ACY-1215 improves cognition in Alzheimer's disease transgenic mice. *J Alzheimer's Dis* 2014;41:1193–205. <https://doi.org/10.3233/JAD-140066>.
- [186] Wang XX, Wan RZ, Liu ZP. Recent advances in the discovery of potent and selective

- HDAC6 inhibitors. *Eur J Med Chem* 2018.
<https://doi.org/10.1016/j.ejmech.2017.10.040>.
- [187] Bahari-Javan S, Sananbenesi F, Fischer A. Histone-acetylation: A link between Alzheimer's disease and post-traumatic stress disorder? *Front Neurosci* 2014.
<https://doi.org/10.3389/fnins.2014.00160>.
- [188] Lu X, Wang L, Yu C, Yu D, Yu G. Histone acetylation modifiers in the pathogenesis of alzheimer's disease. *Front Cell Neurosci* 2015.
<https://doi.org/10.3389/fncel.2015.00226>.
- [189] Mahady L, Nadeem M, Malek-Ahmadi M, Chen K, Perez SE, Mufson EJ. Frontal Cortex Epigenetic Dysregulation during the Progression of Alzheimer's Disease. *J Alzheimer's Dis* 2018. <https://doi.org/10.3233/JAD-171032>.
- [190] Chuang DM, Leng Y, Marinova Z, Kim HJ, Chiu CT. Multiple roles of HDAC inhibition in neurodegenerative conditions. *Trends Neurosci* 2009.
<https://doi.org/10.1016/j.tins.2009.06.002>.
- [191] Walker MP, Laferla FM, Oddo SS, Brewer GJ. Reversible epigenetic histone modifications and Bdnf expression in neurons with aging and from a mouse model of Alzheimer's disease. *Age (Omaha)* 2013. <https://doi.org/10.1007/s11357-011-9375-5>.
- [192] Jeong H, Shin S, Lee JS, Lee SH, Baik JH, Lim S, et al. Pan-HDAC Inhibitors Promote Tau Aggregation by Increasing the Level of Acetylated Tau. *Int J Mol Sci* 2019, Vol 20, Page 4283 2019;20:4283. <https://doi.org/10.3390/IJMS20174283>.
- [193] Fischer A, Sananbenesi F, Wang X, Dobbin M, Tsai LH. Recovery of learning and memory is associated with chromatin remodelling. *Nature* 2007.
<https://doi.org/10.1038/nature05772>.
- [194] Patrick GN, Zukerberg L, Nikolic M, De La Monte S, Dikkes P, Tsai LH. Conversion of p35 to p25 deregulates Cdk5 activity and promotes neurodegeneration. *Nature* 1999.

<https://doi.org/10.1038/45159>.

- [195] Cruz JC, Kim D, Moy LY, Dobbin MM, Sun X, Bronson RT, et al. p25/cyclin-dependent kinase 5 induces production and intraneuronal accumulation of amyloid beta in vivo. *J Neurosci* 2006;26:10536–41. <https://doi.org/10.1523/JNEUROSCI.3133-06.2006>.
- [196] Fischer A, Sananbenesi F, Pang PT, Lu B, Tsai LH. Opposing roles of transient and prolonged expression of p25 in synaptic plasticity and hippocampus-dependent memory. *Neuron* 2005. <https://doi.org/10.1016/j.neuron.2005.10.033>.
- [197] Ricobaraza A, Cuadrado-Tejedor M, Pérez-Mediavilla A, Frechilla D, Del Río J, García-Osta A. Phenylbutyrate ameliorates cognitive deficit and reduces tau pathology in an alzheimer's disease mouse model. *Neuropsychopharmacology* 2009. <https://doi.org/10.1038/npp.2008.229>.
- [198] Fischer A, Sananbenesi F, Mungenast A, Tsai LH. Targeting the correct HDAC(s) to treat cognitive disorders. *Trends Pharmacol Sci* 2010. <https://doi.org/10.1016/j.tips.2010.09.003>.
- [199] Kilgore M, Miller CA, Fass DM, Hennig KM, Haggarty SJ, Sweatt JD, et al. Inhibitors of class 1 histone deacetylases reverse contextual memory deficits in a mouse model of alzheimer's disease. *Neuropsychopharmacology* 2010. <https://doi.org/10.1038/npp.2009.197>.
- [200] Ricobaraza A, Cuadrado-Tejedor M, Marco S, Pérez-Otaño I, García-Osta A. Phenylbutyrate rescues dendritic spine loss associated with memory deficits in a mouse model of Alzheimer disease. *Hippocampus* 2012. <https://doi.org/10.1002/hipo.20883>.
- [201] Sung YM, Lee T, Yoon H, DiBattista AM, Song JM, Sohn Y, et al. Mercaptoacetamide-based class II HDAC inhibitor lowers A β levels and improves learning and memory in a mouse model of Alzheimer's disease. *Exp Neurol* 2013. <https://doi.org/10.1016/j.expneurol.2012.10.005>.

- [202] Govindarajan N, Rao P, Burkhardt S, Sananbenesi F, Schlüter OM, Bradke F, et al. Reducing HDAC6 ameliorates cognitive deficits in a mouse model for Alzheimer's disease. *EMBO Mol Med* 2013. <https://doi.org/10.1002/emmm.201201923>.
- [203] Mahady L, Nadeem M, Malek-Ahmadi M, Chen K, Perez SE, Mufson EJ. HDAC2 dysregulation in the nucleus basalis of Meynert during the progression of Alzheimer's disease. *Neuropathol Appl Neurobiol* 2019;45:380–97. <https://doi.org/10.1111/NAN.12518>.
- [204] Wang Y, Jia A, Ma W. Dexmedetomidine attenuates the toxicity of β -amyloid on neurons and astrocytes by increasing BDNF production under the regulation of HDAC2 and HDAC5. *Mol Med Rep* 2019. <https://doi.org/10.3892/mmr.2018.9694>.
- [205] Wei Z, Meng X, El Fatimy R, Sun B, Mai D, Zhang J, et al. Environmental enrichment prevents A β oligomer-induced synaptic dysfunction through mirna-132 and hdac3 signaling pathways. *Neurobiol Dis* 2020. <https://doi.org/10.1016/j.nbd.2019.104617>.
- [206] Li X, Zhan Z, Zhang J, Zhou F, An L. beta-Hydroxybutyrate Ameliorates Abeta-Induced Downregulation of TrkA Expression by Inhibiting HDAC1/3 in SH-SY5Y Cells. *Am J Alzheimers Dis Other Demen* 2020;35:1533317519883496. <https://doi.org/10.1177/1533317519883496>.
- [207] Huang H-J, Huang H-Y, Hsieh-Li HM. MGCD0103, a selective histone deacetylase inhibitor, coameliorates oligomeric Abeta25-35 -induced anxiety and cognitive deficits in a mouse model. *CNS Neurosci Ther* 2019;25:175–86. <https://doi.org/10.1111/cns.13029>.
- [208] Sharma S, Taliyan R. Targeting Histone Deacetylases: A Novel Approach in Parkinson's Disease. *Parkinsons Dis* 2015. <https://doi.org/10.1155/2015/303294>.
- [209] Guerrero E, Vasudevaraju P, Hegde ML, Britton GB, Rao KS. Recent advances in α -synuclein functions, advanced glycation, and toxicity: implications for Parkinson's

- disease. *Mol Neurobiol* 2013. <https://doi.org/10.1007/s12035-012-8328-z>.
- [210] Hegarty S V., Sullivan AM, O’Keeffe GW. The epigenome as a therapeutic target for Parkinson’s disease. *Neural Regen Res* 2016. <https://doi.org/10.4103/1673-5374.194803>.
- [211] Wu X, Chen PS, Dallas S, Wilson B, Block ML, Wang CC, et al. Histone deacetylase inhibitors up-regulate astrocyte GDNF and BDNF gene transcription and protect dopaminergic neurons. *Int J Neuropsychopharmacol* 2008. <https://doi.org/10.1017/S1461145708009024>.
- [212] Chen SHL, Wu HM, Ossola B, Schendzielorz N, Wilson BC, Chu CH, et al. Suberoylanilide hydroxamic acid, a histone deacetylase inhibitor, protects dopaminergic neurons from neurotoxin-induced damage. *Br J Pharmacol* 2012. <https://doi.org/10.1111/j.1476-5381.2011.01575.x>.
- [213] Ximenes JCM, Neves KRT, Leal LKAM, do Carmo MRS, Brito GA de C, Naffah-Mazzacoratti M da G, et al. Valproic Acid Neuroprotection in the 6-OHDA Model of Parkinson’s Disease Is Possibly Related to Its Anti-Inflammatory and HDAC Inhibitory Properties. *J Neurodegener Dis* 2015. <https://doi.org/10.1155/2015/313702>.
- [214] Kidd SK, Schneider JS. Protection of dopaminergic cells from MPP+-mediated toxicity by histone deacetylase inhibition. *Brain Res* 2010. <https://doi.org/10.1016/j.brainres.2010.07.041>.
- [215] Sharma S, Taliyan R, Singh S. Beneficial effects of sodium butyrate in 6-OHDA induced neurotoxicity and behavioral abnormalities: Modulation of histone deacetylase activity. *Behav Brain Res* 2015. <https://doi.org/10.1016/j.bbr.2015.05.052>.
- [216] St. Laurent R, O’Brien LM, Ahmad ST. Sodium butyrate improves locomotor impairment and early mortality in a rotenone-induced *Drosophila* model of Parkinson’s disease. *Neuroscience* 2013. <https://doi.org/10.1016/j.neuroscience.2013.04.037>.

- [217] Gardian G, Yang L, Cleren C, Calingasan NY, Klivenyi P, Beal MF. Neuroprotective effects of phenylbutyrate against MPTP neurotoxicity. *NeuroMolecular Med* 2004;5:235–41. <https://doi.org/10.1385/NMM:5:3:235>.
- [218] Zhou W, Bercury K, Cumiskey J, Luong N, Lebin J, Freed CR. Phenylbutyrate up-regulates the DJ-1 protein and protects neurons in cell culture and in animal models of Parkinson disease. *J Biol Chem* 2011. <https://doi.org/10.1074/jbc.M110.211029>.
- [219] Canet-Avilés RM, Wilson MA, Miller DW, Ahmad R, McLendon C, Bandyopadhyay S, et al. The Parkinson's disease DJ-1 is neuroprotective due to cysteine-sulfinic acid-driven mitochondrial localization. *Proc Natl Acad Sci U S A* 2004. <https://doi.org/10.1073/pnas.0402959101>.
- [220] Chen PS, Wang CC, Bortner CD, Peng GS, Wu X, Pang H, et al. Valproic acid and other histone deacetylase inhibitors induce microglial apoptosis and attenuate lipopolysaccharide-induced dopaminergic neurotoxicity. *Neuroscience* 2007. <https://doi.org/10.1016/j.neuroscience.2007.06.053>.
- [221] Sanderson L, Taylor GW, Aboagye EO, Alao JP, Latigo JR, Coombes RC, et al. Plasma pharmacokinetics and metabolism of the histone deacetylase inhibitor trichostatin A after intraperitoneal administration to mice. *Drug Metab Dispos* 2004. <https://doi.org/10.1124/dmd.104.000638>.
- [222] Wang Y, Wang X, Liu L, Wang X. HDAC inhibitor trichostatin A-inhibited survival of dopaminergic neuronal cells. *Neurosci Lett* 2009. <https://doi.org/10.1016/j.neulet.2009.10.037>.
- [223] Li G, Jiang H, Chang M, Xie H, Hu L. HDAC6 α -tubulin deacetylase: A potential therapeutic target in neurodegenerative diseases. *J Neurol Sci* 2011. <https://doi.org/10.1016/j.jns.2011.02.017>.
- [224] Seigneurin-Berny D, Verdel A, Curtet S, Lemercier C, Garin J, Rousseaux S, et al.

- Identification of Components of the Murine Histone Deacetylase 6 Complex: Link between Acetylation and Ubiquitination Signaling Pathways. *Mol Cell Biol* 2001. <https://doi.org/10.1128/mcb.21.23.8035-8044.2001>.
- [225] Luxton GWG, Gundersen GG. HDAC6-Pack: Cortactin Acetylation Joins the Brew. *Dev Cell* 2007. <https://doi.org/10.1016/j.devcel.2007.07.014>.
- [226] Valenzuela-Fernández A, Cabrero JR, Serrador JM, Sánchez-Madrid F. HDAC6: a key regulator of cytoskeleton, cell migration and cell-cell interactions. *Trends Cell Biol* 2008. <https://doi.org/10.1016/j.tcb.2008.04.003>.
- [227] Du G, Jiao R. To prevent neurodegeneration: HDAC6 uses different strategies for different challenges. *Commun Integr Biol* 2011. <https://doi.org/10.4161/cib.4.2.14272>.
- [228] Du G, Liu X, Chen X, Song M, Yan Y, Jiao R, et al. Drosophila histone deacetylase 6 protects dopaminergic neurons against α -synuclein toxicity by promoting inclusion formation. *Mol Biol Cell* 2010. <https://doi.org/10.1091/mbc.E10-03-0200>.
- [229] Godena VK, Brookes-Hocking N, Moller A, Shaw G, Oswald M, Sancho RM, et al. Increasing microtubule acetylation rescues axonal transport and locomotor deficits caused by LRRK2 Roc-COR domain mutations. *Nat Commun* 2014. <https://doi.org/10.1038/ncomms6245>.
- [230] Kim T, Song S, Park Y, Kang S, Seo H. HDAC Inhibition by Valproic Acid Induces Neuroprotection and Improvement of PD-like Behaviors in LRRK2 R1441G Transgenic Mice. *Exp Neurobiol* 2019;28:504. <https://doi.org/10.5607/EN.2019.28.4.504>.
- [231] Hsu S-W, Hsu P-C, Chang W-S, Yu C-C, Wang Y-C, Yang J-S, et al. Protective effects of valproic acid on 6-hydroxydopamine-induced neuroinjury. *Environ Toxicol* 2020. <https://doi.org/10.1002/tox.22920>.
- [232] Harrison IF, Powell NM, Dexter DT. The histone deacetylase inhibitor nicotinamide exacerbates neurodegeneration in the lactacystin rat model of Parkinson's disease. *J*

- Neurochem 2019. <https://doi.org/10.1111/jnc.14599>.
- [233] Riccio A. Dynamic epigenetic regulation in neurons: Enzymes, stimuli and signaling pathways. *Nat Neurosci* 2010. <https://doi.org/10.1038/nn.2671>.
- [234] Hsieh J, Nakashima K, Kuwabara T, Mejia E, Gage FH. Histone deacetylase inhibition-mediated neuronal differentiation of multipotent adult neural progenitor cells. *Proc Natl Acad Sci U S A* 2004. <https://doi.org/10.1073/pnas.0407643101>.
- [235] Xylaki M, Atzler B, Outeiro TF. Epigenetics of the Synapse in Neurodegeneration. *Curr Neurol Neurosci Rep* 2019. <https://doi.org/10.1007/s11910-019-0995-y>.
- [236] Stilling RM, Rönicke R, Benito E, Urbanke H, Capece V, Burkhardt S, et al. K-Lysine acetyltransferase 2a regulates a hippocampal gene expression network linked to memory formation. *EMBO J* 2014. <https://doi.org/10.15252/emj.201487870>.
- [237] Xu S, Wilf R, Menon T, Panikker P, Sarthi J, Elefant F. Epigenetic control of learning and memory in drosophila by Tip60 HAT action. *Genetics* 2014. <https://doi.org/10.1534/genetics.114.171660>.
- [238] Peng L, Zhu M, Yang Y, Weng Y, Zou W, Zhu X, et al. Neonatal Lipopolysaccharide Challenge Induces Long-lasting Spatial Cognitive Impairment and Dysregulation of Hippocampal Histone Acetylation in Mice. *Neuroscience* 2019. <https://doi.org/10.1016/j.neuroscience.2018.12.001>.
- [239] Fuller NO, Pirone A, Lynch BA, Hewitt MC, Quinton MS, McKee TD, et al. CoREST Complex-Selective Histone Deacetylase Inhibitors Show Prosynaptic Effects and an Improved Safety Profile to Enable Treatment of Synaptopathies. *ACS Chem Neurosci* 2019. <https://doi.org/10.1021/acchemneuro.8b00620>.
- [240] Joksimovic SM, Osuru HP, Oklopčić A, Beenhakker MP, Jevtovic-Todorovic V, Todorovic SM. Histone deacetylase inhibitor entinostat (MS-275) restores anesthesia-induced alteration of inhibitory synaptic transmission in the developing rat

- hippocampus. *Mol Neurobiol* 2018. <https://doi.org/10.1007/s12035-017-0735-8>.
- [241] Cuadrado-Tejedor M, Garcia-Barroso C, Sánchez-Arias JA, Rabal O, Pérez-González M, Mederos S, et al. A First-in-Class Small-Molecule that Acts as a Dual Inhibitor of HDAC and PDE5 and that Rescues Hippocampal Synaptic Impairment in Alzheimer's Disease Mice. *Neuropsychopharmacology* 2017. <https://doi.org/10.1038/npp.2016.163>.
- [242] Cuadrado-Tejedor M, Garcia-Barroso C, Sanchez-Arias J, Mederos S, Rabal O, Ugarte A, et al. Concomitant histone deacetylase and phosphodiesterase 5 inhibition synergistically prevents the disruption in synaptic plasticity and it reverses cognitive impairment in a mouse model of Alzheimer's disease. *Clin Epigenetics* 2015. <https://doi.org/10.1186/s13148-015-0142-9>.
- [243] Gonzalez-Zuñiga M, Contreras PS, Estrada LD, Chamorro D, Villagra A, Zanlungo S, et al. C-abl stabilizes HDAC2 levels by tyrosine phosphorylation repressing neuronal gene expression in alzheimer's disease. *Mol Cell* 2014. <https://doi.org/10.1016/j.molcel.2014.08.013>.
- [244] Yamakawa H, Cheng J, Penney J, Gao F, Rueda R, Wang J, et al. The Transcription Factor Sp3 Cooperates with HDAC2 to Regulate Synaptic Function and Plasticity in Neurons. *Cell Rep* 2017. <https://doi.org/10.1016/j.celrep.2017.07.044>.
- [245] Figurov A, Pozzo-Miller LD, Olafsson P, Wang T, Lu B. Regulation of synaptic responses to high-frequency stimulation and LTP by neurotrophins in the hippocampus. *Nature* 1996. <https://doi.org/10.1038/381706a0>.
- [246] Huang EJ, Reichardt LF. Neurotrophins: Roles in Neuronal Development and Function. *Annu Rev Neurosci* 2001. <https://doi.org/10.1146/annurev.neuro.24.1.677>.
- [247] Connor B, Young D, Yan Q, Faull RLM, Synek B, Dragunow M. Brain-derived neurotrophic factor is reduced in Alzheimer's disease. *Mol Brain Res* 1997. [https://doi.org/10.1016/S0169-328X\(97\)00125-3](https://doi.org/10.1016/S0169-328X(97)00125-3).

- [248] Kim J, Lee S, Choi BR, Yang H, Hwang Y, Park JHY, et al. Sulforaphane epigenetically enhances neuronal BDNF expression and TrkB signaling pathways. *Mol Nutr Food Res* 2017. <https://doi.org/10.1002/mnfr.201600194>.
- [249] Singh P, Thakur MK. Histone Deacetylase 2 Inhibition Attenuates Downregulation of Hippocampal Plasticity Gene Expression during Aging. *Mol Neurobiol* 2018. <https://doi.org/10.1007/s12035-017-0490-x>.
- [250] Drissi I, Deschamps C, Fouquet G, Alary R, Peineau S, Gosset P, et al. Memory and plasticity impairment after binge drinking in adolescent rat hippocampus: GluN2A/GluN2B NMDA receptor subunits imbalance through HDAC2. *Addict Biol* 2019:e12760. <https://doi.org/10.1111/adb.12760>.
- [251] Luo F, Hu Y, Zhao W, Zuo Z, Yu Q, Liu Z, et al. Maternal exposure of rats to isoflurane during late pregnancy impairs spatial learning and memory in the offspring by Up-Regulating the expression of histone deacetylase 2. *PLoS One* 2016. <https://doi.org/10.1371/journal.pone.0160826>.
- [252] Authement ME, Langlois LD, Kassis H, Gouty S, Dacher M, Shepard RD, et al. Morphine-induced synaptic plasticity in the VTA is reversed by HDAC inhibition. *J Neurophysiol* 2016. <https://doi.org/10.1152/jn.00238.2016>.
- [253] Malvaez M, McQuown SC, Rogge GA, Astarabadi M, Jacques V, Carreiro S, et al. HDAC3-selective inhibitor enhances extinction of cocaine-seeking behavior in a persistent manner. *Proc Natl Acad Sci U S A* 2013. <https://doi.org/10.1073/pnas.1213364110>.
- [254] Whittle N, Schmuckermair C, Gunduz Cinar O, Hauschild M, Ferraguti F, Holmes A, et al. Deep brain stimulation, histone deacetylase inhibitors and glutamatergic drugs rescue resistance to fear extinction in a genetic mouse model. *Neuropharmacology* 2013. <https://doi.org/10.1016/j.neuropharm.2012.06.001>.

- [255] Fujita Y, Morinobu S, Takei S, Fuchikami M, Matsumoto T, Yamamoto S, et al. Vorinostat, a histone deacetylase inhibitor, facilitates fear extinction and enhances expression of the hippocampal NR2B-containing NMDA receptor gene. *J Psychiatr Res* 2012. <https://doi.org/10.1016/j.jpsychires.2012.01.026>.
- [256] Shivakumar M, Subbanna S, Joshi V, Basavarajappa BS. Postnatal Ethanol Exposure Activates HDAC-Mediated Histone Deacetylation, Impairs Synaptic Plasticity Gene Expression and Behavior in Mice. *Int J Neuropsychopharmacol* 2020. <https://doi.org/10.1093/ijnp/pyaa017>.
- [257] Muñoz-Cobo I, Erburu MM, Zwergel C, Cirilli R, Mai A, Valente S, et al. Nucleocytoplasmic export of HDAC5 and SIRT2 downregulation: two epigenetic mechanisms by which antidepressants enhance synaptic plasticity markers. *Psychopharmacology (Berl)* 2018. <https://doi.org/10.1007/s00213-018-4975-8>.
- [258] Erburu M, Muñoz-Cobo I, Domínguez-Andrés J, Beltran E, Suzuki T, Mai A, et al. Chronic stress and antidepressant induced changes in Hdac5 and Sirt2 affect synaptic plasticity. *Eur Neuropsychopharmacol* 2015. <https://doi.org/10.1016/j.euroneuro.2015.08.016>.
- [259] Jaworska J, Ziemka-Nalecz M, Zalewska T. Histone deacetylases 1 and 2 are required for brain development. *Int J Dev Biol* 2015. <https://doi.org/10.1387/ijdb.150071tz>.
- [260] Montgomery RL, Hsieh J, Barbosa AC, Richardson JA, Olson EN. Histone deacetylases 1 and 2 control the progression of neural precursors to neurons during brain development. *Proc Natl Acad Sci U S A* 2009. <https://doi.org/10.1073/pnas.0902750106>.
- [261] Hagelkruys A, Lagger S, Krahmer J, Leopoldi A, Artaker M, Pusch O, et al. A single allele of Hdac2 but not Hdac1 is sufficient for normal mouse brain development in the absence of its paralog. *Dev* 2014. <https://doi.org/10.1242/dev.100487>.

- [262] Tang T, Zhang Y, Wang Y, Cai Z, Lu Z, Li L, et al. HDAC1 and HDAC2 Regulate Intermediate Progenitor Positioning to Safeguard Neocortical Development. *Neuron* 2019. <https://doi.org/10.1016/j.neuron.2019.01.007>.
- [263] Yoo JYJ, Larouche M, Goldowitz D. The expression of HDAC1 and HDAC2 during cerebellar cortical development. *Cerebellum* 2013. <https://doi.org/10.1007/s12311-013-0459-x>.
- [264] Norwood J, Franklin JM, Sharma D, D'Mello SR. Histone deacetylase 3 is necessary for proper brain development. *J Biol Chem* 2014. <https://doi.org/10.1074/jbc.M114.576397>.
- [265] Jiang Y, Hsieh J. HDAC3 controls gap 2/mitosis progression in adult neural stem/progenitor cells by regulating CDK1 levels. *Proc Natl Acad Sci U S A* 2014. <https://doi.org/10.1073/pnas.1411939111>.
- [266] Castelo-Branco G, Lilja T, Wallenborg K, Falcão AM, Marques SC, Gracias A, et al. Neural stem cell differentiation is dictated by distinct actions of nuclear receptor corepressors and histone deacetylases. *Stem Cell Reports* 2014. <https://doi.org/10.1016/j.stemcr.2014.07.008>.
- [267] Sun GQ, Yu RT, Evans RM, Shi Y. Orphan nuclear receptor TLX recruits histone deacetylases to repress transcription and regulate neural stem cell proliferation. *Proc Natl Acad Sci U S A* 2007. <https://doi.org/10.1073/pnas.0704089104>.
- [268] Katayama S, Morii A, Makanga JO, Suzuki T, Miyata N, Inazu T. HDAC8 regulates neural differentiation through embryoid body formation in P19 cells. *Biochem Biophys Res Commun* 2018. <https://doi.org/10.1016/j.bbrc.2018.02.195>.
- [269] Deardorff MA, Porter NJ, Christianson DW. Structural aspects of HDAC8 mechanism and dysfunction in Cornelia de Lange syndrome spectrum disorders. *Protein Sci* 2016. <https://doi.org/10.1002/pro.3030>.

- [270] Brookes E, Riccio A. Location, location, location: nuclear structure regulates gene expression in neurons. *Curr Opin Neurobiol* 2019. <https://doi.org/10.1016/j.conb.2019.03.009>.
- [271] Majdzadeh N, Wang L, Morrison BE, Bassel-Duby R, Olson EN, D’Mello SR. HDAC4 inhibits cell-cycle progression and protects neurons from cell death. *Dev Neurobiol* 2008. <https://doi.org/10.1002/dneu.20637>.
- [272] Price V, Wang L, D’Mello SR. Conditional deletion of histone deacetylase-4 in the central nervous system has no major effect on brain architecture or neuronal viability. *J Neurosci Res* 2013. <https://doi.org/10.1002/jnr.23170>.
- [273] Le TN, Williams SR, Alaimo JT, Elsea SH. Genotype and phenotype correlation in 103 individuals with 2q37 deletion syndrome reveals incomplete penetrance and supports HDAC4 as the primary genetic contributor. *Am J Med Genet Part A* 2019. <https://doi.org/10.1002/ajmg.a.61089>.
- [274] Morrison BE, Majdzadeh N, Zhang X, Lyles A, Bassel-Duby R, Olson EN, et al. Neuroprotection by Histone Deacetylase-Related Protein. *Mol Cell Biol* 2006. <https://doi.org/10.1128/mcb.26.9.3550-3564.2006>.
- [275] Alchini R, Sato H, Matsumoto N, Shimogori T, Sugo N, Yamamoto N. Nucleocytoplasmic Shuttling of Histone Deacetylase 9 Controls Activity-Dependent Thalamocortical Axon Branching. *Sci Rep* 2017. <https://doi.org/10.1038/s41598-017-06243-7>.
- [276] Legube G, Trouche D. Regulating histone acetyltransferases and deacetylases. *EMBO Rep* 2003. <https://doi.org/10.1038/sj.embor.embor941>.
- [277] Tapia M, Wandosell F, Garrido JJ. Impaired function of hdac6 slows down axonal growth and interferes with axon initial segment development. *PLoS One* 2010. <https://doi.org/10.1371/journal.pone.0012908>.

- [278] Walsh ME, Bhattacharya A, Sataranatarajan K, Qaisar R, Sloane L, Rahman MM, et al. The histone deacetylase inhibitor butyrate improves metabolism and reduces muscle atrophy during aging. *Aging Cell* 2015. <https://doi.org/10.1111/ace1.12387>.
- [279] Uittenbogaard M, Brantner CA, Chiaramello A. Epigenetic modifiers promote mitochondrial biogenesis and oxidative metabolism leading to enhanced differentiation of neuroprogenitor cells. *Cell Death Dis* 2018. <https://doi.org/10.1038/s41419-018-0396-1>.
- [280] Tabeshmehr P, Husnain HK, Salmannejad M, Sani M, Hosseini SM, Khorraminejad Shirazi MH. Nicorandil potentiates sodium butyrate induced preconditioning of neurons and enhances their survival upon subsequent treatment with H₂O₂. *Transl Neurodegener* 2017. <https://doi.org/10.1186/s40035-017-0097-1>.
- [281] Kozikowski AP, Chen Y, Subhasish T, Lewin NE, Blumberg PM, Zhong Z, et al. Searching for disease modifiers - PKC activation and HDAC inhibition - A dual drug approach to Alzheimer's disease that decreases A β production while blocking oxidative stress. *ChemMedChem* 2009. <https://doi.org/10.1002/cmdc.200900045>.
- [282] Olson DE, Sleiman SF, Bourassa MW, Wagner FF, Gale JP, Zhang YL, et al. Hydroxamate-based histone deacetylase inhibitors can protect neurons from oxidative stress via a histone deacetylase-independent catalase-like mechanism. *Chem Biol* 2015. <https://doi.org/10.1016/j.chembiol.2015.03.014>.
- [283] Sleiman SF, Olson DE, Bourassa MW, Karuppagounder SS, Zhang YL, Gale J, et al. Hydroxamic acid-based histone deacetylase (HDAC) inhibitors can mediate neuroprotection independent of HDAC inhibition. *J Neurosci* 2014. <https://doi.org/10.1523/JNEUROSCI.1010-14.2014>.
- [284] Lee H, Park JR, Yang J, Kim E, Hong SH, Woo HM, et al. Nicotine inhibits the proliferation by upregulation of nitric oxide and increased HDAC1 in mouse neural stem

- cells. *Vitr Cell Dev Biol - Anim* 2014. <https://doi.org/10.1007/s11626-014-9763-0>.
- [285] Agudelo M, Gandhi N, Saiyed Z, Pichili V, Thangavel S, Khatavkar P, et al. Effects of alcohol on histone deacetylase 2 (HDAC2) and the neuroprotective role of trichostatin A (TSA). *Alcohol Clin Exp Res* 2011. <https://doi.org/10.1111/j.1530-0277.2011.01492.x>.
- [286] Sharma S, Taliyan R, Ramagiri S. Histone Deacetylase Inhibitor, Trichostatin A, Improves Learning and Memory in High-Fat Diet-Induced Cognitive Deficits in Mice. *J Mol Neurosci* 2015. <https://doi.org/10.1007/s12031-014-0461-x>.
- [287] Xu J, Shi J, Zhang J, Zhang Y. Vorinostat: A histone deacetylases (HDAC) inhibitor ameliorates traumatic brain injury by inducing iNOS/Nrf2/ARE pathway. *Folia Neuropathol* 2018. <https://doi.org/10.5114/fn.2018.78697>.
- [288] KV A, Madhana RM, JS IC, Lahkar M, Sinha S, Naidu VGM. Antidepressant activity of vorinostat is associated with amelioration of oxidative stress and inflammation in a corticosterone-induced chronic stress model in mice. *Behav Brain Res* 2018. <https://doi.org/10.1016/j.bbr.2018.02.009>.
- [289] Gaisina IN, Lee SH, Kaidery NA, Ben Aissa M, Ahuja M, Smirnova NN, et al. Activation of Nrf2 and Hypoxic Adaptive Response Contribute to Neuroprotection Elicited by Phenylhydroxamic Acid Selective HDAC6 Inhibitors. *ACS Chem Neurosci* 2018. <https://doi.org/10.1021/acchemneuro.7b00435>.
- [290] Breidert T, Callebert J, Heneka MT, Landreth G, Launay JM, Hirsch EC. Protective action of the peroxisome proliferator-activated receptor- γ agonist pioglitazone in a mouse model of Parkinson's disease. *J Neurochem* 2002. <https://doi.org/10.1046/j.1471-4159.2002.00990.x>.
- [291] Wang X, Wu X, Liu Q, Kong G, Zhou J, Jiang J, et al. Ketogenic Metabolism Inhibits Histone Deacetylase (HDAC) and Reduces Oxidative Stress After Spinal Cord Injury in

<https://doi.org/10.1016/J.NEUROSCIENCE.2017.09.056>.

- [292] Trüe O, Matthias P. Interplay between histone deacetylases and autophagy - From cancer therapy to neurodegeneration. *Immunol Cell Biol* 2012. <https://doi.org/10.1038/icb.2011.103>.
- [293] Jia H, Kast RJ, Steffan JS, Thomas EA. Selective histone deacetylase (HDAC) inhibition imparts beneficial effects in Huntington's disease mice: Implications for the ubiquitin-proteasomal and autophagy systems. *Hum Mol Genet* 2012. <https://doi.org/10.1093/hmg/dd3379>.
- [294] Perez M, Santa-Maria I, De Barreda EG, Zhu X, Cuadros R, Cabrero JR, et al. Tau - An inhibitor of deacetylase HDAC6 function. *J Neurochem* 2009. <https://doi.org/10.1111/j.1471-4159.2009.06102.x>.
- [295] Feng Q, Luo Y, Zhang XN, Yang XF, Hong XY, Sun DS, et al. MAPT/Tau accumulation represses autophagy flux by disrupting IST1-regulated ESCRT-III complex formation: a vicious cycle in Alzheimer neurodegeneration. *Autophagy* 2020. <https://doi.org/10.1080/15548627.2019.1633862>.
- [296] Wu W, Luo M, Li K, Dai Y, Yi H, Zhong Y, et al. Cholesterol derivatives induce dephosphorylation of the histone deacetylases Rpd3/HDAC1 to upregulate autophagy. *Autophagy* 2020. <https://doi.org/10.1080/15548627.2020.1725376>.
- [297] Durham BS, Grigg R, Wood IC. Inhibition of histone deacetylase 1 or 2 reduces induced cytokine expression in microglia through a protein synthesis independent mechanism. *J Neurochem* 2017. <https://doi.org/10.1111/jnc.14144>.
- [298] Faraco G, Pancani T, Formentini L, Mascagni P, Fossati G, Leoni F, et al. Pharmacological Inhibition of Histone Deacetylases by Suberoylanilide Hydroxamic Acid Specifically Alters Gene Expression and Reduces Ischemic Injury in the Mouse

- Brain. *Mol Pharmacol* 2006. <https://doi.org/10.1124/mol.106.027912>.
- [299] Faraco G, Pittelli M, Cavone L, Fossati S, Porcu M, Mascagni P, et al. Histone deacetylase (HDAC) inhibitors reduce the glial inflammatory response in vitro and in vivo. *Neurobiol Dis* 2009. <https://doi.org/10.1016/j.nbd.2009.07.019>.
- [300] Suuronen T, Huuskonen J, Pihlaja R, Kyrylenko S, Salminen A. Regulation of microglial inflammatory response by histone deacetylase inhibitors. *J Neurochem* 2003. <https://doi.org/10.1046/j.1471-4159.2003.02004.x>.
- [301] Marinova Z, Ren M, Wendland JR, Leng Y, Liang MH, Yasuda S, et al. Valproic acid induces functional heat-shock protein 70 via Class I histone deacetylase inhibition in cortical neurons: A potential role of Sp1 acetylation. *J Neurochem* 2009. <https://doi.org/10.1111/j.1471-4159.2009.06385.x>.
- [302] Chen S, Ye J, Chen X, Shi J, Wu W, Lin W, et al. Valproic acid attenuates traumatic spinal cord injury-induced inflammation via STAT1 and NF- κ B pathway dependent of HDAC3. *J Neuroinflammation* 2018. <https://doi.org/10.1186/s12974-018-1193-6>.
- [303] Patnala R, Arumugam T V., Gupta N, Dheen ST. HDAC Inhibitor Sodium Butyrate-Mediated Epigenetic Regulation Enhances Neuroprotective Function of Microglia During Ischemic Stroke. *Mol Neurobiol* 2017. <https://doi.org/10.1007/s12035-016-0149-z>.
- [304] Jaworska J, Zalewska T, Sypecka J, Ziemka-Nalecz M. Effect of the HDAC Inhibitor, Sodium Butyrate, on Neurogenesis in a Rat Model of Neonatal Hypoxia–Ischemia: Potential Mechanism of Action. *Mol Neurobiol* 2019. <https://doi.org/10.1007/s12035-019-1518-1>.
- [305] Chiechio S, Zammataro M, Morales ME, Busceti CL, Drago F, Gereau IV RW, et al. Epigenetic modulation of mGlu2 receptors by histone deacetylase inhibitors in the treatment of inflammatory pain. *Mol Pharmacol* 2009.

<https://doi.org/10.1124/mol.108.054346>.

- [306] Zhang B, West EJ, Van KC, Gurkoff GG, Zhou J, Zhang XM, et al. HDAC inhibitor increases histone H3 acetylation and reduces microglia inflammatory response following traumatic brain injury in rats. *Brain Res* 2008. <https://doi.org/10.1016/j.brainres.2008.05.085>.
- [307] Park MJ, Sohrabji F. The histone deacetylase inhibitor, sodium butyrate, exhibits neuroprotective effects for ischemic stroke in middle-aged female rats. *J Neuroinflammation* 2016. <https://doi.org/10.1186/s12974-016-0765-6>.
- [308] Seo J, Jo SA, Hwang S, Byun CJ, Lee HJ, Cho DH, et al. Trichostatin A epigenetically increases calpastatin expression and inhibits calpain activity and calcium-induced SH-SY5Y neuronal cell toxicity. *FEBS J* 2013. <https://doi.org/10.1111/febs.12572>.
- [309] Ren M, Leng Y, Jeong MR, Leeds PR, Chuang DM. Valproic acid reduces brain damage induced by transient focal cerebral ischemia in rats: Potential roles of histone deacetylase inhibition and heat shock protein induction. *J Neurochem* 2004. <https://doi.org/10.1111/j.1471-4159.2004.02406.x>.
- [310] Jia H, Wang Y, Morris CD, Jacques V, Gottesfeld JM, Rusche JR, et al. The effects of pharmacological inhibition of histone deacetylase 3 (HDAC3) in Huntington's disease mice. *PLoS One* 2016. <https://doi.org/10.1371/journal.pone.0152498>.
- [311] Minamiyama M, Katsuno M, Adachi H, Waza M, Sang C, Kobayashi Y, et al. Sodium butyrate ameliorates phenotypic expression in a transgenic mouse model of spinal and bulbar muscular atrophy. *Hum Mol Genet* 2004. <https://doi.org/10.1093/hmg/ddh131>.
- [312] Xiang C, Zhang S, Dong X, Ma S, Cong S. Transcriptional dysregulation and post-translational modifications in polyglutamine diseases: From pathogenesis to potential therapeutic strategies. *Front Mol Neurosci* 2018. <https://doi.org/10.3389/fnmol.2018.00153>.

- [313] Andreassi C, Angelozzi C, Tiziano FD, Vitali T, De Vincenzi E, Boninsegna A, et al. Phenylbutyrate increases SMN expression in vitro: Relevance for treatment of spinal muscular atrophy. *Eur J Hum Genet* 2004. <https://doi.org/10.1038/sj.ejhg.5201102>.
- [314] Boyault C, Sadoul K, Pabion M, Khochbin S. HDAC6, at the crossroads between cytoskeleton and cell signaling by acetylation and ubiquitination. *Oncogene* 2007. <https://doi.org/10.1038/sj.onc.1210614>.
- [315] Zhang ZY, Schluesener HJ. Oral administration of histone deacetylase inhibitor MS-275 Ameliorates neuroinflammation and cerebral amyloidosis and improves behavior in a mouse model. *J Neuropathol Exp Neurol* 2013. <https://doi.org/10.1097/NEN.0b013e318283114a>.
- [316] Zhang ZY, Schluesener HJ. Oral administration of histone deacetylase inhibitor MS-275 Ameliorates neuroinflammation and cerebral amyloidosis and improves behavior in a mouse model. *J Neuropathol Exp Neurol* 2013. <https://doi.org/10.1097/NEN.0b013e318283114a>.
- [317] Kontopoulos E, Parvin JD, Feany MB. α -synuclein acts in the nucleus to inhibit histone acetylation and promote neurotoxicity. *Hum Mol Genet* 2006. <https://doi.org/10.1093/hmg/ddl243>.
- [318] Cenik B, Sephton CF, Dewey CM, Xian X, Wei S, Yu K, et al. Suberoylanilide hydroxamic acid (vorinostat) up-regulates progranulin transcription: Rational therapeutic approach to frontotemporal dementia. *J Biol Chem* 2011. <https://doi.org/10.1074/jbc.M110.193433>.
- [319] H. S, P. W, J. T, L. C, J. L, D. H, et al. NRSF is an essential mediator for the neuroprotection of trichostatin A in the MPTP mouse model of Parkinson's disease. *Neuropharmacology* 2015. <https://doi.org/http://dx.doi.org/10.1016/j.neuropharm.2015.07.015>.

- [320] Yang W, Chauhan A, Mehta S, Mehta P, Gu F, Chauhan V. Trichostatin A increases the levels of plasma gelsolin and amyloid beta-protein in a transgenic mouse model of Alzheimer's disease. *Life Sci* 2014. <https://doi.org/10.1016/j.lfs.2014.01.064>.
- [321] Paiva I, Pinho R, Pavlou MA, Hennion M, Wales P, Schütz AL, et al. Sodium butyrate rescues dopaminergic cells from alpha-synuclein-induced transcriptional deregulation and DNA damage. *Hum Mol Genet* 2017. <https://doi.org/10.1093/hmg/ddx114>.
- [322] Govindarajan N, Agis-Balboa RC, Walter J, Sananbenesi F, Fischer A. Sodium butyrate improves memory function in an alzheimer's disease mouse model when administered at an advanced stage of disease progression. *J Alzheimer's Dis* 2011. <https://doi.org/10.3233/JAD-2011-110080>.
- [323] Liu H, Zhang JJ, Li X, Yang Y, Xie XF, Hu K. Post-occlusion administration of sodium butyrate attenuates cognitive impairment in a rat model of chronic cerebral hypoperfusion. *Pharmacol Biochem Behav* 2015. <https://doi.org/10.1016/j.pbb.2015.05.012>.
- [324] Roy A, Ghosh A, Jana A, Liu X, Brahmachari S, Gendelman HE, et al. Sodium phenylbutyrate controls neuroinflammatory and antioxidant activities and protects dopaminergic neurons in mouse models of Parkinson's disease. *PLoS One* 2012. <https://doi.org/10.1371/journal.pone.0038113>.
- [325] Monti B, Gatta V, Piretti F, Raffaelli SS, Virgili M, Contestabile A. Valproic acid is neuroprotective in the rotenone rat model of Parkinson's disease: Involvement of α -synuclein. *Neurotox Res* 2010. <https://doi.org/10.1007/s12640-009-9090-5>.
- [326] Kidd SK, Schneider JS. Protective effects of valproic acid on the nigrostriatal dopamine system in a 1-methyl-4-phenyl-1,2,3,6-tetrahydropyridine mouse model of Parkinson's disease. *Neuroscience* 2011. <https://doi.org/10.1016/j.neuroscience.2011.08.010>.
- [327] Pan T, Li X, Xie W, Jankovic J, Le W. Valproic acid-mediated Hsp70 induction and

- anti-apoptotic neuroprotection in SH-SY5Y cells. *FEBS Lett* 2005. <https://doi.org/10.1016/j.febslet.2005.10.067>.
- [328] Su Y, Ryder J, Li B, Wu X, Fox N, Solenberg P, et al. Lithium, a common drug for bipolar disorder treatment, regulates amyloid- β precursor protein processing. *Biochemistry* 2004. <https://doi.org/10.1021/bi035627j>.
- [329] Qing H, He G, Ly PTT, Fox CJ, Staufenbiel M, Cai F, et al. Valproic acid inhibits A β production, neuritic plaque formation, and behavioral deficits in Alzheimer's disease mouse models. *J Exp Med* 2008. <https://doi.org/10.1084/jem.20081588>.
- [330] Zhang J, Liu Y, Lu L. Emerging role of MicroRNAs in peripheral nerve system. *Life Sci* 2018. <https://doi.org/10.1016/j.lfs.2018.06.011>.
- [331] Meng J, Li Y, Camarillo C, Yao Y, Zhang Y, Xu C, et al. The anti-tumor histone deacetylase inhibitor SAHA and the natural flavonoid curcumin exhibit synergistic neuroprotection against amyloid-beta toxicity. *PLoS One* 2014. <https://doi.org/10.1371/journal.pone.0085570>.
- [332] Zhu X, Li Q, Chang R, Yang D, Song Z, Guo Q, et al. Curcumin Alleviates Neuropathic Pain by Inhibiting p300/CBP Histone Acetyltransferase Activity-Regulated Expression of BDNF and Cox-2 in a Rat Model. *PLoS One* 2014;9:e91303.
- [333] Kwon KJ, Kim HJ, Shin CY, Han SH. Melatonin potentiates the neuroprotective properties of resveratrol against beta-amyloid-induced neurodegeneration by modulating AMP-activated protein Kinase pathways. *J Clin Neurol* 2010. <https://doi.org/10.3988/jcn.2010.6.3.127>.
- [334] Bagul PK, Deepthi N, Sultana R, Banerjee SK. Resveratrol ameliorates cardiac oxidative stress in diabetes through deacetylation of NFkB-p65 and histone 3. *J Nutr Biochem* 2015. <https://doi.org/10.1016/j.jnutbio.2015.06.006>.
- [335] Sharma R, Ottenhof T, Rzeczowska PA, Niles LP. Epigenetic targets for melatonin:

- Induction of histone H3 hyperacetylation and gene expression in C17.2 neural stem cells. *J Pineal Res* 2008. <https://doi.org/10.1111/j.1600-079X.2008.00587.x>.
- [336] Li X, Chen X, Zhou W, Ji S, Li X, Li G, et al. Effect of melatonin on neuronal differentiation requires CBP/p300-mediated acetylation of histone H3 lysine 14. *Neuroscience* 2017;364:45–59. <https://doi.org/10.1016/j.neuroscience.2017.07.064>.
- [337] Aranarochana A, Chaisawang P, Sirichoat A, Pannangrong W, Wigmore P, Welbat JU. Protective effects of melatonin against valproic acid-induced memory impairments and reductions in adult rat hippocampal neurogenesis. *Neuroscience* 2019. <https://doi.org/10.1016/j.neuroscience.2019.02.022>.
- [338] Covington HE, Maze I, LaPlant QC, Vialou VF, Ohnishi YN, Berton O, et al. Antidepressant Actions of Histone Deacetylase Inhibitors. *J Neurosci* 2009;29:11451 LP – 11460. <https://doi.org/10.1523/JNEUROSCI.1758-09.2009>.
- [339] Zhang X, Zhao X, Fiskus W, Lin J, Lwin T, Rao R, et al. Coordinated Silencing of MYC-Mediated miR-29 by HDAC3 and EZH2 as a Therapeutic Target of Histone Modification in Aggressive B-Cell Lymphomas. *Cancer Cell* 2012. <https://doi.org/10.1016/j.ccr.2012.09.003>.
- [340] Gu X, Fu C, Lin L, Liu S, Su X, Li A, et al. miR-124 and miR-9 mediated downregulation of HDAC5 promotes neurite development through activating MEF2C-GPM6A pathway. *J Cell Physiol* 2018. <https://doi.org/10.1002/jcp.25927>.
- [341] Nampoothiri SS, Rajanikant GK. miR-9 Upregulation Integrates Post-ischemic Neuronal Survival and Regeneration In Vitro. *Cell Mol Neurobiol* 2019. <https://doi.org/10.1007/s10571-018-0642-1>.
- [342] Lu X, Deng Y, Yu D, Cao H, Wang L, Liu L, et al. Histone acetyltransferase p300 mediates histone acetylation of PS1 and BACE1 in a cellular model of Alzheimer's

- disease. PLoS One 2014. <https://doi.org/10.1371/journal.pone.0103067>.
- [343] Atluri VSR, Tiwari S, Rodriguez M, Kaushik A, Yndart A, Kolishetti N, et al. Inhibition of Amyloid-Beta Production, Associated Neuroinflammation, and Histone Deacetylase 2-Mediated Epigenetic Modifications Prevent Neuropathology in Alzheimer's Disease in vitro Model. *Front Aging Neurosci* 2020;11:342. <https://doi.org/10.3389/FNAGI.2019.00342/BIBTEX>.
- [344] Sreenivasmurthy SG, Iyaswamy A, Krishnamoorthi S, Senapati S, Malampati S, Zhu Z, et al. Protopine promotes the proteasomal degradation of pathological tau in Alzheimer's disease models via HDAC6 inhibition. *Phytomedicine* 2022;96:153887. <https://doi.org/10.1016/J.PHYMED.2021.153887>.
- [345] Cordero JG, García-Escudero R, Avila J, Gargini R, García-Escudero V. Benefit of oleuropein aglycone for Alzheimer's disease by promoting autophagy. *Oxid Med Cell Longev* 2018;2018. <https://doi.org/10.1155/2018/5010741>.
- [346] Zhao YN, Li WF, Li F, Zhang Z, Dai YD, Xu AL, et al. Resveratrol improves learning and memory in normally aged mice through microRNA-CREB pathway. *Biochem Biophys Res Commun* 2013;435:597–602. <https://doi.org/10.1016/j.bbrc.2013.05.025>.
- [347] Gao J, Wang WY, Mao YW, Gräff J, Guan JS, Pan L, et al. A novel pathway regulates memory and plasticity via SIRT1 and miR-134. *Nature* 2010. <https://doi.org/10.1038/nature09271>.
- [348] Chen F, Chen H, Jia Y, Lu H, Tan Q, Zhou X. miR-149-5p inhibition reduces Alzheimer's disease β-amyloid generation in 293/APPsw cells by upregulating H4K16ac via KAT8. *Exp Ther Med* 2020;20:1–1. <https://doi.org/10.3892/ETM.2020.9216>.
- [349] Du W, Lei C, Dong Y. MicroRNA-149 is downregulated in Alzheimer's disease and inhibits β -amyloid accumulation and ameliorates neuronal viability through targeting

- BACE1. *Genet Mol Biol* 2021;44:1–8. <https://doi.org/10.1590/1678-4685-GMB-2020-0064>.
- [350] Ma J, Zhang Y, Ji H, Chen L, Chen T, Guo C, et al. Overexpression of miR-138-5p suppresses MnCl₂-induced autophagy by targeting SIRT1 in SH-SY5Y cells. *Environ Toxicol* 2019;34:539–47. <https://doi.org/10.1002/tox.22708>.
- [351] Sun S, Han X, Li X, Song Q, Lu M, Jia M, et al. MicroRNA-212-5p Prevents Dopaminergic Neuron Death by Inhibiting SIRT2 in MPTP-Induced Mouse Model of Parkinson's Disease. *Front Mol Neurosci* 2018. <https://doi.org/10.3389/fnmol.2018.00381>.
- [352] Ramsay RR, Popovic-Nikolic MR, Nikolic K, Uliassi E, Bolognesi ML. A perspective on multi-target drug discovery and design for complex diseases. *Clin Transl Med* 2018. <https://doi.org/10.1186/s40169-017-0181-2>.
- [353] Iyengar R. Complex diseases require complex therapies. *EMBO Rep* 2013. <https://doi.org/10.1038/embor.2013.177>.
- [354] L. Bolognesi M. Polypharmacology in a Single Drug: Multitarget Drugs. *Curr Med Chem* 2013. <https://doi.org/10.2174/0929867311320130004>.
- [355] Cummings J, Lee G, Mortsdorf T, Ritter A, Zhong K. Alzheimer's disease drug development pipeline: 2017. *Alzheimer's Dement (New York, N Y)* 2017;3:367–84. <https://doi.org/10.1016/j.trci.2017.05.002>.
- [356] Van der Schyf CJ. The use of multi-target drugs in the treatment of neurodegenerative diseases. *Expert Rev Clin Pharmacol* 2011. <https://doi.org/10.1586/ecp.11.13>.
- [357] Weinreb O. The neuroprotective mechanism of action of the multimodal drug ladostigil. *Front Biosci* 2008. <https://doi.org/10.2741/3069>.
- [358] Prati F, Uliassi E, Bolognesi ML. Two diseases, one approach: Multitarget drug discovery in Alzheimer's and neglected tropical diseases. *Medchemcomm* 2014.

- <https://doi.org/10.1039/c4md00069b>.
- [359] Rabal O, Sánchez-Arias JA, Cuadrado-Tejedor M, De Miguel I, Pérez-González M, García-Barroso C, et al. Design, Synthesis, and Biological Evaluation of First-in-Class Dual Acting Histone Deacetylases (HDACs) and Phosphodiesterase 5 (PDE5) Inhibitors for the Treatment of Alzheimer's Disease. *J Med Chem* 2016. <https://doi.org/10.1021/acs.jmedchem.6b00908>.
- [360] Sánchez-Arias JA, Rabal O, Cuadrado-Tejedor M, De Miguel I, Pérez-González M, Ugarte A, et al. Impact of Scaffold Exploration on Novel Dual-Acting Histone Deacetylases and Phosphodiesterase 5 Inhibitors for the Treatment of Alzheimer's Disease. *ACS Chem Neurosci* 2017. <https://doi.org/10.1021/acschemneuro.6b00370>.
- [361] Rabal O, Sánchez-Arias JA, Cuadrado-Tejedor M, de Miguel I, Pérez-González M, García-Barroso C, et al. Design, synthesis, biological evaluation and in vivo testing of dual phosphodiesterase 5 (PDE5) and histone deacetylase 6 (HDAC6)-selective inhibitors for the treatment of Alzheimer's disease. *Eur J Med Chem* 2018. <https://doi.org/10.1016/j.ejmech.2018.03.005>.
- [362] Hu J, An B, Pan T, Li Z, Huang L, Li X. Design, synthesis, and biological evaluation of histone deacetylase inhibitors possessing glutathione peroxidase-like and antioxidant activities against Alzheimer's disease. *Bioorganic Med Chem* 2018. <https://doi.org/10.1016/j.bmc.2018.10.022>.
- [363] Basso M, Chen HH, Tripathy D, Conte M, Apperley KYP, De Simone A, et al. Designing Dual Transglutaminase 2/Histone Deacetylase Inhibitors Effective at Halting Neuronal Death. *ChemMedChem* 2018;13:227–30. <https://doi.org/10.1002/cmdc.201700601>.
- [364] De Simone A, La Pietra V, Betari N, Petraghani N, Conte M, Daniele S, et al. Discovery of the First-in-Class GSK-3 β /HDAC Dual Inhibitor as Disease-Modifying Agent To

- Combat Alzheimer's Disease. *ACS Med Chem Lett* 2019;10:469–74.
<https://doi.org/10.1021/acsmchemlett.8b00507>.
- [365] Orlikova B, Schnekenburger M, Zloh M, Golais F, Diederich M, Tasdemir D. Natural chalcones as dual inhibitors of HDACs and NF- κ B. *Oncol Rep* 2012.
<https://doi.org/10.3892/or.2012.1870>.
- [366] Clough E, Barrett T. The Gene Expression Omnibus database. *Methods Mol Biol* 2016;1418:93. https://doi.org/10.1007/978-1-4939-3578-9_5.
- [367] Piñero J, Saüch J, Sanz F, Furlong LI. The DisGeNET cytoscape app: Exploring and visualizing disease genomics data. *Comput Struct Biotechnol J* 2021;19:2960–7.
<https://doi.org/10.1016/J.CSBJ.2021.05.015>.
- [368] Davis AP, Grondin CJ, Johnson RJ, Sciaky D, Wieggers J, Wieggers TC, et al. Comparative Toxicogenomics Database (CTD): update 2021. *Nucleic Acids Res* 2021;49:D1138–43. <https://doi.org/10.1093/NAR/GKAA891>.
- [369] Alanis-Lobato G, Andrade-Navarro MA, Schaefer MH. HIPPIE v2.0: enhancing meaningfulness and reliability of protein–protein interaction networks. *Nucleic Acids Res* 2017;45:D408. <https://doi.org/10.1093/NAR/GKW985>.
- [370] Zardecki C, Dutta S, Goodsell DS, Voigt M, Burley SK. RCSB Protein Data Bank: A Resource for Chemical, Biochemical, and Structural Explorations of Large and Small Biomolecules. *J Chem Educ* 2016;93:569–75.
https://doi.org/10.1021/ACS.JCHEMED.5B00404/ASSET/IMAGES/LARGE/ED-2015-00404C_0005.JPEG.
- [371] Liu T, Lin Y, Wen X, Jorissen RN, Gilson MK. BindingDB: a web-accessible database of experimentally determined protein–ligand binding affinities. *Nucleic Acids Res* 2007;35:D198. <https://doi.org/10.1093/NAR/GKL999>.
- [372] Pettersen EF, Goddard TD, Huang CC, Couch GS, Greenblatt DM, Meng EC, et al.

- UCSF Chimera--a visualization system for exploratory research and analysis. *J Comput Chem* 2004;25:1605–12. <https://doi.org/10.1002/JCC.20084>.
- [373] Xu D, Zhang Y. Improving the Physical Realism and Structural Accuracy of Protein Models by a Two-Step Atomic-Level Energy Minimization. *Biophysj* 2011;101:2525–34. <https://doi.org/10.1016/j.bpj.2011.10.024>.
- [374] Szklarczyk D, Gable AL, Nastou KC, Lyon D, Kirsch R, Pyysalo S, et al. The STRING database in 2021: customizable protein–protein networks, and functional characterization of user-uploaded gene/measurement sets. *Nucleic Acids Res* 2021;49:D605–12. <https://doi.org/10.1093/NAR/GKAA1074>.
- [375] Shannon P, Markiel A, Ozier O, Baliga NS, Wang JT, Ramage D, et al. Cytoscape: A Software Environment for Integrated Models of Biomolecular Interaction Networks. *Genome Res* 2003;13:2498. <https://doi.org/10.1101/GR.1239303>.
- [376] Bader GD, Hogue CWV. An automated method for finding molecular complexes in large protein interaction networks. *BMC Bioinformatics* 2003;4:1–27. <https://doi.org/10.1186/1471-2105-4-2/FIGURES/12>.
- [377] Chin CH, Chen SH, Wu HH, Ho CW, Ko MT, Lin CY. cytoHubba: identifying hub objects and sub-networks from complex interactome. *BMC Syst Biol* 2014;8 Suppl 4. <https://doi.org/10.1186/1752-0509-8-S4-S11>.
- [378] Chen EY, Tan CM, Kou Y, Duan Q, Wang Z, Meirelles G V., et al. Enrichr: Interactive and collaborative HTML5 gene list enrichment analysis tool. *BMC Bioinformatics* 2013;14:1–14. <https://doi.org/10.1186/1471-2105-14-128/FIGURES/3>.
- [379] Binns D, Dimmer E, Huntley R, Barrell D, O'Donovan C, Apweiler R. QuickGO: a web-based tool for Gene Ontology searching. *Bioinformatics* 2009;25:3045. <https://doi.org/10.1093/BIOINFORMATICS/BTP536>.
- [380] Fabregat A, Sidiropoulos K, Viteri G, Forner O, Marin-Garcia P, Arnau V, et al.

- Reactome pathway analysis: A high-performance in-memory approach. *BMC Bioinformatics* 2017;18:1–9. <https://doi.org/10.1186/S12859-017-1559-2/TABLES/1>.
- [381] Pathan M, Keerthikumar S, Ang CS, Gangoda L, Quek CYJ, Williamson NA, et al. FunRich: An open access standalone functional enrichment and interaction network analysis tool. *Proteomics* 2015;15:2597–601. <https://doi.org/10.1002/PMIC.201400515>.
- [382] Yu CS, Cheng CW, Su WC, Chang KC, Huang SW, Hwang JK, et al. CELLO2GO: A Web Server for Protein subCELLular LOCALization Prediction with Functional Gene Ontology Annotation. *PLoS One* 2014;9:99368. <https://doi.org/10.1371/JOURNAL.PONE.0099368>.
- [383] Fornes O, Castro-Mondragon JA, Khan A, Van Der Lee R, Zhang X, Richmond PA, et al. JASPAR 2020: update of the open-access database of transcription factor binding profiles. *Nucleic Acids Res* 2020;48:D87–92. <https://doi.org/10.1093/NAR/GKZ1001>.
- [384] Zhou G, Soufan O, Ewald J, Hancock REW, Basu N, Xia J. NetworkAnalyst 3.0: a visual analytics platform for comprehensive gene expression profiling and meta-analysis. *Nucleic Acids Res* 2019;47:W234–41. <https://doi.org/10.1093/NAR/GKZ240>.
- [385] Wang D, Liu D, Yuchi J, He F, Jiang Y, Cai S, et al. MusiteDeep: a deep-learning based webserver for protein post-translational modification site prediction and visualization. *Nucleic Acids Res* 2020;48:W140–6. <https://doi.org/10.1093/NAR/GKAA275>.
- [386] Suo SB, Qiu JD, Shi SP, Sun XY, Huang SY, Chen X, et al. Position-specific analysis and prediction for protein lysine acetylation based on multiple features. *PLoS One* 2012;7. <https://doi.org/10.1371/JOURNAL.PONE.0049108>.
- [387] Wei B, Gong X. DeepPLA: a novel deep learning-based model for protein-ligand binding affinity prediction. *BioRxiv* 2021:2021.12.01.470868. <https://doi.org/10.1101/2021.12.01.470868>.

- [388] Thompson JD, Higgins DG, Gibson TJ. CLUSTAL W: improving the sensitivity of progressive multiple sequence alignment through sequence weighting, position-specific gap penalties and weight matrix choice. *Nucleic Acids Res* 1994;22:4673. <https://doi.org/10.1093/NAR/22.22.4673>.
- [389] McGuffin LJ, Bryson K, Jones DT. The PSIPRED protein structure prediction server. *Bioinformatics* 2000;16:404–5. <https://doi.org/10.1093/BIOINFORMATICS/16.4.404>.
- [390] Li Z, Li S, Luo M, Jhong JH, Li W, Yao L, et al. dbPTM in 2022: an updated database for exploring regulatory networks and functional associations of protein post-translational modifications. *Nucleic Acids Res* 2022;50:D471–9. <https://doi.org/10.1093/NAR/GKAB1017>.
- [391] Xu H, Zhou J, Lin S, Deng W, Zhang Y, Xue Y. PLMD: An updated data resource of protein lysine modifications. *J Genet Genomics* 2017;44:243–50. <https://doi.org/10.1016/J.JGG.2017.03.007>.
- [392] Jones DT, Cozzetto D. DISOPRED3: precise disordered region predictions with annotated protein-binding activity. *Bioinformatics* 2015;31:857–63. <https://doi.org/10.1093/BIOINFORMATICS/BTU744>.
- [393] López-Ferrando V, Gazzo A, De La Cruz X, Orozco M, Gelpí JL. PMut: a web-based tool for the annotation of pathological variants on proteins, 2017 update. *Nucleic Acids Res* 2017;45:W222. <https://doi.org/10.1093/NAR/GKX313>.
- [394] Adzhubei I, Jordan DM, Sunyaev SR. Predicting Functional Effect of Human Missense Mutations Using PolyPhen-2. *Curr Protoc Hum Genet* 2013;0 7:Unit7.20. <https://doi.org/10.1002/0471142905.HG0720S76>.
- [395] Mi H, Thomas P. PANTHER Pathway: an ontology-based pathway database coupled with dataanalysis tools. *Methods Mol Biol* 2009;563:123. https://doi.org/10.1007/978-1-60761-175-2_7.

- [396] Hecht M, Bromberg Y, Rost B. Better prediction of functional effects for sequence variants. *BMC Genomics* 2015;16:1–12. <https://doi.org/10.1186/1471-2164-16-S8-S1/FIGURES/4>.
- [397] Rodrigues CHM, Pires DEV, Ascher DB. DynaMut: predicting the impact of mutations on protein conformation, flexibility and stability. *Nucleic Acids Res* 2018;46:W350–5. <https://doi.org/10.1093/NAR/GKY300>.
- [398] Pejaver V, Urresti J, Lugo-Martinez J, Pagel KA, Lin GN, Nam HJ, et al. Inferring the molecular and phenotypic impact of amino acid variants with MutPred2. *Nat Commun* 2020 111 2020;11:1–13. <https://doi.org/10.1038/s41467-020-19669-x>.
- [399] Qiu W, Xu C, Xiao X, Xu D. Computational Prediction of Ubiquitination Proteins Using Evolutionary Profiles and Functional Domain Annotation. *Curr Genomics* 2019;20:389. <https://doi.org/10.2174/1389202919666191014091250>.
- [400] Chang CC, Tung CH, Chen CW, Tu CH, Chu YW. SUMOgo: Prediction of sumoylation sites on lysines by motif screening models and the effects of various post-translational modifications. *Sci Reports* 2018 81 2018;8:1–10. <https://doi.org/10.1038/s41598-018-33951-5>.
- [401] Deng W, Wang C, Zhang Y, Xu Y, Zhang S, Liu Z, et al. GPS-PAIL: prediction of lysine acetyltransferase-specific modification sites from protein sequences. *Sci Rep* 2016;6. <https://doi.org/10.1038/SREP39787>.
- [402] Tokar T, Pastrello C, Rossos AEM, Abovsky M, Hauschild AC, Tsay M, et al. mirDIP 4.1—integrative database of human microRNA target predictions. *Nucleic Acids Res* 2018;46:D360. <https://doi.org/10.1093/NAR/GKX1144>.
- [403] Ludwig N, Leidinger P, Becker K, Backes C, Fehlmann T, Pallasch C, et al. Distribution of miRNA expression across human tissues. *Nucleic Acids Res* 2016;44:3865–77. <https://doi.org/10.1093/NAR/GKW116>.

- [404] Licursi V, Conte F, Fiscon G, Paci P. MIENTURNET: An interactive web tool for microRNA-target enrichment and network-based analysis. *BMC Bioinformatics* 2019;20:1–10. <https://doi.org/10.1186/S12859-019-3105-X/TABLES/1>.
- [405] Li JH, Liu S, Zhou H, Qu LH, Yang JH. starBase v2.0: decoding miRNA-ceRNA, miRNA-ncRNA and protein–RNA interaction networks from large-scale CLIP-Seq data. *Nucleic Acids Res* 2014;42:D92–7. <https://doi.org/10.1093/NAR/GKT1248>.
- [406] Gaulton A, Bellis LJ, Bento AP, Chambers J, Davies M, Hersey A, et al. ChEMBL: a large-scale bioactivity database for drug discovery. *Nucleic Acids Res* 2012;40:D1100. <https://doi.org/10.1093/NAR/GKR777>.
- [407] Morgan HL. The Generation of a Unique Machine Description for Chemical Structures—A Technique Developed at Chemical Abstracts Service. *J Chem Doc* 1965;5:107–13. https://doi.org/10.1021/C160017A018/ASSET/C160017A018.FP.PNG_V03.
- [408] Sander T, Freyss J, Von Korff M, Rufener C. DataWarrior: An open-source program for chemistry aware data visualization and analysis. *J Chem Inf Model* 2015. <https://doi.org/10.1021/ci500588j>.
- [409] Spessard GO. ACD Labs/LogP dB 3.5 and ChemSketch 3.5. *J Chem Inf Comput Sci* 2002. <https://doi.org/10.1021/ci980264t>.
- [410] Shaker B, Yu MS, Song JS, Ahn S, Ryu JY, Oh KS, et al. LightBBB: computational prediction model of blood-brain-barrier penetration based on LightGBM. *Bioinformatics* 2021;37:1135–9. <https://doi.org/10.1093/BIOINFORMATICS/BTAA918>.
- [411] Liu H, Wang L, Lv M, Pei R, Li P, Pei Z, et al. AlzPlatform: An Alzheimer’s disease domain-specific chemogenomics knowledgebase for polypharmacology and target identification research. *J Chem Inf Model* 2014;54:1050–60.

https://doi.org/10.1021/CI500004H/ASSET/IMAGES/LARGE/CI-2014-00004H_0003.JPEG.

- [412] Yang H, Lou C, Sun L, Li J, Cai Y, Wang Z, et al. admetSAR 2.0: web-service for prediction and optimization of chemical ADMET properties. *Bioinformatics* 2019;35:1067–9. <https://doi.org/10.1093/BIOINFORMATICS/BTY707>.
- [413] Backman TWH, Cao Y, Girke T. ChemMine tools: an online service for analyzing and clustering small molecules. *Nucleic Acids Res* 2011;39. <https://doi.org/10.1093/NAR/GKR320>.
- [414] Kochnev Y, Hellemann E, Cassidy KC, Durrant JD. Webina: an open-source library and web app that runs AutoDock Vina entirely in the web browser. *Bioinformatics* 2020;36:4513–5. <https://doi.org/10.1093/BIOINFORMATICS/BTAA579>.
- [415] O’Boyle NM, Banck M, James CA, Morley C, Vandermeersch T, Hutchison GR. Open Babel: An Open chemical toolbox. *J Cheminform* 2011. <https://doi.org/10.1186/1758-2946-3-33>.
- [416] Snider J, Kotlyar M, Saraon P, Yao Z, Jurisica I, Stagljari I. Fundamentals of protein interaction network mapping. *Mol Syst Biol* 2015;11:848. <https://doi.org/10.15252/MSB.20156351>.
- [417] Dai W, Chang Q, Peng W, Zhong J, Li Y. Network Embedding the Protein–Protein Interaction Network for Human Essential Genes Identification. *Genes (Basel)* 2020;11. <https://doi.org/10.3390/GENES11020153>.
- [418] Vella D, Marini S, Vitali F, Silvestre D Di, Mauri G, Bellazzi R. MTGO: PPI Network Analysis Via Topological and Functional Module Identification OPEN. *Sci REPORTs* | 2018;8:5499. <https://doi.org/10.1038/s41598-018-23672-0>.
- [419] Chen S-J, Liao D-L, Chen C-H, Wang T-Y, Chen K-C. Construction and Analysis of Protein-Protein Interaction Network of Heroin Use Disorder. *Sci Reports* 2019 91

- 2019;9:1–9. <https://doi.org/10.1038/s41598-019-41552-z>.
- [420] Friedel CC, Zimmer R. Inferring topology from clustering coefficients in protein-protein interaction networks. *BMC Bioinformatics* 2006;7. <https://doi.org/10.1186/1471-2105-7-519>.
- [421] Xu K, Bezakova I, Bunimovich L, Yi S V. Path lengths in protein-protein interaction networks and biological complexity. *Proteomics* 2011;11:1857–67. <https://doi.org/10.1002/PMIC.201000684>.
- [422] Pavel A, del Giudice G, Federico A, Di Lieto A, Kinaret PAS, Serra A, et al. Integrated network analysis reveals new genes suggesting COVID-19 chronic effects and treatment. *Brief Bioinform* 2021;22:1430–41. <https://doi.org/10.1093/BIB/BBAA417>.
- [423] Gu S, Johnson J, Faisal FE, Milenković T. From homogeneous to heterogeneous network alignment via colored graphlets. *Sci Reports* 2018 81 2018;8:1–16. <https://doi.org/10.1038/s41598-018-30831-w>.
- [424] Ashtiani M, Salehzadeh-Yazdi A, Razaghi-Moghadam Z, Hennig H, Wolkenhauer O, Mirzaie M, et al. A systematic survey of centrality measures for protein-protein interaction networks. *BMC Syst Biol* 2018;12. <https://doi.org/10.1186/S12918-018-0598-2>.
- [425] Koschützki D, Schreiber F. Comparison of Centralities for Biological Networks * n.d.
- [426] Zhou H, Liu J, Li J, Duan W. A density-based approach for detecting complexes in weighted PPI networks by semantic similarity. *PLoS One* 2017;12:e0180570. <https://doi.org/10.1371/JOURNAL.PONE.0180570>.
- [427] NetworkAnalyzer Help n.d. <https://med.bioinf.mpi-inf.mpg.de/netanalyzer/help/2.5/> (accessed August 21, 2021).
- [428] Rong Z, Cheng B, Zhong L, Ye X, Li X, Jia L, et al. Activation of FAK/Rac1/Cdc42-GTPase signaling ameliorates impaired microglial migration response to A β 42 in

- triggering receptor expressed on myeloid cells 2 loss-of-function murine models. *FASEB J* 2020;34:10984–97. <https://doi.org/10.1096/FJ.202000550RR>.
- [429] Huang S, Mao J, Ding K, Zhou Y, Zeng X, Yang W, et al. Polysaccharides from *Ganoderma lucidum* Promote Cognitive Function and Neural Progenitor Proliferation in Mouse Model of Alzheimer's Disease. *Stem Cell Reports* 2017;8:84–94. <https://doi.org/10.1016/J.STEMCR.2016.12.007>.
- [430] Lim S, Kim D, Ju S, Shin S, Cho I, Park S-H, et al. Glioblastoma-secreted soluble CD44 activates tau pathology in the brain. *Exp Mol Med* 2018 504 2018;50:1–11. <https://doi.org/10.1038/s12276-017-0008-7>.
- [431] Neal ML, Boyle AM, Budge KM, Safadi FF, Richardson JR. The glycoprotein GPNMB attenuates astrocyte inflammatory responses through the CD44 receptor. *J Neuroinflammation* 2018 151 2018;15:1–14. <https://doi.org/10.1186/S12974-018-1100-1>.
- [432] Landrock KK, Sullivan P, Martini-Stoica H, Goldstein DS, Graham BH, Yamamoto S, et al. Pleiotropic neuropathological and biochemical alterations associated with Myo5a mutation in a rat Model. *Brain Res* 2018;1679:155–70. <https://doi.org/10.1016/J.BRAINRES.2017.11.029>.
- [433] Bhat G, LaGrave D, Millson A, Herriges J, Lamb AN, Matalon R. Xq11.1-11.2 deletion involving ARHGEF9 in a girl with autism spectrum disorder. *Eur J Med Genet* 2016;59:470–3. <https://doi.org/10.1016/J.EJMG.2016.05.014>.
- [434] Griffin K, Bejoy J, Song L, Hua T, Marzano M, Jeske R, et al. Human Stem Cell-derived Aggregates of Forebrain Astroglia Respond to Amyloid Beta Oligomers. <https://HomeLiebertpubCom/Tea> 2020;26:527–42. <https://doi.org/10.1089/TEN.TEA.2019.0227>.
- [435] Qian G, Ren Y, Zuo Y, Yuan Y, Zhao P, Wang X, et al. Smurf1 represses TNF- α

- production through ubiquitination and destabilization of USP5. *Biochem Biophys Res Commun* 2016;474:491–6. <https://doi.org/10.1016/J.BBRC.2016.04.135>.
- [436] Tsai AP, Lin PBC, Dong C, Moutinho M, Casali BT, Liu Y, et al. INPP5D expression is associated with risk for Alzheimer’s disease and induced by plaque-associated microglia. *Neurobiol Dis* 2021;153:105303. <https://doi.org/10.1016/J.NBD.2021.105303>.
- [437] Esteves IM, Lopes-Aguiar C, Rossignoli MT, Ruggiero RN, Brogгинi ACS, Bueno-Junior LS, et al. Chronic nicotine attenuates behavioral and synaptic plasticity impairments in a streptozotocin model of Alzheimer’s disease. *Neuroscience* 2017;353:87–97. <https://doi.org/10.1016/J.NEUROSCIENCE.2017.04.011>.
- [438] Carvajal-Oliveros A, Domínguez-Baleón C, Zárate R V., Campusano JM, Narváez-Padilla V, Reynaud E. Nicotine suppresses Parkinson’s disease like phenotypes induced by Synphilin-1 overexpression in *Drosophila melanogaster* by increasing tyrosine hydroxylase and dopamine levels. *Sci Reports* 2021 111 2021;11:1–13. <https://doi.org/10.1038/s41598-021-88910-4>.
- [439] Zhang X, Nagai T, Ahammad RU, Kuroda K, Nakamuta S, Nakano T, et al. Balance between dopamine and adenosine signals regulates the PKA/Rap1 pathway in striatal medium spiny neurons. *Neurochem Int* 2019;122:8–18. <https://doi.org/10.1016/J.NEUINT.2018.10.008>.
- [440] Kagawa Y, Umaru BA, Shil SK, Hayasaka K, Zama R, Kobayashi Y, et al. Mitochondrial dysfunction in GnRH neurons impaired GnRH production. *Biochem Biophys Res Commun* 2020;530:329–35. <https://doi.org/10.1016/J.BBRC.2020.07.090>.
- [441] Şişli HB, Hayal TB, Şenkal S, Kıratlı B, Sağraç D, Seçkin S, et al. Apelin Receptor Signaling Protects GT1-7 GnRH Neurons Against Oxidative Stress In Vitro. *Cell Mol Neurobiol* 2020 2020:1–23. <https://doi.org/10.1007/S10571-020-00968-2>.

- [442] Ahmadian E, Eftekhari A, Samiei M, Maleki Dizaj S, Vinken M. The role and therapeutic potential of connexins, pannexins and their channels in Parkinson's disease. *Cell Signal* 2019;58:111–8. <https://doi.org/10.1016/J.CELLSIG.2019.03.010>.
- [443] Xing J, Xu C. Role of connexins in neurodegenerative diseases (Review). *Mol Med Rep* 2021;23:1–6. <https://doi.org/10.3892/MMR.2021.12034>.
- [444] Angeli S, Kousiappa I, Stavrou M, Sargiannidou I, Georgiou E, Papacostas SS, et al. Altered Expression of Glial Gap Junction Proteins Cx43, Cx30, and Cx47 in the 5XFAD Model of Alzheimer's Disease. *Front Neurosci* 2020;0:1060. <https://doi.org/10.3389/FNINS.2020.582934>.
- [445] Maulik M, Vasan L, Bose A, Chowdhury SD, Sengupta N, Sarma J Das. Amyloid- β regulates gap junction protein connexin 43 trafficking in cultured primary astrocytes. *J Biol Chem* 2020;295:15097–111. <https://doi.org/10.1074/JBC.RA120.013705>.
- [446] Wójtowicz S, Strosznajder AK, Jeżyna M, Strosznajder JB. The Novel Role of PPAR Alpha in the Brain: Promising Target in Therapy of Alzheimer's Disease and Other Neurodegenerative Disorders. *Neurochem Res* 2020 455 2020;45:972–88. <https://doi.org/10.1007/S11064-020-02993-5>.
- [447] Dennis DJ, Han S, Schuurmans C. bHLH transcription factors in neural development, disease, and reprogramming. *Brain Res* 2019;1705:48–65. <https://doi.org/10.1016/J.BRAINRES.2018.03.013>.
- [448] Yao Z, Yang W, Gao Z, Jia P. Nicotinamide mononucleotide inhibits JNK activation to reverse Alzheimer disease. *Neurosci Lett* 2017;647:133–40. <https://doi.org/10.1016/J.NEULET.2017.03.027>.
- [449] Wang Y, Lin Y, Wang L, Zhan H, Luo X, Zeng Y, et al. TREM2 ameliorates neuroinflammatory response and cognitive impairment via PI3K/AKT/FoxO3a signaling pathway in Alzheimer's disease mice. *Aging (Albany NY)* 2020;12:20862.

<https://doi.org/10.18632/AGING.104104>.

- [450] Xu X, Wang R, Hao Z, Wang G, Mu C, Ding J, et al. DJ-1 regulates tyrosine hydroxylase expression through CaMKK β /CaMKIV/CREB1 pathway in vitro and in vivo. *J Cell Physiol* 2020;235:869–79. <https://doi.org/10.1002/JCP.29000>.
- [451] Marchese E, Di Maria V, Samengo D, Pani G, Michetti F, Geloso MC. Post-natal Deletion of Neuronal cAMP Responsive-Element Binding (CREB)-1 Promotes Pro-inflammatory Changes in the Mouse Hippocampus. *Neurochem Res* 2017 428 2017;42:2230–45. <https://doi.org/10.1007/S11064-017-2233-9>.
- [452] He T, Shang J, Gao C, Guan X, Chen Y, Zhu L, et al. A novel SIRT6 activator ameliorates neuroinflammation and ischemic brain injury via EZH2/FOXC1 axis. *Acta Pharm Sin B* 2021;11:708–26. <https://doi.org/10.1016/J.APSB.2020.11.002>.
- [453] Emelyanov AK, Lavrinova AO, Litusova EM, Knyazev NA, Kulabukhova DG, Garaeva LA, et al. The Effect of Dopamine on Gene Expression of Alpha-synuclein and Transcription Factors GATA-1, GATA-2, and ZSCAN21 in Parkinson's Disease. *Cell Tissue Biol* 2018 125 2018;12:410–8. <https://doi.org/10.1134/S1990519X18050024>.
- [454] Zhang W, Duan N, Song T, Li Z, Zhang C, Chen X. The Emerging Roles of Forkhead Box (FOX) Proteins in Osteosarcoma. *J Cancer* 2017;8:1619. <https://doi.org/10.7150/JCA.18778>.
- [455] Rahman MR, Islam T, Turanli B, Zaman T, Faruquee HM, Rahman MM, et al. Network-based approach to identify molecular signatures and therapeutic agents in Alzheimer's disease. *Comput Biol Chem* 2019;78:431–9. <https://doi.org/10.1016/J.COMPBIOLCHEM.2018.12.011>.
- [456] Jun GR, Chung J, Mez J, Barber R, Beecham GW, Bennett DA, et al. Transethnic genome-wide scan identifies novel Alzheimer disease loci. *Alzheimers Dement* 2017;13:727. <https://doi.org/10.1016/J.JALZ.2016.12.012>.

- [457] Wang C, Zhao F, Shen K, Wang W, Siedlak SL, Lee H gon, et al. The sterol regulatory element-binding protein 2 is dysregulated by tau alterations in Alzheimer disease. *Brain Pathol* 2019;29:530–43. <https://doi.org/10.1111/BPA.12691>.
- [458] Li H, Liu J. The novel function of HINFP as a co-activator in sterol-regulated transcription of PCSK9 in HepG2 cells. *Biochem J* 2012;443:757–68. <https://doi.org/10.1042/BJ20111645>.
- [459] Lou F, Li M, Liu N, Li X, Ren Y, Luo X. The polymorphism of SREBF1 gene rs11868035 G/A is associated with susceptibility to Parkinson’s disease in a Chinese population. <https://doi.org/10.1080/00207454.2018.1526796> 2019;129:660–5.
- [460] Yuan XQ, Cao B, Wu Y, Chen YP, Wei QQ, Ou RW, et al. Association analysis of SNP rs11868035 in SREBF1 with sporadic Parkinson’s disease, sporadic amyotrophic lateral sclerosis and multiple system atrophy in a Chinese population. *Neurosci Lett* 2018;664:128–32. <https://doi.org/10.1016/J.NEULET.2017.11.015>.
- [461] Zhu X, Asa SL, Ezzat S. Histone-Acetylated Control of Fibroblast Growth Factor Receptor 2 Intron 2 Polymorphisms and Isoform Splicing in Breast Cancer. *Mol Endocrinol* 2009;23:1397. <https://doi.org/10.1210/ME.2009-0071>.
- [462] JL L, MJ W, JY C. Acetylation and activation of STAT3 mediated by nuclear translocation of CD44. *J Cell Biol* 2009;185:949–57. <https://doi.org/10.1083/JCB.200812060>.
- [463] Wei J, Dong S, Yao K, Martinez MFYM, Fleisher PR, Zhao Y, et al. Histone acetyltransferase CBP promotes function of SCF FBXL19 ubiquitin E3 ligase by acetylation and stabilization of its F-box protein subunit. *FASEB J* 2018;32:4284–92. <https://doi.org/10.1096/FJ.201701069R>.
- [464] Pattaroni C, Jacob C. Histone Methylation in the Nervous System: Functions and

- Dysfunctions. *Mol Neurobiol* 2012 472 2012;47:740–56.
<https://doi.org/10.1007/S12035-012-8376-4>.
- [465] Rahman MR, Islam T, Zaman T, Shahjaman M, Karim MR, Huq F, et al. Identification of molecular signatures and pathways to identify novel therapeutic targets in Alzheimer’s disease: Insights from a systems biomedicine perspective. *Genomics* 2020;112:1290–9. <https://doi.org/10.1016/J.YGENO.2019.07.018>.
- [466] Zentner GE, Henikoff S. Regulation of nucleosome dynamics by histone modifications. *Nat Struct Mol Biol* 2013 203 2013;20:259–66. <https://doi.org/10.1038/nsmb.2470>.
- [467] Ram O, Goren A, Amit I, Shoresh N, Yosef N, Ernst J, et al. Combinatorial patterning of chromatin regulators uncovered by genome-wide location analysis in human cells. *Cell* 2011;147:1628. <https://doi.org/10.1016/J.CELL.2011.09.057>.
- [468] Lee J, Ko YU, Chung Y, Yun N, Kim M, Kim K, et al. The acetylation of cyclin-dependent kinase 5 at lysine 33 regulates kinase activity and neurite length in hippocampal neurons. *Sci Reports* 2018 81 2018;8:1–19.
<https://doi.org/10.1038/s41598-018-31785-9>.
- [469] Jin H, Wang M, Wang J, Cao H, Niu W, Du L. Paeonol attenuates isoflurane anesthesia-induced hippocampal neurotoxicity via modulation of JNK/ERK/P38MAPK pathway and regulates histone acetylation in neonatal rat. <https://doi.org/10.1080/1476705820181487396> 2018;33:81–91.
<https://doi.org/10.1080/14767058.2018.1487396>.
- [470] El-Naggar AM, Somasekharan SP, Wang Y, Cheng H, Negri GL, Pan M, et al. Class I HDAC inhibitors enhance YB-1 acetylation and oxidative stress to block sarcoma metastasis. *EMBO Rep* 2019;20:e48375. <https://doi.org/10.15252/EMBR.201948375>.
- [471] Kelly RDW, Chandru A, Watson PJ, Song Y, Blades M, Robertson NS, et al. Histone deacetylase (HDAC) 1 and 2 complexes regulate both histone acetylation and

- crotonylation in vivo. *Sci Reports* 2018 81 2018;8:1–10. <https://doi.org/10.1038/s41598-018-32927-9>.
- [472] Topuz RD, Gunduz O, Tastekin E, Karadag CH. Effects of hippocampal histone acetylation and HDAC inhibition on spatial learning and memory in the Morris water maze in rats. *Fundam Clin Pharmacol* 2020;34:222–8. <https://doi.org/10.1111/FCP.12512>.
- [473] Choi H, Kim HJ, Kim J, Kim S, Yang J, Lee W, et al. Increased acetylation of Peroxiredoxin1 by HDAC6 inhibition leads to recovery of A β -induced impaired axonal transport n.d. <https://doi.org/10.1186/s13024-017-0164-1>.
- [474] Min S-W, Sohn PD, Li Y, Devidze N, Johnson JR, Krogan NJ, et al. SIRT1 Deacetylates Tau and Reduces Pathogenic Tau Spread in a Mouse Model of Tauopathy. *J Neurosci* 2018;38:3680–8. <https://doi.org/10.1523/JNEUROSCI.2369-17.2018>.
- [475] Hansen BK, Gupta R, Baldus L, Lyon D, Narita T, Lammers M, et al. Analysis of human acetylation stoichiometry defines mechanistic constraints on protein regulation. *Nat Commun* 2019 101 2019;10:1–11. <https://doi.org/10.1038/s41467-019-09024-0>.
- [476] Paz JC, Park S, Phillips N, Matsumura S, Tsai W-W, Kasper L, et al. Combinatorial regulation of a signal-dependent activator by phosphorylation and acetylation. *Proc Natl Acad Sci U S A* 2014;111:17116. <https://doi.org/10.1073/PNAS.1420389111>.
- [477] Lu Q, Hutchins AE, Doyle CM, Lundblad JR, Kwok RPS. Acetylation of cAMP-responsive element-binding protein (CREB) by CREB-binding protein enhances CREB-dependent transcription. *J Biol Chem* 2003;278:15727–34. <https://doi.org/10.1074/JBC.M300546200>.
- [478] Gruber JJ, Geller B, Lipchik AM, Chen J, Salahudeen AA, Ram AN, et al. HAT1 Coordinates Histone Production and Acetylation via H4 Promoter Binding. *Mol Cell* 2019;75:711-724.e5. <https://doi.org/10.1016/J.MOLCEL.2019.05.034>.

- [479] Nguyen T Van, Lee JE, Sweredoski MJ, Yang SJ, Jeon SJ, Harrison JS, et al. Glutamine Triggers Acetylation-Dependent Degradation of Glutamine Synthetase via the Thalidomide Receptor Cereblon. *Mol Cell* 2016;61:809–20. <https://doi.org/10.1016/J.MOLCEL.2016.02.032>.
- [480] Son SM, Park SJ, Stamatakou E, Vicinanza M, Menzies FM, Rubinsztein DC. Leucine regulates autophagy via acetylation of the mTORC1 component raptor. *Nat Commun* 2020 11:1–13. <https://doi.org/10.1038/s41467-020-16886-2>.
- [481] A C, Z Z, K R, LA A, I R, LF K, et al. Investigating Crosstalk Among PTMs Provides Novel Insight Into the Structural Basis Underlying the Differential Effects of Nt17 PTMs on Mutant Httex1 Aggregation. *Front Mol Biosci* 2021;8. <https://doi.org/10.3389/FMOLB.2021.686086>.
- [482] Ichiki T. Role of cAMP Response Element Binding Protein in Cardiovascular Remodeling. *Arterioscler Thromb Vasc Biol* 2006;26:449–55. <https://doi.org/10.1161/01.ATV.0000196747.79349.D1>.
- [483] Xu W, Kasper LH, Lerach S, Jeevan T, Brindle PK. Individual CREB-target genes dictate usage of distinct cAMP-responsive coactivation mechanisms. *EMBO J* 2007;26:2890–903. <https://doi.org/10.1038/SJ.EMBOJ.7601734>.
- [484] M S, Y H. Sequence-specific transcriptional repression by an MBD2-interacting zinc finger protein MIZF. *Nucleic Acids Res* 2004;32:590–7. <https://doi.org/10.1093/NAR/GKH249>.
- [485] R M, T B, SK Z, A M-C, JB L, JL S, et al. The histone gene cell cycle regulator HiNF-P is a unique zinc finger transcription factor with a novel conserved auxiliary DNA-binding motif. *Biochemistry* 2008;47:11415–23. <https://doi.org/10.1021/BI800961D>.
- [486] Vettese-Dadey¹ M, Grant PA, Hebbes² TR, Crane-Robinson² C, David Allis⁴ C, Workman⁵ JL. Acetylation of histone H4 plays a primary role in enhancing transcription

- factor binding to nucleosomal DNA in vitro. *EMBO J* 1996;15:2508–18.
- [487] Ina Buchholz, Peter Nestler, Susan Köppen, Mihaela Delcea. Lysine residues control the conformational dynamics of beta 2-glycoprotein I. *Phys Chem Chem Phys* 2018;20:26819–29. <https://doi.org/10.1039/C8CP03234C>.
- [488] Maltsev AS, Ying J, Bax A. Impact of N-Terminal Acetylation of α -Synuclein on Its Random Coil and Lipid Binding Properties. *Biochemistry* 2012;51:5004–13. <https://doi.org/10.1021/BI300642H>.
- [489] Kulemzina I, Ang K, Zhao X, Teh JT, Verma V, Suranthran S, et al. A Reversible Association between Smc Coiled Coils Is Regulated by Lysine Acetylation and Is Required for Cohesin Association with the DNA. *Mol Cell* 2016;63:1044–54. <https://doi.org/10.1016/J.MOLCEL.2016.08.008>.
- [490] Fiumara F, Fioriti L, Kandel ER, Hendrickson WA. Essential role of coiled coils for aggregation and activity of Q/N-rich prions and PolyQ proteins. *Cell* 2010. <https://doi.org/10.1016/j.cell.2010.11.042>.
- [491] Narne P, Pandey V, Simhadri PK, Phanithi PB. Poly(ADP-ribose)polymerase-1 hyperactivation in neurodegenerative diseases: The death knell tolls for neurons. *Semin Cell Dev Biol* 2017. <https://doi.org/10.1016/j.semcdb.2016.11.007>.
- [492] Love S, Barber R, Wilcock GK. Increased poly(ADP-ribosyl)ation of nuclear proteins in Alzheimer's disease. *Brain* 1999. <https://doi.org/10.1093/brain/122.2.247>.
- [493] Abeti R, Abramov AY, Duchen MR. β -amyloid activates PARP causing astrocytic metabolic failure and neuronal death. *Brain* 2011. <https://doi.org/10.1093/brain/awr104>.
- [494] Zhao YJ, Wang JH, Fu B, Ma MX, Li BX, Huang Q, et al. Effects of 3-aminobenzamide on expressions of poly(ADP ribose) polymerase and apoptosis inducing factor in cardiomyocytes of rats with acute myocardial infarction. *Chin Med J (Engl)* 2009. <https://doi.org/10.3760/cma.j.issn.0366-6999.2009.11.016>.

- [495] Yu C, Kim BS, Kim E. FAF1 mediates regulated necrosis through PARP1 activation upon oxidative stress leading to dopaminergic neurodegeneration. *Cell Death Differ* 2016. <https://doi.org/10.1038/cdd.2016.99>.
- [496] Hayakawa F, Towatari M, Ozawa Y, Tomita A, Privalsky ML, Saito H. Functional regulation of GATA-2 by acetylation. *J Leukoc Biol* 2004;75:529–40. <https://doi.org/10.1189/JLB.0603389>.
- [497] Thakur N, Pandey RK, Mehrotra S. Signal transducer and activator of transcription-3 mediated neuroprotective effect of interleukin-6 on cobalt chloride mimetic hypoxic cell death in R28 cells. *Mol Biol Reports* 2021 488 2021;48:6197–203. <https://doi.org/10.1007/S11033-021-06586-5>.
- [498] Li J, Wang J, Wang Y-L, Luo Z, Zheng C, Yu G, et al. NOX2 activation contributes to cobalt nanoparticles-induced inflammatory responses and Tau phosphorylation in mice and microglia. *Ecotoxicol Environ Saf* 2021;225:112725. <https://doi.org/10.1016/J.ECOENV.2021.112725>.
- [499] Yubolphan R, Phuagkhaopong S, Sangpairoj K, Sibmooh N, Power C, Vivithanaporn P. Intracellular nickel accumulation induces apoptosis and cell cycle arrest in human astrocytic cells. *Metallomics* 2021;13. <https://doi.org/10.1093/MTOMCS/MFAA006>.
- [500] Kitazawa M, Hsu H-W, Medeiros R. Copper Exposure Perturbs Brain Inflammatory Responses and Impairs Clearance of Amyloid-Beta. *Toxicol Sci* 2016;152:194–204. <https://doi.org/10.1093/TOXSCI/KFW081>.
- [501] Newcombe EA, Camats-Perna J, Silva ML, Valmas N, Huat TJ, Medeiros R. Inflammation: the link between comorbidities, genetics, and Alzheimer’s disease. *J Neuroinflammation* 2018 151 2018;15:1–26. <https://doi.org/10.1186/S12974-018-1313-3>.
- [502] Bartolotti N, Bennett DA, Lazarov O. Reduced pCREB in Alzheimer’s disease

- prefrontal cortex is reflected in peripheral blood mononuclear cells. *Mol Psychiatry* 2016 219 2016;21:1158–66. <https://doi.org/10.1038/mp.2016.111>.
- [503] Rahman MH, Sarkar B, Islam MS, Abdullah MI. Discovering Biomarkers and Pathways Shared by Alzheimer's Disease and Parkinson's Disease to Identify Novel Therapeutic Targets. *Int J Eng Res Technol* 2020;9.
- [504] Ascolani A, Balestrieri E, Minutolo A, Mosti S, Spalletta G, Bramanti P, et al. Dysregulated NF- κ B Pathway in Peripheral Mononuclear Cells of Alzheimers Disease Patients. *Curr Alzheimer Res* 2012;9:128–37. <https://doi.org/10.2174/156720512799015091>.
- [505] Li H, Wang F, Guo X, Jiang Y. Decreased MEF2A Expression Regulated by Its Enhancer Methylation Inhibits Autophagy and May Play an Important Role in the Progression of Alzheimer's Disease. *Front Neurosci* 2021;0:669. <https://doi.org/10.3389/FNINS.2021.682247>.
- [506] Cong L, Cong Y, Feng N, Liang W, Wu Y. Up-regulated microRNA-132 reduces the cognition-damaging effect of sevoflurane on Alzheimer's disease rats by inhibiting FOXA1. *Genomics* 2021;113:3644–52. <https://doi.org/10.1016/J.YGENO.2021.08.011>.
- [507] Bartolotti N, Lazarov O. CREB signals as PBMC-based biomarkers of cognitive dysfunction: A novel perspective of the brain-immune axis. *Brain Behav Immun* 2019;78:9–20. <https://doi.org/10.1016/j.bbi.2019.01.004>.
- [508] Fielder E, Tweedy C, Wilson C, Oakley F, LeBeau FEN, Passos JF, et al. Anti-inflammatory treatment rescues memory deficits during aging in *nfkb1*^{-/-} mice. *Aging Cell* 2020;19. <https://doi.org/10.1111/accel.13188>.
- [509] Chow N, Bell RD, Deane R, Streb JW, Chen J, Brooks A, et al. Serum response factor and myocardin mediate arterial hypercontractility and cerebral blood flow dysregulation

- in Alzheimer's phenotype. *Proc Natl Acad Sci U S A* 2007;104:823–8.
<https://doi.org/10.1073/pnas.0608251104>.
- [510] Ho WM, Wu YY, Chen YC. Genetic variants behind cardiovascular diseases and dementia. *Genes (Basel)* 2020;11:1–16. <https://doi.org/10.3390/genes11121514>.
- [511] Dancy BM, Cole PA. Protein Lysine Acetylation by p300/CBP. *Chem Rev* 2015;115:2419. <https://doi.org/10.1021/CR500452K>.
- [512] Kang J, Lin C, Chen J, Liu Q. Copper induces histone hypoacetylation through directly inhibiting histone acetyltransferase activity. *Chem Biol Interact* 2004;148:115–23. <https://doi.org/10.1016/J.CBI.2004.05.003>.
- [513] Chen D, Kluz T, Fang L, Zhang X, Sun H, Jin C, et al. Hexavalent Chromium (Cr(VI)) Down-Regulates Acetylation of Histone H4 at Lysine 16 through Induction of Stressor Protein Nupr1 2016. <https://doi.org/10.1371/journal.pone.0157317>.
- [514] Xia B, Yang L qing, Huang H yan, Pang L, Hu G hua, Liu Q cheng, et al. Chromium(VI) causes down regulation of biotinidase in human bronchial epithelial cells by modifications of histone acetylation. *Toxicol Lett* 2011;205:140–5. <https://doi.org/10.1016/J.TOXLET.2011.05.1032>.
- [515] Zhou C, Liu M, Mei X, Li Q, Zhang W, Deng P, et al. Histone hypoacetylation contributes to neurotoxicity induced by chronic nickel exposure in vivo and in vitro. *Sci Total Environ* 2021;783:147014. <https://doi.org/10.1016/J.SCITOTENV.2021.147014>.
- [516] Guo Z, Tang J, Wang J, Zheng F, Zhang C, Wang YL, et al. The negative role of histone acetylation in cobalt chloride-induced neurodegenerative damages in SHSY5Y cells. *Ecotoxicol Environ Saf* 2021;209:111832. <https://doi.org/10.1016/J.ECOENV.2020.111832>.
- [517] Shobana N, Kumar MK, Navin AK, Akbarsha MA, Aruldhas MM. Prenatal exposure to excess chromium attenuates transcription factors regulating expression of androgen and

- follicle stimulating hormone receptors in Sertoli cells of prepuberal rats. *Chem Biol Interact* 2020;328:109188. <https://doi.org/10.1016/J.CBI.2020.109188>.
- [518] Liao MY, Liu HG. Gene expression profiling of nephrotoxicity from copper nanoparticles in rats after repeated oral administration. *Environ Toxicol Pharmacol* 2012;34:67–80. <https://doi.org/10.1016/J.ETAP.2011.05.014>.
- [519] Fujita K, Morimoto Y, Ogami A, Myojyo T, Tanaka I, Shimada M, et al. Gene expression profiles in rat lung after inhalation exposure to C60 fullerene particles. *Toxicology* 2009;258:47–55. <https://doi.org/10.1016/J.TOX.2009.01.005>.
- [520] JA S, RJ B, Y W, A B. Chromium(VI) inhibits the transcriptional activity of nuclear factor-kappaB by decreasing the interaction of p65 with cAMP-responsive element-binding protein-binding protein. *J Biol Chem* 1999;274:36207–12. <https://doi.org/10.1074/JBC.274.51.36207>.
- [521] Gray MJ, Zhang J, Ellis LM, Semenza GL, Evans DB, Watowich SS, et al. HIF-1 α , STAT3, CBP/p300 and Ref-1/APE are components of a transcriptional complex that regulates Src-dependent hypoxia-induced expression of VEGF in pancreatic and prostate carcinomas. *Oncogene* 2005 2419 2005;24:3110–20. <https://doi.org/10.1038/sj.onc.1208513>.
- [522] Wang D, Fei Z, Luo S, Wang H. MiR-335-5p Inhibits β -Amyloid (A β) Accumulation to Attenuate Cognitive Deficits Through Targeting c-jun-N-terminal Kinase 3 in Alzheimer's Disease. *Curr Neurovasc Res* 2020;17:93–101. <https://doi.org/10.2174/1567202617666200128141938>.
- [523] Zeng Z, Liu Y, Zheng W, Liu L, Yin H, Zhang S, et al. MicroRNA-129-5p alleviates nerve injury and inflammatory response of Alzheimer's disease via downregulating SOX6. *Cell Cycle* 2019;18:3095–110. <https://doi.org/10.1080/15384101.2019.1669388>.

- [524] Li Z, Chen Q, Liu J, Du Y. Physical Exercise Ameliorates the Cognitive Function and Attenuates the Neuroinflammation of Alzheimer's Disease via miR-129-5p. *Dement Geriatr Cogn Disord* 2020;49:163–9. <https://doi.org/10.1159/000507285>.
- [525] Fay MJ, Alt LAC, Ryba D, Salamah R, Peach R, Papaeliou A, et al. Cadmium Nephrotoxicity Is Associated with Altered MicroRNA Expression in the Rat Renal Cortex. *Toxics* 2018;6. <https://doi.org/10.3390/TOXICS6010016>.
- [526] Ngalame NNO, Waalkes MP, Tokar EJ. Silencing KRAS Overexpression in Cadmium-Transformed Prostate Epithelial Cells Mitigates Malignant Phenotype. *Chem Res Toxicol* 2016;29:1458. <https://doi.org/10.1021/ACS.CHEMRESTOX.6B00137>.
- [527] Barr I, Weitz SH, Atkin T, Hsu P, Karayiorgou M, Gogos JA, et al. Cobalt (III) protoporphyrin activates the DGCR8 protein and can compensate microRNA processing deficiency. *Chem Biol* 2015;22:793. <https://doi.org/10.1016/J.CHEMBIOL.2015.05.015>.
- [528] Jeon ES, Shin JH, Hwang SJ, Moon GJ, Bang OY, Kim HH. Cobalt chloride induces neuronal differentiation of human mesenchymal stem cells through upregulation of microRNA-124a. *Biochem Biophys Res Commun* 2014;444:581–7. <https://doi.org/10.1016/J.BBRC.2014.01.114>.
- [529] Chiou YH, Liou SH, Wong RH, Chen CY, Lee H. Nickel may contribute to EGFR mutation and synergistically promotes tumor invasion in EGFR-mutated lung cancer via nickel-induced microRNA-21 expression. *Toxicol Lett* 2015;237:46–54. <https://doi.org/10.1016/J.TOXLET.2015.05.019>.
- [530] Wu C-H, Hsiao Y-M, Yeh K-T, Tsou T-C, Chen C-Y, Wu M-F, et al. Upregulation of microRNA-4417 and Its Target Genes Contribute to Nickel Chloride-promoted Lung Epithelial Cell Fibrogenesis and Tumorigenesis. *Sci Reports* 2017 71 2017;7:1–13. <https://doi.org/10.1038/s41598-017-14610-7>.

- [531] Xu M, Yu Z, Hu F, Zhang H, Zhong L, Han L, et al. Identification of differential plasma miRNA profiles in Chinese workers with occupational lead exposure. *Biosci Rep* 2017;37:20171111. <https://doi.org/10.1042/BSR20171111>.
- [532] Ghaffari SH, Bashash D, dizaji MZ, Ghavamzadeh A, Alimoghaddam K. Alteration in miRNA gene expression pattern in acute promyelocytic leukemia cell induced by arsenic trioxide: a possible mechanism to explain arsenic multi-target action. *Tumor Biol* 2011 33:157–72. <https://doi.org/10.1007/S13277-011-0259-1>.
- [533] Jia J, Li T, Yao C, Chen J, Feng L, Jiang Z, et al. Circulating differential miRNAs profiling and expression in hexavalent chromium exposed electroplating workers. *Chemosphere* 2020;260. <https://doi.org/10.1016/J.CHEMOSPHERE.2020.127546>.
- [534] Chandra S, Pandey A, Chowdhuri DK. miRNA profiling provides insights on adverse effects of Cr(VI) in the midgut tissues of *Drosophila melanogaster*. *J Hazard Mater* 2015;283:558–67. <https://doi.org/10.1016/J.JHAZMAT.2014.09.054>.
- [535] Mao H, Huang Q, Liu Y. MEG3 aggravates hypoxia/reoxygenation induced apoptosis of renal tubular epithelial cells via the miR-129-5p/HMGB1 axis. *J Biochem Mol Toxicol* 2021;35:e22649. <https://doi.org/10.1002/JBT.22649>.
- [536] Zhu X, Li Z, Li L, Chen L, Ouyang M, Zhou H, et al. KCTD1 Downregulation Suppresses Hepatocellular Carcinoma by Regulating Angiogenesis and Influencing the HIF-1 α /VEGF Pathway 2021. <https://doi.org/10.21203/rs.3.rs-419484/v1>.
- [537] Belaya Z, Khandaeva P, Nonn L, Nikitin A, Solodovnikov A, Sitkin I, et al. Circulating Plasma microRNA to Differentiate Cushing's Disease From Ectopic ACTH Syndrome. *Front Endocrinol (Lausanne)* 2020;0:331. <https://doi.org/10.3389/FENDO.2020.00331>.
- [538] Yang Y, Gong B, Wu Z-Z, Shuai P, Li D-F, Liu L-L, et al. Inhibition of microRNA-129-5p expression ameliorates ultraviolet ray-induced corneal epithelial cell injury via upregulation of EGFR. *J Cell Physiol* 2019;234:11692–707.

<https://doi.org/10.1002/JCP.27837>.

- [539] Tian J, Song T, Wang W, Wang H, Zhang Z. miR-129-5p Alleviates Neuropathic Pain Through Regulating HMGB1 Expression in CCI Rat Models. *J Mol Neurosci* 2019 701 2019;70:84–93. <https://doi.org/10.1007/S12031-019-01403-Y>.
- [540] Glaesel K, May C, Marcus K, Matschke V, Theiss C, Theis V. miR-129-5p and miR-130a-3p Regulate VEGFR-2 Expression in Sensory and Motor Neurons during Development. *Int J Mol Sci* 2020, Vol 21, Page 3839 2020;21:3839. <https://doi.org/10.3390/IJMS21113839>.
- [541] Li X-Q, Chen F-S, Tan W-F, Fang B, Zhang Z-L, Ma H. Elevated microRNA-129-5p level ameliorates neuroinflammation and blood-spinal cord barrier damage after ischemia-reperfusion by inhibiting HMGB1 and the TLR3-cytokine pathway. *J Neuroinflammation* 2017 141 2017;14:1–12. <https://doi.org/10.1186/S12974-017-0977-4>.
- [542] Li J, Feng Z, Chen L, Wang X, Deng H. MicroRNA-335-5p inhibits osteoblast apoptosis induced by high glucose. *Mol Med Rep* 2016;13:4108–12. <https://doi.org/10.3892/MMR.2016.4994>.
- [543] Yu B, Wang B, Wu Z, Wu C, Ling J, Gao X, et al. LncRNA SNHG8 Promotes Proliferation and Inhibits Apoptosis of Diffuse Large B-Cell Lymphoma via Sponging miR-335-5p. *Front Oncol* 2021;11:650287. <https://doi.org/10.3389/FONC.2021.650287>.
- [544] Yue J, Wang P, Hong Q, Liao Q, Yan L, Xu W, et al. MicroRNA-335-5p Plays Dual Roles in Periapical Lesions by Complex Regulation Pathways. *J Endod* 2017;43:1323–8. <https://doi.org/10.1016/J.JOEN.2017.03.018>.
- [545] Khokhar M, Tomo S, Purohit P. Micro RNA-based regulation of genomics and transcriptomics of inflammatory cytokines in COVID-19. *MedRxiv*

2021:2021.06.08.21258565. <https://doi.org/10.1101/2021.06.08.21258565>.

- [546] Zeng H, Wang J, Chen T, Zhang K, Chen J, Wang L, et al. Downregulation of long non-coding RNA Opa interacting protein 5-antisense RNA 1 inhibits breast cancer progression by targeting sex-determining region Y-box 2 by microRNA-129-5p upregulation. *Cancer Sci* 2019;110:289–302. <https://doi.org/10.1111/cas.13879>.
- [547] Luthra PM. Paradigm of protein folding in neurodegenerative diseases. *Protein Fold.*, 2011.
- [548] Nussbaum RL, Ellis CE. Alzheimer's disease and Parkinson's disease. *N Engl J Med* 2003. <https://doi.org/10.1056/NEJM2003ra020003>.
- [549] Kollmer M, Close W, Funk L, Rasmussen J, Bsoul A, Schierhorn A, et al. Cryo-EM structure and polymorphism of A β amyloid fibrils purified from Alzheimer's brain tissue. *Nat Commun* 2019 10:1–8. <https://doi.org/10.1038/s41467-019-12683-8>.
- [550] Bu X-L, Xiang Y, Jin W-S, Wang J, Shen L-L, Huang Z-L, et al. Blood-derived amyloid- β protein induces Alzheimer's disease pathologies. *Mol Psychiatry* 2018 239 2017;23:1948–56. <https://doi.org/10.1038/mp.2017.204>.
- [551] Zheng T, Zhang Z. Activated microglia facilitate the transmission of α -synuclein in Parkinson's disease. *Neurochem Int* 2021;148:105094. <https://doi.org/10.1016/J.NEUINT.2021.105094>.
- [552] Chang C-W, Yang S-Y, Yang C-C, Chang C-W, Wu Y-R. Plasma and Serum Alpha-Synuclein as a Biomarker of Diagnosis in Patients With Parkinson's Disease. *Front Neurol* 2020;0:1388. <https://doi.org/10.3389/FNEUR.2019.01388>.
- [553] Si X, Tian J, Chen Y, Yan Y, Pu J, Zhang B. Central Nervous System-Derived Exosomal Alpha-Synuclein in Serum May Be a Biomarker in Parkinson's Disease. *Neuroscience* 2019;413:308–16. <https://doi.org/10.1016/J.NEUROSCIENCE.2019.05.015>.

- [554] Bao J, Zheng L, Zhang Q, Li X, Zhang X, Li Z, et al. Deacetylation of TFEB promotes fibrillar A β degradation by upregulating lysosomal biogenesis in microglia. *Protein Cell* 2016. <https://doi.org/10.1007/s13238-016-0269-2>.
- [555] Luca C, Garamszegi S, Eldick D, Singer C, Mash D. Altered SIRT4 Expression Is Associated with Lewy Body Pathology (P01.209). *Neurology* 2012. https://doi.org/10.1212/wnl.78.1_meetingabstracts.p01.209.
- [556] Wang L, Shi F-X, Li N, Cao Y, Lei Y, Wang J-Z, et al. AMPK Ameliorates Tau Acetylation and Memory Impairment Through Sirt1. *Mol Neurobiol* 2020 5712 2020;57:5011–25. <https://doi.org/10.1007/S12035-020-02079-X>.
- [557] Fusco S, Leone L, Barbati SA, Samengo D, Piacentini R, Maulucci G, et al. A CREB-Sirt1-Hes1 Circuitry Mediates Neural Stem Cell Response to Glucose Availability. *Cell Rep* 2016;14:1195–205. <https://doi.org/10.1016/J.CELREP.2015.12.092>.

LIST OF PUBLICATIONS

Cumulative Impact Factor

Cumulative impact factor of all publications	=	106.03
h-index and i-10 index	=	6 and 3
Cumulative citation index	=	187

PUBLICATIONS FROM THESIS

1. **Rohan Gupta** and Pravir Kumar, “Computational Analysis Indicates That PARP1 Acts as a Histone Deacetylases Interactor Sharing Common Lysine Residues for Acetylation, Ubiquitination, and SUMOylation in Alzheimer’s and Parkinson’s Disease”, *ACS Omega*, DOI: <https://doi.org/10.1021/acsomega.0c06168>. **IF: 4.13** (ACS).
2. **Rohan Gupta** and Pravir Kumar, “CREB1^{K292} and HINFP^{K330} as Putative Common Therapeutic Targets in Alzheimer’s and Parkinson’s Disease”, *ACS Omega*, DOI: <https://doi.org/10.1021/acsomega.1c05827>. **IF: 4.13** (ACS).
3. **Rohan Gupta** and Pravir Kumar, “Integrative analysis of OIP5-AS1/miR-129-5p/CREBBP axis as a potential therapeutic candidate in the pathogenesis of metal toxicity-induced Alzheimer's disease”, *Gene Reports*, DOI: <http://dx.doi.org/10.1016/j.genrep.2021.101442>. **IF:1.51** (Elsevier)
4. **Rohan Gupta**, Mehar Sahu, Devesh Srivastava, Swati Tiwari, Rashmi K Ambasta, and Pravir Kumar, “Post-translational modifications: Regulators of neurodegenerative proteinopathies”, *Ageing Research Reviews*, DOI: <https://doi.org/10.1016/j.arr.2021.101336>. **IF: 11.12** (Elsevier).
5. **Rohan Gupta**, Rashmi K Ambasta, and Pravir Kumar, “Multifaced role of protein deacetylase sirtuins in neurodegenerative disease”, *Neuroscience and Biobehavioral Reviews*, DOI: <https://doi.org/10.1016/j.neubiorev.2021.10.047>. **IF: 9.05** (Elsevier).
6. **Rohan Gupta**, Rashmi K Ambasta, and Pravir Kumar, “Pharmacological intervention of histone deacetylase enzymes in the neurodegenerative disorders”, *Life Sciences*, DOI:

<https://doi.org/10.1016/j.lfs.2020.117278>. **IF: 6.78** (Elsevier).

7. **Rohan Gupta**, Rashmi K Ambasta, and Pravir Kumar, “Histone deacetylase in neuropathology”, *Advances in Clinical Chemistry*, DOI: <https://doi.org/10.1016/bs.acc.2020.09.004>. **IF: 6.30** (Elsevier).

OTHER PUBLICATIONS

1. **Rohan Gupta**, Rashmi K Ambasta, and Pravir Kumar, “Identification of novel class I and class IIb histone deacetylase inhibitor for Alzheimer's disease therapeutics”, *Life Sciences*, DOI: <https://doi.org/10.1016/j.lfs.2020.117912>. **IF: 6.78** (Elsevier).
2. **Rohan Gupta**, Mehar Sahu, Rahul Tripathi, Rashmi K Ambasta, and Pravir Kumar, “Protein S-sulfhydration: Unravelling the prospective of hydrogen sulfide in the brain, vasculature and neurological manifestations”, *Ageing Research Reviews*, DOI: <https://doi.org/10.1016/j.arr.2022.101579>. **IF: 11.12** (Elsevier).
3. **Rohan Gupta**, Rashmi K Ambasta, and Pravir Kumar, “Autophagy and apoptosis cascade: which is more prominent in neuronal death?”, *Cellular and Molecular Life Sciences*, DOI: <https://doi.org/10.1007/s00018-021-04004-4>. **IF: 9.20** (Springer).
4. **Rohan Gupta**, Ankita Jha, Rashmi K Ambasta, and Pravir Kumar, “Regulatory mechanism of cyclins and cyclin-dependent kinases in post-mitotic neuronal cell division”, *Life Sciences*, DOI: <https://doi.org/10.1016/j.lfs.2021.120006>. **IF: 6.78** (Elsevier).
5. **Rohan Gupta**, Mehar Sahu, Devesh Srivastava, Swati Tiwari, Rashmi K Ambasta, and Pravir Kumar, “Artificial intelligence to deep learning: Machine intelligence approach for drug discovery”, *Molecular Diversity*, DOI: <https://doi.org/10.1007/s11030-021-10217-3>. **IF: 3.36** (Springer).
6. Mehar Sahu, **Rohan Gupta**, Rashmi K Ambasta, Pravir Kumar, “Artificial intelligence and machine learning in precision medicine: A paradigm shift in big data analysis”, *Progress in Molecular Biology and Translational Science*. **IF: 4.07** (Elsevier)

7. Rahul Tripathi, **Rohan Gupta**, Mehar Sahu, Devesh Srivastava, Ankita Das, Rashmi K Ambasta, and Pravir Kumar, “Free radical biology in neurological manifestations: mechanisms to therapeutics interventions”, *Environmental Science and Pollution Research*, DOI: <https://doi.org/10.1007/s11356-021-16693-2>. **IF: 5.19** (Springer).
8. Vaibhav Oli, **Rohan Gupta**, and Pravir Kumar, “FOXO and related transcription factors binding elements in the regulation of neurodegenerative disorders”, *Journal of Chemical Neuroanatomy*, DOI: <https://doi.org/10.1016/j.jchemneu.2021.102012>. **IF: 3.09** (Elsevier).
9. Nishtha Malhotra, **Rohan Gupta**, and Pravir Kumar, “Pharmacological relevance of CDK inhibitors in Alzheimer's disease” *Neurochemistry International*, DOI: <https://doi.org/10.1016/j.neuint.2021.105115>. **IF: 4.29** (Elsevier).
10. Dia Advani, **Rohan Gupta**, Rahul Tripathi, Sudhanshu Sharma, Rashmi K Ambasta, and Pravir Kumar, “Protective role of anticancer drugs in neurodegenerative disorders: a drug repurposing approach”, *Neurochemistry International*, DOI: <https://doi.org/10.1016/j.neuint.2020.104841>. **IF: 4.29** (Elsevier).
11. Rashmi K Ambasta, **Rohan Gupta**, Dhiraj Kumar, Saurabh Bhattacharya, Aditi Sarkar, and Pravir Kumar, “Can luteolin be a therapeutic molecule for both colon cancer and diabetes?”, *Briefings in Functional Genomics*, DOI: <https://doi.org/10.1093/bfpg/ely036>. **IF: 4.84** (Oxford).

BOOK CHAPTERS

1. **Rohan Gupta**, Rashmi K Ambasta, and Pravir Kumar, “Mitochondrial dysfunction and autophagy in neurodegeneration”, “Mitochondrial Dysfunction and Nanotherapeutics (Elsevier); Aging, Diseases, and Nanotechnology-Related Strategies in Mitochondrial Medicine”
2. Dia Advani, Sudhanshu Sharma, Rahul Tripathi, **Rohan Gupta**, Asmita Jaiswal, Rashmi K Ambasta, and Pravir Kumar, “Mitochondrial dysfunction in metabolic disorders”,

“Mitochondrial Dysfunction and Nanotherapeutics (Elsevier), Aging, Diseases, and Nanotechnology-Related Strategies in Mitochondrial Medicine”

CONFERENCES AND WORKSHOPS

1. **Rohan Gupta** and Pravir Kumar (2019), mi-RNA regulatory pathway network and associate biomarkers in Alzheimer's Disease, SSCI October 2019, Jamia Hamdard, Delhi, India. [Poster presentation]
2. **Rohan Gupta**, Rashmi K Ambasta, and Pravir Kumar (2018), Novel inhibitor of histone deacetylase for Alzheimer's disease therapy using machine learning based virtual screening, Punjab university, Patiala, Punjab, India. [Poster presentation]

ROHAN GUPTA,

Phone: +91-9711803142, +91-8700101539

E-Mail: rohangupta_phd2k19@dtu.ac.in, rohangupta1394@gmail.com

Corresponding Address:

Molecular Neuroscience and Functional Genomics Laboratory, Department of Biotechnology, Delhi Technological University, Shahbad Daultapur, Bawana Road, Delhi: 110042

Current Status: PhD thesis is in submission stage

EDUCATIONAL BACKGROUND

2019-present	Delhi Technological University	Ph.D.	Molecular Neurobiology, Biotechnology
2016-2018	Delhi Technological University	M.Tech.	Bioinformatics
2012-2016	Dr. B R Ambedkar National Institute of Technology (NIT), Jalandhar	B.Tech.	Biotechnology

PERSONAL STATEMENT

My scientific research interests involve the mechanism of lysine-induced post-translational mechanism and its associated enzymes in the pathogenesis of neurodegenerative diseases through the involvement of multiple signaling pathways. My academic training, research experience, teaching assistance, and scientific training experience have provided me with excellent background on multiple discipline, such as computational biology, neuroinformatics, biomedical informatics, drug designing, drug discovery, proteomic studies, genetics, and molecular biology. As a master's student, I was feeling lucky to work under the supervision of Prof. Pravir Kumar on the identification of novel histone deacetylase inhibitor as a therapeutic approach for Alzheimer's disease. I gained the expertise in the machine learning models, network biology, and transcriptional regulation of disease progression. As a doctoral student under the supervision of Prof. Pravir Kumar, I was able to implement my experience of computational biology, machine learning, bioinformatics tools, network and structural biology in identification of acetylation and HDACs mechanism in the pathogenesis of neurodegenerative disease, especially AD and PD. In my doctoral training, I published several first author papers in major journals, namely ageing research reviews, neuroscience and biobehavioral reviews, cellular and molecular life sciences, life sciences, molecular diversity, ACS omega, and many others. In my recent publication, I concluded the importance of critical lysine residues and its corresponding transcription factors binding element. I also aim to identify crosstalk between different post-translational modifications, such as ubiquitination, acetylation, and SUMOylation on HDAC interactor, namely PARP in the crosstalk of AD and PD. Further, we also aim to identify the potential micro-RNAs and long non-coding RNAs that interfere with acetylation mechanism in the pathogenesis of AD and PD, simultaneously. Later on, we aim to identify potential HDAC multi-target drug ligand through machine learning and molecular docking approach that will be act as potential therapeutic agent in AD and PD. In my doctoral training, I received research excellence award in 2020 and 2021, organized by Delhi Technological University. For my postdoctoral training, I will continue to build on my

previous training on regulation of disease progression through involvement of post-translational modification and multiple signaling pathways.

POSITIONS AND TRAINING

Teaching Assistant:

- **ADVANCED GENETIC ENGINEERING LABORATORY (BIO5402)**
The subject focusses on the techniques in genetic engineering, namely DNA and RNA isolation, DNA gel electrophoresis, RNA gel electrophoresis, and polymerase chain reaction (PCR).
- **ADVANCED PROTEOMICS LABORATORY (BIO503)**
The subject was taught to master students that focusses on the techniques of proteomics studies, namely protein isolation and electrophoresis, immunofluorescence techniques, EMSA, and others.
- **CELL AND MOLECULAR BIOLOGY LABORATORY (BIO6405)**
The subject discusses the different experimental techniques based on DNA and RNA isolation, gel electrophoresis, DNA and RNA quantification.
- **GENETIC ENGINEERING LABORATORY (MSBT106)**
The subject taught the experimental methods employed in genetic engineering, namely DNA and RNA isolation, DNA gel electrophoresis, RNA gel electrophoresis, and polymerase chain reaction (PCR).

Training Experience

- Post-conference workshop on "Neurological Disorders: Advances in Research Techniques and Translational Applications", 13th to 19th October 2019, SNCI, Jamia Hamdard, Delhi, India.
- International E-Workshop on Bioinformatics sponsored by DTU, 14th to 18th December, 2020, Department of Biotechnology, Delhi Technological University, Delhi, India.
- 5 Day Online Workshop in Drug Discovery Technology organized by BDG Lifesciences, 21st to 25th December, 2020.
- One Day Workshop on "Big Data in Genomics" Organized by the Center for Computational Biology, 4th Feb, 2017, by IIIT-Delhi, Delhi, India.
- TEQIP-II Sponsored Conference on "Application of Biotechnology in Industry and Society (ABIS-2016) Organized by Department of Biotechnology, Dr. B R Ambedkar National Institute of Technology, 12th to 14th April, 2016, Jalandhar, Punjab, India.

CONTRIBUTION TO SCIENCE

1. **Early Career:** My early career focusses on identification of novel therapeutic agent against histone deacetylases that reverses the progression of AD through computational analysis, including machine learning models. The study incorporated four different machine learning model and train the model on over 3000 compounds and classify over 5000 compounds into HDAC inhibitors and non-inhibitors. Screening of potential inhibitor compounds yield ChEMB11834473 as potential class I and class IIb HDAC isoform inhibitor.
2. **Doctoral Career:** In doctoral career, I forwarded my initially studies to a next level and working on the project entitled "HDAC enzymes in NDDs" and "Machine learning and

artificial intelligence in drug discovery. I am interested to dissect the role of lysine-induced post-translational modification, especially acetylation, ubiquitination, and SUMOylation in gene regulation through involvement of multiple signaling events and signaling molecules. I originally reported the role of HDAC interactor PARP's critical lysine residue that will reverse the disease progression and rescue neuronal apoptosis. In addition, I reported the role of OIP5-AS1/miR-129-5p/CREBBP axis as a potential therapeutic candidate in the pathogenesis of Alzheimer's disease.

PUBLICATIONS AND PRESENTATIONS

Cumulative Impact Factor

Cumulative impact factor of all publications	=	106.03
h-index and i-10 index	=	6 and 3
Cumulative citation index	=	187

First Author Publications

8. **Rohan Gupta**, Rashmi K Ambasta, and Pravir Kumar, "Identification of novel class I and class IIb histone deacetylase inhibitor for Alzheimer's disease therapeutics", *Life Sciences*, DOI: <https://doi.org/10.1016/j.lfs.2020.117912>. **IF: 6.78** (Elsevier).
9. **Rohan Gupta** and Pravir Kumar, "Computational Analysis Indicates That PARP1 Acts as a Histone Deacetylases Interactor Sharing Common Lysine Residues for Acetylation, Ubiquitination, and SUMOylation in Alzheimer's and Parkinson's Disease", *ACS Omega*, DOI: <https://doi.org/10.1021/acsomega.0c06168>. **IF: 4.13** (ACS).
10. **Rohan Gupta** and Pravir Kumar, "CREB1^{K292} and HINFP^{K330} as Putative Common Therapeutic Targets in Alzheimer's and Parkinson's Disease", *ACS Omega*, DOI: <https://doi.org/10.1021/acsomega.1c05827>. **IF: 4.13** (ACS).
11. **Rohan Gupta** and Pravir Kumar, "Integrative analysis of OIP5-AS1/miR-129-5p/CREBBP axis as a potential therapeutic candidate in the pathogenesis of metal toxicity-induced Alzheimer's disease", *Gene Reports*, DOI: <http://dx.doi.org/10.1016/j.genrep.2021.101442>. **IF:1.51** (Elsevier).
12. **Rohan Gupta**, Mehar Sahu, Devesh Srivastava, Swati Tiwari, Rashmi K Ambasta, and Pravir Kumar, "Post-translational modifications: Regulators of neurodegenerative proteinopathies", *Ageing Research Reviews*, DOI: <https://doi.org/10.1016/j.arr.2021.101336>. **IF: 11.12** (Elsevier).
13. **Rohan Gupta**, Mehar Sahu, Rahul Tripathi, Rashmi K Ambasta, and Pravir Kumar, "Protein S-sulfhydration: Unravelling the prospective of hydrogen sulfide in the brain, vasculature and neurological manifestations", *Ageing Research Reviews*, DOI: <https://doi.org/10.1016/j.arr.2022.101579>. **IF: 11.12** (Elsevier).
14. **Rohan Gupta**, Rashmi K Ambasta, and Pravir Kumar, "Autophagy and apoptosis cascade: which is more prominent in neuronal death?", *Cellular and Molecular Life Sciences*, DOI: <https://doi.org/10.1007/s00018-021-04004-4>. **IF: 9.20** (Springer).
15. **Rohan Gupta**, Rashmi K Ambasta, and Pravir Kumar, "Multifaced role of protein deacetylase sirtuins in neurodegenerative disease", *Neuroscience and Biobehavioral Reviews*, DOI: <https://doi.org/10.1016/j.neubiorev.2021.10.047>. **IF: 9.05** (Elsevier).
16. **Rohan Gupta**, Ankita Jha, Rashmi K Ambasta, and Pravir Kumar, "Regulatory mechanism of cyclins and cyclin-dependent kinases in post-mitotic neuronal cell division", *Life Sciences*, DOI: <https://doi.org/10.1016/j.lfs.2021.120006>. **IF: 6.78** (Elsevier).

17. **Rohan Gupta**, Mehar Sahu, Devesh Srivastava, Swati Tiwari, Rashmi K Ambasta, and Pravir Kumar, "Artificial intelligence to deep learning: Machine intelligence approach for drug discovery", *Molecular Diversity*, DOI: <https://doi.org/10.1007/s11030-021-10217-3>. **IF: 3.36** (Springer).
18. **Rohan Gupta**, Rashmi K Ambasta, and Pravir Kumar, "Pharmacological intervention of histone deacetylase enzymes in the neurodegenerative disorders", *Life Sciences*, DOI: <https://doi.org/10.1016/j.lfs.2020.117278>. **IF: 6.78** (Elsevier).
19. **Rohan Gupta**, Rashmi K Ambasta, and Pravir Kumar, "Histone deacetylase in neuropathology", *Advances in Clinical Chemistry*, DOI: <https://doi.org/10.1016/bs.acc.2020.09.004>. **IF: 6.30** (Elsevier).

Co-Author Publications

1. Mehar Sahu, **Rohan Gupta**, Rashmi K Ambasta, Pravir Kumar, "Artificial intelligence and machine learning in precision medicine: A paradigm shift in big data analysis", *Progress in Molecular Biology and Translational Science*. **IF: 4.07** (Elsevier)
2. Rahul Tripathi, **Rohan Gupta**, Mehar Sahu, Devesh Srivastava, Ankita Das, Rashmi K Ambasta, and Pravir Kumar, "Free radical biology in neurological manifestations: mechanisms to therapeutics interventions", *Environmental Science and Pollution Research*, DOI: <https://doi.org/10.1007/s11356-021-16693-2>. **IF: 5.19** (Springer).
3. Vaibhav Oli, **Rohan Gupta**, and Pravir Kumar, "FOXO and related transcription factors binding elements in the regulation of neurodegenerative disorders", *Journal of Chemical Neuroanatomy*, DOI: <https://doi.org/10.1016/j.jchemneu.2021.102012>. **IF: 3.09** (Elsevier).
4. Nishtha Malhotra, **Rohan Gupta**, and Pravir Kumar, "Pharmacological relevance of CDK inhibitors in Alzheimer's disease" *Neurochemistry International*, DOI: <https://doi.org/10.1016/j.neuint.2021.105115>. **IF: 4.29** (Elsevier).
5. Dia Advani, **Rohan Gupta**, Rahul Tripathi, Sudhanshu Sharma, Rashmi K Ambasta, and Pravir Kumar, "Protective role of anticancer drugs in neurodegenerative disorders: a drug repurposing approach", *Neurochemistry International*, DOI: <https://doi.org/10.1016/j.neuint.2020.104841>. **IF: 4.29** (Elsevier).
6. Rashmi K Ambasta, **Rohan Gupta**, Dhiraj Kumar, Saurabh Bhattacharya, Aditi Sarkar, and Pravir Kumar, "Can luteolin be a therapeutic molecule for both colon cancer and diabetes?", *Briefings in Functional Genomics*, DOI: <https://doi.org/10.1093/bfpg/ely036>. **IF: 4.84** (Oxford).

Book Chapters

- **Rohan Gupta**, Rashmi K Ambasta, and Pravir Kumar, "Mitochondrial dysfunction and autophagy in neurodegeneration", "Mitochondrial Dysfunction and Nanotherapeutics (Elsevier); Aging, Diseases, and Nanotechnology-Related Strategies in Mitochondrial Medicine"
- Dia Advani, Sudhanshu Sharma, Rahul Tripathi, **Rohan Gupta**, Asmita Jaiswal, Rashmi K Ambasta, and Pravir Kumar, "Mitochondrial dysfunction in metabolic disorders", "Mitochondrial Dysfunction and Nanotherapeutics (Elsevier), Aging, Diseases, and Nanotechnology-Related Strategies in Mitochondrial Medicine"

Presentations in National/International Conferences

- **Rohan Gupta** and Pravir Kumar (2019), mi-RNA regulatory pathway network and associate biomarkers in Alzheimer's Disease, SNCI October 2019, Jamia Hamdard, Delhi, India. [Poster presentation]
- **Rohan Gupta**, Rashmi K Ambasta, and Pravir Kumar (2018), Novel inhibitor of

histone deacetylase for Alzheimer's disease therapy using machine learning based virtual screening, Punjab university, Patiala, Punjab, India. [Poster presentation]

REFERENCES

1. Prof. Pravir Kumar, PhD

Professor and Head, Department of Biotechnology
Molecular Neuroscience and Functional Genomics Laboratory
Former Dean, Delhi Technological University (Formerly Delhi College of Engineering)
Former Faculty, Tufts University School of Medicine, Boston, MA, USA
Room# FW4TF3, Mechanical Engineering Building
Shahbad Daulatpur, Bawana Road, Delhi 110042; Phone: +91- 9818898622
Email: pravirkumar@dtu.ac.in; kpravir@gmail.com

2. Dr. Rashmi K Ambasta, PhD

CSIR Scientific Pool Officer
Former Principal Investigator of SERB-DST at DTU
Email: rashmiambasta@gmail.com

3. Dr. Nirala Ramchiary, PhD

Assistant Professor
Room: 229, School of Life Sciences
Jawaharlal Nehru University, Delhi
Email: nramchiary@mail.jnu.ac.in

DECLARATION

I hereby declare that the given above information is accurate to the best of my knowledge and belief and can be supported with reliable documents when needed.

Rohan Gupta
Date: 08.08.2022
Place: New Delhi

PAPER NAME

Acetylation Mechanism and HDAC Enzymes in Neurodegenerative Diseases

AUTHOR

Rohan Gupta 2K18/PHDBT/501

WORD COUNT

63398 Words

CHARACTER COUNT

409763 Characters

PAGE COUNT

281 Pages

FILE SIZE

9.3MB

SUBMISSION DATE

Sep 14, 2022 2:39 PM GMT+5:30

REPORT DATE

Sep 14, 2022 2:44 PM GMT+5:30

● **6% Overall Similarity**

The combined total of all matches, including overlapping sources, for each database.

- 3% Internet database
- 3% Publications database
- Crossref database
- Crossref Posted Content database
- 4% Submitted Works database

● **Excluded from Similarity Report**

- Bibliographic material
- Quoted material
- Cited material
- Small Matches (Less than 8 words)
- Manually excluded sources

● **6% Overall Similarity**

Top sources found in the following databases:

- 3% Internet database
- Crossref database
- 4% Submitted Works database
- 3% Publications database
- Crossref Posted Content database

TOP SOURCES

The sources with the highest number of matches within the submission. Overlapping sources will not be displayed.

1	Vels University on 2017-05-29 Submitted works	1%
2	rj-robbins.com Internet	<1%
3	ouci.dntb.gov.ua Internet	<1%
4	link.springer.com Internet	<1%
5	University of Sheffield on 2021-12-09 Submitted works	<1%
6	Erasmus University of Rotterdam on 2021-05-16 Submitted works	<1%
7	Masha G. Savelieff, Geewoo Nam, Juhye Kang, Hyuck Jin Lee, Misun L... Crossref	<1%
8	Vaibhav Oli, Rohan Gupta, Pravir Kumar. "FOXO and related transcriptio... Crossref	<1%

- 9

"Handbook of Nutrition, Diet, and Epigenetics", Springer Science and B...

Crossref

<1%
- 10

Ágnes Kasza. "Rodent models of Alzheimer's disease", University of Sz...

Crossref posted content

<1%
- 11

University of Sydney on 2019-07-02

Submitted works

<1%
- 12

Systems Biology of Free Radicals and Antioxidants, 2014.

Crossref

<1%
- 13

Rohan Gupta, Rashmi K. Ambasta, Pravir Kumar. "Multifaced role of pr...

Crossref

<1%
- 14

Anglia Ruskin University on 2020-04-30

Submitted works

<1%
- 15

hdl.handle.net

Internet

<1%
- 16

Swinburne University of Technology on 2015-09-03

Submitted works

<1%
- 17

Rohan Gupta, Mehar Sahu, Rahul Tripathi, Rashmi K. Ambasta, Pravir K...

Crossref

<1%
- 18

"The DNA, RNA, and Histone Methylomes", Springer Science and Busin...

Crossref

<1%
- 19

Eli J. Cornblath, John L. Robinson, Virginia M.-Y. Lee, John Q. Trojano...

Crossref posted content

<1%
- 20

Marmara University on 2021-04-27

Submitted works

<1%

- 21

"Chemical Epigenetics", Springer Science and Business Media LLC, 2020

Crossref

<1%
- 22

University of Sydney on 2018-11-08

Submitted works

<1%
- 23

uni-muenster.de

Internet

<1%
- 24

Phuong H. Nguyen, Ayyalusamy Ramamoorthy, Bikash R. Sahoo, Jie Z...

Crossref

<1%
- 25

University of Wales central institutions on 2019-11-14

Submitted works

<1%
- 26

fjfsdata01prod.blob.core.windows.net

Internet

<1%
- 27

Universidad Internacional de la Rioja on 2020-12-27

Submitted works

<1%
- 28

"Neuroimmune Pharmacology", Springer Science and Business Media ...

Crossref

<1%
- 29

Jing Huang, Xiu-Juan Jiang, Wei Yu, Yan Xu, Bo Xiong, Jun Qian, Ya-Ke...

Crossref posted content

<1%
- 30

"Brain Iron Metabolism and CNS Diseases", Springer Science and Busin...

Crossref

<1%
- 31

brenda-enzymes.org

Internet

<1%
- 32

Orkid Coskuner-Weber, Ozan Mirzanli, Vladimir N. Uversky. "Intrinsicall...

Crossref

<1%

- 33

Rohan Gupta, Devesh Srivastava, Mehar Sahu, Swati Tiwari, Rashmi K. ... <1%

Crossref
- 34

Craig, Nancy. "Molecular Biology- Principles of Genome Function", Oxf... <1%

Publication
- 35

Fatemeh Ataellahi, Raheleh Masoudi, Mohammad Haddadi. "Differenti... <1%

Crossref posted content
- 36

Cardiff University on 2021-03-03 <1%

Submitted works
- 37

dokumen.pub <1%

Internet
- 38

"Multi-Target Drug Design Using Chem-Bioinformatic Approaches", Spr... <1%

Crossref
- 39

ebin.pub <1%

Internet
- 40

Md. Rezanur Rahman, Tania Islam, Toyfiqz Zaman, Md. Shahjaman et... <1%

Crossref posted content
- 41

Universidade Estadual Paulista on 2022-05-10 <1%

Submitted works
- 42

Birla Institute of Technology and Science Pilani on 2017-09-30 <1%

Submitted works
- 43

Associatie K.U.Leuven on 2022-06-16 <1%

Submitted works
- 44

Basavaraj Vastrad, Chanabasayya Vastrad. "Screening key genes and s... <1%

Crossref posted content

45	National University of Singapore on 2021-12-01	<1%
	Submitted works	
46	d-nb.info	<1%
	Internet	
47	Manipal University on 2022-05-12	<1%
	Submitted works	
48	Universiti Teknologi MARA on 2021-08-04	<1%
	Submitted works	
49	Dia Advani, Rohan Gupta, Rahul Tripathi, Sudhanshu Sharma, Rashmi K...	<1%
	Crossref	
50	academic.oup.com	<1%
	Internet	
51	"Biological, Diagnostic and Therapeutic Advances in Alzheimer's Disea...	<1%
	Crossref	
52	"Role of Nutrients in Neurological Disorders", Springer Science and Bus...	<1%
	Crossref	
53	Vishal Kumar, Satyabrata Kundu, Arti Singh, Shamsheer Singh. "Underst...	<1%
	Crossref	
54	Ying Han, Le Chen, Jingyun Liu, Chunyang Wang, Yu Guo, Xuebin Yu, C...	<1%
	Crossref posted content	
55	tel.archives-ouvertes.fr	<1%
	Internet	
56	bioRxiv.org	<1%
	Internet	

57	mbfbioscience.com	<1%
	Internet	
58	Lei Li, Xiang-Hui Wu, Xiao-Jing Zhao, Lu Xu, Cai-Long Pan, Zhi-Yuan Zh...	<1%
	Crossref posted content	
59	University of East London on 2020-06-01	<1%
	Submitted works	
60	University of Hong Kong on 2021-07-29	<1%
	Submitted works	
61	University of Portsmouth on 2022-05-23	<1%
	Submitted works	

● Excluded from Similarity Report

- Bibliographic material
- Cited material
- Manually excluded sources
- Quoted material
- Small Matches (Less than 8 words)

EXCLUDED SOURCES

Rohan Gupta, Pravir Kumar. "Integrative analysis of OIP5-AS1/miR-129-5p/CR... 13%
Crossref

Rohan Gupta, Pravir Kumar. " CREB1 and HINFP as Putative Common Therap... 11%
Crossref

Rohan Gupta, Pravir Kumar. "Computational Analysis Indicates That PARP1 A... 11%
Crossref

ncbi.nlm.nih.gov 10%
Internet

Rohan Gupta, Rashmi K. Ambasta, Pravir Kumar. "Pharmacological interventio... 6%
Crossref

Rohan Gupta, Rashmi K. Ambasta, Pravir Kumar. "Histone deacetylase in neur... 4%
Crossref

Rohan Gupta, Mehar Sahu, Devesh Srivastava, Swati Tiwari, Rashmi K. Ambas... 2%
Crossref

CREB1^{K292} and HINFP^{K330} as Putative Common Therapeutic Targets in Alzheimer's and Parkinson's Disease

Rohan Gupta and Pravir Kumar*

Cite This: *ACS Omega* 2021, 6, 35780–35798

Read Online

ACCESS |



Metrics & More

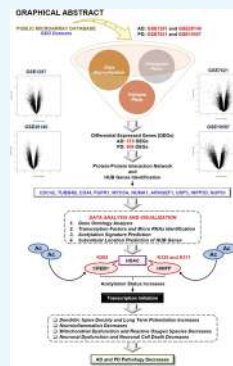


Article Recommendations



Supporting Information

ABSTRACT: Integration of omics data and deciphering the mechanism of a biological regulatory network could be a promising approach to reveal the molecular mechanism involved in the progression of complex diseases, including Alzheimer's and Parkinson's. Despite having an overlapping mechanism in the etiology of Alzheimer's disease (AD) and Parkinson's disease (PD), the exact mechanism and signaling molecules behind them are still unknown. Further, the acetylation mechanism and histone deacetylase (HDAC) enzymes provide a positive direction toward studying the shared phenomenon between AD and PD pathogenesis. For instance, increased expression of HDACs causes a decrease in protein acetylation status, resulting in decreased cognitive and memory function. Herein, we employed an integrative approach to analyze the transcriptomics data that established a potential relationship between AD and PD. Data preprocessing and analysis of four publicly available microarray datasets revealed 10 HUB proteins, namely, CDC42, CD44, FGFR1, MYOSA, NUMA1, TUBB4B, ARHGEF9, USP5, INPP5D, and NUP93, that may be involved in the shared mechanism of AD and PD pathogenesis. Further, we identified the relationship between the HUB proteins and transcription factors that could be involved in the overlapping mechanism of AD and PD. CREB1 and HINFP were the crucial regulatory transcription factors that were involved in the AD and PD crosstalk. Further, lysine acetylation sites and HDAC enzyme prediction revealed the involvement of 15 and 27 potential lysine residues of CREB1 and HINFP, respectively. Our results highlighted the importance of HDAC1(K292) and HDAC6(K330) association with CREB1 and HINFP, respectively, in the AD and PD crosstalk. However, different datasets with a large number of samples and wet lab experimentation are required to validate and pinpoint the exact role of CREB1 and HINFP in the AD and PD crosstalk. It is also possible that the different datasets may or may not affect the results due to analysis parameters. In conclusion, our study potentially highlighted the crucial proteins, transcription factors, biological pathways, lysine residues, and HDAC enzymes shared between AD and PD at the molecular level. The findings can be used to study molecular studies to identify the possible relationship in the AD–PD crosstalk.



1. INTRODUCTION

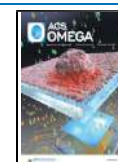
Neurodegenerative diseases (NDDs) such as Alzheimer's disease (AD) and Parkinson's disease (PD) are forms of dementia characterized by the progressive loss of neuronal cells due to the accumulation of toxic protein aggregates. Further, excessive neuronal cell death due to protein aggregates causes synaptic dysfunction, memory impairment, and cognitive defects.¹ AD is the most prevalent form of dementia best characterized by the presence of amyloid plaques and neurofibrillary tangles produced by unsystematic proteolytic processing of amyloid peptide-protein and hyperphosphorylation of the tau protein.² For example, Kollmer et al., 2019, demonstrated that β -amyloid ($A\beta$) fibrils from meningeal Alzheimer's brain tissue are polymorphic but consist of similarly structured protofibrils.³ Similarly, Bu et al., 2017, concluded that blood-derived $A\beta$ protein induces AD pathologies that result in the functional impairment of neurons.⁴ In contrast, PD, which is the second most common NDDs, is characterized by the progressive loss of dopaminergic neurons in the substantia nigra *pars compacta*. The pathological feature of PD is the accumulation of the toxic α -synuclein⁵ protein and the formation of Lewy bodies, which cause neuronal cell death and ultimately lead to synaptic

dysfunction and memory loss.^{6,7} Mounting evidence suggests the common overlapping molecular phenomenon in the pathology of AD and PD. However, the exact molecular pathways and signaling molecules being involved are poorly understood. Moreover, the active treatment of AD and PD is still unknown due to a lack of understanding of the molecular mechanism of disease progression. Accumulating evidence suggests that protein acetylation and deacetylation play a significant role in the pathogenesis of AD and PD.^{8–10} For instance, Choi et al., 2019, demonstrated that acetylation of tau facilitated the recruitment of Hsp40, Hsp70, and Hsp110, which causes tau association with E3 ligases and results in its degradation through a proteasomal pathway.¹¹ Similarly, Wang et al., 2020, concluded that AMPK reduces tau acetylation

Received: October 18, 2021

Accepted: December 7, 2021

Published: December 16, 2021



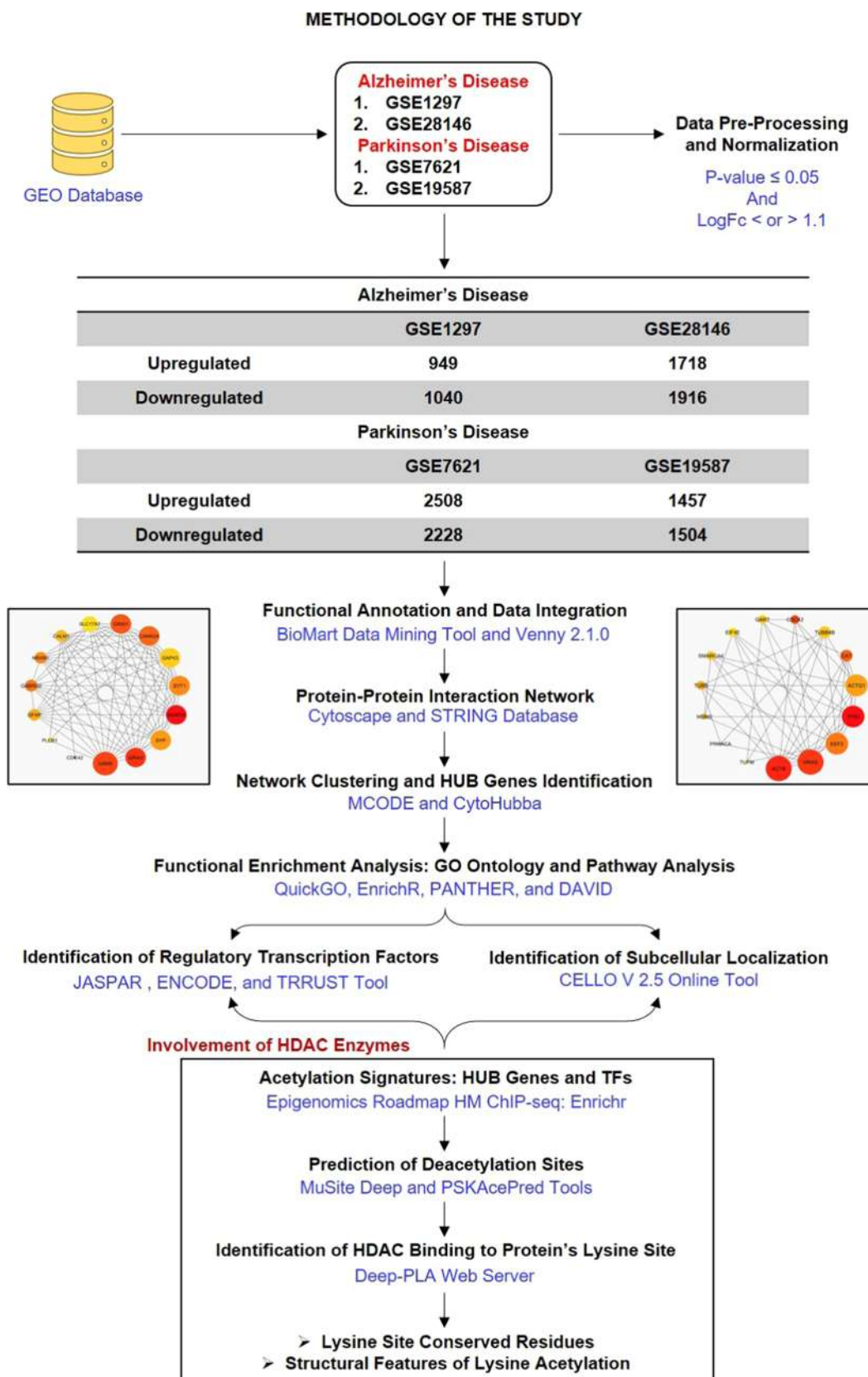


Figure 1. Methodology of the study: workflow and steps that were considered along with the datasets collected and processed to identify shared molecular signatures between AD and PD. The figure also highlights the involvement of the acetylation mechanism and HDAC enzymes in the AD and PD crosstalk.

and rescues memory impairment by activating sirtuin 1 in APP/PS1 mice.¹² Further, Fan et al., 2020, concluded that PGC-1 α

translocation due to its acetylation promotes neuroprotection from oxidative damage in a PD experimental model.¹³

Table 1. Datasets Obtained from the GEO Database for AD and PD

GEO accession number	platform	sample source	total samples	control samples	disease samples	total DEGs	upregulated DEGs	downregulated DEGs
Alzheimer's Disease								
GSE1297	Affymetrix Human Genome U133A Array	hippocampal region	31	9	22	1989	949	1040
GSE28146	Affymetrix Human Genome U133 Plus 2.0 Array	hippocampal region	30	8	22	3634	1718	1916
Parkinson's Disease								
GSE7621	Affymetrix Human Genome U133 Plus 2.0 Array	Substantia nigra	25	9	16	4736	2508	2228
GSE19587	Affymetrix Human Genome U133A 2.0 Array	Substantia nigra	22	10	12	2961	1457	1504

In the pathogenesis of NDDs such as AD and PD, HDACs/HATs are involved in the regulation of biological processes such as apoptosis and autophagy, cell-cycle arrest, inflammatory and immune response, oxidative stress, and mitochondrial dysfunction, which cause neuronal cell death and lead to memory impairment and cognitive defects.^{14–18} Different experimental studies have confirmed the role of HDAC and its inhibitors in the pathogenesis of AD and PD. For instance, the over-expression of HDAC3 in the hippocampus increases spatial memory deficits and amyloid plaque load, whereas HDAC2 dysregulation in the nucleus basalis of Meynert was observed during the progression of AD.^{19,20} Similarly, the inhibition of HDAC through valproic acid increases histone acetylation levels and decreases the expression of proinflammatory biomarkers in the LRRK2 R1441G mice model of PD.²¹ Further, the inhibition of HDAC4/5 with the administration of LMK235 protects dopaminergic neurons against 1-methyl-4-phenylpyridinium (MPP⁺) and α -synuclein-induced neuronal cell death.²² Apart from HDAC and its inhibitors, acetylated lysine residues of histone and non-histone substrates also play a crucial role in AD and PD pathogenesis. For example, Yakhine-Diop et al., 2018, demonstrated the acetylation of H4 at K5, K8, and K12 and its increased expression in IPD cells in PD pathogenesis. The authors also confirmed the acetylation of α -tubulin at K40 and the role of PCAF/p300 in α -tubulin acetylation.¹⁵ Similarly, Pilkington et al., 2020, concluded that the acetylation of A β at K16 and K28 promotes the extent of aggregation and inhibits fibril formation and oligomerization. However, the authors concluded that the acetylation of A β at K16 is preferred over the acetylation at K28.²³ A recent study demonstrated the crucial role of lysine residues in the PTM crosstalk, namely, acetylation, ubiquitination, and SUMOylation in AD and PD pathogenesis. The authors concluded that the inhibition of PARP1 acetylation (K249, K331, K337, K528, K600, K637, K700, and K796) and the simultaneous activation of ubiquitination and SUMOylation at identical lysine residues rescue neuronal cell death.²⁴ Further, lysine residues are also crucial for subcellular localization of proteins, where the loss of K304 resulted in CREB nuclear localization and modification of HDAC1 at K444 and K476, resulting in increased biological activity.^{25,26} In addition, Kirsh et al., 2002, demonstrated that SUMOylation of HDAC4 at K559 takes place at a nuclear pore complex RanBP2 and is coupled to its nuclear import.²⁷ Thus, the identification of crucial lysine acetylating/deacetylating residues in novel pathological biomarkers provide considerable significance in unraveling a novel therapeutic approach for the treatment of AD and PD. Extensive research is ongoing on proteomics, transcriptomics, and epigenetic-based approaches to determine the molecular signatures and pathways involved in disease

progression using a network biology approach based on microarray datasets. This will enable us to understand the molecular basis of the disease and the exact mechanism of disease progression.

Further, the acetylation and deacetylation of transcription factors (TFs) play a vital role in regulating cellular and molecular processes, which activate different neuronal signal transduction pathways such as PI3K/Akt and MAPK pathways, cAMP/PKA pathways, and Ca²⁺/CaMK cascade. For instance, Fusco et al., 2016, concluded that the acetylation of CREB1 at K122 increases Hes-1 expression under low glucose concentrations, facilitating neurogenesis by removing sirtuin 1 on the Hes-1 promoter region.²⁸ Similarly, Paz et al., 2014, demonstrated that the acetylation of CREB at K136 facilitated its interaction with the CBP bromodomain that augmented the recruitment of this coactivator to the promoter.²⁹ Thus, these pieces of evidence concluded the importance of acetylation of TFs in gene regulation.

Herein, we aim to investigate the potential conventional biomarkers and regulatory TFs involved in the pathogenesis of AD and PD simultaneously with the help of microarray datasets and the network biology approach. The identified proteomic and transcriptomic signatures were further analyzed to investigate the potential lysine residue for acetylation and deacetylation activity, along with the determination of the type of HDAC enzyme being involved in the disease progression. Lastly, the study focuses on investigating conserved amino acid residues involved in the lysine acetylation/deacetylation process along with the structural selectivity of molecular signatures, which could be crucial for protein acetylation or deacetylation activity.

2. RESULTS AND DISCUSSION

2.1. Transcriptomic Signatures of AD and PD. The obtained datasets were normalized through quantile normalization and log₂ transformation. Statistically, in microarray data, the intensity values are relative numbers, and thus log₂ transformation is necessary to make variations similar across the order of magnitude. Boxplots of data before normalization and after normalization were created to check the background corrections in the datasets (Supplementary Figure 1). Further, independent histograms of normalized data with a color intensity such as green for control and red for the disease were prepared to check the variation in the required datasets (Supplementary Figure 2B). Our results identified 4736 (GSE7621), 2961 (GSE19587), 1989 (GSE1297), and 3634 (GSE28146) differentially expressed genes (DEGs) (Figure 1) (Table 1). Independent volcano plots of different datasets were used to measure the extent of DEGs in AD and PD

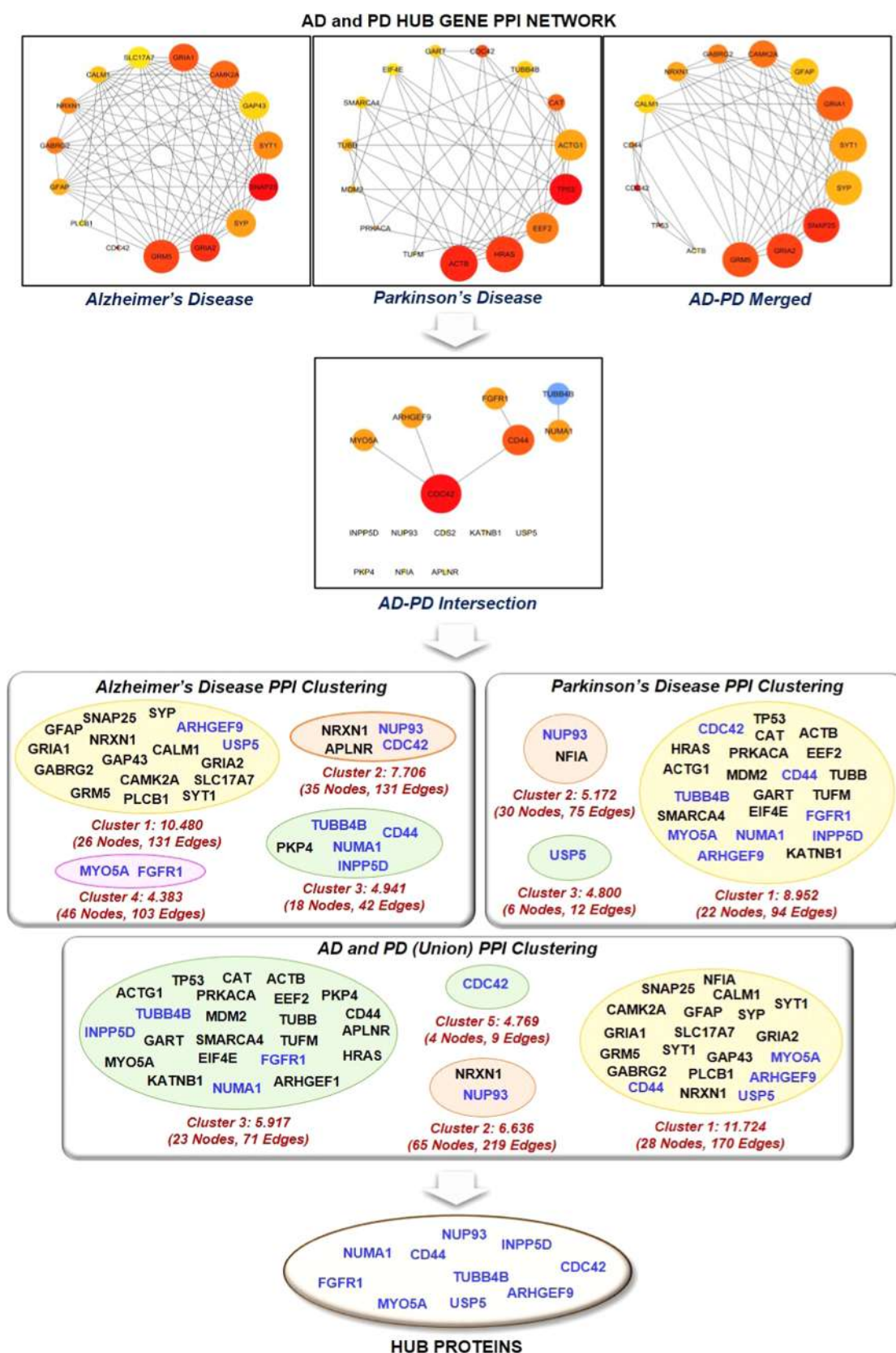


Figure 2. It represents the protein–protein interaction network of the top 15 ranked or HUB genes involved in Alzheimer’s disease, Parkinson’s disease, Alzheimer’s disease–Parkinson’s disease union merged network, and Alzheimer’s disease–Parkinson’s disease intersection merged network. Further, the top 15 proteins of the individual network were mapped against the clusters of AD, PD, AD–PD intersection, and AD–PD union network to extract HUB proteins.

Table 2. Role of HUB Genes in the Pathogenesis of Alzheimer's Disease and Parkinson's Disease Identified with the Help of MalaCards

HUB genes	description	involvement in Alzheimer's disease	involvement in Parkinson's disease
CDC42	Cell Division Cycle 42	establishes neuron polarity, regulates cell morphology and mortality, and regulates cell cycle	inhibits the activating features of microglia
TUBB4B	Tubulin β 4B	regulates inflammatory response	serves as a target for PD-associated toxins
CD44	CD44 Molecule (Indian Blood Group)	interacts with mutant p53 activity	causes α -synuclein-induced migration of BV-2 microglial cells
FGFR1	Fibroblast Growth Factor Receptor 1	involved in axonal projection and inhibits apoptosis	elevates DA levels and protects the specific midbrain neurons
MYO5A	Myosin VA (Heavy-Chain, Myosin)	induces cell motility	mutant MYO5A exhibits alterations in dopamine metabolism
NUMA1	Nuclear Mitotic Apparatus Protein 1	identifies transported MSC in the brain	helps in mitotic spindle formation
ARHGEF9	CDC42 Guanine Nucleotide Exchange Factor (GEF) 9	plays a role in integrin signaling and axon guidance signaling	encodes synaptic proteins, and loss of function results in intellectual disability
USP5	Ubiquitin-Specific Peptidase 5	compromises tau levels	deletion causes increased p53 activity
INPP5D	Inositol Polyphosphate-5-Phosphatase, 145 kDa	modulates inflammatory response	involved in immune response
NUP93	Nucleoporin 93 kDa	promotes nuclear accumulation of mRNA	inhibits mRNA transport

(Supplementary Figure 2A). After identifying DEGs, the probe IDs were converted into respective gene symbols, and then Venn analysis of DEGs was performed. Venn analysis results demonstrated 579 DEGs in AD while 406 DEGs in PD.

2.2. PPI Interaction Analysis. PPI interaction analysis confirmed the presence of 492 proteins with 2335 physical interactions and 311 proteins and 1014 physical interactions in the AD and PD network, respectively. The clustering coefficients of AD and PD networks were found to be 0.244 and 0.248, respectively, which implies a higher coexpression of DEGs in AD networking than in PD networking. Further, the characteristic path lengths of AD and PD networks were 3.504 and 3.390, respectively. Herein, the network centralization was found to be 0.107 and 0.200, whereas the network heterogeneity was found to be 1.028 and 1.057 for AD and PD PPI networks, respectively. The analysis found that the network densities of AD and PD networks are 0.019 and 0.021, respectively, which indicates that a particular node in the PD PPI network has more participants compared to the AD PPI network (Figure 2).

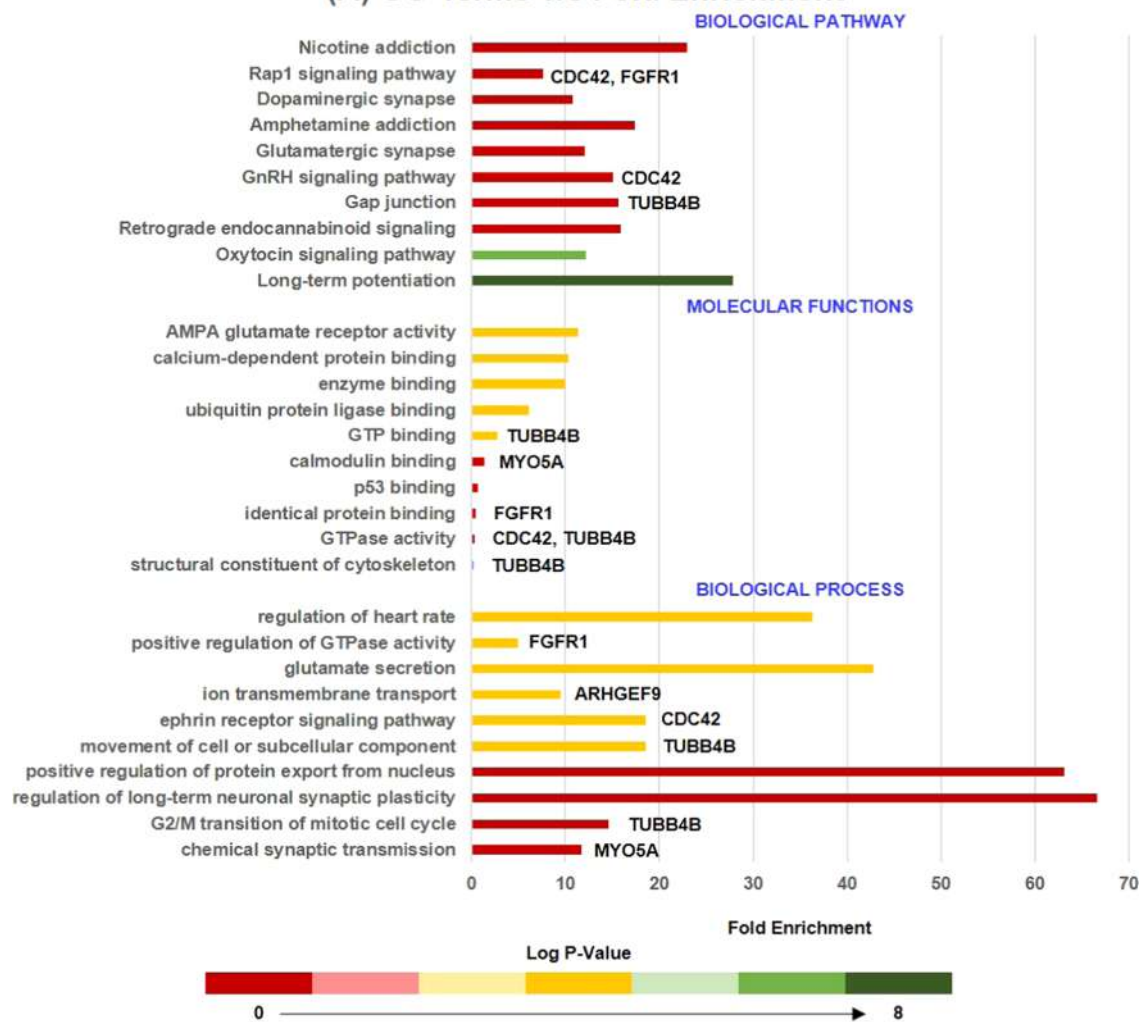
Further, network biology using PPI networking becomes an important tool to establish a relationship between two proteins and identify the interactive pattern of proteomics data.³⁰ In addition, PPI networking provides an in-depth understanding of the biological characteristics of proteins encoded through DEGs and helps in estimating their biological significance.^{31,32} The PPI network is characterized by the presence of nodes and edges along with other topological features, namely, clustering coefficient, characteristic path length, network density, and network centralization.³³ The protein in the networks were represented as nodes marked in a circle, while their biological association with other proteins were represented as edges marked as lines.³⁴ The clustering of the network determines the extent to which genes in the network coexpressed in biological conditions based on distance calculation. Thus, the higher the clustering coefficient, the lower the probability of proteins coexpressing in the biological network.³⁵ The characteristic path length denotes the best possible configuration of the biological network.³⁶ Network homogeneity refers to a nonuniformity in character,^{37,38} while network centralization or centrality identifies the network's essential vertices or proteins.^{39,40} Another essential feature of biological networks is network density, which measures the average number of connections of a particular protein or node divided by the total number of participant proteins in the network.⁴¹ Statistically, the

topological coefficient is a relative measure for the extent to which a particular protein in the given network shares neighbors with other proteins. The proteins that have one or no neighbors are assigned a topological coefficient of zero.⁴² The topological analysis of the PPI network provides a way to identify HUB proteins, which pass signaling stimulus to other proteins or nodes in the network. Subsequently, HUB proteins were identified based on topological features of the PPI network, especially node degree (number of proteins interacting with single protein), which may serve as potential biomarkers in AD and PD therapeutics.

2.3. Network Clustering and Proteomic Signatures of AD and PD. The merging of two PPI networks was done in two steps. In the first step, the PPI networks of AD and PD were combined by a union to ensure complete coverage of relevant proteins involved in the study, followed by extraction of common proteins (nodes) of the individual PPI network. The AD–PD union PPI network consists of 784 proteins and 3344 physical/functional interactions, while the AD–PD intersection biological network consists of 19 proteins and five physical/functional interactions (Figure 2). The top 15 highly connected proteins of individual AD, PD, AD–PD (union), and AD–PD (intersection) PPI networks were extracted. The HUB proteins were marked according to their presence in the respective PPI cluster. CDC42, CD44, FGFR1, MYO5A, NUMA1, TUBB4B, ARHGEF9, USP5, INPP5D, and NUP93 were found to be the most prominent proteins found in clusters of AD, PD, and AD–PD (union) PPI networks. Table 2 describes the role of HUB proteins in the pathogenesis of AD and PD (Supplementary Table 1). Here, our network analysis study demonstrates the involvement of CDC42, CD44, FGFR1, MYO5A, NUMA1, TUBB4B, ARHGEF9, USP5, INPP5D, and NUP93 in the onset and progression of AD and PD. Studies demonstrated that these proteins were associated with different biological processes. For instance, the activation of FAK/Rac1/CDC42-GTPase signaling rescued the impaired microglial migration response to $A\beta$ 42 in triggering the receptor expressed on myeloid cells 2 loss-of-function.⁴³ Similarly, the inhibition of FGFR1 effectively blocked the GLP-promoted NPC proliferation in the mouse model of AD.⁴⁴ However, the exact role of FGFR1 and CDC42 in the AD and PD crosstalk is still missing. In addition, Lim et al., 2018, concluded that CD44 activates tau pathology, whereas Neal et al., 2018, concluded that GPNMB attenuates astrocyte inflammatory response through the CD44 receptor.^{45,46}

FUNCTIONAL ENRICHMENT ANALYSIS OF DEG's IN AD and PD

(A) GO Terms v/s Fold Enrichment



(B) LOG P-VALUE OF CELLULAR COMPONENTS

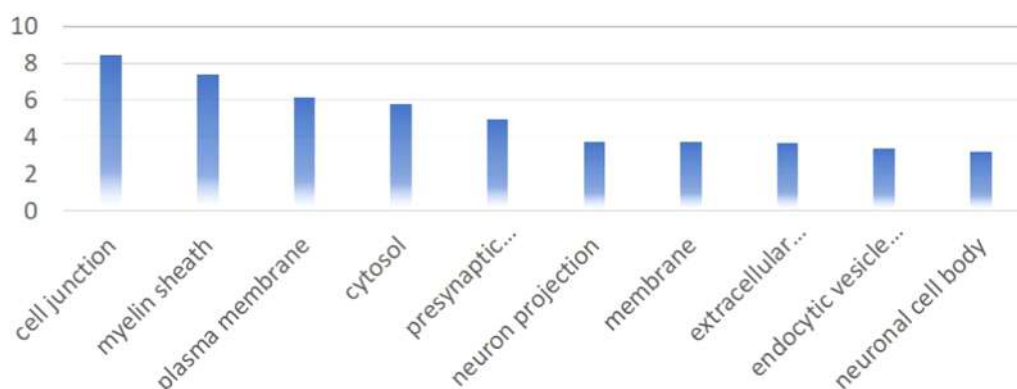


Figure 3. Represents the bar graph of the top 10 biological processes, molecular functions, and biological pathways of HUB proteins along with their p -value and involved HUB proteins. The axis of the bar represents the p -value. The figures also represent the critical cellular components in which HUB proteins lie with their corresponding p -value. Terms with a P -value ≤ 0.05 were considered significant.

Further, loss of MYO5A resulted in structural and functional alterations in the rat brain through alterations in dopamine

metabolism, whereas TUBB4B may be a part of the signaling cascade involved in the etiology of PD and is related to an

Table 3. Biological Significance of Top Interacting Transcription Factors in the Progression of Alzheimer's Disease and Parkinson's Disease, along with Their Degree of Node and Interacting Partners

Transcription Factor	Degree	Interacting Partners	Network Centrality	Topological Coefficient	Role in Neuropathology
FOXC1	8	INPP5D, CDC42, NUP93, FGFR1, USP5, CD44, ARHGEF9, MYO5A	0.8235	0.1585	Required for cell viability and resistance to oxidative stress
GATA2	5	INPP5D, FGFR1, TUBB4B, GATA2, ARHGEF9,	0.7137	0.2800	Regulates the proliferation of neuronal progenitors
CREB1	4	CDC42, USP5, CD44, INPP5D	0.6509	0.2826	Induces cognitive dysfunction
FOXL1	3	ARHGEF9, NUMA1, INPP5D	0.6274	0.3968	Involved in synaptic assembly and neural circuit development
NFIC	3	TUBB4B, NUMA1, USP5	0.5569	0.3888	Regulates differentiation of human neural progenitors to astrocytes
HINFP	3	TUBB4B, NUMA1, CD44	0.5568	0.4166	Regulates gene expression patterns
SREBF1	3	TUBB4B, ARHGEF9, CD44	0.5960	0.3921	Involved in DNA repair mechanism, regulates development of CNS

inflammatory response.^{47,48} ARHGEF9 encodes collybistin involved in the postsynaptic clustering of glycine and inhibitor γ -aminobutyric acid receptors.⁴⁹ Further, Griffin et al., 2020, concluded the upregulation of ARHGEF9 during astroglia response to $A\beta$ oligomers.⁵⁰ USP5, a stress granule protein, increases TNF α expression through the ubiquitin-proteasome pathway and regulates inflammatory response through Smurf1.⁵¹ Recently, Tsai et al., 2021, demonstrated that INPP5D was positively associated with amyloid plaque density in the human brain.⁵² Thus, these pieces of evidence concluded that the abovementioned HUB proteins are associated with neurological diseases in some manner through the regulation of different biological phenomena, yet their relationship in the AD and PD crosstalk is still missing. Further, HUB proteins, namely, NUMA1 and NUP93, lack the potential involvement in the pathogenesis of either AD and PD.

2.4. Gene-Set Enrichment Analysis and Pathway Analysis. To identify the complicated relationship between the highly dense connected components of PPI networks (AD, PD, AD–PD union, and AD–PD intersection), pathway analysis and GO analysis were performed. Moreover, we extracted the top 10 biological pathways, cellular components, and molecular functions of highly interconnected proteins involved in neurodegeneration, as demonstrated in Figure 3. Moreover, after GO analysis, the extracted highly interconnected proteins were subjected to pathway analysis, which enables the identification of the molecular pathway, followed by the interconnected proteins in the progression of AD and PD. Figure 3 demonstrates the top 10 biological pathways in which these proteins were involved. Gap junction (TUBB4B), GnRH signaling pathway (CDC42), and Rap1 signaling pathway (CDC42 and FGFR1) were critical pathways in which HUB proteins were involved and may be potential biological pathway targets for the AD and PD crosstalk. For instance, Esteves et al., 2017, demonstrated that nicotine effectively prevented prefrontal long-term potentiation and memory deficits induced by streptozotocin in AD,⁵³ whereas Carvajal-Oliveros et al., 2021, demonstrated that nicotine suppresses the PD-like phenotype induced by synphilin-1 overexpression through

increased dopamine levels.⁵⁴ Similarly, a study concluded that the balance between dopamine and adenosine signals regulates the PKA/Rap1 pathway in spiny neurons, where D1R and A2AR agonist enhanced PKA-mediated Rap1 phosphorylation *in vivo* and *in vitro*.⁵⁵ Further, studies demonstrated that impaired GnRH production is directly linked to oxidative stress and mitochondrial dysfunction in neurons.^{56,57} Another significantly enriched pathway is the gap junction that is involved in the pathogenesis of AD and PD.^{58,59} For instance, Angeli et al., 2020, demonstrated the altered expression of glial gap junction proteins, namely, Cx43, Cx30, and Cx47, in the 5XFAD model of AD,⁶⁰ whereas Maulik et al., 2020, concluded that $A\beta$ regulates the gap junction protein connexin 43 in cultured primary astrocytes.⁶¹ Consistent with this, the results demonstrated the importance of CDC42, TUBB4B, and FGFR1 in the pathogenesis of AD and PD. Further, these three HUB proteins were a potential target for identifying the relationship between AD and PD.

2.5. CREB1 and HINFP: Essential Regulatory Molecules in AD and PD Crosstalk with High Acetylation Marks. The functions of a particular protein depend on its subcellular location. Mounting evidence demonstrated that acetylation was highly observed on nuclear proteins involved in chromatin regulation and transcription. This observation is consistent with the known nuclear function of acetyltransferase, deacetylase, and acetylated lysine-binding bromodomain proteins.⁶² For instance, a study demonstrated that in response to oxidative stress, TyrRS becomes highly acetylated, which causes its nuclear translocation, where sirtuin 1 and PCAF/p300 regulate its nuclear translocation in an acetylation-dependent manner.⁶³ Further, Zhao et al., demonstrated that silica nanoparticle-mediated sirtuin 1 suppression markedly increased p53 acetylation and cytoplasmic localization.⁶⁴

Herein, we analyzed the cellular location of HUB proteins with CELLO version 2.5: subCELLular LOcalization predictor. Among the 10 HUB proteins extracted, 40% were cytoplasmic proteins, 50% were nuclear proteins, and 10% were extracellular proteins. CD44 (1.974), FGFR1 (2.078), INPP5D (3.954), MYO5A (3.300), and NUMA1 (1.858) were predicted as

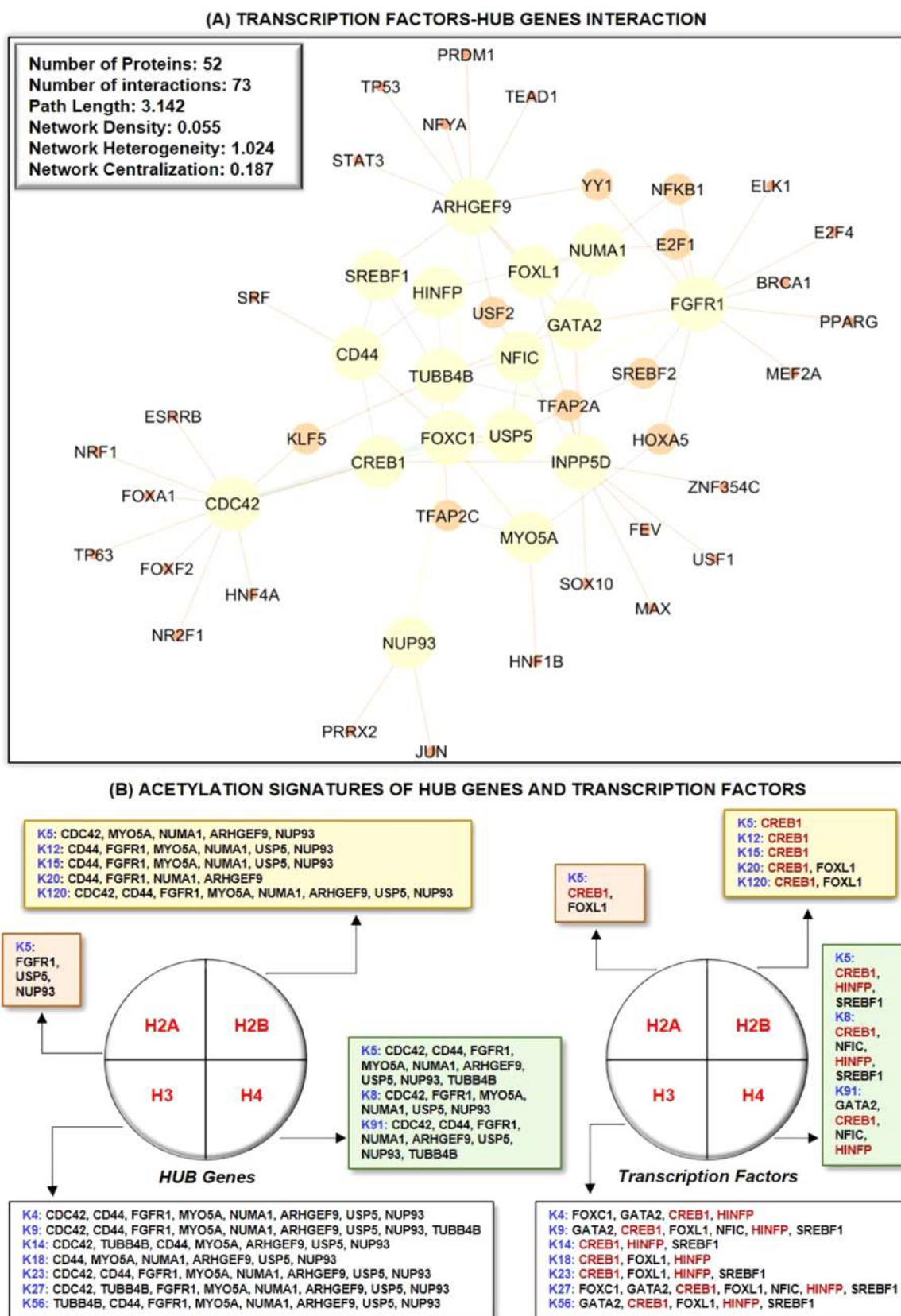


Figure 4. (A) PPI network of HUB genes with associated regulatory transcription factors. Among the transcription factors, FOXC1 (8) has the highest number of interacting proteins, followed by GATA2 (5), CREB1 (4), FOXL1 (3), NFIC (3), HINFP (3), and SREBF1 (3). The total number of proteins and physical/functional interaction in HUB proteins and transcription factors in protein–protein interaction networks are 52 and 73. (B) Acetylation signatures of non-histone protein substrates, such as HUB genes and transcription factors. CREB1 and HINFP are the most prominent acetylated transcription factors, whereas CDC42, CD44, and TUBB4B are the most crucial non-histone protein acetylating substrates.

nuclear proteins, while CDC42 (2.037) was predicted as an extracellular protein. Similarly, ARHGEF (2.770), NUP93 (2.534), TUBB4B (3.682), and USP5 (2.207) were predicted as cytoplasmic proteins. Studies demonstrated that acetylation activates STAT3 through the nuclear translocation of CD44, whereas the acetylation of histone proteins controls FGFR1 polymorphisms and isoform splicing.^{65,66} In addition, lysine acetylation of SCF FBXL19 ubiquitin E3 ligase increases its activity and stabilization that targets CDC42 for its ubiquitination and degradation.⁶⁷

Further, we identified HUB protein–TF interaction and detected central regulatory molecules using topological features. Thus, we extracted seven regulatory TFs, namely, FOXC1 (8), GATA2 (5), CREB1 (4), FOXL1 (3), NFIC (3), HINFP (3), and SREBF1 (3). Subsequently, the cross-validation of TFs in the pathogenesis of AD and PD was identified with the help of MalaCards, as demonstrated in Table 3. TFs are transcriptional regulators that are involved in the pathogenesis of AD and PD.^{68–71} In this study, we also studied the potential relationship between TFs and HUB proteins to identify mutual transcriptional regulators of the identified HUB proteins. The identified TFs are FOXC1, GATA2, CREB1, FOXL1, NFIC, HINFP, and SREBF1 as a regulator of HUB proteins commonly expressed in AD and PD pathogenesis (Figure 4A). For instance, Xu et al., 2019, concluded that the deletion of CREB1 diminishes the effect of DJ1 on TH regulation through the deregulation of the CaMKK β /CaMIV/CREB1 pathway.⁷² Similarly, the deletion of CREB1 promotes proinflammatory changes in the mouse hippocampus.⁷³ Moreover, He et al. concluded that the deacetylation of EZH2 through SIRT6 causes an increased association between EZH2 and FOXC1 that exerts anti-inflammatory response, whereas Emelyanov et al., 2018, concluded the positive correlation between dopamine and GATA2 expression in PD.^{74,75} FOXL1 is implemented in the pathogenesis of NDDs, while NFIC was identified as novel loci in AD.^{76–78} Studies demonstrated that HINFP is a coactivator in the sterol-regulated transcription of PCSK9, a target gene of SREBP2 involved in the tau alterations, which contribute to disturbed cholesterol homeostasis in AD.^{79,80} Lastly, genetic mutation analysis concluded that genetic polymorphism rs11868035 was associated with susceptibility to PD in the Chinese population.^{81,82} Thus, the evidence mentioned above proves the potential link of identified TFs in the progression and pathogenesis of AD and PD and acts as a specific biomarker for their therapeutics. However, their potential role in the AD and PD crosstalk is still missing.

Moreover, HUB genes and TFs were analyzed for their acetylation signature to understand the involvement of acetylation and deacetylation processes associated with HUB genes and TFs in the pathogenesis of AD and PD. Herein, CDC42 (10), CD44 (11), FGFR1 (11), MYO5A (13), NUMA1 (14), ARHGEF9 (11), USP5 (14), and NUP93 (15) were predicted as the most non-histone acetylating substrates among HUB proteins, while CREB1 (16) and HINFP (10) were predicted as non-histone acetylating substrates among TFs (Figure 4B) (Supplementary Figure 3). Lately, to study the epigenetic regulation of HUB proteins and TFs, we investigated histone modification sites found in the coding region of HUB proteins and TFs implicated with NDDs and identified a range of sites.^{83,84} Thus, this raises the possibility that PTMs, namely, acetylation, deacetylation, ubiquitination, SUMOylation, methylation, and others, are the primary means of alteration in these proteins that need further investigation. Further, histone

acetylation signatures are primarily related to the markers of activity at regulatory elements, namely, promoters and enhancers.⁸⁵ Moreover, understanding the specific role of histone acetylation at different genomic elements has the potential to improve disease therapeutics by increasing the target specificity.⁸⁶ In addition, histone signatures enable us to understand the biological phenomenon, namely, chromosome packaging, transcriptional activation, and DNA packaging. Further, studies demonstrated the correlation between histone acetylation levels and gene expression *in vivo* and *in vitro* studies. For instance, curcumin, a CREB HAT activity inhibitor, causes a reduction in acetylation levels of both histone H4 and H3, whereas HDAC inhibitors, namely, butyric acid and valproic acid, inhibit the H4 acetylation and CREB1 activity *in vivo*.^{87,88} Similarly, Guo et al., 2011, demonstrated that excessive alcohol exposure decreases CREB-binding protein expression and acetylation status of both H3 and H4 in the cerebellum of ethanol-induced rats.⁸⁹ Similarly, another study identified that GATA1 displaces GATA2, which is associated with transcriptional repression, and causes a reduction in the histone H3K4 acetylation status.⁹⁰ In addition, Li and Liu et al. concluded that HINFP forms a complex with NPAT that recruits the HAT cofactor TRRAP to facilitate H4 acetylation at the PCSK9 promoter, whereas Gruber et al. concluded that the requirement for the acetyltransferase activity of HAT1 for proliferation might point to the HAT1-dependent acetylation of non-histone substrates, for example, Hinfp, a factor also shown to bind H4 promoters.^{91,92} Forma et al., 2018, demonstrated that an increased expression of FOXA1 and FOXC1 was associated with increased acetylation levels of histone H3, whereas He et al. concluded that increased FOXC1 protein levels in RAW246.7 cells were associated with altered levels of H3 acetylation.^{74,93}

2.6. Potential Lysine Residues for Protein Acetylation.

The correlation between acetylation and HDAC enzymes has been studied extensively in the past.^{94–96} For instance, MS-275, a class I HDAC inhibitor, promotes rapid acetylation of the YB-1 RNA-binding protein at K81,⁹⁷ whereas the HDAC1 complex is able to regulate histone H3 acetylation at K18.⁹⁸ Further, Topuz et al., 2019, demonstrated that administration of the HDAC inhibitor, namely, sodium butyrate, increases H2B acetylation at K5 that leads to increased spatial learning and long-term memory in the rat hippocampus.⁹⁹ Similarly, Choi et al., 2017, demonstrated that increased acetylation of peroxiredoxin 1 at K197 through HDAC6 inhibition leads to the recovery of A β -induced impaired axonal transport.¹⁰⁰ In addition, the role of SIRT1 in regulating pathogenic tau acetylation at K174 and in suppressing the spread of tau pathology has been demonstrated in a mouse model of tauopathy.¹⁰¹ Thus, based on the abovementioned evidence, we identified acetylation sites and HDAC enzymes of CREB1 and HINFP through two online tools, namely, MuSite deep and PSKAcePred. For MuSite Deep, statistically, a high confidence score relates to the high probability of lysine acetylation at a particular lysine amino acid. A score above 0.5 is considered as a high confidence score and a high probability of lysine acetylation, whereas a score below 0.2 is considered as a low confidence score where the probability of lysine acetylation is negligible, and a score between 0.2 and 0.5 is considered as the site with moderate probability. Further, for PSKAcePred, a score above 0.7 is considered a high confidence score and the probability of lysine acetylation is very high, whereas a score between 0.5 and 0.7 is considered a moderate confidence score and the probability of lysine acetylation is relatively less as compared to acetylation at a

high confidence score lysine site. The CREB1 peptide sequence (P16220.2) has 15 potential acetylating lysine residues. The respective acetylation-site prediction scores were determined with the help of MuSite deep and PSKAcePred, as shown in [Supplementary Table 2](#). MuSite predicted K330 as an essential lysine acetylation site with a high confidence score of 0.557. Similarly, PSKAcePred predicted K94, K292, K303, K304, and K309 as potential protein acetylation lysine residues with a high confidence score of 0.872, 0.737, 0.856, 0.924, and 0.994, respectively. From the protein acetylation-site prediction of CREB1, it may be concluded that K304, K309, and K330 were essential for acetylating lysine residues. The type of HDAC enzymes involved in the deacetylation of CREB1 was predicted and found that HDAC1, HDAC2, and SIRT7 were important in CREB1 deacetylation, where HDAC1 was involved in K292 (3.35) deacetylation, HDAC2 involved in K330 (10.67), and SIRT7 involved in K94 (13.26), K303 (12.54), and K304 (12.90) deacetylation. The results demonstrated that the binding propensity of SIRT7 and HDAC2 is very low as compared to the binding propensity of HDAC1. Thus, the results show that K292 is a critical lysine residue for CREB1 acetylation and deacetylation processes with HDAC1 as its deacetylating enzyme involved in the pathogenesis of AD and PD. In addition, Hansen et al., 2019,⁶² demonstrated the acetylation of CREB1 at K330 and K136, whereas Paz et al., 2014, demonstrated that sirtuin 1 directly downregulates the CREB transcriptional activity by binding and deacetylating CREB at K136, thereby reducing CREB interaction with CBP.¹⁰² Further, Lu et al., 2003, confirmed the acetylation of CREB1 at K91, K94, and K136 within the activation domain through CBP. However, they also concluded that a single mutation of the putative CBP acetylation sites has no significant effect on the transactivation potential of CREB.¹⁰³ Thus, these pieces of evidence suggest the possibility of CREB1 acetylation and its binding with HDAC enzymes in the regulation of gene transcription.

Moreover, HINFP (AAH17234.1) consists of 27 potential acetylating lysine residues such as K6, K10, K31, K94, K96, K164, K174, K181, K185, K197, K213, K236, K256, K285, K294, K301, K330, K335, K346, K352, K366, K367, K371, K382, K439, K446, and K504, as observed in [Supplementary Table 3](#). MuSite Deep predicted all 27 sites as potential acetylating lysine residues with no residue of high confidence score. However, five sites were predicted as potential acetylation sites with a moderate score as follows: K6, 0.318; K213, 0.311; K330, 0.420; K371, 0.354; and K382, 0.269. Thus, predicted acetylation sites were essential for triggering protein acetylation results in transcription initiation. Among the predicted acetylating lysine residues, HDAC6 (K6 and K330), HDAC1 (K382), and SIRT1 (K371) were important deacetylating residues involved in protein deacetylation, resulting in the progression of AD and PD. However, the binding score of HDAC6 (2.74 and 3.84) was predicted higher than HDAC1 (6.53) and SIRT1 (7.01). Similarly, PSKAcePred predicted 15 potential lysine acetylation sites, of which eight sites were predicted as potential lysine acetylation sites with a high confidence score: K31, 0.730; K96, 0.766; K174, 0.779; K330, 0.726; K335, 0.930; K367, 0.904; K371, 0.911; and K446, 0.719. Further, the HDAC enzyme prediction tool predicted that SIRT1 (K31, 6.51 and K371, 7.01), SIRT2 (K446, 0.95), SIRT7 (K174, 13.26), HDAC1 (K367, 4.23), and HDAC6 (K330, 3.84 and K335, 2.74) were crucial enzymes involved in the regulation of HINFP deacetylating activity. A comparative analysis of both

the acetylation prediction tools and the type of deacetylating enzyme reflected that K330 and K371 were crucial proteins acetylating lysine residues with HDAC6 and SIRT1 as their interacting partners. However, the confidence score of SIRT1 is lower than that of HDAC6, while the confidence of K330 is higher than that of K371. Thus, it will be concluded that K330 interacts with HDAC6 to carry out HINFP deacetylation in AD and PD progression. Further, until now, no proteomic study has investigated the implementation of acetylation sites and HDAC binding residues in the activation domain of HINFP. However, mounting evidence suggests that HAT1, an acetyltransferase binding to HINFP promoters, has a specific stimulatory effect on H4 gene transcription. In addition, the authors concluded that HAT1 promotes the accumulation of newly synthesized H4 dimers without affecting the levels of histones embedded in the nucleosome.⁹² Another study concluded that HINFP forms a functional complex with NPAT that recruits the HAT cofactor TRRAP to facilitate the histone 4 acetylation at the PCSK9 promoter.⁹¹ Thus, this *in silico* analysis could be a milestone in providing an avenue for identifying crucial acetylation or deacetylation patterns of CREB1 and HINFP to minimize AD and PD progression ([Table 4](#)).

Table 4. List of Common Crucial Lysine Residues in CREB1 and HINFP

CREB1		
lysine residue		interactor
K94		SIRT7
K292		HDAC1
K303		SIRT7
K304		SIRT7
HINFP		
K31		SIRT1
K174		SIRT7
K330		HDAC6
K335		HDAC6
K367		HDAC1
K371		SIRT1

2.7. Glutamic Acid and Leucine Predominately Conserved Residues at Protein Acetylation Sites. The predicted protein acetylation sites were analyzed for the conserved lysine residues, which could be crucial for lysine selectivity and specificity for the acetylation process and binding of deacetylating enzymes. CREB1 has 15 potential lysine residues represented by 16220.2, while HINFP has 27 potential lysine residues represented by AAH17234.1. The multiple sequence alignment (MSA) analysis of predicted lysine residues for acetylation revealed the conservation of negatively charged glutamic acid (E) and neutrally charged leucine (L), methionine (M), valine (V), and glutamine (Q) in close association with the positively charged lysine residue, as shown in [Figure 5A](#). These conserved residues provided a suitable environment and favorable conditions for associated potential lysine residues for the acetylation process, thus imparting lysine selectivity and specificity for the acetylation and deacetylation. However, further investigations are required to determine the potential of conserved residues in the acetylation and deacetylation processes of CREB1 and HINFP. However, glutamic acid is most prominent compared to other conserved amino acids as it decreases the overall positive charge of lysine and imparts a negative charge to the lysine site, which will promote acetylation

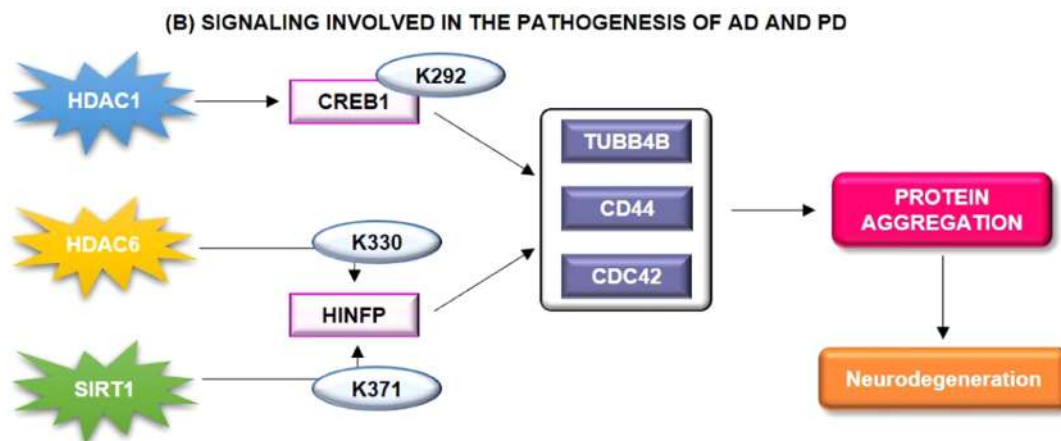
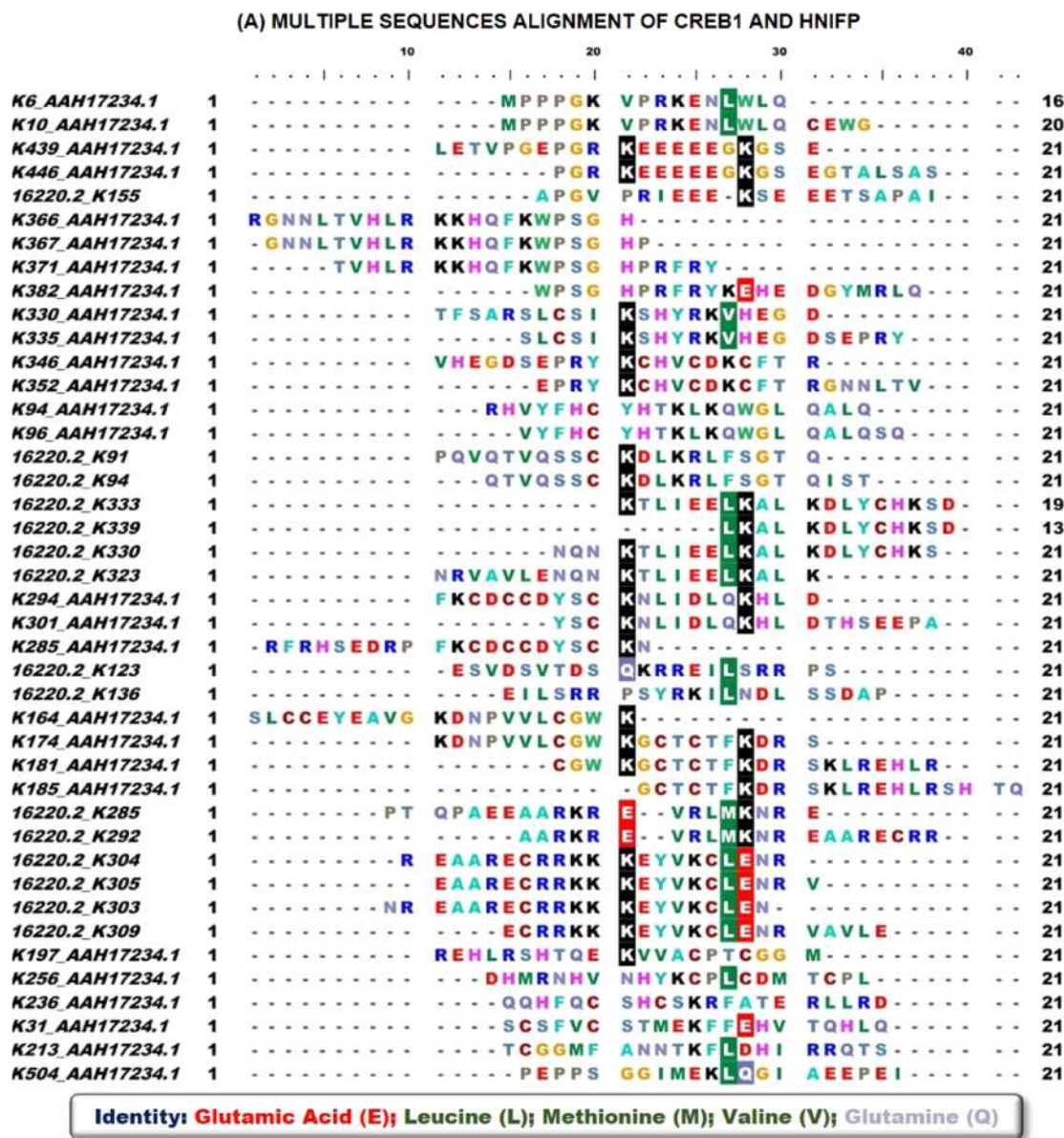


Figure 5. (A) Multiple sequence analysis of potential acetylation/deacetylation lysine residues by taking 21 window sizes. 21 window size was taken by lysine at the center with ten amino acids on both sides. (B) Proposed action of mechanism or the signaling transduction pathway in CREB1- and HINFP-mediated neurodegeneration.

and deacetylation reactions. For instance, Nguyen et al., 2016, concluded that glutamine triggers acetylation-dependent

degradation of glutamine synthetase, whereas Son et al., 2020, demonstrated that leucine regulates autophagy through

acetylation of the mTORC1.^{104,105} Moreover, the role of methionine involvement in lysine acetylation is not studied so far in AD and PD, but yet at the same time demonstrated the potential relationship between methionine and lysine acetylation in other neurological defects. For instance, Chiki et al., 2021, concluded that the presence of oxidation of methionine at position 8 and acetylation at K6 resulted in the dramatic inhibition of Httex1 fibrilization.¹⁰⁶ Thus, these studies correlate with our results and suggest that glutamic acid (E), leucine (L), methionine (M), valine (V), and glutamine (Q) could be critical amino acid residues in acetylation and HDAC binding.

Further, structural information of CREB reveals that it consists of 11 exons and three isoforms that are produced through alternative splicing.¹⁰⁷ Primary structure studies of CREB identified the presence of four functional domains, namely, Q1 basal transcriptional activity domain, kinase inducible domain, a glutamine-rich region, and basic region/leucine zipper domain.¹⁰⁸ Thus, this relates to the importance of glutamine in the structural activity of CREB1. Similarly, structural information of HINFP confirms that the interaction of HINFP produced TF with methyl-CpG-binding protein-2, a component of the HDAC complex, and plays an important role in transcription repression. Sekimata et al., 2004, demonstrated that HINFP, through its DNA-binding activity, acts as a sequence-specific (conserved CCGAC core) transcriptional repressor,¹⁰⁹ whereas Medina et al. concluded that the PSCR motif is required for the activation of histone H4 gene transcription and promotes its binding with DNA.¹¹⁰ Further, the study revealed the presence of acetylated H4 histone in the binding activity of HINFP to USF and GAL4-AH.¹¹¹ In addition, a study concluded that lysine residues control the conformational dynamics of proteins.¹¹² Thus, it is equally important to identify the structural features of CREB1 and HINFP that were involved in the acetylation mechanism. Thus, the potential and possible acetylation lysine residues were analyzed for their structural selectivity for lysine recognition pattern and potential deacetylating enzyme attachment, as discussed in [Supplementary Table 4](#). The structural pattern of the putative deacetylating enzyme attachment binding to potential acetylation or deacetylation lysine residues revealed the presence of α -helix, strand, and coil region in the CREB1 and HINFP peptide. However, an in-depth analysis of the structural configuration of CREB1 and HINFP revealed that the helix region is predominant over the strand/coil region in the acetylation of CREB1. A study by Maltsev et al., 2012, concluded the involvement of the helical structure in the acetylation process, where acetylation increases α -helicity of the first six residues of α -synuclein.¹¹³ Similarly, the coil region is dominant over the helix/strand region in the potential lysine acetylation of HINFP. The results correlate with the study by Kulemzina et al., 2016, which concluded that lysine acetylation promotes interactions between Smc coiled coils that are required for cohesion ring assembly.¹¹⁴ Further, the results were analyzed precisely and revealed the involvement of structural selectivity in the acetylation and deacetylation of CREB1 and HINFP. In addition, the results also provide an avenue of helix and coil regions in the acetylation of predicted lysine residues of CREB1 and HINFP, respectively ([Figure 5B](#)). However, due to limited structural information of CREB1 and HINFP and the potential effect of acetylation on CREB1 and HINFP structural changes, these results need to be verified *in vitro*.

3. MATERIALS AND METHODS

3.1. Data Collection and Identification of Differentially Expressed Genes (DEGs). The microarray gene expression datasets for AD (GSE1297¹¹⁵ and GSE28146¹¹⁶) and PD (GSE7621¹¹⁷ and GSE19587¹¹⁸) were obtained from the NCBI-GEO database (<https://www.ncbi.nlm.nih.gov/geo/>),¹¹⁹ irrespective of the population. The datasets were analyzed in an R-environment for data normalization and data preprocessing. Further, Limma was used to identify DEGs in both AD and PD compared to controls. The p -value < 0.05 and $\text{ILog } 2F_c > 1.1$ was regarded as cutoff criteria to screen for significant DEGs. The significance for the selection of $\text{Log } 2F_c$ is that the expression is slightly more than twice for both upregulated and downregulated genes. The BioMart data-mining tool (<https://m.ensembl.org/info/data/biomart/index.html>)¹²⁰ was applied to convert probe symbols into gene symbols. Lastly, Venn analysis was performed using the online tool called Venny 2.1 (<https://bioinfoq.cnb.csic.es/tools/venny/>)¹²¹ to identify common DEGs from the four datasets.

3.2. Protein–Protein Interaction Network Analysis and Visualization. The interrelation between different DEGs of AD and PD was obtained from STRING database version 11.0 (<https://string-db.org/>).¹²² The search criteria in the STRING database are limited to a confidence score of 0.5. The obtained networks were imported into Cytoscape software version 3.8.0 (<https://cytoscape.org/>)¹²³ for protein data integration, PPI network visualization, and PPI network analysis. Subsequently, node degree, number of edges, clustering coefficient, network homogeneity, shortest path length, and network density of AD and PD PPI networks were calculated.

3.3. PPI Network Clustering and Identification of HUB Proteins. The AD and PD networks were merged using a network merging tool of Cytoscape based on two methods, namely, network union and network intersection. Afterward, network clustering was performed through molecular complex detection (MCODE) (<http://apps.cytoscape.org/apps/mcode>)¹²⁴ plugin of Cytoscape software. The clusters so formed were analyzed and visualized on different parameters such as the number of proteins (nodes) and physical interactions between them (Edges), network clustering coefficient, characteristics of path length, network centralization and homogeneity, and network density. The clusters of all PPI networks were statistically analyzed and ranked separately based on node degree. Lastly, the HUB proteins were identified using CytoHubba (<http://apps.cytoscape.org/apps/cytohubba>)¹²⁵ through default parameters. Subsequently, the HUB proteins were mapped from all PPI network clusters individually, which include AD, PD, and AD–PD union PPI networks.

3.4. Functional Enrichment and Pathway Analysis of HUB Proteins. HUB protein overrepresentation was performed through the bioinformatics resource EnrichR (<http://amp.pharm.mssm.edu/Enrichr/>)¹²⁶ and QuickGO (<https://www.ebi.ac.uk/QuickGO/>)¹²⁷ to identify the molecular function, biological process, and cellular function. Further, pathway analysis of HUB proteins was carried out using freely accessible online databases and tools such as the REACTOME database (<https://reactome.org/>)¹²⁸ and FunRich version 3.1.3 (<http://funrich.org/>).¹²⁹ For statistical assessment of GO analysis and pathway analysis, a p -value less than 0.05 was considered significant, and a fold-enrichment value was considered. Here, the p -value reflects the chance of observing “ n ” number of genes in a gene list annotated to a specific term, whereas fold

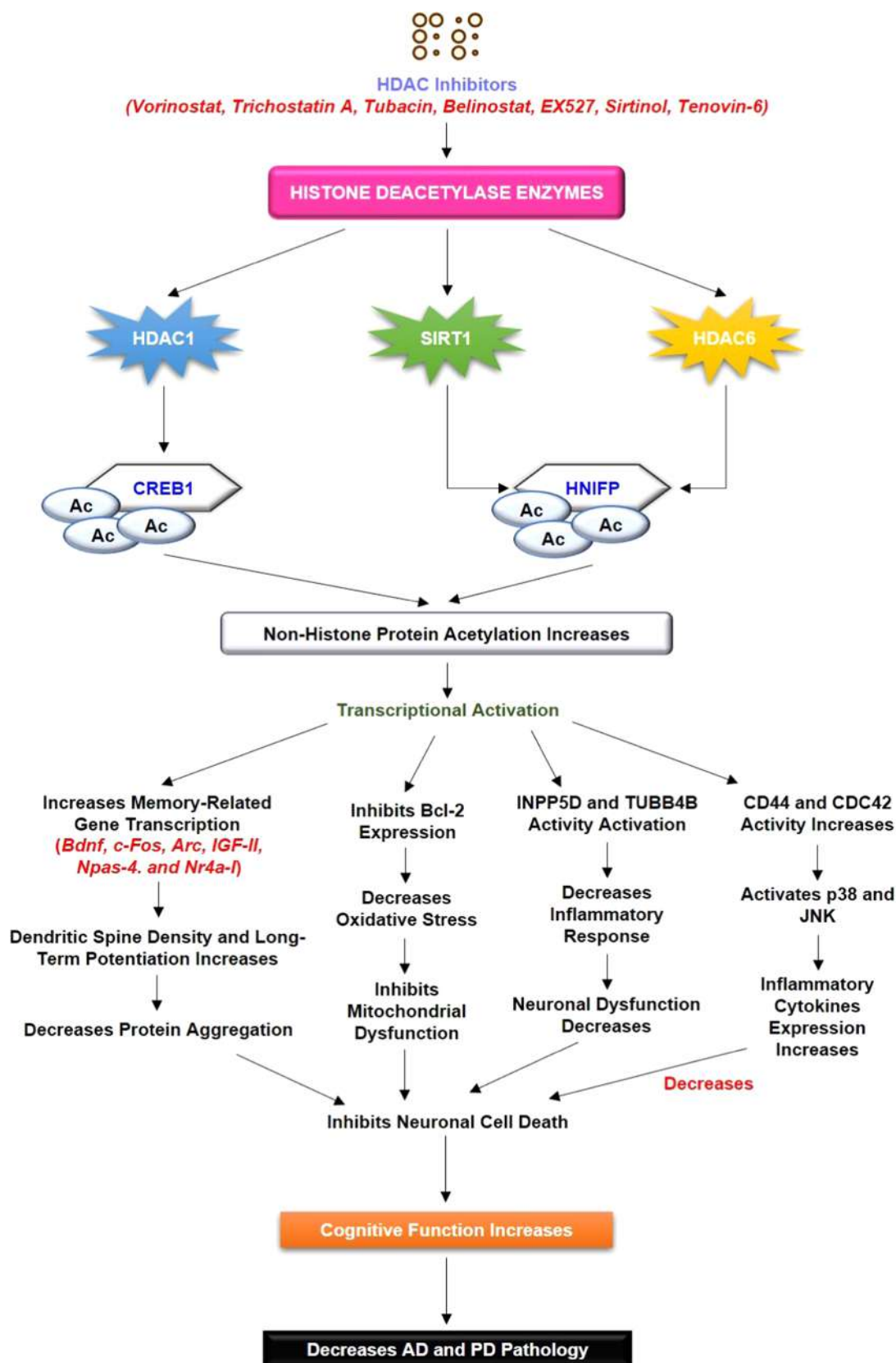


Figure 6. Literature validation of the involvement of HDAC interaction with CREB1 and HINFP. HDAC inhibitors cause a decrease in HDAC activity, followed by the increased acetylation status of CREB1, and HINFP causes positive transcriptional regulation. Increased transcriptional activity causes an increase in the transcription of memory-associated genes, and Bcl-2 expression leads to an increase in cognitive function and memory function. The increased acetylation status of CREB1 and HINFP causes INPP5D and TUBB4B activation, which decreases neuronal cell death and leads to neuroprotection.

enrichment of a term was designated as overrepresented compared to the background, where overrepresentation is denoted as positive fold enrichment.

3.5. HUB Proteins–Transcription Factors (TFs) Interaction and Prediction of Protein Subcellular Localization. The subcellular localization of HUB genes was calculated to understand the mechanism of action of protein and its associated functions using CELLO version 2.5: subCELLular LOcalization predictor (<http://cello.life.nctu.edu.tw/>).¹³⁰ To identify the TFs that control the HUB proteins at a transcriptional level, TF-target interactions were obtained from JASPAR version 8 (<http://jaspar.genereg.net/>)¹³¹ and an interaction network between TFs and HUB proteins was created using NetworkAnalyst tool version 3.0 (<https://www.networkanalyst.ca/home.xhtml>).¹³²

3.6. Identification of Histone Lysine Signatures and Prediction of Protein Deacetylating Enzymes. Based on the previous experimental studies, it was evident that acetylation signatures were associated with the pathogenesis of AD and PD by altering gene expression patterns. Thus, we used the Epigenomics Roadmap CHIP-seq dataset, which is an inbuilt feature of EnrichR for their potential acetylation marks of HUB proteins. Moreover, acetylation sites in CREB1 and HINFP have been predicted through machine learning algorithm-based, freely accessible online tools such as MuSite Deep (<https://www.musite.net/>)¹³³ and PSKAcePred (http://bioinfo.ncu.edu.cn/inquiries_PSKAcePred.aspx).¹³⁴ Lastly, the type of deacetylating enzyme associated with CREB and HINFP was predicted with the help of a freely accessible online web server named Deep-PLA (<http://deeppla.cancerbio.info/index.html>).¹³⁵

3.7. Prediction of Conserved Lysine Residues and Structural Features for HDAC's Binding. The conserved sequence was predicted using a multiple sequence alignment (MSA) of 21 window size of lysine site residues that includes 10 residues on both the left and the right end and containing a lysine acetylating site in the middle for both CREB1 and HINFP using ClustalW MSA tool (<https://www.genome.jp/tools-bin/clustalw>).¹³⁶ Additionally, the structural selectivity of lysine acetylating sites has been predicted with the help of PSIPRED: protein structure prediction server (<http://bioinf.cs.ucl.ac.uk/psipred/>).¹³⁷ Subsequently, the secondary structure of the protein has been correlated with their respective protein acetylating sites.

4. CONCLUSIONS

In conclusion, the present study focuses on the crosstalk between AD and PD at the molecular level. Through this study, we identified the relationship between DEGs, HUB proteins, TFs, acetylation, and HDAC enzymes in the shared pathogenesis of AD and PD. Our findings highlighted the crucial role of CDC42, TUBB4B, and FGFR1 in the AD and PD crosstalk through Gap junction (TUBB4B), GnRH signaling pathway (CDC42), and Rap1 signaling pathway (CDC42 and FGFR1). In addition, the present study identified the potential TFs that regulate the expression of HUB proteins at the transcriptional level through biological network analysis. Our analysis identified FOXC1, GATA2, CREB1, FOXL1, NFIC, HINFP, and SREBF1 as potential TFs that regulate the activity of HUB proteins shared between AD and PD. Our bioinformatic analysis also revealed the effect of subcellular localization of HUB proteins and TFs in the AD and PD crosstalk. Lately, the study identified the 15 potential lysine residues and 27 potential lysine

residues in CREB1 and HINFP, respectively. The study revealed that among 15 possible lysine residues of CREB1, only four lysine residues, namely, K91, K94, K136, and K330, had been studied in the past, while K123, K155, K285, K292, K303, K304, K305, K309, K323, K333, and K339 have been reported first time for their role in the acetylation process. Similarly, among HINFP, all 27 lysine residues have been reported for the first time. Further, the *in silico* analysis of CREB1 and HINFP revealed the importance of HDAC1 for its deacetylation activity at K292 of CREB1 and HDAC6 for its deacetylation activity at K330 of HINFP. This will provide a way to study the role of acetylation and HDAC enzymes in the transcriptional activity of CREB1 and HINFP in the AD and PD crosstalk. Further, the computational analysis identified the importance of negatively charged glutamic acid (E) and neutrally charged leucine (L), methionine (M), valine (V), and glutamine (Q) amino acid residues in the acetylation mechanism of CREB1 and HINFP in the AD and PD crosstalk. The study also highlighted the importance of the helix region over the strand/coil region in the acetylation of CREB1. Similarly, the coil region is dominant over the helix/strand region in the potential lysine acetylation of HINFP. Thus, this study highlighted the importance of two prominent biological pathways for the progression of AD and PD simultaneously, such as HDAC1-CREB1-TUBB4B/CDC42/CD44 and HDAC6-HINFP-TUBB4B/CDC42/CD44 (Figure 6). Further studies are required to generate the potential treatments targeting the abovementioned biological pathways to treat the adverse effects of AD and PD. Further, the current study is associated with some sort of limitation as the study uses only microarray data, which is not as comprehensive as transcriptomics data analysis. Thus, there is a growing need to simultaneously analyze the different types of AD and PD datasets, namely, microarray data, epigenetic data, and RNA data, to extract the novel biomarkers involved in disease pathology. Further, there should be a greater number of control as well as disease samples to conclude a general discussion. In addition, samples from different tissues could be more beneficial in understanding the molecular mechanism and role of HDAC in AD and PD simultaneously. In the current study, using Bioinformatics tools, we identified that CREB1 and HINFP are putative targets in the pathogenesis of AD and PD simultaneously; however, the different datasets with a large number of samples and wet lab experimentation are absolutely necessary to establish the molecular signature and validate the role of CREB1 and HINFP in AD and PD.

■ ASSOCIATED CONTENT

SI Supporting Information

The Supporting Information is available free of charge at <https://pubs.acs.org/doi/10.1021/acsomega.1c05827>.

Box plot, volcano plots, relative expression of HUB genes, list of HUB genes, putative lysine residues in CREB1 and HINFP, and secondary structure of acetylated lysine residues (PDF)

■ AUTHOR INFORMATION

Corresponding Author

Pravir Kumar – Molecular Neuroscience and Functional Genomics Laboratory, Department of Biotechnology, Delhi Technological University (Formerly DCE), Delhi 110042, India; orcid.org/0000-0001-7444-2344; Phone: +91-

9818898622; Email: pravirkumar@dtu.ac.in, kpravir@gmail.com

Author

Rohan Gupta – Molecular Neuroscience and Functional Genomics Laboratory, Department of Biotechnology, Delhi Technological University (Formerly DCE), Delhi 110042, India

Complete contact information is available at:

<https://pubs.acs.org/10.1021/acsomega.1c05827>

Author Contributions

P.K. and R.G. conceived and designed the manuscript. R.G. collected, analyzed, and critically evaluated these data. R.G. prepared the figures and tables. P.K. and R.G. analyzed the entire data and wrote the manuscript.

Notes

The authors declare no competing financial interest.

ACKNOWLEDGMENTS

The authors thank the senior management of Delhi Technological University for constant support and encouragement.

REFERENCES

- (1) Luthra, P. M. Paradigm of Protein Folding in Neurodegenerative Diseases. *Protein Res. J.* **2011**, *2*, 479.
- (2) Nussbaum, R. L.; Ellis, C. E. Alzheimer's Disease and Parkinson's Disease. *N. Engl. J. Med.* **2003**, *348*, 1356–1364.
- (3) Kollmer, M.; Close, W.; Funk, L.; Rasmussen, J.; Bsoul, A.; Schierhorn, A.; Schmidt, M.; Sigurdson, C. J.; Jucker, M.; Fändrich, M. Cryo-EM Structure and Polymorphism of A β Amyloid Fibrils Purified from Alzheimer's Brain Tissue. *Nat. Commun.* **2019**, *10*, No. 4760.
- (4) Bu, X.-L.; Xiang, Y.; Jin, W.-S.; Wang, J.; Shen, L.-L.; Huang, Z.-L.; Zhang, K.; Liu, Y.-H.; Zeng, F.; Liu, J.-H.; Sun, H.-L.; Zhuang, Z.-Q.; Chen, S.-H.; Yao, X.-Q.; Giunta, B.; Shan, Y.-C.; Tan, J.; Chen, X.-W.; Dong, Z.-F.; Zhou, H.-D.; Zhou, X.-F.; Song, W.; Wang, Y.-J. Blood-Derived Amyloid- β Protein Induces Alzheimer's Disease Pathologies. *Mol. Psychiatry* **2018**, *23*, 1948–1956.
- (5) Zheng, T.; Zhang, Z. Activated Microglia Facilitate the Transmission of α -Synuclein in Parkinson's Disease. *Neurochem. Int.* **2021**, *148*, No. 105094.
- (6) Chang, C.-W.; Yang, S.-Y.; Yang, C.-C.; Chang, C.-W.; Wu, Y.-R. Plasma and Serum Alpha-Synuclein as a Biomarker of Diagnosis in Patients With Parkinson's Disease. *Front. Neurol.* **2020**, *10*, 1388.
- (7) Si, X.; Tian, J.; Chen, Y.; Yan, Y.; Pu, J.; Zhang, B. Central Nervous System-Derived Exosomal Alpha-Synuclein in Serum May Be a Biomarker in Parkinson's Disease. *Neuroscience* **2019**, *413*, 308–316.
- (8) Bao, J.; Zheng, L.; Zhang, Q.; Li, X.; Zhang, X.; Li, Z.; Bai, X.; Zhang, Z.; Huo, W.; Zhao, X.; Shang, S.; Wang, Q.; Zhang, C.; Ji, J. Deacetylation of TFEB Promotes Fibrillar A β Degradation by Upregulating Lysosomal Biogenesis in Microglia. *Protein Cell* **2016**, *7*, 417–433.
- (9) Min, S. W.; Cho, S. H.; Zhou, Y.; Schroeder, S.; Haroutunian, V.; Seeley, W. W.; Huang, E. J.; Shen, Y.; Masliah, E.; Mukherjee, C.; Meyers, D.; Cole, P. A.; Ott, M.; Gan, L. Acetylation of Tau Inhibits Its Degradation and Contributes to Tauopathy. *Neuron* **2010**, *67*, 953–966.
- (10) Luca, C.; Garamszegi, S.; Eldick, D.; Singer, C.; Mash, D. Altered SIRT4 Expression Is Associated with Lewy Body Pathology (P01.209). *Neurology* **2012**, *78*, P01.209.
- (11) Choi, H.; Kim, H. J.; Yang, J.; Chae, S.; Lee, W.; Chung, S.; Kim, J.; Choi, H.; Song, H.; Lee, C. K.; Jun, J. H.; Lee, Y. J.; Lee, K.; Kim, S.; Sim, H.; Il Choi, Y.; Ryu, K. H.; Park, J.-C.; Lee, D.; Han, S.-H.; Hwang, D.; Kyung, J.; Mook-Jung, I. Acetylation Changes Tau Interactome to Degrade Tau in Alzheimer's Disease Animal and Organoid Models. *Aging Cell* **2020**, *19*, No. e13081.
- (12) Wang, L.; Shi, F.-X.; Li, N.; Cao, Y.; Lei, Y.; Wang, J.-Z.; Tian, Q.; Zhou, X.-W. AMPK Ameliorates Tau Acetylation and Memory Impairment Through Sirt1. *Mol. Neurobiol.* **2020**, *57*, 5011–5025.
- (13) Fan, F.; Li, S.; Wen, Z.; Ye, Q.; Chen, X.; Ye, Q. Regulation of PGC-1 α Mediated by Acetylation and Phosphorylation in MPP+ Induced Cell Model of Parkinson's Disease. *Aging* **2020**, *12*, 9461.
- (14) Shi, X.; Pi, L.; Zhou, S.; Li, X.; Min, F.; Wang, S.; Liu, Z.; Wu, J. Activation of Sirtuin 1 Attenuates High Glucose-Induced Neuronal Apoptosis by Deacetylating P53. *Front. Endocrinol.* **2018**, *9*, 274.
- (15) Yakhine-Diop, S. M. S.; Niso-Santano, M.; Rodríguez-Arribas, M.; Gómez-Sánchez, R.; Martínez-Chacón, G.; Uribe-Carretero, E.; Navarro-García, J. A.; Ruiz-Hurtado, G.; Aiastui, A.; Cooper, J. M.; López de Munaín, A.; Bravo-San Pedro, J. M.; González-Polo, R. A.; Fuentes, J. M. Impaired Mitophagy and Protein Acetylation Levels in Fibroblasts from Parkinson's Disease Patients. *Mol. Neurobiol.* **2019**, *56*, 2466–2481.
- (16) Zhang, W.; Feng, Y.; Guo, Q.; Guo, W.; Xu, H.; Li, X.; Yi, F.; Guan, Y.; Geng, N.; Wang, P.; Cao, L.; O'Rourke, B. P.; Jo, J.; Kwon, J.; Wang, R.; Song, X.; Lee, I. H.; Cao, L. SIRT1 Modulates Cell Cycle Progression by Regulating CHK2 Acetylation–phosphorylation. *Cell Death Differ.* **2020**, *27*, 482–496.
- (17) Wu, C. C.; Lee, P. T.; Kao, T. J.; Chou, S. Y.; Su, R. Y.; Lee, Y. C.; Yeh, S. H.; Liou, J. P.; Hsu, T. L.; Su, T. P.; Chuang, C. K.; Chang, W. C.; Chuang, J. Y. Upregulation of Zn179 Acetylation by SAHA Protects Cells against Oxidative Stress. *Redox Biol.* **2018**, *19*, 74–80.
- (18) Lee, J.; Kim, Y.; Liu, T.; Hwang, Y. J.; Hyeon, S. J.; Im, H.; Lee, K.; Alvarez, V. E.; McKee, A. C.; Um, S.-J.; Hur, M.; Mook-Jung, I.; Kowall, N. W.; Ryu, H. SIRT3 Deregulation Is Linked to Mitochondrial Dysfunction in Alzheimer's Disease. *Aging Cell* **2018**, *17*, No. e12679.
- (19) Zhu, X.; Wang, S.; Yu, L.; Jin, J.; Ye, X.; Liu, Y.; Xu, Y. HDAC3 Negatively Regulates Spatial Memory in a Mouse Model of Alzheimer's Disease. *Aging Cell* **2017**, *16*, 1073–1082.
- (20) Mahady, L.; Nadeem, M.; Malek-Ahmadi, M.; Chen, K.; Perez, S. E.; Mufson, E. J. HDAC2 Dysregulation in the Nucleus Basalis of Meynert during the Progression of Alzheimer's Disease. *Neuropathol. Appl. Neurobiol.* **2019**, *45*, 380–397.
- (21) Kim, T.; Song, S.; Park, Y.; Kang, S.; Seo, H. HDAC Inhibition by Valproic Acid Induces Neuroprotection and Improvement of PD-like Behaviors in LRRK2 R1441G Transgenic Mice. *Exp. Neurobiol.* **2019**, *28*, 504.
- (22) Mazzocchi, M.; Goulding, S. R.; Wyatt, S. L.; Collins, L. M.; Sullivan, A. M.; O'Keefe, G. W. LMK235, a Small Molecule Inhibitor of HDAC4/5, Protects Dopaminergic Neurons against Neurotoxin- and α -Synuclein-Induced Degeneration in Cellular Models of Parkinson's Disease. *Mol. Cell. Neurosci.* **2021**, *115*, No. 103642.
- (23) Pilkington, A. W.; Schupp, J.; Nyman, M.; Valentine, S. J.; Smith, D. M.; Legleiter, J. Acetylation of A β 40 Alters Aggregation in the Presence and Absence of Lipid Membranes. *ACS Chem. Neurosci.* **2020**, *11*, 146–161.
- (24) Gupta, R.; Kumar, P. Computational Analysis Indicates That PARP1 Acts as a Histone Deacetylases Interactor Sharing Common Lysine Residues for Acetylation, Ubiquitination, and SUMOylation in Alzheimer's and Parkinson's Disease. *ACS Omega* **2021**, *6*, 5739–5753.
- (25) Comerford, K. M.; Leonard, M. O.; Karhausen, J.; Carey, R.; Colgan, S. P.; Taylor, C. T. Small Ubiquitin-Related Modifier-1 Modification Mediates Resolution of CREB-Dependent Responses to Hypoxia. *Proc. Natl. Acad. Sci. U.S.A.* **2003**, *100*, 986.
- (26) David, G.; Neptune, M. A.; Depinho, R. A. SUMO-1 Modification of Histone Deacetylase 1 (HDAC1) Modulates Its Biological Activities. *J. Biol. Chem.* **2002**, *277*, 23658–23663.
- (27) Kirsh, O.; Seeler, J. S.; Pichler, A.; Gast, A.; Müller, S.; Miska, E.; Mathieu, M.; Harel-Bellan, A.; Kouzarides, T.; Melchior, F.; Dejean, A. The SUMO E3 Ligase RanBP2 Promotes Modification of the HDAC4 Deacetylase. *EMBO J.* **2002**, *21*, 2682–2691.
- (28) Fusco, S.; Leone, L.; Barbat, S. A.; Samengo, D.; Piacentini, R.; Maulucci, G.; Toietta, G.; Spinelli, M.; McBurney, M.; Pani, G.; Grassi, C. A CREB-Sirt1-Hes1 Circuitry Mediates Neural Stem Cell Response to Glucose Availability. *Cell Rep.* **2016**, *14*, 1195–1205.

- (29) Paz, J. C.; Park, S.; Phillips, N.; Matsumura, S.; Tsai, W.-W.; Kasper, L.; Brindle, P. K.; Zhang, G.; Zhou, M.-M.; Wright, P. E.; Montminy, M. Combinatorial Regulation of a Signal-Dependent Activator by Phosphorylation and Acetylation. *Proc. Natl. Acad. Sci. U.S.A.* **2014**, *111*, 17116–17121.
- (30) Snider, J.; Kotlyar, M.; Saraon, P.; Yao, Z.; Jurisica, I.; Staglar, I. Fundamentals of Protein Interaction Network Mapping. *Mol. Syst. Biol.* **2015**, *11*, 848.
- (31) Capriotti, E.; Ozturk, K.; Carter, H. Integrating Molecular Networks with Genetic Variant Interpretation for Precision Medicine. *Wiley Interdiscip. Rev.: Syst. Biol. Med.* **2019**, *11*, No. e1443.
- (32) Dai, W.; Chang, Q.; Peng, W.; Zhong, J.; Li, Y. Network Embedding the Protein–Protein Interaction Network for Human Essential Genes Identification. *Genes* **2020**, *11*, 153.
- (33) Vella, D.; Marini, S.; Vitali, F.; Di Silvestre, D.; Mauri, G.; Bellazzi, R. MTGO: PPI Network Analysis Via Topological and Functional Module Identification OPEN. *Sci. Rep.* **2018**, *8*, No. 5499.
- (34) Chen, S.-J.; Liao, D.-L.; Chen, C.-H.; Wang, T.-Y.; Chen, K.-C. Construction and Analysis of Protein-Protein Interaction Network of Heroin Use Disorder. *Sci. Rep.* **2019**, *9*, No. 4980.
- (35) Friedel, C. C.; Zimmer, R. Inferring Topology from Clustering Coefficients in Protein-Protein Interaction Networks. *BMC Bioinf.* **2006**, *7*, 519.
- (36) Xu, K.; Bezakova, I.; Bunimovich, L.; Yi, S. V. Path Lengths in Protein-Protein Interaction Networks and Biological Complexity. *Proteomics* **2011**, *11*, 1857–1867.
- (37) Pavel, A.; del Giudice, G.; Federico, A.; Di Lieto, A.; Kinaret, P. A. S.; Serra, A.; Greco, D. Integrated Network Analysis Reveals New Genes Suggesting COVID-19 Chronic Effects and Treatment. *Briefings Bioinf.* **2021**, *22*, 1430–1441.
- (38) Gu, S.; Johnson, J.; Faisal, F. E.; Milenković, T. From Homogeneous to Heterogeneous Network Alignment via Colored Graphlets. *Sci. Rep.* **2018**, *8*, No. 12524.
- (39) Ashtiani, M.; Salehzadeh-Yazdi, A.; Razaghi-Moghadam, Z.; Hennig, H.; Wolkenhauer, O.; Mirzaie, M.; Jafari, M. A Systematic Survey of Centrality Measures for Protein-Protein Interaction Networks. *BMC Syst. Biol.* **2018**, *12*, 80.
- (40) Koschützki, D.; Schreiber, F. Comparison of Centralities for Biological Networks*. (41) Zhou, H.; Liu, J.; Li, J.; Duan, W. A Density-Based Approach for Detecting Complexes in Weighted PPI Networks by Semantic Similarity. *PLoS One* **2017**, *12*, No. e0180570.
- (42) NetworkAnalyzer Help, <https://med.bioinf.mpi-inf.mpg.de/netanalyzer/help/2.5/> (accessed Aug 21, 2021).
- (43) Rong, Z.; Cheng, B.; Zhong, L.; Ye, X.; Li, X.; Jia, L.; Li, Y.; Shue, F.; Wang, N.; Cheng, Y.; Huang, X.; Liu, C.-C.; Fryer, J. D.; Wang, X.; Zhang, Y.; Zheng, H. Activation of FAK/Rac1/Cdc42-GTPase Signaling Ameliorates Impaired Microglial Migration Response to A β 42 in Triggering Receptor Expressed on Myeloid Cells 2 Loss-of-Function Murine Models. *FASEB J.* **2020**, *34*, 10984–10997.
- (44) Huang, S.; Mao, J.; Ding, K.; Zhou, Y.; Zeng, X.; Yang, W.; Wang, P.; Zhao, C.; Yao, J.; Xia, P.; Pei, G. Polysaccharides from *Ganoderma lucidum* Promote Cognitive Function and Neural Progenitor Proliferation in Mouse Model of Alzheimer's Disease. *Stem Cell Rep.* **2017**, *8*, 84–94.
- (45) Lim, S.; Kim, D.; Ju, S.; Shin, S.; Cho, I.; Park, S.-H.; Grailhe, R.; Lee, C.; Kim, Y. K. Glioblastoma-Secreted Soluble CD44 Activates Tau Pathology in the Brain. *Exp. Mol. Med.* **2018**, *50*, 1–11.
- (46) Neal, M. L.; Boyle, A. M.; Budge, K. M.; Safadi, F. F.; Richardson, J. R. The Glycoprotein GPNMB Attenuates Astrocyte Inflammatory Responses through the CD44 Receptor. *J. Neuroinflammation* **2018**, *15*, 73.
- (47) Landrock, K. K.; Sullivan, P.; Martini-Stoica, H.; Goldstein, D. S.; Graham, B. H.; Yamamoto, S.; Bellen, H. J.; Gibbs, R. A.; Chen, R.; D'Amelio, M.; Stoica, G. Pleiotropic Neuropathological and Biochemical Alterations Associated with Myo5a Mutation in a Rat Model. *Brain Res.* **2018**, *1679*, 155–170.
- (48) Liu, X.; Cheng, R.; Ye, X.; Verbitsky, M.; Kisselev, S.; Mejia-Santana, H.; Louis, E. D.; Cote, L. J.; Andrews, H. F.; Waters, C. H.; Ford, B.; Fahn, S.; Marder, K.; Lee, J. H.; Clark, L. N. Increased Rate of Sporadic and Recurrent Rare Genic Copy Number Variants in Parkinson's Disease among Ashkenazi Jews. *Mol. Genet. Genomic Med.* **2013**, *1*, 142.
- (49) Bhat, G.; LaGrave, D.; Millson, A.; Herriges, J.; Lamb, A. N.; Matalon, R. Xq11.1-11.2 Deletion Involving ARHGEP9 in a Girl with Autism Spectrum Disorder. *Eur. J. Med. Genet.* **2016**, *59*, 470–473.
- (50) Griffin, K.; Bejoy, J.; Song, L.; Hua, T.; Marzano, M.; Jeske, R.; Sang, Q.-X. A.; Li, Y. Human Stem Cell-Derived Aggregates of Forebrain Astroglia Respond to Amyloid Beta Oligomers. *Tissue Eng., Part A* **2020**, *26*, 527–542.
- (51) Qian, G.; Ren, Y.; Zuo, Y.; Yuan, Y.; Zhao, P.; Wang, X.; Cheng, Q.; Liu, J.; Zhang, L.; Guo, T.; Liu, C.; Zheng, H. Smurf1 Represses TNF- α Production through Ubiquitination and Destabilization of USPS. *Biochem. Biophys. Res. Commun.* **2016**, *474*, 491–496.
- (52) Tsai, A. P.; Lin, P. B. C.; Dong, C.; Moutinho, M.; Casali, B. T.; Liu, Y.; Lamb, B. T.; Landreth, G. E.; Oblak, A. L.; Nho, K. INPP5D Expression Is Associated with Risk for Alzheimer's Disease and Induced by Plaque-Associated Microglia. *Neurobiol. Dis.* **2021**, *153*, No. 105303.
- (53) Esteves, I. M.; Lopes-Aguiar, C.; Rossignoli, M. T.; Ruggiero, R. N.; Brogini, A. C. S.; Bueno-Junior, L. S.; Kandratavicius, L.; Monteiro, M. R.; Romcy-Pereira, R. N.; Leite, J. P. Chronic Nicotine Attenuates Behavioral and Synaptic Plasticity Impairments in a Streptozotocin Model of Alzheimer's Disease. *Neuroscience* **2017**, *353*, 87–97.
- (54) Carvajal-Oliveros, A.; Domínguez-Baleón, C.; Zárate, R. V.; Campusano, J. M.; Narváez-Padilla, V.; Reynaud, E. Nicotine Suppresses Parkinson's Disease like Phenotypes Induced by Synphilin-1 Overexpression in *Drosophila melanogaster* by Increasing Tyrosine Hydroxylase and Dopamine Levels. *Sci. Rep.* **2021**, *11*, No. 9579.
- (55) Zhang, X.; Nagai, T.; Ahammad, R. U.; Kuroda, K.; Nakamura, S.; Nakano, T.; Yukinawa, N.; Funahashi, Y.; Yamahashi, Y.; Amano, M.; Yoshimoto, J.; Yamada, K.; Kaibuchi, K. Balance between Dopamine and Adenosine Signals Regulates the PKA/Rap1 Pathway in Striatal Medium Spiny Neurons. *Neurochem. Int.* **2019**, *122*, 8–18.
- (56) Kagawa, Y.; Umaru, B. A.; Shil, S. K.; Hayasaka, K.; Zama, R.; Kobayashi, Y.; Miyazaki, H.; Kobayashi, S.; Suzuki, C.; Katori, Y.; Abe, T.; Owada, Y. Mitochondrial Dysfunction in GnRH Neurons Impaired GnRH Production. *Biochem. Biophys. Res. Commun.* **2020**, *530*, 329–335.
- (57) Şişli, H. B.; Hayal, T. B.; Şenkal, S.; Kıratlı, B.; Sağraç, D.; Seçkin, S.; Özpolat, M.; Şahin, F.; Yılmaz, B.; Doğan, A. Apelin Receptor Signaling Protects GT1-7 GnRH Neurons Against Oxidative Stress In Vitro. *Cell. Mol. Neurobiol.* **2020**, DOI: 10.1007/S10571-020-00968-2.
- (58) Ahmadian, E.; Eftekhari, A.; Samiei, M.; Maleki Dizaj, S.; Vinken, M. The Role and Therapeutic Potential of Connexins, Pannexins and Their Channels in Parkinson's Disease. *Cell. Signalling* **2019**, *58*, 111–118.
- (59) Xing, J.; Xu, C. Role of Connexins in Neurodegenerative Diseases (Review). *Mol. Med. Rep.* **2021**, *23*, 1–6.
- (60) Angeli, S.; Kousiappa, I.; Stavrou, M.; Sargiannidou, I.; Georgiou, E.; Papacostas, S. S.; Kleopa, K. A. Altered Expression of Glial Gap Junction Proteins Cx43, Cx30, and Cx47 in the 5XFAD Model of Alzheimer's Disease. *Front. Neurosci.* **2020**, *14*, 582934.
- (61) Maulik, M.; Vasan, L.; Bose, A.; Chowdhury, S. D.; Sengupta, N.; Sarma, J. D. Amyloid- β Regulates Gap Junction Protein Connexin 43 Trafficking in Cultured Primary Astrocytes. *J. Biol. Chem.* **2020**, *295*, 15097–15111.
- (62) Hansen, B. K.; Gupta, R.; Baldus, L.; Lyon, D.; Narita, T.; Lammers, M.; Choudhary, C.; Weinert, B. T. Analysis of Human Acetylation Stoichiometry Defines Mechanistic Constraints on Protein Regulation. *Nat. Commun.* **2019**, *10*, No. 1055.
- (63) Cao, X.; Li, C.; Xiao, S.; Tang, Y.; Huang, J.; Zhao, S.; Li, X.; Li, J.; Zhang, R.; Yu, W. Acetylation Promotes TyrRS Nuclear Translocation to Prevent Oxidative Damage. *Proc. Natl. Acad. Sci. U.S.A.* **2017**, *114*, 687–692.
- (64) Zhao, X.; Wu, Y.; Li, J.; Li, D.; Jin, Y.; Zhu, P.; Liu, Y.; Zhuang, Y.; Yu, S.; Cao, W.; Wei, H.; Wang, X.; Han, Y.; Chen, G. JNK Activation-Mediated Nuclear SIRT1 Protein Suppression Contributes to Silica

- Nanoparticle-Induced Pulmonary Damage via P53 Acetylation and Cytoplasmic Localisation. *Toxicology* **2019**, *423*, 42–53.
- (65) Zhu, X.; Asa, S. L.; Ezzat, S. Histone-Acetylated Control of Fibroblast Growth Factor Receptor 2 Intron 2 Polymorphisms and Isoform Splicing in Breast Cancer. *Mol. Endocrinol.* **2009**, *23*, 1397.
- (66) Lee, J. L.; Wang, M. J.; Chen, J. Y. Acetylation and Activation of STAT3 Mediated by Nuclear Translocation of CD44. *J. Cell Biol.* **2009**, *185*, 949–957.
- (67) Wei, J.; Dong, S.; Yao, K.; Martinez, M. F. Y. M.; Fleisher, P. R.; Zhao, Y.; Ma, H.; Zhao, J. Histone Acetyltransferase CBP Promotes Function of SCF FBXL19 Ubiquitin E3 Ligase by Acetylation and Stabilization of Its F-Box Protein Subunit. *FASEB J.* **2018**, *32*, 4284–4292.
- (68) Wójtowicz, S.; Strosznajder, A. K.; Jeżyna, M.; Strosznajder, J. B. The Novel Role of PPAR Alpha in the Brain: Promising Target in Therapy of Alzheimer's Disease and Other Neurodegenerative Disorders. *Neurochem. Res.* **2020**, *45*, 972–988.
- (69) Dennis, D. J.; Han, S.; Schuurmans, C. BHLH Transcription Factors in Neural Development, Disease, and Reprogramming. *Brain Res.* **2019**, *1705*, 48–65.
- (70) Yao, Z.; Yang, W.; Gao, Z.; Jia, P. Nicotinamide Mononucleotide Inhibits JNK Activation to Reverse Alzheimer Disease. *Neurosci. Lett.* **2017**, *647*, 133–140.
- (71) Wang, Y.; Lin, Y.; Wang, L.; Zhan, H.; Luo, X.; Zeng, Y.; Wu, W.; Zhang, X.; Wang, F. TREM2 Ameliorates Neuroinflammatory Response and Cognitive Impairment via PI3K/AKT/FoxO3a Signaling Pathway in Alzheimer's Disease Mice. *Aging* **2020**, *12*, 20862.
- (72) Xu, X.; Wang, R.; Hao, Z.; Wang, G.; Mu, C.; Ding, J.; Sun, W.; Ren, H. DJ-1 Regulates Tyrosine Hydroxylase Expression through CaMKK β /CaMKIV/CREB1 Pathway in Vitro and in Vivo. *J. Cell. Physiol.* **2020**, *235*, 869–879.
- (73) Marchese, E.; Di Maria, V.; Samengo, D.; Pani, G.; Michetti, F.; Geloso, M. C. Post-Natal Deletion of Neuronal CAMP Responsive-Element Binding (CREB)-1 Promotes Pro-Inflammatory Changes in the Mouse Hippocampus. *Neurochem. Res.* **2017**, *42*, 2230–2245.
- (74) He, T.; Shang, J.; Gao, C.; Guan, X.; Chen, Y.; Zhu, L.; Zhang, L.; Zhang, C.; Zhang, J.; Pang, T. A Novel SIRT6 Activator Ameliorates Neuroinflammation and Ischemic Brain Injury via EZH2/FOXO1 Axis. *Acta Pharm. Sin. B* **2021**, *11*, 708–726.
- (75) Emelyanov, A. K.; Lavrinova, A. O.; Litusova, E. M.; Knyazev, N. A.; Kulabukhova, D. G.; Garaeva, L. A.; Milyukhina, I. V.; Berkovich, O. A.; Pchelina, S. N. The Effect of Dopamine on Gene Expression of Alpha-Synuclein and Transcription Factors GATA-1, GATA-2, and ZSCAN21 in Parkinson's Disease. *Cell Tissue Biol.* **2018**, *12*, 410–418.
- (76) Zhang, W.; Duan, N.; Song, T.; Li, Z.; Zhang, C.; Chen, X. The Emerging Roles of Forkhead Box (FOX) Proteins in Osteosarcoma. *J. Cancer* **2017**, *8*, 1619.
- (77) Rahman, M. R.; Islam, T.; Turanli, B.; Zaman, T.; Faruquee, H. M.; Rahman, M. M.; Mollah, M. N. H.; Nanda, R. K.; Arga, K. Y.; Gov, E.; Moni, M. A. Network-Based Approach to Identify Molecular Signatures and Therapeutic Agents in Alzheimer's Disease. *Comput. Biol. Chem.* **2019**, *78*, 431–439.
- (78) Jun, G. R.; Chung, J.; Mez, J.; Barber, R.; Beecham, G. W.; Bennett, D. A.; Buxbaum, J. D.; Byrd, G. S.; Carrasquillo, M. M.; Crane, P. K.; Cruchaga, C.; Jager, P.; De; Ertekin-Taner, N.; Evans, D.; Fallin, M. D.; Foroud, T. M.; Friedland, R. P.; Goate, A. M.; Graff-Radford, N. R.; Hendrie, H.; Hall, K. S.; Hamilton-Nelson, K. L.; Inzelberg, R.; Kamboh, M. I.; Kauwe, J. S.; Kukull, W. A.; Kunkle, B. W.; Kuwano, R.; Larson, E. B.; Logue, M. W.; Manly, J. J.; Martin, E. R.; Montine, T. J.; Mukherjee, S.; Naj, A.; Reiman, E. M.; Reitz, C.; Sherva, R.; George-Hyslop, S. P. H.; Thornton, T.; Winkler, S. G.; Vardarajan, B. N.; Wang, L.-S.; Wendlund, J. R.; Winslow, A. R.; Consortium, A. D. G.; Haines, J.; Mayeux, R.; Pericak-Vance, M. A.; Schellenberg, G.; Lunetta, K. L.; Farrer, L. A.; et al. Transethnic Genome-Wide Scan Identifies Novel Alzheimer Disease Loci. *Alzheimer's Dement.* **2017**, *13*, 727.
- (79) Wang, C.; Zhao, F.; Shen, K.; Wang, W.; Siedlak, S. L.; Lee, H.-G.; Phelix, C. F.; Perry, G.; Shen, L.; Tang, B.; Yan, R.; Zhu, X. The Sterol Regulatory Element-Binding Protein 2 Is Dysregulated by Tau Alterations in Alzheimer Disease. *Brain Pathol.* **2019**, *29*, 530–543.
- (80) Li, H.; Liu, J. The Novel Function of HINFP as a Co-Activator in Sterol-Regulated Transcription of PCSK9 in HepG2 Cells. *Biochem. J.* **2012**, *443*, 757–768.
- (81) Lou, F.; Li, M.; Liu, N.; Li, X.; Ren, Y.; Luo, X. The Polymorphism of SREBF1 Gene Rs11868035 G/A Is Associated with Susceptibility to Parkinson's Disease in a Chinese Population. *Int. J. Neurosci.* **2019**, *129*, 660–665.
- (82) Yuan, X. Q.; Cao, B.; Wu, Y.; Chen, Y. P.; Wei, Q. Q.; Ou, R. W.; Yang, J.; Chen, X. P.; Zhao, B.; Song, W.; Shang, H. F. Association Analysis of SNP Rs11868035 in SREBF1 with Sporadic Parkinson's Disease, Sporadic Amyotrophic Lateral Sclerosis and Multiple System Atrophy in a Chinese Population. *Neurosci. Lett.* **2018**, *664*, 128–132.
- (83) Pattaroni, C.; Jacob, C. Histone Methylation in the Nervous System: Functions and Dysfunctions. *Mol. Neurobiol.* **2013**, *47*, 740–756.
- (84) Rahman, M. R.; Islam, T.; Zaman, T.; Shahjaman, M.; Karim, M. R.; Huq, F.; Quinn, J. M. W.; Holsinger, R. M. D.; Gov, E.; Moni, M. A. Identification of Molecular Signatures and Pathways to Identify Novel Therapeutic Targets in Alzheimer's Disease: Insights from a Systems Biomedicine Perspective. *Genomics* **2020**, *112*, 1290–1299.
- (85) Zentner, G. E.; Henikoff, S. Regulation of Nucleosome Dynamics by Histone Modifications. *Nat. Struct. Mol. Biol.* **2013**, *20*, 259–266.
- (86) Ram, O.; Goren, A.; Amit, I.; Shoshitaishvili, N.; Yosef, N.; Ernst, J.; Kellis, M.; Gymrek, M.; Issner, R.; Coyne, M.; Durham, T.; Zhang, X.; Donaghey, J.; Epstein, C. B.; Regev, A.; Bernstein, B. E. Combinatorial Patterning of Chromatin Regulators Uncovered by Genome-Wide Location Analysis in Human Cells. *Cell* **2011**, *147*, 1628.
- (87) Shen, H. Y.; Kalda, A.; Yu, L.; Ferrara, J.; Zhu, J.; Chen, J. F. Additive Effects of Histone Deacetylase Inhibitors and Amphetamine on Histone H4 Acetylation, CAMP Responsive Element Binding Protein Phosphorylation and Δ FosB Expression in the Striatum and Locomotor Sensitization in Mice. *Neuroscience* **2008**, *157*, 644–655.
- (88) Yildirim, F.; Ji, S.; Kronenberg, G.; Barco, A.; Olivares, R.; Benito, E.; Dirnagl, U.; Gertz, K.; Endres, M.; Harms, C.; Meisel, A. Histone Acetylation and CREB Binding Protein Are Required for Neuronal Resistance against Ischemic Injury. *PLoS One* **2014**, *9*, No. e95465.
- (89) Guo, W.; Crossey, E. L.; Zhang, L.; Zucca, S.; George, O. L.; Valenzuela, C. F.; Zhao, X. Alcohol Exposure Decreases CREB Binding Protein Expression and Histone Acetylation in the Developing Cerebellum. *PLoS One* **2011**, *6*, No. e19351.
- (90) Grass, J. A.; Boyer, M. E.; Pal, S.; Wu, J.; Weiss, M. J.; Bresnick, E. H. GATA-1-Dependent Transcriptional Repression of GATA-2 via Disruption of Positive Autoregulation and Domain-Wide Chromatin Remodeling. *Proc. Natl. Acad. Sci. U.S.A.* **2003**, *100*, 8811–8816.
- (91) Li, H.; Liu, J. The Novel Function of HINFP as a Co-Activator in Sterol-Regulated Transcription of PCSK9 in HepG2 Cells. *Biochem. J.* **2012**, *443*, 757–768.
- (92) Gruber, J. J.; Geller, B.; Lipchik, A. M.; Chen, J.; Salahudeen, A. A.; Ram, A. N.; Ford, J. M.; Kuo, C. J.; Snyder, M. P. HAT1 Coordinates Histone Production and Acetylation via H4 Promoter Binding. *Mol. Cell* **2019**, *75*, 711–724.e5.
- (93) Forma, E.; Józwiak, P.; Ciesielski, P.; Zaczek, A.; Starska, K.; Bryś, M.; Krześlak, A. Impact of OGT Dereglulation on EZH2 Target Genes FOXA1 and FOXO1 Expression in Breast Cancer Cells. *PLoS One* **2018**, *13*, No. e0198351.
- (94) Wang, X.; Wu, X.; Liu, Q.; Kong, G.; Zhou, J.; Jiang, J.; Wu, X.; Huang, Z.; Su, W.; Zhu, Q. Ketogenic Metabolism Inhibits Histone Deacetylase (HDAC) and Reduces Oxidative Stress After Spinal Cord Injury in Rats. *Neuroscience* **2017**, *366*, 36–43.
- (95) Lee, J.; Ko, Y. U.; Chung, Y.; Yun, N.; Kim, M.; Kim, K.; Oh, Y. J. The Acetylation of Cyclin-Dependent Kinase 5 at Lysine 33 Regulates Kinase Activity and Neurite Length in Hippocampal Neurons. *Sci. Rep.* **2018**, *8*, No. 13676.
- (96) Jin, H.; Wang, M.; Wang, J.; Cao, H.; Niu, W.; Du, L. Paeonol Attenuates Isoflurane Anesthesia-Induced Hippocampal Neurotoxicity via Modulation of JNK/ERK/P38MAPK Pathway and Regulates Histone Acetylation in Neonatal Rat. *J. Matern.-Fetal. Neonat. Med.* **2020**, *33*, 81–91.

- (97) El-Naggar, A. M.; Somasekharan, S. P.; Wang, Y.; Cheng, H.; Negri, G. L.; Pan, M.; Wang, X. Q.; Delaidelli, A.; Rafn, B.; Cran, J.; Zhang, F.; Zhang, H.; Colborne, S.; Gleave, M.; Mandinova, A.; Kedersha, N.; Hughes, C. S.; Surdez, D.; Delattre, O.; Wang, Y.; Huntsman, D. G.; Morin, G. B.; Sorensen, P. H. Class I HDAC Inhibitors Enhance YB-1 Acetylation and Oxidative Stress to Block Sarcoma Metastasis. *EMBO Rep.* **2019**, *20*, No. e48375.
- (98) Kelly, R. D. W.; Chandru, A.; Watson, P. J.; Song, Y.; Blades, M.; Robertson, N. S.; Jamieson, A. G.; Schwabe, J. W. R.; Cowley, S. M. Histone Deacetylase (HDAC) 1 and 2 Complexes Regulate Both Histone Acetylation and Crotonylation in Vivo. *Sci. Rep.* **2018**, *8*, No. 14690.
- (99) Topuz, R. D.; Gunduz, O.; Tastekin, E.; Karadag, C. H. Effects of Hippocampal Histone Acetylation and HDAC Inhibition on Spatial Learning and Memory in the Morris Water Maze in Rats. *Fundam. Clin. Pharmacol.* **2020**, *34*, 222–228.
- (100) Choi, H.; Kim, H. J.; Kim, J.; Kim, S.; Yang, J.; Lee, W.; Park, Y.; Hyeon, S. J.; Lee, D.-S.; Ryu, H.; Chung, J.; Mook-Jung, I. Increased Acetylation of Peroxiredoxin1 by HDAC6 Inhibition Leads to Recovery of β -Induced Impaired Axonal Transport. *Mol. Neurodegener.* **2017**, *12*, 23.
- (101) Min, S.-W.; Sohn, P. D.; Li, Y.; Devidze, N.; Johnson, J. R.; Krogan, N. J.; Masliah, E.; Mok, S.-A.; Gestwicki, J. E.; Gan, L. SIRT1 Deacetylates Tau and Reduces Pathogenic Tau Spread in a Mouse Model of Tauopathy. *J. Neurosci.* **2018**, *38*, 3680–3688.
- (102) Paz, J. C.; Park, S.; Phillips, N.; Matsumura, S.; Tsai, W.-W.; Kasper, L.; Brindle, P. K.; Zhang, G.; Zhou, M.-M.; Wright, P. E.; Montminy, M. Combinatorial Regulation of a Signal-Dependent Activator by Phosphorylation and Acetylation. *Proc. Natl. Acad. Sci. U.S.A.* **2014**, *111*, 17116.
- (103) Lu, Q.; Hutchins, A. E.; Doyle, C. M.; Lundblad, J. R.; Kwok, R. P. S. Acetylation of CAMP-Responsive Element-Binding Protein (CREB) by CREB-Binding Protein Enhances CREB-Dependent Transcription. *J. Biol. Chem.* **2003**, *278*, 15727–15734.
- (104) Van Nguyen, T.; Lee, J. E.; Sweredoski, M. J.; Yang, S. J.; Jeon, S. J.; Harrison, J. S.; Yim, J. H.; Lee, S. G.; Handa, H.; Kuhlman, B.; Jeong, J. S.; Reitsma, J. M.; Park, C. S.; Hess, S.; Deshaies, R. J. Glutamine Triggers Acetylation-Dependent Degradation of Glutamine Synthetase via the Thalidomide Receptor Cereblon. *Mol. Cell* **2016**, *61*, 809–820.
- (105) Son, S. M.; Park, S. J.; Stamatakou, E.; Vicinanza, M.; Menzies, F. M.; Rubinsztein, D. C. Leucine Regulates Autophagy via Acetylation of the MTORC1 Component Raptor. *Nat. Commun.* **2020**, *11*, No. 3148.
- (106) Chiki, A.; Zhang, Z.; Rajasekhar, K.; Abriata, L. A.; Rostami, I.; Krapp, L. F.; Boudeffa, D.; Dal Peraro, M.; Lashuel, H. A. Investigating Crosstalk Among PTMs Provides Novel Insight Into the Structural Basis Underlying the Differential Effects of Nt17 PTMs on Mutant Httex1 Aggregation. *Front. Mol. Biosci.* **2021**, *8*, 686086.
- (107) Ichiki, T. Role of CAMP Response Element Binding Protein in Cardiovascular Remodeling. *Arterioscler., Thromb., Vasc. Biol.* **2006**, *26*, 449–455.
- (108) Xu, W.; Kasper, L. H.; Lerach, S.; Jeevan, T.; Brindle, P. K. Individual CREB-Target Genes Dictate Usage of Distinct CAMP-Responsive Coactivation Mechanisms. *EMBO J.* **2007**, *26*, 2890–2903.
- (109) Sekimata, M.; Homma, Y. Sequence-Specific Transcriptional Repression by an MBD2-Interacting Zinc Finger Protein MIZF. *Nucleic Acids Res.* **2004**, *32*, 590–597.
- (110) Medina, R.; Buck, T.; Zaidi, S. K.; Miele-Chamberland, A.; Lian, J. B.; Stein, J. L.; Van Wijnen, A. J.; Stein, G. S. The Histone Gene Cell Cycle Regulator HiNF-P Is a Unique Zinc Finger Transcription Factor with a Novel Conserved Auxiliary DNA-Binding Motif. *Biochemistry* **2008**, *47*, 11415–11423.
- (111) Vetteese-Dadey, M.; Grant, P. A.; Hebbes2', T. R.; Crane-Robinson2, C.; David Allis4, C.; Workman5, J. L. Acetylation of Histone H4 Plays a Primary Role in Enhancing Transcription Factor Binding to Nucleosomal DNA in Vitro. *EMBO J.* **1996**, *15*, 2508–2518.
- (112) Buchholz, I.; Nestler, P.; Köppen, S.; Delcea, M. Lysine Residues Control the Conformational Dynamics of Beta 2-Glycoprotein I. *Phys. Chem. Chem. Phys.* **2018**, *20*, 26819–26829.
- (113) Maltsev, A. S.; Ying, J.; Bax, A. Impact of N-Terminal Acetylation of α -Synuclein on Its Random Coil and Lipid Binding Properties. *Biochemistry* **2012**, *51*, 5004–5013.
- (114) Kulemzina, I.; Ang, K.; Zhao, X.; Teh, J. T.; Verma, V.; Suranthran, S.; Chavda, A. P.; Huber, R. G.; Eisenhaber, B.; Eisenhaber, F.; Yan, J.; Ivanov, D. A Reversible Association between Smc Coiled Coils Is Regulated by Lysine Acetylation and Is Required for Cohesin Association with the DNA. *Mol. Cell* **2016**, *63*, 1044–1054.
- (115) Landfield, P. W.; Geddes, J. W.; Chen, K. C.; Blalock, E. M.; Porter, N. M.; Markesbery, W. R. Incipient Alzheimer's Disease: Microarray Correlation Analyses Reveal Major Transcriptional and Tumor Suppressor Responses. *Proc. Natl. Acad. Sci. U.S.A.* **2004**, *101*, 2173–2178.
- (116) Blalock, E. M.; Buechel, H. M.; Popovic, J.; Geddes, J. W.; Landfield, P. W. Microarray Analyses of Laser-Captured Hippocampus Reveal Distinct Gray and White Matter Signatures Associated with Incipient Alzheimer's Disease. *J. Chem. Neuroanat.* **2011**, *42*, 118–126.
- (117) Lesnick, T. G.; Papapetropoulos, S.; Mash, D. C.; Ffrench-Mullen, J.; Shehadeh, L.; De Andrade, M.; Henley, J. R.; Rocca, W. A.; Ahlskog, J. E.; Maraganore, D. M. A Genomic Pathway Approach to a Complex Disease: Axon Guidance and Parkinson Disease. *PLoS Genet.* **2007**, *3*, No. e98.
- (118) Lewandowski, N. M.; Ju, S.; Verbitsky, M.; Ross, B.; Geddie, M. L.; Rockenstein, E.; Adame, A.; Muhammad, A.; Vonsattel, J. P.; Ringe, D.; Cote, L.; Lindquist, S.; Masliah, E.; Petsko, G. A.; Marder, K.; Clark, L. N.; Small, S. A. Polyamine Pathway Contributes to the Pathogenesis of Parkinson Disease. *Proc. Natl. Acad. Sci. U.S.A.* **2010**, *107*, 16970–16975.
- (119) Edgar, R. Gene Expression Omnibus: NCBI Gene Expression and Hybridization Array Data Repository. *Nucleic Acids Res.* **2002**, *30*, 207.
- (120) Smedley, D.; Haider, S.; Durinck, S.; Pandini, L.; Provero, P.; Allen, J.; Arnaiz, O.; Awedh, M. H.; Baldock, R.; Barbiera, G.; Bardou, P.; Beck, T.; Blake, A.; Bonierbale, M.; Brookes, A. J.; Bucci, G.; Buetti, I.; Burge, S.; Cabau, C.; Carlson, J. W.; Chelala, C.; Chrysostomou, C.; Cittaro, D.; Collin, O.; Cordova, R.; Cutts, R. J.; Dassi, E.; Di Genova, A.; Djari, A.; Esposito, A.; Estrella, H.; Eyraes, E.; Fernandez-Banet, J.; Forbes, S.; Free, R. C.; Fujisawa, T.; Gadaleta, E.; Garcia-Manteiga, J. M.; Goodstein, D.; Gray, K.; Guerra-Assunção, J. A.; Haggarty, B.; Han, D. J.; Han, B. W.; Harris, T.; Harshbarger, J.; Hastings, R. K.; Hayes, R. D.; Hoede, C.; Hu, S.; Hu, Z. L.; Hutchins, L.; Kan, Z.; Kawaji, H.; Kellet, A.; Kerhornou, A.; Kim, S.; Kinsella, R.; Klopp, C.; Kong, L.; Lawson, D.; Lazarevic, D.; Lee, J. H.; Letellier, T.; Li, C. Y.; Lio, P.; Liu, C. J.; Luo, J.; Maass, A.; Mariette, J.; Maurel, T.; Merella, S.; Mohamed, A. M.; Moreews, F.; Nabihoudine, I.; Ndegwa, N.; Noirot, C.; Perez-Llamas, C.; Primig, M.; Quattrone, A.; Quesneville, H.; Rambaldi, D.; Reecy, J.; Riba, M.; Rosanoff, S.; Sadiq, A. A.; Salas, E.; Sallou, O.; Shepherd, R.; Simon, R.; Sperling, L.; Spooner, W.; Staines, D. M.; Steinbach, D.; Stone, K.; Stupka, E.; Teague, J. W.; Dayem Ullah, A. Z.; Wang, J.; Ware, D.; Wong-Erasmus, M.; Youens-Clark, K.; Zadissa, A.; Zhang, S. J.; Kasprzyk, A. The BioMart Community Portal: An Innovative Alternative to Large, Centralized Data Repositories. *Nucleic Acids Res.* **2015**, *43*, W589.
- (121) Oliveros, J. C. VENNY. An interactive tool for comparing lists with Venn Diagrams. <http://bioinfogp.cnb.csic.es/tools/venny/index.html>.
- (122) Szklarczyk, D.; Gable, A. L.; Lyon, D.; Junge, A.; Wyder, S.; Huerta-Cepas, J.; Simonovic, M.; Doncheva, N. T.; Morris, J. H.; Bork, P.; Jensen, L. J.; Von Mering, C. STRING V11: Protein-Protein Association Networks with Increased Coverage, Supporting Functional Discovery in Genome-Wide Experimental Datasets. *Nucleic Acids Res.* **2019**, *47*, D607.
- (123) Excoffier, L.; Gouy, A.; Daub, J. T.; Shannon, P.; Markiel, A.; Ozier, O.; Baliga, N. S.; Wang, J. T.; Ramage, D.; Amin, N.; Schwikowski, B.; Ideker, T. Cytoscape: A Software Environment for Integrated Models of Biomolecular Interaction Networks. *Nucleic Acids Res.* **2017**, *45*, e149.

(124) Bader, G. D.; Hogue, C. W. V. An Automated Method for Finding Molecular Complexes in Large Protein Interaction Networks. *BMC Bioinf.* **2003**, *4*, 2.

(125) Chin, C. H.; Chen, S. H.; Wu, H. H.; Ho, C. W.; Ko, M. T.; Lin, C. Y. CytoHubba: Identifying Hub Objects and Sub-Networks from Complex Interactome. *BMC Syst. Biol.* **2014**, *8*, 41.

(126) Kuleshov, M. V.; Jones, M. R.; Rouillard, A. D.; Fernandez, N. F.; Duan, Q.; Wang, Z.; Koplev, S.; Jenkins, S. L.; Jagodnik, K. M.; Lachmann, A.; McDermott, M. G.; Monteiro, C. D.; Gunderson, G. W.; Ma'ayan, A. Enrichr: A Comprehensive Gene Set Enrichment Analysis Web Server 2016 Update. *Nucleic Acids Res.* **2016**, *44*, W90.

(127) Dimmer, E. C.; Huntley, R. P.; Barrell, D. G.; Binns, D.; Draghici, S.; Camon, E. B.; Hubank, M.; Talmud, P. J.; Apweiler, R.; Lovering, R. C. The Gene Ontology - Providing a Functional Role in Proteomic Studies. *Proteomics* **2008**, DOI: 10.1002/pmic.200800002.

(128) Jassal, B.; Matthews, L.; Viteri, G.; Gong, C.; Lorente, P.; Fabregat, A.; Sidiropoulos, K.; Cook, J.; Gillespie, M.; Haw, R.; Loney, F.; May, B.; Milacic, M.; Rothfels, K.; Sevilla, C.; Shamovsky, V.; Shorsler, S.; Varusai, T.; Weiser, J.; Wu, G.; Stein, L.; Hermjakob, H.; D'Eustachio, P. The Reactome Pathway Knowledgebase. *Nucleic Acids Res.* **2020**, *48*, D498–D503.

(129) Pathan, M.; Keerthikumar, S.; Ang, C. S.; Gangoda, L.; Quek, C. Y. J.; Williamson, N. A.; Mouradov, D.; Sieber, O. M.; Simpson, R. J.; Salim, A.; Bacic, A.; Hill, A. F.; Stroud, D. A.; Ryan, M. T.; Agbinya, J. L.; Mariadason, J. M.; Burgess, A. W.; Mathivanan, S. FunRich: An Open Access Standalone Functional Enrichment and Interaction Network Analysis Tool. *Proteomics* **2015**, *15*, 2597.

(130) Yu, C. S.; Chen, Y. C.; Lu, C. H.; Hwang, J. K. Prediction of Protein Subcellular Localization. *Proteins* **2006**, *64*, 643.

(131) Bryne, J. C.; Valen, E.; Tang, M. H. E.; Marstrand, T.; Winther, O.; Da piedade, I.; Krogh, A.; Lenhard, B.; Sandelin, A. JASPAR, the Open Access Database of Transcription Factor-Binding Profiles: New Content and Tools in the 2008 Update. *Nucleic Acids Res.* **2007**, *36*, D102–D106.

(132) Zhou, G.; Soufan, O.; Ewald, J.; Hancock, R. E. W.; Basu, N.; Xia, J. NetworkAnalyst 3.0: A Visual Analytics Platform for Comprehensive Gene Expression Profiling and Meta-Analysis. *Nucleic Acids Res.* **2019**, *47*, W234.

(133) Wang, D.; Liu, D.; Yuchi, J.; He, F.; Jiang, Y.; Cai, S.; Li, J.; Xu, D. MusiteDeep: A Deep-Learning Based Webserver for Protein Post-Translational Modification Site Prediction and Visualization. *Nucleic Acids Res.* **2020**, *48*, W140–W146.

(134) Suo, S.-B.; Qiu, J.-D.; Shi, S.-P.; Sun, X.-Y.; Huang, S.-Y.; Chen, X.; Liang, R.-P. Position-Specific Analysis and Prediction for Protein Lysine Acetylation Based on Multiple Features. *PLoS One* **2012**, *7*, No. e49108.

(135) Yu, K.; Zhang, Q.; Liu, Z.; Du, Y.; Gao, X.; Zhao, Q.; Cheng, H.; Li, X.; Liu, Z.-X. Deep Learning Based Prediction of Reversible HAT/HDAC-Specific Lysine Acetylation. *Briefings Bioinf.* **2020**, *21*, 1798–1805.

(136) Thompson, J. D.; Gibson, T. J.; Higgins, D. G. Multiple Sequence Alignment Using ClustalW and ClustalX. *Curr. Protoc. Bioinf.* **2003**, 151.

(137) McGuffin, L. J.; Bryson, K.; Jones, D. T. The PSIPRED Protein Structure Prediction Server. *Bioinformatics* **2000**, *16*, 404.

Recommended by ACS

Effect of Probiotic Fungi against Cognitive Impairment in Mice via Regulation of the Fungal Microbiota–Gut–Brain Axis

Tao Ye, Jing Sun, *et al.*

JULY 14, 2022

JOURNAL OF AGRICULTURAL AND FOOD CHEMISTRY

READ 

Extracellular Matrix Muscle Arm Development Defective Protein Cooperates with the One Immunoglobulin Domain Protein To Suppress Precocious Synaptic Remodeling

Chunhong Chen, Haijun Tu, *et al.*

MAY 21, 2021

ACS CHEMICAL NEUROSCIENCE

READ 

Testing Amyloid Cross-Toxicity in the Vertebrate Brain

Gabriela Henríquez, Mahesh Narayan, *et al.*

JUNE 15, 2020

ACS OMEGA

READ 

Contrasting Effects of Ferric and Ferrous Ions on Oligomerization and Droplet Formation of Tau: Implications in Tauopathies and Neurodegeneration

Sandipan Mukherjee and Dulal Panda

NOVEMBER 16, 2021

ACS CHEMICAL NEUROSCIENCE

READ 

Get More Suggestions >


Computational Analysis Indicates That PARP1 Acts as a Histone Deacetylases Interactor Sharing Common Lysine Residues for Acetylation, Ubiquitination, and SUMOylation in Alzheimer's and Parkinson's Disease

Rohan Gupta and Pravir Kumar*

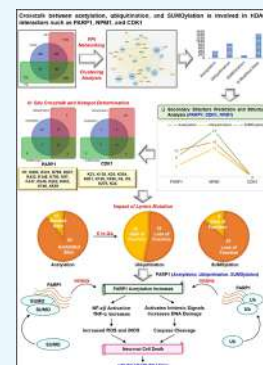
Cite This: *ACS Omega* 2021, 6, 5739–5753

Read Online

ACCESS |

 Metrics & More Article Recommendations

ABSTRACT: *Aim/Hypothesis:* Lysine residues are known for the post-translational modifications (PTMs) such as acetylation, ubiquitination, and SUMOylation. In acetylation, histone deacetylase (HDAC) and its interactors cause transcriptional deregulation and cause mitochondrial dysfunction, apoptosis, inflammatory response, and cell-cycle impairment that cause brain homeostasis and neuronal cell death. Other regulatory PTMs involved in the pathogenesis of neurodegenerative diseases (NDDs) are ubiquitination and SUMOylation for the degradation of the misfolded proteins. Thus, we aim to investigate the potential acetylation/ubiquitination/SUMOylation crosstalk sites in the HDAC interactors, which cause NDDs. Furthermore, we aim to identify the influence of PTMs on the structural features of proteins and the impact of putative lysine mutation on disease susceptibility. Last, we aim to examine the impact of the putative mutation on acetylated lysine for ubiquitination and SUMOylation. *Results:* Herein, we integrate 1455 genes, 3094 genes, and 1940 genes related to HDAC interactors, Alzheimer's disease (AD), and Parkinson's disease (PD), respectively. Furthermore, the protein–protein interaction and PTM integrations from different databases identified 32 proteins that are associated with HDAC, AD, and PD with 1489 potential lysine-modified sites. HDAC interactors poly(ADP-ribose) polymerase 1 (PARP1), nucleophosmin (NPM1), and cyclin-dependent kinase 1 (CDK1) involved in the progression of NDDs and 64 and 75% of PTM sites in PARP1, NPM1, and CDK1 fall into coiled and ordered regions, respectively. Moreover, 15 putative lysine sites have been found in the crosstalk and K148, K249, K528, K637, K700, and K796 of PARP1 are crosstalk hotspots. *Conclusion:* The loss of acetylated hotspot sites results in the loss of ubiquitination and SUMOylation function on nearby sites, which is relatively higher when compared to the gain of function.



1. INTRODUCTION

Neurodegenerative diseases (NDDs) such as Alzheimer's disease (AD), Parkinson's disease (PD), Huntington's disease (HD), amyotrophic lateral sclerosis (ALS), frontotemporal dementia, and multiple sclerosis occur due to the progressive loss of neuronal cells, which causes synaptic dysfunction and memory impairment. AD and PD are the two most prevalent forms of NDDs in older people.¹ Recent studies demonstrated the potential role of post-translational modifications (PTMs) such as acetylation/deacetylation, methylation/demethylation, ubiquitination, SUMOylation, phosphorylation, and others in the pathogenesis of NDDs.² These PTMs cause transcriptional alteration, which leads to mitochondrial dysfunction, apoptosis and autophagic cell death, DNA damage response, inflammatory response, cell-cycle dysregulation, stress response, and microglial activation, which are prominent features of AD and PD.^{3,4} Among different PTMs, acetylation of essential regulatory proteins via lysine acetyltransferase (HATs/KATs) promotes the euchromatin structure and leads to transcriptional activation.^{5–8} Acetylation of lysine residues neutralizes

the charges on histone proteins, increasing the chromatin accessibility for transcription factors, which is called euchromatin or relaxed chromatin structure.⁹ Transcriptional activation of regulatory proteins reverses cellular processes' impairment, which restores synaptic functions and learning ability.¹⁰

On the contrary, histone deacetylases (HDACs) are a class of lysine deacetylases that reverse the process of acetylation and cause transcriptional repression, which causes neurodegeneration.¹¹ Along with acetylation, ubiquitination and SUMOylation are two other significant PTMs, which are involved in the pathogenesis of NDDs. Ubiquitination plays an essential role in the clearance of accumulated toxic proteins in

Received: December 18, 2020

Accepted: February 12, 2021

Published: February 19, 2021



Table 1. Mechanism of HDAC Interactors Involved in AD and PD Pathogenesis in Acetylation, Ubiquitination, and SUMOylation

HDAC interactor	acetylation	ubiquitination	SUMOylation
NPM1	NPM1 acetylation through p300 modulates its subcellular localization and promotes its binding with transcriptionally active RNA polymerase II. ²¹	impaired BRCA1-BARD1 ubiquitin ligase causes NPM1 downregulation through p-STATs, which in turn enhances cell survival. ²²	ARF and TRIM28 coexpression enhances NPM1 SUMOylation and alters its centrosomal localization, which suppressed the centrosome amplification. ²³
HIF1A	acetylation of HIF1A at K709 through p300 increases its stability and decreases polyubiquitination. ²⁴	HIF1A ubiquitination at K63 through STUB1 causes its proteasomal degradation. ²⁵	SUMOylation of HIF1A changes its turnover rate through E3 SUMO ligase, which reduces its transcriptional activity. ²⁶
CASP8	HDAC inhibitor increases Ku70 acetylation and thus decreases FLIP/Ku70 association and increases caspase 8 activation. ²⁷	increased Ku70 acetylation triggers FLIP polyubiquitination and causes its degradation through the proteasome. ²⁷	SUMOylation of caspase 8 at K156 alters its nuclear localization but does not interfere in its activation. ²⁸
ERK1	acetylated ERK1 at K72 enhances the enzymatic activity and affects ATP binding. ²⁹	PHD domain of E3 ligase MEK1 acts as an upstream activator of ERK1 and JNK, which promotes their degradation through the proteasomal pathway. ³⁰	SUMOylation of nNOS at K725 and K739 enhances NO production, which is required for ERK1/2 activity in nNOS-positive neurons. ³¹
PARP1	P300/CREB-induced PARP1 acetylation causes coactivation of NF- κ B-dependent transcription. ³²	polyubiquitination of PARP1 at K48 regulates its degradation. ³³	SUMOylation of PARP1 at K486 through SUMO1 and SUMO3 decreases its p300-mediated acetylation, which restrains transcriptional coactivator functions. ³⁴
AKT1	acetylation of Akt at K163 and K377 increases the neuronal differentiation. ³⁵	E3 Ligase TRAF6 promotes Akt1 polyubiquitination at K63 and promotes membrane localization and its phosphorylation. ³⁶	decreases Akt SUMOylation at K276 and K301 and affects Akt-induced Bcl-X alternative splicing. ³⁷
ERBB2	acetylation of ERBB2 increases its stability. ³⁸	ubiquitination of ERBB2 through E3 ligase CHIP decreases its stability and facilitates its proteasomal degradation. ³⁹	SUMOylation of ERBB2 at K23 promotes its transcriptional repression. ⁴⁰
DNMT1	DNMT1 is destabilized with Tip60-induced acetylation. ⁴¹	acetylation of DNMT1 triggers ubiquitination with UHRF1 and promotes its proteasomal degradation. ⁴¹	SUMOylation of DNMT1 enhances demethylase activity <i>in vivo</i> and modulates its interaction with HDAC. ⁴²
MYC	P300-mediated Myc acetylation increases the transcriptional activity and control Myc protein turnover. ⁴³	USP28-induced Myc ubiquitination promotes its stability and promotes its degradation through interaction with FBW7. ⁴⁴	K52, K148, K157, and K317 SUMOylation of Myc promotes its degradation regulated by PIAS1 and RNF4. ⁴⁵
APP	increased H3 and H4 acetylation of APP enhances its transcriptional activity, which increases EGRI and c-FOS expression. ⁴⁶	enhanced ubiquitination of APP decreases its full-length expression and thus decreases A β generation. ⁴⁷	SUMOylation of APP decreases A β production, whereas SENP1 and SENP2 decrease APP SUMOylation. ⁴⁸
GAPDH	GAPDH acetylation at K256 increases its activity in glucose response. ⁴⁹	S-nitrosylation of B23 at cysteine 275 enhances b23-SIAH1 binding through the decreased E3 ligase activity of SIAH1 and exerts neuroprotective effects. ⁵⁰	
CDK1	acetylation of CDK1 at K33 requires CDK1: cyclin B binding. ⁵¹	CDK master target of SUMOylation. Inhibition of CDK1 SUMOylation alters its status on CDK1 and its interacting proteins. Decreased CDK1 SUMOylation enhances its activity. ⁵²	TRAP1 silencing enhances CDK1 ubiquitination, increases MAD2 degradation, and decreases nuclear translocation of the CDK1/cyclin B complex. ⁵³

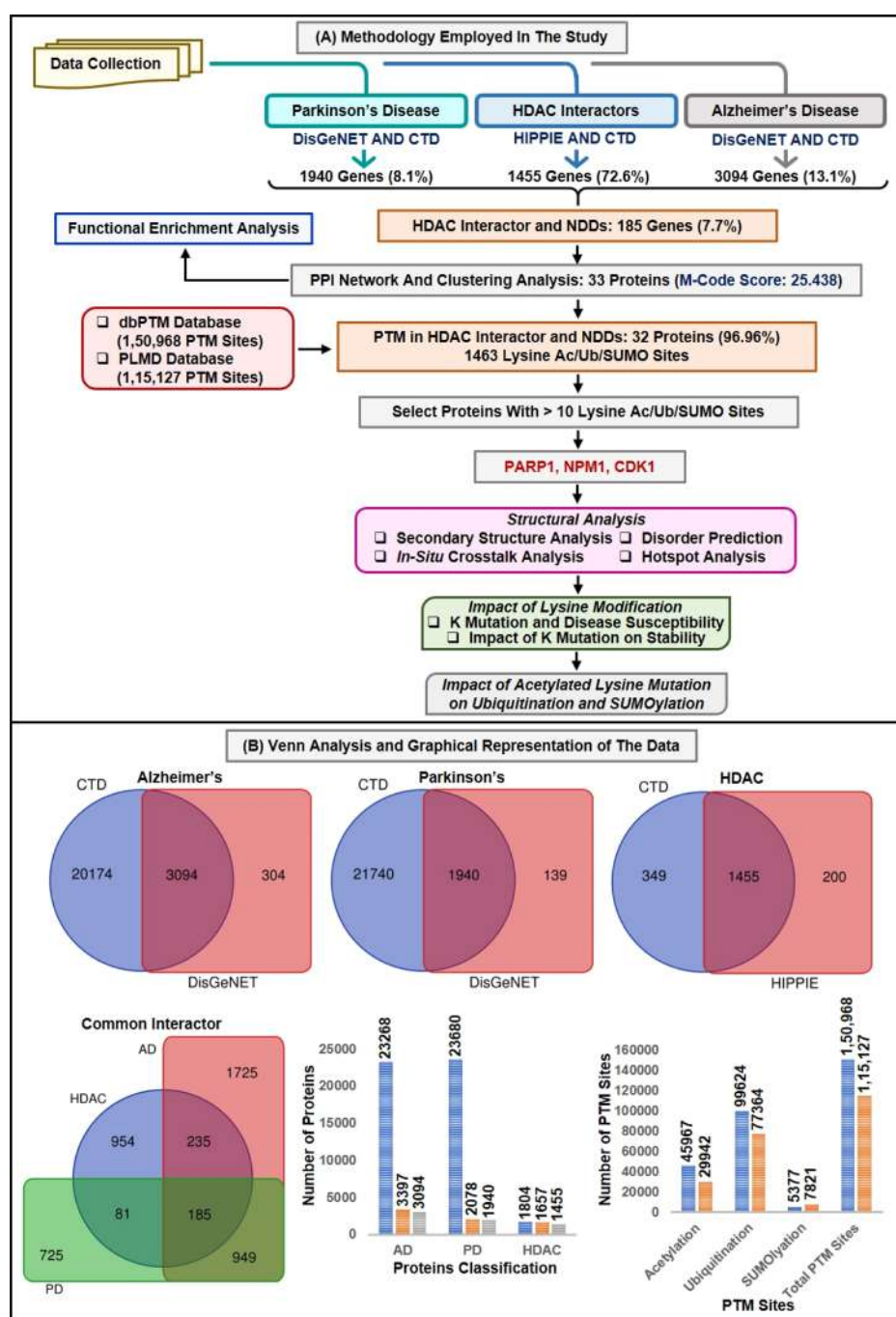


Figure 1. (A) Brief description of the methodology in the current study and (B) interactive Venn analysis of AD, PD, and HDAC interactors collected during the data extraction from different databases. For AD and PD, databases such as CTD and DisGeNET were used, whereas for HDAC interactors, databases such as CTD and HIPPIE were used. The figure also shows the Venn analysis of common genes involved in AD, PD, and HDAC interactors. Later on, bar graph analysis of protein extracted from databases for AD, PD, and HDAC interactors is given in the figure. The blue color in the graph represents the CTD database. The orange color represents the DisGeNET database for AD and PD and the HIPPIE database for HDAC interactors. Similarly, gray color represents the common among them. In the second bar graph, the blue color denotes the dbPTM database, whereas the orange color represents the PLMD database.

the brain through the ubiquitin–proteasome system (UPS), where any impairment in ubiquitination is known to exaggerate the neurodegenerative malignancies.¹² Similarly, SUMOylation is a process that involves the addition of a small ubiquitin-related modifier (SUMO) protein to the lysine side chain of regulatory proteins, which assists in protein folding and the clearance of toxic protein aggregates through chaperone-mediated autophagy, macroautophagy, and proteolytic sys-

tems.¹³ Thus, targeting acetylation, ubiquitination, and SUMOylation pathways provides a new mechanism toward neuroprotection. Recent studies demonstrated the implementation of PTM crosstalk in the progression of NDDs, where negative crosstalk at the same site between different lysine modifications or commonly called as *in situ* crosstalk, has been highlighted on different occasions.^{14,15} Previous studies confirmed that HDAC and its interactors play a crucial role

in the PTMs, such as acetylation, ubiquitination, and SUMOylation in neurodegeneration. For example, the non-covalent attachment of SUMO-2 to repressor element-1 silencing the transcription factor corepressor 1 (CoREST1) causes transcriptional activation and changes the acetylation level of coREST1/lysine (K)-specific demethylase 1 (LSD1)/HDAC target genes.¹⁶ Similarly, decreased HDAC activity promotes the acetylation of Htt protein and also causes an increase in Ube2e3, SUMO2, and USp28 expression. Furthermore, decreased HDAC expression causes increased proteasomal degradation of mHtt aggregates due to the increased activity of HDAC interactor IκappaB kinase (IKK).¹⁷ Tao et al. (2017) demonstrated that in APP/PS1 mice, acute Aβ increases the protein inhibitor of activated STAT 1 (PIAS1) and Mcl-1 expression through MAPK/ERK signaling activation. Increased PIAS1 expression enhances HDAC1 SUMOylation in rat hippocampus.¹⁸ Table 1 describes the mechanism of different HDAC interactors in acetylation, ubiquitination, and SUMOylation. Our previous studies confirmed the role of lysine residues in ubiquitination¹⁹ and acetylation,²⁰ which enables us to investigate the crosstalk between acetylation, ubiquitination, and SUMOylation at HDAC interactors. Moreover, acetylation, ubiquitination, and SUMOylation individual *in situ* crosstalk have been demonstrated in different large-scale proteome studies. However, crosstalk between the three has not been discussed until now, and the possible effect of acetylation on ubiquitination and SUMOylation is still unexplored.

Herein, we integrated AD- and PD-related genes with HDAC interactors and identified the HUB genes through the protein–protein interaction (PPI) network and clustering analysis. Furthermore, we examined the molecular functions and biological pathways in which shared genes (AD, PD, and HDAC) were involved. Last, PTM data were integrated through dbPTM and PLMD databases on 32 proteins, which are the regulatory sequences. Afterward, the proteins with high frequency for acetylation, ubiquitination, and SUMOylation were extracted among the 32 selected proteins. Finally, structural features and crosstalk sites were identified along with the impact of putative lysine mutation on disease susceptibility and protein stability. Last, our study investigates the potential implementation of the loss of crucial lysine residues on ubiquitination and SUMOylation function. Thus, to the best of our knowledge, this is the first study that deals with the crosstalk of acetylation with ubiquitination and SUMOylation simultaneously among HDAC interactors.

2. MATERIALS AND METHODS

2.1. Integration of PPI of HDAC, AD, and PD Genes.

Data from two databases, such as DisGeNET (<https://www.disgenet.org/>)⁵⁴ and The Comparative Toxicogenomics Database (CTD) (<http://ctdbase.org/>),⁵⁵ were collected for genes associated with the progression of AD and PD. Similarly, information related to HDAC interactors was extracted from two databases, such as CTD and HIPPIE (<http://cbdm-01.zdv.uni-mainz.de/~mschaefer/hippie/>).⁵⁶ The databases were searched for duplicates, and redundancy in data was removed manually (Figure 1A). The proteins that were common in two databases were selected, and Venn analysis was carried out through Bioinformatics & Evolutionary Genomics Venn creator (<http://bioinformatics.psb.ugent.be/webtools/Venn/>) in order to identify common proteins in AD, PD, and HDAC interactors (Figure 1B). Furthermore, the PPI network and

clustering analysis of proteins were carried out with the STRING database (<https://string-db.org/>)⁵⁷ and The Cytoscape Software (<https://cytoscape.org/>).⁵⁸

2.2. Molecular Function and Biological Pathway Analysis of HDAC Interactors. Gene set enrichment analysis was performed to extract the information related to molecular functions and biological pathways in which the defined set of genes (HDAC interactors) were involved. The gene set's molecular functions were determined through a freely available software known as FunRich (<http://www.funrich.org/>).⁵⁹ Furthermore, signal transduction pathways in which the genes were involved were determined with the Kyoto encyclopedia of genes and genomes (KEGG) pathway database (<https://www.genome.jp/kegg/>).⁶⁰

2.3. Integration of PTM Sites. Two databases, such as dbPTM (<http://dbptm.mbc.nctu.edu.tw/>)⁶¹ and protein lysine modification database (PLMD) (<http://plmd.biocuckoo.org/>),⁶² were used to extract the information of PTM (acetylation, ubiquitination, and SUMOylation) on regulatory proteins. Once the data were extracted, they were combined manually, and redundancy in PTM sites was removed. The PTM sites are sorted out according to PTM and modification sites.

2.4. Structural Analysis of Regulatory Proteins.

2.4.1. Secondary Structure Prediction. PTM influences the secondary structure of the protein, which regulates its biological functions. We extracted the protein secondary structure information from DISOPRED3 (<http://bioinf.cs.ucl.ac.uk/psipred/>)⁶³ on both PTM and nonPTM lysine residues. DISOPRED3 is an open-source tool created by the UCL Department of Computer Science: Bioinformatics Group. The output was classified into three categories, such as coiled, helix, and strand.

2.4.2. Disorder Prediction. The sequences for regulatory proteins containing PTMs were extracted from the PLMD database. Structural order and disorder for these proteins were predicted through DISOPRED3, which uses PSIPRED software for disorder prediction. The extracted data were separated into two categories, such as the ordered region and the disordered region, as analyzed from the output.

2.4.3. PTM Crosstalk. *In situ* crosstalk analysis was performed to check the competition of PTMs on the same site. Data collected from PLMD and dbPTM were used to identify different PTMs on the same amino acid residues. The residues which have more than one PTM were selected for further analysis.

2.4.4. Hotspot Analysis. For all the identified PTM crosstalk sites, a motif of +7 and −6 amino acid stretch was extracted from the PLMD database from the corresponding protein sequence. For each identified acetylation site, the frequency of the probable PTM site was calculated in the vicinity for the defined motif. Every motif containing ≥2 lysine residues, excluding the central lysine residue, was called a PTM hotspot region. Furthermore, if a motif contained ≥2 PTMs on the same site, it will be considered a PTM crosstalk hotspot.

2.5. Impact of Lysine Modification. **2.5.1. Acetylated Lysine Mutation and Disease Susceptibility.** The functional impact of lysine mutations was studied with the help of online tools such as PMut (<http://mmb.irbbarcelona.org/PMut/>),⁶⁴ PolyPhen2 (<http://genetics.bwh.harvard.edu/pph2/>),⁶⁵ PANTHER (<http://www.pantherdb.org/tools/csnpscoreform.jsp>),⁶⁶ and SNAP2 (<https://roslab.org/services/snap/>).⁶⁷ The obtained results were transformed into numerical values

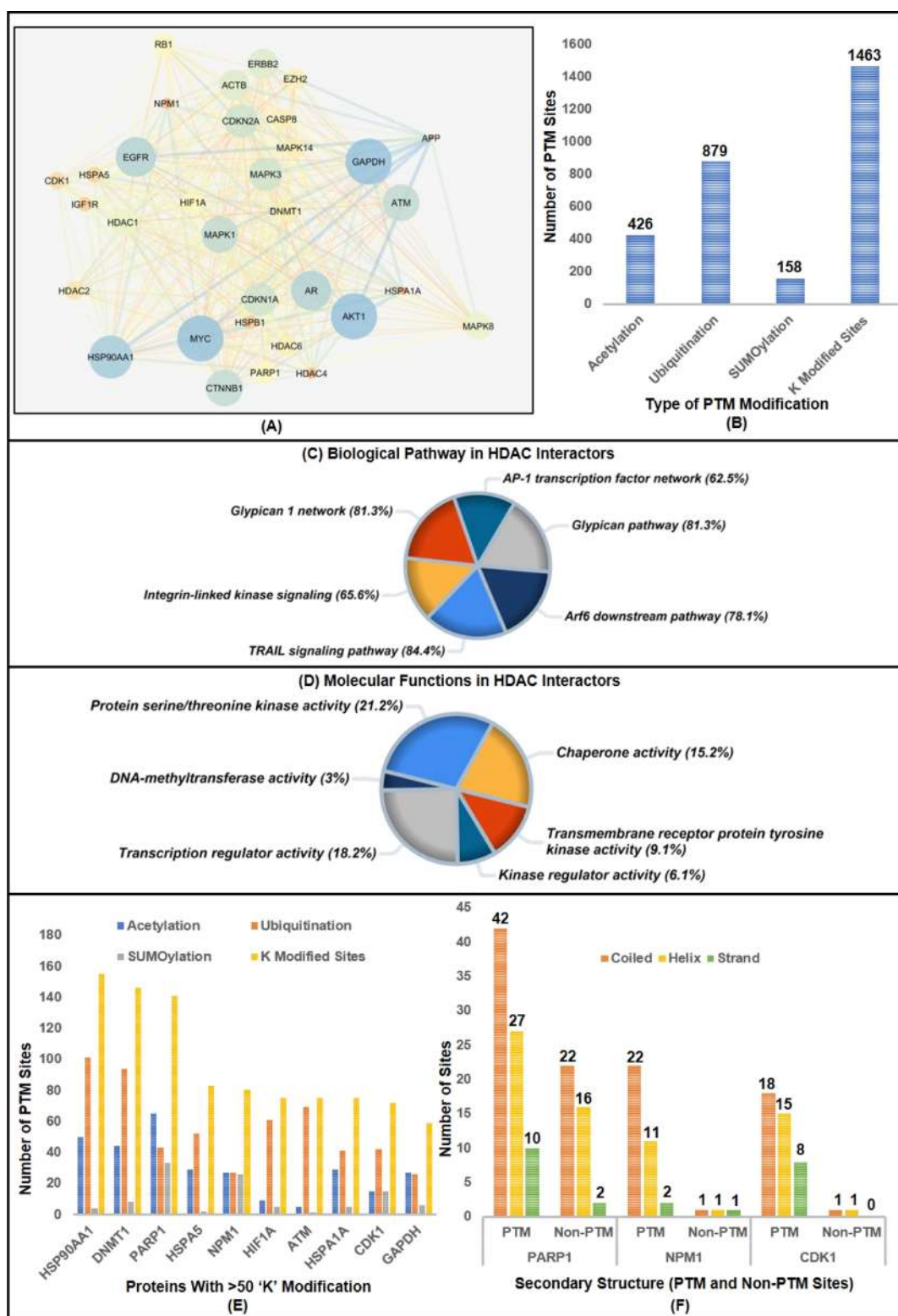


Figure 2. (A) PPI network of cluster 1 including 33 proteins extracted from the core PPI network after clustering analysis, (B) graphical representation of acetylation, ubiquitination, and SUMOylation sites in the protein present in cluster 1, (C) molecular functions of top 33 proteins involved in HDAC interactors, AD, and PD, (D) biological pathway analysis of HDAC interactors involved in the pathogenesis of AD and PD, (E) stack-bar representation of “K”-modified sites, and (F) secondary structure representation in PARP1, CDK1, and NPM1.

in order to visualize them on the stack bar graph. The particular mutation is said to be disease susceptible if its confidence score is greater than or equal to “3”, which is called a threshold value.

2.5.2. Involvement of Acetylated Lysine Mutation on Protein Stability. The protein structure was analyzed for force field energy upon lysine mutation. The lysine residue was mutated into glutamine (Q) and leucine (L), and their total

Table 2. Functional Enrichment Analysis (Biological Pathways and Molecular Functions) Involved in Top Interacting HDAC Interactors^a

Molecular Function	Number of Genes	Percentage of Genes	Fold Enrichment	P-Value	Mapped Genes
MOLECULAR FUNCTION					
Protein serine/threonine kinase activity	7	21.21	12.78	9.58384E-07	ATM; CDK1; MAPK8; AKT1; MAPK1; MAPK3; MAPK14;
Transcription regulator activity	6	18.18	3.96	0.0035	HDAC1; EZH2; HDAC2; HDAC4; RB1; HDAC6;
Transcription factor activity	2	6.06	1.31	0.45	MYC; HIF1A;
Transmembrane receptor protein tyrosine kinase activity	3	9.09	29.50	0.000142	IGF1R; ERBB2; EGFR;
Chaperone activity	5	15.15	21.83	3.04388E-06	HSPB1; HSPA5; NPM1; HSPA1A; HSP90AA1;
DNA-methyltransferase activity	1	3.03	138.29	0.0072	DNMT1;
BIOLOGICAL PATHWAY					
Glypican pathway	26	81.25	3.82	6.10568E-13	AR; HSPB1; ATM; CDK1 ; NPM1 ; CTNNB1; HSPA1A; MAPK8; MYC; IGF1R; HDAC1; HIF1A; APP; AKT1; HDAC2; CASP8; MAPK1; ERBB2; MAPK3; CDKN2A; RB1; HSP90AA1; EGFR; CDKN1A; GAPDH; MAPK14;
TRAIL signaling pathway	27	84.37	4.00	2.91586E-14	AR; HSPB1; ATM; CDK1 ; NPM1 ; CTNNB1; HSPA1A; MAPK8; MYC; IGF1R; HDAC1; PARP1 ; HIF1A; APP; AKT1; HDAC2; CASP8; MAPK1; ERBB2; MAPK3; CDKN2A; RB1; HSP90AA1; EGFR; CDKN1A; GAPDH; MAPK14;
Glypican 1 network	26	81.25	3.94	2.93211E-13	AR; HSPB1; ATM; CDK1 ; NPM1 ; CTNNB1; HSPA1A; MAPK8; MYC; IGF1R; HDAC1; HIF1A; APP; AKT1; HDAC2; CASP8; MAPK1; ERBB2; MAPK3; CDKN2A; RB1; HSP90AA1; EGFR; CDKN1A; GAPDH; MAPK14;
Integrin-linked kinase signaling	21	65.62	6.31	7.17368E-14	AR; HSPB1; ATM; CDK1 ; NPM1 ; CTNNB1; MAPK8; MYC; HDAC1; PARP1 ; HIF1A; AKT1; HDAC2; CASP8; MAPK1; MAPK3; CDKN2A; RB1; HSP90AA1; CDKN1A; MAPK14;
AP-1 transcription factor network	20	62.5	6.33	4.19493E-13	AR; HSPB1; ATM; CDK1 ; NPM1 ; CTNNB1; MAPK8; MYC; HDAC1; HIF1A; AKT1; HDAC2; CASP8; MAPK1; MAPK3; CDKN2A; RB1; HSP90AA1; CDKN1A; MAPK14;
Arf6 downstream pathway	25	78.12	3.82	3.54199E-12	AR; HSPB1; ATM; CDK1 ; NPM1 ; CTNNB1; HSPA1A; MAPK8; MYC; IGF1R; HDAC1; HIF1A; AKT1; HDAC2; CASP8; MAPK1; ERBB2; MAPK3; CDKN2A; RB1; HSP90AA1; EGFR; CDKN1A; GAPDH; MAPK14;

^aIn the above table, the blue color highlights the involvement of key HDAC interactors such as PARP1, CDK1, and NPM1 in the biological pathways. The table observed that CDK1 and NPM1 were involved in the glypican pathway, glypican 1 network, AP-1 transcription factor network, and Arf6 downstream pathway. Similarly, CDK1, PARP1, and NPM1 were involved in the TRAIL signaling pathway and integrin-linked kinase signaling.

energy was calculated with the help of an online prediction tool, that is, DynaMut (<http://biosig.unimelb.edu.au/dynamut/>).⁶⁸ The variation in the energy was estimated to observe the impact of lysine mutation on poly(ADP-ribose) polymerase 1 (PARP1) protein stability.

2.6. Crosstalk Analysis of Acetylated Lysine with Ubiquitination and SUMOylation. To investigate the contribution of lysine in acetylation, ubiquitination, and SUMOylation on the nearby sites, substitute lysine residue to glutamine (Q) and leucine (L). MutPred2 (<http://mutpred.mutdb.org/>),⁶⁹ an online tool, was used to predict the physical significance of lysine mutation on acetylation, ubiquitination, and SUMOylation. The same tool was also used to predict the affected motifs and pathogenic score upon lysine mutation with either glutamine or leucine. Furthermore, BDM-PUB (<http://bdmpub.biocuckoo.org/>)⁷⁰ and SUMOgo (<http://predictor.nchu.edu.tw/SUMOgo/>)⁷¹ were employed to predict the potential ubiquitination and SUMOylation on nearby sites, respectively. The sites which are affected due to modification of lysine by either glutamine or leucine were tallied. The affected sites were classified into two groups that are gain in function on nearby sites and loss of function on nearby sites.

3. RESULTS AND DISCUSSION

3.1. Integration of Data and PTM Sites. After collecting data for HDAC interactors from two databases, such as HIPPIE and CTD, Venn analysis was performed to investigate the common interactors among both databases. A total of 1657 proteins were obtained from HIPPIE, and 1804 proteins were collected from the CTD database. The HDAC interactors were associated with class I, class II, and class IV HDACs. Venn analysis demonstrated that there are 1455 (72.6%) proteins that were common in both the databases. Similarly, for AD- and PD-associated protein, data were collected from CTD and DisGeNET. In CTD, 23268 and 23680 proteins were associated with AD and PD, respectively, whereas in DisGeNET, 3397 and 2078 proteins were involved in the pathogenesis of AD and PD, respectively. Furthermore, Venn analysis demonstrated the involvement of 3094 (13.1%) and 1940 (8.1%) proteins that were common in both the databases. Furthermore, HDAC interactor, AD, and PD data were combined manually to check the common proteins among them. A total of 185 proteins (7.7%) were found to be involved in the pathogenesis of AD and PD, which are associated with HDAC interactors.

Moreover, the PPI network and clustering analysis demonstrated the involvement of 33 proteins as top-ranked proteins (Figure 2A), which are associated with HDAC

Table 3. List of HDAC Interactors Having More Than 50 Lysine-Modified Sites (Acetylation, Ubiquitination, and SUMOylation)^a

	Acetylation	Ubiquitination	SUMOylation	K Modified Sites
HSP90AA1	50	101	4	155
DNMT1	44	94	8	146
PARP1	65	43	33	141
HSPA5	29	52	2	83
NPM1	27	27	26	80
HIF1A	9	61	5	75
ATM	5	69	1	75
HSPA1A	29	41	5	75
CDK1	15	42	15	72
GAPDH	27	26	6	59

^aThe proteins marked in blue color and filled with gray color indicate that proteins have individual acetylation, ubiquitination, and SUMOylation sites more than 10.

interactors and the pathogenesis of NDDs. Furthermore, 150,968 PTM sites and 115,127 PTM sites were collected from the dbPTM database and PLMD database, respectively. A total of 45,967 and 29,942 acetylation sites, 99,624 and 77,364 ubiquitination sites, and 5377 and 7821 SUMOylation sites were extracted from the dbPTM and PLMD database. The extracted PTM sites were mapped to respective proteins. A total of 1463 potential acetylation (426), ubiquitination (879), and SUMOylation (158) sites were identified among 32 potential proteins for crosstalk analysis (Figure 2B).

3.2. Different Molecular Functions and Biological Pathways Followed by Top Interacting HDAC Partners.

A total of 33 proteins identified through clustering analysis involving HDAC interactors, AD, and PD were subjected to the gene set enrichment analysis. Through this, molecular functions and biological processes involved in the pathogenesis of AD and PD through HDAC interaction were determined. The cutoff *p*-value for identifying the molecular function and biological pathways was set at less than 0.05, as shown in Table 2. Among molecular functions, protein serine/threonine kinase activity (21.21%), transcription regulator activity (18.18%), transcription factor activity (6.06%), transmembrane receptor protein tyrosine kinase activity (9.09%), chaperone activity (15.15%), and DNA-methyltransferase activity (3.03%) were highly enriched having a *p*-value less than 0.05 (Figure 2C). Similarly, among different biological pathways, glypican pathway (81.25%), TNF-related apoptosis-inducing ligand (TRAIL) signaling pathway (84.37%), glypican 1 network (81.25%), integrin-linked kinase signaling (65.62%), AP-1 transcription factor network (62.50%), and ADP-ribosylation factor 6 (Arf6) downstream pathway (78.12%) (Figure 2D). However, from Table 1, it is observed that only two pathways, such as the TRAIL signaling pathway and integrin-linked kinase signaling, constitute nucleophosmin (NPM1), cyclin-dependent kinase 1 (CDK1), and PARP1 (highlight in blue script with a green fill). Thus, the above-said pathways were crucial in the AD and PD pathogenesis with HDAC interactors.

3.3. Structural Characterization of PARP1, NPM1, and CDK1. For crosstalk analysis, a protein should be selected on the basis that the individual frequency of acetylation, ubiquitination, and SUMOylation is ≥ 10 (Table 3). Thus, PARP1, NPM1, and CDK1 were found to be the most prominent proteins for crosstalk between acetylation, ubiquitination, and SUMOylation (Figure 2E). Secondary structure analysis of PARP1, NPM1, and CDK1 revealed the importance of the coiled structure as compared to helix and strand in the PTM region. A coiled region regulates protein interactions and

aggregation propensity, and thus mutations, which impair coiled regions and deregulate aggregation and protein activity, whereas mutations, which increase the coiled structure, enhance aggregation propensity.⁷² In PARP1, 42 PTM sites fall into the coiled region, whereas 22 and 18 PTM sites formed a coiled structure in NPM1 and CDK1, respectively. Furthermore, our analysis demonstrates that the frequency of the helix structure is greater in PARP1 (27), NPM1 (11), and CDK1 (15) PTM sites as compared to that in nonPTM sites (Figure 2F) (Table 4). However, in NPM1, the frequency of strands is almost equal in both PTM and nonPTM sites.

Table 4. List of PTM and NonPTM Sites of PARP1, NPM1, and CDK1 (HDAC Interactors) in Coiled, Helix, and Strand Regions

	PARP1		NPM1		CDK1	
	PTM	nonPTM	PTM	nonPTM	PTM	nonPTM
coiled	42	22	22	1	18	1
helix	27	16	11	1	15	1
strand	10	2	2	1	8	0

PTMs preferred disordered regions as compared to the ordered region, which affect their functions and interactions. Furthermore, the involvement of PTM in the disordered region influences disorder to order transition, thus altering protein's stability and its associated mechanisms. This mechanism could be beneficial in diversifying the functional effect of protein by forming new structural sites or PPI by proving a binding region. Interestingly, our analysis of PTM sites revealed that 75% of sites fall in the ordered region, whereas 25% of sites fall in the disordered region (Figure 3A). Our data suggest that there is no PTM site in the disordered region for CDK1. Similarly, PARP1 has 12 acetylation, 9 SUMOylation, and 5 ubiquitination sites falling in the disordered region, whereas NPM1 has 16 acetylation, 21 SUMOylation, and 13 ubiquitination sites falling in the disordered region. Although previous studies reported that acetylation, ubiquitination, and SUMOylation preferred the ordered region, and thus, PARP1 has more acetylation and ubiquitination sites in the ordered region, which is 53 and 38, respectively. However, in NPM1, the number of acetylation sites in the ordered region is less than that of the disordered region, whereas the number of ubiquitination sites in the ordered region (18) is higher than that of ubiquitination sites in the disordered region (13). Similarly, the SUMOylation sites of PARP1 in the ordered region (24) are greater than that in the disordered region (9), whereas the SUMOylation sites

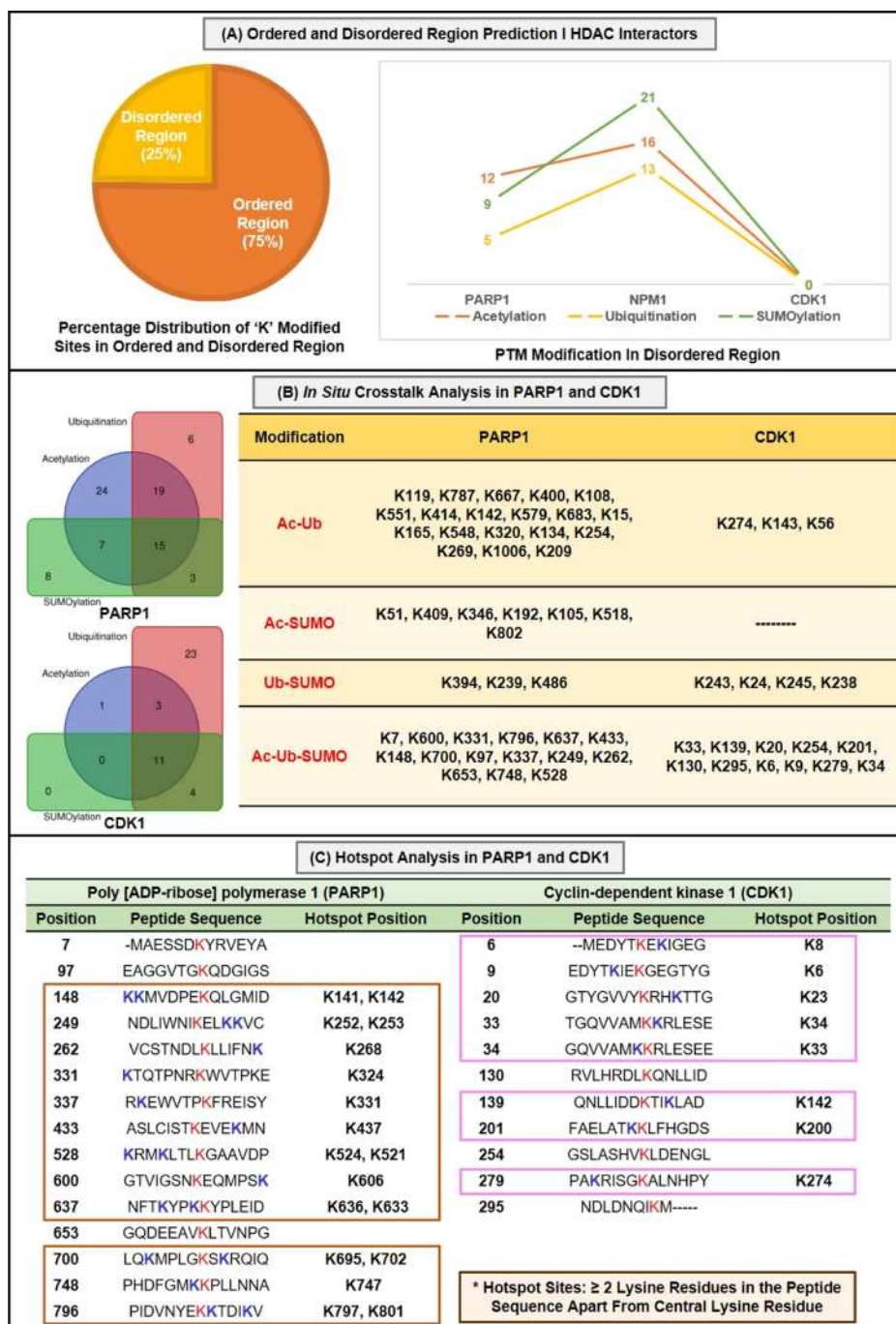


Figure 3. (A) Classification of PTM sites of PARP1, NPM1, and CDK1 into the ordered and disordered region, (B) crosstalk analysis between acetylation, ubiquitination, and SUMOylation in PARP1, CDK1, and NPM1, and (C) identification of hotspot regions in PARP1 and CDK1.

of NPM1 in the ordered region (5) are less than that in the disordered region (21). Thus, our study demonstrates the deviation in NPM1, whereas PARP1 data go well with the previously reported literature for acetylation, ubiquitination, and SUMOylation. Moreover, to identify PTM hotspots and crosstalk hotspots and their susceptibility to neurodegeneration, we separated the proteins based on PTM sites and hotspot sites. *In situ* crosstalk analysis in PARP1 revealed 15 potential acetylation/ubiquitination/SUMOylation sites, 19 acetylation/ubiquitination sites, 7 acetylation/SUMOylation sites, and 3 ubiquitination/SUMOylation sites. Similarly, in CDK1, there are 11 acetylation/ubiquitination/SUMOylation sites, 3 acetylation/ubiquitination sites, and 4 ubiquitination/

SUMOylation sites (Figure 3B). The acetylation/ubiquitination/SUMOylation crosstalk sites of CDK1 and PARP1 were selected to identify crosstalk hotspots. Later on, we selected high-density stretches containing the +7 and -6 motif starch, excluding the central PTM. Our analysis observed that K148, K249, K528, K637, K700, and K796 have crosstalk hotspots in PARP1, whereas no such hotspot has been observed in CDK1 (Figure 3C).

3.4. Impact of Lysine Mutation on PARP1. The disease susceptibility of putative lysine mutation, either with glutamine or with leucine, was investigated through mutational analysis tools such as PANTHER, PMut, PolyPhen2, and SNAP2. Our results observed that all sites have an impact on disease

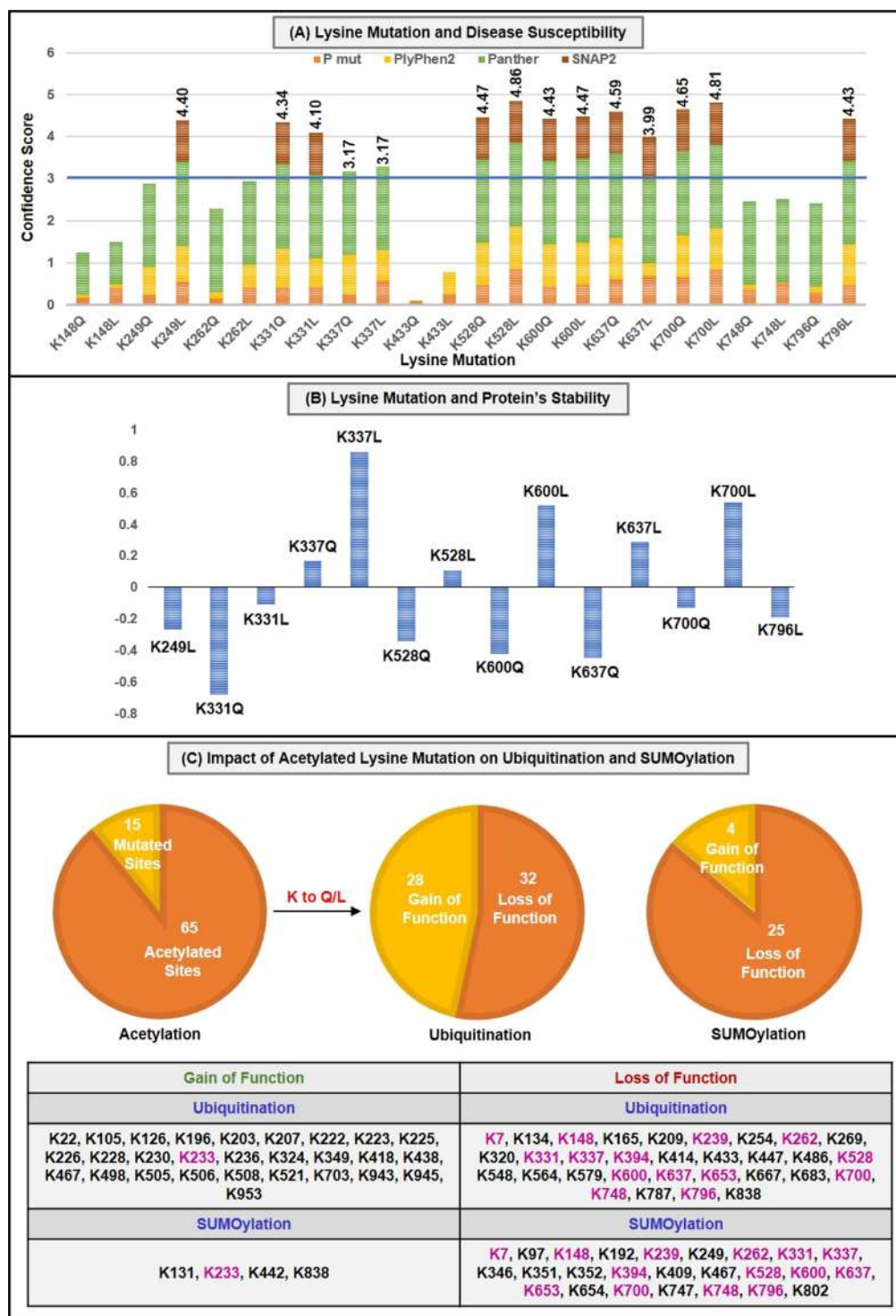


Figure 4. (A) Impact of lysine mutation in hotspot sites on disease susceptibility. The selected lysine residues such as K148, K249, K262, K331, K337, K433, K528, K600, K637, K700, K748, and K796 were subjected to mutation with both glutamine and leucine. Afterward, the mutations were checked for their impact on disease susceptibility. The results indicate that mutations such as K249L, K331Q, K331L, K337Q, K337L, K528Q, K528L, K600Q, K600L, K637Q, K637L, K700Q, K700L, and K796L have a pathogenic score above 3 (taken as reference). (B) Impact of lysine mutation on protein stability. Afterward, the selected disease-susceptible mutations were subjected to investigate their impact on protein structure stability. The results indicate that mutations such as K337Q, K337L, K528L, K600L, K637L, and K700L have a positive energy value and increase the protein stability. Similarly, K249L, K331Q, K331L, K528Q, K600Q, K637Q, K700Q, and K796L have a negative energy value and thus decrease the stability of the protein. (C) Investigation of acetylated lysine residue mutations on ubiquitination and SUMOylation. Here, the results suggest that out of a total of 65 potential lysine sites, 15 sites were mutated and predicted the change in ubiquitination and SUMOylation states of the PARP1. The results suggested that a total of 28 sites result in a gain of ubiquitination, whereas 32 sites exhibit loss of ubiquitination when mutated with either glutamine or leucine. Similarly, 4 sites result in a gain of SUMOylation, whereas 25 sites exhibit loss of SUMOylation when mutated with both glutamine and leucine. Furthermore, K233 exhibits gain of both ubiquitination and SUMOylation, whereas 14 sites result in a loss of both ubiquitination and SUMOylation as represented with pink color in the figure.

susceptibility. However, K249, K331, K337, K528, K600, K637, K700, and K796 have a high confidence score on disease susceptibility. The highly intolerant mutation that is disease susceptible is shown in Figure 4A and Table 5. The mutational

Table 5. Impact of PARP1's "K" Putative Mutation to Either Q or L on Disease Susceptibility Predicted with the Help of PMut, PolyPhen2, Panther, and SNAP2

Residue	Pmut	PolyPhen2	Panther	SNAP2	Confidence
K148Q	0.16	0.075	1	0	1.235
K148L	0.39	0.097	1	0	1.487
K249Q	0.23	0.656	2	0	2.886
K249L	0.54	0.86	2	1	4.4
K262Q	0.15	0.138	2	0	2.288
K262L	0.42	0.529	2	0	2.949
K331Q	0.42	0.924	2	1	4.344
K331L	0.41	0.696	2	1	4.106
K337Q	0.24	0.935	2	0	3.175
K337L	0.56	0.731	2	0	3.291
K433Q	0.08	0.005	0	0	0.085
K433L	0.26	0.522	0	0	0.782
K528Q	0.47	1	2	1	4.47
K528L	0.86	1	2	1	4.86
K600Q	0.43	1	2	1	4.43
K600L	0.48	0.999	2	1	4.479
K637Q	0.61	0.988	2	1	4.598
K637L	0.68	0.318	2	1	3.998
K700Q	0.66	0.997	2	1	4.657
K700L	0.84	0.979	2	1	4.819
K748Q	0.38	0.084	2	0	2.464
K748L	0.51	0.01	2	0	2.52
K796Q	0.28	0.148	2	0	2.428
K796L	0.47	0.961	2	1	4.431

"Probably Begin" and "Neutral" Marked as 0
 "Possible Damage" Marked as 1
 "Probably Damaging" and "Effect" Marked as 2

analysis study also revealed that the mutation of K249, K331, and K796 residue with leucine decreases PARP1 stability, whereas the mutation of K331, K528, K600, K637, and K700 with glutamine decreases PARP1 stability. However, the decrease in PARP1 stability at K331 is higher when mutated with glutamine as compared to mutation with leucine (Figure 4B). Thus, the investigation suggests that mutation with glutamine on crosstalk sites impacts the stability of PARP1 to a great extent as compared to leucine.

3.5. Crosstalk between Acetylation, Ubiquitination, and SUMOylation. Herein, we investigated the impact of an acetylated lysine residue on ubiquitination and SUMOylation, either at the same location or at the nearby sites. Our data revealed that putative mutation in 15 lysine-acetylated sites (K7, K97, K148, K249, K262, K331, K337, K433, K528, K600, K637, K653, K700, K748, and K796) out of a total of 65 acetylated sites in PARP1 affects the process of ubiquitination to a great extent as compared to SUMOylation (Table 6). Table 6 demonstrates the functional impact of putative lysine residue mutation on acetylation, ubiquitination, and SUMOylation. Furthermore, the collective results depict the role of putative lysine mutation on other cellular functions. The results revealed that mutation in K7, K249, K337, K528, and K796 results in loss of acetylation on the same site, whereas the loss of lysine on K637 results in loss of acetylation at K633. Similarly, the loss of putative lysine residue on K7 results in loss of ubiquitination at K7, whereas the loss of putative lysine residue on K600 results in the loss of SUMOylation at K600. Furthermore, our analysis demonstrates that putative mutation in lysine either with glutamine or with leucine at K528 results in loss of acetylation at K528, loss of ubiquitination at K528, and loss of SUMOylation at K524 with ELME000051,

ELME000231, ELME000336, and PS00005 as the affected motifs. The results collectively show the importance of K528 of PARP1, which regulates acetylation, ubiquitination, and SUMOylation collectively in NDDs such as AD and PD. Furthermore, SUMOgo and BDM-PUB predict 117 SUMOylation sites and 80 ubiquitination sites, respectively. The cutoff value for SUMOylation and ubiquitination prediction was set at 0.5 and 1.5, respectively, which filters 12 SUMOylation sites and 39 ubiquitination sites in PARP1. Through the *in silico* approach, we substitute the lysine residue with glutamine and leucine, which promotes the neutral side chain and hydrophobic side chain, respectively. The predicted residues were then compared with the integrated ubiquitination and SUMOylation residues.

Here, we classified the affected ubiquitination and SUMOylation sites into two groups, which are the gain of function on nearby sites and loss of function on nearby sites. Our prediction demonstrated that the loss of crucial lysine residue alters the ubiquitination function to a great extent as compared to SUMOylation. In ubiquitination, 28 sites resulted in a gain of function, whereas 32 sites resulted in the loss of function. Similarly, in SUMOylation, only 4 sites were predicted to gain in function, whereas 25 sites resulted in the loss of function (Figure 4C). Furthermore, our results suggest that the loss of lysine residue at crucial sites either with glutamine or with leucine resulted in both ubiquitination and SUMOylation gain in function at K233. Similarly, 14 sites (K7, K148, K239, K262, K331, K337, K394, K528, K600, K637, K653, K700, K748, and K798) predicted to the loss in function for both ubiquitination and SUMOylation upon lysine substitution with either glutamine or leucine.

4. CONCLUSIONS

NDDs such as AD and PD are best characterized as progressive loss of neuronal cells leading to memory deficits and cognitive dysfunction. Mounting evidence suggests the possible implementation of PTMs in the pathogenesis of NDDs. One important PTM is acetylation, which is the process of the addition of the acetyl group to the N-terminal lysine residue. Acetylation and deacetylation are reversible processes, which are carried out with the help of HATs and HDAC enzymes, respectively. HATs/HDACs promote euchromatin and heterochromatin structure, respectively, which is involved in the transcriptional regulation. Apart from acetylation, ubiquitination and SUMOylation are two important PTMs, which help in the removal of misfolded toxic protein aggregates such as β -amyloid ($A\beta$) and α -synuclein. The common characteristic feature of acetylation, ubiquitination, and SUMOylation is the involvement of the lysine (K) residue, and thus, crosstalk between three PTMs becomes a fascinating topic for research. Studies indicate that the acetylation of PARP1 leads to its hyperactivation, which will intensify oxidative stress and cause mitochondrial dysfunction and subsequently neuronal cell death through parthanatos. Mounting evidence indicates that PARP1 acetylation increases $A\beta$ and α -synuclein aggregates, which increases neurotoxicity.⁷⁸ Studies demonstrated that the activation of PARP1 decreases $A\beta$ clearance and increases AIF expression. Love et al. (1999) first reported the activation of PARP1 in brain samples of AD patients. The authors conducted immunostaining analysis, which indicated the increased levels of PAR in AD patients in frontal and temporal lobes as compared to control patients.⁷⁹ Similarly, Abeti et al. (2011) in mixed cultures of

Table 6. Physical Significance of Lysine (K) Residue in PARP1 Acetylation, Ubiquitination, and SUMOylation through an Online Analysis Tool Known as MutPred2 (<http://mutpred.mutdb.org/>)^a

lysine residue	mutation	affected molecular mechanism ($p \leq 0.05$)	affected motifs	pathogenic score
K7	Lys(K)-Gln(Q)			0.273
	Lys(K)-Leu(L)	loss of intrinsic disorder, loss of acetylation at K7 , loss of phosphorylation at Y9, loss of methylation at K7, loss of ubiquitination at K7	ELME000149, PS00005	0.517
K97	Lys(K)-Gln(Q)			0.196
	Lys(K)-Leu(L)			0.383
K148	Lys(K)-Gln(Q)		ELME000155, PS00347	0.545
	Lys(K)-Leu(L)	gain of loop, altered transmembrane protein		0.742
K249	Lys(K)-Gln(Q)			0.479
	Lys(K)-Leu(L)	altered coiled, loss of intrinsic disorder, gain of loop, loss of helix, altered disordered interface, loss of acetylation at K249	ELME000002	0.737
K262	Lys(K)-Gln(Q)			0.453
	Lys(K)-Leu(L)	altered coiled		0.771
K331	Lys(K)-Gln(Q)			0.272
	Lys(K)-Leu(L)	altered transmembrane protein		0.575
K337	Lys(K)-Gln(Q)	loss of acetylation at K337	ELME000064, ELME000117, ELME000133, ELME000136, ELME000159	0.694
	Lys(K)-Leu(L)	loss of acetylation at K337		0.825
K433	Lys(K)-Gln(Q)			0.113
	Lys(K)-Leu(L)			0.385
K528	Lys(K)-Gln(Q)			0.370
	Lys(K)-Leu(L)	loss of intrinsic disorder, loss of acetylation at K528 , loss of strand, loss of helix, loss of SUMOylation at K524 , loss of ubiquitination at K528 , loss of methylation at K528	ELME000051, ELME000231, ELME000336, PS00005	0.687
K600	Lys(K)-Gln(Q)	loss of SUMOylation at K600 , gain of GPI-anchor amidation at N599	PS00005	0.718
	Lys(K)-Leu(L)	loss of SUMOylation at K600		0.862
K637	Lys(K)-Gln(Q)	gain of strand, loss of acetylation at K633 , altered transmembrane protein	ELME000163, ELME000233	0.713
	Lys(K)-Leu(L)	loss of acetylation at K633 , altered transmembrane protein	ELME000120, ELME000233	0.886
K653	Lys(K)-Gln(Q)			0.273
	Lys(K)-Leu(L)			0.489
K700	Lys(K)-Gln(Q)			0.499
	Lys(K)-Leu(L)	altered coiled	ELME000333	0.768
K748	Lys(K)-Gln(Q)			0.562
	Lys(K)-Leu(L)	altered coiled		0.775
K796	Lys(K)-Gln(Q)	loss of acetylation at K796 , altered transmembrane protein, altered coiled, gain of proteolytic cleavage at D791	ELME000020, ELME000120, ELME000173, ELME000233	0.546
	Lys(K)-Leu(L)	altered ordered interface, loss of acetylation at K796 , altered transmembrane protein, altered coiled, gain of proteolytic cleavage at D791		0.776

^aIn the given table, the pathogenic score represents the probability that the amino acid substitution is pathogenic. A score threshold of 0.50 would suggest pathogenic for a particular substitution. However, a threshold of 0.68 yields a false positive rate of 10%, whereas a threshold of 0.80 yields a false positive rate of 5%.

hippocampal neurons and glial cells from a Sprague-Dawley rat concluded that PARP1 activation leads to oxidative stress in the presence of A β and causes metabolic failure and neuronal death.⁸⁰ Furthermore, Li et al. (2010) in ischemic mice demonstrated that PARP1 causes nuclear translocation of AIF, which results in neuronal cell death, whereas in another study conducted on rats, it was concluded that PARP1 increased expression causes suppression of the AIF protein expression.⁸¹ In the 1-methyl-4-phenyl-1,2,3,6-tetrahydropyridine mouse model of PD, FAF1 plays a key role in PARP-1-dependent necrosis in response to oxidative stress. Furthermore, FAF1 depletion prevented PARP1-linked downstream events such as mitochondrial depolarization and nuclear translocation of AIF.⁸² (Figure 5A).

In this study, we have examined the PTMs and their crosstalk in HDAC interactors, which are involved in the progression of NDDs such as AD and PD. The interactors of HDAC and proteins involved in AD and PD were collected from different databases such as HIPPIE, CTD, and

DisGeNET. Venn analysis and PPI interaction of HDAC interactors, AD, and PD demonstrated the involvement of the top 33 proteins. Gene set enrichment analysis of 33 proteins confirmed the involvement of six different molecular functions and biological pathways in the pathogenesis of AD and PD through HDAC interactors. Protein serine/threonine kinase activity (21.21%), transcription regulator activity (18.18%), transcription factor activity (6.06%), transmembrane receptor protein tyrosine kinase activity (9.09%), chaperone activity (15.15%), and DNA-methyltransferase activity (3.03%) were the top-ranked molecular functions performed by HDAC interactors having a p -value less than 0.05. Similarly, glypican pathway (81.25%), TRAIL signaling pathway (84.37%), glypican 1 network (81.25%), integrin-linked kinase signaling (65.62%), AP-1 transcription factor network (62.50%), and Arf6 downstream pathway (78.12%) were the top-ranked biological pathways involved in the pathogenesis of AD and PD. Lately, 150,968 PTM sites from dbPTM and 115,127 PTM sites from PLMD were integrated to 32 proteins in which

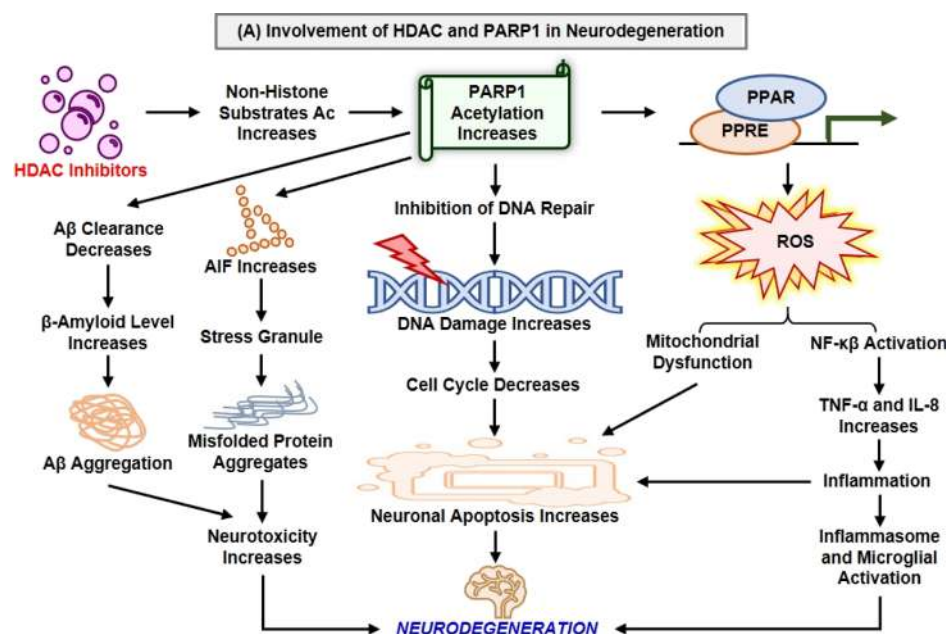


Figure 5. (A) Mechanism of PARP1 acetylation in NDDs. HDAC inhibitors increase the level of PARP1 acetylation and lead to PARP1 activation. This level is involved in the pathogenesis of AD.^{73,74} Increased PARP1 acetylation levels induce increased levels of AIF expression and decreased levels of Aβ clearance, which in turn increase neurotoxicity by increasing the levels of misfolded protein aggregates.^{75–77} Similarly, the increased PARP1 acetylation causes inhibition of DNA repair and increased ROS activity, which decreases the cell-cycle activity and increases the mitochondrial dysfunction, respectively. The decreased cell-cycle regulation and increased mitochondrial dysfunction cause increased neuronal apoptosis, which results in memory impairment and cognitive defects. Increased ROS activity by increased PARP1 acetylation leads to NF-κB activation, which increases proinflammatory cytokine release and results in microglial activation.

1489 were acetylation, ubiquitination, and SUMOylation sites. Among the 32 proteins, only three proteins, such as PARP1, NPM1, and CDK1, have individual acetylation, ubiquitination, and SUMOylation frequency greater than 10. Secondary structure prediction confirmed that 42, 22, and 18 PTM sites formed coiled structure in PARP1, NPM1, and CDK1, respectively, demonstrating that the probability of the PTM site is higher in the coiled region as compared to that in the helix and strand region. However, in NPM1, the probability of forming a strand region is higher as compared to that in PARP1 and CDK1. Further investigation revealed that 75% of PTM sites were associated with the ordered region, whereas 25% of PTM sites were associated with the disordered region. Thus, it will be concluded that the PTM distribution is higher in the ordered region as compared to that in the disordered region. Furthermore, crosstalk analysis of acetylation, ubiquitination, and SUMOylation sites in PARP1 revealed that 19 PTM sites were associated with acetylation and ubiquitination crosstalk. Similarly, acetylation-SUMOylation (7 sites), ubiquitination-SUMOylation (3 sites), and acetylation-ubiquitination-SUMOylation (15 sites) were identified. Hotspot analysis identified that K148, K249, K528, K637, K700, and K796 have potential crosstalk sites having ≥ 2 potential lysine residue in the vicinity of +7 and -6 motif sequence. In order to predict crucial crosstalk sites, the impact of putative lysine mutation on disease susceptibility was predicted, which demonstrated that among hotspot sites, K249L, K528Q, K528L, K637Q, K637L, K700Q, K700L, and K796L were involved in the progression of NDDs. Furthermore, our study investigated the role of putative lysine mutation on ubiquitination and SUMOylation, which shows that putative mutation in the lysine residue will result in the loss of SUMOylation and ubiquitination function. However, the gain of function after putative lysine mutation

will also be observed, but the frequency is low as compared to the loss of function. In conclusion, K249, K331, K337, K528, K600, K637, K700, and K796 of PARP1 play a vital role in ubiquitination, acetylation, and SUMOylation crosstalk, which can potentially be useful for newer leads into acetylation mechanism, HDAC interactions, disease progression, biomarkers, or as a therapeutic target. Furthermore, from this study, we also concluded that site-specific inhibition of PARP1 acetylation (K249, K331, K337, K528, K600, K637, K700, and K796) and simultaneous activation of ubiquitination and SUMOylation at the same residues rescue neuronal cell death that is involved in AD pathology..

■ AUTHOR INFORMATION

Corresponding Author

Pravir Kumar – Molecular Neuroscience and Functional Genomics Laboratory, Department of Biotechnology, Delhi Technological University (Formerly DCE), Delhi 110042, India; orcid.org/0000-0001-7444-2344; Phone: +91-9818898622; Email: pravirkumar@dtu.ac.in, kpravir@gmail.com

Author

Rohan Gupta – Molecular Neuroscience and Functional Genomics Laboratory, Department of Biotechnology, Delhi Technological University (Formerly DCE), Delhi 110042, India

Complete contact information is available at: <https://pubs.acs.org/10.1021/acsoomega.0c06168>

Author Contributions

P.K. and R.G. conceived and designed the manuscript. R.G. has collected, analyzed, and critically evaluated these data. P.K.

and R.G. have prepared figures and tables. P.K and R.G. analyzed the entire data and wrote the manuscript.

Notes

The authors declare no competing financial interest.

ACKNOWLEDGMENTS

We would like to thank the senior management of the Delhi Technological University for constant support and encouragement. This study was funded by the Delhi Technological University (Established under Govt. of Delhi Act 6 of 2009), Delhi-110042, India.

ABBREVIATIONS

PTMs, post-translational modifications; HDAC, histone deacetylase; NDDs, neurodegenerative diseases; PARP1, poly(ADP-ribose) polymerase 1; NPM1, nucleophosmin; CDK1, cyclin-dependent kinase 1; AD, Alzheimer's disease; PD, Parkinson's disease; HD, Huntington's disease; ALS, amyotrophic lateral sclerosis; HATs, histone acetyltransferases; HDACs, histone deacetylases; UPS, ubiquitin proteasome system; SUMO, small ubiquitin-related modifier; CoREST1, repressor element-1 silencing transcription factor corepressor 1; LSD1, lysine (K)-specific demethylase 1; IKK, I κ B kinase; PIAS1, protein inhibitor of activated STAT 1; CTD, Comparative Toxicogenomics Database; KEGG, Kyoto Encyclopedia of Genes and Genomes; PLMD, protein lysine modifications database; Arf6, ADP-ribosylation factor 6; TRAIL, TNF-related apoptosis-inducing ligand; HSP90AA1, heat shock protein 90 α ; DNMT1, DNA methyltransferase 1; HSPAS, heat shock protein family A (Hsp70) member 5; HIF1A, hypoxia-inducible factor 1- α ; ATM, ataxia-telangiectasia mutated; HSPA1A, heat shock 70 kDa protein 1; GAPDH, glyceraldehyde 3-phosphate dehydrogenase

REFERENCES

- (1) Dawson, T. M.; Golde, T. E.; Lagier-Tourenne, C. Animal Models of Neurodegenerative Diseases. *Nat. Neurosci.* **2018**, *21*, 1370.
- (2) Didonna, A.; Benetti, F. Post-Translational Modifications in Neurodegeneration. *AIMS Biophys.* **2016**, *3*, 27.
- (3) Barrett, P. J.; Timothy Greenamyre, J. Post-Translational Modification of α -Synuclein in Parkinson's Disease. *Brain Res.* **2015**, *1628*, 247.
- (4) Buuh, Z. Y.; Lyu, Z.; Wang, R. E. Interrogating the Roles of Post-Translational Modifications of Non-Histone Proteins. *J. Med. Chem.* **2018**, *61*, 3239.
- (5) Bannister, A. J.; Kouzarides, T. Regulation of Chromatin by Histone Modifications. *Cell Res.* **2011**, *21*, 381.
- (6) Eberhartner, A.; Becker, P. B. Histone Acetylation: A Switch between Repressive and Permissive Chromatin. Second in Review on Chromatin Dynamics. *EMBO Rep* **2002**, *3*, 224.
- (7) Görisch, S. M.; Wachsmuth, M.; Tóth, K. F.; Lichter, P.; Rippe, K. Histone Acetylation Increases Chromatin Accessibility. *J. Cell Sci.* **2005**, *118*, 5825.
- (8) Hassan, A. H.; Prochasson, P.; Neely, K. E.; Galasinski, S. C.; Chandy, M.; Carozza, M. J.; Workman, J. L. Function and Selectivity of Bromodomains in Anchoring Chromatin-Modifying Complexes to Promoter Nucleosomes. *Cell* **2002**, *111*, 369.
- (9) Mujtaba, S.; He, Y.; Zeng, L.; Yan, S.; Plotnikova, O.; Sachidanand; Sanchez, R.; Zeleznik-Le, N. J.; Ronai, Z.; Zhou, M. M. Structural Mechanism of the Bromodomain of the Coactivator CBP in P53 Transcriptional Activation. *Mol. Cell* **2004**, *13*, 251.
- (10) Esteves, A. R.; Palma, A. M.; Gomes, R.; Santos, D.; Silva, D. F.; Cardoso, S. M. Acetylation as a Major Determinant to Microtubule-Dependent Autophagy: Relevance to Alzheimer's and Parkinson

Disease Pathology. *Biochim. Biophys. Acta, Mol. Basis Dis.* **2019**, *1865*, 2008.

(11) Sharma, S.; Sarathlal, K. C.; Taliyan, R. Epigenetics in Neurodegenerative Diseases: The Role of Histone Deacetylases. *CNS Neurol. Disord.—Drug Targets* **2019**, *18*, 11.

(12) Kumar, D.; Ambasta, R. K.; Kumar, P. Ubiquitin Biology in Neurodegenerative Disorders: From Impairment to Therapeutic Strategies. *Ageing Res. Rev.* **2020**, *12*, 101078.

(13) Yau, T.-Y.; Molina, O.; Courey, A. J. SUMOylation in Development and Neurodegeneration. *Development* **2020**, *147*, dev175703.

(14) Olsen, C. A. An Update on Lysine Deacylases Targeting the Expanding "Acylome". *ChemMedChem* **2014**, *9*, 434.

(15) Sabari, B. R.; Zhang, D.; Allis, C. D.; Zhao, Y. Metabolic Regulation of Gene Expression through Histone Acylations. *Nat. Rev. Mol. Cell Biol.* **2017**, *18*, 90.

(16) Ouyang, J.; Shi, Y.; Valin, A.; Xuan, Y.; Gill, G. Direct Binding of CoREST1 to SUMO-2/3 Contributes to Gene-Specific Repression by the LSD1/CoREST1/HDAC Complex. *Mol. Cell* **2009**, *34*, 145.

(17) Jia, H.; Kast, R. J.; Steffan, J. S.; Thomas, E. A. Selective Histone Deacetylase (HDAC) Inhibition Imparts Beneficial Effects in Huntington's Disease Mice: Implications for the Ubiquitin-Proteasomal and Autophagy Systems. *Hum. Mol. Genet.* **2012**, *21*, 5280.

(18) Tao, C. C.; Hsu, W. L.; Ma, Y. L.; Cheng, S. J.; Lee, E. H. Epigenetic Regulation of HDAC1 SUMOylation as an Endogenous Neuroprotection against A β Toxicity in a Mouse Model of Alzheimer's Disease. *Cell Death Differ.* **2017**, *24*, 597.

(19) Kumar, D.; Kumar, P. Integrated Mechanism of Lysine 351, PARK2, and STUB1 in A β PP Ubiquitination. *J. Alzheimer's Dis.* **2019**, *68*, 1125.

(20) Gupta, R.; Ambasta, R. K.; Kumar, P. Identification of Novel Class I and Class IIb Histone Deacetylase Inhibitor for Alzheimer's Disease Therapeutics. *Life Sci* **2020**, *256*, 117912.

(21) Shandilya, J.; Swaminathan, V.; Gadad, S. S.; Choudhari, R.; Kodaganur, G. S.; Kundu, T. K. Acetylated NPM1 Localizes in the Nucleoplasm and Regulates Transcriptional Activation of Genes Implicated in Oral Cancer Manifestation. *Mol. Cell Biol.* **2009**, *29*, 5115.

(22) Ren, Z.; Aerts, J. L.; Vandenplas, H.; Wang, J. A.; Gorbenko, O.; Chen, J. P.; Giron, P.; Heirman, C.; Goyvaerts, C.; Zacksenhaus, E.; Minden, M. D.; Stambolic, V.; Breckpot, K.; De Grève, J. Phosphorylated STAT5 Regulates P53 Expression via BRCA1/BARD1-NPM1 and MDM2. *Cell Death Dis.* **2016**, *7*, No. e2560.

(23) Neo, S. H.; Itahana, Y.; Alagu, J.; Kitagawa, M.; Guo, A. K.; Lee, S. H.; Tang, K.; Itahana, K. TRIM28 Is an E3 Ligase for ARF-Mediated NPM1/B23 SUMOylation That Represses Centrosome Amplification. *Mol. Cell Biol.* **2015**, *35*, 2851.

(24) Geng, H.; Liu, Q.; Xue, C.; David, L. L.; Beer, T. M.; Thomas, G. V.; Dai, M. S.; Qian, D. Z. HIF1 α Protein Stability Is Increased by Acetylation at Lysine 709. *J. Biol. Chem.* **2012**, *287*, 35496.

(25) Ferreira, J. V.; Soares, A. R.; Ramalho, J. S.; Pereira, P.; Giraó, H. K63 Linked Ubiquitin Chain Formation Is a Signal for HIF1A Degradation by Chaperone-Mediated Autophagy. *Sci. Rep.* **2015**, *5*, 1.

(26) Berta, M. A.; Mazure, N.; Hattab, M.; Pouyssegur, J.; Brahimi-Horn, M. C. SUMOylation of Hypoxia-Inducible Factor-1 α Reduces Its Transcriptional Activity. *Biochem. Biophys. Res. Commun.* **2007**, *360*, 646.

(27) Kerr, E.; Holohan, C.; McLaughlin, K. M.; Majkut, J.; Dolan, S.; Redmond, K.; Riley, J.; McLaughlin, K.; Stasik, I.; Crudden, M.; Van Schaebroeck, S.; Fenning, C.; O'Connor, R.; Kiely, P.; Sgobba, M.; Haigh, D.; Johnston, P. G.; Longley, D. B. Identification of an Acetylation-Dependent Ku70/FLIP Complex That Regulates FLIP Expression and HDAC Inhibitor-Induced Apoptosis. *Cell Death Differ* **2012**, *19*, 1317.

(28) Besnault-Mascard, L.; Leprince, C.; Auffredou, M. T.; Meunier, B.; Bourgeade, M. F.; Camonis, J.; Lorenzo, H. K.; Vazquez, A. Caspase-8 Sumoylation Is Associated with Nuclear Localization. *Oncogene* **2005**, *24*, 3268.

- (29) Wu, J. Y.; Xiang, S.; Zhang, M.; Fang, B.; Huang, H.; Kwon, O. K.; Zhao, Y.; Yang, Z.; Bai, W.; Bepeler, G.; Mary Zhang, X. Histone Deacetylase 6 (HDAC6) Deacetylates Extracellular Signal-Regulated Kinase 1 (ERK1) and Thereby Stimulates ERK1 Activity. *J. Biol. Chem.* **2018**, *293*, 1976.
- (30) Lu, Z.; Xu, S.; Joazeiro, C.; Cobb, M. H.; Hunter, T. The PHD Domain of MEKK1 Acts as an E3 Ubiquitin Ligase and Mediates Ubiquitination and Degradation of ERK1/2. *Mol. Cell* **2002**, *9*, 945.
- (31) Du, C. P.; Wang, M.; Geng, C.; Hu, B.; Meng, L.; Xu, Y.; Cheng, B.; Wang, N.; Zhu, Q. J.; Hou, X. Y. Activity-Induced SUMOylation of Neuronal Nitric Oxide Synthase Is Associated with Plasticity of Synaptic Transmission and Extracellular Signal-Regulated Kinase 1/2 Signaling. *Antioxid. Redox Signaling* **2020**, *32*, 18.
- (32) Hassa, P. O.; Haenni, S. S.; Buerki, C.; Meier, N. I.; Lane, W. S.; Owen, H.; Gersbach, M.; Imhof, R.; Hottiger, M. O. Acetylation of Poly(ADP-Ribose) Polymerase-1 by P300/CREB-Binding Protein Regulates Coactivation of NF- κ B-Dependent Transcription. *J. Biol. Chem.* **2005**, *280*, 40450.
- (33) Wang, T.; Simbulan-Rosenthal, C. M.; Smulson, M. E.; Chock, P. B.; Yang, D. C. H. Polyubiquitylation of PARP-1 through Ubiquitin K48 Is Modulated by Activated DNA, NAD⁺, and Dipeptides. *J. Cell. Biochem.* **2008**, *104*, 318.
- (34) Messner, S.; Schuermann, D.; Altmeyer, M.; Kassner, I.; Schmidt, D.; Schär, P.; Müller, S.; Rottiger, M. O. Sumoylation of Poly(ADP-ribose) Polymerase 1 Inhibits Its Acetylation and Restrains Transcriptional Coactivator Function. *FASEB J* **2009**, *23*, 3978.
- (35) Iaconelli, J.; Lalonde, J.; Watmuff, B.; Liu, B.; Mazitschek, R.; Haggarty, S. J.; Karmacharya, R. Lysine Deacetylation by HDAC6 Regulates the Kinase Activity of AKT in Human Neural Progenitor Cells. *ACS Chem. Biol.* **2017**, *12*, 2139.
- (36) Yang, W.-L.; Wang, J.; Chan, C.-H.; Lee, S.-W.; Campos, A. D.; Lamothe, B.; Hur, L.; Grabner, B. C.; Lin, X.; Darnay, B. G.; Lin, H.-K. The E3 Ligase TRAF6 Regulates Akt Ubiquitination and Activation. *Science* **2009**, *325*, 1134–1138.
- (37) Risso, G.; Pelisch, F.; Pozzi, B.; Mammi, P.; Blaustein, M.; Colman-Lerner, A.; Srebrow, A. Modification of Akt by SUMO Conjugation Regulates Alternative Splicing and Cell Cycle. *Cell Cycle* **2013**, *12*, 3354.
- (38) Scott, G. K.; Marx, C.; Berger, C. E.; Saunders, L. R.; Verdin, E.; Schäfer, S.; Jung, M.; Benz, C. C. Destabilization of ERBB2 Transcripts by Targeting 3' Untranslated Region Messenger RNA Associated HuR and Histone Deacetylase-6. *Mol. Cancer Res.* **2008**, *6*, 1250.
- (39) Xu, W.; Marcu, M.; Yuan, X.; Mimnaugh, E.; Patterson, C.; Neckers, L. Chaperone-Dependent E3 Ubiquitin Ligase CHIP Mediates a Degradative Pathway for c-ErbB2/Neu. *Proc. Natl. Acad. Sci. U.S.A.* **2002**, *99*, 12874.
- (40) Brix, D. M.; Tvingsholm, S. A.; Hansen, M. B.; Clemmensen, K. B.; Ohman, T.; Siino, V.; Lambrugh, M.; Hansen, K.; Puustinen, P.; Gromova, I.; James, P.; Papaleo, E.; Varjosalo, M.; Moreira, J.; Jäättelä, M.; Kallunki, T. Release of Transcriptional Repression via ErbB2-Induced, SUMO-Directed Phosphorylation of Myeloid Zinc Finger-1 Serine 27 Activates Lysosome Redistribution and Invasion. *Oncogene* **2019**, *3*, ra80.
- (41) Du, Z.; Song, J.; Wang, Y.; Zhao, Y.; Guda, K.; Yang, S.; Kao, H. Y.; Xu, Y.; Willis, J.; Markowitz, S. D.; Sedwick, D.; Ewing, R. M.; Wang, Z. DNMT1 Stability Is Regulated by Proteins Coordinating Deubiquitination and Acetylation-Driven Ubiquitination. *Sci. Signal.* **2010**, *3*, ra80.
- (42) Lee, B.; Muller, M. T. SUMOylation Enhances DNA Methyltransferase 1 Activity. *Biochem. J.* **2009**, *421*, 449.
- (43) Faiola, F.; Liu, X.; Lo, S.; Pan, S.; Zhang, K.; Lyman, E.; Farina, A.; Martinez, E. Dual Regulation of C-Myc by P300 via Acetylation-Dependent Control of Myc Protein Turnover and Coactivation of Myc-Induced Transcription. *Mol. Cell. Biol.* **2005**, *25*, 10220.
- (44) Popov, N.; Wanzel, M.; Madiredjo, M.; Zhang, D.; Beijersbergen, R.; Bernards, R.; Moll, R.; Elledge, S. J.; Eilers, M. The Ubiquitin-Specific Protease USP28 Is Required for MYC Stability. *Nat. Cell Biol.* **2007**, *9*, 765.
- (45) González-Prieto, R.; Cuijpers, S. A. G.; Kumar, R.; Hendriks, I. A.; Vertegaal, A. C. O. C-Myc Is Targeted to the Proteasome for Degradation in a SUMOylation-Dependent Manner, Regulated by PIAS1, SENP7 and RNF4. *Cell Cycle* **2015**, *14*, 1859.
- (46) Hendrickx, A.; Pierrot, N.; Tasiaux, B.; Schakman, O.; Kienlen-Campard, P.; De Smet, C.; Octave, J. N. Epigenetic Regulations of Immediate Early Genes Expression Involved in Memory Formation by the Amyloid Precursor Protein of Alzheimer Disease. *PLoS One* **2014**, *9*, No. e99467.
- (47) Scuderi, C.; Steardo, L.; Esposito, G. Cannabidiol Promotes Amyloid Precursor Protein Ubiquitination and Reduction of Beta Amyloid Expression in SHSY5YAPP+ Cells through PPAR γ Involvement. *Phyther. Res.* **2014**, *28*, 1007.
- (48) Maruyama, T.; Abe, Y.; Niikura, T. SENP1 and SENP2 Regulate SUMOylation of Amyloid Precursor Protein. *Heliyon* **2018**, *4*, No. e00601.
- (49) Li, T.; Liu, M.; Feng, X.; Wang, Z.; Das, I.; Xu, Y.; Zhou, X.; Sun, Y.; Guan, K. L.; Xiong, Y.; Lei, Q. Y. Glyceraldehyde-3-Phosphate Dehydrogenase Is Activated by Lysine 254 Acetylation in Response to Glucose Signal. *J. Biol. Chem.* **2014**, *289*, 3775.
- (50) Lee, S. B.; Kim, C. K.; Lee, K. H.; Ahn, J. Y. S-Nitrosylation of B23/Nucleophosmin by GAPDH Protects Cells from the SIAH1-GAPDH Death Cascade. *J. Cell Biol.* **2012**, *199*, 65.
- (51) Deota, S.; Rathnachalam, S.; Namrata, K.; Boob, M.; Fulzele, A.; Radhika, S.; Ganguli, S.; Balaji, C.; Kaypee, S.; Vishwakarma, K. K.; Kundu, T. K.; Bhandari, R.; Gonzalez de Peredo, A.; Mishra, M.; Venkatramani, R.; Kolthur-Seetharam, U. Allosteric Regulation of Cyclin-B Binding by the Charge State of Catalytic Lysine in CDK1 Is Essential for Cell-Cycle Progression. *J. Mol. Biol.* **2019**, *431*, 2127.
- (52) Xiao, Y.; Lucas, B.; Molcho, E.; Schiff, T.; Vigodner, M. Inhibition of CDK1 Activity by Sumoylation. *Biochem. Biophys. Res. Commun.* **2016**, *478*, 919.
- (53) Sisinni, L.; Maddalena, F.; Condelli, V.; Pannone, G.; Simeon, V.; Li Bergolis, V.; Lopes, E.; Piscazzi, A.; Matassa, D. S.; Mazzoccoli, C.; Nozza, F.; Lettini, G.; Amoroso, M. R.; Bufo, P.; Esposito, F.; Landriscina, M. TRAP1 Controls Cell Cycle G2–M Transition through the Regulation of CDK1 and MAD2 Expression/Ubiquitination. *J. Pathol.* **2017**, *243*, 123.
- (54) Piñero, J.; Bravo, A.; Queralt-Rosinach, N.; Gutiérrez-Sacristán, A.; Deu-Pons, J.; Centeno, E.; García-García, J.; Sanz, F.; Furlong, L. I. DisGeNET: A Comprehensive Platform Integrating Information on Human Disease-Associated Genes and Variants. *Nucleic Acids Res* **2017**, *45*, D833–D839.
- (55) Davis, A. P.; Grondin, C. J.; Johnson, R. J.; Sciaky, D.; McMorran, R.; Wieggers, J.; Wieggers, T. C.; Mattingly, C. J. The Comparative Toxicogenomics Database: Update 2019. *Nucleic Acids Res* **2019**, *47*, D948.
- (56) Alanis-Lobato, G.; Andrade-Navarro, M. A.; Schaefer, M. H. HIPPIE v2.0: Enhancing Meaningfulness and Reliability of Protein-Protein Interaction Networks. *Nucleic Acids Res* **2017**, *45*, D408–D414.
- (57) Szklarczyk, D.; Morris, J. H.; Cook, H.; Kuhn, M.; Wyder, S.; Simonovic, M.; Santos, A.; Doncheva, N. T.; Roth, A.; Bork, P.; Jensen, L. J.; Von Mering, C. The STRING Database in 2017: Quality-Controlled Protein-Protein Association Networks, Made Broadly Accessible. *Nucleic Acids Res* **2017**, *45*, D362–D368.
- (58) Cline, M. S.; Smoot, M.; Cerami, E.; Kuchinsky, A.; Landys, N.; Workman, C.; Christmas, R.; Avila-Campilo, I.; Creech, M.; Gross, B.; Hanspers, K.; Isserlin, R.; Kelley, R.; Killcoyne, S.; Lotia, S.; Maere, S.; Morris, J.; Ono, K.; Pavlovic, V.; Pico, A. R.; Vailaya, A.; Wang, P. L.; Adler, A.; Conklin, B. R.; Hood, L.; Kuiper, M.; Sander, C.; Schmulevich, I.; Schwikowski, B.; Warner, G. J.; Ideker, T.; Bader, G. D. Integration of Biological Networks and Gene Expression Data Using Cytoscape. *Nat. Protoc.* **2007**, *2*, 2366.
- (59) Pathan, M.; Keerthikumar, S.; Ang, C. S.; Gangoda, L.; Quek, C. Y. J.; Williamson, N. A.; Mouradov, D.; Sieber, O. M.; Simpson, R. J.; Salim, A.; Bacic, A.; Hill, A. F.; Stroud, D. A.; Ryan, M. T.; Agbinya, J. I.; Mariadason, J. M.; Burgess, A. W.; Mathivanan, S.

FunRich: An Open Access Standalone Functional Enrichment and Interaction Network Analysis Tool. *Proteomics* **2015**, *15*, 2597.

(60) Kanehisa, M.; Furumichi, M.; Tanabe, M.; Sato, Y.; Morishima, K. KEGG: New Perspectives on Genomes, Pathways, Diseases and Drugs. *Nucleic Acids Res* **2017**, *45*, D353.

(61) Huang, K. Y.; Lee, T. Y.; Kao, H. J.; Ma, C. T.; Lee, C. C.; Lin, T. H.; Chang, W. C.; Huang, H. Da. DbPTM in 2019: Exploring Disease Association and Cross-Talk of Post-Translational Modifications. *Nucleic Acids Res* **2019**, *47*, D298.

(62) Xu, H.; Zhou, J.; Lin, S.; Deng, W.; Zhang, Y.; Xue, Y. PLMD: An Updated Data Resource of Protein Lysine Modifications. *J. Genet. Genom.* **2017**, *44*, 243.

(63) Jones, D. T.; Cozzetto, D. DISOPRED3: Precise Disordered Region Predictions with Annotated Protein-Binding Activity. *Bioinformatics* **2015**, *31*, 857.

(64) López-Ferrando, V.; Gazzo, A.; De La Cruz, X.; Orozco, M.; Gelpi, J. L. PMut: A Web-Based Tool for the Annotation of Pathological Variants on Proteins, 2017 Update. *Nucleic Acids Res.* **2017**, *45*, W222.

(65) Adzhubei, I.; Jordan, D. M.; Sunyaev, S. R. Predicting Functional Effect of Human Missense Mutations Using PolyPhen-2. *Curr. Protoc. Hum. Genet.* **2013**, *76*, 7.

(66) Mi, H.; Huang, X.; Muruganujan, A.; Tang, H.; Mills, C.; Kang, D.; Thomas, P. D. PANTHER Version 11: Expanded Annotation Data from Gene Ontology and Reactome Pathways, and Data Analysis Tool Enhancements. *Nucleic Acids Res* **2017**, *45*, D183.

(67) Hecht, M.; Bromberg, Y.; Rost, B. Better Prediction of Functional Effects for Sequence Variants. *BMC Genom.* **2015**, *16*, 1.

(68) Rodrigues, C. H. M.; Pires, D. E. V.; Ascher, D. B. DynaMut: Predicting the Impact of Mutations on Protein Conformation, Flexibility and Stability. *Nucleic Acids Res* **2018**, *46*, W350.

(69) Pejaver, V.; Urresti, J.; Lugo-Martinez, J.; Pagel, K. A.; Lin, G. N.; Nam, H. J.; Mort, M.; Cooper, D. N.; Sebat, J.; Iakoucheva, L. M.; Mooney, S. D.; Radivojac, P. Inferring the molecular and phenotypic impact of amino acid variants with MutPred2. *Nat. Commun.* **2020**, *11*, 5918.

(70) Cai, B.; Jiang, X. Computational Methods for Ubiquitination Site Prediction Using Physicochemical Properties of Protein Sequences. *BMC Bioinf.* **2016**, *17*, 1.

(71) Chang, C. C.; Tung, C. H.; Chen, C. W.; Tu, C. H.; Chu, Y. W. SUMOgo: Prediction of Sumoylation Sites on Lysines by Motif Screening Models and the Effects of Various Post-Translational Modifications. *Sci. Rep.* **2018**, *8*, 1.

(72) Fiumara, F.; Fioriti, L.; Kandel, E. R.; Hendrickson, W. A. Essential Role of Coiled Coils for Aggregation and Activity of Q/N-Rich Prions and PolyQ Proteins. *Cell* **2010**, *143*, 1121.

(73) Martire, S.; Mosca, L.; d'Erme, M. PARP-1 Involvement in Neurodegeneration: A Focus on Alzheimer's and Parkinson's Diseases. *Mech. Ageing Dev.* **2015**, *146*, 53.

(74) Cohen-Armon, M.; Visochek, L.; Rozensal, D.; Kalal, A.; Geistrikh, I.; Klein, R.; Bendetz-Nezer, S.; Yao, Z.; Seger, R. DNA-Independent PARP-1 Activation by Phosphorylated ERK2 Increases Elk1 Activity: A Link to Histone Acetylation. *Mol. Cell* **2007**, *25*, 297.

(75) Strosznajder, J. B.; Czapski, G. A.; Adamczyk, A.; Strosznajder, R. P. Poly(ADP-Ribose) Polymerase-1 in Amyloid Beta Toxicity and Alzheimer's Disease. *Mol. Neurobiol.* **2012**, *46*, 78.

(76) Kauppinen, T. M.; Suh, S. W.; Higashi, Y.; Berman, A. E.; Escartin, C.; Won, S. J.; Wang, C.; Cho, S. H.; Gan, L.; Swanson, R. A. Poly(ADP-Ribose) Polymerase-1 Modulates Microglial Responses to Amyloid β . *J. Neuroinflammation* **2011**, *8*, 1.

(77) Gorman, A. M. Neuronal Cell Death in Neurodegenerative Diseases: Recurring Themes around Protein Handling. *J. Cell Mol. Med.* **2008**, *12*, 2263.

(78) Narne, P.; Pandey, V.; Simhadri, P. K.; Phanithi, P. B. Poly(ADP-Ribose) Polymerase-1 Hyperactivation in Neurodegenerative Diseases: The Death Knell Tolls for Neurons. *Semin. Cell Dev. Biol.* **2017**, *63*, 154.

(79) Love, S.; Barber, R.; Wilcock, G. K. Increased Poly(ADP-Ribosyl)ation of Nuclear Proteins in Alzheimer's Disease. *Brain* **1999**, *122*, 247.

(80) Abeti, R.; Abramov, A. Y.; Duchen, M. R. β -Amyloid Activates PARP Causing Astrocytic Metabolic Failure and Neuronal Death. *Brain* **2011**, *134*, 1658.

(81) Zhao, Y. J.; Wang, J. H.; Fu, B.; Ma, M. X.; Li, B. X.; Huang, Q.; Yang, B. F. Effects of 3-Aminobenzamide on Expressions of Poly(ADP Ribose) Polymerase and Apoptosis Inducing Factor in Cardiomyocytes of Rats with Acute Myocardial Infarction. *Chin. Med. J.* **2009**, *122*, 1322.

(82) Yu, C.; Kim, B. S.; Kim, E. FAF1 Mediates Regulated Necrosis through PARP1 Activation upon Oxidative Stress Leading to Dopaminergic Neurodegeneration. *Cell Death Differ* **2016**, *23*, 1873.



Integrative analysis of OIP5-AS1/miR-129-5p/CREBBP axis as a potential therapeutic candidate in the pathogenesis of metal toxicity-induced Alzheimer's disease

Rohan Gupta, Pravir Kumar^{*}

Molecular Neuroscience and Functional Genomics Laboratory, Department of Biotechnology, Delhi Technological University (Formerly DCE), Delhi 110042, India

ARTICLE INFO

Keywords:

Neurodegenerative diseases
Alzheimer's disease
OIP5-AS1
miR-129-5p
miR-335-5p
CREBBP
Lysine acetylation
Post-translational modification
Metal toxicity

ABSTRACT

Neurodegenerative disease, namely Alzheimer's disease (AD), is characterized by the accumulation of toxic β -amyloid aggregates and insoluble tau tangles. Mounting evidence demonstrated that heavy metals, such as copper, chromium, cobalt, and nickel, increase the β -amyloid and tau aggregation in the pathogenesis of AD by activating different signaling events. For instance, copper induces the formation of reactive oxygen species to cause mitochondrial dysfunction and DNA damage, whereas, chromium elevates neuroinflammatory response and neuronal apoptosis. Similarly, cobalt increases tau hyperphosphorylation and promotes tau aggregation, whereas, nickel elevates β -amyloid aggregation. Further, acetylation, a lysine-specific post-translational modification, has been linked to transcriptional activation, which regulates the transcription of genes associated with metal toxicity-induced AD. However, micro-RNAs (miRNAs) can reduce the activity of acetyltransferase, which decreases the transcriptional activation and thus inhibits the pathogenesis of AD. In contrast, long non-coding RNAs modulate the expression of specific miRNA and serve as a sponge to particular miRNA. In this study, we aim to identify the crucial proteins involved in metal toxicity-induced AD through network biology, followed by identifying regulatory transcription factors associated with crucial proteins. Further, we aim to determine the critical lysine residue and the role of CREBBP-induced acetylation on transcription factors. Lately, we have focused on identifying miRNAs associated with CREBBP and transcription factors simultaneously. Lastly, we aim to identify the potential long non-coding RNA, serving as a sponge to miRNAs. Our results demonstrated that the OIP5-AS1/miR-129-5p/CREBBP axis is a potential therapeutic target in metal toxicity-induced Alzheimer's disease pathogenesis.

1. Introduction

Neurodegenerative diseases (NDDs) such as Alzheimer's disease (AD) and Parkinson's disease (PD) are disorders of the central nervous system characterized by excessive loss of neuronal cells due to toxic protein aggregates. The aggregation of toxic proteins inside the brain causes disturbance in cellular and molecular processes, which leads to mitochondrial dysfunction, immunological response, oxidative stress, autophagy and apoptosis, and cell-cycle dysregulation, ultimately causes neuronal cell death (Soldan et al., 2016). AD is the most prevalent NDDs

that occurs mainly in people aged above 65 years, which is characterized by neurofibrillary tangles and amyloid- β ($A\beta$) aggregates due to hyperphosphorylation of tau and irregular proteolytic processing of amyloid peptide protein (Weller and Budson, 2018). Despite having extensive research on the subject information regarding the exact etiology of the disease, the mechanism of disease progression, the involvement of different biomarkers, and therapeutic interventions remain unelucidated. Moreover, environmental risk factors such as excessive exposure to toxic metals play an essential role in the pathogenesis of AD. For example, several studies demonstrated that excessive concentration of

Abbreviations: NDDs, neurodegenerative disease; AD, Alzheimer's disease; PD, Parkinson's disease; $A\beta$, amyloid- β ; GSK3 β , glycogen synthase kinase 3 beta; CREBBP, cAMP response element-binding protein; miRNAs, micro-RNAs; CREB, cyclic AMP-responsive element-binding protein; PI3K, phosphoinositide 3-kinases; Akt, protein kinase B; BACE1, beta-secretase 1; CTD, comparative toxicogenomics database; GO, gene ontology; KEGG, Kyoto Encyclopedia of Genes and Genomes; PPI, protein-protein interaction; TFs, transcription factors; PTM, post-translational modification; JNK3, c-Jun N-terminal kinase 3; SOX6, SRY-box transcription factor 6.

^{*} Corresponding author at: Molecular Neuroscience and Functional Genomics Laboratory, Shahbad Daultapur, Bawana Road, Delhi 110042, India.

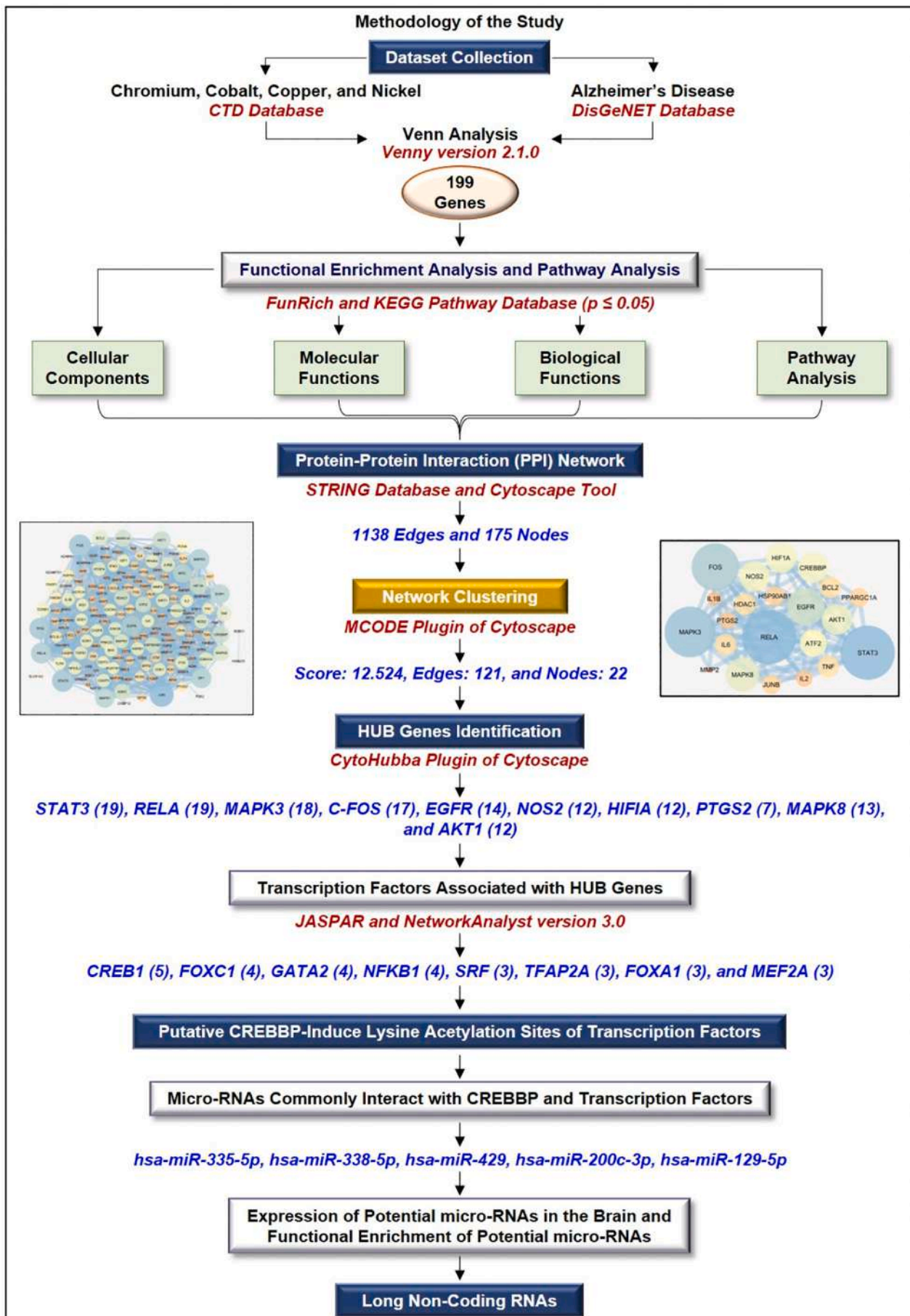
E-mail address: pravirkumar@dtu.ac.in (P. Kumar).

<https://doi.org/10.1016/j.genrep.2021.101442>

Received 14 July 2021; Received in revised form 2 November 2021; Accepted 15 November 2021

Available online 24 November 2021

2452-0144/© 2021 Elsevier Inc. All rights reserved.



(caption on next page)

Fig. 1. Methodology of the current study: firstly, datasets related to chromium, cobalt, copper, and nickel were extracted from the CTD database, while the dataset related to the AD was obtained from the DisGeNET database. Venn analysis through Venny 2.1.0 identified 199 common genes among metal toxicity and AD. Further, functional enrichment analysis of identified genes was carried out to identify the cellular components, molecular function, biological functions, and pathways followed by the common genes. Later on, a protein-protein interaction network through the STRING database and the Cytoscape tool, followed by the network clustering, identified the potential biological network with 22 nodes and 121 edges. Furthermore, CytoHubba identified 10 HUB genes involved in the metal toxicity-induced AD, such as STAT3 (19), RELA (19), MAPK3 (18), C-FOS (17), EGFR (14), NOS2 (12), HIF1A (12), PTGS2 (7), MAPK8 (13), and AKT1 (12). Transcription factors associated with HUB genes were identified with the help of JASPAR and NetworkAnalyst version 3.0. Furthermore, putative CREBBP binding sites and micro-RNAs interact with CREBBP, and potential transcription factors were identified. hsa-miR-335-5p, hsa-miR-338-5p, hsa-miR-429, hsa-miR-200c-3p, hsa-miR-129-5p were putative micro-RNAs regulates the expression and activity of CREBBP and identified transcription factors. Lastly, long non-coding RNAs that alter the binding activity of putative micro-RNAs to target genes were identified.

chromium, nickel, cobalt, and copper causes oxidative stress and mitochondrial DNA damage, which leads to mitochondrial dysfunction and, ultimately, neuronal apoptosis and neuroinflammation (Huat et al., 2019). In addition, excessive accumulation of copper initiates A β aggregation, the formation of neurite plaques and cell damage due to excessive generation of reactive oxygen species, decreases hydrogen peroxide, and decreases in ATP production (Mayes et al., 2014).

Similarly, chromium, another trace metal inferred with genes involved in the inflammatory response and apoptotic cell death through increasing caspase 3 expressions, elevating tumor necrosis factor-alpha and interleukin 6 activity and decreasing phosphorylation of glycogen synthase kinase 3 beta (GSK3 β) (Ge et al., 2008; Padmavathi et al., 2010; Park et al., 1997; Rafael et al., 2007). Moreover, a high lead concentration in neuronal cells inhibits calcium homeostasis, decreases nitric oxide generation, and increases inflammatory action in glial cells. Further, the dose-dependent administration of copper elevates reactive oxygen species, which leads to mitochondrial dysfunction and inhibits DNA repair response (P. Chen et al., 2016). Cobalt exposure damages the brain's structure and functions, impairing visual learning transmission to the brain. Cobalt administration leads to promotes tau hyperphosphorylation and induces tau aggregates, which causes neuronal cell death (Gorantla et al., 2019). Furthermore, the dose-dependent administration of nickel elevates amyloid deposition and amyloid aggregation, which leads to neuronal apoptosis (Kim et al., 2012).

Further, different studies demonstrated that cAMP response element-binding protein (CREBBP) or CBP-mediated lysine acetylation plays a crucial role in the pathogenesis of AD (Barral et al., 2014; Caccamo et al., 2010; Chatterjee et al., 2013; Song et al., 2015). For instance, Chen et al., 2020 demonstrated that p300/CBP activated in tauopathies, which degraded the autophagy-lysosomal pathway and caused excessive secretion of insoluble tau aggregates (Chen et al., 2020). Similarly, Schueller et al., 2020 concluded that CBP or CREBBP-induces histone acetylation was dysregulated in the hippocampus and frontal cortex of AD patients (Schueller et al., 2020). Further, Portillo et al., 2021 demonstrated that excessive DNA damage or absence of sirtuin 6 increases Tau(K174) acetylation through CREBBP or CBP, which leads to Tau accumulation (Portillo et al., 2021). Moreover, post-transcriptional regulators, namely micro-RNAs (miRNAs) and long non-coding RNAs, regulate the expression pattern of proteins either upregulated or downregulated, which causes the pathogenesis of AD (Ahmadi et al., 2020; Catana et al., 2020; Doxtater et al., 2020; Kou et al., 2020; Kumar and Reddy, 2020; Wei et al., 2020; Zoltowska et al., 2020). For example, reduced miR-134 levels increase cyclic AMP-responsive element-binding protein (CREB) activity, increasing BDNF expression and improving synaptic plasticity, whereas, increasing miR-34c activity targets sirtuin 1, which results in memory impairment (Bourassa and Ratan, 2014; Zhao et al., 2013). Similarly, L. Li et al. (2020) demonstrated that overexpression of long non-coding RNAs, namely MALAT1 or CNR1, reduced neuronal injury in rat hippocampus and decreased the activity of pro-inflammatory cytokines, such as interleukin-6 and tumor necrosis factor-alpha. Further, the authors demonstrated that MALAT1 could be served as a sponge to miR-30b, which upregulated CNR1 expression and activated the phosphorylation of phosphoinositide 3-kinases (PI3K) and

protein kinase B (Akt) (L. Li et al., 2020). Recently, Yue et al., 2020 concluded that silencing of long non-coding RNA, such as XIST, rescued from AD progression through miR124-induced deregulation of beta-secretase 1 (BACE1) (Yue et al., 2020). Thus, from the accumulating evidence, it might be concluded that metal toxicity leads to the pathogenesis of AD and deregulation in acetylation levels of non-histone substrates elevates AD progression. Further, miRNA and long non-coding RNAs regulate the expression of CREBBP or CBP acetyltransferase, which might alter the pathogenesis of AD. Thus, in this study, we aim to identify the mechanism of CREBBP acetyltransferase in the pathogenesis of metal toxicity-induced AD. Further, we aim to determine the potential miRNA regulates the acetylation level of non-histone substrates through the regulation of CREBBP. Lastly, we aim to identify the potential long non-coding RNA, serving as a sponge to miRNA.

2. Materials and methodology

2.1. Data collection and data integration

The AD-related dataset was obtained from a publicly available gene-disease association database known as DisGeNET version 7.0 (<https://www.disgenet.org/>), containing information about the complicated biological relationship between 30,170 diseases and 21,671 genes (Piñero et al., 2020). Similarly, the datasets related to trace elements such as chromium, cobalt, copper, and nickel were obtained from the online freely accessible comparative toxicogenomics database (CTD) version 2019 (<http://ctdbase.org/>). The reason for selection of trace metals, such as chromium, cobalt, copper, and nickel are the negligence of these metals as compared to heavy metals, namely iron, cadmium, mercury, arsenic, and other. Further, accumulation of these metals leads to the pathological conditions. CTD is an online database that contains information regarding associations between genes, disease, chemicals, and phenotypes (Davis et al., 2019). Furthermore, after datasets collection, chemical data (chromium, cobalt, copper, and nickel) were integrated, followed by integration with AD-related datasets using an online Venn analysis tool known as Venny version 2.1.0 (<https://bioinfo.gp.cnb.csic.es/tools/venny/>) (Oliveros, 2007).

2.2. Gene set enrichment analysis and pathway analysis

To extract the exact biological, molecular, and cellular functions of genes involved in heavy metal toxicity induced AD, functional enrichment analysis of genes was performed. Gene ontology (GO) was identified through an online web-server for functional enrichment analysis of gene sets known as FunRich (<http://www.funrich.org/>) (Pathan et al., 2015). Further, pathways followed by shared genes between metal toxicity and AD were identified using the Kyoto Encyclopedia of Genes and Genomes (KEGG) pathway analysis with the help of the KEGG pathway database (<https://www.genome.jp/kegg/>) (Ogata et al., 1999). KEGG is an online database for understanding the exact biological function of the cell. Further, the common molecular signatures of metal toxicity-induced AD were imported into BUSCA: Bologna Unified Sub-cellular Component Annotator (<http://busca.biocomp.unibo.it/>)

Table 1

Gene set enrichment analysis (GO analysis and pathway analysis) of 199 common genes related to metal toxicity and AD.

Name	Fold enrichment	P-value	Genes mapped
<i>Biological process</i>			
Apoptosis	4.206953589	0.000145225	TP53; CASP3; MAPK9; BCL2; BAX; CASP7; BBC3; CASP9; BCL2L11; CASP8;
Regulation of cell cycle	8.125736768	0.000372966	MAPK9; CDKN1A; CCNE2; CHEK2; KLF4;
Anti-apoptosis	11.58336557	0.000376289	SOD2; GPX1; FAS; IGF1;
Protein metabolism	1.747940437	0.004511294	PARP1; MMP1; MMP2; ADAMTS1; EIF4A1; HSPA5; MMP13; ANPEP; BMP1; CALR; CCT2; DNAJB1; DPP4; F3; HSPA9; HSPB1; HSPH1; HYOU1; PDIA6; RPL15; SERPINA1; SERPINC1; SERPING1; SQSTM1; THOP1;
Metabolism	1.593812016	0.008086365	CAT; NQO1; GSR; SOD1; HMOX1; PTGS2; GPT; NOS2; TXN; GSK3B; LYZ; G6PD; HMGCR; NAT10; ACHE; ALDH1L1; CD36; CYCS; FDPS; GCHFR; GPX4; IDH2; LDHA; NME1; PHYHD1; PRDX1; PSAT1; SIRT1; TXNRD1;
Signal transduction	1.339959419	0.009037422	MAPK8; MAPK1; AKT1; MAPK3; TNF; MAPK9; VEGFA; CCND1; FYN; IRS1; PLK1; CDK1; MAP2K4; EGFR; ICAM1; CHEK2; LDLR; NOTCH1; PLK2; SGK1; TGFB1; TGFB1; AGT; ARHGEF2; ATM; BMP4; CCL5; CD44; CD68; CXCR4; DENR; DKK1; DUSP6; EDN1; FAS; FGFR4; FZD4; GDF15; GPNMB; HSP90A1; IGF1; IGF2; IL1RL1; MAPK14; NTS; PGF; PHB; PRKCD; RAB31; RGCC; RGS2; S100A6; ST13; STIP1; TAX1BP1; TGFB2; TLR4;
<i>Cellular component</i>			
Extracellular	3.124166679	3.33129E-21	CAT; SOD1; IL6; TNF; CXCL8; CDKN1A; VEGFA; GPT; GPX1; STAT3; TF; IFNG; TIMP1; TXN; APOA1; EGFR; ICAM1; IL1B; LYZ; MMP1; MMP2; MT2A; TFRC; VIM; ADAMTS1; C3; EGR1; FABP3; G6PD; HMGCR; IL4; MMP13; TGFB1; TGFB1; ACHE;

(Savojarado et al., 2018), an online web-server to predict the subcellular localization of molecular signatures.

2.3. Protein-protein interaction network analysis and visualization

To identify the complex biological association between the genes involved in both metal toxicity and AD, an online freely available database STRING version 11.0 (<https://string-db.org/>) (Szklarczyk et al., 2019) was used. The confidence score of the protein-protein interaction (PPI) network in STRING was set to >0.4, which is medium confidence. Furthermore, to visualize the network and identification of network characteristics, a freely available software, Cytoscape version 3.8.0 (<https://cytoscape.org/>) (Excoffier et al., 2017), was used, which draws complex biological interactions between them.

2.4. PPI network clustering and HUB genes identification

After extracting the information related to the interaction between genes, and the visualization of parameters, the clustering of the network was done to minimize the network nodes. The Cytoscape software plugin MCODE (<https://apps.cytoscape.org/apps/mcode>) (Bader and Hogue, 2003) was used to cluster the PPI network. MCODE identifies the highly-dense regions of a given PPI network based on network topology. Furthermore, to determine the HUB genes from a given network, the Cytoscape software plugin CytoHubba (<https://apps.cytoscape.org/apps/cytohubba>) (Chin et al., 2014) was used. The CytoHubba identifies the central elements of a given network and sub-network identification based on characteristic features of a complex interactome. The CytoHubba plugin predictions were based on two algorithms, such as maximum neighborhood component and maximal clique centrality.

2.5. Identification of regulatory transcription factors interacts with HUB genes

It is a well-established fact that regulatory biomolecules, such as transcription factors (TFs), play a crucial role in gene regulation. TFs determine the transcriptional fate of target genes and, based on that, activate or deactivate the transcriptional activity of a particular gene. HUB genes were analyzed with JASPAR (<http://jaspar.genereg.net/>) (Bryne et al., 2008), an open-source and online database of curated TFs. The information extracted from JASPAR was imported into NetworkAnalyst version 3.0 (<https://www.networkanalyst.ca/>) (Zhou et al., 2019), an online freely available tool to form an interaction network between genes-TFs. Top interacting nodes were selected for further investigation and analysis.

2.6. Identification of putative lysine acetylation sites in identified transcription factors

Acetylation is a lysine-specific post-transcriptional modification (PTM), which promotes euchromatin structure and activates the transcription process. To find out the potential acetylated lysine residues of identified transcription factors, two online web-servers, such as Deep PLA (<http://deeptla.cancerbio.info/>) (Yu et al., 2020) and GPS-PAIL (<http://pail.biocuckoo.org/>) (Deng et al., 2016) were used. The study is restricted to identify the potential CREBBP induced acetylation sites. Deep PLA is a deep neural network-based online prediction tool, where four models are combined into one complete connection layer. Similarly, GPS-PAIL is a machine learning-based online prediction tool, which predicts acetylated sites of seven different acetyltransferases.

2.7. Prediction of potential micro-RNA interacts with acetylated transcription factors

miRNAs are post-transcriptional regulators, which regulate the expression of particular proteins. To predict the putative miRNAs bound

Table 1 (continued)

Name	Fold enrichment	P-value	Genes mapped
Extracellular space	5.943226358	3.12411E-16	ADM; AGT; ALB; ANPEP; APOB; APOC3; BMP1; BMP4; CALR; CCL2; CCL5; CFB; CFI; CXCL1; DKK1; DPP4; EDN1; F3; FAS; FGFR4; FN1; GDF15; HMGB1; HSP90AB1; IGF1; IGF2; IL10; IL1RL1; IL2; NME1; NTS; PDIA6; PGF; PHB; RGS2; SERPINA1; SERPINC1; SERPING1; SHBG; THOP1; TXNRD1; SOD1; IL6; HMOX1; TNF; CXCL8; VEGFA; APOA1; EGFR; ICAM1; IL1B; LYZ; MMP2; IL4; MMP13; TGFB1; TGFB2; ADM; AGT; ALB; APOC3; CALR; CCL2; CXCL1; EDN1; F3; FN1; HMGB1; IGF1; IL10; IL2; SERPINA1; SERPINC1; TP53; CASP3; GSR; SOD1; HMOX1; MAPK8; MAPK1; AKT1; MAPK3; CDKN1A; CCND1; FYN; GPX1; IRS1; RELA; BCL2; HDAC1; BAX; CASP7; PLK1; CASP9; CDK1; MAP2K4; NOS2; TXN; GSK3B; TCF4; VIM; BCL2L11; CASP8; CCNE2; EIF4A1; G6PD; NOTCH1; ARHGEP2; CALR; CCT2; CYCS; DNAJB1; FAS; GART; HSP90AB1; HSPH1; LDHA; MAPK14; PPIA; PRKCD; PSAT1; RPL15; S100A6; SQSTM1; TXNRD1; NQO1; GSR; SOD1; GPT; TF; BAX; CASP9; CDK1; TXN; APOA1; EGFR; ICAM1; LYZ; SLC2A1; TFRC; VIM; C3; EIF4A1; FABP3; G6PD; HSPA5; NOTCH1; PCNA; TGFB1; TGFB2; AGT; ALB; ALDH1L1; ANPEP; APOB; CALR; CCT2; CD36; CD44; CFI; CXCR4; DNAJB1; DPP4; FAS; FDPS; FN1; GART; GPX4; HSP90AB1; HSPA9; HSPB1; HSPH1; HYOU1; LDHA; NME1; OPTN; PDIA6; PHB; PPIA; PRDX1; PRKCD; PSAT1; RBM3; RPL15; S100A6; SERPINA1; SERPING1; SLC2A3; SQSTM1; ST13;
Cytosol	3.311818965	4.53947E-15	
Exosomes	2.533787837	3.15643E-14	

with CREBBP and identified TFs simultaneously, we used an online integrated miRNA target database known as mirDIP (<https://ophid.utoronto.ca/mirDIP/>) (Tokar et al., 2018). Only those miRNAs with confidence scores high (top 5%) and very high (top 1%) were selected for further studies. Further, the Venny tool was used to identify the common miRNAs among CREBBP, NFKB1, CREB1, GATA2, and FOXA1. Moreover, the predicted miRNAs were subjected to TissueAtlas (<https://ccb-web.cs.uni-saarland.de/tissueatlas/>) (Ludwig et al., 2016), an online web server to identify the potential of predicted miRNAs for expressing in healthy brain tissues (Fig. 1).

2.8. Validation of predicted micro-RNA's through disease ontology and reactome pathway analysis

It is crucial to validate that the predicted miRNAs are involved in the pathogenesis of AD and central nervous system diseases. MIENTURNET (<http://userver.bio.uniroma1.it/apps/mienturnet/>) (Licursi et al., 2019), an online web tool devised for miRNA functional enrichment analysis and miRNA-target prediction. Similarly, miRNAs involved in signaling transduction were predicted using the MIENTURNET web tool. Further, it is a well-established notion that gene expression is regulated by non-coding RNAs, such as long non-coding RNAs and circular RNAs. Thus, it is equally important to identify the long non-coding RNAs that will regulate the activity of selected miRNAs in the pathogenesis of AD. StarBase V2.0 (<http://starbase.sysu.edu.cn/>) (Li et al., 2014) was used to identify the potential non-coding RNA that simultaneously binds with selected miRNAs.

3. Results

3.1. Common genes involved in metal toxicity and AD

Data extraction from the CTD database identified that genes involved in chromium, cobalt, copper, and nickel toxicity are 2149, 4804, 5862, and 7649, respectively. The Venn analysis of the genes revealed that 376 genes were common among them. Similarly, a total of 3397 genes involved in AD pathogenesis were extracted from the DisGeNET database. Furthermore, Venn analysis of metal toxicity linked genes and AD-related genes identified 199 shared genes.

3.2. Functional enrichment analysis of common genes: GO analysis, pathway analysis, and subcellular localization

A total of 199 common genes identified in metal toxicity and AD were subjected to functional enrichment analysis such as GO analysis and pathway analysis. Gene set enrichment analysis of common genes enables identifying cellular functions, molecular functions, biological processes, and pathways. The cut-off p-value for identifying cellular, molecular, biological, and pathway functions was set at less than 0.05, as shown in Table 1. Among biological processes, apoptosis (5.1%), regulation of cell cycle (2.6%), anti-apoptosis (2%), protein metabolism (12.8%), and metabolism (14.8%) were top 5 ranked processes. Similarly, extracellular (39.2%), extracellular space (16.5%), cytosol (26.8%), exosomes (35.6%), and nucleoplasm (14.4%) were top-ranked cellular components, while protein serine/threonine kinase activity (7.1%), peroxidase activity (2%), metalloproteinase activity (3.6%), cytokine activity (3.6%), and superoxide dismutase activity (1%) were top-ranked molecular functions of common genes.

Further, pathway analysis of common genes demonstrated the involvement of AP-1 transcription factor network (43.2%), Integrin-linked kinase signaling (43.8%), TRAIL Signaling pathway (59.8%), VEGF and VEGFR signaling cascade (59.2%), and VEGFR1 and VEGFR2 mediated signaling cascade (58.6%). Moreover, the fold enrichment value of the above-described cellular pathways is 4.375, 4.211, 2.837, 2.860, and 2.849, respectively. Thus, the results concluded that the common genes were mainly involved in apoptosis, and cell-cycle

Table 1 (continued)

Name	Fold enrichment	P-value	Genes mapped
Nucleoplasm	4.679352988	9.37804E-12	STIP1; TAX1BP1; TPM1; TXNRD1; TP53; CASP3; JUN; MAPK8; MAPK1; AKT1; MAPK3; MAPK9; CDKN1A; CCND1; RELA; MYC; CASP7; PLK1; CDK1; ATF2; CCNE2; MCM2; PCNA; ATM; DUSP6; HMGB1; MAPK14; PHB; PPARGC1A; SFPQ; SIRT1; SQSTM1;
Cytoplasm	1.61016101	1.28598E-11	CAT; TP53; NQO1; CASP3; GSR; HIF1A; SOD1; JUN; MAPK8; MAPK1; PTGS2; AKT1; MAPK3; MAPK9; PARP1; CDKN1A; VEGFA; CCND1; FYN; GPT; GPX1; IRS1; RELA; STAT3; TF; BCL2; HDAC1; BAX; CASP7; NFE2L2; PLK1; BBC3; CASP9; CDK1; MAP2K4; NOS2; TXN; AHR; APOA1; ATF2; EGFR; GSK3B; ICAM1; IL1B; MT2A; SLC2A1; VIM; BCL2L11; C3; CASP8; CHEK2; CREBBP; EIF4A1; ESR1; FABP3; G6PD; HSPA5; PCNA; PLK2; PPARA; SGK1; SLC11A2; SLC40A1; TGFB1; TGFB1; ADM; AGT; ALB; ALDH1L1; ARHGFE2; ATM; BMP1; C1QBP; CALR; CCL5; CCT2; CD36; CD44; CXCR4; CYCS; DHFR; DNAJB1; DUSP6; EDN1; FAS; FDPS; FZD4; GCHFR; GPX4; HMGB1; HSP90A1; HSPA9; HSPB1; HSPH1; HYOU1; IGF1; KLF4; LDHA; MAPK14; NFIA; NME1; OPTN; PHB; PPIA; PRDX1; PRKCD; RAB31; RGCC; RGS2; S100A6; SERPINA1; SFPQ; SIRT1; SQSTM1; ST13; STIP1; TAX1BP1; TGFB2; THOP1; TLR4; TPM1; TXNRD1;
Molecular functions			
Protein serine/threonine kinase activity	4.303851101	5.27737E-06	MAPK8; MAPK1; AKT1; MAPK3; MAPK9; PLK1; CDK1; GSK3B; CHEK2; PLK2; SGK1; ATM; MAPK14; PRKCD;
Peroxidase activity	18.53093404	5.61002E-05	PTGS2; GPX1; GPX4; PRDX1;
Metallopeptidase activity	6.417319661	0.000113325	MMP1; MMP2; ADAMTS1; MMP13;

regulation causes neuronal cell death in metal toxicity induced AD. Fig. 2(A) demonstrated the functional enrichment analysis of common genes such as cellular components, biological processes, molecular functions, and pathways. Further, subcellular localization prediction of shared genes involved in metal toxicity-induced AD indicates the crucial role of cytoplasm (60 genes: 30.2%). The analysis found that the percentage of genes present in the extracellular space (58 genes: 29.1%) is almost comparable to that of the cytoplasm. In addition, apart from the cytoplasm and extracellular space, the shared genes were found in the nucleus (35 genes: 17.6%), plasma membrane (21 genes: 10.6%), mitochondria (14 genes: 7.0%), endomembrane system (6 genes: 3.0%), and organelle membrane (5 genes: 2.5%) Fig. 2(B).

3.3. PPI network of common genes and HUB genes in the network

To construct a global PPI network of common genes involved in metal toxicity and AD, the genes were entered as a list in the STRING database with a medium confidence score. The obtained output was imported into the Cytoscape software as input with the help of the Reactome FI plugin for data visualization. The results of the PPI network show 175 nodes and 1138 edges in the network (Fig. 3(A)). Nodes represent the protein signature, while edges are the interaction between different signatures. The size of the particular node decreases as the degree of the node decreases. Similarly, the edge thickness depends on the experimental validation of the interaction among two different nodes. The characteristics and parameters of the PPI network are given in Table 2.

Further, the global PPI network clustering was carried out to extract the highly-dense connected region of the network with the help of M-Code (Fig. 3(B)). Cluster 1 with an MCode score of 11.524, the number of nodes equal to 22, and the number of edges equal to 121 were selected for further investigations. Herein, we selected cluster 1 as it has a higher MCODE score and, thus, higher accuracy and biological significance than other predicted clusters. The density, centralization, and heterogeneity of the cluster network are 0.524, 0.419, and 0.385, respectively. Other parameters and characteristics of the cluster network are given in Table 2. Furthermore, the top 10 proteomic signatures or HUB genes were selected from the cluster network with the help of the CytoHubba. STAT3 (19), RELA (19), MAPK3 (18), C-FOS (17), EGFR (14), NOS2 (12), HIF1A (12), PTGS2 (7), MAPK8 (13), and AKT1 (12) were identified as HUB genes in the network (Fig. 3(C)). The network density, network centralization, and network heterogeneity of the HUB genes network are 0.889, 0.139, and 0.148, respectively.

3.4. Regulatory TFs involved in the regulation of HUB genes expression

The selected HUB genes were further analyzed to identify transcriptional signatures that are TFs involved in regulating metal toxicity induced AD. The HUB genes were analyzed with the JASPAR tool to identify regulatory TFs, and then with the help of network analyst interaction networks between HUB genes and TFs, were identified (Fig. 4(A)). Analysis of the HUB genes-TFs network demonstrated 47 nodes and 73 edges in the network. Table 2 describes the parameters of the HUB genes-TFs interaction network. 47 TFs were identified, which regulate the transcriptional activity of HUB genes. To minimize the number of transcriptional signatures, the TFs with node degrees equal to or greater than 3 were selected for further investigations. The rationale behind selecting transcription factors with node degrees equal to or greater than 3 is to minimize the number of transcription factors for further analysis. Another necessary explanation for selecting transcription factors with node degree equal to 3 or greater than 3 is to remove irrelevant transcription factors associated with molecular signatures of metal toxicity-induced AD. The node degree equal or greater than three signifies that a particular transcription factor is associated with either 3 molecular signatures or above 3 molecular signatures involved in metal toxicity-induced AD. Thus, these transcription factors have a higher

Table 1 (continued)

Name	Fold enrichment	P-value	Genes mapped
Cytokine activity	6.057503589	0.000162709	ANPEP; BMP1; THOP1; IL6; CXCL8; IFNG; IL1B; IL4; IL10; IL2; SOD1; SOD2;
Superoxide dismutase activity	61.74895155	0.000346553	
Chaperone activity	5.144142997	0.00044355	HSPA5; CALR; CCT2; HSP90A1; HSPA9; HSPB1; HYOU1;
<i>Biological pathways</i>			
AP-1 transcription factor network	4.375449634	1.06375E-30	TP53; CASP3; HIF1A; IL6; JUN; HMOX1; MAPK8; MAPK1; PTGS2; AKT1; MAPK3; TNF; CXCL8; MAPK9; CDKN1A; VEGFA; CCND1; FYN; RELA; STAT3; TF; BCL2; HDAC1; IFNG; MYC; BAX; CDK1; MAP2K4; NOS2; TIMP1; TXN; ATF2; FOS; GSK3B; ICAM1; MMP1; MMP2; MT2A; SLC2A1; TCF4; TFRC; BCL2L11; CASP8; CREBBP; DDIT3; EGR1; ESRI; IL4; SGK1; SP1; TGFB1; ACHE; ADM; AGT; ATM; BHLHE40; CCL2; CXCR4; DKK1; EDN1; GJA1; HSPB1; IL10; IL2; JUNB; KLF4; LDHA; MAPK14; NTS; PPARGC1A; PRDX1; PRKCD; TGFBR2;
Integrin-linked kinase signaling	4.21157898	4.56458E-30	TP53; CASP3; HIF1A; IL6; JUN; HMOX1; MAPK8; MAPK1; PTGS2; AKT1; MAPK3; TNF; CXCL8; MAPK9; PARP1; CDKN1A; VEGFA; CCND1; FYN; RELA; STAT3; TF; BCL2; HDAC1; IFNG; MYC; BAX; CDK1; MAP2K4; NOS2; TIMP1; TXN; ATF2; FOS; GSK3B; ICAM1; MMP1; MMP2; MT2A; SLC2A1; TCF4; TFRC; BCL2L11; CASP8; CREBBP; DDIT3; EGR1; ESRI; IL4; SGK1; SP1; TGFB1; ACHE; ADM; AGT; ATM; BHLHE40; CCL2; CXCR4; DKK1; EDN1; GJA1; HSPB1; IL10; IL2; JUNB; KLF4; LDHA; MAPK14; NTS; PPARGC1A; PRDX1; PRKCD; TGFBR2;
TRAIL signaling pathway	2.837162097	1.33272E-28	CAT; TP53; CASP3; HIF1A; IL6; JUN; HMOX1; MAPK8; MAPK1; PTGS2; AKT1; MAPK3; TNF; CXCL8; MAPK9; PARP1; CDKN1A;

weightage or higher probability of being involved in metal toxicity-induced AD. Thus, CREB1 (5), FOXC1 (4), GATA2 (4), NFKB1 (4), SRF (3), TFAP2A (3), FOXA1 (3), and MEF2A (3) were identified as top interacting TFs (Table 3).

3.5. Literature validation of regulatory molecules and protein sub-cellular localization

Transcriptomics signatures and post-transcriptomics signatures were further investigated and validated to identify their potential role in regulating HUB genes or involvement in disease pathogenesis. The TFs were analyzed with MalaCards to extract the role of regulatory molecules in the progression of the disease (Table 3). Furthermore, HUB genes were analyzed for their sub-cellular localization. Among the HUB genes, 50% were cytoplasmic (MAPK3, RELA, NOS2, MAPK8, AKT1), 30% were nuclear proteins (STAT3, C-FOS, HIF1A), 10% were endoplasmic reticulum complex protein (PTGS2), and 10% were Golgi complex proteins (EGFR).

3.6. CREBBP-induces CREB1, GATA2, NFKB1, and FOXA1 acetylation at K122, K399, K967, and K350

Acetylation of TFs at specific lysine residues causes transcriptional activation and thus promotes the cellular and biological processes. The identified TFs, such as CREB1, FOXC1, GATA2, NFKB1, SRF, TFAP2A, FOXA1, and MEF2A, were analyzed with Deep-PLA and GPS-PAIL to determine the crucial common CREBBP-induced acetylated lysine residues with high confidences score. For Deep-PLA, if the score is less than 5%, it must be said as acetylated lysine residue with high confidence, whereas, for GPS-PAIL, if the score is greater than 1.0, it is said to be acetylated lysine residue with high confidence. Our analysis identified a total of 4 acetylated lysine residues with high confidence, each one in four identified TFs. CREB1 (K122), GATA2 (K399), FOXA1 (K350), and NFKB1 (K967) were identified as critical lysine residues (Table 4). FOXC1, SRF, TFAP2A, and MEF2A did not have any common acetylated lysine residue and thus were excluded for further analysis. Further, our prediction of CREBBP-induced acetylation sites for CREB coincides with the previously reported study. For instance, Lu et al., 2003 reported that the acetylation of CREB at K91, K94, K122, and K136 by CREBBP enhanced CREB-dependent transcription (Lu et al., 2003). In addition, a previously published study identified the GATA2 acetylation on K399 by p300, where the authors concluded that acetylation of GATA2 in 293T cells increases its DNA-binding activity (Hayakawa et al., 2004).

3.7. hsa-miR-129-5p and hsa-miR-335-5p are putative micro-RNAs involved in the pathogenesis of AD

miRNAs are post-transcriptional regulators, which regulate the activity of a particular gene. Moving forward, we aim to identify the critical miRNAs that regulate the expression of CREBBP, CREB1, GATA2, NFKB1, and FOXA1. mirDIP, an online miRNA-target prediction tool, identified 379 miRNAs, 640 miRNAs, 145 miRNAs, 127 miRNAs, and 223 miRNAs in CREBBP, CREB1, GATA2, NFKB1, and FOXA1, respectively. Further, miRNAs having confidence score high or very high with a particular target, such as CREBBP (85 very high and 294 high), CREB1 (220 very high and 420 high), GATA2 (36 very high and 109 high), NFKB1 (32 very high and 95 high), and FOXA1 (71 very high and 152 high) were selected for further analysis. Moreover, Venn analyses were carried to identify the common miRNAs associated with CREBBP, CREB1, GATA2, NFKB1, and FOXA1 (Fig. 4(B)). Our analysis identified five miRNAs, such as hsa-miR-338-5p, hsa-miR-335-5p, hsa-miR-429, hsa-miR-200c-3p, and hsa-miR-129-5p, were important miRNAs associated with all five selected targets. Furthermore, it is equally important to check whether the selected miRNA was expressed in brain tissues or not. For this, we analyzed the expression of putative miRNA in brain tissue samples from TissueAtlas, where we identified the expression of

Table 1 (continued)

Name	Fold enrichment	P-value	Genes mapped
			SOD2; VEGFA; CCND1; FYN; GPX1; IRS1; RELA; STAT3; TF; BCL2; HDAC1; IFNG; MYC; BAX; CASP7; PLK1; BBC3; CASP9; CDK1; MAP2K4; NOS2; TIMP1; TXN; ATF2; EGFR; FOS; GSK3B; ICAM1; MMP1; MMP2; MT2A; SLC2A1; TCF4; TFRC; VIM; BCL2L11; CASP8; CHEK2; CREBBP; DDIT3; EGR1; EIF4A1; ESR1; IL4; MMP13; PCNA; SGK1; SP1; TGFB1; ACHE; ADM; AGT; ATM; BHLHE40; BMP4; CCL2; CCL5; CXCR4; CYCS; DKK1; DUSP6; EDN1; FAS; FGFR4; FN1; GDF15; GJA1; HSPB1; IGF1; IGF2; IL10; IL2; JUNB; KLF4; LDHA; MAPK14; NME1; NTS; PPARGC1A; PRDX1; PRKCD; RGCC; SIRT1; TGFB2;
VEGF and VEGFR signaling network	2.860893735	1.62998E-28	CAT; TP53; CASP3; HIF1A; IL6; JUN; HMOX1; MAPK8; MAPK1; PTGS2; AKT1; MAPK3; TNF; CXCL8; MAPK9; CDKN1A; SOD2; VEGFA; CCND1; FYN; GPX1; IRS1; RELA; STAT3; TF; BCL2; HDAC1; IFNG; MYC; BAX; PLK1; BBC3; CASP9; CDK1; MAP2K4; NOS2; TIMP1; TXN; ATF2; EGFR; FOS; GSK3B; ICAM1; MMP1; MMP2; MT2A; SLC2A1; TCF4; TFRC; BCL2L11; CASP8; CHEK2; CREBBP; DDIT3; EGR1; EIF4A1; ESR1; IL4; MMP13; PCNA; SGK1; SP1; TGFB1; ACHE; ADM; AGT; ATM; BHLHE40; BMP4; CCL2; CCL5; CXCR4; CYCS; DKK1; DUSP6; EDN1; FAS; FGFR4; FN1; GDF15; GJA1; HSP90A1; HSPB1; IGF1; IGF2; IL10; IL2; JUNB; KLF4; LDHA; MAPK14; NME1; NTS; PGF; PPARGC1A; PRDX1; PRKCD; RGCC; SIRT1; TGFB2;
Signaling events mediated by VEGFR1 and VEGFR2	2.849811345	5.67443E-28	CAT; TP53; CASP3; HIF1A; IL6; JUN; HMOX1; MAPK8; MAPK1; PTGS2;

particular miRNA in the brain. hsa-miR-338-5p (23.09484), hsa-miR-335-5p (169.42783), hsa-miR-429 (4.26456), hsa-miR-200c-3p (2.72829), and hsa-miR-129-5p (251.58495) were expressed in 43, 46, 21, 28, and 47 brain tissue samples, respectively (Fig. 4(B)). Further, we checked the role of putative miRNAs in the pathogenesis of AD. Our study identified that miRNAs, such as hsa-miR-335-5p (169.42783) and hsa-miR-129-5p (251.58495), were significantly enriched in the AD pathway with a p-value less than 0.05 (Fig. 4(B)). Thus, hsa-miR-338-5p (23.09484), hsa-miR-429 (4.26456), and hsa-miR-200c-3p (2.72829) were excluded from further analysis.

3.8. OIP5-AS1 regulates the expression and activity of hsa-miR-129-5p and hsa-miR-335-5p in the pathogenesis of metal toxicity-induced AD

Apart from AD, it is equally important to analyze the role of identified miRNAs in the pathogenesis and progression of brain diseases. hsa-miR-335-5p is involved in AD (0.03), developmental disorder of mental health (0.2), and tauopathy (0.03), whereas, hsa-miR-129-5p is involved in the pathogenesis of AD (0.002), dementia (0.107), Lewy body dementia (0.03), Parkinson's disease (0.13), and tauopathy (0.002). Thus, the analysis concluded that both hsa-miR-335-5p and hsa-miR-129-5p are significantly involved in the pathogenesis of AD and tauopathy (Fig. 5(A)). Further, our study also concluded that hsa-miR-338-5p is significantly enriched in the pathogenesis of Ataxia Telangiectasia (0.019), whereas, hsa-miR-429 is significantly enriched in autism spectrum disorder (0.020), brain edema (0.03), brain ischemia (0.001), CNS vasculitis (0.004), a developmental disorder of mental health (0.026), and peripheral nervous system disease (0.02). Similarly, hsa-miR-200c-3p is significantly enriched in ARMD (0.007), autism spectrum disorder (0.003), brain ischemia (0.005), CNS vasculitis (0.013), cerebral arterial disease (0.006), dementia (0.04), developmental disorder of mental health (0.0008), diabetic neuropathy (0.005), and macular degeneration (0.007).

Further, we analyzed the signaling mechanism followed by hsa-miR-335-5p and hsa-miR-129-5p in the pathogenesis of AD. Our results demonstrated that hsa-miR-129-5p significantly enriches corticotropin-releasing hormone pathway (9.91805E-05), IL17 signaling pathway (0.000468125), EGF/EGFR signaling pathway (0.000533398), Interleukin-11 signaling pathway (0.000945926), and VEGFA-VEGFR2 (0.001582748) signaling pathway. Similarly, the TGF-beta signaling pathway (5.90563E-06), IL-2 signaling pathway (8.98756E-06), ErbB signaling pathway (9.29391E-05), B cell receptor signaling pathway (0.000115973), and IL-7 signaling pathway (0.000302961) are the top 5 signaling cascade in the hsa-miR-335-5p (Fig. 5(B)).

It is well-known that non-coding RNAs, namely long non-coding RNAs and circular RNAs, bind to the miRNA response element and alter the binding activity of miRNA to a target gene. Thus, keeping this in mind, we analyzed the putative long non-coding RNAs that alter the activity of five identified miRNAs. OIP5-AS1 is identified as long non-coding RNAs that alter the binding affinity of hsa-miR-335-5p and hsa-miR-129-5p to CREBBP in the pathogenesis of AD.

4. Discussion and conclusion

In the following study, we utilized a publicly accessible database, the CTD database and the DisGeNET database were used to identify common molecular signatures in metal toxicity and AD. The Venn analysis of genes involved in copper, chromium, cobalt, and nickel toxicity identified 376 shared genes. Furthermore, the Venn analysis of shared metal toxicity genes with the genes expressed in the AD revealed the presence of 199 common molecular genes that has been linked to heavy metal toxicity and AD. The gene set enrichment analysis of shared molecular targets identified the involvement of apoptosis, regulation of cell cycle, anti-apoptosis, protein metabolism, metabolism, signal transduction as the crucial biological process followed by shared molecular targets. Moreover, pathway analysis of common molecular targets identified the

Table 1 (continued)

Name	Fold enrichment	P-value	Genes mapped
IFN-gamma pathway	2.849811345	5.67443E-28	AKT1; MAPK3; TNF; CXCL8; MAPK9; CDKN1A; SOD2; VEGFA; CCND1; FYN; GPX1; IRS1; RELA; STAT3; TF; BCL2; HDAC1; IFNG; MYC; BAX; PLK1; BBC3; CASP9; CDK1; MAP2K4; NOS2; TIMP1; TXN; ATF2; EGFR; FOS; GSK3B; ICAM1; MMP1; MMP2; MT2A; SLC2A1; TCF4; TFRC; BCL2L11; CASP8; CHEK2; CREBBP; DDIT3; EGR1; EIF4A1; ESR1; IL4; MMP13; PCNA; SGK1; SP1; TGFB1; ACHE; ADM; AGT; ATM; BHLHE40; BMP4; CCL2; CCL5; CXCR4; CYCS; DKK1; DUSP6; EDN1; FAS; FGFR4; FN1; GDF15; GJA1; HSP90AB1; HSPB1; IGF1; IGF2; IL10; IL2; JUNB; KLF4; LDHA; MAPK14; NME1; NTS; PPARGC1A; PRDX1; PRKCD; RGCC; SIRT1; TGFB2; CAT; TP53; CASP3; HIF1A; IL6; JUN; HMOX1; MAPK8; MAPK1; PTGS2; AKT1; MAPK3; TNF; CXCL8; MAPK9; CDKN1A; SOD2; VEGFA; CCND1; FYN; GPX1; IRS1; RELA; STAT3; TF; BCL2; HDAC1; IFNG; MYC; BAX; PLK1; BBC3; CASP9; CDK1; MAP2K4; NOS2; TIMP1; TXN; ATF2; EGFR; FOS; GSK3B; ICAM1; IL1B; MMP1; MMP2; MT2A; SLC2A1; TCF4; TFRC; BCL2L11; CASP8; CHEK2; CREBBP; DDIT3; EGR1; EIF4A1; ESR1; IL4; MMP13; PCNA; SGK1; SP1; TGFB1; ACHE; ADM; AGT; ATM; BHLHE40; BMP4; CCL2; CCL5; CXCR4; CYCS; DKK1; DUSP6; EDN1; FAS; FGFR4; FN1; GDF15; GJA1; HSPB1; IGF1; IGF2; IL10; IL2; JUNB; KLF4; LDHA; MAPK14; NME1; NTS; PPARGC1A; PRDX1; PRKCD; RGCC; SIRT1; TGFB2;

potential involvement of AP-1 transcription factor network (43.2%), Integrin-linked kinase signaling (43.8%), TRAIL Signaling pathway (59.8%), VEGF and VEGFR signaling cascade (59.2%), and VEGFR1 and VEGFR2 mediated signaling cascade (58.6%). Further, the common molecular targets were analyzed to identify associated proteomic signatures, highly dense regions of the network, and highly connected nodes with the help of network biology. The protein-protein interaction network has 175 nodes, and 1138 edges, where nodes were mapped according to their degree of nodes and edges were mapped according to FI score. Clustering of global PPI network identified highly dense regions with a clustering score of 11.524 with 22 nodes and 121 edges. Further investigation identified HUB genes in the cluster network, which are STAT3, MAPK3, RELA, C-FOS, EGFR, NOS2, HIF1A, PTGS2, MAPK8, and AKT1. PPI network analysis of HUB genes identified that the network has 10 nodes and 40 edges with network density and clustering coefficient of 0.889 and 0.916, respectively. Apart from identified 10 nodes or proteomic signatures or HUB genes, other nodes of cluster 1, such as IL2, IL6, Bcl-2, HDAC1, TNF, IL1 β , ATF2, and others were found to be associated with AD pathways through metal toxicity. For instance, Cobalt chloride mimics hypoxia in R28 cells, which causes mitochondrial membrane potential disruption and activation of caspase 3 and ultimately leads to neuronal cell death. The same study also concluded that IL6 mediated its pro-survival effect against cobalt toxicity via STAT3 phosphorylation and activation of anti-apoptotic proteins (Thakur et al., 2021). Similarly, another study demonstrated that administration of cobalt nanoparticles causes an increase in inflammation-related proteins, such as NLRP3 and IL1 β in C57BL/6J mice brain, suggesting the role of microglia-involved inflammation (J. Li et al., 2021). Further, Yubolphan et al., 2021 demonstrated that administration of nickel at 600.60 μ M and >1000 μ M in astrocytoma cells and primary human astrocytes, respectively, triggered apoptotic pathway through decreased activity of Bcl-2 and increased activity of caspase 3 (Yubolphan et al., 2021). Kitazawa et al., 2016 concluded that the copper-A β complex inhibits microglial phagocytosis and increases TNF α and IL1 β clearance, leading to decreased activity of LRP1, which activates the inflammatory pathway (Kitazawa et al., 2016; Newcombe et al., 2018).

Further, CREB1 (5), FOXC1 (4), GATA2 (4), NFKB1 (4), SRF (3), TFAP2A (3), FOXA1 (3), and MEF2A (3) were identified as top interacting TFs, which regulates the expression activity of HUB genes. Lately, literature validation confirmed the role of identified TFs in the pathogenesis and progression of AD (Ascolani et al., 2012; Bartolotti et al., 2016; Cong et al., 2021; H. Li et al., 2021; Rahman et al., 2020, 2019). For instance, activation of CREB1 and acquisition of transcription co-factors, such as CREBBP, is crucial for memory formation, whereas, deficiency of NFKB1 causes early onset of memory loss (Bartolotti and Lazarov, 2019; Fielder et al., 2020). Similarly, silencing SRF reversed contractile protein content and rescued from a hypercontractile phenotype in AD, while TFAP2A is involved in the genetic variants associated with a high risk of dementia (Chow et al., 2007; Ho et al., 2020). Lately, we identified the CREBBP-induced acetylation sites of the eight TFs. CREBBP, also called CBP or KAT3A is involved in acetylation by modulating different signaling pathways, such as calcium signaling, notch signaling, response to hypoxia, and NF κ B signaling (Dancy and Cole, 2015). Recent studies demonstrated the potential link between metal toxicity and the acetylation process. For instance, Kang et al., 2004 concluded that copper at both toxic and non-toxic levels (100 or 200 μ M) causes histone hypoacetylation in Hep3B cultured cells through inhibiting specific histone acetyltransferase activity (Kang et al., 2004). Further, it was concluded that administration of hexavalent chromium (10 μ M) downregulates histone H4 acetylation at K16 through activation of stressor protein Nupr1 (D. Chen et al., 2016). Similarly, chromium (12.5 μ M) administration causes inhibition of biotinidase, which could be reversed by increased acetylation levels (Xia et al., 2011). Recently, Zhou et al., 2021 demonstrated that administration of nickel causes a reduction in H3K9 acetylation levels, which leads to repression

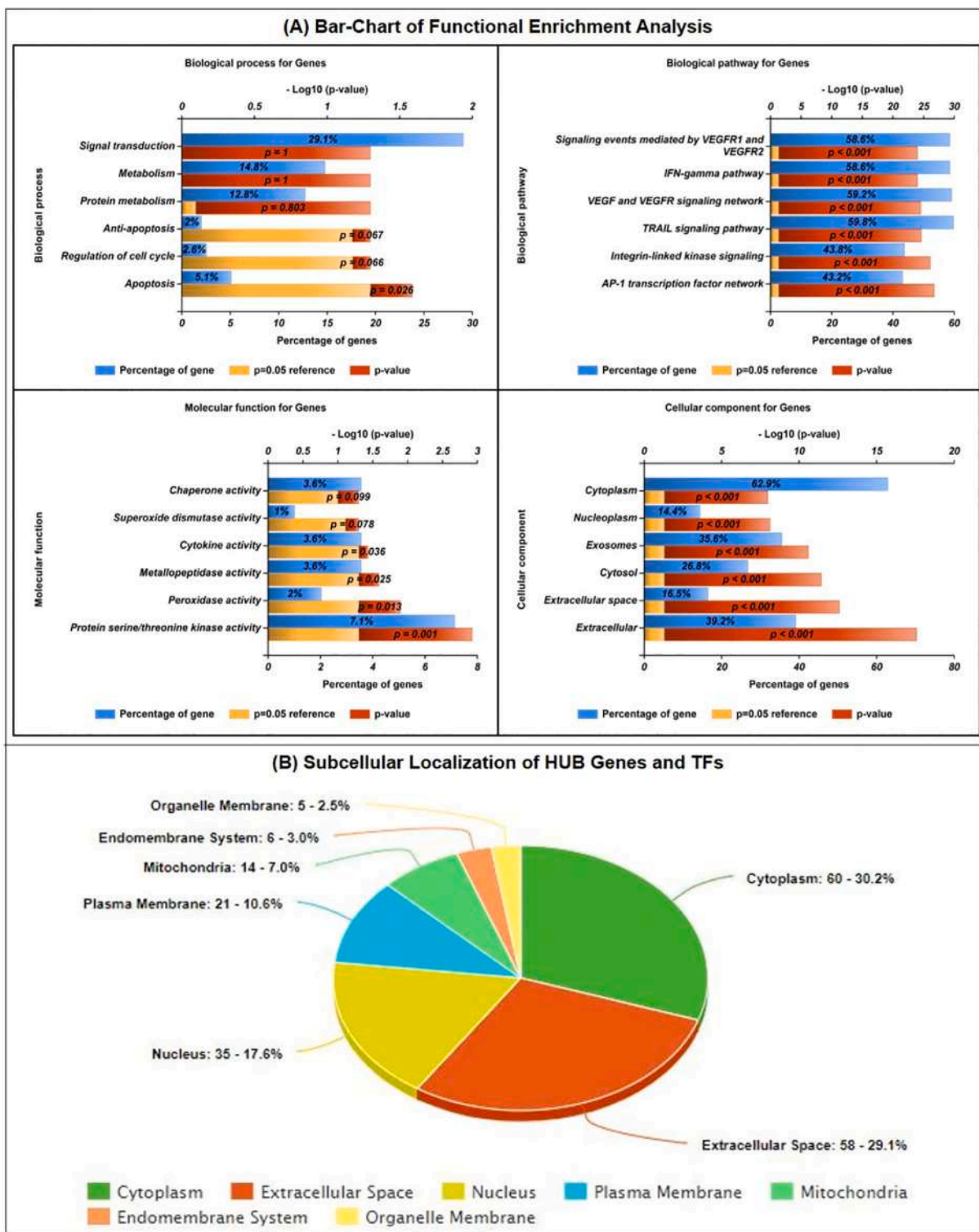


Fig. 2. Gene set enrichment analysis of common genes between chromium, cobalt, copper, and nickel-associated Alzheimer's disease (FunRich and KEGG pathway database). (A) represents the bar-graph of biological process, cellular components, molecular function, and associated pathway. Among the biological process, signal transduction, metabolism, protein metabolism, anti-apoptosis, apoptosis, and cell cycle regulation with p-value 1, 1, 0.803, 0.067, 0.066, and 0.026 were top-ranked. Similarly, chaperon's activity, superoxide dismutase activity, cytokine activity, metalloproteinase activity, peroxidase activity, and protein serine/threonine activity were top-ranked molecular functions. At the same time, cytoplasm, nucleoplasm, exosomes, cytosol, extracellular space, and extracellular were top-ranked cellular components. Moreover, signaling events mediated by VEGFR1 and VEGFR2 (58.6%), IFN-gamma pathway (58.6%), VEGF and VEGFR signaling network (59.2%), TRAIL signaling pathway (59.8%), integrin-linked kinase signaling (43.8%), and AP-1 transcription factor network (43.2%) were top-ranked biological pathway associated with shared genes. (B) Subcellular localization of the shared genes involved in metal toxicity-induced AD through BUSCA: Bologna Unified Subcellular Component Annotator.

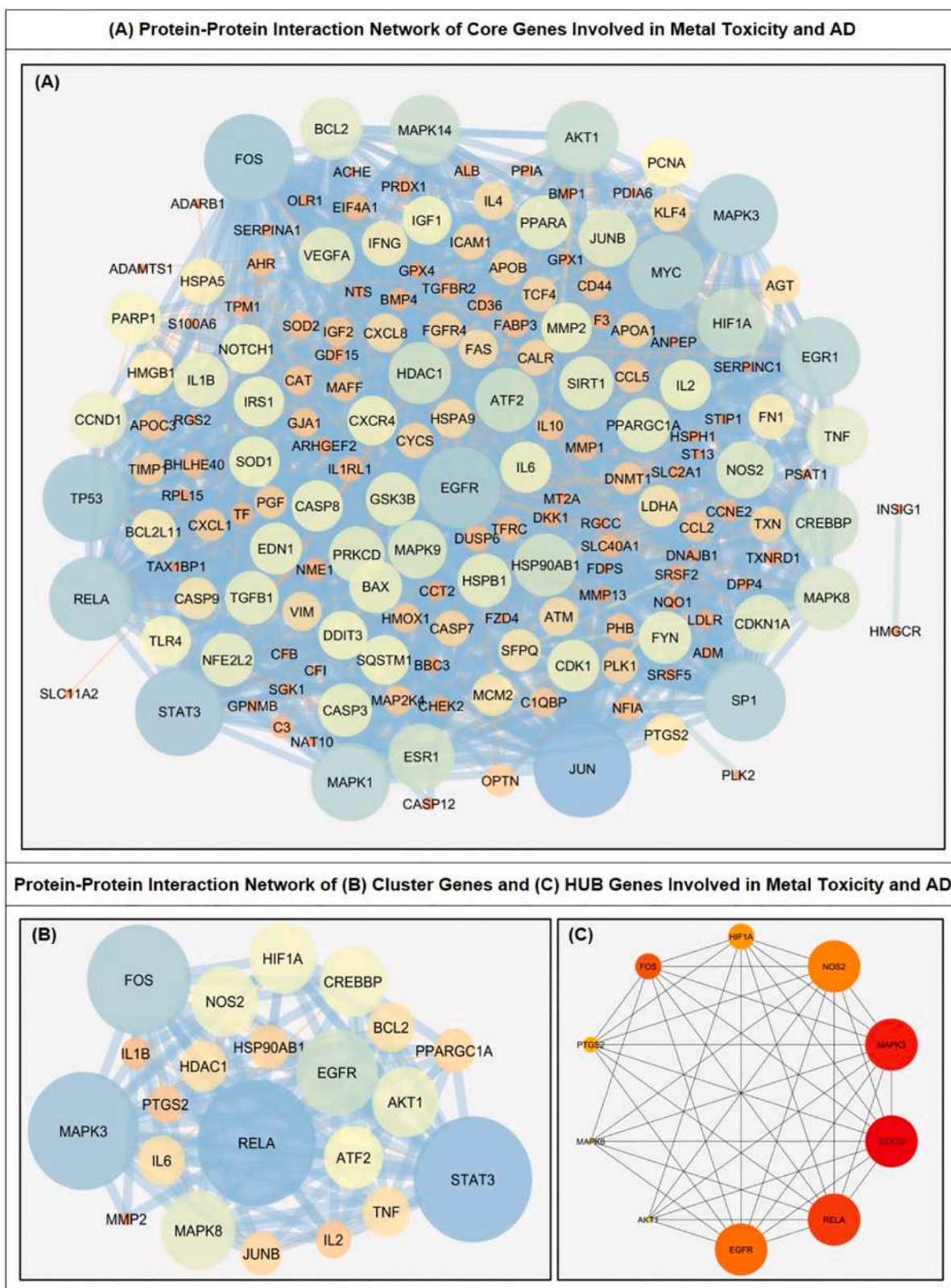


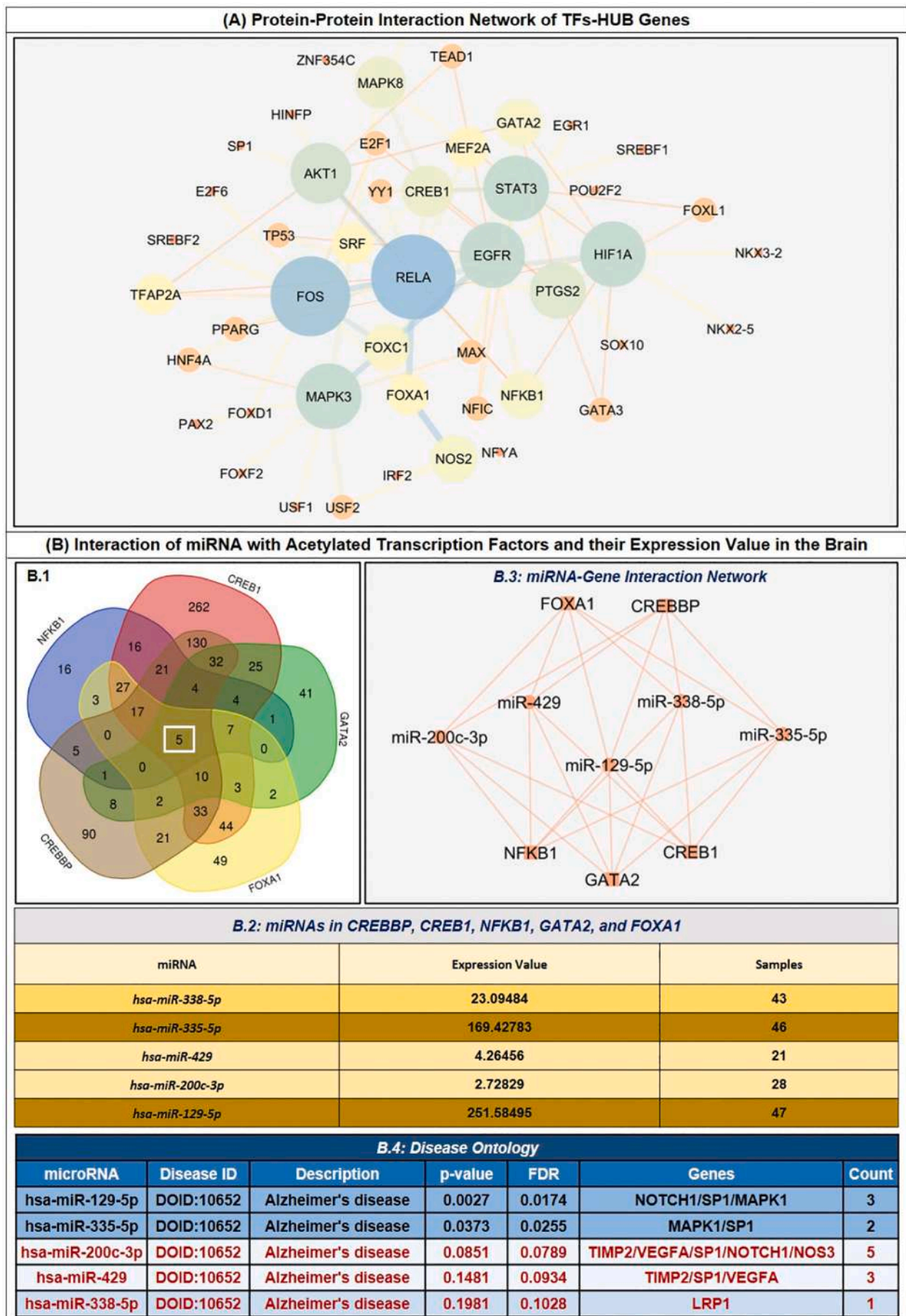
Fig. 3. (A) It represents the protein-protein interaction network of 199 common genes between chromium, cobalt, copper, and nickel associated metal toxicity induced Alzheimer's disease. The nodes in the network were ranked according to their degree. The size of the node decreases as the degree of the node decreases. Similarly, the color of the node increases from a light color to dark color as the degree of the node decreases. Furthermore, the size of the edge between nodes depends on edge betweenness. (B) It represents the clustering protein-protein interaction network and aims to identify the highly-dense or connected region in the global biological interaction network. (C) It represents the top 10 ranked HUB genes in the network. Here, darker is the color of the node; more is the rank of the HUB gene.

Table 2
Characteristics and parameters of core, cluster, HUB genes, transcription factors, and miRNA PPI network.

Network	Number of nodes	Number of edges	Clustering coefficient	Network density	Network centralization	Network heterogeneity	Characteristics path length	Average no of neighbors
Core PPI	175	1138	0.422	0.075	0.36.	1.14	2.426	13.006
Cluster (11.524)	22	121	0.713	0.524	0.419	0.385	0.419	11
HUB genes	10	40	0.916	0.889	0.139	0.148	1.111	8
Transcription factors	47	73	0.071	0.068	0.202	0.896	3.192	3.106

of H3K9-modulate neural genes expression (Zhou et al., 2021). Apart from nickel, copper, and chromium, another metal that interferes with acetylation is cobalt. Evidence suggests the potential relationship between cobalt and acetylation status. For example, Guo et al., 2021 demonstrated that cobalt chloride administration at 400 μM for 24 h in the SHSY5Y cell culture model inhibits H3 and H4 acetylation (Guo et al., 2021). The same study concluded that cobalt chloride selectively decreased the activity of histone acetyltransferases and did not alter the activity of histone deacetylase. Thus, these evidences validate the role of metal toxicity and acetylation status. Further different studies also investigated the role of metal exposure on the expression of CREBBP. For example, administration of chromium hexavalent ion results in decreased expression of CREBBP protein, whereas, exposure to copper caused decreased expression of CREBBP mRNA (Liao and Liu, 2012; Shobana et al., 2020). However, in another study, it was concluded that administration of nickel monoxide results in increased expression of CREBBP mRNA (Fujita et al., 2009). Further, some evidences suggest the role of metal exposure on the activity of CREBBP and its targets. For instance, chromium inhibits the transcriptional activity of NF- κ B by decreasing the interaction between p65 and CBP (JA et al., 1999). Similarly, Cobalt causes increased activity of SRC protein, which activates HIF1A/STAT3/VEGFA and leads to binding of APEX1 to CREBBP promoter (Gray et al., 2005). Thus, these evidences demonstrated the potential link between metal exposure and CREBBP and acetylation. However, no study was reported that concluded the exact role of metal exposure in CREBBP and its target acetylation. Thus, we aim to identify the potential targets of CREBBP involved in metal toxicity and AD pathogenesis. Our study identified that CREBBP-Induces CREB1, GATA2, NFKB1, and FOXA1 acetylation at K122, K399, K967, and K350. Thus, K122 of CREB1, K399 of GATA2, K967 of NFKB1, and K350 of FOXA1 were considered crucial lysine residues for the acetylation process in the pathogenesis of AD. In addition, post-transcriptional signatures, namely miRNA and long non-coding RNAs, regulate the expression of proteins, where long non-coding RNAs serve as a sponge for miRNA. Our results identified five potential miRNAs that were associated with CREBBP and identified TFs simultaneously, such as hsa-miR-338-5p, hsa-miR-335-5p, hsa-miR-429, hsa-miR-200c-3p, and hsa-miR-129-5p. However, hsa-miR-335-5p and hsa-miR-129-5p, having expression values of 169.427 and 251.584, respectively, in the brain tissue, were selected for further studies. In addition, literature validation suggests the potential applicability of hsa-miR-335-5p and hsa-miR-129-5p in the pathogenesis and progression of AD. For instance, Wang et al., 2020 demonstrated that overexpression of miR-335-5p significantly decreased the expression of c-Jun N-terminal kinase 3 (JNK3) and $\text{A}\beta$ and thus, inhibited the neuronal apoptosis in SH-SY5Y/APPsw cells (Wang et al., 2020). Similarly, overexpression of miR-129-5p rescued nerve injury and inflammatory response through decreased expression of SRY-box transcription factor 6 (SOX6) in the $\text{A}\beta_{25-35}$ -induced AD rat model (Z. Zeng et al., 2019). In addition, Z. Li et al. concluded that knockdown of miR-129-5p decreased the neuroprotective effects of

exercise on cognition and neuroinflammation in the AD mice model (Z. Li et al., 2020). Thus, it could be concluded that overexpression of both hsa-miR-335-5p and hsa-miR-129-5p promotes neuroprotection. Furthermore, disease ontology confirmed the involvement of hsa-miR-335-5p and hsa-miR-129-5p in the pathogenesis of AD, having a p-value of 0.0373 and 0.0027, respectively. Further, mounting evidence suggests the potential link between metal toxicity and miRNA expression. For instance, administration of cadmium at 0.6 mg/kg increased the expression levels of miR-21-5p, miR-34a-5p, miR-224-5p, miR-451-5p, and miR-1949, whereas, administration of cadmium in human prostrate epithelial cells at 10 μM increases the expression of miR-96, miR-134, and miR-9 (Fay et al., 2018; Ngalamé et al., 2016). Similarly, administration of cobalt increases the pri-miRNA processing activity of DGCR8, which enhanced the expression of miR-9 (Barr et al., 2015). Further, Jeon et al., 2014 concluded that administration of cobalt chloride-induced neuronal differentiation of human mesenchymal stem cells through upregulation of miR-124a, which inhibits the expression of SCP1 and SOX9 (Jeon et al., 2014). Chiou et al., 2015 demonstrated that administration of nickel contributes to EGFR mutation and miR-21 overexpression, whereas, Wu et al., 2017 concluded that upregulation of miR-4417 contributes to nickel-induced fibrogenesis (Chiou et al., 2015; Wu et al., 2017). Another study identified that administration of arsenic in Patu8988 cells at 3 $\mu\text{mol/l}$ causes increased expression of miR-330-5p, whereas, administration of lead in blood samples of battery factory workers causes and upregulation of miR-520c-3p, miR-148a, miR-141, and miR-211 (Ghaffari et al., 2011; Xu et al., 2017). Jia et al., 2020 reported that chromium in exposed electroplating workers causes upregulation of miR-941 and miR-590-3p, whereas, Chandra et al., 2015 concluded that administration of chromium at 10 and 20 $\mu\text{g/ml}$ for 24 h upregulated the expression of miR-34-5p (Chandra et al., 2015; Jia et al., 2020). Further, studies demonstrated that exposure to cobalt chloride regulates the expression of miR-129-5p and its target genes (Mao et al., 2021; Zhu et al., 2021). Moreover, pathway analysis demonstrated the possible pathways through which hsa-miR-335-5p and hsa-miR-129-5p are involved in the pathogenesis of AD (Z. Li et al., 2020; Wang et al., 2020). hsa-miR-129-5p is involved in corticotropin-releasing hormone pathway, IL17 signaling pathway, EGF/EGFR signaling pathway, Interleukin signaling pathway, and VEGFA-VEGFR2 signaling pathway (Belaya et al., 2020; Glaesel et al., 2020; Li et al., 2017; Tian et al., 2019; Yang et al., 2019), whereas, hsa-miR-335-5p is involved in TGF-beta signaling pathway, IL-2 signaling pathway, ErbB signaling pathway, B cell receptor signaling pathway, and IL-7 signaling pathway (Khokhar et al., 2021; Li et al., 2016; Tang and Qin, 2019; Yu et al., 2021; Yue et al., 2017). Lastly, we identified the potential long non-coding RNA that is OPI5-AS1 that regulates the activity of hsa-miR-335-5p and hsa-miR-129-5p. Literature analysis validated our results as downregulation of OPI5-AS1 causes upregulation of has-miR-129-5p (H. Zeng et al., 2019). Thus, we concluded that downregulation of OPI5-AS1 causes upregulation of miR-129-5p, which modulate CREBBP-induced hyperacetylation of CREB1, GATA2, NFKB1, and FOXA1 acetylation at K122,



(caption on next page)

Fig. 4. (A) Protein-protein interaction network of transcription factors-HUB genes through Cytoscape Software: network analysis from network analyst identified the potential transcription factors associated with HUB genes. Among transcription factors, CREB1 (5), FOXC1 (4), GATA2 (4), NFκβ (4), SRF (3), TFAP2A (3), FOXA1 (3), and MEF2A (3) were the top interacting partners of HUB genes. Similarly, among HUB genes, FOS (11), RELA (9), MAPK3 (8), STAT3 (8), EGFR (8), HIF1A (8), AKT1 (6), PTGS2 (6), MAPK8 (5), and NOS2 (4) interacting partners. (B.1) Further, micro-RNAs interacting with putative acetylated transcription factors and acetylating enzyme CREBBP were identified. Five micro-RNAs, such as hsa-miR-338-5p, hsa-miR-335-5p, hsa-miR-429, hsa-miR-200c-3p, and hsa-miR-129-5p, were common micro-RNAs interacting with acetylated transcription factors and CREBBP with the help of Venny 2.0 Software. (B.2) Expression analysis of the predicted micro-RNAs in the brain tissue identified that micro-RNAs, namely hsa-miR-335-5p (146.427, 46 samples) and hsa-miR-129-5p (251.584, 47 samples), have the highest expression in the brain tissue among all five predicted micro-RNAs. (B.3) network analysis of predicted micro-RNAs with identified transcription factors through Cytoscape software. (B.4) Moreover, disease ontology analysis confirmed the involvement of hsa-miR-335-5p and hsa-miR-129-5p in the pathogenesis of Alzheimer's disease with the significantly enriched p-value of 0.0373 and 0.0174, respectively.

Table 3

Top interacting transcriptional regulatory factors involved in metal toxicity induced AD.

TFs	Degree	Partners	Role in disease pathogenesis
CREB1	5	C-FOS, RELA, MAPK8, PTGS2, STAT3	Reduction in CREB1 activation promotes memory impairment
FOXC1	4	C-FOS, STAT3, EGFR, MAPK3	Mutation in FOXC1 cause neurodevelopmental disorder
GATA2	4	HIF1A, PTGS2, EGFR, AKT1	Reduction in GATA2 expression decreases neuroglobin expression
NFKB1	4	RELA, EGFR, AKT1, HIF1A	Regulate immunological response
SRF	3	MAPK3, MAPK8, C-FOS	Regulate LRP mediate amyloid-β clearance
TFAP2A	3	AKT1, RELA, C-FOS	Regulate the proliferation and apoptosis of neuronal cells
FOXA1	3	C-FOS, RELA, NOS2	Required for adult dopamine neuronal cells maintenance and functioning
MEF2A	3	RELA, MAPK8, HIF1A	Reduction in MEF2A expression causes decreased activity of anti-apoptotic genes

Table 4

Prediction of CREBBP-induced acetylation sites of identified transcription factors through Deep PLA and GPS-PAIL.

TF	Acetylation (CREBBP)		Common K sites
	Deep PLA (score < 5%)	GPS-PAIL (score: >1.0)	
CREB1	122	122, 271, 278, 289, 295, 316, 325	122
FOXC1	256	181, 552	–
GATA2	102, 281, 285, 399	324, 378, 389, 390, 399, 403, 405, 406,	399
NFKB1	277, 431, 967	362, 425, 448, 896, 967	967
SRF	147, 154	506	–
TFAP2A	271	411, 427, 431, 434, 437	–
FOXA1	316, 350, 389	6, 350	350
MEF2A	Nil	403, 498	–

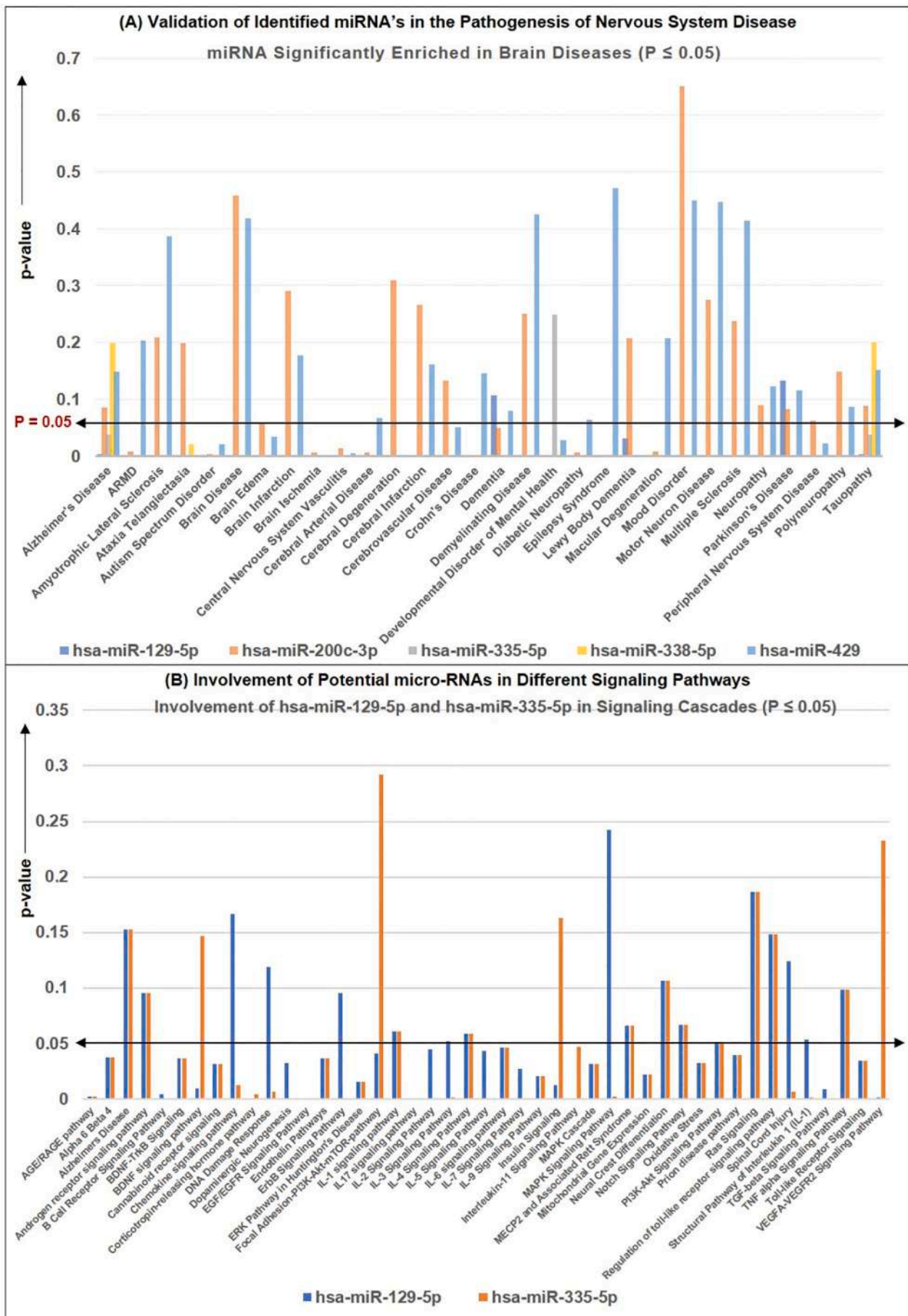
K399, K967, and K350. Regulation of hyperacetylation of CREB1, GATA2, NFKB1, and FOXA1 modulate their transcriptional activation, neuroinflammation, Wnt Signaling, and MAOA gene regulation, respectively, which inhibits neuronal cell death. In addition, decreased neuronal cell death rescued memory impairment and cognitive defects, which inhibits the pathogenesis of AD. Thus, the OIP5-AS1/miR-129-5p/CREBBP axis could be a possible therapeutic target in metal toxicity-induced AD. Further, these results provide a gateway for the future *in vivo* and *in vitro* studies targeting OIP5-AS1/miR-129-5p/CREBBP axis in a metal toxicity-induced AD.

CRedit authorship contribution statement

P.K. and R.G. conceived and designed the manuscript. R.G. has collected, analyzed, and critically evaluated these data. P.K. and R.G. have prepared figures and tables. P.K and R.G. analyzed the entire data and wrote the manuscript.

Declaration of competing interest

The authors declare that they have no known competing financial interests or personal relationships that could have appeared to influence the work reported in this paper.



(caption on next page)

Fig. 5. (A) Involvement of predicted micro-RNAs, such as hsa-miR-338-5p, hsa-miR-335-5p, hsa-miR-429, hsa-miR-200c-3p, and hsa-miR-129-5p in the brain disease, such as Alzheimer's disease, Parkinson's disease, tauopathy, neuropathy, brain ischemia, brain edema, autism spectrum disorder, cerebral degeneration, and others through mirDIP database. (B) Pathway analysis of hsa-miR-335-5p and hsa-miR-129-5p with the help of TissueAtlas database: hsa-miR-129-5p is significantly enriched in corticotropin-releasing hormone pathway (9.91805E-05), IL17 signaling pathway (0.000468125), EGF/EGFR signaling pathway (0.000533398), Interleukin-11 signaling pathway (0.000945926), and VEGFA-VEGFR2 (0.001582748) signaling pathway, whereas, hsa-miR-335-5p is significantly enriched in TGF-beta signaling pathway (5.90563E-06), IL-2 signaling pathway (8.98756E-06), ErbB signaling pathway (9.29391E-05), B cell receptor signaling pathway (0.000115973), and IL-7 signaling pathway (0.000302961).

Acknowledgement

We would like to thank the senior management of Delhi Technological University for constant support and encouragement.

References

- Ahmadi, S., Zobeiri, M., Bradburn, S., 2020. Molecular mechanisms underlying actions of certain long noncoding RNAs in Alzheimer's disease. *Metab. Brain Dis.* <https://doi.org/10.1007/s11011-020-00564-9>.
- Ascolani, A., Balestrieri, E., Minutolo, A., Mosti, S., Spalletta, G., Bramanti, P., Mastino, A., Caltagirone, C., Macchi, B., 2012. Dysregulated NF- κ B pathway in peripheral mononuclear cells of alzheimer's disease patients. *Curr. Alzheimer Res.* 9, 128–137. <https://doi.org/10.2174/156720512799015091>.
- Bader, G.D., Hogue, C.W.V., 2003. An automated method for finding molecular complexes in large protein interaction networks. *BMC Bioinformatics.* <https://doi.org/10.1186/1471-2105-4-2>.
- Barr, I., Weitz, S.H., Atkin, T., Hsu, P., Karayiorgou, M., Gogos, J.A., Weiss, S., Guo, F., 2015. Cobalt (III) protoporphyrin activates the DGCR8 protein and can compensate microRNA processing deficiency. *Chem. Biol.* 22, 793. <https://doi.org/10.1016/j.CHEMBIOL.2015.05.015>.
- Barral, S., Reitz, C., Small, S.A., Mayeux, R., 2014. Genetic variants in a "cAMP element binding protein" (CREB)-dependent histone acetylation pathway influence memory performance in cognitively healthy elderly individuals. *Neurobiol. Aging* 35, 2881.e7–2881.e10. <https://doi.org/10.1016/j.neurobiolaging.2014.06.024>.
- Bartolotti, N., Bennett, D.A., Lazarov, O., 2016. Reduced pCREB in Alzheimer's disease prefrontal cortex is reflected in peripheral blood mononuclear cells. *Mol. Psychiatry* 219 (21), 1158–1166. <https://doi.org/10.1038/mp.2016.111>, 2016.
- Bartolotti, N., Lazarov, O., 2019. CREB signals as PBMC-based biomarkers of cognitive dysfunction: a novel perspective of the brain-immune axis. *Brain Behav. Immun.* <https://doi.org/10.1016/j.bbi.2019.01.004>.
- Belaya, Z., Khandava, P., Nonn, L., Nikitin, A., Solodovnikov, A., Sitkin, I., Grigoriev, A., Pikunov, M., Lapshina, A., Rozhinskaya, L., Melnichenko, G., Dedov, I., 2020. Circulating plasma microRNA to differentiate cushing's disease from ectopic ACTH syndrome. *Front. Endocrinol. (Lausanne)* 0, 331. <https://doi.org/10.3389/FENDO.2020.00331>.
- Bourassa, M.W., Ratan, R.R., 2014. The interplay between microRNAs and histone deacetylases in neurological diseases. *Neurochem. Int.* <https://doi.org/10.1016/j.neuint.2014.03.012>.
- Byrne, J.C., Valen, E., Tang, M.H.E., Marstrand, T., Winther, O., Krogh, A., Lenhard, B., Sandelin, A., Da Piedade, I., 2008. jasp, the open access database of transcription factor-binding profiles: new content and tools in the 2008 update. *Nucleic Acids Res.* <https://doi.org/10.1093/nar/gkm955>.
- Caccamo, A., Maldonado, M.A., Bokov, A.F., Majumder, S., Oddo, S., 2010. CBP gene transfer increases BDNF levels and ameliorates learning and memory deficits in a mouse model of Alzheimer's disease. *Proc. Natl. Acad. Sci. U. S. A.* 107, 22687–22692. <https://doi.org/10.1073/pnas.1012851108>.
- Catana, C.S., Crisjan, C.A., Opre, D., Berindan-Neagoe, I., 2020. Diagnostic and prognostic value of microRNAs for Alzheimer's disease: a comprehensive metaanalysis. *Med. Pharm. Rep.* 93, 53–61. <https://doi.org/10.15386/mpr-1393>.
- Chandra, S., Pandey, A., Chowdhuri, D.K., 2015. miRNA profiling provides insights on adverse effects of Cr(VI) in the midgut tissues of *Drosophila melanogaster*. *J. Hazard. Mater.* 283, 558–567. <https://doi.org/10.1016/j.jhazmat.2014.09.054>.
- Chatterjee, S., Mizar, P., Cassel, R., Neidl, R., Ruthrotha Selvi, B., Mohankrishna, D.V., Vedamurthy, B.M., Schneider, A., Bousiges, O., Mathis, C., Cassel, J.C., Eswaramoorthy, M., Kundu, T.K., Boutilier, A.L., 2013. A novel activator of CBP/p300 acetyltransferases promotes neurogenesis and extends memory duration in adult mice. *J. Neurosci.* 33, 10698–10712. <https://doi.org/10.1523/JNEUROSCI.5772-12.2013>.
- Chen, D., Kluz, T., Fang, L., Zhang, X., Sun, H., Jin, C., Costa, M., 2016. Hexavalent Chromium (Cr(VI)) Down-Regulates Acetylation of Histone H4 at Lysine 16 through Induction of Stressor Protein Nupr1. <https://doi.org/10.1371/journal.pone.0157317>.
- Chen, P., Miah, M.R., Aschner, M., 2016. Metals and neurodegeneration. *F1000Research.* <https://doi.org/10.12688/f1000research.7431.1>.
- Chen, X., Li, Y., Wang, C., Tang, Y., Mok, S.A., Tsai, R.M., Rojas, J.C., Karydas, A., Miller, B.L., Boxer, A.L., Gestwicki, J.E., Arkin, M., Cuervo, A.M., Gan, L., 2020. Promoting tau secretion and propagation by hyperactive p300/CBP via autophagy-lysosomal pathway in tauopathy. *Mol. Neurodegener.* 15, 1–19. <https://doi.org/10.1186/s13024-019-0354-0>.
- Chin, C.H., Chen, S.H., Wu, H.H., Ho, C.W., Ko, M.T., Lin, C.Y., 2014. cytoHubba: identifying hub objects and sub-networks from complex interactome. *BMC Syst. Biol.* <https://doi.org/10.1186/1752-0509-8-54-S11>.
- Chiou, Y.H., Liou, S.H., Wong, R.H., Chen, C.Y., Lee, H., 2015. Nickel may contribute to EGFR mutation and synergistically promotes tumor invasion in EGFR-mutated lung cancer via nickel-induced microRNA-21 expression. *Toxicol. Lett.* 237, 46–54. <https://doi.org/10.1016/j.toxlet.2015.05.019>.
- Chow, N., Bell, R.D., Deane, R., Streb, J.W., Chen, J., Brooks, A., Van Nostrand, W., Miano, J.M., Zlokovic, B.V., 2007. Serum response factor and myocardin mediate arterial hypercontractility and cerebral blood flow dysregulation in Alzheimer's phenotype. *Proc. Natl. Acad. Sci. U. S. A.* 104, 823–828. <https://doi.org/10.1073/pnas.0608251104>.
- Cong, L., Cong, Y., Feng, N., Liang, W., Wu, Y., 2021. Up-regulated microRNA-132 reduces the cognition-damaging effect of sevoflurane on Alzheimer's disease rats by inhibiting FOXA1. *Genomics* 113, 3644–3652. <https://doi.org/10.1016/j.YGENO.2021.08.011>.
- Dancy, B.M., Cole, P.A., 2015. Protein lysine acetylation by p300/CBP. *Chem. Rev.* 115, 2419. <https://doi.org/10.1021/CR500452K>.
- Davis, A.P., Grondin, C.J., Johnson, R.J., Sciaky, D., McMorran, R., Wieggers, J., Wieggers, T.C., Mattingly, C.J., 2019. The comparative toxicogenomics database: update 2019. *Nucleic Acids Res.* <https://doi.org/10.1093/nar/gky868>.
- Deng, W., Wang, C., Zhang, Y., Xu, Y., Zhang, S., Liu, Z., Xue, Y., 2016. GPS-PAIL: prediction of lysine acetyltransferase-specific modification sites from protein sequences. *Sci. Rep.* 6, 1–10. <https://doi.org/10.1038/srep39787>.
- Doxtater, K., Tripathi, M., Khan, M., 2020. Recent advances on the role of long non-coding RNAs in Alzheimer's disease. *Neural Regen. Res.* <https://doi.org/10.4103/1673-5374.284990>.
- Excoffier, L., Gouy, A., Daub, J.T., Shannon, P., Markiel, A., Ozier, O., Baliga, N.S., Wang, J.T., Ramage, D., Amin, N., Schwikowski, B., Ideker, T., 2017. Cytoscape: a software environment for integrated models of biomolecular interaction networks. *Nucleic Acids Res.* <https://doi.org/10.1093/nar/gkx626>.
- Fay, M.J., Alt, L.A.C., Ryba, D., Salamah, R., Peach, R., Papaeliou, A., Zawadzka, S., Weiss, A., Patel, N., Rahman, A., Stubbs-Russell, Z., Lamar, P.C., Edwards, J.R., Prozialek, W.C., 2018. Cadmium nephrotoxicity is associated with altered MicroRNA expression in the rat renal cortex. *Toxicol.* 6. <https://doi.org/10.3390/TOXICS6010016>.
- Fielder, E., Tweedy, C., Wilson, C., Oakley, F., LeBeau, F.E.N., Passos, J.F., Mann, D.A., von Zglinicki, T., Jurk, D., 2020. Anti-inflammatory treatment rescues memory deficits during aging in nfkb1-/- mice. *Aging Cell* 19. <https://doi.org/10.1111/acel.13188>.
- Fujita, K., Morimoto, Y., Ogami, A., Myojo, T., Tanaka, I., Shimada, M., Wang, W.N., Endoh, S., Uchida, K., Nakazato, T., Yamamoto, K., Fukui, H., Horie, M., Yoshida, Y., Iwahashi, H., Nakanishi, J., 2009. Gene expression profiles in rat lung after inhalation exposure to C60 fullerene particles. *Toxicology* 258, 47–55. <https://doi.org/10.1016/j.tox.2009.01.005>.
- Ge, X., Liu, Z., Qi, W., Shi, X., Zhai, Q., 2008. Chromium (VI) induces insulin resistance in 3T3-L1 adipocytes through elevated reactive oxygen species generation. *Free Radic. Res.* <https://doi.org/10.1080/10715760802155113>.
- Ghaffari, S.H., Bashash, D., Ghavamzadeh, A., Alimoghaddam, K., Dizaji, M.Z., 2011. Alteration in miRNA gene expression pattern in acute promyelocytic leukemia cell induced by arsenic trioxide: a possible mechanism to explain arsenic multi-target action. *Tumor Biol.* 331 (33), 157–172. <https://doi.org/10.1007/S13277-011-0259-1>, 2011.
- Glaeser, K., May, C., Marcus, K., Matschke, V., Theiss, C., Theis, V., 2020. miR-129-5p and miR-130a-3p regulate VEGFR-2 expression in sensory and motor neurons during development, 2020 *Int. J. Mol. Sci.* 21, 3839. <https://doi.org/10.3390/IJMS21113839>, 21, 3839.
- Gorantla, N.V., Landge, V.G., Nagaraju, P.G., Priyadarshini Cg, P., Balaraman, E., Chinnathambi, S., 2019. Molecular Cobalt(II) complexes for tau polymerization in Alzheimer's disease. *ACS Omega.* <https://doi.org/10.1021/acsomega.9b00692>.
- Gray, M.J., Zhang, J., Ellis, L.M., Semenza, G.L., Evans, D.B., Watowich, S.S., Gallick, G.E., 2005. HIF-1 α , STAT3, CBP/p300 and Ref-1/APE are components of a transcriptional complex that regulates Src-dependent hypoxia-induced expression of VEGF in pancreatic and prostate carcinomas. *Oncogene* 2419 (2005), 3110–3120. <https://doi.org/10.1038/sj.onc.1208513>.
- Guo, Z., Tang, J., Wang, J., Zheng, F., Zhang, C., Wang, Y.L., Cai, P., Shao, W., Yu, G., Wu, S., Li, H., 2021. The negative role of histone acetylation in cobalt chloride-induced neurodegenerative damages in SHSY5Y cells. *Ecotoxicol. Environ. Saf.* 209, 111832. <https://doi.org/10.1016/j.ecoenv.2020.111832>.
- Hayakawa, F., Towatari, M., Ozawa, Y., Tomita, A., Privalsky, M.L., Saito, H., 2004. Functional regulation of GATA-2 by acetylation. *J. Leukoc. Biol.* 75, 529–540. <https://doi.org/10.1189/JLB.0603389>.
- Ho, W.M., Wu, Y.Y., Chen, Y.C., 2020. Genetic variants behind cardiovascular diseases and dementia. *Genes (Basel).* <https://doi.org/10.3390/genes11121514>.
- Huat, T.J., Camats-Perna, J., Newcombe, E.A., Valmas, N., Kitazawa, M., Medeiros, R., 2019. Metal toxicity links to Alzheimer's disease and neuroinflammation. *J. Mol. Biol.* <https://doi.org/10.1016/j.jmb.2019.01.018>.
- JA, S., RJ, B., Y., W., A., B., 1999. Chromium(VI) inhibits the transcriptional activity of nuclear factor-kappaB by decreasing the interaction of p65 with cAMP-responsive

- element-binding protein-binding protein. *J. Biol. Chem.* 274, 36207–36212. <https://doi.org/10.1074/JBC.274.51.36207>.
- Jeon, E.S., Shin, J.H., Hwang, S.J., Moon, G.J., Bang, O.Y., Kim, H.H., 2014. Cobalt chloride induces neuronal differentiation of human mesenchymal stem cells through upregulation of microRNA-124a. *Biochem. Biophys. Res. Commun.* 444, 581–587. <https://doi.org/10.1016/j.bbrc.2014.01.114>.
- Jia, J., Li, T., Yao, C., Chen, Junfei, Feng, L., Jiang, S., Shi, L., Liu, J., Chen, Junqiang, Lou, J., 2020. Circulating differential miRNAs profiling and expression in hexavalent chromium exposed electroplating workers. *Chemosphere* 260. <https://doi.org/10.1016/j.chemosphere.2020.127546>.
- Kang, J., Lin, C., Chen, J., Liu, Q., 2004. Copper induces histone hypoacetylation through directly inhibiting histone acetyltransferase activity. *Chem. Biol. Interact.* 148, 115–123. <https://doi.org/10.1016/j.cbi.2004.05.003>.
- Khokhar, M., Tomo, S., Purohit, P., 2021. Micro RNA-based regulation of genomics and transcriptomics of inflammatory cytokines in COVID-19. medRxiv. <https://doi.org/10.1101/2021.06.08.21258565>.
- Kim, S.H., Knight, E.M., Saunders, E.L., Cuevas, A.K., Popovech, M., Chen, L.C., Gandy, S., 2012. Rapid doubling of Alzheimer's amyloid- β 40 and 42 levels in brains of mice exposed to a nickel nanoparticle model of air pollution. *F1000Research*. <https://doi.org/10.12688/f1000research.1-70.v1>.
- Kitazawa, M., Hsu, H.-W., Medeiros, R., 2016. Copper exposure perturbs brain inflammatory responses and impairs clearance of amyloid-beta. *Toxicol. Sci.* 152, 194–204. <https://doi.org/10.1093/toxsci/kfw081>.
- Kou, X., Chen, D., Chen, N., 2020. The regulation of microRNAs in Alzheimer's disease. *Front. Neurol.* <https://doi.org/10.3389/fneur.2020.00288>.
- Kumar, S., Reddy, P.H., 2020. The role of synaptic microRNAs in Alzheimer's disease. *Biochim. Biophys. Acta - Mol. Basis Dis.* <https://doi.org/10.1016/j.bbdis.2020.165937>.
- Li, H., Wang, F., Guo, X., Jiang, Y., 2021. Decreased MEF2A expression regulated by its enhancer methylation inhibits autophagy and may play an important role in the progression of Alzheimer's disease. *Front. Neurosci.* 669. <https://doi.org/10.3389/fnins.2021.682247>.
- Li, J., Feng, Z., Chen, L., Wang, X., Deng, H., 2016. MicroRNA-335-5p inhibits osteoblast apoptosis induced by high glucose. *Mol. Med. Rep.* 13, 4108–4112. <https://doi.org/10.3892/mmr.2016.4994>.
- Li, J., Wang, J., Wang, Y.-L., Luo, Z., Zheng, C., Yu, G., Wu, S., Zheng, F., Li, H., 2021. NOX2 activation contributes to cobalt nanoparticles-induced inflammatory responses and tau phosphorylation in mice and microglia. *Ecotoxicol. Environ. Saf.* 225, 112725. <https://doi.org/10.1016/j.ecoenv.2021.112725>.
- Li, J.H., Liu, S., Zhou, H., Qu, L.H., Yang, J.H., 2014. StarBase v2.0: decoding miRNA-cRNA, miRNA-mRNA and protein-RNA interaction networks from large-scale CLIP-seq data. *Nucleic Acids Res.* 42, D92–D97. <https://doi.org/10.1093/nar/gkt1248>.
- Li, L., Xu, Y., Zhao, M., Gao, Z., 2020. Neuro-protective roles of long non-coding RNA MALAT1 in Alzheimer's disease with the involvement of the microRNA-30b/CNR1 network and the following PI3K/AKT activation. *Exp. Mol. Pathol.* 117, 104545. <https://doi.org/10.1016/j.yexmp.2020.104545>.
- Li, X.-Q., Chen, F.-S., Tan, W.-F., Fang, B., Zhang, Z.-L., Ma, H., 2017. Elevated microRNA-129-5p level ameliorates neuroinflammation and blood-spinal cord barrier damage after ischemia-reperfusion by inhibiting HMGB1 and the TLR3-cytokine pathway. *J. Neuroinflammation* 141 (14), 1–12. <https://doi.org/10.1186/S12974-017-0977-4>, 2017.
- Li, Z., Chen, Q., Liu, J., Du, Y., 2020. Physical exercise ameliorates the cognitive function and attenuates the neuroinflammation of Alzheimer's disease via miR-129-5p. *Dement. Geriatr. Cogn. Disord.* 49, 163–169. <https://doi.org/10.1159/000507285>.
- Liao, M.Y., Liu, H.G., 2012. Gene expression profiling of nephrotoxicity from copper nanoparticles in rats after repeated oral administration. *Environ. Toxicol. Pharmacol.* 34, 67–80. <https://doi.org/10.1016/j.etap.2011.05.014>.
- Licursi, V., Conte, F., Fison, G., Paci, P., 2019. MIENTURNET: an interactive web tool for microRNA-target enrichment and network-based analysis. *BMC Bioinformatics* 20, 1–10. <https://doi.org/10.1186/s12859-019-3105-x>.
- Lu, Q., Hutchins, A.E., Doyle, C.M., Lundblad, J.R., Kwok, R.P.S., 2003. Acetylation of cAMP-responsive element-binding protein (CREB) by CREB-binding protein enhances CREB-dependent transcription. *J. Biol. Chem.* <https://doi.org/10.1074/jbc.M300546200>.
- Ludwig, N., Leidinger, P., Becker, K., Backes, C., Fehlmann, T., Pallasch, C., Rheinheimer, S., Meder, B., Stähler, C., Meese, E., Keller, A., 2016. Distribution of miRNA expression across human tissues. *Nucleic Acids Res.* 44, 3865–3877. <https://doi.org/10.1093/nar/gkw116>.
- Mao, H., Huang, Q., Liu, Y., 2021. MEG3 aggravates hypoxia/reoxygenation induced apoptosis of renal tubular epithelial cells via the miR-129-5p/HMGB1 axis. *J. Biochem. Mol. Toxicol.* 35, e22649. <https://doi.org/10.1002/jbt.22649>.
- Mayes, J., Tinker-Mill, C., Kolosov, O., Zhang, H., Tabner, B.J., Allsop, D., 2014. β -amyloid fibrils in alzheimer disease are not inert when bound to copper ions but can degrade hydrogen peroxide and generate reactive oxygen species. *J. Biol. Chem.* <https://doi.org/10.1074/jbc.M113.525212>.
- Newcombe, E.A., Camats-Perna, J., Silva, M.L., Valmas, N., Huat, T.J., Medeiros, R., 2018. Inflammation: the link between comorbidities, genetics, and Alzheimer's disease. *J. Neuroinflammation* 151 (15), 1–26. <https://doi.org/10.1186/S12974-018-1313-3>, 2018.
- Ngalame, N.N.O., Waalkes, M.P., Tokar, E.J., 2016. Silencing KRAS overexpression in cadmium-transformed prostate epithelial cells mitigates malignant phenotype. *Chem. Res. Toxicol.* 29, 1458. <https://doi.org/10.1021/ACS.CHEMRETOX.6B00337>.
- Ogata, H., Goto, S., Sato, K., Fujibuchi, W., Bono, H., Kanehisa, M., 1999. KEGG: Kyoto encyclopedia of genes and genomes. *Nucleic Acids Res.* <https://doi.org/10.1093/nar/27.1.29>.
- Oliveros, J.C., 2007. VENNY. An Interactive Tool for Comparing Lists With Venn Diagrams [WWW Document]. <http://bioinfogp.cnb.csic.es/tools/venny/index.html>. <http://p://bioinfogp.cnb.csic.es/tools/venny/index.html>.
- Padmavathi, I.J.N., Rao, K.R., Venu, L., Ganeshan, M., Kumar, K.A., Rao, C.N., Harishankar, N., Ismail, A., Raghunath, M., 2010. Chronic maternal dietary chromium restriction modulates visceral adiposity: probable underlying mechanisms. *Diabetes*. <https://doi.org/10.2337/db09-0779>.
- Park, Y., Albright, K.J., Liu, W., Storkson, J.M., Cook, M.E., Pariza, M.W., 1997. Effect of conjugated linoleic acid on body composition in mice. *Lipids*. <https://doi.org/10.1007/s11745-997-0109-x>.
- Pathan, M., Keerthikumar, S., Ang, C.S., Gangoda, L., Quek, C.Y.J., Williamson, N.A., Mouradov, D., Sieber, O.M., Simpson, R.J., Salim, A., Bacic, A., Hill, A.F., Stroud, D. A., Ryan, M.T., Agbinya, J.I., Mariadason, J.M., Burgess, A.W., Mathivanan, S., 2015. FunRich: an open access standalone functional enrichment and interaction network analysis tool. *Proteomics*. <https://doi.org/10.1002/pmic.201400515>.
- Piñero, J., Ramírez-Anguita, J.M., Saúch-Pitarch, J., Ronzano, F., Centeno, E., Sanz, F., Furlong, L.L., 2020. The DisGenET knowledge platform for disease genomics: 2019 update. *Nucleic Acids Res.* <https://doi.org/10.1093/nar/gkz1021>.
- Portillo, M., Eremenko, E., Kaluski, S., Garcia-Venzor, A., Onn, L., Stein, D., Slobodnik, Z., Zaretsky, A., Ueberham, U., Einav, M., Brückner, M.K., Arendt, T., Toiber, D., 2021. SIRT6-CBP-dependent nuclear tau accumulation and its role in protein synthesis. *Cell Rep.* 35, 109035. <https://doi.org/10.1016/j.celrep.2021.109035>.
- Rafael, A.I., Almeida, A., Santos, P., Parreira, I., Madeira, V.M.S., Alves, R., Cabrita, A.M. S., Alpoim, M.C., 2007. A role for transforming growth factor- β apoptotic signaling pathway in liver injury induced by ingestion of water contaminated with high levels of Cr(VI). *Toxicol. Appl. Pharmacol.* <https://doi.org/10.1016/j.taap.2007.07.004>.
- Rahman, M.H., Sarkar, B., Islam, M.S., Abdullah, M.I., 2020. Discovering biomarkers and pathways shared by Alzheimer's disease and Parkinson's disease to identify novel therapeutic targets. *Int. J. Eng. Res. Technol.* 9.
- Rahman, M.R., Islam, T., Turanli, B., Zaman, T., Faruquee, H.M., Rahman, M.M., Mollah, M.N.H., Nanda, R.K., Arga, K.Y., Gov, E., Moni, M.A., 2019. Network-based approach to identify molecular signatures and therapeutic agents in Alzheimer's disease. *Comput. Biol. Chem.* 78, 431–439. <https://doi.org/10.1016/j.compbiolchem.2018.12.011>.
- Savojardo, C., Martelli, P.L., Fariselli, P., Profitti, G., Casadio, R., 2018. BUSCA: an integrative web server to predict subcellular localization of proteins. *Nucleic Acids Res.* 46, W459–W466. <https://doi.org/10.1093/NAR/GKY320>.
- Schueler, E., Paiva, I., Blanc, F., Wang, X.L., Cassel, J.C., Boutilier, A.L., Bousiges, O., 2020. Dysregulation of histone acetylation pathways in hippocampus and frontal cortex of Alzheimer's disease patients. *Eur. Neuropsychopharmacol.* 33, 101–116. <https://doi.org/10.1016/j.euroneuro.2020.01.015>.
- Shobana, N., Kumar, M.K., Navin, A.K., Akbarsha, M.A., Aruldas, M.M., 2020. Prenatal exposure to excess chromium attenuates transcription factors regulating expression of androgen and follicle stimulating hormone receptors in sertoli cells of prepubertal rats. *Chem. Biol. Interact.* 328, 109188. <https://doi.org/10.1016/j.cbi.2020.109188>.
- Soldan, A., Gazes, Y., Stern, Y., 2016. Alzheimer's disease. In: *The Curated Reference Collection in Neuroscience and Biobehavioral Psychology*. <https://doi.org/10.1016/B978-0-12-809324-5.06319-7>.
- Song, H., Moon, M., Choe, H.K., Han, D.H., Jang, C., Kim, A., Cho, S., Kim, K., Mook-Jung, I., 2015. β -induced degradation of BMAL1 and CBP leads to circadian rhythm disruption in Alzheimer's disease. *Mol. Neurodegener.* 10, 1–15. <https://doi.org/10.1186/s13024-015-0007-x>.
- Szklarczyk, D., Gable, A.L., Lyon, D., Junge, A., Wyder, S., Huerta-Cepas, J., Simonovic, M., Doncheva, N.T., Morris, J.H., Bork, P., Jensen, L.J., Von Mering, C., 2019. STRING v11: protein-protein association networks with increased coverage, supporting functional discovery in genome-wide experimental datasets. *Nucleic Acids Res.* <https://doi.org/10.1093/nar/gky1131>.
- Tang, X.-W., Qin, Q.-X., 2019. miR-335-5p induces insulin resistance and pancreatic islet β -cell secretion in gestational diabetes mellitus mice through VASH1-mediated TGF- β signaling pathway. *J. Cell. Physiol.* 234, 6654–6666. <https://doi.org/10.1002/jcp.27406>.
- Thakur, N., Pandey, R.K., Mehrotra, S., 2021. Signal transducer and activator of transcription-3 mediated neuroprotective effect of interleukin-6 on cobalt chloride mimetic hypoxic cell death in R28 cells. *Mol. Biol. Reports* 488 (48), 6197–6203. <https://doi.org/10.1007/S11033-021-06586-5>, 2021.
- Tian, J., Song, T., Wang, W., Wang, H., Zhang, Z., 2019. miR-129-5p alleviates neuropathic pain through regulating HMGB1 expression in CCI Rat Models. *J. Mol. Neurosci.* 701 (70), 84–93. <https://doi.org/10.1007/S12031-019-01403-Y>, 2019.
- Tokar, T., Pastrello, C., Rossos, A.E.M., Abovsky, M., Hauschild, A.C., Tsay, M., Lu, R., Jurisica, I., 2018. MirDIP 4.1 - integrative database of human microRNA target predictions. *Nucleic Acids Res.* 46, D360–D370. <https://doi.org/10.1093/nar/gkx1144>.
- Wang, D., Fei, Z., Luo, S., Wang, H., 2020. MiR-335-5p inhibits β -amyloid ($A\beta$) accumulation to attenuate cognitive deficits through targeting c-Jun-N-terminal kinase 3 in Alzheimer's disease. *Curr. Neurovasc. Res.* 17, 93–101. <https://doi.org/10.2174/1567202617666200128141938>.
- Wei, W., Wang, Z.Y., Ma, L.N., Zhang, T.T., Cao, Y., Li, H., 2020. MicroRNAs in Alzheimer's disease: function and potential applications as diagnostic biomarkers. *Front. Mol. Neurosci.* <https://doi.org/10.3389/fnmol.2020.00160>.
- Weller, J., Budson, A., 2018. Current understanding of Alzheimer's disease diagnosis and treatment. *F1000Research*. <https://doi.org/10.12688/f1000research.14506.1>.
- Wu, C.-H., Hsiao, Y.-M., Yeh, K.-T., Tsou, T.-C., Chen, C.-Y., Wu, M.-F., Ko, J.-L., 2017. Upregulation of microRNA-4417 and its target genes contribute to nickel chloride-

- promoted lung epithelial cell fibrogenesis and tumorigenesis. *Sci. Reports* 71 (7), 1–13. <https://doi.org/10.1038/s41598-017-14610-7>, 2017.
- Xia, B., Yang, Xiong, Z., Zhuang, Bin, Y., Xia, Jun, J., Liu, Hui, J., Yuan, Cheng, Q., Liu, Hua, G., Hu, Pang, L., Yan, H., Huang, Qing, L., 2011. Chromium(VI) causes down regulation of biotinidase in human bronchial epithelial cells by modifications of histone acetylation. *Toxicol. Lett.* 205, 140–145. <https://doi.org/10.1016/J.TOXLET.2011.05.1032>.
- Xu, M., Yu, Z., Hu, F., Zhang, Hongbing, Zhong, L., Han, L., An, Y., Zhu, B., Zhang, Hengdong, 2017. Identification of differential plasma miRNA profiles in chinese workers with occupational lead exposure. *Biosci. Rep.* 37, 20171111. <https://doi.org/10.1042/BSR20171111>.
- Yang, Y., Gong, B., Wu, Z.-Z., Shuai, P., Li, D.-F., Liu, L.-L., Yu, M., 2019. Inhibition of microRNA-129-5p expression ameliorates ultraviolet ray-induced corneal epithelial cell injury via upregulation of EGFR. *J. Cell. Physiol.* 234, 11692–11707. <https://doi.org/10.1002/JCP.27837>.
- Yu, B., Wang, B., Wu, Z., Wu, C., Ling, J., Gao, X., Zeng, H., 2021. LncRNA SNHG8 promotes proliferation and inhibits apoptosis of diffuse large B-cell lymphoma via sponging miR-335-5p. *Front. Oncol.* 11, 650287 <https://doi.org/10.3389/FONC.2021.650287>.
- Yu, K., Zhang, Q., Liu, Z., Du, Y., Gao, X., Zhao, Q., Cheng, H., Li, X., Liu, Z.X., 2020. Deep learning based prediction of reversible HAT/HDAC-specific lysine acetylation. *Brief. Bioinform.* 21, 1798–1805. <https://doi.org/10.1093/bib/bbz107>.
- Yubolphan, R., Phuagkhaopong, S., Sangpairoj, K., Sibmooh, N., Power, C., Vivithanaporn, P., 2021. Intracellular nickel accumulation induces apoptosis and cell cycle arrest in human astrocytic cells. *Metallomics* 13. <https://doi.org/10.1093/MTOMCS/MFAA006>.
- Yue, D., Guanqun, G., Jingxin, L., Sen, S., Shuang, L., Yan, S., Minxue, Z., Ping, Y., Chong, L., Zhuobo, Z., Yafen, W., 2020. Silencing of long noncoding RNA XIST attenuated Alzheimer's disease-related BACE1 alteration through miR-124. *Cell Biol. Int.* 44, 630–636. <https://doi.org/10.1002/cbin.11263>.
- Yue, J., Wang, P., Hong, Q., Liao, Q., Yan, L., Xu, W., Chen, X., Zheng, Q., Zhang, L., Huang, D., 2017. MicroRNA-335-5p plays dual roles in periapical lesions by complex regulation pathways. *J. Endod.* 43, 1323–1328. <https://doi.org/10.1016/J.JOEN.2017.03.018>.
- Zeng, H., Wang, J., Chen, T., Zhang, K., Chen, J., Wang, L., Li, H., Tuluhong, D., Li, J., Wang, S., 2019. Downregulation of long non-coding RNA opa interacting protein 5-antisense RNA 1 inhibits breast cancer progression by targeting sex-determining region Y-box 2 by microRNA-129-5p upregulation. *Cancer Sci.* 110, 289–302. <https://doi.org/10.1111/cas.13879>.
- Zeng, Z., Liu, Y., Zheng, W., Liu, L., Yin, H., Zhang, S., Bai, H., Hua, L., Wang, S., Wang, Z., Li, X., Xiao, J., Yuan, Q., Wang, Y., 2019. MicroRNA-129-5p alleviates nerve injury and inflammatory response of Alzheimer's disease via downregulating SOX6. *Cell Cycle* 18, 3095–3110. <https://doi.org/10.1080/15384101.2019.1669388>.
- Zhao, Y.N., Li, W.F., Li, F., Zhang, Z., Dai, Y.D., Xu, A.L., Qi, C., Gao, J.M., Gao, J., 2013. Resveratrol improves learning and memory in normally aged mice through microRNA-CREB pathway. *Biochem. Biophys. Res. Commun.* 435, 597–602. <https://doi.org/10.1016/j.bbrc.2013.05.025>.
- Zhou, C., Liu, M., Mei, X., Li, Q., Zhang, W., Deng, P., He, Z., Xi, Y., Tong, T., Pi, H., Lu, Y., Chen, C., Zhang, L., Yu, Z., Zhou, Z., He, M., 2021. Histone hypoacetylation contributes to neurotoxicity induced by chronic nickel exposure in vivo and in vitro. *Sci. Total Environ.* 783, 147014 <https://doi.org/10.1016/J.SCITOTENV.2021.147014>.
- Zhou, G., Soufan, O., Ewald, J., Hancock, R.E.W., Basu, N., Xia, J., 2019. NetworkAnalyst 3.0: a visual analytics platform for comprehensive gene expression profiling and meta-analysis. *Nucleic Acids Res.* <https://doi.org/10.1093/nar/gkz240>.
- Zhu, X., Li, Z., Li, L., Chen, L., Ouyang, M., Zhou, H., Xiao, K., Lin, L., Chu, P.K., Zhou, C., Xun, C., Yang, L., Huang, W., Ding, X., 2021. KCTD1 Downregulation Suppresses Hepatocellular Carcinoma by Regulating Angiogenesis and Inuencing the HIF-1 α /VEGF Pathway. <https://doi.org/10.21203/rs.3.rs-419484/v1>.
- Zoltowska, K.M., Laskowska-Kaszub, K., Nagaraj, S., Wojda, U., 2020. Implication of microRNAs in Alzheimer's disease pathogenesis. In: *Genetics, Neurology, Behavior, and Diet in Dementia*. Elsevier, pp. 131–145. <https://doi.org/10.1016/b978-0-12-815868-5.00009-8>.